Microglial and neurochemical mechanisms of seizure-induced central autonomic cardiovascular dysfunction

Amol Mohan Bhandare

Master of Pharmacy in Pharmacology

Department of Biomedical Sciences

Faculty of Medicine and Health Sciences

Macquarie University

This thesis is presented for the degree of Doctorate of Philosophy in Advanced Medicine

June 2016

Table of Contents

Summary

Epilepsy is a chronic paroxysmal neurological disorder characterised by seizures. Central autonomic cardiovascular dysfunction is established as a major cause of sudden unexpected death in epilepsy (SUDEP). Cardiovascular autonomic function is controlled by nuclei present in the brainstem, including the rostral ventrolateral medulla (RVLM). The RVLM gives projection to presympathetic neurons in the intermediolateral cell column (IML) of the spinal cord, which in turn controls the sympathetic nerve activity (SNA) of post-ganglionic neurons and thus the cardiovascular system.

Microglia are the principal resident immune cells of the CNS that react to pathological or physiological disturbances in the brain, such as seizures, to produce pro-inflammatory or anti-inflammatory effects. Levels of the peptide pituitary adenylate cyclase-activating polypeptide (PACAP) increase during and after seizures, and it has neuroprotective as well as sympathoexcitatory properties, while glutamate, which is the principal cardiovascular autonomic neurotransmitter in the RVLM, plays an important role in the development of seizures.

The major aims of this thesis were to investigate the role of microglia, PACAP and glutamate in the RVLM and/or IML in the progression of seizure-induced autonomic cardiovascular dysfunction during acute and chronic epilepsy in rats.

The findings suggest that: 1) Kainic acid (KA)-induced acute seizures cause significant and dose-dependent increase in SNA, mean arterial pressure and heart rate and a prolongation of the QT interval in the ECG. 2) Intrathecal (IT) infusion of PACAP antagonist (PACAP(6-38)) or microglial antagonist (minocycline and doxycycline) worsens the cardiovascular responses of acute seizures, whereas IT PACAP agonist (PACAP-38) has no significant effect. 3) Acute seizure-induced cardiovascular responses, including prolongation of the QT interval, are driven by activation of glutamatergic receptors in the RVLM as these effects are abolished with glutamate receptor antagonist (kynurenic acid) microinjection. The activity of PACAP and microglia in the RVLM do not alter SNA, but mediate prolongation of the QT interval. 4) In the vicinity of the RVLM neurons, microglia are in a surveillance state with no change in their number of anti-inflammatory M2 phenotype during acute seizures. 5) In rats with KA-induced chronic temporal lobe epilepsy, spontaneous seizures cause significant tachycardia with long-lasting prolongation of QT interval. The antagonism of microglial activation, but not PACAP, at the level of the IML significantly reduces SNA and proarrhythmogenic effects of chronic seizure activity. Neither PACAP nor microglia regulate baroreflex or peripheral and central chemoreflex responses during chronic epilepsy in rats. 6) In chronic epileptic rats, microglia are in surveillance state and their number of anti-inflammatory M2 phenotype remains unchanged in the vicinity of the RVLM neurons.

Statement

I declare that the work in this thesis entitled "Microglial and neurochemical mechanisms of seizure-induced central autonomic cardiovascular dysfunction" has not previously been submitted for a degree nor has it been submitted as part of requirements for a degree to any other university or institution other than Macquarie University.

I also declare that the thesis is written by me and it contains no material previously published or written by another person, except where due reference is stated otherwise. I have acknowledged all the assistance and help that I received during this research work and the preparation of this thesis itself. I acknowledge Prof. Terence J O'Brien and his research group at the University of Melbourne for conducting experiments to generate "chronic epileptic rats" and Ms Komal Kapoor for performing immunohistochemical experiments.

The majority of content from Chapter 1 (Literature Review) has been published in the "Respiratory Physiology and Neurobiology" journal (Appendix 1). Chapter 3 and Chapter 4 have been published, and fluorescence image has been illustrated as a cover art, in the "Journal of Neuroscience-An Official Journal of Society for Neuroscience", as a separate entity (Appendix 1). Findings presented in Chapter 5 have been submitted in the "Journal of Neuroscience", and manuscript is under review.

In addition, I certify that all information sources and literature used are indicated in the thesis.

The research presented in the thesis was approved by the Animal Care, and Ethics Committee of Macquarie University (2013/017), the Sydney Local Health District (2013/082 and 2014/024) and The University of Melbourne (14/072/UM).

Amol Mohan Bhandare

Department of Biomedical Sciences

Faculty of Medicine and Health Sciences

Macquarie University

9th June 2016

Acknowledgements

My first and foremost appreciation goes to my Adjunct Supervisor Prof. Paul Pilowsky, Principal Supervisor Prof. Jacqueline Phillips, and Associate Supervisor Dr Melissa Farnham. Thank you so much Paul for initially adopting me as a PhD candidate in your group, and then giving me all the freedom and support that I required to reveal my scientific strengths and talent. Whenever I knocked on your office door for assistance, you were always hospitable with a charming face. This appreciation is just not enough for the way you have helped me; as being strongly standing with me in my scientific and personal difficulties. So thank you so much!!

My second biggest thanks to Jackie for helping me across my PhD and being supportive especially during early part my PhD when I was changing my supervisor. You were always supportive and advised me throughout my PhD journey. Thank you so much!

My special thanks to Melissa, who taught me the electrophysiology experiment. Melissa, you were incredibly patient to answer my crazy questions during training. Thanks for initially staying late, when I was learning electrophysiology techniques, and being there to stay back at ASAM during our move to HRI, just so that I can get my experiments done. Huge thank you Melissa.

I am also thankful to our collaborators at "University of Melbourne" Terry, Kim, Emma, Pablo and their research team for their help with this project.

I would like to thank animal house facility personnel at Macquarie University and at the HRI, Kim, Jessica, Katja, and Jashmi, for looking after my rats and taking care of them.

I am greatly thankful to Suja for teaching me molecular techniques. Suja and Polina, thank you for your company for a cup of tea, sharing laughs and organising weekly lunches, which were much required during my PhD journey. So thank you both of you.

It was my great pleasure to have Komal as my laboratory buddy and PhD colleague. Komal, you have contributed a lot in my scientific success. Thank you for listening to my practice presentations, and giving your thoughtful feedback. We had a lot of fun during last three years and especially during conferences, and I am sure that we will continue it.

Seungjae and Zohra, you were the best buddies in the rig room. Thanks for giving me a chance to answer your questions and asking for the technical help, which enabled me to acquire the supervisory skills. VJ, Steve, Lei, Sarah, Myf, YeonJae, Thara and Seren, you are the best friends I have made across my PhD. Thanks for your company and help that I received. I am also thankful to my friends at Macquarie University, and Karthik-Nandini, Asim-Nadia, Saju, and my flatmate Jo and Jude, who made my PhD journey memorable.

My very special thanks to my family for being my motivation and courage during my PhD. Mum-Dad and Nana-Nani, thank you so much! Whatever I have achieved is only because of your support and encouragement. I dedicate this thesis to my family. My brothers and sisters-in-law and little nieces, Mahika, Aarohi and Anushree, you were my happiness during my PhD. So thank you so much all of you!! Love you so much!

Publications and Presentations

Publications directly related to thesis that are produced during the course of candidature

1. **Bhandare AM**, Mohammed S, Pilowsky PM, Farnham MMJ (2015) Antagonism of PACAP or microglia function worsens the cardiovascular consequences of kainic acid-induced seizures in rats. J Neurosci 35:2191-2199.

2. **Bhandare AM**, Kapoor K, Pilowsky PM, Farnham MMJ (2016) Seizure-induced sympathoexcitation is caused by activation of glutamatergic receptors in RVLM that also causes proarrhythmogenic changes mediated by PACAP and microglia in rats. J Neurosci 36:506-517.

3. **Bhandare AM**, Kapoor K, Farnham MMJ, Pilowsky PM (2016) Microglia PACAP and glutamate: Friends or foes in seizure-induced autonomic dysfunction and SUDEP? Respir Physiol Neurobiol 226:39-50.

Under Review

4. **Bhandare AM**, Kapoor K, Powell KL, Braine E, Casillas-Espinosa P, O'Brien TJ, Farnham MMJ, Pilowsky PM Microglial activation in the spinal cord mediates sympathoexcitatory and proarrhythmogenic changes in rats with chronic temporal lobe epilepsy. J Neurosci *Under review*.

Other publications produced during the course of candidature

5. Kapoor K, **Bhandare AM**, Farnham MMJ, Pilowsky PM (2016) Alerted microglia and the sympathetic nervous system: A novel form of microglia in the development of hypertension. Respir Physiol Neurobiol 226:51-62.

6. Nedoboy PE, Mohammed S, Kapoor K, **Bhandare AM**, Farnham MMJ, Pilowsky PM (2016) pSer40 tyrosine hydroxylase immunohistochemistry identifies the anatomical location of C1 neurons in rat RVLM that are activated by hypotension. Neurosci 317:162-172.

7. Kapoor K, **Bhandare AM**, Nedoboy PE, Mohammed S, Farnham MMJ, Pilowsky PM (2016) Dynamic changes in the relationship of microglia to cardiovascular neurons in response to increases and decreases in blood pressure. Neurosci 329:12-29.

8. Kapoor K, **Bhandare AM**, Mohammed S, Farnham MMJ, Pilowsky PM (2016) Microglial number is related to the number of tyrosine hydroxylase neurons in SHR and normotensive rats. Auton Neurosci-Basic 198:10-18.

9. **Bhandare AM**, Vyawahare NS, Kshirsagar AD (2015) Anti-migraine effect of Areca catechu L. nut extract in bradykinin induced plasma protein extravasation and vocalisation in rats. J Ethnopharmacol 171:121-124.

In Preparation or Under Review

10. Kapoor K, **Bhandare AM**, Mohammed S, Farnham MMJ, Pilowsky PM Microglial response to changes in blood pressure in the rostral ventrolateral medulla is exaggerated in spontaneously hypertensive rats. *In Preparation*.

11. Filipe E, Santos M, Matthews L, Hung J, **Bhandare AM,** Ng M, Rnjak-Kovacina J, Wise S Electrospun silk is a versatile biomaterial for vascular grafts. ACS Biomaterials Science and Engineering *Under Review*.

Presentations during the course of candidature

1. **Bhandare AM**, Kapoor K, Mohammed S, Farnham MMJ, Pilowsky PM Central autonomic and cardiovascular dysfunction in seizure and sudden unexpected death in epilepsy. Presented at Central Cardiovascular and Respiratory Control: Future Directions, Melbourne, AMREP Education Centre, 15-16 September 2014.

2. **Bhandare AM**, Kapoor K, Mohammed S, Farnham MMJ, Pilowsky PM Kainic acid-induced seizure causes dose-dependent cardiorespiratory changes. Presented at The 13th Oxford Breathing Meeting, Respiratory and Cardiovascular, October 26-31, 2014, Sydney Australia.

3. **Bhandare AM**, Kapoor K, Mohammed S, Farnham MMJ, Pilowsky PM Antagonism of PACAP or microglia function worsens the cardiovascular consequences of kainic acid (KA)-induced seizures in rats. Presented at 25th Meeting of the International Society for Neurochemistry (ISN)-Asian Pacific Society for Neurochemistry (APSN)-Joint Biennial Meeting in conjunction with Australasian Neuroscience Society (ANS), Cairns, Australia, August 23-28, 2015.

4. **Bhandare AM**, Kapoor K, Farnham MMJ, Pilowsky PM Seizure-induced sympathoexcitation is caused by activation of glutamatergic receptors in RVLM that also causes proarrhythmogenic changes mediated by PACAP and microglia in

rats. Presented at Neuroscience 2015, the 45th annual meeting of the Society for Neuroscience (SfN), October 17-21, 2015, Chicago, IL, USA.

List of Figures

List of Tables

Glossary of Abbreviations

AMPA	α-amino-3-hydroxy-5-methyl-4-isoxazolepropionic acid
ANOVA	analysis of variance
ANS	autonomic nervous system
AP	arterial pressure
ATP	adenosine triphosphate
AUC	area under curve
BDNF	brain-derived neurotrophic factor
BötC	Bötzinger complex
BP	blood pressure
bpm	beats per minute
cAMP	cyclic adenosine monophosphate
CD	cluster of differentiation
CNS	central nervous system
CSF	cerebrospinal fluid
CVLM	caudal ventrolateral medulla
Cy	cyanine dye
DBA/2	dilute Brown Non-Agouti/2
DMV	dorsal motor nucleus of the vagus
EAAT	excitatory amino acid transporter
ECG	electrocardiogram
EEG	electroencephalogram
ETCO$_2$	end-tidal CO_2
GABA	gamma (γ)-aminobutyric acid
GLAST	glutamate aspartate transporter
GLT-1	glutamate transporter-1
GPCR	G-protein coupled receptor
HCl	hydrochloric acid
HR	heart rate
i.p.	intraperitoneal
i.v.	intravenous
Iba1	ionised calcium-binding adapter molecule-1
iGluRs	ionotropic glutamate receptors
IL	interleukin
IML	intermediolateral cell column
ir	immunoreactive
IT	intrathecal
IU	international units
JNK	c-Jun N-terminal kinase
KA	kainic acid
KYNA	kynurenic acid
MAP	mean arterial pressure
MAPK	mitogen-activated protein kinase
mGluRs	metabotropic glutamate receptors

mRNA	messenger ribonucleic acid
NaCl	sodium chloride
NGF	nerve growth factor
NMDA	N-methyl-D-aspartate
NO	nitric oxide
NTS	nucleus of the solitary tract
PACAP	pituitary adenylate cyclase-activating polypeptide
PaCO$_2$	partial pressure of carbon dioxide
PAG	periaqueductal gray
PBN	parabrachial nucleus
PBS	phosphate-buffered saline
PFA	paraformaldehyde
PKA	protein kinase A
PKC	protein kinase C
PNA	phrenic nerve activity
PNF	phrenic nerve frequency
pre-BötC	pre-Bötzinger complex
PSNS	parasympathetic nervous system
PSPs	postsynaptic potentials
PVN	paraventricular nucleus
QTc	corrected QT
RTN	retrotrapezoid nucleus
RVLM	rostral ventrolateral medulla
SAPK	stress activated protein kinase
SD	Sprague-Dawley
SE	status epilepticus
SNA	sympathetic nerve activity
SNS	sympathetic nervous system
SUDEP	sudden unexpected death in epilepsy
TGF-β	transforming growth factor-β
TH	tyrosine hydroxylase
TLE	temporal lobe epilepsy
TNF-α	tumor necrosis factor-α
VIP	vasoactive intestinal peptide
VLM	ventrolateral medulla

Chapter 1
Literature Review

Table of Contents

1.1. <u>Introduction</u>

The word "epilepsy" is derived from the Greek "epilambanein", meaning to be seized, or overwhelmed by surprise. Epilepsy is one of the most common disorders of the brain, affecting about 50 million people worldwide (WHO, 2005). It is a paroxysmal neurological disorder caused by a variety of pathological processes in the brain. It is characterised by occasional, excessive, and disorderly discharge of neurons that leads to clinical manifestations and/or changes in electroencephalogram (EEG) activity (McNamara, 1994; McNamara, 1999; Browne and Holmes, 2008).

Sudden unexpected death in epilepsy (SUDEP) is an important but poorly-appreciated phenomenon (Massey et al., 2014) that accounts for 5-17% of deaths in people with epilepsy, and 50% in refractory epilepsy (Ficker et al., 1998; Holst et al., 2013). The mounting evidence suggests that the seizure-induced central autonomic and cardiorespiratory dysfunctions are the leading cause of SUDEP (Figure 1. 1). In humans, seizures are commonly associated with profound apnoea and oxygen desaturation (Langan et al., 2000; Bateman et al., 2008; Bateman et al., 2010; Ryvlin et al., 2013; Dlouhy et al., 2015). Central apnoea and hypoventilation were also evident in an animal model of seizure (Johnston et al., 1995; Johnston et al., 1997). Cardiac sympathovagal imbalance with sympathetic dominance, baroreflex dysfunction and tachycardia or bradycardia with severe ictal electrocardiogram (ECG) abnormalities are common in epilepsy patients (Nei et al., 2000; Nei et al., 2004; Brotherstone et al., 2010; Ponnusamy et al., 2012; Ryvlin et al., 2013) and animals (Sakamoto et al., 2008; Metcalf et al., 2009b; Metcalf et al., 2009a). Cardiac and respiratory autonomic dysfunctions are considered as possible cause of SUDEP, but the underlying neuronal mechanism remains obscure.

The central nervous system (CNS) exerts a profound regulatory effect on peripheral organs and tissues. It tightly regulates integrated cardiac and respiratory function by influencing the activity of autonomic nervous system (ANS) via neuroendocrine regulation of target glands and organs. The overall autonomic output to the cardiorespiratory system is determined by medullary reflexes and influence of the cerebral cortex. The precise central autonomic regulation is coordinated through the sympathetic and parasympathetic nervous systems (SNS and PSNS), and influenced by the sensory feedback from peripheral organs such as carotid and aortic bodies, carotid sinus and aortic arch (Pilowsky and Goodchild, 2002; Guyenet, 2006; Pilowsky et al., 2009; Guyenet, 2014). Importantly, major neurotransmitters, neuropeptides and glia influence the autonomic output (SNS and PSNS) to the cardiorespiratory system (Miyawaki et al., 1996a; Lai et al., 1997; Du et al., 2015).

Autonomic responses to environmental or homeostatic challenges (produced through behavioural or endocrine changes) are regulated through ionotropic and/or metabotropic receptors that are essential for regulating cardiorespiratory activity and reflexes (Ross et al., 1984a; Suzuki et al., 1997; Ivy and Scott, 2015). Glutamate, gamma-aminobutyric acid (GABA) and glycine are three major neurotransmitters in the CNS. Antagonism of any of these three neurotransmitter systems causes major, or even complete, disruption of central cardiorespiratory control (Ross et al., 1984a; Miyawaki et al., 1996a; Ito and Sved, 1997; Suzuki et al., 1997; Araujo et al., 1999; Sakima et al., 2000). For example, microinjection of the broad-spectrum ionotropic glutamate receptors (iGluRs) antagonist, kynurenic acid (KYNA), into major cardiorespiratory autonomic nuclei, such as nucleus of the solitary tract (NTS) or ventrolateral medulla (VLM), reduces the vagal and sympathetic baroreflex and chemoreflex responses (Guyenet et al., 1987; Koshiya et al., 1993; Moraes et al., 2012). Selective inhibition of N-methyl-D-aspartate (NMDA) and α-amino-3-hydroxy-5-methyl-4-isoxazolepropionic acid (AMPA)/kainate receptors in the caudal ventrolateral medulla (CVLM) has a similar effect (Miyawaki et al., 1996a; Miyawaki et al., 1997).

Additionally, other neurotransmitters and peptides, including pituitary adenylate cyclase-activating polypeptide (PACAP), play a significant role in modulating cardiorespiratory function, and reflexes (Callera et al., 1997; Miyawaki et al., 2002b; Kashihara et al., 2008; Pilowsky et al., 2009; Farnham et al., 2011; Rahman et al., 2011; Shahid et al., 2011). PACAP and its three receptors are present in the brainstem and the spinal cord autonomic nuclei that are important in central cardiorespiratory regulation (Légrádi et al., 1994; Sundler et al., 1996; Das et al., 2007; Farnham et al., 2008). PACAP is positively coupled to act on its membrane-bound receptors, and activate adenylyl cyclase, to generate increased intracellular levels of cyclic adenosine monophosphate (cAMP). Since the discovery of PACAP, many studies have emphasised its neuroprotective, and anti-inflammatory role in *in vivo* and *in vitro* models of neurodegenerative diseases (Shioda et al., 1998; Delgado et al., 1999; Brifault et al., 2015). In cardiovascular regulation, PACAP acts as an excitatory neurotransmitter at central autonomic nuclei in the brainstem and spinal cord (Farnham et al., 2008; Inglott et al., 2011; Farnham et al., 2012).

Microglia are the principal resident immune cells of the CNS and contribute ~10% of total brain population (Kettenmann et al., 2011; Benarroch, 2013). Microglia are categorised into two types based on their function and morphology; surveilling and activated.
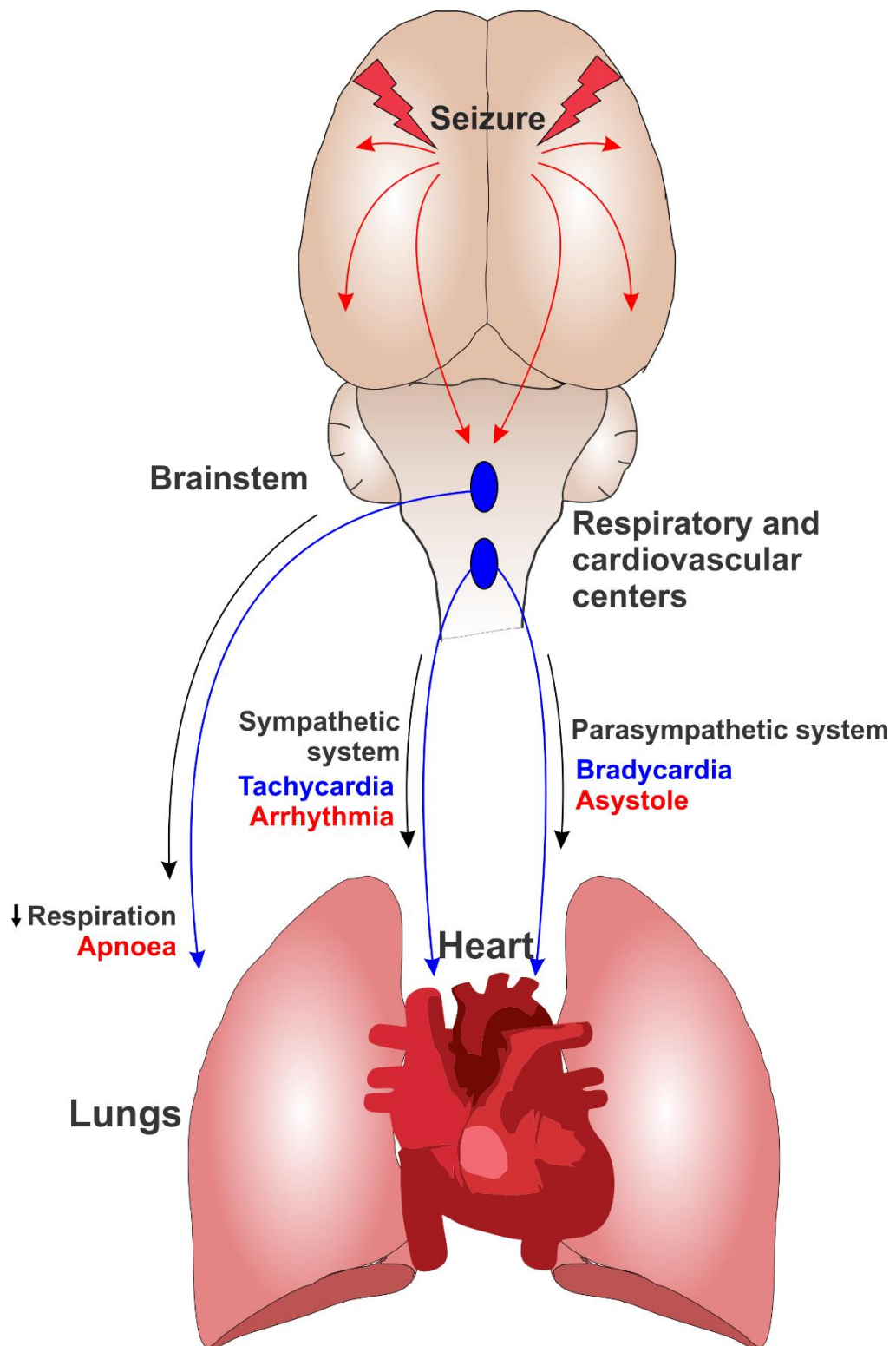
Figure 1. 1: A schematic diagram to show how the spread of seizures could result in central autonomic cardiorespiratory dysfunction.

Seizures propagate from higher brain region into the cardiorespiratory brainstem autonomic nuclei, and disturb the normal cardiorespiratory activity and reflexes. Seizure-induced excitation of sympathetic neurons leads to tachycardia and arrhythmia, whereas activation of parasympathetic system causes bradycardia and asystole. Moreover, spread of seizures could results in postictal coma, and loss of protective airway reflexes eventually causing decreased respiratory drive, apnoea and hypoventilation.

Surveilling microglia (also known as "resting") are present in healthy CNS, and are vigilant towards changes in their microenvironment. Using *in vivo* two photon imaging of fluorescently labelled neurons and microglia in mice, it has been shown that resting microglia continuously survey their microenvironment for the homeostatic conditions by making brief and direct contact with synapses (Wake et al., 2009). The frequency of microglial contact is directly proportional to neuronal activity, and reflects the functional status of the synapses (Wake et al., 2009; Tremblay et al., 2010). Such a dynamic and careful reorganisation of microglia is believed to enable them to scan the brain parenchyma every few hours without disturbing the fine-wired neuronal circuits. "Activated" microglia are ramified, with an amoeboid morphology, and acquire their phenotype depending on the type of the stimulus; participating in either neuroprotection or neurotoxicity (Ayoub and Salm, 2003). Microglia maintain synaptic and neuronal homeostasis during normal and diseased CNS conditions (Wake et al., 2009; Kettenmann et al., 2011).

Pituitary adenylate cyclase-activating polypeptide produces a neuroprotective effect (Shioda et al., 1998; Ohtaki et al., 2006), and its expression increases in central autonomic nuclei, such as paraventricular nucleus (PVN), in kainic acid (KA)-induced seizure rats (Nomura et al., 2000). Microglia can be pro-inflammatory or anti-inflammatory in animal models of diseases such as epilepsy (Shapiro et al., 2008; Mirrione et al., 2010; Vinet et al., 2012). During seizures, there is extensive activation of microglia both in humans and in animals (Beach et al., 1995; Shapiro et al., 2008; Eyo et al., 2014). Moreover, there are reports suggesting that PACAP can modulate the activated microglial state (Wada et al., 2013; Brifault et al., 2015). This important relationship between PACAP, microglia and seizure-induced increase in its expression or activation in cardiovascular autonomic nuclei makes them a very promising target in the development of treatment strategies for seizure-induced sympathoexcitation and cardiorespiratory autonomic dysfunction.

In addition, brain glutamate levels are increased in epilepsy patients and animal models of temporal lobe epilepsy (TLE) (Meldrum et al., 1999; Blümcke et al., 2000). Increased glutamate synthesis and release play a major pathogenic role in neuronal hyperexcitability, which could disturb the homeostasis of cardiorespiratory neurons. Collectively, the central autonomic cardiorespiratory dysfunction during seizure could be driven by increased glutamate turnover. However, the glutamatergic drive is not important for maintenance of blood pressure (BP) or basal tonic activity of catecholaminergic (C1 and non-C1) rostral ventrolateral medulla (RVLM) neurons as the KYNA microinjection into the RVLM on its own does not affect the basal BP and sympathetic nerve activity (SNA) (Guyenet et al.,

1987; Araujo et al., 1999; Sved et al., 2002). Thus, it is possible to abolish the sympathoexcitation during seizure by glutamate antagonist microinjection into RVLM without affecting basal sympathetic output and BP.

Hence, the aims of this thesis are to investigate the effect of PACAP, microglia and glutamate on central autonomic cardiorespiratory neurons during acute and chronic epilepsy in rats. The study is designed to identify whether the modulation of PACAP, microglia and/or glutamatergic receptors has a beneficial effects on cardiorespiratory dysfunction during seizure, and could provide future therapeutic strategies to prevent SUDEP. To achieve these aims we used a combination of electrophysiological and neuroanatomical approaches with KA-induced acute and chronic seizures in rats.

1.2. <u>Autonomic nervous system (ANS)</u>

The CNS maintains and regulates homeostasis by regulation of peripheral organ systems. Normally, the short-term cardiorespiratory homeostasis is precisely regulated by the CNS through modulation of sympathetic and parasympathetic divisions of the ANS (Pilowsky and Goodchild, 2002; Michael Spyer and Gourine, 2009). The SNS and PSNS are responsive to sensory feedback from the periphery, such as changes in mean arterial pressure (MAP), blood oxygen saturation, fluid volume, temperature, diet, salt intake and different types of nociception (DiBona, 1986; Koshiya et al., 1993; Hirooka et al., 1997b; Armitage et al., 2012; Nijs et al., 2012; Simmonds et al., 2014; Shibasaki et al., 2015). To perform such an integrated function, the CNS requires dynamic and responsive neuronal circuits that can provide and control effective autonomic output. Medullary reflexes manipulate and provide a neuronal network to control autonomic output to the cardiorespiratory system (Figure 1. 2) (Westerhaus and Loewy, 2001; Guo et al., 2002). Transneuronal tracing using neurotropic viruses, which are retrogradely or anterogradely transported through synaptically connected neuronal chains, has significantly contributed to identify these neuronal circuits. The findings in rats after pseudorabies virus injection in cardiac sympathetic target organs, such as adrenal gland and stellate ganglion, showed that higher brain centres exert a descending control on autonomic outflow to the heart (Westerhaus and Loewy, 2001). Stimulation of cardiac sympathetic afferents in cats, which evokes excitatory cardiovascular reflexes, confirmed that the neurons in the medulla, especially VLM, regulate the cardiovascular sympathetic reflexes (Guo et al., 2002).

The CNS controls the autonomic function through the regulation of activity of sympathetic and parasympathetic neurons in the brain and the spinal cord (Sun, 1995). The groups of

neurons in the brainstem and limbic forebrain directly control the activity of sympathetic and parasympathetic preganglionic neurons (Jansen et al., 1995b; Jansen et al., 1995a). These preganglionic neurons provide central regulatory information to neurons in peripheral ganglia (post-ganglionic neurons), which in turn innervate the organs and tissues that are under autonomic control. The sympathetic and parasympathetic outflows are regulated in highly complex and organised manner so that the overall autonomic output is appropriate for the response required at any particular time.

1.2.1. Parasympathetic nervous system (PSNS)

Activation of the PSNS promotes digestive movement and decreases heart rate (HR), and is known as "rest and digest" stage. Parasympathetic output to the heart is mediated by the vagus nerve in the medulla, which originates from the dorsal motor nucleus of the vagus (DMV) and nucleus ambiguus (Figure 1. 3) (Ter Horst et al., 1996). Respiratory centres in the brainstem provide an input to vagal efferent fibres, which increases vagus nerve activity decreasing HR, atrioventricular conduction and ventricular excitability. These vagal efferent fibres innervate airways and cause contraction of airway smooth muscles (Haxhiu et al., 1993; Jones et al., 1998). In many experimental protocols aimed at examining the SNS, animals are vagotomised, paralysed and injected with atropine, to eliminate the parasympathetic drive to the cardiorespiratory system (Zanzinger et al., 1994b; Moreira et al., 2006). This approach was used for the experiments detailed in this thesis and consequently, from here onward the focus will be only on the sympathetic component, even though the PSNS drive is essential in cardiorespiratory control.

1.2.2. Sympathetic nervous system (SNS)

The ANS controls the primary "fight or flight" response through increased HR and decreased digestive movement mediated by the SNS and PSNS (Jansen et al., 1995b). The excitation of the SNS increases HR by increased synthesis and release of catecholamines, whereas excitation of the PSNS has opposite effect through acetylcholine (McGrattan et al., 1987; Jansen et al., 1995a). The sympathetic preganglionic neurons are organised in a very complex manner, which allows target specific regulation of sympathetically innervated organs and tissues (Morrison, 2001). For example, extensive axonal branching of sympathetic premotor neurons projecting to intermediolateral cell column (IML), targets the same organ tissue at multiple levels of the thoracic spinal cord (Barman and Gebber, 1985). This organisation of the SNS is essential for organ specific control of peripheral autonomic functions.
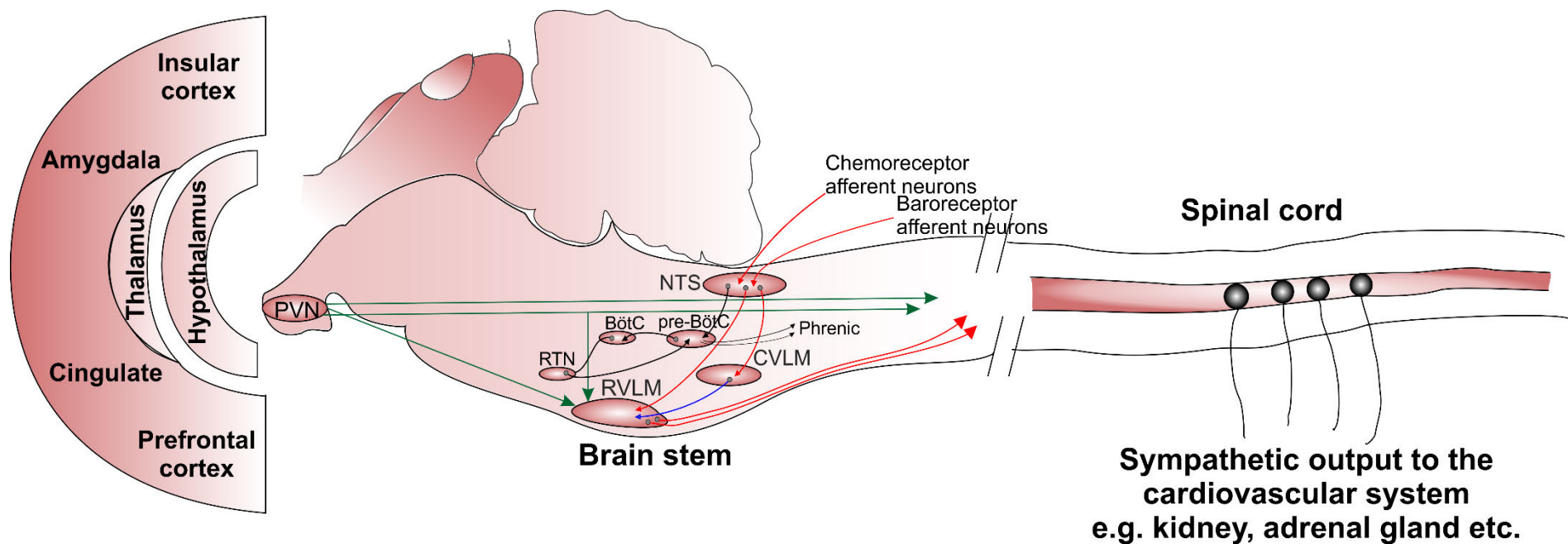
Figure 1. 2: Neuronal network to control autonomic output to the cardiorespiratory system.

Cardiorespiratory homeostasis is maintained by autonomic output, which is determined by the balance of medullary reflexes, and influence of cerebral cortex. The sympathetic output to the heart is mediated by neurons from the RVLM through their direct projections to the IML (red). The PVN affects sympathetic output through three different pathways; first, a direct descending projections to the IML, secondly, a projection to the vasomotor neurons of the RVLM, and thirdly, collateral projections to both IML and RVLM (green). Arterial baroreceptors are situated in the aortic arch and carotid sinus, and peripheral chemoreceptors are located in carotid and aortic bodies, providing afferent signals to NTS (red). The NTS integrates afferent information and relays it to activate (red) inhibitory neurons in the CVLM that in turn inhibit (blue) neurons in the RVLM. Astrocytes and RTN neurons act as central respiratory chemoreceptors that are exquisitely sensitive to changes in CO_2. Peripheral chemosensory afferents in NTS provide information to the pre-BötC influencing the rate and shape of respiratory rhythm, which in turn regulates respiratory motoneurons including the phrenic, intercostal and hypoglossal neurons. Bulbar respiratory interneurons also modulate the activity of cardiovascular neurons.

Transneuronal viral tracer and many other classical studies have identified neurons that project to sympathetic preganglionic neurons (Strack et al., 1989b; Strack et al., 1989a). Although the innervating presympathetic neurons are present in different regions of the brainstem and limbic area, the precise map of supraspinal groups of neurons and their axonal terminal is obscure. The interneuronal network within the spinal cord provides an indirect descending input that can influence sympathetic outflow. This network is identified with retrograde transport of pseudorabies virus injected in the kidney of rats (Tang et al., 2004). The cardiorespiratory autonomic nuclei, from which projections to the sympathetic preganglionic neurons originate, contain neurochemically diverse types of neurons (Strack et al., 1989a). This neurochemical heterogeneity suggests that within single nucleus there are functionally heterogeneous neurons, and different nuclei are involved in controlling even closely related autonomic functions. These important cell groups regulating cardiovascular functions are discussed in details in further sections.

1.2.3. Central autonomic nuclei regulating cardiorespiratory activity

The brainstem and spinal cord play a critical role in the regulation of cardiovascular and respiratory autonomic function, mainly by regulating SNA and phrenic nerve activity (PNA), and other spinal motoneurons. Brainstem autonomic neurons extend rostrally to the pontomedullary junction and caudally to the junction with the cervical spinal cord (Figure 1. 3 and Figure 1. 4). Functionally and anatomically, these neurons can be mapped by transneuronal viral tracing, observing physiological responses to localised neuronal excitation or inhibition, expression of the early response gene c-Fos, and establishing electrophysiological or neuroanatomical connections to other important cardiovascular and respiratory nuclei.

The cardiovascular autonomic nuclei modulate sympathetic output directly or indirectly and are grouped into two types. The first group includes "preautonomic" cell groups such as RVLM, A5 cell group, PVN, lateral hypothalamic area and parapyramidal area (Figure 1. 3). These cell groups directly regulate autonomic output through input to preganglionic sympathetic neurons. The second cell groups include CVLM, A1 adrenergic cell group, parabrachial nucleus (PBN), periaqueductal gray (PAG), dorsomedial hypothalamic nucleus, bed nucleus of stria terminalis, central nucleus of the amygdala and cerebral cortex that indirectly control the sympathetic output via projections to "preautonomic" nuclei (Figure 1. 3).
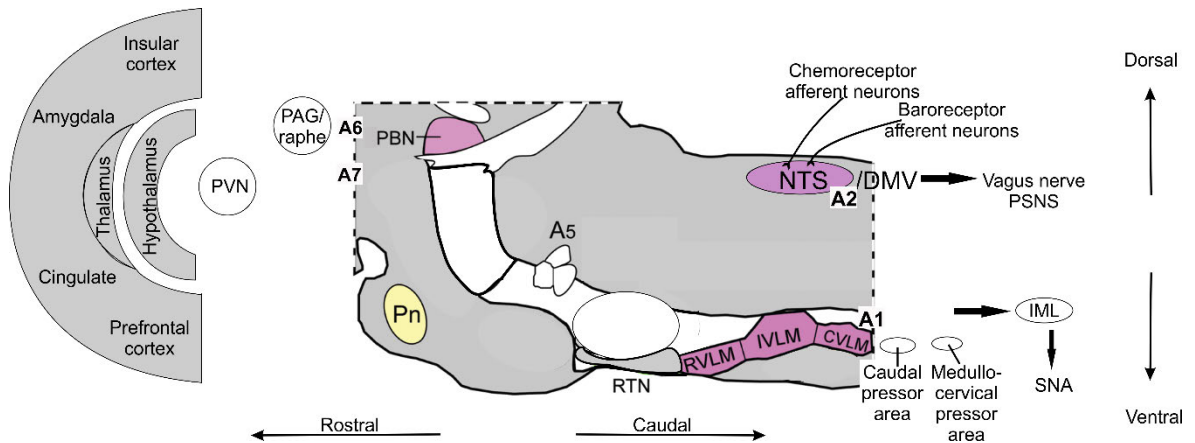
Figure 1. 3: Medullary regions responsible for controlling cardiovascular activity.

Parasagittal section of higher brain, pons and medulla in rodent. Figure modified from (Guyenet, 2014). The major autonomic nuclei generating cardiovascular autonomic output are represented in magenta. Abbreviations: Pn- pontine nuclei; IVLM-intermediate ventrolateral medulla.
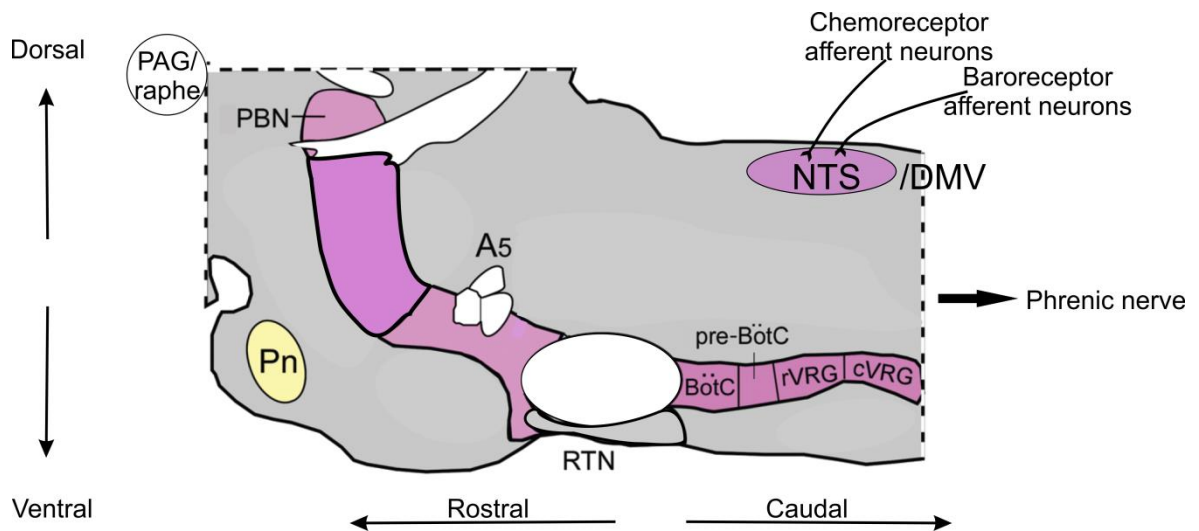
Figure 1. 4: Medullary regions responsible for generating respiratory rhythm.

Parasagittal section of pons and medulla in rodent. Figure modified from (Guyenet, 2014). The autonomic nuclei generating respiratory rhythm are highlighted in magenta. Abbreviations: Pn- pontine nuclei; rVRG-rostral ventral respiratory groups; cVRG-caudal ventral respiratory groups.

Brainstem autonomic nuclei are also responsible for generating respiratory rhythm (Haxhiu et al., 1993; Chitravanshi and Sapru, 1999; Mutolo et al., 2005; Rosin et al., 2006). These cell groups include pontine nuclei, retrotrapezoid nucleus (RTN) or parafacial respiratory group, Bötzinger complex (BötC), pre-Bötzinger complex (pre-BötC), rostral and caudal ventral respiratory groups, NTS and raphe nuclei (Figure 1. 4). Findings in the rabbit show that the respiratory rhythm is generated by glutamatergic interneurons, where the broad-spectrum iGluRs antagonist, KYNA, in pre-BötC or BötC induces a pattern of breathing characterised by low-amplitude and high-frequency irregular oscillations, superimposed on tonic PNA (Mutolo et al., 2005). The respiratory interneurons project to bulbar, phrenic, and other spinal motoneurons (Chitravanshi and Sapru, 1999). Peripheral chemoreceptors are located in the carotid body and monitor blood chemistry (e.g. CO_2, O_2, H^+, glucose) to maintain homeostasis through the initiation of respiratory and cardiovascular reflexes (Heeringa et al., 1979; Moraes et al., 2014). Astrocytes and neurons in the RTN act as central respiratory chemoreceptors (Wenker et al., 2010). Serotonin (5-hydroxytryptamine) (Massey et al., 2015) and many neuropeptides (Pilowsky et al., 2009; Rahman et al., 2011) can modify the excitability of central chemoreceptors.

1.2.3.1. Nucleus of the solitary tract (NTS)

The central autonomic cardiorespiratory neurons dynamically respond to homeostatic and environmental challenges. In this paradigm, sensory feedback is essential at all levels. The sensory afferents originate from multiple sources and provide input to central autonomic control circuitry at different levels. The NTS is the major recipient of the primary cardiorespiratory sensory afferents and receives sensory information from all innervated target organs and tissues. The NTS lies in the dorsal caudal brainstem, adjacent to the DMV and the area postrema (Figure 1. 3 and Figure 1. 4), where the bilateral column forms a "V" shape (Figure 1. 5). Glutamatergic NTS neurons excite both the RVLM and CVLM neurons, and the GABAergic CVLM neurons inhibit the sympathetic activity of RVLM neurons (Figure 1. 5) (Suzuki et al., 1997). The NTS plays a critical integrative role in the regulation of cardiovascular and respiratory system since it is an initial step in processing barosensory and chemosensory information that culminates in homeostatic reflex responses (Finley and Katz, 1992; Lawrence and Jarrott, 1996; Callera et al., 1997; Andresen et al., 2001). Arterial baroreceptors, situated in the aortic arch and carotid sinus, and peripheral chemoreceptors, located in the carotid and aortic bodies, respond to changes in BP and blood chemicals to provide afferent signals to NTS (Guo et al., 1982).
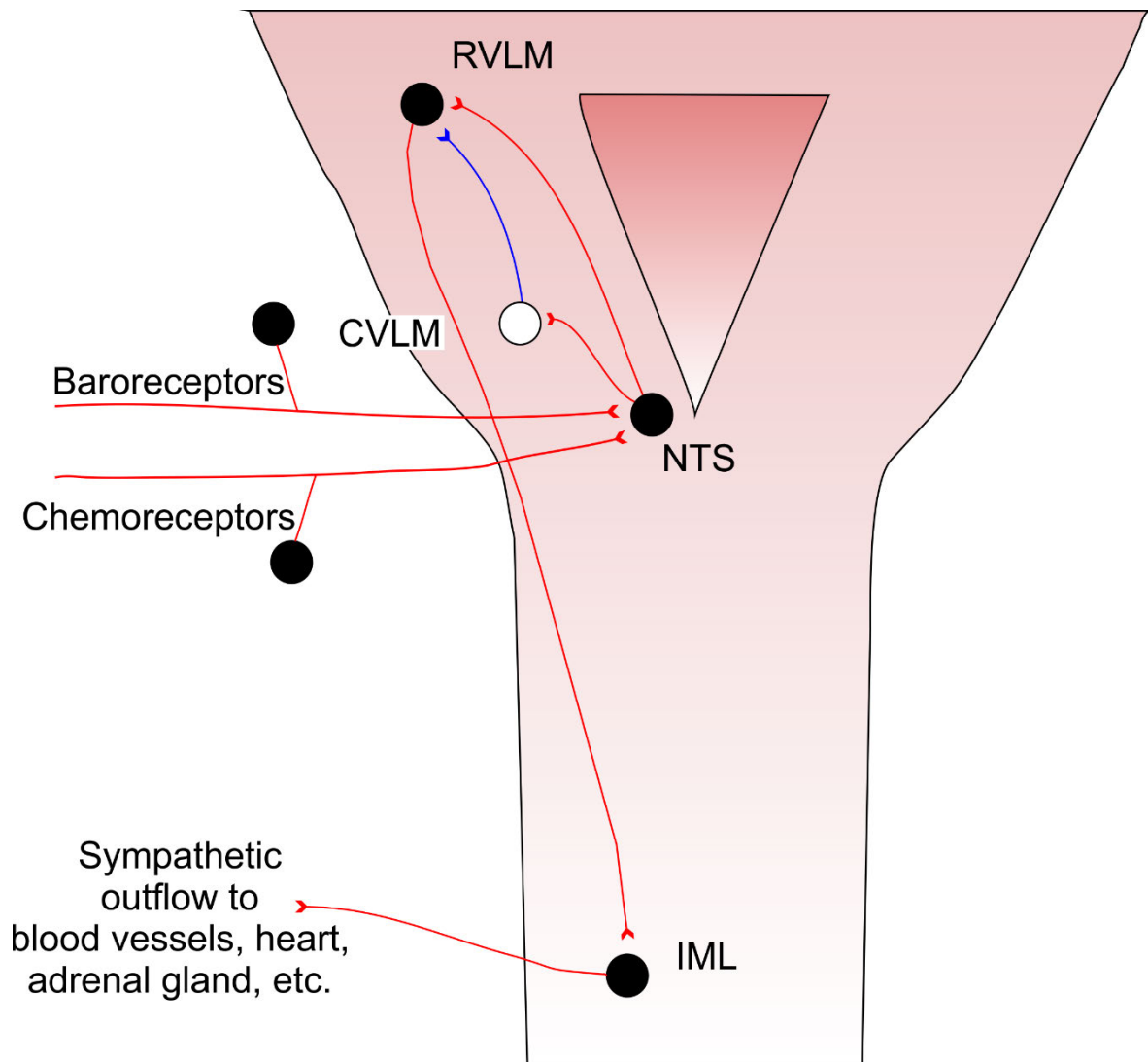
Figure 1. 5: Schematic diagram showing the major pathways involved in cardiovascular reflex mechanisms.

Excitatory pathways are in red and inhibitory pathways are in blue. Open circle indicates inhibitory neurons and filled circles indicate excitatory neurons. Figure modified from (Pilowsky and Goodchild, 2002).

The NTS interneurons perform an integrative function of processing sensory information by connecting different NTS subnuclei. The NTS also receives afferents from almost all of the brain sites that participate in regulating autonomic function (Haxhiu et al., 1993; Hermes et al., 2006). These sites include the RVLM, the A5 noradrenergic cell group, the parapyramidal region, the lateral hypothalamic area, the PVN, area postrema, the PBN, the PAG, the dorsomedial hypothalamic nucleus, the central nucleus of amygdala, the insular cortex and infralimbic area of the medial prefrontal cortex (Jansen et al., 1995a; Pyner and Coote, 2000; Chen and Toney, 2010). This complex circuitry allows NTS to integrate and coordinate the activity of various NTS output neurons. The growing evidence suggests that NTS is a complex integrative centre that can influence outflow either through local brainstem circuits or projections to other, more distal central autonomic sites, where it influences more complex and integrated control over peripheral responses (Castle et al., 2005).

1.2.3.2. Rostral ventrolateral medulla (RVLM)

The RVLM neurons, C1 and non-C1, are pressor and maintain sympathetic vasomotor tone and BP through their direct projections to the IML (Card et al., 2006; Guyenet et al., 2013). The RVLM is tonically active and gives rise to SNA to increase arterial pressure (AP) and HR. Sympathetic reflex responses such as baroreflex, chemoreflex and somatosympathetic-reflex are regulated by the RVLM neurons (Miyawaki et al., 2001; Madden and Sved, 2003a; Guyenet, 2014). The detailed structural and functional characteristics of the RVLM are described in section 1.2.4.

Another pressor cell group in the VLM, distinct from the RVLM, referred as the caudal pressor area, which is situated 1-2 mm caudal to the CVLM and its properties are not well known (Figure 1. 3). Neurons in caudal pressor area project to several medullary regions associated with autonomic control, but not directly to the spinal cord (Sun and Panneton, 2005). Pressor responses evoked by the caudal pressor area are sympathetically mediated and require activation of presympathetic RVLM neurons. Recently, further caudal to the caudal pressor area, at the junction of the medulla and the cervical spinal cord, another pressor nucleus termed the medullo-cervical pressor area was reported (Figure 1. 3) (Seyedabadi et al., 2006). The medullo-cervical pressor area neurons do not contribute to the basal sympathetic activity and their functional properties are yet to be investigated.

1.2.3.3. A5 cell group

The A5 noradrenergic cell group of the ventrolateral pons sends descending projections to the IML (Figure 1. 3). A catecholamine neurotoxin (6-hydroxydopamine)-induced lesion study in rats confirmed that more than 90% of A5 noradrenergic neurons project to the thoracic spinal cord (Byrum et al., 1984). A retrograde study with pseudorabies virus injection into peripheral sympathetic target organs confirmed the dense projections of A5 neurons to the spinal cord (Sved et al., 2001). Although the findings support the idea that A5 neurons have a little tonic influence on the SNA, these neurons do play a crucial role in the sympathetic chemoreflex response (Koshiya and Guyenet, 1994; Maiorov et al., 2000). Inhibition of the neuronal activity of A5 cell group by microinjection of the GABA receptor agonist, muscimol, attenuates the sympathetic chemoreflex by 65% in rats (Koshiya and Guyenet, 1994). Moreover, muscimol microinjection in A5 cell group in rabbits under normoxia has no effect whereas under the hypoxic condition it attenuated the sympathetic reflex response (Maiorov et al., 2000). A5 neurons also influence the parasympathetic outflow.

1.2.3.4. Paraventricular nucleus (PVN)

Although the PVN of the hypothalamus is primarily concerned with blood volume regulation, transneuronal viral tracing studies confirmed that the PVN neurons innervate the sympathetic preganglionic neurons (Jansen et al., 1995a). The PVN integrates the specific afferent inputs to generate a differential sympathetic output (Figure 1. 2). The PVN affects the sympathetic output (Allen, 2002) through three different pathways; projections to the RVLM (Pyner and Coote, 1999), direct descending projections to the IML and collateral projections to both IML and RVLM (Shafton et al., 1998; Pyner and Coote, 2000). The functional study identified the role of PVN in hypertension and heart failure. The firing rate of PVN neurons is higher in heart failure animals (Zhang et al., 2002), while the bilateral inhibition of the PVN in spontaneously hypertensive rats produces a large decrease in AP (Allen, 2002).

Another cell group similar to the PVN, called lateral hypothalamic area, also influences autonomic function through direct descending projections to the preganglionic cell groups. The lateral hypothalamic area contains neurochemically different types of neurons, which have been confirmed with immunohistochemical and tract-tracing studies (Jansen et al., 1995a).

1.2.3.5. Parapyramidal area

The parapyramidal area consists of caudal raphe cell groups (raphe pallidus and raphe magnus) and gigantocellular and paragigantocellular nuclei. Parapyramidal neurons give projections to other central autonomic supraspinal nuclei (Tóth et al., 2006; Kung et al., 2010). Serotonin is the major neurotransmitter of these cell groups and is involved in compensatory responses (to maintain oxygenation of peripheral tissues) that develop during severe blood loss by inhibiting presympathetic RVLM neurons (Kung et al., 2010).

1.2.3.6. Caudal ventrolateral medulla (CVLM)

The CVLM is a depressor region, which is immediately caudal to the RVLM (Figure 1. 3). CVLM GABAergic neurons are intermingled with the A1 noradrenergic cell group (Schreihofer and Guyenet, 2002). The CVLM is an essential component of the brainstem circuitry responsible for reflex control of arterial BP. Baroreceptor afferents synapse on a subpopulation of glutamatergic NTS neurons that excite neurons in the CVLM (Figure 1. 5). These GABAergic CVLM neurons, in turn, project to RVLM and produce a reduction in arterial BP by inhibiting RVLM neurons that innervate sympathetic preganglionic neurons. The CVLM is more than a simple relay of baroreceptor reflex and discussed in more detail in section 1.2.4.

1.2.3.7. A1 noradrenergic cell group

The A1 noradrenergic cell group is intermingled with the CVLM neurons in the caudal brainstem (Figure 1. 3) (Schreihofer and Guyenet, 2002). The A1 neurons are distinct from the CVLM neurons as they innervate different targets and are catecholaminergic instead of CVLM GABAergic neurons. The A1 neurons play an important role in hypovolemia-induced release of vasopressin from the posterior pituitary (Day et al., 1992; Gieroba et al., 1994). Haemorrhage-induced activation of A1 neurons produces compensatory response via vasopressin release (Gieroba et al., 1994). The major preautonomic cell groups, such as the lateral hypothalamic area, PVN, PBN and NTS, receive dense innervations from A1 cell group and control autonomic functions (McKellar and Loewy, 1982).

1.2.3.8. Parabrachial nucleus (PBN)

The primary role of the PBN is to distribute the sensory information to regulate output from other cell groups involved in central autonomic regulation (Figure 1. 3). The PBN heavily innervates preautonomic cell groups and receives afferents from NTS (Hermann et

al., 1997; Hermes et al., 2006). Stimulation of internal subdivision of the PBN, which receives innervation from the NTS, produces sympathoexcitation and rise in BP suggestive of its role in the regulation of SNA (Chamberlin and Saper, 1992). The PBN also gives reciprocal innervations to NTS subnuclei, the medullary reticular formation, the central nucleus of the amygdala, the bed nucleus of stria terminalis and hypothalamic nuclei involved in autonomic regulation (Fulwiler and Saper, 1984).

Haemorrhage-induced hypotension studies outlined the role of PBN in autonomic regulation, where initial blood loss decreases arterial BP, unloading baroreceptors and causing a reduction in inhibition of RVLM presympathetic neurons by GABAergic CVLM neurons so that AP is increased. The reduction in BP due to further blood loss causes the PAG to induce bradycardia and reduced sympathetic drive (Dean, 2004). Finally, in the third phase of the response, ventrolateral PBN neurons restore normal BP by reinstituting sympathetic vasomotor drive, presumably through projections to the RVLM (Blair and Mickelsen, 2006).

The PAG is functionally similar to the PBN and divided into dorsomedial, dorsolateral, lateral and ventrolateral columns (Hermann et al., 1997). As explained above, PAG plays a crucial role during haemorrhage-induced bradycardia and hypotensive responses.

1.2.3.9. Dorsomedial hypothalamic nucleus

Microinjection of a GABA antagonist or excitatory amino acid into dorsomedial hypothalamic nucleus produces tachycardia and pressor responses, and these effects are reversed with microinjection of GABA agonist muscimol (DiMicco et al., 2002). The dorsomedial hypothalamic nucleus mediates cardiovascular responses through RVLM, as inhibition of the RVLM reduces the sympathoexcitation induced with activation of the dorsomedial hypothalamic nucleus (Horiuchi et al., 2004b). The dorsomedial hypothalamic nucleus gives innervation to the PVN that activates the hypothalamic-pituitary-adrenal axis and plays a crucial role in stress-induced activation of the autonomic and endocrine system (Das et al., 2007).

1.2.3.10. Barrington's nucleus

Viral labelling from tissues that receive only sympathetic innervations, such as the spleen and brown adipose tissue, identified a role for Barrington's nucleus in controlling sympathetic outflow (Cano et al., 2001; Cano et al., 2003). Moreover, Barrington's nucleus densely innervates the parasympathetic preganglionic neurons in the lumbosacral cord and

classically known as the "pontine micturition centre" (Sasaki, 2005). Collectively, Barrington's nucleus is involved in coordinating the activity of both the SNS and the PSNS.

1.2.3.11. Bed nucleus of stria terminalis

The bed nucleus of stria terminalis receives dense noradrenergic innervations from the A2 neurons in the NTS and A1 neurons in the caudal medulla (Shin et al., 2008). This nucleus integrates information from cortical, limbic and subcortical nuclei including the amygdala and the medial prefrontal cortex, and gives input to the PVN, lateral hypothalamic area, Barrington's nucleus, the NTS, and influence SNS and PSNS (Dong and Swanson, 2006).

The central nucleus of the amygdala is highly interconnected to the bed nucleus of the stria terminalis. The GABAergic neurons of the lateral and medial subnucleus of the central nucleus of the amygdala target multiple cardiovascular autonomic nuclei such as hypothalamic area, PAG, and the dorsal vagal complex (Sah et al., 2003).

1.2.3.12. Cerebral cortex

The insular cortex and the medial prefrontal cortex innervate preautonomic nuclei, such as the hypothalamus, PBN, NTS, RVLM, PAG, lateral hypothalamic area, nucleus of the amygdala, bed nucleus of the stria terminalis and regulate autonomic function (Westerhaus and Loewy, 2001; Gabbott et al., 2005).

1.2.4. <u>RVLM, CVLM and spinal cord in autonomic regulation</u>

Presympathetic RVLM neurons are located 1.8 mm lateral from the midline, 2-3 mm rostral and ~3.2-3.6 mm ventral to calamus scriptorius in rats. The RVLM neurons are ventral and slightly medial to the nucleus ambiguus with some neurons located near the ventral surface, and the majority lying within 300 µm of it (Figure 1. 6)(Farnham et al., 2008; Nedoboy et al., 2016). The GABAergic CVLM neurons are approximately 1.5 mm caudal to the facial nucleus or 1 mm rostral to calamus scriptorius (Miyawaki et al., 1996a; Miyawaki et al., 1997; Paxinos and Watson, 2007).

The RVLM gives projections to excitatory presympathetic neurons to maintain basal sympathetic vasomotor tone and integrates reflex responses mediated through changes in SNA and arterial BP (Figure 1. 6 and Figure 1. 7) (Guyenet et al., 1989; Madden and Sved, 2003a; Guyenet, 2006). Excitation of the RVLM markedly increases SNA, arterial BP and HR (Araujo et al., 1999). The RVLM neurons are extremely sensitive to changes in AP,
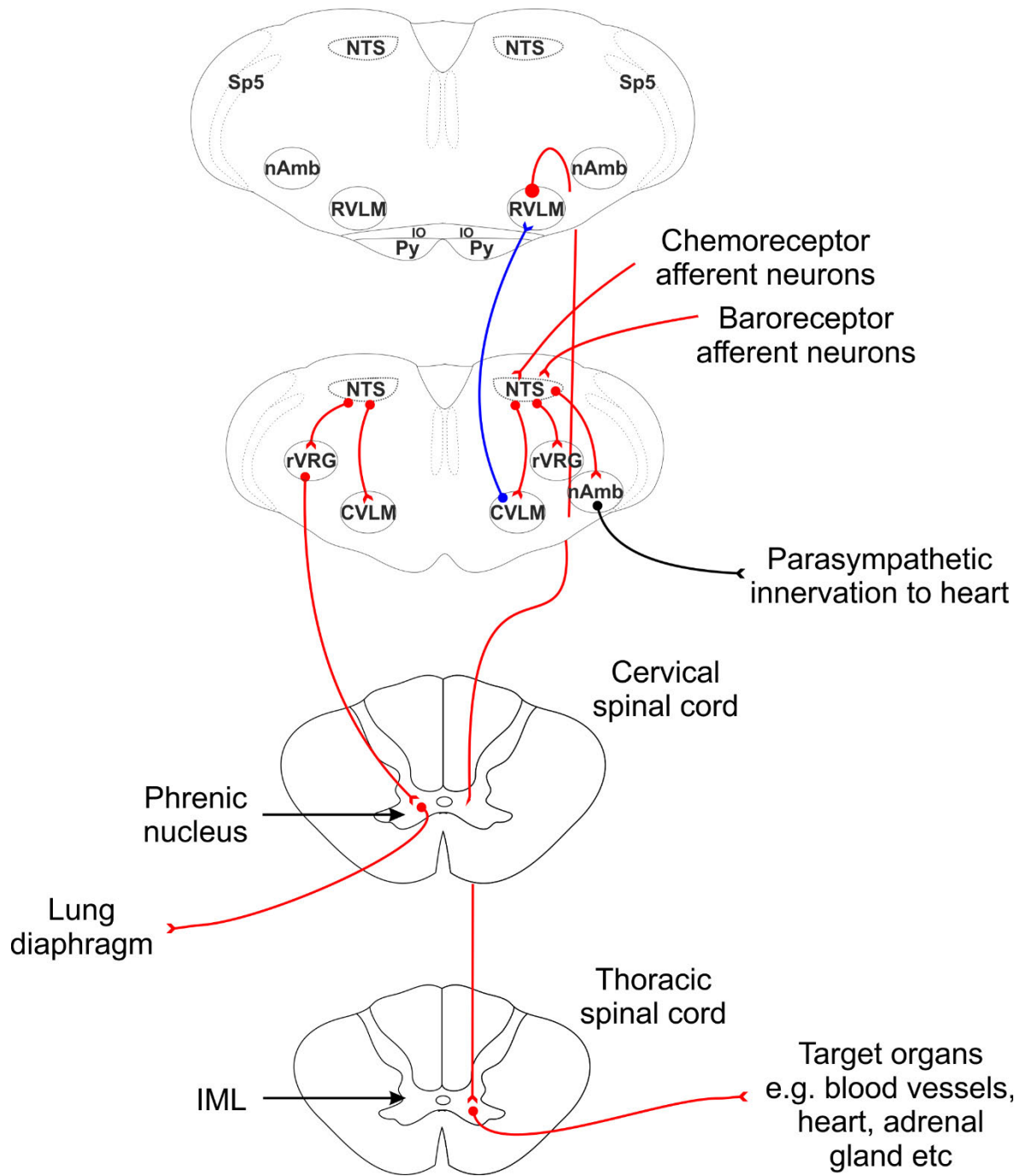
Figure 1. 6: The anatomical locations of major cardiorespiratory autonomic nuclei.

Excitatory pathways are in red and inhibitory pathways are in blue. Abbreviations: IO- inferior olive, Py- pyramids, Sp5- spinal trigeminal tract.

which is identified through baroreceptors. Pressor responses silence baroreceptors with decrease in the SNA (Ross et al., 1984a; Pilowsky and Goodchild, 2002; Schreihofer and Guyenet, 2002).

Although two theories are proposed to explain the mechanism of generation of sympathetic vasomotor tone by presympathetic RVLM neurons, the mechanism is still unclear. Guyenet and colleagues proposed "Pacemaker theory", which suggests that under certain conditions, presympathetic RVLM neurons can display pacemaker-like activity and generate an action potential that is independent of synaptic inputs (Sun et al., 1988a; Sun et al., 1988b). This theory was challenged by a second theory, which proposed that synaptic inputs are required to generate the sympathetic vasomotor tone by RVLM neurons, and these neurons lack known pacemaker activity (Kangrga and Loewy, 1995; Lipski et al., 1996). This was based on *in vivo* and *in vitro* experiments, which showed that the action potential in the RVLM neurons is preceded by excitatory postsynaptic potentials (PSPs) produced by synaptic inputs with no sign of pacemaker activity (Lipski et al., 1996; Piguet and Schlichter, 1998). It is still not clear whether the activity of RVLM neurons is determined by synaptic input or by intrinsic pacemaker potential as there are evidences to support both theories (Lipski et al., 2002; Almado et al., 2014).

The RVLM receives dense afferent inputs and gives rise to efferent innervations to multiple targets that signify its critical role in autonomic cardiovascular regulation. It receives dense inputs from NTS (Koshiya and Guyenet, 1996), CVLM (Li et al., 1992b), PVN of the hypothalamus (Shafton et al., 1998; Pyner and Coote, 2000; Chen and Toney, 2010), caudal pressor area (Sun and Panneton, 2005), contralateral RVLM (McMullan and Pilowsky, 2012), dorsomedial hypothalamic nucleus (Horiuchi et al., 2004b), raphe nuclei (Cao and Morrison, 2003; Horiuchi et al., 2004b), paratrigeminal nucleus (De Sousa Buck et al., 2001), PAG (Chen and Aston-Jones, 1995; Farkas et al., 1998), A1 cell group (Woulfe et al., 1990) and prefrontal cortex (Gabbott et al., 2007) (Figure 1. 7).

The RVLM inputs play an essential role in presympathetic neuronal output and modulate sympathetic activity however, their precise role is still unclear. On the other hand, RVLM neurons project to multiple targets including the IML in thoracic spinal cord (Minson et al., 1991; Morrison et al., 1991; Card et al., 2006), raphe pallidus (Card et al., 2006), hypothalamic PVN (vasopressin response to haemorrhage) (Swanson et al., 1981; Cunningham Jr et al., 1990), PAG (Herbert and Saper, 1992), locus coeruleus and A1 and A2 noradrenergic cell groups (involved in psychological stress) (Holloway et al., 2013).
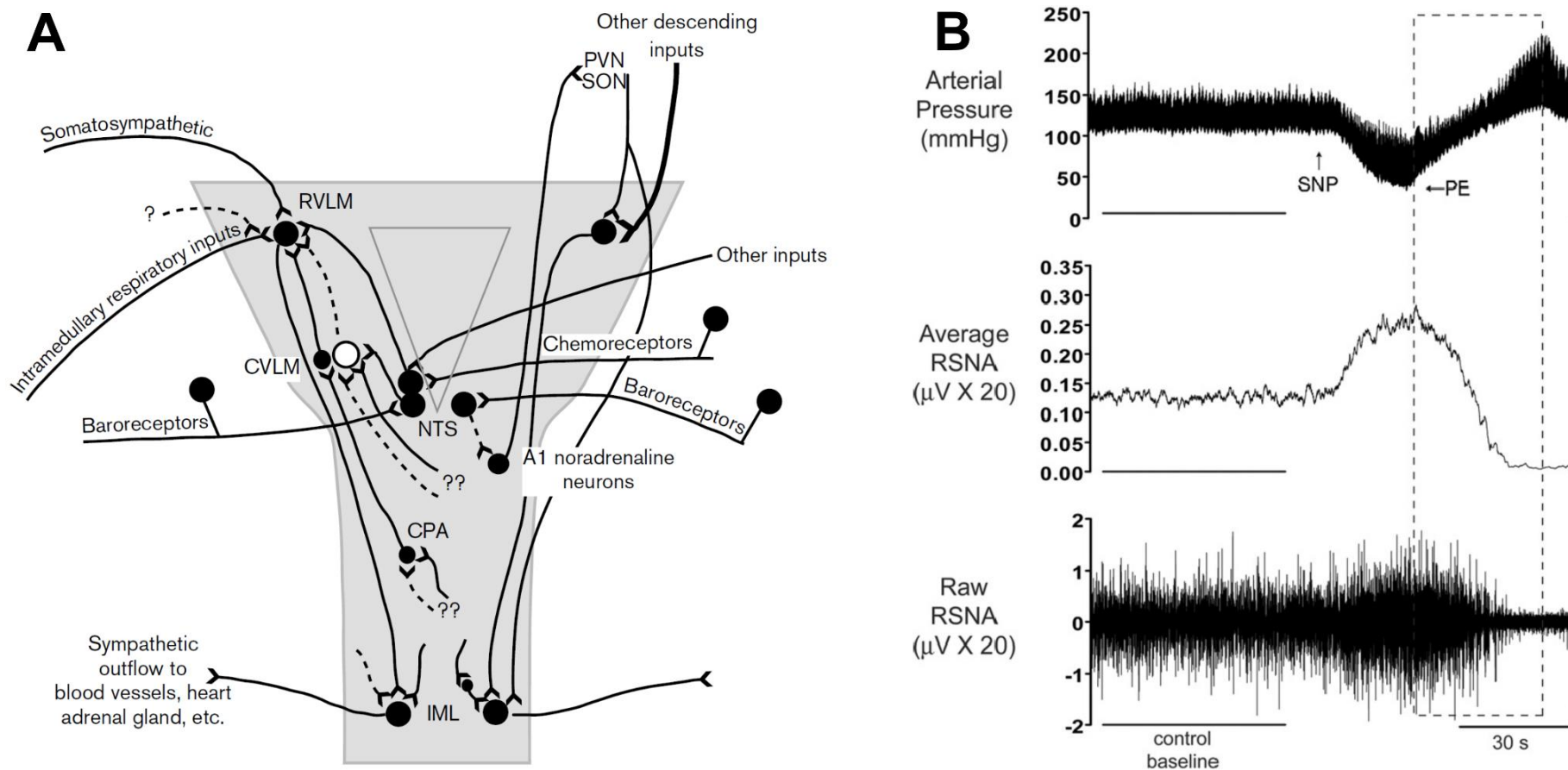
Figure 1. 7: Medullary reflex pathways.

A) Sympathetic reflexes are mediated through the baroreceptor and chemoreceptor pathways that influence the activity of major cardiorespiratory autonomic nuclei including NTS, RVLM, CVLM and pre-ganglionic and postganglionic neurons. Figure modified from (Pilowsky and Goodchild, 2002). B) The activity of presympathetic RVLM neurons is directly correlated with SNA, which is tightly controlled by pressure sensitive baroreceptors. The activity of presympathetic RVLM neurons increases during lowest AP (with i.v. SNP), and decrease with increase in AP (with i.v. PE). Figure modified from (Zahner and Schramm, 2011). SNP- sodium nitroprusside; PE- phenylephrine; RSNA- renal SNA.

Presympathetic RVLM neurons which project through the lateral horn of the spinal cord are excitatory to sympathetic preganglionic neurons innervating cardiac and vasoconstrictor targets such as adrenal gland, blood vessels and heart (Figure 1. 6 and Figure 1. 7) (Pilowsky et al., 1985; Guyenet et al., 1989; Pilowsky and Goodchild, 2002). The activity of presympathetic RVLM neurons is directly correlated with SNA, which is tightly controlled by pressure sensitive baroreceptors (Figure 1. 7). For example, RVLM efferent nerve activity increases during lowest AP, and vice versa, which shows rhythmicity between the SNA and BP changes (Figure 1. 7) (Guo et al., 2009) . The RVLM has two subsets of neurons; a catecholaminergic phenotype called as C1 cell group (C1 neurons) and non-catecholaminergic phenotype called non-C1 neurons that are located slightly more rostrally (Phillips et al., 2001; Madden and Sved, 2003b).

The bulbospinal RVLM neurons are more likely to be glutamatergic as the majority of them express one of the isoforms of vesicular glutamate transporter (Stornetta et al., 2002a; Stornetta et al., 2002b). Injection of a broad-spectrum glutamate receptor antagonist, KYNA, into the subarachnoid space at the thoracic sympathetic column blocks pressor responses evoked by electrical stimulation of the RVLM (Mills et al., 1990). Microinjection of glutamate into the RVLM causes pressor responses and sympathoexcitation that are completely blocked by KYNA (Ito and Sved, 1997; Araujo et al., 1999; Dampney et al., 2003). However, KYNA microinjection into the RVLM on its own does not affect basal BP and SNA (Guyenet et al., 1987; Kiely and Gordon, 1994; Araujo et al., 1999). Subsequently, Ito and Sved observed that if the CVLM (inhibitory drive to the RVLM) is inhibited first, subsequent blockade of glutamate receptor in the RVLM markedly reduces BP (Ito and Sved, 1997). In this paradigm, glutamatergic input to the RVLM directly excite presympathetic neurons and indirectly inhibit GABAergic inhibition of the RVLM, and the lack of change in AP with KYNA in the RVLM reflects the balance of these two actions. Miyawaki and colleagues also observed that after blockade of GABAergic input within the RVLM, injection of KYNA produced inhibition of splanchnic and lumbar SNA (Miyawaki et al., 2002a). Together these findings illustrate that there is a tonic glutamatergic input with the existence of additional sources of neurotransmitter drive to RVLM neurons.

Angiotensin II is another major neurotransmitter that has an excitatory effect on presympathetic RVLM neurons (Averill et al., 1994; Hirooka et al., 1997a). Similar to glutamate, the role of angiotensin II in the generation of tonic vasomotor activity is not yet clear.

Presympathetic neurons synthesise and release other neuropeptides, such as PACAP (Chiba et al., 1996; Farnham et al., 2008), opioids (Strack et al., 1989a; Chalmers and Pilowsky, 1991; Jansen et al., 1995a; Guyenet et al., 2002; Miyawaki et al., 2002b), substance P (Strack et al., 1989a), neuropeptide Y (Strack et al., 1989a; Jansen et al., 1995a), somatostatin (Strack et al., 1989a; Jansen et al., 1995a), vasoactive intestinal peptide (VIP) (Jansen et al., 1995a), galanin (Melander et al., 1986) and orexin (Peyron et al., 1998), which suggest that these neuropeptides modulate the activity of sympathetic preganglionic neurons. The role of PACAP in regulating the activity of presympathetic neurons is elaborated in further section 1.9. In addition, superoxides, cocaine, and amphetamine-like compounds also modify the RVLM neuronal activity (Burman et al., 2004; Guo et al., 2009). Thoracic region of the spinal cord showed the presence of noradrenaline and non-detectable adrenaline, which suggest that presympathetic C1 neurons may use noradrenaline as a neurotransmitter when catecholamines are released (Sved, 1989). The precise role of catecholamine as a neurotransmitter still remains the matter of investigation even though 50-70% of presympathetic RVLM neurons are catecholaminergic.

The CVLM is a major inhibitory control mechanism of presympathetic RVLM neurons (Agarwal et al., 1990; Miyawaki et al., 1997; Chan and Sawchenko, 1998). Juxtacellular labelling of baro-activated CVLM neurons paired with *in situ* hybridisation histochemistry for GAD67 (glutamic acid decarboxylase-67) messenger ribonucleic acid (mRNA) demonstrates that CVLM neurons are GABAergic (Schreihofer and Guyenet, 2003). Excitation of the CVLM neurons decrease SNA and MAP through activation of GABAergic CVLM neurons which inhibit the RVLM neurons (Willette et al., 1987), whereas inhibition of the CVLM produces pressor and sympathoexcitatory responses (Figure 1. 5 and Figure 1. 7) (Ito and Sved, 1997; Horiuchi et al., 2004a). GABAergic CVLM neurons control the activity of presympathetic RVLM neurons and overall sympathetic output to maintain the normal AP. More importantly, all sympathoinhibitory reflexes produced by inhibition of the RVLM are mediated through activation of GABAergic CVLM neurons (Agarwal et al., 1990; Chan and Sawchenko, 1998). For example, activated baroreceptor afferents, due to an increase in AP, activate second-order neurons in the NTS which in turn excite GABAergic interneurons in the CVLM via a glutamatergic input (Chan and Sawchenko, 1998). These baro-activated GABAergic CVLM neurons most likely inhibit presympathetic RVLM neurons, thereby inhibiting SNA and returning AP to normal levels (Figure 1. 7). Conversely, hypotension causes

unloading of baroreceptors that is associated with a reduction in the activity of baro-activated GABAergic CVLM neurons that coincides with an increase in SNA (Figure 1. 7) (Mandel and Schreihofer, 2008). Overall, changes in the GABAergic CVLM neurons in either direction have profound effects on the SNA that regulates cardiovascular function. The RVLM is the major integration site for generation of reflexes, mediated through the NTS-CVLM-RVLM circuit, and are discussed in detail in section 1.2.5.

The NTS-mediated excitation of CVLM neurons plays an essential role in passing inhibitory signals to RVLM, and providing required inhibitory link in reflex pathways (Agarwal et al., 1990; Miyawaki et al., 1996a; Chan and Sawchenko, 1998). The NTS integrates the afferent inputs and generates the differential excitatory output to either RVLM or CVLM. The NTS is a major source of glutamate input to GABAergic CVLM neurons (Suzuki et al., 1997; Chan and Sawchenko, 1998). Inhibition of the CVLM continues to increase the SNA even after lowering AP below baroreceptor threshold, which suggest that GABAergic CVLM neurons are tonically active independent of arterial baroreceptor activity (Cravo and Morrison, 1993; Mandel and Schreihofer, 2008). The baroreceptors-independent drive to the CVLM appears to be glutamatergic because unloading of baroreceptors by hypotension or blockade of glutamatergic input in the NTS produces a smaller rise in AP than blockade of glutamatergic input in the CVLM (Mandel and Schreihofer, 2008). It is possible that the PVN is a source of remaining glutamatergic drive to the CVLM, as the stimulation of the PVN produces depressor responses that coincides with the activation of the baro-activated, pulse modulated CVLM neurons (Yang and Coote, 1999). Evidence also suggests that central respiratory-related neurons may be another possible source of excitatory drive to CVLM neurons (Mandel and Schreihofer, 2006). The activity of CVLM neurons is modulated in relation to the cardiac cycle, as most of their activity is occurring during the rising phase of systole (Mobley et al., 2006). In addition, baro-activated CVLM neurons display patterns of central respiratory modulation that appear to be inversely related to patterns observed in presympathetic RVLM neurons (Schreihofer and Guyenet, 2003).

1.2.5. <u>Central autonomic reflexes</u>

Central autonomic reflexes are vital in the maintenance of normal cardiovascular function. Disturbances in homeostasis conditions, such as a sudden rise in AP, a drop in oxygen content or prediction of defensive behaviour, produce reflex responses that are mediated through changes in the SNA, which modifies and regulates the cardiovascular functions.

Glutamate plays an essential role in almost all sympathoexcitatory reflexes through activation of presympathetic RVLM neurons (Miyawaki et al., 1996a; Moraes et al., 2012). In contrast, GABAergic CVLM neurons are crucial for passing baroreceptor reflex related inhibitory input from NTS to RVLM (Chan and Sawchenko, 1998; Schreihofer and Guyenet, 2003).

1.2.5.1. Baroreflex

The central baroreflex mechanism is crucial for regulation of AP. It is the first line defence mechanism against abnormal BP and any abnormalities in baroreflex function lead to uncontrolled AP and cardiovascular damage. High threshold arterial baroreceptors are situated in the carotid sinus and aortic arch, whereas low threshold baroreceptors are found in the atria and ventricles (McMahon et al., 1996). These receptors continuously monitor the changes in BP, and are activated when there is increased vessel wall pressure to provide moment-to-moment information to the NTS (Figure 1. 8) (Chan and Sawchenko, 1998; Andresen et al., 2001). The reflex circuitry in the brain detects these changes, and sends signals back to the circulatory system to dilate the peripheral blood vessels, reduce the force and rate of heart beat and adjust vasopressin secretion (Figure 1. 8).

Disruption or impairment of this reflex mechanism is associated with impairment of short-term BP control and ultimately hypertension and cardiovascular dysfunction (Billman et al., 1982; Pilowsky and Goodchild, 2002). The arterial baroreceptors can scan the wide range of physiological pressures in rabbit (30-300 mmHg), where individual receptor differs in upper and lower range (Chen et al., 2014). The high threshold carotid sinus baroreceptors are divided into two types depending on their role in the regulation of either acute change in BP; type I, or tonic and baseline BP change; type II (Seagard et al., 1990), and contain myelinated A- and C-fibres (Fan et al., 1999).

Lesion or chemical inhibition of the medial NTS instantly increases AP and SNA through the elimination of baroreflex response (Moreira et al., 2005). In contrast, electrical stimulation of the same area produces a decrease in activity of presympathetic neurons (Agarwal et al., 1990). Glutamic acid is considered as a major neurotransmitter for baroreceptor afferent neurons that carry baroreflex information and terminate on NTS neurons (Reis et al., 1981). The electrophysiological studies to demonstrate the baroreflex mechanism are carried out with either electrical stimulation of the baroreceptor afferents (such as aortic depressor nerve) or by intravenous (i.v.) administration of a vasoconstrictive agents (Fan et al., 1999; Kashihara et al., 2008; Abbott and Pilowsky,

2009). The aortic depressor nerve contains no functional chemoreceptor afferents, hence its electrical stimulation is the most widely used method to test the baroreflex function (Figure 5. 1). There are certain limitations of this technique, such as stimulation of aortic depressor nerve does not replicate the natural firing pattern of the baroreceptors. Alternatively, baroreflex response is produced by systemic administration of vasoconstrictive substances such as phenylephrine (Figure 1. 7B). In this method, the observed effect on SNA or AP may not be entirely secondary to changes in AP. The vasoconstrictive substances may affect the activity of the neurons that are directly or indirectly involved in the reflex responses through undefined central and/or peripheral mechanisms.

1.2.5.2. Chemoreflex

Oxygen content in blood is carefully monitored and sensed by peripheral and central chemoreceptors. Decrease in oxygen saturation rapidly triggers highly coordinated central reflex pathways to adjust the cardiorespiratory responses (Figure 1. 9) (Rosin et al., 2006; Michael Spyer and Gourine, 2009). Carotid bodies are the most important peripheral chemoreceptors as they are sensitive to natural stimuli, which include hypoxic, anemic, metabolic and respiratory acidosis and osmolar and temperature changes, whereas aortic bodies play a minimal role in hypoxic chemoreception (Heeringa et al., 1979; Michael Spyer and Gourine, 2009). Carotid body is a small organ located in the vicinity of the common carotid artery bifurcation. In *in vivo* animal studies, chemoreflexes are activated by a moderate reduction of PaO_2 below the normal resting level of 80-100 mmHg, and functions maximally when haemoglobin is half saturated (Gonzalez et al., 1994). The discharge of chemoreceptor afferent nerves rises sharply when PaO_2 falls to 60-75 mmHg, and reaches maximum when PaO_2 is about 5-10 mmHg. Type I glomus cells are the functional chemoreceptors in carotid bodies, which are round or ovoid cells with a diameter of 10-12 µm. The rat and cat carotid bodies contain about 1000 and 10,000 type I glomus cells, respectively. Carotid bodies receive continuous innervations from carotid sinus nerve and a thin branch of the glossopharyngeal nerve as well as a small filament of the vagus nerve join the carotid sinus nerve on its way to carotid bodies (Gonzalez et al., 1994). The chemical transmission between glomus cells and sensory nerve endings (carotid sinus) is mediated by numerous neurotransmitters, including acetylcholine, dopamine, noradrenaline, adenosine triphosphate (ATP) and opioids (Kato et al., 2013; Kåhlin et al., 2014; Yokoyama et al., 2015). Hypoxia triggers glomus cells to release neurotransmitters and excite chemoreceptor afferents that further lead to changes in cardiorespiratory responses (Figure 1. 9) (Gonzalez et al., 1994).
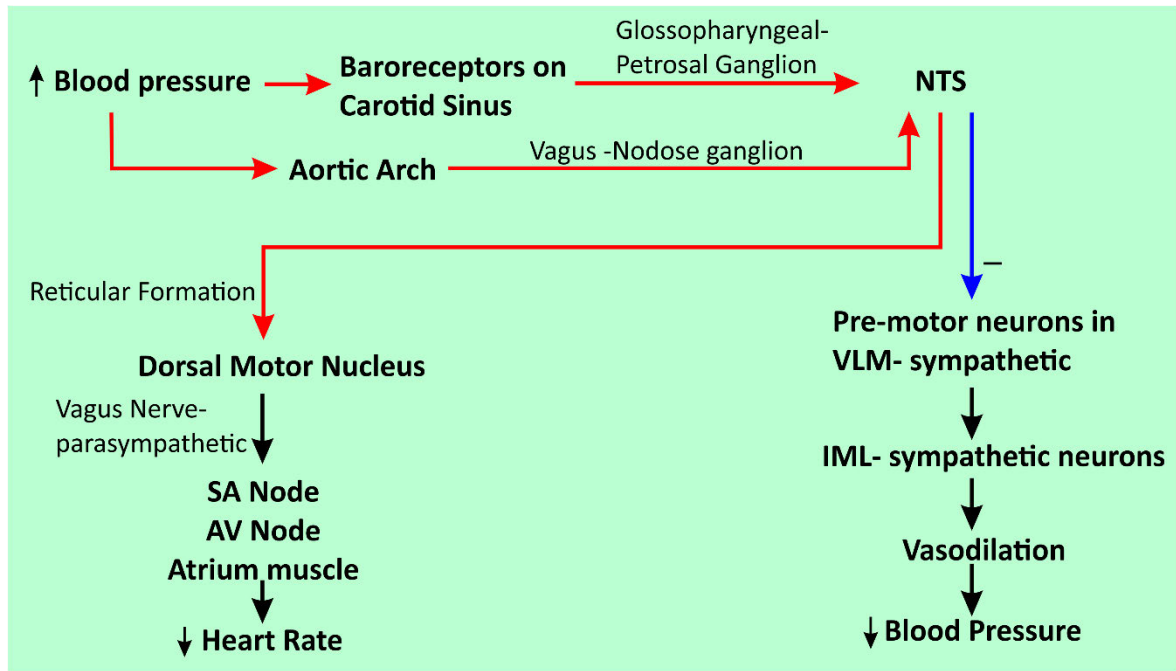
Figure 1. 8: Baroreflex pathway.

Excitatory pathways are in red and inhibitory pathway is in blue.
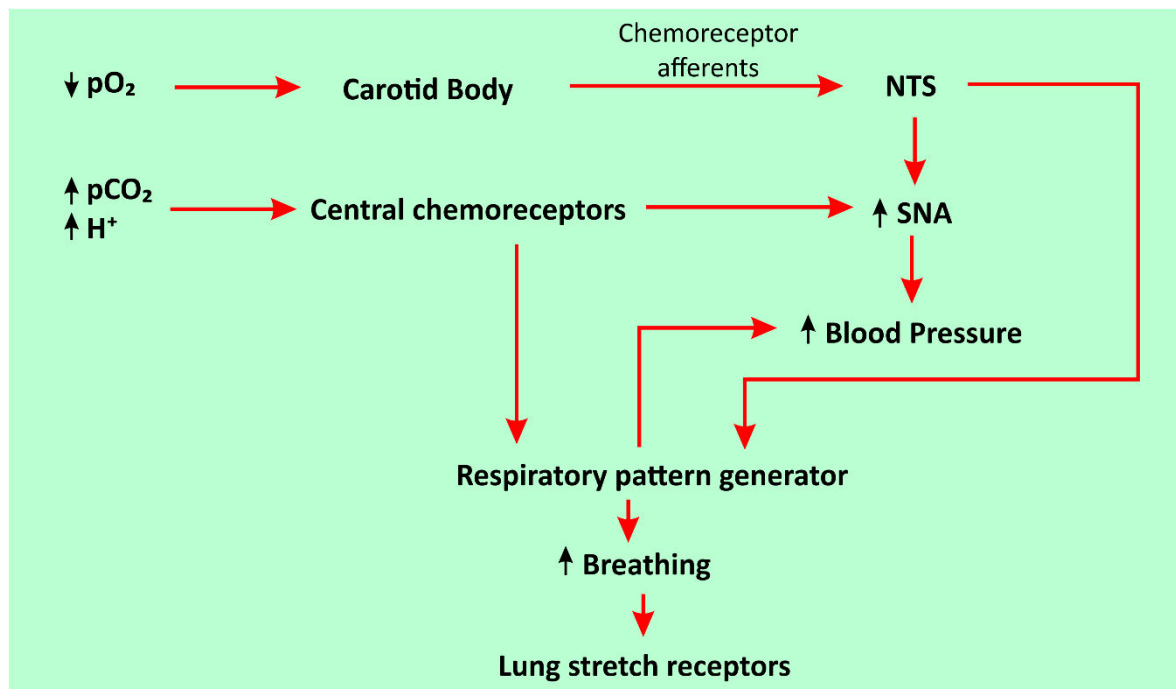
Figure 1. 9: Chemoreflex pathway.

Excitatory pathways are in red.

The RTN is a prominent central respiratory chemoreceptor (Guyenet, 2014). The absence of RTN causes severe central apnoea in diseases such as congenital central hypoventilation syndrome (Amiel et al., 2009). Central respiratory chemosensitivity is caused by direct effects of acid on neurons and indirect effects of CO_2 via astrocytes (Figure 1. 9).

Stimulation of central and carotid chemoreceptors raises AP primarily by increasing sympathetic outflow to vasculature that is also mediated through increased activity of respiratory pattern generator (Figure 1. 9). The respiratory pattern generator increases breathing, which activates lung stretch receptors that in turn exerts a feedback regulation on the respiratory pattern generator. The central chemoreflex-mediated sympathoexcitatory response is relayed by RVLM spinal vasomotor neurons. Microinjection of KYNA into the RVLM eliminates the sympathoexcitatory chemoreflex response (Moreira et al., 2006).

The chemoreflex response produced by stimulation of carotid chemoreceptors with isotonic solution of inorganic phosphate might elicit a release of vasopressin since i.v. administration of a vasopressin receptor antagonist inhibited the small pressor response evoked by chemoreceptor activation in rats (Li et al., 1992a).

Chemoreceptor afferents arising from the carotid bodies terminate most densely in the commissural subnucleus and the medial subnucleus of the NTS (Finley and Katz, 1992). Their termination site is more caudal and medial compared to arterial baroreceptor afferents. Chemoreceptor afferents also project to the CVLM in the region of the nucleus retroambiguus and few projections to the DMV and area postrema (Finley and Katz, 1992).

1.2.5.3. Somatosympathetic reflex

The somatosympathetic reflex includes early spinal and late supraspinal reflex components (Zanzinger et al., 1994b). The spinal reflex component is mediated through descending inhibition from medullary brainstem region including the RVLM (Dembowsky et al., 1981). The supraspinal somatosympathetic reflexes, both inhibitory and excitatory appear to be mediated by the vasomotor neurons located in the RVLM as well through neurons in the CVLM (Zanzinger et al., 1994b; Zanzinger et al., 1994a). The sympathetic responses to somatic stimuli, induced through sciatic nerve stimulation, mediated by RVLM are non-uniform and depend on specific sympathetic output; e.g. biphasic and monophasic response in splanchnic and cervical SNA, respectively (McMullan et al., 2008). These responses are evoked due to a specific activity of myelinated and unmyelinated nociceptors to the medulla (Figure 1. 10). The somatosympathetic reflex was mediated through synaptic activation of non-NMDA receptors in the RVLM (Kiely and Gordon, 1993).
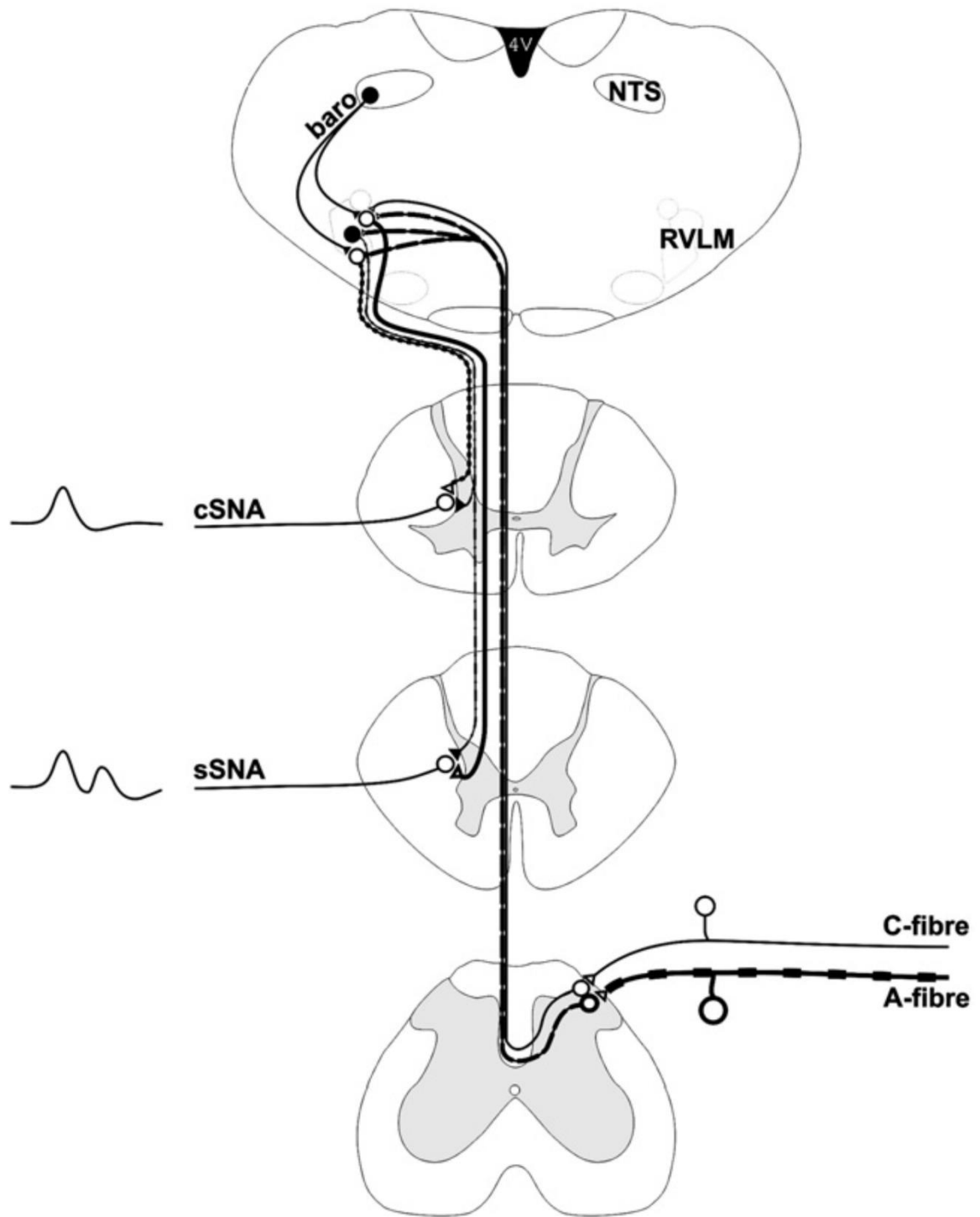
Figure 1. 10: Schematic of different somatosympathetic reflex responses generated by splanchnic and cervical sympathetic nerves (sSNA and cSNA).

Figure modified from (McMullan et al., 2008). 4V: fourth ventricle.

1.3. <u>Epilepsy</u>

Seizure is a characteristic of epilepsy, which is a chronic brain disorder arising from excessively synchronous, and sustained discharge of groups of neurons in the brain (McNamara, 1994; McNamara, 1999). Approximately 150,000 Australians and 50 million people worldwide have epilepsy (WHO, 2005; Hackett et al., 2011). Seizure may remain localised and restricted to certain part of the brain, or it can spread to other brain areas. A clinical seizure occurs when the discharge area is of sufficient size; otherwise they remain asymptomatic, and localised. The expression of seizure is determined by the area of brain affected.

1.3.1. Epilepsy terminologies

The actual duration of seizure is called as "*ictal* or *ictus period*". The time immediately after seizure is referred as "*post-ictal period*", whereas the interval between seizures is called as "*inter-ictal period*". "*Aura*" is the time before an actual seizure, and is the only event remembered by the patient.

The "status epilepticus" is defined as a condition in which seizures occur very frequently, and the patient does not recover fully from one seizure before having another. A seizure lasting for more than 5 min is normally considered as status epilepticus (SE). There are different types of SE depending on the clinical signs of the seizure and tonic-clonic SE is the most common and most life-threatening (Sutter et al., 2013).

1.4. <u>Classification of epileptic seizures and epilepsies</u>

Epileptic seizures and epilepsies are classified independently (Dreifuss et al., 1981; McNamara, 1994; Browne and Holmes, 2008; Berg et al., 2010). The classification of epileptic seizures is based on clinical signs and symptoms, where each seizure is considered as a separate event (Dreifuss et al., 1981; McNamara, 1999). The classification of epilepsies considers all types of seizures as same, and is based on etiology, genetics, age at epilepsy onset, and evidence of brain pathology (Browne and Holmes, 2008; Berg et al., 2010). The classification of epileptic seizures and epilepsies are described in brief in following sections.

1.4.1. Classification of epileptic seizures

Table 1.1 summarises the International Classification of epileptic seizures proposed in 1981 (Dreifuss et al., 1981). Accordingly, seizures are categorised into two broad types:

1) Partial seizures (seizures begin in a relatively small location of the brain) and 2) Generalised seizures (seizures are bilaterally symmetric and without local onset). These seizures are further sub-classified according to their clinical and EEG manifestations (Table 1. 1) (Dreifuss et al., 1981; Berg et al., 2010). All the definations are derived from (Browne and Holmes, 2008).

1. Partial (focal/ local) seizures
   A. Simple partial seizures (consciousness not impaired)
      a. With motor signs
      b. With sensory symptoms
      c. With autonomic symptoms or signs
      d. With psychic symptoms
   B. Complex partial seizures (temporal lobe; consciousness impaired)
      a. Simple partial onset, followed by impairment of consciousness
         i. With simple partial features followed by impaired consciousness
         ii. With automatism
      b. With impairment of consciousness at onset
         i. With impairment of consciousness only
         ii. With automatism
   C. Partial seizures evolving to secondarily generalised seizures (tonic-clonic, tonic or clonic)
      a. Simple partial seizures evolving to generalised seizures
      b. Complex partial seizures evolving to generalised seizures
      c. Simple partial seizures evolving to complex partial seizure, evolving to generalised seizures
2. Generalised seizures
   A. Absence (petit mal) seizures
   B. Myoclonic seizures
   C. Tonic seizures
   D. Atonic seizures
   E. Clonic seizures
   F. Tonic-clonic (grand mal) seizures
3. Unclassified epileptic seizures (cannot be classified as either focal or generalised)

Table 1. 1: International classification of epileptic seizures.
Table modified from (Browne and Holmes, 2008).

1.4.1.1. Partial/focal/local seizures

Simple partial seizures

Simple partial seizures are caused by a local discharge of neurons in the brain, which results in seizure symptoms without impairment of consciousness. Simple partial seizures are sub-classified and may consist of motor, sensory, autonomic, or psychic signs or symptoms (Table 1.1).

Complex partial seizures

Consciousness is impaired in complex partial seizures (Table 1.1). Initially, the signs or symptoms of a simple partial seizure may occur without impairment of consciousness providing an aura, followed by an impairment of consciousness. No other signs or symptoms may present during the period of impaired consciousness. The attack characteristically ends gradually with a period of post-ictal drowsiness or confusion.

Partial seizures evolving to secondarily generalised seizures

Secondarily generalised seizures commence in one part of the brain like simple partial seizures and then spread throughout the brain to become a generalised seizure.

1.4.1.2. Generalised seizures

Generalised seizure is an outcome of simultaneous abnormal activity in both hemispheres of the brain, which normally, but not necessarily, results in loss of consciousness at the onset of a seizure (Dreifuss et al., 1981; Berg et al., 2010).

Absence (petit mal) seizures

These seizures start suddenly and last only for few seconds, although they can occur multiple times in a day, and accompanied by a unique 3-Hz spike-wave-EEG pattern. Absence seizures appear like a daydreaming, and therefore often remain unnoticed. These seizures first manifest between 5-12 years of age, and often stop in teens.

Myoclonic

Myoclonic seizures are characterised by uncontrolled muscle jerks and a brief loss of consciousness. These seizures do not cause impairment of consciousness, but if several seizures occur over a short period of time the person may feel slightly confused or drowsy.

Tonic seizures

Tonic seizures are characterised by muscles stiffening and falling to the ground. Consciousness is usually partially or completely lost. These seizures frequently occur in clusters during sleep. Tonic seizures are relatively rare and occur between 1-7 years of age.

Atonic

Atonic seizures consist of sudden loss of muscle tone. The loss of muscle tone may be confined to a group of muscles, such as the neck, resulting in a head drop. Alternatively, atonic seizures may involve all trunk muscles, leading to a fall on the ground.

Clonic seizures

Clonic seizures occur almost exclusively in early childhood. The attack begins with the loss of consciousness associated with sudden hypotonia or a brief generalised tonic spasm, which is followed by one to several minutes of bilateral jerks.

Tonic-clonic (grand mal seizures)

These seizures are characterised by two main phases: a tonic phase when person stiffens and falls to the ground, and a clonic phase during which body begins strong jerking. Prominent autonomic phenomena occur during the tonic-clonic phase. The patient awakens by passing through stages of coma, confusional state and drowsiness.

1.4.2. Classification of epilepsies

Epilepsies are classified according to their etiology: idiopathic, symptomatic, or genetic (Browne and Holmes, 2008; Berg et al., 2010). Idiopathic means arising spontaneously from an obscure or unknown cause. Symptomatic epilepsies arise as symptoms of a known brain abnormality. Genetic means arising from a known gene defect. Three special categories of epilepsy are also included such as reflex epilepsies, epileptic encephalopathies, and progressive myoclonic epilepsies. Moreover, some conditions may result in seizures but are not likely to result in epilepsy, and are called as chronic unprovoked seizures.

Based on these categories, epilepsies are divided into eight groups (Table 1. 2), and within each group there are number of specific epilepsy syndromes based on clustering of specific seizure type, specific etiology, genetics, age and evidence of brain pathology (Browne and Holmes, 2008; Berg et al., 2010).

1. Idiopathic focal epilepsies of infancy and childhood	Benign infantile seizures (non-genetic) Benign childhood epilepsy with centrotemporal spikes Early-onset benign childhood occipital epilepsy Late-onset childhood occipital epilepsy (Gastaut type)
2. Genetic (autosomal dominant) focal epilepsies	Benign genetic neonatal seizures Benign genetic infantile seizures Autosomal dominant nocturnal frontal lobe epilepsy Genetic TLE Genetic focal lobe epilepsy with variable foci

3. Unclassified epileptic seizures	Limbic epilepsies
	    Mesial TLE with hippocampal sclerosis
	    Mesial TLE defined by specific etiology
	    Other types defined by location and etiology
	Neocortical epilepsies
	    Rasmussen syndrome
	    Hemiconvulsion-hemiplegia syndrome
	    Other types defined by location and etiology
	Migrating partial seizure of early infancy

4. Idiopathic generalised epilepsies	Benign myoclonic epilepsy in infancy
	Epilepsy with myoclonic astatic seizures
	Childhood absence epilepsy
	Epilepsy with myoclonic absences
	Idiopathic generalised epilepsies with variable phenotypes
	    Juvenile absence epilepsy
	    Juvenile myoclonic epilepsy
	    Epilepsy with generalised tonic-clonic seizures only
	Generalised epilepsy with febrile seizures plus (GEFS+)

5. Reflex epilepsies	Idiopathic photosensitive occipital lobe epilepsy Other visual sensitive epilepsies Primary reading epilepsy Startle epilepsy
6. Epileptic encephalopathies (in which the epileptiform abnormalities may contribute to progressive dysfunction)	Early myoclonic encephalopathy Ohtahara syndrome West syndrome Dravet syndrome (known as myoclonic epilepsy in infancy) Myoclonic status in non-progressive encephalopathies Lenox-Gastaut syndrome Landau-Kleffner syndrome Epilepsy with continuous spike-waves during slow-wave sleep
7. Progressive myoclonus epilepsies	
8. Seizure not necessarily requiring a diagnosis of epilepsy	Benign neonatal seizures Febrile seizures Reflex seizures Alcohol withdrawal seizures Drug or other chemically induced seizures Immediate and early post-traumatic seizures Single seizure or isolated clusters of seizures Rarely repeated seizures (oligoepilepsy)

Table 1. 2: International classification of epilepsy syndromes.
Table modified from (Browne and Holmes, 2008).

1.5. <u>Pathophysiology of epilepsy</u>

Epilepsy is a paroxysmal neuronal disorder characterised by a persistent increase in neuronal excitability causing abnormal neuronal discharges. Paroxysmal neuronal discharge occurs, when the neuronal membrane-firing-threshold decreases below the intrinsic membrane-threshold-stabilising potential to prevent firing (McNamara, 1994; McNamara, 1999). Although there are different causes of epilepsy, such as trauma (Annegers et al., 1998), tumour (Beaumont and Whittle, 2000), infection (Ho et al., 2015), oxygen deprivation, and metabolic derangements (Herman, 2002), the fundamental disorder is secondary to either abnormal neuronal membrane potentials or an imbalance between excitatory and inhibitory mechanisms (Wong, 2005; Li et al., 2015; Williams et al., 2015). Although microglial function is not associated with a particular type of seizure nor with a specific seizure generation mechanism, the following mechanisms are closely related to the chosen potential targets (in this thesis) of the central autonomic cardiorespiratory dysfunction in epilepsy.

1.5.1. <u>Ictogenesis (generation of seizure activity)</u>

Neuronal excitability, a key feature of ictogenesis, may originate from an individual neuron, neuronal environment or a population of neurons (Traub et al., 1996). Each neuron has a resting membrane potential that represents the separation of positive and negative charges across the cell membrane (Figure 1. 11). Sodium (Na^+) and chloride (Cl^-) ions are present in the extracellular space along the membrane, whereas K^+ is dominant in the intracellular space. This generates an excess of positive charges outside, and negative charges inside the cell with resting membrane potential of approximately -50 to -80 mV. Change in membrane permeability causing Na^+ to enter the cell leads to depolarisation, whereas K^+ outflow or Cl^- entry into the cell result in hyperpolarisation (Figure 1. 11). Activation of GABA (ionotropic or metabotropic) receptors increase Cl^- conductance and give rise to inhibitory PSPs, which results in greater intracellular negativity than baseline (hyperpolarisation). The action of excitatory amino acids acting on their receptors increases Na^+ and Ca^{2+} permeability that give rise to excitatory PSPs, leaving a relatively negative extracellular environment (depolarisation). Whether a neuron generates an action potential or not is determined by the relative balance of excitatory PSPs and inhibitory PSPs (Browne and Holmes, 2008).

The EEG does not record an activity from a single neuron, and is dependent on the summation of thousands to millions of PSPs, and therefore represents activity from a large

neuronal population. During an ictal discharge, neurons generate high-voltage (approximately 10-15 mV), and relatively long depolarisation (100-200 µsec) causing bursts of spike activity (Browne and Holmes, 2008). This depolarisation is much longer than the depolarisation during excitatory PSPs, which is in the range of 10-16 µsec. The EEG activity is based on conduction volume of ionic currents generated by nerve cells from summated excitatory and inhibitory PSPs. The long depolarisation generates a train of action potentials that are conducted away from the neuronal cell body along the axon and called the paroxysmal depolarisation shift (Browne and Holmes, 2008).

1.5.2. Mechanisms of interictal-ictal transition

The event that leads from interictal to ictal state is poorly understood. It may include disturbances in neuronal membrane function (nonsynaptic mechanism) or balance between excitatory or inhibitory neurotransmitters (synaptic mechanism) (Wendling et al., 2005). The decrease in synaptic inhibition, an increase in synaptic excitation, alteration in K^+ or Ca^{2+} currents, or changes in the extracellular ion concentration may trigger prolonged depolarisation. These changes may occur in microenvironment at the epilepticus focus as well as at distant sites through synaptic pathways. This mechanism could be responsible for generalisation and spread of seizures to the central autonomic nuclei in the brainstem.

1.5.2.1. Nonsynaptic mechanisms

Alterations in ionic microenvironment and transport

The nonsynaptic mechanisms of development of seizure activity include changes in postsynaptic receptor proteins, activity of Na^+-K^+ pump, number of Ca^{2+} channels, and Cl^--K^+ co-transport. Functional and structural changes in postsynaptic membrane alter characteristics of the receptor protein (conductance channels), which favours the development of paroxysmal depolarisation shift and enhanced excitability (Wyneken et al., 2001). In epileptic neurons, the number of Ca^{2+} channels is chronically elevated that increases Ca^{2+} conductance (Yaari et al., 2007). Activation of Na^+-K^+ pump is important for regulation of neuronal excitability during excessive neuronal discharges (Ayala et al., 1970). Hypoxia or ischemia can result in Na^+-K^+ pump failure that promotes interictal-ictal transition (Florence et al., 2009). A Cl^--K^+ co-transport mechanism controls the intracellular Cl^- concentration, and the Cl^- gradient across the cell membrane, which regulates effectiveness of GABA-activated inhibitory Cl^- currents. However, interference in this process could cause a progressive decrease in the effectiveness of GABAergic inhibition leading to increased excitability (Kaila et al., 1997; Pavlov et al., 2013).
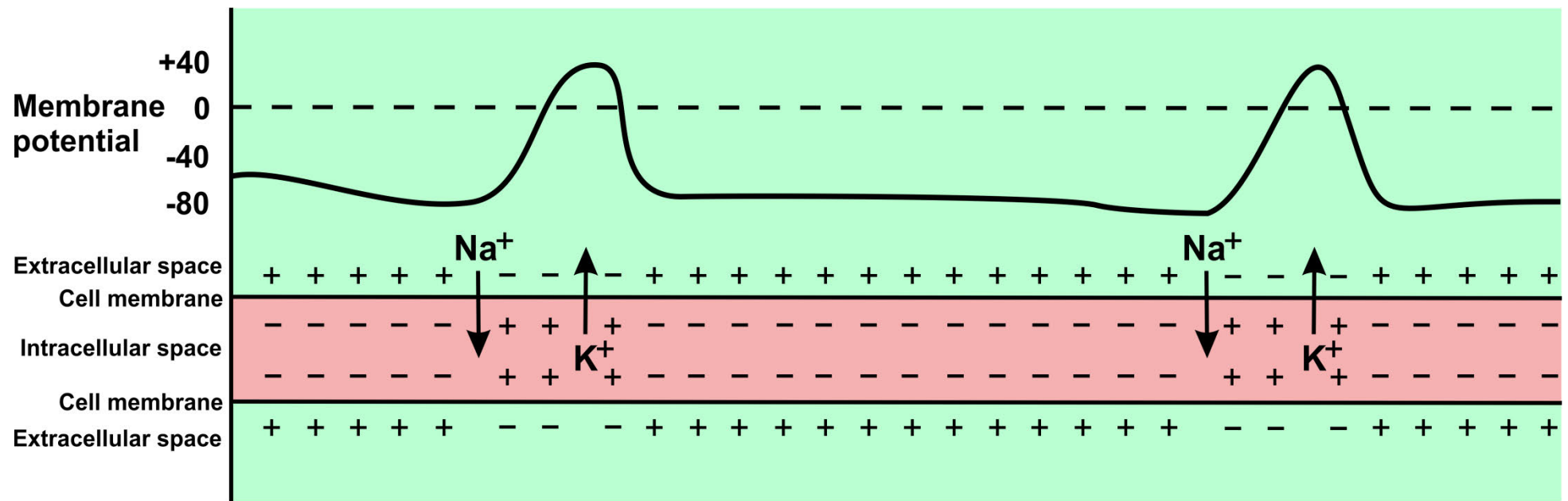
Figure 1. 11: Propagation of action potential along the axon as a result of changing membrane potential.

Figure modified from (Browne and Holmes, 2008).

Excitability arising from neuronal microenvironment

Excessive extracellular K^+ depolarises neurons that lead to spike discharge. Endogenously, astrocytes are able to clear neurotransmitters from the extracellular space, and to buffer K^+ thus, correcting the increased extracellular K^+ concentrations that occur during seizures. However, the structural changes in glia (astrogliosis) affect their K^+ buffering capacity, and may contribute to seizure generation (Coulter and Eid, 2012; Devinsky et al., 2013; Seidel et al., 2015).

The epileptic neuronal population

Mossy fiber sprouting is an example of neuronal alterations during seizures (Kharatishvili et al., 2006; Gurbanova et al., 2008). Normally, the dentate granule cells control the seizure propagation through the hippocampal network. However, the formation of recurrent excitatory synapses between dentate granule cells (mossy fiber sprouting) transforms them into an epileptogenic population of neurons (Sharma et al., 2007). Ephaptic interactions also produced when currents from activated neurons excite adjacent neurons in the absence of synaptic connections (Jefferys et al., 2012).

1.5.2.2. Synaptic mechanisms (neurochemical mechanisms)

Two neurochemical mechanisms are involved in the pathophysiology of epilepsy: decreased effectiveness of inhibitory synaptic mechanisms or facilitation of excitatory synaptic events. The major neurotransmitters in the synaptic mechanism are discussed below.

Gamma (γ)-aminobutyric acid (GABA)

Gamma-aminobutyric acid is a major inhibitory neurotransmitter in the CNS. Decrease in GABAergic inhibition causes seizures, whereas an enhancement of GABAergic inhibition results in an anti-epileptic effect (Domann et al., 1994; Wong, 2005). Several studies have shown that GABA is involved in the pathophysiology of epilepsy in both animal models and patients suffering from epilepsy (Sato et al., 1990; Wendling et al., 2005). Low GABA levels and increased antibodies to glutamic acid decarboxylase (a catalytic enzyme that converts glutamate into GABA) are evidenced in patients with chronic epilepsy (Stagg et al., 2010). Glutamic acid decarboxylase levels are decreased in the substantia nigra of amygdale-kindled rats (Löscher and Schwark, 1987). Seizure frequency is positively correlated with a reduction in benzodiazepine receptor (allosteric modulatory sites on $GABA_A$ receptors) in epilepsy patients (Savic et al., 1996). There are decreased levels of

GABA in the epileptic model in dogs (Hasegawa et al., 2004). Mice with a genetic susceptibility to audiogenic seizures have a lower number of GABA receptors than animals of the same strain that are not seizure prone (Horton et al., 1982). The convulsant agent, such as bicuculline, inhibits GABAergic transmission, whereas anti-epileptic drugs are GABA analogues, such as valproate, and block GABA metabolism.

Glutamate (refer section 1.10 for detail)

Glutamate is a major excitatory neurotransmitter in the CNS that plays an important role in epileptogenesis. Activation of both postsynaptic iGluRs and metabotropic glutamate receptors (mGluRs) is proconvulsant. Antagonism of NMDA receptors produces powerful anticonvulsant effects in animal models of epilepsy (Smolders et al., 1997; Rice and Delorenzo, 1998). NMDA receptor function is altered in acquired animal models of epilepsy and in humans (Brines et al., 1997; Rice and Delorenzo, 1998). Hippocampal neuronal cultures showed a time-dependent increase in neuronal death with increasing duration of SE. This causes an enhanced entry of Ca^{2+} into neurons and increased excitatory PSPs. The neuronal death was significantly reduced by addition of NMDA receptor antagonist (Deshpande et al., 2008). Moreover, in patients with epilepsy, plasma and cerebrospinal fluid (CSF) glutamate levels were found to be significantly increased (Rainesalo et al., 2004).

Glutamate is also a major neurotransmitter in cardiovascular autonomic neuronal function, and reflex responses (section 1.10.2). Therefore, this study was designed to evaluate the significance of increased glutamate levels in epilepsy, and their correlation with the central autonomic cardiovascular dysfunction.

Catecholamines

Abnormal catecholamine levels in the CNS have been reported in several genetic models of epilepsy (Szot et al., 1996; Weinshenker and Szot, 2002). Low levels of dopamine in nucleus caudatus and higher levels of noradrenaline in midbrain and brainstem are reported in spontaneous epileptic rats (Hara et al., 1993). Dopamine is also decreased in epileptic foci of epilepsy patients (Mori et al., 1987). Overall, increased levels of noradrenaline and adrenaline in patients and animal models of epilepsy might account for increased SNA.

1.6. <u>Sudden unexpected death in epilepsy (SUDEP)</u>

Sudden unexpected death in epilepsy is operationally defined as "sudden, unexpected, witnessed or unwitnessed, non-traumatic and non-drowning death in patients with epilepsy, with or without evidence of a seizure, and excluding documented SE, where post-mortem examination does not reveal a toxicological or anatomical cause of death" (Nashef, 1997). The mechanism of SUDEP is still unknown and is the major hurdle in finding the best therapeutic solution for its prevention. Plausible mechanisms of SUDEP include ictal arrhythmias (Darbin et al., 2002; Auerbach et al., 2013), ictal and postictal central apnoea (Bateman et al., 2008; Seyal et al., 2010), acute neurogenic pulmonary oedema (Kennedy et al., 2015), and autonomic dysfunction (Naggar et al., 2014) for each of which case reports have been documented and described further in detail (sections 1.6.1 and 1.6.2). SUDEP in epilepsy monitoring units showed an early postictal, centrally mediated, severe alteration of respiratory and cardiac function induced by generalised tonic-clonic seizures followed by terminal apnoea then cardiac arrest (Ryvlin et al., 2013). It therefore seems unlikely that SUDEP is a failure of a single system; rather it is more likely to be due to the collapse of multiple systems leading to fatal cardiac and respiratory dysfunction.

1.6.1. <u>Cardiovascular dysfunction in seizure</u>

1.6.1.1. Acute cardiac changes in epilepsy

Studies into the mechanisms of SUDEP in humans and animals, show that seizure causes major cardiovascular changes with significant sympathovagal imbalance, tachycardia (Figure 1. 12) or bradycardia (Ryvlin et al., 2013), and abnormal changes in the ECG (Ponnusamy et al., 2012; Naggar et al., 2014). Acute seizure causes an increase in sympathetic activity, pressor effects, tachycardia (Figure 1. 12), and prolongation of the QT interval in rats (Sakamoto et al., 2008; Naggar et al., 2014). The increase in both sympathetic and parasympathetic activity, baroreflex dysfunction, and hypoperfusion of brain and heart is evidenced as the major cause of death in seizure-induced rats (Sakamoto et al., 2008). Pilocarpine-induced SE causes severe shifts in sympathovagal balance towards a sympathetic predominance in rats (Metcalf et al., 2009a). KA-induced chronic seizures in rats showed decreased vagal tone, increased QT dispersion, and eccentric cardiac hypertrophy without significant cardiac fibrosis (Naggar et al., 2014). Peri-ictal and ictal ECG changes are potential features that can be used to detect seizure risk. In patients with refractory or well-controlled TLE, HR variation during normal breathing and tilting was lower compared to control subjects (Ansakorpi et al., 2000). In TLE patients, heart

rate variability changes (RR interval, low and high-frequency domain analysed from ictal ECG recording) were significantly lower and cardiosympathetic index was higher compared to patients with psychogenic nonepileptic seizures (Ponnusamy et al., 2012).

Sudden unexpected death in epilepsy is closely linked to ictal cardiovascular changes. ECG abnormalities, including ST-segment elevation or depression and T-wave inversion occur in around 49% of patients during or after epileptic discharges and are common in generalised seizures (Nei et al., 2000; Opherk et al., 2002). Tachycardia is present in 76 to 99% patients that suffer convulsive and non-convulsive seizures in epilepsy monitoring unit (Figure 1. 12) (Opherk et al., 2002; Moseley et al., 2011). Activation of the central autonomic cardiovascular network, including the RVLM, causes cardiac changes observed in epilepsy (Silveira et al., 2000; Tsai et al., 2012). Overall, epileptic discharges are thought to propagate to the central autonomic nuclei in the brainstem and disturb the normal autonomic control through sympathetic and parasympathetic pathways (Figure 1. 1).

1.6.1.2. Chronic cardiac changes in epilepsy

Neurocardiac channelopathies are the most significant chronic cardiovascular changes in patients with epilepsy. These changes lead to altered membrane excitability both in the brain and the heart (Ludwig et al., 2003), and pose an increased risk of autonomic dysfunction and cardiac arrhythmia (Biet et al., 2015). Patch-clamp recordings reveal that, as in the brain, epilepsy is associated with an increased expression of the neuronal isoform Nav1.1 (voltage-gated sodium channel) in cardiomyocytes (Biet et al., 2015). In mice, the HCN (hyperpolarisation-activated cyclic nucleotide-gated) channel plays a physiological role in regulating the resting membrane potential, required for regular cardiac and neuronal rhythmicity (Ludwig et al., 2003). In Genetic Absence Epilepsy Rats from Strasbourg (GAERS) and acquired TLE rats, a significant reduction in HCN2 (hyperpolarisation-activated cyclic nucleotide-gated2) mRNA and protein expression in heart is the mechanism for abnormal cardiac electrophysiology (Powell et al., 2014c).

Genetic mutations in the *KCNQ1* gene cause familial long QT syndrome due to prolonged cardiac action potentials (Goldman et al., 2009). Mutations in the *KCNQ1* gene in forebrain neuronal networks, and in the brainstem autonomic nuclei can produce seizures, and dysregulate the autonomic control of the heart (Goldman et al., 2009).

Dravet syndrome (Table 1.2) is associated with a loss of function mutation in gene *SCN1A* encoding for voltage-gated sodium channel Nav1.5 that leads to ECG abnormalities.

Increased excitability, prolongation of action potential duration, and triggered activity was recorded in isolated Dravet syndrome ventricular myocytes (Auerbach et al., 2013). Patients with Dravet syndrome have reduced heart rate variability that shows an imbalance in autonomic cardiac function (Delogu et al., 2011). The findings in *SCN1A* heterozygous knockout mice show that an increase in parasympathetic activity following tonic-clonic seizures causes bradycardia and subsequently SUDEP (Kalume et al., 2013). *SCN1A* mutant mice have a lower threshold for spreading depression that causes bradycardia, apnoea, and SUDEP (Aiba and Noebels, 2015).

Loss of function mutations in the *SCN5A* gene causes Brugada syndrome (Table 1.2), and is characterised by ECG abnormalities including ST-segment elevation, syncope as well as seizures and sleep abnormalities (Wang et al., 2015).

Heart rate variability is used as a functional tool to investigate the state of the ANS. Reduced heart rate variability is seen in epilepsy patients compared to their controls (Ponnusamy et al., 2012) and is associated with increased mortality in patients with heart failure. Abnormal BP variability with higher vasomotor tone is observed in patients with chronic epilepsy (Devinsky et al., 1994).

1.6.2. Respiratory dysfunction in seizure

In epilepsy patients with severe respiratory dysfunction, as demonstrated using video-EEG telemetry, the ictal hypoventilation period is associated with a severe hypercapnic hypoxia (Figure 1. 12) (Bateman et al., 2008; Seyal et al., 2010).

Ictal and post-ictal end-tidal CO_2 ($ETCO_2$) increased above 50 mmHg in 11 out of the 33 epilepsy patients with the post-ictal increase in respiratory rate, and amplitude (Seyal et al., 2010). In humans, peri-ictal respiratory disturbances are likely to play a critical role in the pathophysiology of SUDEP (Dlouhy et al., 2015).

In audiogenic seizure-prone dilute Brown Non-Agouti (DBA)/2 mice, death due to a respiratory arrest can be prevented by mechanical ventilation (Venit et al., 2004). Interestingly, SUDEP in DBA/2 mice can also be prevented by treatment with a selective serotonin reuptake inhibitor (Tupal and Faingold, 2006). Serotonergic and/or glutamatergic neuronal abnormalities are associated with central respiratory dysfunction (Hodges et al., 2008; Hodges et al., 2009). Impaired ventilatory responses to hypercapnia may lead to SUDEP by adversely affecting patients' ability to reposition their head when prone after convulsion.
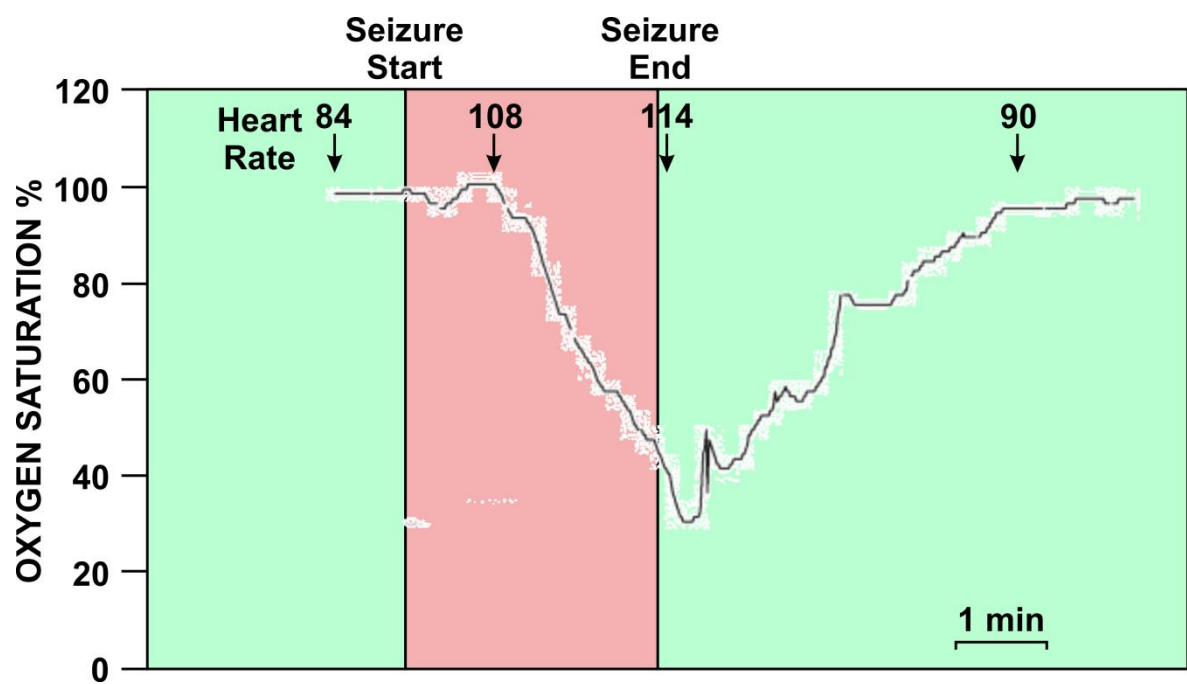
Figure 1. 12: Oxygen saturation falling below 40% in a 19-year-old male patient with a complex partial seizure without generalisation.

Figure modified from (Bateman et al., 2008).

Clinical evidence suggests that post-ictal pulmonary oedema, which may be mediated by vasoconstriction induced by massive seizure-related sympathetic outburst with increased pulmonary vascular resistance, could be associated with the pathophysiology of SUDEP (Kennedy et al., 2015). Forensic autopsies of 52 cases of SUDEP showed marked pulmonary congestion and oedema with an average combined lung weight of 1182 g, compared with the normal average combined lung weight of 840 g in men (Zhuo et al., 2012). In epileptic baboons that died suddenly without apparent cause, 96% had pulmonary congestion or oedema, whereas only 12% of the control animals had pulmonary oedema (Ákos Szabó et al., 2009).

1.7. <u>**Animal models of seizures and epilepsy**</u>

Animal models of seizures and epilepsy have played a significant role in advancing and understanding the mechanism of seizure and SUDEP. Epilepsy models can be used as models of seizures (e.g. mutant animals with inherent epilepsy), whereas a pure seizure model in a nonepileptic animal cannot be used as a model of chronic epilepsy (e.g. maximal electroshock-induced seizures in rats). There are several animal models of epilepsy and epileptic seizures. These animal models can be assigned into different categories, e.g. models with spontaneously occurring seizures versus chemically or electrically-induced seizures, models with recurrent seizures versus models with single seizures (i.e., chronic versus acute models), models with partial seizures versus models with generalised seizures and models with convulsive seizures versus models with non-convulsive seizures. Animal models of partial seizures versus generalised seizures are shown in Figure 1. 13.

In this thesis, a model of KA-induced TLE in rats is used (Figure 1. 14). The KA model of TLE is described in detail in the following section and was chosen due to following factors. This study was designed to investigate the effect of seizures on central autonomic cardiorespiratory system, and its possible mechanism, which is considered as a major cause of SUDEP (Glasscock et al., 2010; Auerbach et al., 2013; Naggar et al., 2014; Aiba and Noebels, 2015). KA-induced seizures provide a useful way to initiate seizure activity in a model where one can also record the central autonomic cardiorespiratory activity. The systemic injection of KA requires a considerable amount of time before a seizure propagates to the central autonomic nuclei (Lévesque et al., 2009) (Figure 4. 2), which allows researchers to differentiate between the times of onset of seizure, and autonomic cardiorespiratory changes.
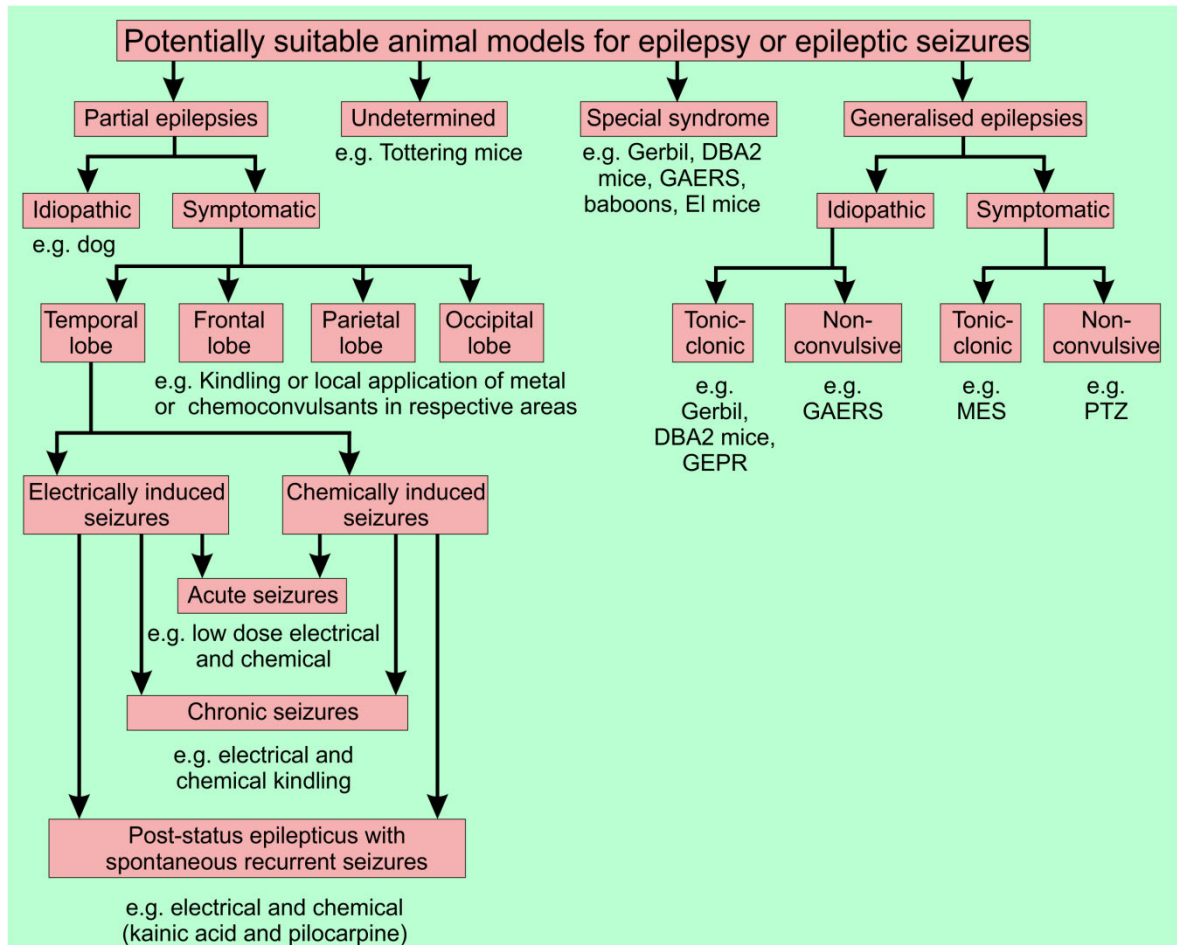
Figure 1. 13: Animal models of epilepsy or epileptic seizures.
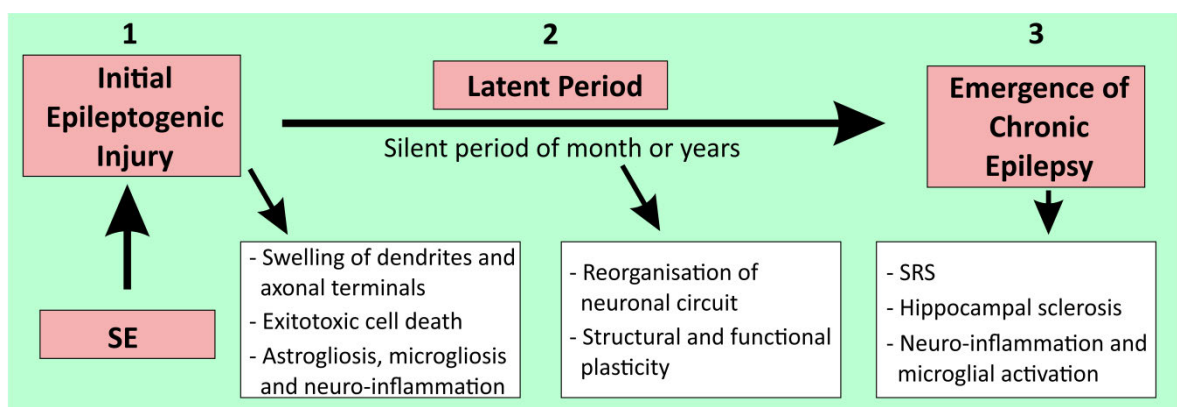
Figure 1. 14: KA-induced acute and chronic TLE model in rat.

Pathophysiological changes occur during acute, latent and chronic phase of epilepsy and contribute to observed behavioural manifestations.

1.7.1. <u>Kainic acid-induced TLE in rats</u>

The KA model of TLE has contributed greatly to understand the molecular, cellular and pharmacological mechanisms of epileptogenesis and ictogenesis. This model presents neuropathological and EEG features of TLE in humans (Nadler, 1981; Ben-Ari, 1985). The KA model is characterised by a latent period that follows the initial precipitating injury (i.e. SE) until the appearance of recurrent seizures, as observed in humans (Figure 1. 14). KA provides an easy way of induction of seizures, through systemic, intrahippocampal or intra-amygdaloid injection, in a variety of species (Lévesque and Avoli, 2013).

1.7.1.1. Kainic acid (KA)

Kainic acid, a cyclic analog of glutamate, is an ionotropic kainate receptor agonist. It was first isolated and extracted in early 1950s from red algae (*Digenea simplex*), and was known as digenic acid. KA induces robust neuronal depolarisation and eventually cell death, which is a central phenomenon in TLE (Nadler et al., 1978; Ben-Ari et al., 1981; Lothman and Collins, 1981; Sperk et al., 1983). These findings helped to develop an animal model of TLE characterised by a latent period followed by spontaneous seizures.

1.7.1.2. Kainic acid receptors

Kainic acid receptors are present in multiple regions in the brain, such as the hippocampus, amygdala, pyriform cortex, striatum and cerebellum (Unnerstall and Wamsley, 1983). They are highly expressed in the hippocampus on both presynaptic and postsynaptic neuronal membranes (Wisden and Seeburg, 1993; Carta et al., 2014).

KA1 and KA2 subunits of the KA receptor are differentially expressed by subsets of specific neurons in the brain. KA1 subunits (known as GluK4) are highly expressed in CA3 pyramidal cells of the hippocampus and dentate gyrus, but weakly expressed in CA1 cells, cortical layers and white matters (Wisden and Seeburg, 1993). KA2 (known as GluK5) subunits are instead highly expressed in both CA1 and CA3 pyramidal cells as well as in dentate granule cells, the bed nucleus of stria terminalis, ventral medial hypothalamic nuclei, dorsal raphe, locus coeruleus and cerebellar granule cells (Wisden and Seeburg, 1993). Therefore, the high affinity of KA1 and KA2 receptors to glutamate and their high concentration in CA3 region of the hippocampus render this region highly susceptible to the excitotoxic damage induced by KA. This often makes the hippocampus a seizure onset zone in this model (Ben-Ari et al., 1981; Lothman and Collins, 1981; Lothman et al., 1981; Sperk et al., 1983; Medvedev et al., 2000).

Other KA receptor subunits (GluR5 and GluR6 subunits or GluK1 and GluK2, respectively) also contribute to the excitatory action of KA. GluR6 subunits are highly expressed in CA3 pyramidal cells and dentate granule cells of the hippocampus, while GluR5 are highly expressed in cingulate and prefrontal cortex (Wisden and Seeburg, 1993; Carta et al., 2014). Moreover, the formation of the epileptic cell population, such as mossy fiber sprouting (section 1.5.2.1), is mediated through KA receptor mechanism and correlated to GluR5 upregulation, and is observed in histological brain samples of epileptic patients and animals (Darstein et al., 2003; Li et al., 2010). Overall, KA receptors are highly involved in the generation of epileptiform activity and used as a major tool in the development of model of epilepsy.

1.7.1.3. Features of KA-induced seizures

Systemic (i.v./ intraperitoneal (i.p.)/subcutaneous) or local administration of KA leads to a series of clinical manifestations, and pathological changes in rodents (Lévesque and Avoli, 2013). The clinical manifestations include recurrent seizures with behavioral changes (Lothman and Collins, 1981; Mikulecká et al., 1999), accompanied by pathological changes to neurons and glia including oxidative stress, generation of reactive oxygen species and reactive nitrogen species (Penkowa et al., 2001; Wang et al., 2005), hippocampal neuronal death and glial (astrocytes and microglia) activation (Figure 1. 14) (Sperk et al., 1983; Drexel et al., 2012). The main advantage of using systemic administration of KA compared to intracerebral injection is that many animals can be injected at one time and it does not require surgical procedures, which therefore eliminates post-surgical complications or damage to the brain tissue made by the cannula. However, its main disadvantage is that one cannot control the bio-availability of KA in the brain, thus, some animals require multiple systemic injections to induce SE (Hellier et al., 1998).

1.7.1.4. Behavioural manifestations

During SE-period, KA-treated animals show behavioural features that can be scored with modified Racine scale (Racine, 1972). During seizures animals show automatism with a catatonic posture such as facial movement and head bobbing (i.e. class I and II seizures) that often progresses to forelimbs clonus (class III), rearing with concomitant forelimb clonus (class IV), and forelimb clonus with rearing and falling (class V) (section 2.2.5) (Sperk et al., 1983; Hellier et al., 1998).

Systemic injection of KA in the range of 6-15 mg/kg, to induce SE in rats, produces 5-30% mortality (Sperk et al., 1983; Hellier et al., 1998; Sharma et al., 2008). However, multiple

doses of 5 mg/kg/h of KA until the occurrence of SE can reduce the mortality rate significantly. Moreover, initial 5 mg/kg dose of KA following by a half dose (2.5 mg/kg) administered depending on the severity of behavioural symptoms induced by the initial injection further help to reduce the mortality rate (Hellier et al., 1998).

1.7.1.5. EEG features

The epileptiform EEG changes occur during first 30 min following a systemic administration of KA (Ben-Ari et al., 1981; Lothman and Collins, 1981; Lothman et al., 1981). Immediately after KA injection, the incidence of "wet-dog shakes" increases, which later gets masked by convulsions (Ben-Ari et al., 1981). Ictal discharges then appear in the CA3 region and in the amygdala, followed by propagation to the thalamus, the CA1 region, and the frontal cortex. However, these ictal discharges are observed only on the EEG signals and are not associated with any clinical signs, besides "wet-dog shakes" (Lothman and Collins, 1981). The hippocampal EEG activity is characterised by an increase in the gamma frequency range (25-30 Hz) (Medvedev et al., 2000). During seizures, hippocampal gamma oscillations occur, which explains that the hippocampus is the seizure onset zone in KA-induced seizures (Medvedev et al., 2000; Lévesque et al., 2009). Overall, findings suggest that as with the intra-cerebral administration of KA, the hippocampus plays a central role in the onset of seizures in systemic KA injection model (Ben-Ari et al., 1981; Ben-Ari and Cossart, 2000). Thus, the KA-induced seizure in rats is an ideal animal model to perform studies which aim to understand the neuronal mechanisms of central autonomic cardiovascular dysfunction during seizures.

1.7.1.6. Neuropathological changes

Kainic acid-induced seizures produce a wide range of pathological changes ranging from acute neuroexcitation to chronic necrotic cell death that depends on the seizure duration and severity (Figure 1. 14) (Sperk et al., 1983). During the first 3 h after SE, swelling of dendrites and axonal terminals occur, and is accompanied by signs of oedema across the brain. Twenty-four hour after SE, neuropathological findings show incomplete tissue necrosis with loss of nerve cells, oligodendrocytes and astroglial scar in pyriform cortex, amygdala, hippocampus and gyrus and bulbus olfactorius (Sperk et al., 1983). At low doses of intra-cerebral injection of KA (0.1 µg), more specific loss of hippocampal CA3 pyramidal cells occur, which extend into CA1, CA2 and CA4 pyramidal cells at higher doses (0.8 µg) (Nadler et al., 1978). This hierarchy explains the vulnerability of hippocampal neurons to KA-induced SE. An extra hippocampal damage is seen only in

animals presenting robust convulsions during SE, and is not caused by the KA toxicity, but depends on the propagation of epileptiform activity (Nadler et al., 1978).

More importantly, astrocytes and microglia activate 24 h after SE, which become more prominent 8 days after SE, and remain high even after 30 days and during chronic epilepsy (Figure 1. 14) (Drexel et al., 2012). Seizure causes microglial activation, and neuroinflammation in patients and animal models (Beach et al., 1995; Shapiro et al., 2008; Eyo et al., 2014), which persist for many years during chronic epilepsy (Beach et al., 1995; Papageorgiou et al., 2015). Microglia can play pro-inflammatory or anti-inflammatory role in epilepsy (section 1.11) (Shapiro et al., 2008; Mirrione et al., 2010; Vinet et al., 2012). Although pro-inflammatory or anti-inflammatory action of activated microglia is a topic of debate, there is strong support for their dual role (Hanisch and Kettenmann, 2007; Loane and Byrnes, 2010). Short-term microglial activation is considered as beneficial (Mirrione et al., 2010; Vinet et al., 2012), whereas chronic microglial activation is deleterious, and might produce a damaging response to injury (Qin et al., 2007; Loane et al., 2014).

1.7.1.7. Epileptogenesis

Approximately 10-30 days after SE, 60-80% of animals develop convulsive and non-convulsive seizures that can be confirmed with video-EEG recordings (Figure 1. 14) (Hellier et al., 1998; Sharma et al., 2008; Drexel et al., 2012). The rate of interictal spikes during the latent period is higher in rats that develop chronic seizures compared to rats that do not become epileptic, which suggests that in the KA model, interictal spikes are markers of pathological network activity in limbic networks (White et al., 2010).

1.8. <u>Neurotransmitters involved both in seizure and autonomic cardiovascular regulation</u>

Glutamate, GABA, and glycine are the three major neurotransmitters within the CNS that are responsible for regulating cardiorespiratory activity and reflexes (Ross et al., 1984a; Suzuki et al., 1997). Antagonism of any of these three neurotransmitter systems causes major, or even complete, disruption of central cardiorespiratory control (Ross et al., 1984a). Microinjection of the broad-spectrum iGluRs antagonist, KYNA, into either the NTS, or VLM, reduces the vagal and sympathetic baroreflex (Guyenet et al., 1987). Selective inhibition of NMDA, AMPA and kainate receptors in the CVLM has a similar effect (Miyawaki et al., 1996a; Miyawaki et al., 1996b; Miyawaki et al., 1997). On the other hand, as explained in section 1.5.2.2, the glutamate-GABA imbalance in the CNS is primarily responsible for ictogenesis (Wong, 2005). GABA analogues (e.g. valproate) act as antiepileptics; whereas drugs that block GABAergic transmission can be convulsant (e.g. bicuculline). Expression of NMDA and AMPA receptors is increased in the hilus and CA1 region in hippocampal foci removed from TLE patients (Brines et al., 1997). This suggests that enhanced sensitivity to glutamate plays an important role in the pathophysiology of epilepsy.

Other neurotransmitters and peptides, such as serotonin, catecholamines, PACAP, opioids, substance P, neuropeptide Y, somatostatin, galanin, orexin and angiotensin II play a significant role in modulating cardiorespiratory function and reflexes (Callera et al., 1997; Miyawaki et al., 2002b; Kashihara et al., 2008; Pilowsky et al., 2009; Farnham et al., 2011; Rahman et al., 2011; Shahid et al., 2011). PACAP is a pleiotropic neuropeptide with autocrine neuroprotective and paracrine anti-inflammatory properties (Shioda et al., 1998; Reglodi et al., 2000; Chen et al., 2006; Baxter et al., 2011; Seaborn et al., 2011). In cardiovascular regulation, PACAP acts as an excitatory neurotransmitter at central autonomic nuclei in the brainstem, and the spinal cord (Farnham et al., 2008; Farnham et al., 2011; Inglott et al., 2011; Farnham et al., 2012; Inglott et al., 2012). More importantly, PACAP expression increases in KA-induced seizure rats in the central autonomic cardiovascular nuclei such as PVN (Nomura et al., 2000). The potential role of PACAP and glutamate in the regulation of central autonomic cardiorespiratory activity during seizure and SUDEP is discussed in further sections.

1.9. <u>Pituitary adenylate cyclase-activating polypeptide (PACAP)</u>

Pituitary adenylate cyclase-activating polypeptide was originally isolated from an ovine hypothalamic tissue (Miyata et al., 1989) and stimulates cAMP formation in rat pituitary cells. PACAP is a 38 amino acid pleiotropic neuropeptide (Joo et al., 2004). It belongs to the glucagon-secretin-VIP superfamily of peptides. PACAP is positively coupled to act on its membrane-bound receptors and activate adenylyl cyclase to generate increased intracellular levels of cAMP (Gordon et al., 2007). Subsequently, the increased level of cAMP leads to enhanced phosphorylation and changes in intracellular proteins expression. It inhibits the MAP kinase proteins (inhibit activation of c-Jun N-terminal kinase (JNK)/ stress activated protein kinase (SAPK), while it activates extracellular signal-regulated kinase (ERK)), and stimulates interleukin (IL)-6 secretion (Shioda et al., 1998; Shoge et al., 1999). PACAP achieves all these effects through three different G-protein coupled receptors (GPCR) (PAC1, VPAC1, and VPAC2) (Joo et al., 2004). Since the discovery of PACAP, many studies have emphasised its neuroprotective and anti-inflammatory roles in *in vivo* and *in vitro* models of neurodegenerative diseases (Shioda et al., 1998; Delgado et al., 1999; Brifault et al., 2015), and are discussed in section 1.9.3.

1.9.1. <u>Types of PACAP receptors</u>

PACAP exerts its actions through three different GPCRs: PAC1, VPAC1, and VPAC2. The biological effects of PACAP and VIP are mediated through common receptors due to the high degree of sequence homology between these two peptides. PACAP binds to PAC1 receptors with high affinity and VIP has a lower affinity for it. Both PACAP and VIP bind equally to VPAC1 and VPAC2 receptors (Buscail et al., 1990). These three receptors are GPCRs with 7 transmembrane domains and are positively coupled to stimulative regulative G-protein (Gs) (Holighaus et al., 2011). PACAP receptors also exert their effects through phospholipase C and phospholipase D (Kuri et al., 2009; Roy et al., 2013).

<u>PAC1 receptor</u>

The PAC1 receptor is specific for PACAP and binds to PACAP-27 and PACAP-38 with equal affinity, whereas it has 1000-fold lower affinity for VIP (Miyata et al., 1989; Buscail et al., 1990). The predominant intracellular signalling pathway of the PAC1 receptor is via Gs-coupled to adenylate cyclase leading to an increase in protein kinase A (PKA) (Holighaus et al., 2011). PAC1 coupling to Gq activates the phospholipase C-inositol trisphosphate pathway causing release of intracellular stores of calcium and an increase in protein kinase C (PKC) and/or phospholipase D (Spengler et al., 1993; Kuri et al., 2009).

VPAC1/VPAC2 receptors

VPAC1 and VPAC2 receptors have equal affinity for PACAP-38, PACAP-27 and VIP, and act primarily to increase cAMP through Gs-coupled receptors (Alexandre et al., 1999; Dickson and Finlayson, 2009). The two VPAC receptors are able to activate the phospholipase C pathway through Gq and Gi coupling (Dickson and Finlayson, 2009).

1.9.2. Distribution of PACAP and its receptors

PACAP immunoreactivity is found in specific regions of the brainstem and spinal cord. PACAP-immunoreactive (ir) fibres innervate the PVN (Hannibal et al., 1995; Das et al., 2007), the RVLM (Farnham et al., 2008), the ventromedial hypothalamus (Maekawa et al., 2006), the arcuate nucleus (Dürr et al., 2007), and the IML (Chiba et al., 1996), which are major cardiorespiratory autonomic nuclei. PACAP is present in the brainstem, and spinal cord autonomic nuclei that are important in central cardiorespiratory regulation (Farnham et al., 2008). PAC and VPAC receptors are present at specific locations throughout the CNS, on both neurons and glia (Delgado, 2002a; Joo et al., 2004). PAC1 and VPAC1 (but not VPAC2) receptors are present on microglia (Kim et al., 2000; Delgado, 2002b, a; Pocock and Kettenmann, 2007; Nunan et al., 2014). Astrocytes express all three types of VIP/PACAP receptors, whereas only PAC1 receptors are present in the oligodendrocytes (Joo et al., 2004). PAC1 receptors have a more restricted pattern and are densely present in the cerebellar cortex, deep cerebellar nuclei, epithalamus, hypothalamus, brainstem and white matter of many brain regions. VPAC1 receptors are expressed in the cerebral cortex, hippocampal formation, deep cerebellar nuclei, thalamus, hypothalamus, and brainstem. VPAC2 receptors are concentrated in the cerebral cortex, hippocampal formation, amygdalar regions, cerebellar cortex, deep cerebellar nuclei, hypothalamus, and brainstem (Joo et al., 2004). The presence of PACAP/VIP receptors in the brainstem and spinal cord suggests that they play a role in the regulation of autonomic cardiorespiratory function.

1.9.3. PACAP in the context of cardiovascular autonomic dysfunction in seizure and SUDEP

PACAP activates adenylyl cyclase and produces both excitatory, through phosphorylation of tyrosine hydroxylase (TH) at serine 40 (Bobrovskaya et al., 2007), and anti-inflammatory effects (Shioda et al., 1998; Delgado et al., 1999; Kim et al., 2000; Kim et al., 2002), which signifies its importance in the cardiovascular autonomic function during seizures. The KA-induced seizures increase PACAP expression in PVN of the hypothalamus in rats (Nomura et al., 2000). PACAP has excitatory effect on both the

RVLM and preganglionic sympathetic neurons in rats, and produces pressor and tachycardia responses (Lai et al., 1997; Farnham et al., 2008; Kuri et al., 2009; Farnham et al., 2011; Inglott et al., 2011; Farnham et al., 2012; Inglott et al., 2012). There are a number of possibilities that could explain the way in which PACAP is exerting its protective and excitatory effects on neurons. First, PACAP may produce neuroprotective, and anti-inflammatory effects to keep the neuronal firing threshold under control, and keep them in healthy condition (Shioda et al., 1998; Dejda et al., 2011). Secondly, action of PACAP on microglial PAC1 and VPAC1 receptors may polarise microglia towards an M2 (anti-inflammatory) phenotype, and increase the endogenous production of anti-inflammatory cytokines, such as transforming growth factor-β (TGF-β), and IL-10 (Suk et al., 2004; Brifault et al., 2015). Thirdly, as reported earlier, PACAP may produce an excitatory effect on the catecholaminergic neurons (Lai et al., 1997; Farnham et al., 2008), and mediate sympathoexcitatory responses along with major effects on the ECG.

First, PACAP is anti-inflammatory and protects neurons against various *in vitro* toxic insults (Delgado et al., 1999; Kim et al., 2000). Following ischemia, PACAP treatment inhibits the activation of JNK/SAPK and increases secretion of IL-6, which further inhibits activation of JNK/SAPK (Shioda et al., 1998). The protective effect of PACAP is also seen in *in vivo* models of cerebral ischemia where its expression increases after ischemic injury in rats and mice (Skoglösa et al., 1999b; Chen et al., 2006). PACAP is upregulated following sciatic nerve injury, suggesting a role for PACAP in the post-injury recovery of the nervous system (Zhang et al., 1996). PACAP also influences the development of the nervous system; specifically, it has neurotrophic action on primary culture of a mesencephalic dopaminergic neurons (Takei et al., 1998; Skoglösa et al., 1999a). The survival of the immature sympathetic neuron depends on nerve growth factor (NGF), and in its absence neurons undergo a decrease in intracellular cAMP levels, and programmed cell death (Chang and Korolev, 1997; Przywara et al., 1998). However, treatment with PACAP can increase the cAMP levels, and delay neuronal death caused by NGF deprivation (Przywara et al., 1998). The study suggest that PACAP can rescue chick embryonic sympathetic neurons from apoptosis when the supply of NGF is compromised (Przywara et al., 1998). These findings indicate that under normal conditions, PACAP might not play a major role as a neurotrophic molecule for sympathetic neuroblasts because NGF is sufficient, and is a dominant neurotrophic factor. However, if neurons become vulnerable, as a result of unavailable NGF, PACAP released from presynaptic sites could prevent neurons from apoptosis. Also caspases 3, 6 and 7 cleave protein substrates

within the cell to trigger the final phase of apoptosis. PACAP inhibits caspase 3 in NGF-deprived chicken sympathetic embryonic neuroblasts, which could be mediated through PKA and PKC, but not by ERK-type mitogen-activated protein kinase (MAPK) transduction pathways (Vaudry et al., 1998).

PACAP has a protective effect against glutamate-induced toxicity *in vitro* (Shoge et al., 1999). In cultured retinal neurons, a 10 min exposure to 1 mM glutamate followed by further 24 h incubation in 0.25% trypsin diluted in dissecting solution significantly decreases cell viability. Application of PACAP simultaneously with glutamate attenuates the glutamate-induced neurotoxicity and prevents the decrease in viability, via cAMP/PKA/MAPK pathways (Shoge et al., 1999). Glutamate transporters play an important role in the rapid clearance of synaptically released excess glutamate. Reverse transcription polymerase chain reaction analysis of PACAP mRNA shows that PACAP is synthesised exclusively by neurons, and not by glia. The exposure of cortical astrocytes to PACAP increases the maximal velocity of glutamate uptake by promoting the expression of glutamate transporter-1 (GLT-1) and glutamate aspartate transporter (GLAST) (Figiel and Engele, 2000), and could be a mechanism of action of PACAP against glutamate-induced neurotoxicity. PACAP-induced increased expression of glial glutamate transporter by astrocytes is likely mediated through activation of cAMP-dependant pathways (Swanson et al., 1997). PACAP also induces expression of glutamine synthetase, which metabolises glutamate into glutamine. Results suggest that PACAP regulates glutamate transport and metabolism that could produce neuroprotective effect on cardiorespiratory neurons during seizures, as the increased synaptic glutamate mediates the development of seizure and neuronal excitation (section 1.5.2.2). This hypothesis is evaluated in Chapter 4.

Secondly, PACAP can produce a neuroprotective effect through its action on microglial PAC1 and VPAC1 receptors (Kim et al., 2000), causing the release of substances such as IL-10, and TGF-β, compounds that protect neurons from overexcitation. PACAP suppresses NMDA-induced cell loss in the ganglion cell layer of the retina and significantly elevates the mRNA levels of anti-inflammatory cytokines IL-10, and TGF-β by increasing the number of microglia and macrophages (Wada et al., 2013). PACAP inhibits activated microglia-induced production of tumor necrosis factor-α (TNF-α) by a cAMP-dependent pathway in *in vivo*, and *in vitro* (Kim et al., 2000). The action of PACAP on microglial cell surface receptors increases IL-10 protein expression, causing downregulation of costimulatory molecules cluster of differentiation (CD)40, and B7

mRNA that are important in the further activation of microglia, and thereby acts as a potent anti-inflammatory agent (Delgado et al., 1999; Kim et al., 2002). PACAP increases IL-10 expression, both in *in vivo* and *in vitro*, through PAC1 and VPAC1 receptors present on microglia (Delgado et al., 1999). PACAP inhibits the activation of the MAPK family such as JNK (Shioda et al., 1998; Delgado, 2002b), stimulates the secretion of IL-6 in CSF (Gottschall et al., 1994; Shioda et al., 1998), and inhibits NF-κB (nuclear factor kappa B) in activated microglia (Delgado, 2002a) to produce an anti-inflammatory effect. Under hypoxic condition, PACAP attenuates transition of microglia into an inflammatory state and protects co-cultured PC12 cells from microglial neurotoxicity via reduction of hypoxia-induced activation of p38 MAPK (Suk et al., 2004). Activated microglia can polarise into two different phenotypes depending on the type of the stimulus, and participate in either neuroprotection or neurotoxicity (section 1.11.2). PACAP administration after permanent cerebral ischemia by electrocauterisation of middle cerebral artery improves function and recovery in mice (Brifault et al., 2015). Findings suggest that PACAP treatment can redirect microglia towards a neuroprotective M2 phenotype in the late phase of brain ischemia, suggesting its neuroprotective effect on activated microglia (Brifault et al., 2015). Altogether, the actions of PACAP and its increased expression in post-ictal period may produce a neuroprotective effect on cardiorespiratory neurons in the brainstem and spinal cord during neurotoxic insults such as epilepsy.

A third possibility also occurs when increased PACAP expression during seizures excites catecholaminergic neurons, and mediate sympathoexcitatory responses along with ECG abnormalities. PACAP infusion into the intrathecal (IT) space (Lai et al., 1997; Farnham et al., 2011), or microinjection into RVLM (Farnham et al., 2012) has long-lasting sympathoexcitatory effects along with variable pressor responses in rats. Systemic administration of low doses of PACAP in rats decreases the threshold for the development of febrile convulsions. Conversely, administration of higher doses of PACAP increased the threshold (Chepurnova et al., 2002). The observed effect is most likely to be an indirect effect of PACAP-induced arginine vasopressin expression, where arginine vasopressin is known to mediate the hypothermia-induced seizures (Kasting et al., 1981). In these circumstances, PACAP seems to mediate the induction of seizures and acts as an excitatory neurotransmitter, which may cause further sympathoexcitatory effects.

The investigation of the role of PACAP during seizure, and its effect on cardiovascular autonomic function is a major aim of this thesis.

1.10. <u>Glutamate</u>

Glutamate is the principal excitatory neurotransmitter of the CNS and is found in high concentration (10 mM) throughout the brain (Meldrum, 2000). It is synthesised in presynaptic terminals, predominantly from glutamine by phosphate-activated glutaminase, which is also expressed in the brainstem cardiovascular and respiratory neurons (Minson et al., 1991; Pilowsky et al., 1997). Glutamate is accumulated in synaptic vesicles, and released by vesicular transporters controlled by Mg^{2+}-ATP and the proton gradient that requires Cl^- (Danbolt, 2001). Glutamate, released into the synaptic cleft, exerts its action through distinct classes of receptors, the iGluRs and the G-protein coupled mGluRs. Glutamate-induced activation of the ionotropic NMDA and AMPA receptors leads to an influx of Ca^{2+} and Na^+ (Mayer and Miller, 1990). During prolonged excitation, glutamate causes neurotoxic insults through disruption of ionic homeostasis, and increase in oxidative stress (Michaels and Rothman, 1990; Hartley et al., 1993). Glutamate also binds to presynaptic and postsynaptic mGluRs and to neuronal and glial glutamate transporters (Biber et al., 1999; Alexander and Godwin, 2006b). Glutamate transporters play an important role in the rapid clearance of the synaptically released glutamate (Swanson et al., 1997). High affinity sodium-dependant glutamate transporters include GLAST/ excitatory amino acid transporter (EAAT)-1, GLT-1/EAAT2, EAAC1 (excitatory amino acid carrier-1)/EAAT3, EAAT4, and EAAT5. The GLAST and GLT-1 are expressed predominantly by glia (Swanson et al., 1997). These two transporters are known to perform over 90% of glutamate uptake in the brain, and unlike neurons, are capable of metabolising incorporated glutamate into glutamine by glutamine synthetase, which diffuses through the extracellular space back to neurons (Petr et al., 2015). EAAT3 and EAAT4 are expressed by neurons, whereas EAAT5 are primarily localised to photoreceptors and bipolar neurons in the retina (Lehre and Danbolt, 1998). The extracellular concentration of glutamate is normally very low. (Danbolt, 2001). Glutamate is responsible for fast excitatory PSPs at most synapses in the brain. It is also responsible for induction of paroxysmal depolarisation shift characteristically recorded intracellularly in association with epileptic discharges (Sun et al., 2001). Thus, the abnormalities in the transport of glutamate or in glutamate receptor expression or function or in the synaptic release of glutamate could contribute to neuronal excitation and epileptic phenomena.

1.10.1. <u>Types of glutamate receptors and transporters</u>

There are three families of iGluRs with intrinsic cation-permeable channels (NMDA, AMPA and kainate) and eight metabotropic GPCR (mGluR). The mGluR are categorised

into three groups that modify neuronal and glial excitability through G protein subunits, and second messengers such as diacylglycerol and cAMP.

Ionotropic glutamate receptors (iGluRs): AMPA, NMDA and kainate

The iGluRs are ligand-gated ion channels that mediate the majority of excitatory neurotransmission in the brain. The iGluRs comprise the AMPA, NMDA and kainate families of receptors. The NMDA receptors are more permeable to Ca^{2+}, whereas non-NMDA receptors (AMPA and kainate) are permeable to Na^+ and Ca^{2+} (Macdermott et al., 1986). The different genes encode the iGluRs; AMPA family is composed of GRIA 1-4, NMDA family include GRIN1, GRIN2(A-D) and GRIN3A-B and kainate include GRIK 1-5 (Boulter et al., 1990). The heteromeric structures of iGluRs are composed of four to five subunits, where their biophysical properties (sensitivity to Na^+, K^+ and Ca^{2+}) and pharmacological sensitivities are determined by their subunit composition, the splice variants and mRNA editing (Pellegrini-Giampietro et al., 1997). For example, alterations in the expression of GluR2 mRNA subunit in AMPA receptor, important for Ca^{2+} ion flux, serve as a molecular switch leading to the formation Ca^{2+} permeable AMPA receptors, and play a role in epilepsy and acute neurodegenerative processes (Pellegrini-Giampietro et al., 1997; Vandenberghe et al., 2000).

NMDA receptors are highly permeable to Ca^{2+} ions (Macdermott et al., 1986) and are primarily present on neurons and also on microglia (Gottlieb and Matute, 1997). However, glial and neuronal NMDA receptors are functionally and structurally different.

AMPA receptors are involved in fast glutamatergic neurotransmission that corresponds to Ca^{2+} influx. However, native AMPA receptor channel permeability to Ca^{2+} is determined by GluR2 subunit. The Ca^{2+} permeability of the GluR2 subunit is controlled by post-transcriptional editing of the GluR2 mRNA, which changes a single amino acid glutamine (Q) to arginine (R) and is called as Q/R editing (Vandenberghe et al., 2000). The edited subunit, GluR2 (Q), is permeable to Ca^{2+}, but GluR2 is not. Generally, all the GluR2 protein expressed in the CNS are in the GluR2(R) form that give rise to Ca^{2+} impermeable AMPA receptors.

The kainate receptors have a close structural homology with AMPA receptors, but they serve quite different functions. Although the kainate receptors are distributed throughout the CNS, they are more localised in hippocampus and striatum and suggested to play an important role in the generation of seizure. Findings have shown the role of postsynaptic kainate receptors in the generation of chronic epileptic seizures (Epsztein et al., 2005;

Artinian et al., 2011). However, whether kainate receptors play any role in the pathophysiology of TLE is not known (Vincent and Mulle, 2009).

Metabotropic glutamate receptors (mGluRs)

Metabotropic glutamate receptors are members of GPCR that are activated by extracellular ligand and convert into intracellular signal via interaction with G protein. These receptors contain an extracellular N-terminal domain, seven transmembrane-spanning domains and an intracellular C-terminus (Conn and Pin, 1997; Niswender and Conn, 2010). mGluR are subclassified into three groups according to their sequence homology, G-protein coupling, and ligand selectivity. Group I includes mGluR 1 and 5, group II includes mGluR 2 and 3, and group III includes mGluR 4, 6, 7 and 8 (Niswender and Conn, 2010). mGluR are broadly distributed throughout the CNS and are specifically localised at synaptic and extrasynaptic sites on both neurons and glia (Biber et al., 1999; Niswender and Conn, 2010). Activation of mGluRs leads to a wide variety of immediate and delayed effects on neuronal excitability and synaptic transmission by modulation of ion channels and other regulatory and signalling proteins. Group I mGluR are often localised postsynaptically and their activation leads to cell depolarisation and an increase in neuronal excitability (Zhao et al., 2015). The neuronal excitability results from the modulation of a number of ion channels, and NMDA and AMPA responses, and can range from robust excitation to subtle changes in the pattern of frequency of cell firing. Glutamate release can be enhanced by mGlu1 activation (Anwyl, 1999). In contrast, group II and group III mGluRs are often localised on presynaptic terminals or preterminal axon where they inhibit neurotransmitter release (Niswender and Conn, 2010). They inhibit the excitatory (glutamatergic), inhibitory (GABAergic), and neuromodulatory (i.e. monoamine, ACh and peptides) synapses. Thus, the selective agonists of Group I mGluR are convulsant and antagonists are anticonvulsant in rodent models (Tizzano et al., 1995). Conversely, Group II and III agonists produce anticonvulsant effects (Ghauri et al., 1996).

Glutamate transporters

Sodium-dependent glutamate transporters in the plasma membranes of neurons and glia remove glutamate from the extracellular fluid and modify the time course of synaptic excitatory potentials. These transporters are responsible for the long-term maintenance of low and non-toxic concentration of glutamate in extracellular space. As mentioned above, the GLAST and GLT-1 (homologous with EAAT1 and EAAT2 in humans) are expressed predominantly by glia (Swanson et al., 1997) and perform the majority of glutamate uptake

in the brain (Petr et al., 2015). These transporters co-transport Na$^+$ and H$^+$ with glutamate and counter transport K$^+$. The excess Na$^+$ ions generate a net positive inward current that drives the transport (Levy et al., 1998; Danbolt, 2001). Glutamate transporters located in the plasma membrane of neurons and glia are different from vesicular glutamate transporters located on synaptic vesicles within presynaptic terminals. In contrast to sodium-dependent glutamate transporters, the vesicular transporters selectively concentrate glutamate into synaptic vesicle in Na$^+$ independent and ATP-dependent manner that requires Cl$^-$ (Bai et al., 2001). Glutamate binding to the transporter is very rapid but transport is slower (Otis and Jahr, 1998), therefore, it is binding to the transporter that initially removes glutamate from the synaptic cleft. The glial glutamate transporters are differentially expressed according to the brain region, with GLT-1 (EAAT2) predominating (4:1) over GLAST in the hippocampus and GLAST over GLT-1 (6:1) in the molecular layer of the cerebellum (Lehre and Danbolt, 1998). The extent to which astrocytic processes surround each synaptic cleft is responsible for the differences in synaptic cross talks in some part of the brain compared to the other. The functional activity of transporters is influenced by their expression, their location and their phosphorylation (Lortet et al., 1999).

1.10.2. Glutamate as major neurotransmitter in cardiovascular regulation

There is abundant evidence to demonstrate that sympathetic premotor RVLM neurons use glutamate as the primary excitatory neurotransmitter, as explained in detail in previous sections 1.2.4 and 1.2.5. Collectively, all evidence suggest that glutamatergic excitatory inputs to RVLM presympathetic neurons is essential for regulation of cardiovascular system and is originated from a variety of sources within the brainstem and forebrain.

1.10.3. Glutamate: Role in neurotoxicity, and seizure-induced autonomic dysfunction and SUDEP

Glutamate produces acute neurotoxicity and is involved in the development of chronic neurological and psychiatric disorders, such as epilepsy, motor neuron disease, Huntington's, Alzheimer's, Parkinson's, stroke and traumatic brain injury, psychiatric disturbances and pain (Coyle and Puttfarcken, 1993; Wagster et al., 1994; Bal-Price and Brown, 2001; Mandal et al., 2011). Glutamate acting on NMDA, AMPA, kainate or group I metabotropic receptors induces severe stress leading to necrotic cell death, whereas if it is less severe, apoptosis may be the consequence (Sun et al., 2016). The relative contribution of these different classes of receptors varies according to the neurons involved and

multiple other factors. For example, the acute neurodegeneration after transient global or focal cerebral ischemia is likely to be dependent on AMPA and not on NMDA receptors (Nellgard and Wieloch, 1992; Sheardown et al., 1993). On the contrary, selective neuronal death subsequent to SE appears to be highly dependent on NMDA receptor activation (Rice and Delorenzo, 1998; Deshpande et al., 2008). Neuronal susceptibility to excitotoxic cell death is under genetic control, such as single-gene defect may enhance vulnerability, as in the case of superoxide dismutase (Boillée et al., 2006). The genetic background can be protective, such as C57BL/6 and BALB/c mice are relatively insensitive to the excitotoxic effect of KA in the hippocampus (Schauwecker and Steward, 1997). The primary mechanism involved in neuronal cell death is ionic disequilibrium related to the excessive entry of Na^+ and Ca^{2+} through ligand-gated and voltage-sensitive channels. There is a complex interaction between the ionic changes, altered energy metabolism with mitochondrial toxicity and oxidative or free radical mediated damage (Coyle and Puttfarcken, 1993).

Glutamate acting on AMPA, NMDA and probably mGluR1 receptors is thought to play an important role in cell death in neurodegenerative diseases including epilepsy (Nellgard and Wieloch, 1992; Sacaan and Schoepp, 1992; Brines et al., 1997; Arias et al., 1999; Takeuchi et al., 2008). The predominant effect of group I mGluR receptor activation is excitatory. Extracellular glutamate exposure to mouse hippocampal slices facilitates group I mGluR activation and epileptogenesis (Zhao et al., 2015). However, activation of group II mGluR reduced behavioural and electrographic seizures in pilocarpine-induced seizure in mice, which suggest that group I receptor antagonists can produce a neuroprotective effect in models of neurodegenerative diseases (Caulder et al., 2014).

Glutamatergic pathways are involved in acute and chronic neurodegenerative diseases including epilepsy. Seizure elevates glutamate levels in the extracellular fluid of the rat hippocampus (Rainesalo et al., 2004; Kanamori and Ross, 2011) and produces down-regulation and functional failure of glutamate transporters (Tanaka et al., 1997; Ueda et al., 2001; Petr et al., 2015). Induction of seizures in rat with mild or no behavioural manifestations causes 2- to 6-fold increase in extracellular glutamate levels, which also suggest that the rate of glutamate release is faster than its uptake during seizures (Kanamori and Ross, 2011). In addition, patients with acute and chronic epilepsy showed increased levels of glutamate both in CSF and plasma (Rainesalo et al., 2004). The homozygous mice lacking GLT-1 are highly prone to spontaneous seizures and acute cortical injury, which is attributed to elevated levels of glutamate in the brain (Tanaka et

al., 1997). This is also supported by the findings in which conditional deletion of GLT-1 from astrocytes in mouse resulted in excess mortality, lower body weight and seizures (Petr et al., 2015). Activation of both iGluRs and mGluRs is pro-convulsant (Faingold et al., 1992; Sacaan and Schoepp, 1992; Brines et al., 1997; Deshpande et al., 2008; Zhao et al., 2015). In genetically-epilepsy prone rat, development of audiogenic seizures was blocked by NMDA and non-NMDA receptor antagonist microinjection in the inferior colliculus, where NMDA receptor antagonist was 200 times more effective that non-NMDA (Faingold et al., 1992). KA-induced seizures in rats modify and increase the postsynaptic density of NMDA receptor protein (Wyneken et al., 2001). In hippocampus foci from TLE patients, hilus and CA1 region showed increased NMDA and AMPA receptor density (Brines et al., 1997). Subsequently, the activation of group I mGluR mediates the induction of seizures, which can be blocked with specific antagonist treatment (Sacaan and Schoepp, 1992; Zhao et al., 2015). On the contrary, activation of group II mGluR reduces behavioural electrographic manifestations of pilocarpine-induced SE in mice, suggestive of the protective role of group II mGluR during seizures (Alexander and Godwin, 2006a; Caulder et al., 2014).

The RVLM contains sympathetic premotor neurons responsible for maintaining tonic excitation of sympathetic preganglionic neurons involved in cardiovascular regulation as detailed in section 1.2.4. The activity of presympathetic RVLM neurons is directly correlated with SNA, and stimulation of neuronal cell bodies in the RVLM with glutamate produces dose-dependent increases in AP, that is sympathetically mediated (Madden and Sved, 2003a). It is likely that increased glutamate levels during seizure induces excito-neurotoxicity of presympathetic RVLM neurons or preganglionic IML neurons, and may contribute to cardiovascular autonomic dysfunction in epilepsy as detailed in section 1.6.1. Extracellular glutamate activates either AMPA, NMDA or group I metabotropic receptors, resulting in oxidative stress and cellular excitability causing sympathoexcitation during epilepsy, and on long-term, this might lead to neurodegeneration, and inflammation (Coyle and Puttfarcken, 1993; Mueller et al., 2014). Moreover, increased oxidative stress, and inflammation in RVLM during seizure (Tsai et al., 2012) could be mediated through increased glutamate levels or functional failure of glutamate transporters on astrocytes (Ueda et al., 2001). Overall, seizure-induced increase in glutamate might cause sympathoexcitation and other cardiovascular autonomic changes, which could be reversed with the glutamate receptor antagonist microinjection into the RVLM, and is one of the major aims of this study.

1.11. <u>Microglia</u>

1.11.1. <u>Role of microglia in the CNS</u>

Microglia are the principal resident immune cells of the CNS, contributing ~10% of total brain population (Hanisch and Kettenmann, 2007; Mosser and Edwards, 2008; Kettenmann et al., 2011; Benarroch, 2013; Biber et al., 2014). Since the first morphological characterisation of microglia, enormous research has been conducted; however, their precise role in the healthy and diseased CNS remains unclear. Initially, microglia were classified into two types, "resting" microglia, which are "inactive", and present in uninjured CNS; and "activated" microglia that are present in response to injury. However, recent work suggests that this classical active/inactive classification is misleading. Using *in vivo* two photon imaging of fluorescently-labelled neurons and microglia in mice, it is shown that resting microglia continuously survey their microenvironment for maintaining homeostatic conditions by making brief and direct contact with synapses. The frequency of microglial contact is directly proportional to neuronal activity, and also reflects the functional status of the synapses (Nimmerjahn et al., 2005; Wake et al., 2009; Kapoor et al., 2016a; Kapoor et al., 2016b; Kapoor et al., 2016c). On the other hand, resting microglia undergo drastic changes, and transform into an activated state. Activated microglia are ramified, with an amoeboid morphology, and acquire their phenotype depending on the type of the stimulus; participating in either neuroprotection or neurotoxicity (Ayoub and Salm, 2003; Li et al., 2007; Lai and Todd, 2008; Beck et al., 2010; Pisanu et al., 2014). The important role of highly dynamic microglial cells is to maintain synaptic and neuronal homeostasis during both normal and diseased CNS conditions.

Microglia play a key role in healthy and diseased brain. During early development, microglia clear apoptotic neurons, promote survival of cortical neurons, and prune synapses (Awasaki and Ito, 2004), whereas in the mature CNS they perform highly dynamic functions. The interaction between neuron and microglia is crucial for network formation in developing brain (Katz and Shatz, 1996; Paolicelli et al., 2011; Ueno et al., 2013). However, their role in developed brain has remained elusive, as they are capable of inducing both neuroprotective (Eleuteri et al., 2008; Neumann et al., 2008; Mirrione et al., 2010; Vinet et al., 2012; Eyo et al., 2014) and neurodegenerative responses (Gao et al., 2011; Loane et al., 2014). Exquisitely motile processes and stationary somata of microglial cells make contacts with neurons, and synapses to constantly survey the microenvironment (Wake et al., 2009). Microglia express almost all types of receptors such as, PACAP

receptors (Delgado, 2002b, a; Nunan et al., 2014), mGluRs (Biber et al., 1999; Taylor et al., 2002; Taylor et al., 2003), iGluRs (Noda et al., 2000; Hagino et al., 2004), P2Y receptors (Eyo et al., 2014; Du et al., 2015), EAAT1 (Chrétien et al., 2004), Ccr2 (El Khoury et al., 2007), fractalkine receptors (Cardona et al., 2006) and many more others (Pocock and Kettenmann, 2007). Microglial processes are closely associated with dendritic spines and their activity can modulate the neuronal synapses through different chemokines. These chemokines are expressed by neurons whose receptors are present on microglia such as CX3CL1 (fractalkine receptor) (Paolicelli et al., 2011), caspase 3 and 8 (Burguillos et al., 2011), and ATP (Davalos et al., 2005). With regard to this thesis, two most significant types of receptors/transporters expressed by microglia are PACAP receptors and GLT-1 transporter. PACAP produces a neuroprotective effect (as explained previously in section 1.9.3) that is partly mediated through its action on microglial PAC1 and VPAC1 receptors. PACAP acts on microglia and inhibit CD40 expression (Kim et al., 2002), TNF-α production (Kim et al., 2000), MAPK and JNK activity (Delgado, 2002b) or nuclear factor-κB (Delgado, 2002a). However, recently it has shown that PACAP can also promote microglial neurotoxic function in amyotrophic lateral sclerosis (Ringer et al., 2013).

The substantial amount of experimental evidence suggests that activated microglia express a high amount of GLT-1 (Swanson et al., 1997; Persson et al., 2006). This provides a neuronal defence mechanism from toxic insults such as facial nerve axotomy (López-Redondo et al., 2000) and herpes simplex virus infection (Persson et al., 2007). Findings suggest that activated microglia can regulate the neurotoxicity through increased uptake of excess synaptic glutamate that can be converted back into glutathione and prevent neuronal overexcitation (López-Redondo et al., 2000; Persson et al., 2007).

1.11.2. Neurotoxic M1 and neuroprotective M2 phenotypes

In healthy brain, microglia are in the resting, or quiescent state with ramified morphology (Kettenmann et al., 2011). This morphology with thin and long processes, allows them to quickly assess and respond to CNS injury or pathogens. As a consequence of excitotoxic insult or inflammation, such as brain injury, infection or diseases, microglia become activate and polarise into either "neurodegenerative M1" phenotype (produces pro-inflammatory cytokines) or "neuroprotective M2" phenotype (produces anti-inflammatory cytokines) (Kettenmann et al., 2011; Benarroch, 2013). Microglia acquire either M1 or M2 phenotype, depending on the type of injury, severity, neuronal microenvironment and other multiple factors, and produce "beneficial" or "deleterious"

effects on neurons (Li et al., 2007; Lai and Todd, 2008; Pisanu et al., 2014). Activated microglia retract their processes and change into round amoeboid morphology, which become proliferative and migratory (Hellwig et al., 2013). Microglia perform a neurotoxic function once they acquire the amoeboid shape through increased pro-inflammatory cytokines (Bal-Price and Brown, 2001; Cunningham et al., 2005; El Khoury et al., 2007). However, studies performed with tetracycline derivatives, minocycline and doxycycline, which are microglial activation antagonists through inhibition of MAPK pathway (Tikka et al., 2001), have shown their wide range of functions (from neuroprotective to neurodestructive) under different experimental conditions, such as ischemia (Yrjänheikki et al., 1998), excitotoxic stimulus (He et al., 2001; Tikka et al., 2001; Filipovic and Zecevic, 2008), inflammation-induced hyperalgesia (Hua et al., 2005; LeBlanc et al., 2011), Alzheimer's disease (Seabrook et al., 2006) and amyotrophic lateral sclerosis (Gordon et al., 2007). Tetracycline derivatives do not alter the neuronal function and thus can be exquisitely used to modify the microglial activation (Filipovic and Zecevic, 2008).

Activated microglia can perform a neurotoxic function during conditions such as inflammation, where they produce NADPH oxidase, and dopaminergic neurodegeneration during Parkinson's disease (Gao et al., 2011) or neurodegeneration after traumatic brain injury (Loane et al., 2014). On the contrary, microglia can protect neurons through local tissue repair by phagocytosing injured neurons and neuronal debris, such as amyloid-β in Alzheimer's disease (El Khoury et al., 2007). Microglia facilitate this through initial mobilisation of cells near the site of injury and recruitment of distant microglia into the damaged area, which release pro-inflammatory mediators. At appropriately minimal and transient microglial activation, this process is ultimately neuroprotective (Vilhardt, 2005). However, neuronal hyperactivity and release of toxic factors, such as nitric oxide (NO), peroxynitrite, and reactive oxygen species, may result in excessive oxidative stress and polarisation of microglia into M1 phenotype. The polarisation of microglia into M1 phenotype further causes neuroinflammation by recruitment of peripheral immune cells into the damaged brain, and might occur through a compromised blood-brain-barrier as seen in epilepsy (Van Vliet et al., 2007; Orihuela et al., 2016).

Activated microglia secrete anti-inflammatory or pro-inflammatory mediators upon activation, including IL-6, IL-10, brain-derived neurotrophic factor (BDNF), NGF, IL-β, TNF-α, prostaglandins, tissue plasminogen activator, monocyte chemo-attractant protein-1 (MCP-1), vascular endothelial growth factor (VEGF), lymph toxin, matrix metalloproteinases (MMPs), and macrophage inflammatory protein-1α (MIP-1α) (Ajmone-

Cat et al., 2003; Taylor et al., 2005; Qin et al., 2007; Benarroch, 2013). The quantity and duration of release of these factors can widely vary based on the specific injury. Some of these molecules can be toxic in high amounts, whereas others promote neuronal stability and certainly can have a direct impact on neuronal function during conditions including epilepsy (Mirrione et al., 2010; Eyo et al., 2014). Microglia produce a neuroprotective effect during glutamate-induced neuro-excitotoxicity through the removal of excess glutamate (López-Redondo et al., 2000; Persson et al., 2007). Activated microglia express the high affinity glutamate transporter GLT-1, and thus, can contribute to ~10% of glutamate recycling (Swanson et al., 1997; Van Landeghem et al., 2001; Persson et al., 2006; Persson et al., 2007), which may become more important under pathological conditions, such as seizure (Ueda et al., 2001), especially if astrocytes are overburdened or impaired. Neuroprotective properties of activated microglia were also evidenced with marked increases in infarct size and neuronal apoptosis when the proliferation of resident microglia was selectively ablated in a mouse model of cerebral ischemia (Lalancette-Hébert et al., 2007). Similar findings were observed in *in vitro* studies, where ablation of ramified microglia severely enhanced NMDA-induced neuronal cell death (Vinet et al., 2012). Microglia also produce a neuroprotective effect by building tolerance to autoimmune self-antigens that could involve priming or preconditioning of microglia cells. Preconditioning of microglia with lipopolysaccharide modulates seizures (Mirrione et al., 2010). With lipopolysaccharide preconditioning, microglia could attain the neuroprotective M2 phenotype and release neurotrophins, such as NGF and BDNF. Moreover, the exogenous application of microglia during ischemia can produce a protective effect (Suzuki et al., 2001; Kitamura et al., 2004; Kitamura et al., 2005; Imai et al., 2007). Overall, the primary role of activated microglia is to return injured tissue to homeostasis.

1.11.3. Role of microglia in cardiovascular dysfunction during seizure and SUDEP

Extensive microglial activation is well described in animal models of seizures (Drage et al., 2002; Borges et al., 2003; Shapiro et al., 2008; Drexel et al., 2012), as well as in humans (Beach et al., 1995). Patients with intractable seizures display an 11-fold increase in microglial reactivity in the hippocampus suggesting that microglia change their state in response to altered neuronal activity (Beach et al., 1995).

Brainstem and spinal cord autonomic nuclei are important in central cardiorespiratory regulation (section 1.2.4) whose function is disturbed in seizure cases (Schauwecker and Steward, 1997; Sakamoto et al., 2008; Naggar et al., 2014). Microglia are closely

associated with sympathetic premotor RVLM neurons (Figure 1. 15), and help to maintain normal homeostasis. During seizure, microglial responses are not necessarily neurotoxic. Ablation of preconditioned hippocampal microglia in mice causes significant increases in acute seizure scores compared to non-ablated and preconditioned microglia in control mice, suggestive of a protective effect of microglia (Mirrione et al., 2010). However, neurotoxic effects of microglia can occur in cases of overshooting, and uncontrolled stimulation, and are widely attributed to the release of cytokines such as caspases, TNF-α and IL-1β (Li et al., 2007; Burguillos et al., 2011). Activated microglia are major contributors to neuroinflammation, via secretion of pro-inflammatory cytokines, and chemokines, in addition to non-specific inflammatory mediators such as reactive oxygen species, and NO. However, there is little information available about the effect of seizure on microglial activation in the brainstem, and spinal cord cardiovascular autonomic nuclei, and their possible neuroprotective or neurotoxic role.

Recent findings provide increasing evidence for microglial communication with neurons (Wake et al., 2009). There is increasing evidence suggesting a direct role of microglia in the regulation of homeostasis of cardiovascular autonomic neurons. During myocardial infarction in rats, microglial activation in the PVN mediates the production of pro-inflammatory cytokine that further drives the sympathoexcitation (Du et al., 2015). Neurogenic hypertension in rats involves the activation of microglia and increase in pro-inflammatory cytokines in the PVN suggestive of the role of microglia in regulation of central cardiovascular activity (Shi et al., 2010). The substantial amount of evidence suggests central autonomic cardiorespiratory neurons are active during seizure (Kanter, 1995; Kanter et al., 1996; Silveira et al., 2000), which causes the dysfunction in a sympathovagal imbalance in favour of sympathetic activity. The disturbed cardiovascular autonomic function is considered as one of the major mechanisms of the SUDEP. However, the effect of activated microglia during seizure on presympathetic and preganglionic neurons remains elusive. Therefore, investigation of the role microglia in regulation and modulation of sympathetic and cardiovascular activity, during acute and chronic seizures, is the major aim of this thesis.
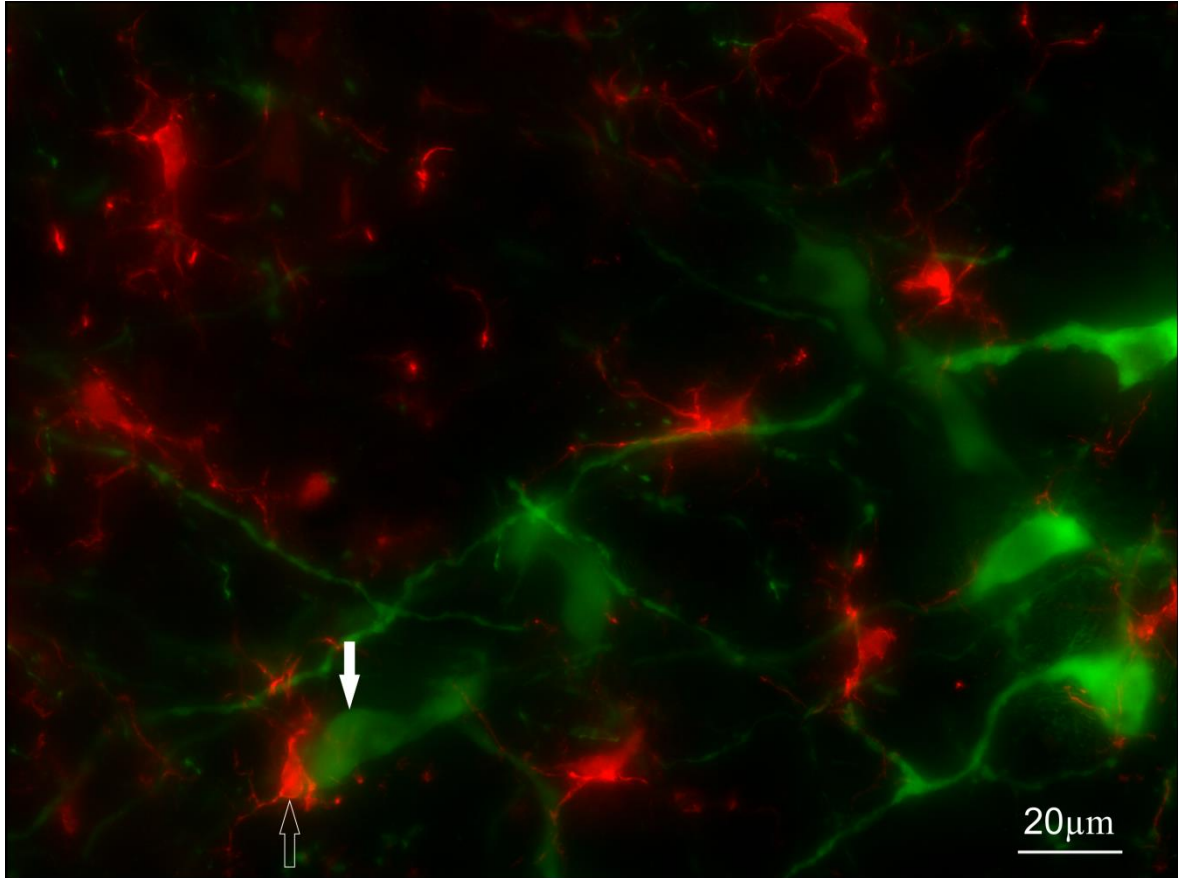
Figure 1. 15: Image illustrating close relationship between microglia and sympathetic premotor RLVM neurons.

Microglia (Iba1-ir; red) with a round cell body and normal processes with few ramifications are closely associated and distributed in the vicinity of premotor TH-ir RVLM neurons (green). Sympathetic premotor RVLM neurons (green) are shown with a closed arrow and microglia (red) with open arrow. Image was acquired from brainstem section of ~300 g SD rat using a Zeiss Axio Imager Z2 at 40X magnification. Image was acquired and processed by Ms Komal Kapoor.

71

Glutamate plays a crucial role in the development of seizures and is a major neurotransmitter in cardiorespiratory reflexes. Increased glutamate levels in seizure activates neuronal NMDA and non-NMDA receptors followed by calcium influx, and ATP release, which attracts microglial processes through activation of P2Y12 receptor (Eyo et al., 2014). Normally, astroglial glutamate transporters, GLT-1, and GLAST, perform the majority of glutamate uptake in the brain to mediate a high signal to noise ratio in synaptic signalling. However, in pathological conditions, such as epilepsy, astroglial glutamate transporter proteins are downregulated, causing excitotoxicity (Ueda et al., 2001). It is possible that microglia may be neuroprotective during seizure by increasing glutamate transporter (GLT-1) expression, and reducing synaptic glutamate concentrations, as demonstrated during facial nerve axotomy (López-Redondo et al., 2000), infectious diseases (Persson et al., 2007), and neurodegenerative diseases (Chrétien et al., 2004). Collectively, findings support the notion that during seizures, microglia might exert a neuroprotective effect on cardiovascular neurons in the brainstem that could be partly mediated by PACAP.

1.12. <u>Aims</u>

Overall, the aims of this thesis were to investigate the role of PACAP, microglia and glutamate during acute and chronic epilepsy and their effects on central autonomic cardiorespiratory function in rats. These aims are investigated in the following three chapters, which contain specific sub-aims.

<u>Chapter 3:</u>

Evaluate the dose-response of KA-induced seizures, and its effect on autonomic cardiorespiratory function in rats.

Investigate the effect of IT administration of (1) PACAP and the PACAP antagonist, PACAP(6-38); and (2) microglial antagonists, minocycline and doxycycline, on acute seizure-induced cardiovascular responses in rats.

<u>Chapter 4:</u>

Identify the significance of PACAP, microglia and glutamatergic receptors in the RVLM to regulate the catecholaminergic neuronal hyperexcitability and other cardiovascular changes in rats that occur following a low dose KA-induced acute seizures.

Characterise the changes in microglial morphology and the expression of the anti-inflammatory M2 microglial phenotype in the vicinity of RVLM catecholaminergic neurons in response to 2 and 10 mg/kg KA-induced acute seizures in rats.

<u>Chapter 5:</u>

Investigate the role of PACAP and microglia, at the IT level, in the regulation of SNA, reflex responses, and arrhythmogenic changes in rats with chronic TLE.

Characterise the changes in microglial morphology and the expression of the anti-inflammatory M2 microglial phenotype in the vicinity of RVLM catecholaminergic neurons in chronic TLE and control rats.

Chapter 2
General Methods

Table of Contents

2.1. <u>Animals</u>

The acute seizure electrophysiology experiments were performed on adult male Sprague-Dawley (SD) rats weighing between 250-350 g. Animals were resourced from Animal Resource Centre, Perth, WA, and housed in the animal house facility at the Heart Research Institute, Sydney NSW Australia.

To generate chronic seizures, continuous seizure activity (status epilepticus) was induced in 12 weeks old male Wistar rats, also resourced from Animal Resource Centre, Perth, WA. Initially, Wistar rats were housed at the Melbourne Brain Centre, The University of Melbourne, Parkville Vic. Australia, where chronic seizures were induced as detailed in section 2.2.5 and 2.2.7. After confirmation of spontaneous recurrent seizures with video-electroencephalogram (EEG)- electrocardiogram (ECG) recording (section 2.2.7), rats were transported to the animal house facility at the Heart Research Institute. The chronic seizure electrophysiology experiments were performed on 19-20 weeks old chronic epileptic rats at the Heart Research Institute.

Sprague-Dawley and Wistar rats were housed in small groups ($\leq$ 3 animal per cage), whereas post-status epilepticus (post-SE) and non-epileptic control Wistar rats that had EEG-ECG head mount were housed in individual cages. Animals were housed under the standard temperature controlled conditions (i.e. at 22 ± 2^0C, humidity: 50-55% and 12 h light/dark cycle) and fed with the standard chow pellet and water *ad libitum*.

2.1.1. <u>Ethics</u>

The animal usage and protocols were in accordance with the Australian code of practice for the care and use of animals for scientific purposes. The protocols were approved by the Animal Care and Ethics Committee of Macquarie University (2013/017), The University of Melbourne (15/072/UM) and the Sydney Local Health District (2013/082 and 2014/024) (Appendix 3).

2.2. <u>General procedures</u>

The specific details of all chemicals, reagents, materials, equipment and recording software used and mentioned in this section are listed in Appendix 2.

2.2.1. <u>Tail cuff</u>

Systolic and diastolic blood pressure (BP) was measured with non-invasive BP measurement technique in chronic epileptic and control rats at least 2-3 days prior to the

electrophysiology experiments. IITC software was used for recording of BP, which records, analyses and reports systolic, diastolic and mean BP and heart rate (HR) values, and can be imported into a spreadsheet at the end of the test.

The tail cuff system was turned "ON" at least for half an hour before the measurement of the BP. This allows measurement chamber and rat holder to adjust the set temperature. Rats were individually removed from the cage and sedated with isoflurane, and immediately placed in an animal holder pre-warmed at 32^0C. Chronic epileptic rats are aggressive compared to other normal strains and therefore they were sedated during placement into the holder. Sedation helps to avoid the stress that rat experiences during handling and positioning into the chamber, and animal recovers within 10-20 s. Animals were kept in the chamber for 5-10 min with a cuff attached to their tail and allowed to acclimatise to the chamber. The software setup was adjusted for cuff inflation pressure to reach up to 200 mmHg. The BP was recorded when rats were stable and comfortable inside the chamber and was acquired in triplicate and averaged. The BP was re-recorded whenever there was a noise or rat movement artefact. The total amount of time rats were kept in the chamber was 10-15 min. The systolic and diastolic BP was recorded from the waveform. The HR and mean BP was derived from the BP waveform channel. At the end of the test, rats were carefully removed from the holder and placed back into their cages.

2.2.2. Induction of anesthesia

Rats were anesthetised with different anesthetics depending on the purpose of the experiment. For all electrophysiology experiments (both acute and chronic seizure models), rats were anesthetised with urethane (ethyl carbamate). Rats used for acute seizure histology experiments were anesthetised with sodium pentobarbital. After injection of anesthetic, rats were placed on the heating pad until they were surgically anesthetised. Subsequently, rats were placed on a homeothermic blanket, and the body temperature was recorded with a rectal probe and maintained between 36.5 and 37.5^0C throughout the experiment. The depth of anesthesia was monitored by observing reflex responses (withdrawal or pressor >10 mmHg) to nociceptive stimuli (periodic tail/paw pinches). If reflex responses were observed, additional anesthetic was injected intraperitoneally or intravenously depending on the accessible route. Atropine sulfate (100 μg/kg, intraperitoneal (i.p.)) was administered with the first dose of anesthetic (urethane or sodium pentobarbital) to ensure the complete blockage of parasympathetic activity and prevent bronchial secretions.

In non-epileptic control and post-SE rats, EEG-ECG electrode implantation surgeries were performed under isoflurane anesthesia (section 2.2.2.3).

2.2.2.1. Urethane

Urethane is a long acting anesthetic with an average half-life of 15 h. It produces minimal effects on the cardiovascular and pulmonary system and spinal reflex responses (Maggi and Meli, 1986). Rats used for the electrophysiology experiments were anesthetised with urethane (1.3-1.5 g/kg). Urethane (10%) was dissolved in 0.9% saline (0.9% sodium chloride (NaCl)) to reduce peritoneal irritation, and injected into the peritoneal cavity using a 26 G needle. If required, additional top-ups were injected (30-40 mg, 10% urethane; i.p. or intravenous (i.v.)).

2.2.2.2. Sodium pentobarbital

Sodium pentobarbital was used as an anesthetic for the acute seizure histology experiments (50 mg/kg). Sodium pentobarbital offers fast induction, short action and stimulates the least c-Fos in the brain compared to other anesthetics (Takayama et al., 1994). Three percent sodium pentobarbital solution (50 mg/kg) was prepared by diluting stock solution in 0.9% saline and injected i.p. using a 26 G needle. The depth of anesthesia was monitored as mentioned above in section 2.2.2, and additional anesthetic was injected as and when required (1.5-2.0 mg sodium pentobarbital; i.p. or i.v.).

2.2.2.3. Isoflurane

Isoflurane was used as a general inhalational anesthetic for recovery surgeries in rats to implant ECG-EEG electrodes. Isoflurane offers a large margin of safety, ease of control of anesthesia and quick recovery. Initially, isoflurane flow was connected to an induction chamber with 5% isoflurane combined with 2.0 L/min oxygen. Rats were placed in the induction chamber and monitored until recumbent. Rats were removed from the induction chamber and positioned into a nose cone and gas flow initiated with isoflurane at 1.5-2.5% at a flow rate of 0.5-1.0 L/min oxygen. Rats were monitored for the respiration and response to the stimulus during surgical procedure and the vaporiser was adjusted accordingly. After completion of the surgical procedure (section 2.3.7), the vaporiser was turned off and rats were allowed to breathe supplied oxygen until they began to awaken.

2.2.3. Collection of blood samples and plasma catecholamine analysis

At the conclusion of electrophysiology experiments, 3-4 ml of blood was withdrawn from post-SE and control rats for the analysis of plasma adrenaline and noradrenaline. Blood

samples were withdrawn from the carotid artery over a minute and collected in heparinised tubes containing additive metabisulphite. Blood samples were immediately centrifuged at 4^0C for 10 min at 900 g, and collected plasma samples were stored at -20^0C until analysis.

The plasma catecholamine analysis was performed by the pathology laboratory at Royal Price Alfred hospital. In brief, adrenaline and noradrenaline content in plasma samples were extracted onto activated alumina in a buffered environment. The alumina bound catecholamines were washed and isolated. The extracted catecholamines were then separated by high-performance liquid chromatography on a reverse phase C18 column. Peak height response as measured by electrochemical detection is proportional to catecholamine concentration. The analyte peak heights from samples of unknown concentration were compared with the peak heights from calibrators with known concentrations. The concentrations of unknown samples were calculated with the use of an internal standard.

2.2.4. Transcardial perfusion

At the conclusion of electrophysiology and histology experiments, rats were over-anesthetised with urethane (1 ml of 10% solution) and sodium pentobarbital (0.5 ml of 3% solution), respectively. Rats were heparinised with 1 ml of heparin (5000 international units (IU)/ml) through the venous line and the chest opened to expose the heart. An 18 G needle connected to a peristaltic pump was inserted through the left ventricle into the aorta and secured with a haemostat. Ice-cold phosphate-buffered saline (PBS) (10 mM sodium phosphate buffer and 0.9% NaCl at pH 7.4) was infused using a peristaltic pump followed by incision of the right atrium. Approximately 400 ml of ice-cold PBS was infused and then animals were perfused with a 4% paraformaldehyde (PFA) fixative solution (approximately 400 ml). Brain and spinal cord were removed and post-fixed overnight in the same fixative for 18-24 h at 4^0C. Subsequently, samples were transferred into PBS with merthiolate (PBSm) (10mM sodium phosphate buffer, 0.9% NaCl, 0.1% merthiolate at pH 7.4) until further processing.

2.2.4.1. Paraformaldehyde (PFA) solution (4%)

Paraformaldehyde solution was prepared a day before the animal perfusion. Milli-Q water (300 ml) was heated to 60^0C on a heater with a magnetic stirrer. Sixteen grams of PFA powder was added to the water and stirred to dissolve. Sodium hydroxide (NaOH) (1N) was added with a dropper until the solution was clear. Sodium phosphate monobasic (1.28 g) and sodium phosphate dibasic (4.36 g) were added to the solution and stirred to

dissolve. The solution was cooled down to room temperature and pH was adjusted to 7.4 with 1N hydrochloric acid (HCl). The final volume was adjusted to 400 ml with milli-Q water and the solution was stored at 4^0C until use.

2.2.5. <u>Induction of status epilepticus (SE)</u>

The procedure described in this section and section 2.2.7, 2.3.7 were performed at the Melbourne Brain Centre, The University of Melbourne, Parkville Vic. Australia, by our collaborator Prof. Terence J. O'Brien and his research team.

The post-SE model of acquired epilepsy was generated by i.p. injection of the glutamate receptor agonist, kainic acid (KA), to induce a period of continuous seizure activity (status epilepticus) in non-epileptic rats as described previously (Hellier et al., 1998; Powell et al., 2008b; Jupp et al., 2012; Powell et al., 2014b; Vivash et al., 2014). This model reflects many features of temporal lobe epilepsy (TLE) in humans, including histopathologic changes in limbic structures, a "latent period" following the initiating insult, and the eventual occurrence of both non-convulsive and convulsive spontaneous seizures.

On the day of induction of SE, twelve weeks old male Wistar rats were collected from animal holding room and placed in individual cages. Repeated i.p. injections of KA were given with a 26 G needle (5 mg/kg, i.p., followed by 2.5 mg/kg, i.p., injections once per hour) until animals exhibited the first stage 4/5 seizure, as defined by the Racine scale (Table 2.1) (Racine, 1972). Stage 4 or 5 for ≥ 4 h was considered when rats had at least one stage 4 or 5 seizure during each consecutive one-hour period. After four hours of SE, all rats were given diazepam injection (5mg/kg i.p.) to terminate the SE. At the conclusion of behavioural monitoring, rats were monitored until their full recovery (ambulatory and eating pellets). Rats were returned to their home cages in animal house and maintained with normal animal house care and diet. Rats were monitored twice daily from next day. Normally, all post-SE rats develop spontaneous seizures, and none were observed in control rats.

Stage	Behavioural change
0	No any obvious change
1	Mouth and facial movement
2	Head bobbing
3	Forelimb clonus
4	Forelimb clonus with rearing
5	Forelimb clonus with rearing and falling

Table 2. 1: Racine scale.

2.2.6. <u>Induction of acute seizures</u>

After recording of baseline activities, acute seizures were generated by i.p. injection of KA in anesthetised, paralysed and artificially ventilated SD rats. In pilot study, nine different doses of KA enabled to generate a dose-response curve and decide the lowest dose (used in further studies), which induces seizures and produces significant effect on cardiovascular system. Responses were recorded for at least 2 h post-KA injection, during which continuous monitoring of EEG was used to identify the development of seizures. To quantify the EEG, the area under curve (AUC) between gamma frequencies (25-45 Hz) at 60 and 120 min after the KA injection relative to the area before the injection was calculated (explained in section 2.5.1) (Olsson et al., 2006; Gurbanova et al., 2008). A seizure was considered to have occurred if the AUC increased by at least 50%.

In the histology study, two doses of KA (2 and 10 mg/kg; i.p.) were used to elicit mild and severe seizures in rats to analyse their effects on the microglial morphology in the vicinity of the rostral ventrolateral medulla (RVLM) catecholaminergic neurons. Two mg/kg is the lowest dose of KA required to induce seizure and sympathoexcitation (Figure 3. 2), whereas 10 mg/kg KA induces SE with generalised tonic-clonic seizures (Nadler, 1981; Sperk et al., 1983). However, in our study rats were paralysed and had no behavioural seizures. EEG activity was recorded as explained above. To investigate the duration of seizure-induced cardiovascular responses, 2 mg/kg KA-induced seizures were recorded until cardiovascular parameters returned to baseline.

2.2.7. <u>Video-EEG-ECG recording in post-SE and control rats</u>

One week after recovery from the surgery (section 2.3.7), a continuous 24 h video-EEG-ECG recording was acquired for one week using Compumedics EEG acquisition software digitised at 2048 Hz as previously described (Powell et al., 2008b; Powell et al., 2014b). Each recording was reviewed for seizure activity, and the start and end of a seizure was manually marked on the EEG to allow quantification of the number of seizures and seizure duration. Seizure activity on the EEG was defined as the development of high-amplitude, rhythmic discharges that clearly represented a new pattern of tracing (Kharatishvili et al., 2006; Bouilleret et al., 2011). This included repetitive spikes, spike-and-wave discharges, and slow waves. The event must have lasted at least 5 s and showed an evolution in the dominant frequency, and be accompanied by behavioural change observable on the video recording consistent with a seizure. Almost all post-SE rats were documented to have spontaneous seizures, and none were observed in control rats.

2.3. <u>General surgical procedures</u>

The general surgical procedures were performed on rats as shown in Figure 2. 1, and explained in detail in following sections. Rats were anesthetised with general anesthetic urethane, sodium pentobarbital or isoflurane depending on the purpose of the experiment (section 2.2.2).

2.3.1. <u>Cannulation of artery and vein</u>

In rats, the carotid artery and right jugular vein were cannulated during electrophysiology and histology experiments for the recording of BP, and for the administration of drugs and fluids, respectively. The jugular vein was isolated and freed from the connective tissues. Polyethylene tubing (internal diameter = 0.50 mm; outer diameter = 0.90 mm) was filled with 0.9% saline and inserted through a slit in vein wall and secured in place with silk thread. The right carotid artery was located, cleared of the connective tissue and cannulated similar to the jugular vein with polyethylene tubing filled with heparinised 0.9% saline (5 IU heparin/ml) to prevent blood clotting.

2.3.2. <u>Cannulation of trachea to allow artificial ventilation</u>

Tracheostomy was performed to enable mechanical ventilation. The trachea was isolated from the neck region from the same area of cannulated carotid artery. Blood vessels and muscles were cleared off the trachea. A small slit was given between two cartilages and a 14 G catheter was slit through the trachea and secured in place with silk threads. The other end of tracheal tube was kept open until rat was vagotomised and paralysed. Subsequently, the open end of the tracheal tube was connected to the ventilator and rat was artificially ventilated with oxygen-enriched room air. To analyse the expired CO_2, another tube was connected to the expiratory line and expired air was monitored with the CO_2 analyser. Arterial blood gases were analysed with an electrolyte and blood gas analyser. A ventilator stroke volume and frequency were adjusted to keep the blood gases and pH in physiological range. Partial pressure of carbon dioxide ($PaCO_2$) was maintained at 40 ± 2 and pH between 7.35-7.45.

2.3.3. <u>Paralysing animal</u>

After rats were vagotomised and artificially ventilated, they were paralysed with pancuronium bromide (0.4 mg given as a 0.2 ml bolus i.v. injection) followed by an infusion of 10% pancuronium in 0.9% saline at a rate of 2 ml/h.

Figure 2. 1: Schematic of general surgical procedure in rat.

Rat was anesthetised and body temperature was monitored and controlled with rectal probe and homethermic heating pad. Carotid artery and jugular vein were cannulated with polyethylene tubing for recording of BP and administration of drugs and fluids, respectively. Trachea was cannulated to allow the artificial ventilation and recording of expired CO_2. Rats were fixed in a stereotaxic frame. EEG electrodes were implanted and recorded. ECG was recorded with three wire electrodes and HR was derived from it. Phrenic and splanchnic nerves were isolated and recorded with a bipolar stainless steel electrodes. Aortic depressor nerve and sciatic nerve were isolated and stimulated to generate baroreflex and somatosympathetic reflex.

CO₂
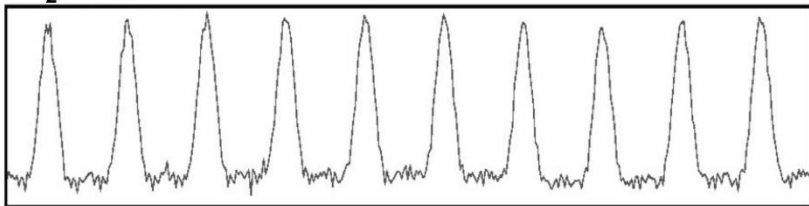
EEG activity

Phrenic nerve activity
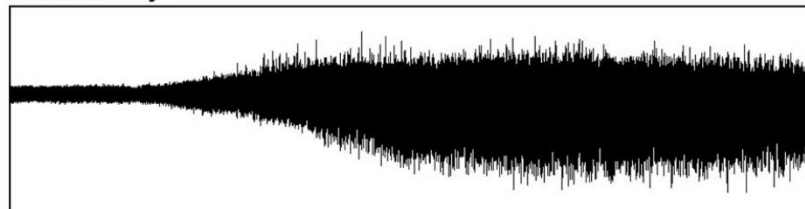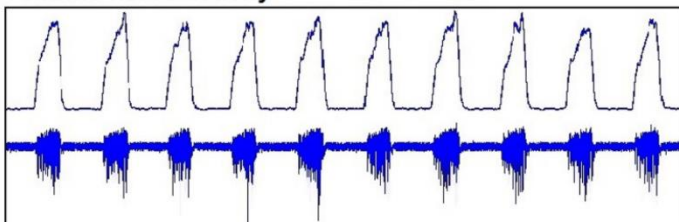
Sympathetic nerve activity

Heart rate

Blood pressure

Body temperature

ECG

To ventilator

EEG actvivity

Jugular vein cannula

Carotid artery cannula

Brain stem

ADN nerve

Phrenic Nerve

Heart

Splanchnic Nerve

Kidney

Bladder

Tail

Rectal probe

Sciatic nerve
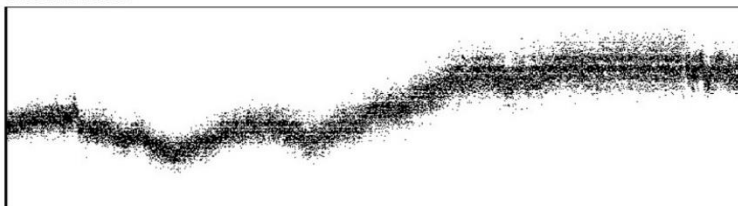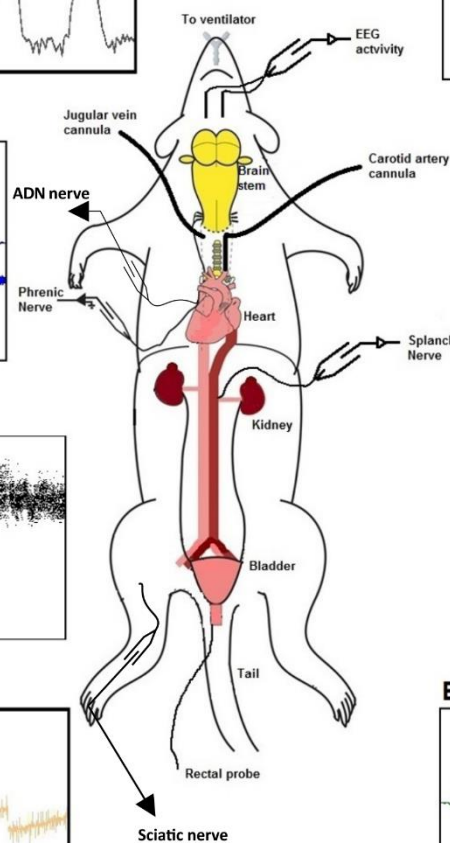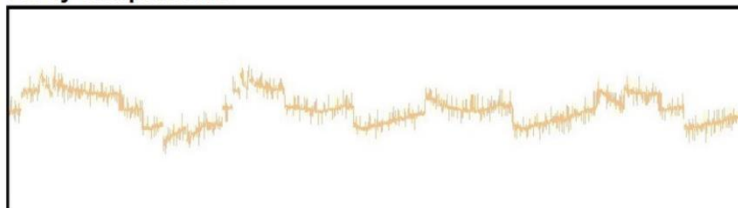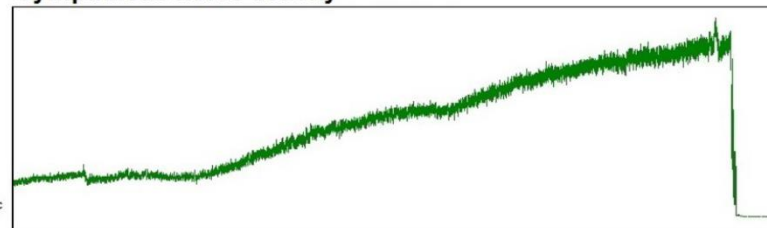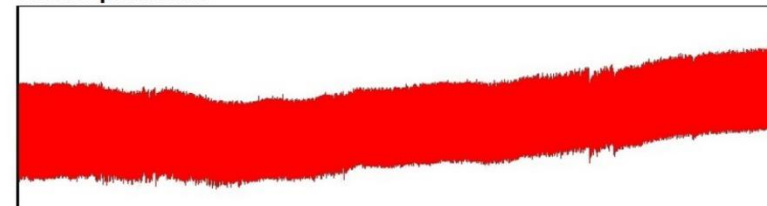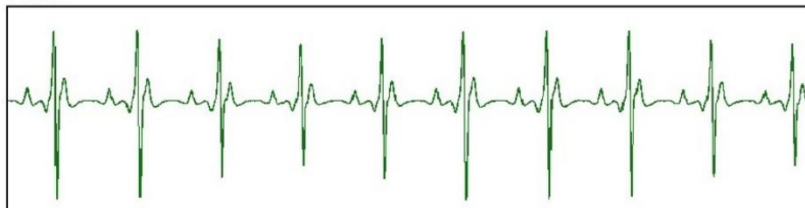
2.3.4. <u>Electrocardiogram (ECG)</u>

A three lead ECG was recorded, where two silver electrodes were inserted into the front paws and ground electrode into the exposed muscle on the back of rat. The signals were recorded and amplified. HR was derived from the peak of the R-wave and drawn as an event channel. After the completion of the general surgical procedure, rats were secured in a stereotaxic frame and body temperature was recorded and maintained between 36.5 and 37.5^0C throughout the experiment using a homeothermic blanket.

2.3.5. <u>Isolation and preparation of nerves</u>

2.3.5.1. Vagus nerve transection

The right vagus nerve was located, isolated and cut at the time of right carotid artery cannulation. Left vagus nerve was located from the dorsomedial approach from the neck at the time of isolation of phrenic nerve. The nerve was cut only after all surgical procedures were completed and rat was ready for artificial ventilation.

2.3.5.2. Greater splanchnic nerve

The left greater splanchnic sympathetic nerve at a site proximal to the coeliac ganglion was isolated after the strat of artificial ventilation through dorsomedial approach, dissected, tied with 5/0 silk thread and cut distally. The greater splanchnic nerve enables good measurement of sympathetic output to the adrenal gland. The nerve was placed on a bipolar stainless steel electrode, electrically isolated and recorded (section 2.3.6).

2.3.5.3. Phrenic nerve

The phrenic nerve was isolated with a dorsomedial approach from a neck region before the start of artificial ventilation. The nerve was cleared of connective tissue and tied with 5/0 silk thread and cut distally. The nerve was placed on a bipolar stainless steel electrode, electrically isolated and recorded as explained in section 2.3.6.

2.3.5.4. Aortic depressor nerve

For the stimulation of baroreflex response in post-SE and control rats, the aortic depressor nerve was isolated from the same cavity as phrenic and left vagus nerve before the strat of artificial ventilation. The aortic depressor nerve was isolated, confirmed with a sound similar to trains of HR, tied with suture and cut distal to the knot. The nerve was placed on a stimulating stainless steel bipolar electrode and fixed with silgel. The electrode was connected to a stimulator and operated through pulser Spike2 software (section 2.4.1).

2.3.5.5. Sciatic nerve

The sciatic nerve was isolated at the mid-thigh, cleared of tissues and tied with silk thread before the start of artificial ventilation. The nerve was cut distal to the silk tie. Subsequently, it was placed on a stimulating electrode similar to the aortic depressor nerve and stimulated using pulser Spike2 software (section 2.4.1).

2.3.6. Nerve recordings

The isolated phrenic and splanchnic nerves were placed across a bipolar stainless steel electrodes and recorded. The nerves were electrically isolated either with paraffin oil or silgel. Signals were amplified with bioamplifiers (sampling rate: 6 kHz, gain: 2,000, filtering: 30-3,000 Hz) and 50/60-Hz frequency noise was eliminated (Humbug).

2.3.7. Implantation of EEG and ECG electrodes in post-SE and control rats

Seven weeks after KA-induced SE ($n = 15$) (or saline administered controls ($n = 9$)), two ECG and four EEG electrodes were implanted in each rat under isoflurane anesthesia (section 2.2.2.3). Two small incisions were made to expose the thoracic muscle directly above the heart, and to expose the muscle overlying the xiphoid process of the sternum. The distal end of an ECG lead was sutured to each muscle using polypropylene (4-0). The leads of both ECG electrodes were then tunnelled up through the left side of the neck subcutaneously and the skin layer was sutured. A single midline incision was then made on the scalp. Two ECG leads were located and tunneled through the neck and protruded through the incision. Each rat was then placed into a stereotaxic frame, and four extradural electrodes comprised of gold-plated sockets attached to stainless steel screws (outer diameter 1 mm) were implanted into the skull: one on each side approximately 2 mm from the midline, 3 mm anterior to the Bregma, one at approximately the centre of the midline and another 6 mm posterior to the Bregma, 4 mm right of midline. These EEG coordinates (chronic seizures) used in Prof. O'Brien's laboratory are different from one used for acute seizure study that were performed at HRI. The electrodes were fixed to the skull using dental cement. The gold-plated sockets were fixed into the small plastic barrel (Figure 2. 2) that was fixed on the skull surface with dental cement and animals observed until recovery. Rats were left to recover for at least one week before EEG-ECG recordings were taken.

2.3.8. Implantation of EEG electrodes during acute seizure recordings

For the placement of EEG electrodes during acute seizure experiments, the scalp over the dorsal surface of the skull was incised, the skin retracted, and the periosteum scraped from

the skull surface. Burr holes were drilled bilaterally for recording over the dorsal hippocampus (5.2 mm anterior to lambda, 3 mm lateral to midline and 2-3 mm below the skull surface). Teflon-insulated stainless steel wire (75 µm) was inserted into each hole using stereotaxic manipulator and fixed with superglue. Signals were amplified, band-pass filtered from 1 Hz to 10 kHz, and digitised at 6 kHz (Chapter 3) or 20 kHz (Chapter 4 and 5) with a 100x gain.

2.3.8.1. EEG electrodes site confirmation

The fixed hippocampal brain samples were coronally sectioned (100 µm). The sections were stained with cresyl violet method (section 2.7.2) and bright field images were acquired using Zeiss microscope. The tip of EEG electrode was identified and the position was confirmed.

2.3.9. Intrathecal (IT) drug administration

2.3.9.1. Intrathecal catheterisation

The skin cut for the phrenic and vagus nerve was extended rostrally up to the skull. The muscles overlying occipital bone were gently cauterised to prevent any bleeding and removed. The next muscle layer attached to the occipital bone was carefully scraped with the cotton swabs to expose the membrane over the atlanto-occipital junction. The membrane was cleared of any blood stain and the slit was made with the sharp edge of a 26 G needle. The surge of cerebrospinal fluid (CSF) provided the confirmation of correct site and was stopped by holding dry cotton swab. A catheter (polyethylene tubing, outer diameter = 0.50 mm; internal diameter = 0.20 mm) with a dead space of ~6 µl was inserted into the IT space through a slit in the dura and advanced caudally to the level of T5/6. A micro-syringe was attached to the silastic on the other end of the catheter and CSF was pulled out up to the tip of the catheter. This gives the confirmation of the IT catheterisation and fills the void space with the CSF.

2.3.9.2. Drug administration protocol

IT injections were made after stable baseline recordings. Drugs were dissolved in PBS, and if required pH was adjusted to 7.4. A 25 µl syringe was filled with 6 µl of PBS followed by 1 µl void space and then 10 µl of drug solution. The void space between drug and PBS separates them. A 10 µl of drug was administered slowly over 10 to 15 s. Six µl of PBS flushes the drugs from IT catheter into the subarachnoid space. Followings drugs were administered intrathecally.
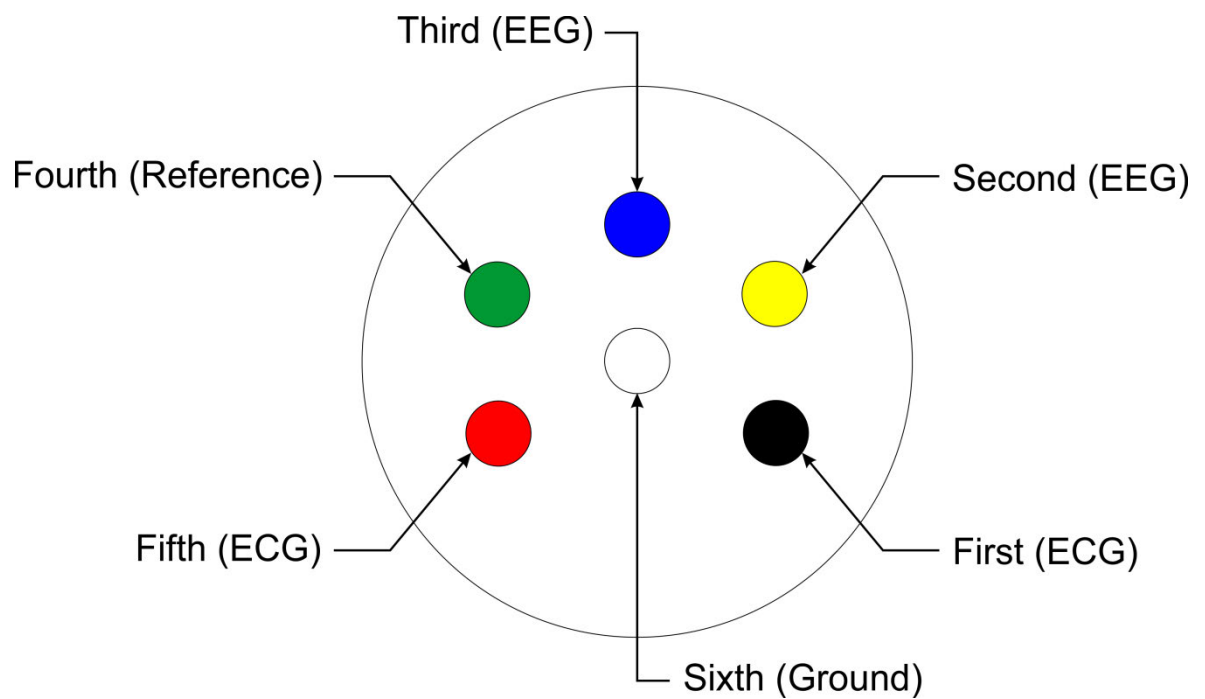
Figure 2. 2: A small plastic barrel with EEG and ECG electrode positions on the rat skull.

Drug	Concentration	Volume	Specific action
PBS	10 mM	10 µl	Vehicle control
PACAP-38	300 µmol/L	10 µl	PACAP receptor agonist
PACAP(6-38)	1 mM	10 µl	PAC1 and VPAC2 receptor antagonist
Minocycline	10 mg/ml	10 µl	Microglial antagonist
Doxycycline	10 mg/ml	10 µl	Microglial antagonist

Table 2. 2: List of drugs administered intrathecally.

2.3.9.3. Validation of site of injection

At the end of experiment and death level recording, 10 µl of Chicago Sky Blue was injected intrathecally and flushed with 6 µl of PBS. The spinal cord was exposed from the dorsal side, and position of the tip of the cannula and dye were recorded and noticed with reference to the position of the thoracic vertebrae.

2.3.10. RVLM microinjection

2.3.10.1. Occipital craniotomy and confirmation of the RVLM site

The dorsal surface of the medulla oblongata was exposed similar to the IT catheterisation as explained above. The occipital bone was cleared, broken into small pieces with a fine rongeur and bone pieces were removed carefully. After completion of the craniotomy, the dura was removed with fine forceps and scissors. The bilateral RVLM stereotaxic coordinates were measured with reference to the calamus scriptorius and confirmed if a 50 nl microinjection of 100 mM glutamate increased BP > 30 mmHg. After glutamate confirmation, stable baseline parameters were recorded at least for 30 min before the start of the protocol.

2.3.10.2. Drugs microinjection protocol

Micropipettes were pulled from borosilicate capillaries with internal diameter 0.58 mm and outer diameter 1 mm. A laser pipette puller was used to pull fine and straight tip pipettes. Then micropipettes were placed in eppendorf tubes containing drug solution with their tip facing upward. Drug solution sucks into the micropipette in 5-10 min with capillary action.

Micropipettes were attached to a long silastic tubing with 5 ml syringe on the other end and fixed into the stereotaxic manipulator. The upper meniscus of drug solution was matched with grading on the manipulator. At the time of drug microinjection, a syringe piston was pushed carefully and lower meniscus level was monitored for the amount of drug administered. The piston pressor was controlled manually to inject the desired amount of drug into the RVLM. Following drugs were microinjected into the RVLM.

Drug	Concentration	Volume	Specific action
PBS	10 mM	50 nl	Vehicle control
Kynurenic acid (KYNA)	100 mM	50 nl	Glutamate receptor antagonist
PACAP(6-38)	15 pmol	50 nl	PAC1 and VPAC2 receptor antagonist
Minocycline	10 mg/ml	50 nl	Microglial antagonist

Table 2. 3: List of drugs microinjected into the RVLM.

2.3.10.3. RVLM microinjection site confirmation

At the conclusion of the experiment, Chicago Sky Blue (50 nl) was microinjected into each RVLM, rats were perfused and brainstems were fixed. The brainstem was sectioned at 100 μm and cresyl violet staining was performed (section 2.7.2). The microinjection sites were checked and confirmed with reference to the rat atlas (Paxinos and Watson, 2007).

2.3.11. Euthanasia

Rats were euthanised after the electrophysiology experiments when the tissue collection was not required. A 0.5 ml bolus injection of 3M potassium chloride (KCl) solution was infused via jugular vein. Subsequently, the recordings were continued and monitored for 10-15 min to record the death level and background noise in nerve activity.

2.4. Sympathetic reflex responses protocols

2.4.1. Baroreflex and somatosympathetic reflex

The effect of stimulation of aortic depressor and sciatic nerve on splanchnic sympathetic nerve activity (SNA) was assessed to estimate the baroreflex and somatosympathetic reflex function in post-SE and control rats. Stimuli were generated by isolated stimulators controlled by a Spike2 script. Stimulus threshold was determined by increasing or decreasing the stimulus voltage until no response was observed. During the experimental protocol, the aortic depressor nerve was stimulated at 4 times the threshold (1-10 V, 0.2-ms pulse width, 100 cycles at 1 Hz across 100 s) and the average SNA response was analysed before and 60, 90 and 120 min after IT treatment. The left sciatic nerve was stimulated to generate the somatosympathetic response. Stimulus threshold was determined as above, and sciatic nerve was stimulated at 4 times the threshold (1-20 V, 0.2 ms pulse width, 100 pulses at 0.4 Hz across 250 s). The average SNA response was analysed before and 60, 90 and 120 min after IT treatment. The voltage was kept constant across both the protocols.

2.4.2. Peripheral and central chemoreflex

Peripheral chemoreceptors were stimulated by ventilating rats with 10% O_2 in N_2 for 45 s. Central chemoreceptors were stimulated by ventilating animals with 5% CO_2 in O_2 for

3 min. Under these conditions, the observed reflex responses are generated due to stimulation of the central chemoreceptors as the oxygenation of the blood was maintained throughout the challenge. Both the central and peripheral chemoreflex responses were generated (with the same minute ventilation as used for the baseline) prior to IT treatment and 60, and 120 min after the treatment.

2.5. <u>Data analysis</u>

Data were acquired using a CED 1401 ADC system and Spike2 acquisition and analysis software. The SNA, phrenic nerve activity (PNA), EEG, ECG, mean arterial pressure (MAP) and HR were analysed as below.

2.5.1. <u>Electroencephalogram (EEG)</u>

The EEG activity raw data was filtered for the zero Hz frequency to remove the low frequency component (DC removed). The power in the gamma frequency range (25-45 Hz) was analysed, as shown previously (Olsson et al., 2006; Gurbanova et al., 2008). A power spectrum analysis was done from 5-min blocks taken 1 min before the drug treatment and 60 and 120 min after the treatment. The percent change in power spectrum area was calculated for each rat at 60 and 120 min post i.p. injection compared to the pre-treatment area (taken as 100%), and grouped together.

The video-EEG data in chronic epileptic and control rats was analysed as explained above in section 2.2.7.

2.5.2. <u>Phrenic nerve activity (PNA)</u>

Phrenic nerve activity was rectified and smoothed (τ 0.5 s). The PNA was analysed from 1-min blocks taken 1 min before and 60 and 120 min after the treatment. The percent change in PNA AUC was analysed at 60 and 120 min post-treatment and compared to the pre-treatment area (taken as 100%).

2.5.3. <u>Sympathetic nerve activity (SNA)</u>

Sympathetic nerve activity was rectified, smoothed (τ 2 s) and normalised to zero by subtracting the residual activity 5-10 min after death or after nerve pinch. The integrated SNA trace was calibrated (baseline as 100%) and analysed by two different methods. The AUC between 60 to 120 min after the treatment was analysed and compared with the pre-treatment AUC (considered as 100%) for results presented in Chapter 4 and 5. The sigmoid curve was fitted to the SNA processed channel and % low, % high, % range and

%/s slope were calculated for results presented in Chapter 3. Both the sigmoid curve-fit and AUC methods provide accurate measures of changes in SNA. The AUC provides the total change in the activity, whereas sigmoid curve-fit provides change in activity (% range) as well as its rate (%/s slope). However, the sigmoid curve fit method requires the smooth nerve recording preferably in a sigmoid shape. The results presented in Chapter 3 were more suitable to analyse with the sigmoid curve-fit methods, whereas results in Chapter 4 and 5 were not and analysed with the AUC method.

2.5.4. Mean arterial pressure (MAP) and heart rate (HR)

Mean arterial pressure and HR were analysed from 1-min blocks taken 1 min before the treatment and 30, 60, 90 and 120 min after the treatment (only 120 min results are shown in graphs). MAP and HR results presented in Chapter 3 were analysed whenever the respective values were at their maximum during the two-hour recording period and compared with the pre-treatment period.

2.5.5. Baroreflex and somatosympathetic reflex responses

Baroreflex and somatosympathetic reflex responses were analysed before, and 60, 90 and 120 min after IT treatment. The percent change in baroreflex response (AUC) was calculated considering pre-treatment response as 100%. The somatosympathetic reflex response was analysed with a sigmoid curve fit analysis. A sigmoid curve was fitted to the averaged waveform of the somatosympathetic response curve (both fast conducting A-fibre and slow conducting C-fibre response). The low, high, range, and slope values were calculated (only range is shown in graphs). The pre-treatment range is considered as 100% response, and percent change is calculated at 60, 90 and 120 min post-treatment.

2.5.6. Chemoreflex responses

Peripheral and central chemoreflex responses were analysed as percent change in SNA at 60 and 120 min post-treatment compared to the pre-treatment response. The pre-treatment response was considered as 100%.

2.5.7. End-tidal CO_2 (ETCO$_2$), and core temperature

End-tidal CO_2 and core temperature were analysed from 1-min blocks taken 1 min before the treatment and 30, 60, 90, and 120 min after the treatment. In all animals, arterial blood gas levels (PaCO$_2$, and pH) were measured 10 min before the treatment and 120 min after the treatment or before the end of the experiment.

2.5.8. Duration of KA-induced seizures

In rats used to investigate the duration of KA-induced seizures, the duration of effect was analysed from the time of i.p. KA injection up to the point where SNA, MAP, and HR returned to baseline. Changes in EEG activity were analysed at the point where SNA returned to baseline and compared to the pre-KA (control) and 60 min post-KA injection (seizure control) period. A log transformation was applied to EEG raw values since variances were not normally distributed, and/or heterogeneous.

2.5.9. Calculation of corrected QT (QTc) interval

The QT interval values change in proportion with change in HR. The increased HR shortens the duration of QT interval in proportion with the RR interval (heart beat/HR). Hence, to compare QT interval values at two different time points, it is essential to correct the QT interval at a specific HR.

QT, PR, and RR intervals were calculated from the ECG recordings. ECG raw data was processed (DC remove), wherever baseline fluctuations were prominent. QTc interval was calculated by dividing the QT interval in seconds by the square root of the RR interval in seconds (Bazett, 1920). The QTc was obtained before and 120 min after vehicle or KA injection. Additionally, QTc was analysed at the different time points depending on the protocol and specific aims.

2.6. **Statistical analysis**

Statistical analysis was carried out in GraphPad Prism software. Statistical significance was determined using one-way analysis of variance (ANOVA) followed by t-tests with the Dunnett's correction for dose response study and with the Holm-Šídák correction for the rest of the studies. Multiple comparisons were done between groups. $p \leq 0.05$ was considered significant.

2.7. **General molecular procedures**

2.7.1. Tissue collection and storage

The brainstem was removed from PFA solution after an overnight period of fixation and rinsed in PBS. Brainstems were sectioned coronally (40 µm thick) with a vibrating microtome, collected sequentially into five different pots containing a cryoprotectant solution (30% sucrose, 30% ethylene glycol, 1% polyvinylpyrrolidone in 0.1 M sodium phosphate buffer at pH 7.4) and stored at -20^0C until further processing.

2.7.2. Cresyl violet staining protocol

The cerebrum and brainstem were sectioned coronally (100 µm) and stained with cresyl violet for histological verification of the EEG electrode positions in the hippocampus and microinjection site in the RVLM, respectively.

Sections were washed three times in PBS if they were stored in cryoprotectant. Free-floating sections were mounted on gelatinised slides and slides were air-dried. Sections were dehydrated by immersing slides in graded ethanol 50%, 70%, 95% and 100% for 5 min. Subsequently, slides were delipidated in chloroform, and then immersed in decreasing grades of ethanol (100%, 95%, 70% and 50%) for 5 min. Sections were rehydrated by immersing in deionised water. Subsequently, slides were immersed in cresyl violet stain (5% solution in water) for 2 min and in deionised water twice for 1 min. Slides were again immersed in graded ethanol to rehydrate them (50%, 70%, 95% and 100% for 5 min) followed by glacial acetic acid in 95% ethanol which is a clearing agent (makes unstained part of the tissue transparent). Finally, slides were immersed in 95% ethanol for 5 min followed by xylene for 10 min. Slides were coverslipped with DPX (dibutylphthalate polystyrene xylene) and allowed to set.

2.7.3. Immunohistochemistry protocol

Free-floating sections were used for all immunohistological procedures. Sections stored in cryoprotectant solution were washed three times, for 30 min each, in 0.1 M PBS containing 0.3% Triton X-100 at room temperature. Sections were incubated for > 48 h in TTPBSm (10 mM Tris-HCl, 10 mM sodium phosphate buffer, 0.9% NaCl, 0.3% Triton X-100, 0.1% merthiolate at pH 7.4), 10% normal donkey serum and primary antibodies as mentioned in Table 2.4, at 4^0C while shaking.

Subsequently, sections were washed three times (30 min each) in TPBS (10 mM Tris-HCl, 10 mM sodium phosphate buffer, 0.9% NaCl at pH 7.4) and incubated overnight with secondary antibodies, as mentioned in Table 2.4, in TPBSm (10 mM Tris-HCl, 10 mM sodium phosphate buffer, 0.9% NaCl, 0.1% merthiolate at pH 7.4) with 2% donkey serum at room temperature while shaking. The binding of secondary antibodies revealed the tyrosine hydroxylase (TH) (C1 neurons), cluster of differentiation (CD)206 (a mannose receptor present on M2 phenotype of microglia) and ionised calcium-binding adapter molecule-1(Iba1) (a microglia/macrophage specific calcium binding protein) immunoreactivity. Sections were washed three times in TPBS at room temperature,

sequentially mounted on glass slides, and coverslipped with Vectashield (H-1000) and sealed with clear nail polish.

Antibody	Primary/ Secondary	Concentration	Supplier
Mouse anti-TH	Primary	1:500	Sigma-Aldrich and Avanti Antibodies
Rabbit anti-CD206	Primary	1:2000	Abcam
Goat anti-Iba1	Primary	1:1000	Novus Biologicals
cyanine dye (Cy)5-conjugated donkey anti-mouse	Secondary	1:500	Jackson Immunoresearch Laboratories
Alexa Fluor 488-conjugated donkey anti-rabbit CD206	Secondary	1:500	Jackson Immunoresearch Laboratories
Cy3-conjugated donkey anti-goat Iba1	Secondary	1:500	Jackson Immunoresearch Laboratories

Table 2. 4: List of antibodies.

2.8. Microscopy

All images were acquired using a Zeiss Axio Imager Z2 (Zen software, Zeiss, Germany). Images were captured at 20X and 40X magnifications. The RVLM is defined as a triangular area ventral to the nucleus ambiguus, medial to the spinal trigeminal tract (Sp5), and lateral to the inferior olive or the pyramidal tracts (Figure 1. 6 and Figure 4. 9).

2.9. Morphological analysis of microglia

A 0.16 mm^2 box was placed within the imaged RVLM and this area was used for analysis. The morphological analysis (branch length and a number of endpoint processes) of Iba1-labelled microglial cells in the vicinity of TH-labelled RVLM neurons was carried out using ImageJ plugin software (Kapoor et al., 2016b; Kapoor et al., 2016c).

2.10. Histology statistical analysis

GraphPad Prism was used for chi-square test for goodness of fit to analyse the difference between the number of microglia. The proportions of CD206 labelled anti-inflammatory M2 microglia in the RVLM of treatment group of rats were compared with the vehicle-treated group. The proportion of M2 microglia is equal to the number of M2 microglia divided by the total number of microglia multiplied by 100. GraphPad Prism was used to analyse differences between % CD206 microglia and their morphological changes. The statistical significance was determined using nonparametric Kruskal-Wallis or Mann-Whitney test (Sokal and Rohlf, 2012).

Chapter 3
Antagonism of PACAP or microglia function worsens the cardiovascular consequences of kainic acid-induced seizures in rats

The work in this Chapter is published in the "Journal of Neuroscience-An Official Journal of Society for Neuroscience".

Bhandare AM, Mohammed S, Pilowsky PM, Farnham MMJ (2015) Antagonism of PACAP or microglia function worsens the cardiovascular consequences of kainic acid induced seizures in rats. J Neurosci 35:2191 2199.

"The candidate designed experiments, performed all experiments, analysed data and interpreted results. Candidate was the major contributor to the manuscript writing, editing, figures drawing and revision. Paul Pilowsky, Melissa Farnham and Suja Mohammed contributed to design of experiments, interpretation of results and editing, revision and final approval of manuscript."

Table of Contents

3.1. <u>Abstract</u>

Seizures are accompanied by cardiovascular changes that are a major cause of sudden unexpected death in epilepsy (SUDEP). Seizures activate inflammatory responses in the cardiovascular nuclei of the medulla oblongata and increase neuronal excitability. Pituitary adenylate cyclase-activating polypeptide (PACAP) is a neuropeptide with autocrine and paracrine neuroprotective properties. Microglia are key players in inflammatory responses in the central nervous system (CNS). We sought to determine whether PACAP and microglia mitigate the adverse effects of seizure on cardiovascular function in a rat model of temporal lobe epilepsy (TLE). Kainic acid (KA)-induced seizures increased splanchnic sympathetic nerve activity (SNA) by 97%, accompanied by an increase in heart rate (HR) but not blood pressure (BP). Intrathecal (IT) infusion of the PACAP antagonist PACAP(6-38) or microglial antagonists minocycline and doxycycline augmented sympathetic responses to KA-induced seizures. PACAP(6-38) caused a 161% increase, whereas minocycline and doxycycline caused a 225% and 215% increase, respectively. In IT PACAP antagonist treated rats both BP and HR increased, whereas, after treatment with microglial antagonists only BP was significantly increased compared with control. Our findings support the idea that PACAP and its action on microglia at the level of the spinal cord elicit cardioprotective effects during seizure. However, IT PACAP did not show additive effects, suggesting that the agonist effect was at maximum. The protective effect of microglia may occur by the adoption of an M2 phenotype and expression of factors such as transforming growth factor-β (TGF-β) and interleukin (IL)-10 that promote neuronal quiescence. In summary, therapeutic interventions targeting PACAP and microglia could be a promising strategy for preventing SUDEP.

3.2. <u>Introduction</u>

Epileptic seizures are commonly accompanied by autonomic changes that include disturbances in BP, HR, and heart rhythm (Wannamaker, 1985; Darbin et al., 2002; Müngen et al., 2010; Pansani et al., 2011). These cardiovascular changes may be dramatic and lead to SUDEP, a syndrome that accounts for 5-17% of deaths in people with epilepsy (Sakamoto et al., 2008; Brotherstone et al., 2010; Tolstykh and Cavazos, 2013).

PACAP is a 38 amino acid peptide that activates three receptors: PAC1R, VPAC1R, and VPAC2R. The canonical pathway in each case is activation of adenylate cyclase, leading to two main effects on neurons. First, it is able to act as an excitatory neurotransmitter (Lai et al., 1997; Farnham et al., 2008; Farnham et al., 2011; Farnham et al., 2012), and second, as a neuroprotective and anti-inflammatory agent by inhibiting the activation of mitogen-activated protein kinase (MAPK) family and by stimulating secretion of IL-6 (Shioda et al., 1998). In patients who are recovering from tonic-clonic seizure, there is an upregulation of MAPK in the hippocampus, and IL-6 is elevated in cerebrospinal fluid (CSF) (Peltola et al., 2000). Conversely, IL-6 knock-out mice are more susceptible to seizure-induced hippocampal damage (Penkowa et al., 2001), suggesting that IL-6 is neuroprotective. Nomura et al. (2000) showed that PACAP gene expression increases in the paraventricular nucleus (PVN) of the hypothalamus after KA-induced TLE in rats. Based on these findings, we hypothesised that PACAP itself or its action on activated microglia might have neuroprotective effects that inhibit seizure-induced neuronal excitation and protect against the adverse autonomic effects of seizure. Activated microglia are associated with neurodegeneration both in patients and animal models of TLE (Mirrione et al., 2010; Ahmadi et al., 2013); however, their action as either neurotoxic or neuroprotective in the brainstem and spinal cord cardiovascular nuclei remains unclear. A number of recent studies suggest that microglia may acquire the neuroprotective M2 phenotype, and increase endogenous production of TGF-β and IL-10 (Li et al., 2007; Mosser and Edwards, 2008; Neumann et al., 2008; Loane and Byrnes, 2010; Vinet et al., 2012). These findings led to our second hypothesis that microglia in cardiovascular nuclei may be neuroprotective and provide a defense mechanism by attenuating sympathoexcitatory cardiovascular responses during seizure.

This study, therefore, aimed to investigate the role of PACAP and microglia in seizure-induced cardiovascular responses. Specifically, the aims of this study were to determine the effect of IT administration of PACAP and the PACAP antagonist PACAP(6-38) and microglial antagonists minocycline and doxycycline on seizure-induced

cardiovascular responses. We used *in vivo* physiological and pharmacological approaches in anesthetised rats using the KA-induced seizure model (Sakamoto et al., 2008).

3.3. <u>Materials and methods</u>

3.3.1. <u>Animals</u>

All protocols were approved by the Animal Care and Ethics Committee of Macquarie University and the Sydney Local Health District (section 2.1.1). All experiments were conducted on adult male Sprague-Dawley (SD) rats (250-350 g) in accordance with the Australian code of practice for the care and use of animals for scientific purposes.

3.3.2. <u>Surgical preparation</u>

Rats ($n = 64$) were anesthetised with 10% urethane (1.3-1.5 g/kg, intraperitoneal (i.p.)) and additional top-ups were given as required (section 2.2.2). Atropine sulfate (100 µg/kg, i.p.) was administered with the first dose of urethane to prevent bronchial secretions. After the completion of the general surgical procedures described below, rats were secured in a stereotaxic frame. Core body temperature was monitored with a rectal thermometer and maintained between 36.5 and 37.5^0C throughout the experiment.

3.3.3. <u>General surgical procedures</u>

The right carotid artery and jugular vein were cannulated for the recording of BP, and for the administration of drugs and fluids, respectively (section 2.3.1). Tracheostomy was performed to enable mechanical ventilation (section 2.3.2). Electrocardiogram (ECG) was recorded from leads connected to the forepaws of the rat and HR was derived (section 2.3.4). Rats were vagotomised (section 2.3.5.1), artificially ventilated with oxygen enriched room air, and paralysed with pancuronium bromide (section 2.3.3). Arterial blood gases were analysed with an electrolyte and blood gas analyser, and partial pressure of carbon dioxide ($PaCO_2$) and pH were maintained at 40.0 ± 2 and 7.35-7.45, respectively. The left greater splanchnic sympathetic nerve at a site proximal to the celiac ganglion (section 2.3.5.2) and the left phrenic nerves (section 2.3.5.3) were isolated, dissected, and tied with 5/0 silk thread. Nerve activity was recorded with bipolar stainless steel electrodes and signals were amplified and filtered with a 50/60-Hz line filter (section 2.3.6).

3.3.4. <u>Intrathecal (IT) catheter placement</u>

The atlanto-occipital junction was exposed and a catheter with a dead space of ~6 µl was inserted into the IT space of all rats through a slit in the dura and advanced caudally to the level of T5/6 (section 2.3.9.1).

3.3.5. Electroencephalogram (EEG) electrode placement

Bilateral EEG electrodes were placed over the dorsal surface of the skull (section 2.3.8). A single electrode wire was inserted into each hole using stereotaxic manipulator. Signals were amplified, band-pass filtered from 1 Hz to 10 kHz, amplified 100X, and digitised at 6 kHz.

3.3.6. Seizure induction

Intraperitoneal injection of KA was used to generate seizures and KA dose-response curve in SD rats (section 2.2.6). Responses were recorded for at least 2 h after KA injection, during which continuous monitoring of EEG was used to identify the development of seizures (section 2.5.1). To determine the presence or absence of seizure, the amplitude of the area under curve (AUC) of the EEG before and after KA administration was measured. The log-transformation was applied to EEG data as variance was very high.

The dose-response study showed that 2 mg/kg dose of KA was sufficient to induce seizure and a significant increase in SNA (Figure 3. 1 and Figure 3. 2) and was used for the rest of the study. At the conclusion of the experiment, rats were killed with 0.5 ml of 3 M potassium chloride (KCl, intravenous (i.v.)) (section 2.3.11) or deeply anesthetised and perfused with 400 ml of ice-cold 0.9% saline followed by 400 ml of 4% paraformaldehyde (PFA) solution (section 2.2.4). Brains were removed from the perfused rats and postfixed in the same fixative overnight. Brains were sectioned coronally (100 µm) and stained with cresyl violet for histological verification of the electrode positions (section 2.7.2).

3.3.7. IT drug administration protocol

The drugs were administered intrathecally as mentioned in section 2.3.9.2. Briefly, in all dose-response studies, a control injection of 10 µl of 10 mM phosphate-buffered saline (PBS) was washed in with 6 µl PBS 10 min before the i.p. injection of KA. The same IT PBS infusion protocol was followed for the vehicle control group of rats, 10 min before i.p. PBS injection.

Ten microliters of 1 mM PACAP(6-38), 300µmol/l PACAP, minocycline (100µg/10µl) or doxycycline (100µg/10µl) were administered intrathecally and flushed in with 6µl of PBS in respective groups. In all groups of rats, IT infusion was made 10 min before i.p. KA or PBS injection. All infusions were made over a 10 to 15 s period. At the conclusion of experiments, rats were euthanised and post-mortem verification of the position of catheter tip was carried out (section 2.3.9.3).

3.3.8. Data acquisition and analysis

Data were acquired using a CED 1401 ADC system and Spike2 acquisition and analysis software. The EEG activity raw data was DC removed. The power of the gamma range was analysed with power spectrum analysis from 5-min blocks taken 1 min before IT infusion and 60 and 120 min after i.p. injection of either KA or PBS (section 2.5.1). Phrenic nerve activity (PNA) was rectified and smoothed (τ 0.5 s). PNA was analysed from 1-min blocks taken 1 min before IT infusion and 60 and 120 min after i.p. injection of either KA or PBS (section 2.5.2). SNA raw data was rectified and smoothed (τ 2 s) and normalised to zero by subtracting the residual activity 5-10 min after death. SNA was analysed with a sigmoid curve-fit analysis method. The % low, % high, % range, and slope (%/s) were calculated (only % range is showed in graphs) (section 2.5.3). Mean arterial pressure (MAP) and HR were analysed from 1-min blocks taken 1 min before IT infusion and the time at which it was peaked (section 2.5.4). End-tidal CO_2 ($ETCO_2$) and core temperature were analysed from 1-min blocks taken 1 min before IT infusion and 30, 60, 90 and 120 min after i.p. injection of either KA or PBS (section 2.5.7). Arterial blood gas levels ($PaCO_2$, and pH) were measured 10 min before IT infusion and 120 min after KA or PBS injections in all animals (section 2.5.7). Log transformation was applied to EEG and SNA raw values where necessary if variances were not normally distributed, or heterogeneous. Statistical analysis was carried out in GraphPad Prism software. Statistical significance was determined using one-way analysis of variance (ANOVA) followed by t-tests with Dunnett's correction for dose-response studies and with the Holm-Šídák correction for the rest of the study. Multiple comparisons were done between groups. $p \leq$ 0.05 was considered significant (section 2.6). Because the length of the QT interval can be affected by HR, corrected QT (QTc) interval was calculated (Bazett, 1920). The QTc was obtained in all rats before and after vehicle or KA injection (section 2.5.9).

3.4. Results

3.4.1. KA-induced seizures cause sympathoexcitation, tachycardia, and pressor responses

Intraperitoneal injection of KA in urethane-anesthetised rats (Figure 3. 1) was used to determine the most effective dose for use in this study (Figure 3. 2). One-way ANOVA of peak EEG AUC responses revealed that the 2 mg/kg was the lowest dose of KA effective in significantly elevating EEG (120 min after KA: 64.0 ± 17.7%; $p \leq$ 0.0001; Figure 3. 2D, E), SNA (% range: 97.2 ± 7.4%; $p \leq$ 0.001; Figure 3. 2A) and HR (ΔHR: 46.5 ± 4.8 beats per minute (bpm); $p \leq$ 0.05; Figure 3. 2C). Therefore, a 2 mg/kg dose of KA was

used in the rest of the study. SNA percentage low was same in all groups, whereas percentage high was significantly different in 2 mg/kg (194.3 ± 6.0%; $p \leq 0.05$) and in all higher doses of KA compared to the vehicle-treated group. The change in MAP was significantly higher only in 8 (ΔMAP: 48.3 ± 4.5 mmHg; $p \leq 0.0001$) and 12 mg/kg (ΔMAP: 28.2 ± 14.6 mmHg; $p \leq 0.05$) doses of KA compared to vehicle control (Figure 3. 2B), whereas the change in HR was significantly different in 2 mg/kg and all higher doses of KA compared to vehicle control (Figure 3. 2C). There were no significant differences in PNA (as shown in supplementary results in section 3.6.1; Figure 3. 8C-D), expired CO_2 and rectal temperature in any of the groups studied. Blood gas analysis revealed that blood $PaCO_2$ and pH were within a normal physiological range in all animals ($PaCO_2$ was 40.0 ± 2 and pH between 7.35 and 7.45). There was no significant change in pre-treatment and post-treatment blood $PaCO_2$ and pH levels (results not shown). A 2 mg/kg i.p. injection of KA increased EEG amplitude beyond 50% above the baseline and was classified as a seizure. The EEG seizure response was followed by an increase in SNA (Figure 3. 1). Importantly, SNA did not begin to increase before the first instance of seizure, eliminating the possibility of the increase in SNA being due to a peripheral effect of KA. The EEG activity started to increase at 25.6 ± 3.6 min after KA injection, followed by SNA, MAP, and HR. SNA, EEG, and HR were significantly increased post-KA injection compared to the vehicle-treated group.

3.4.2. Antagonism of PACAP exacerbates the cardiovascular effects of seizure

The PACAP antagonist PACAP(6-38) was administered intrathecally, 10 min before i.p. KA injection, to test the hypothesis that PACAP has a neuroprotective and anti-inflammatory role in KA-induced seizure rats that might be responsible for attenuating the seizure-induced sympathoexcitation. The seizure-induced cardiovascular responses were significantly increased by infusing PACAP(6-38) in KA-induced seizure rats compared with the KA control group (SNA high: 255.1 ± 15.3%; $p \leq 0.01$, SNA range: 160.8 ± 16.0%; $p \leq 0.01$, Figure 3. 3A; SNA slope: 0.043 ± 0.0095%/s; $p \leq 0.01$, ΔMAP: 31.84 ± 3.5 mmHg; $p \leq 0.05$, Figure 3. 3B; and ΔHR: 56.1 ± 4.9 beats/min; $p \leq 0.05$, Figure 3. 3C). IT infusion of 300 µmol/l PACAP had no effect on the SNA increase in response to KA-induced seizures (Figure 3. 3A). IT PACAP agonist and antagonist treatment had no effect on EEG activity in seizure-induced rats compared with the KA control group (Figure 3. 3D).
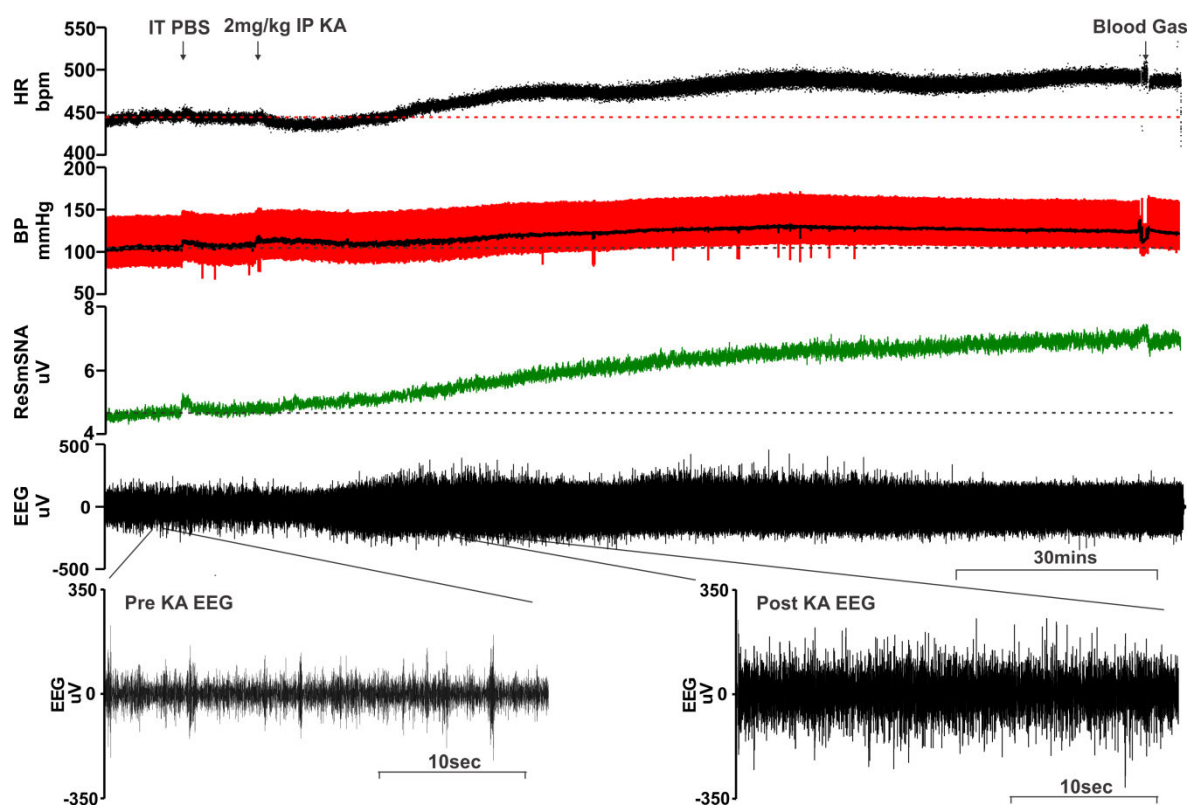
Figure 3. 1: Effect of IT PBS (10 μl) followed by 2 mg/kg i.p. KA in an anesthetised rat.

From the top: HR (bpm), BP (mmHg), SNA (μV), and EEG (μV). Time of administration of IT PBS and i.p. KA are marked with an arrow. Pre-KA EEG and post-KA EEG refer to the expanded periods as indicated.

Figure 3. 2: Dose-response curve for i.p. KA.

Change in SNA (log transform of percentage range) (A), maximum change in MAP (on y-axis) at respective time point after i.p. PBS or KA injection (on x-axis) (B), maximum change in HR (on y-axis) at respective time point after i.p. PBS or KA injection (on x-axis) (C) and log transform of percentage change in AUC of EEG activity at 60 min (D) and 120 min (E) after i.p. PBS or KA injection, in PBS ($n = 5$) and 0.1 ($n = 3$), 0.3 ($n = 3$), 1 ($n = 3$), 2 ($n = 5$), 3 ($n = 3$), 5 ($n = 3$), 8 ($n = 3$), 10 ($n = 3$), and 12 ($n = 3$) mg/kg i.p. KA-treated rats. Statistical significance was determined using one-way ANOVA followed by t tests and Dunnett's correction to compare effects with the control value. Data are expressed as mean ± SEM. ****$p \leq$ 0.0001; ***$p \leq 0.001$; **$p \leq 0.01$ and *$p \leq 0.05$ compared with vehicle control group.
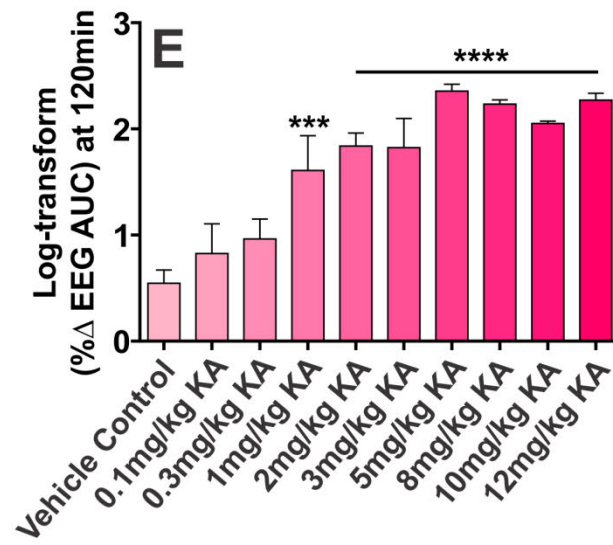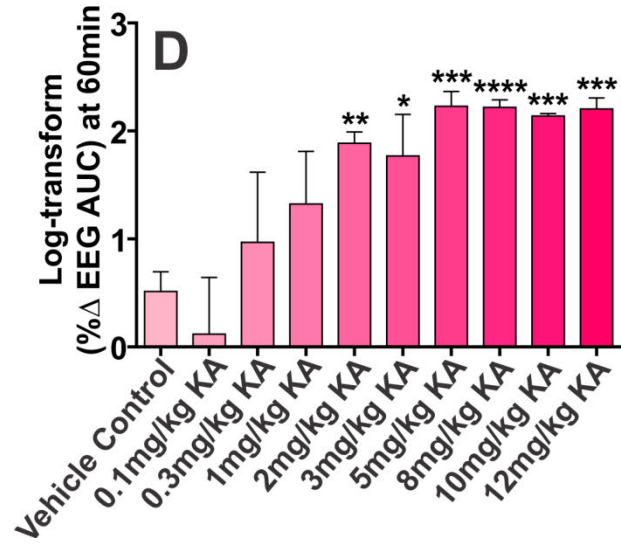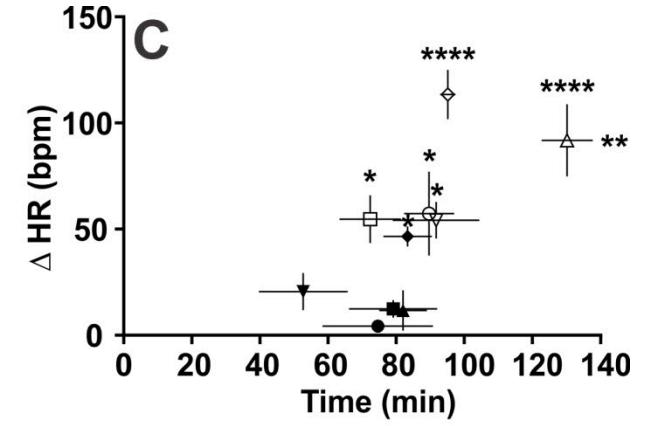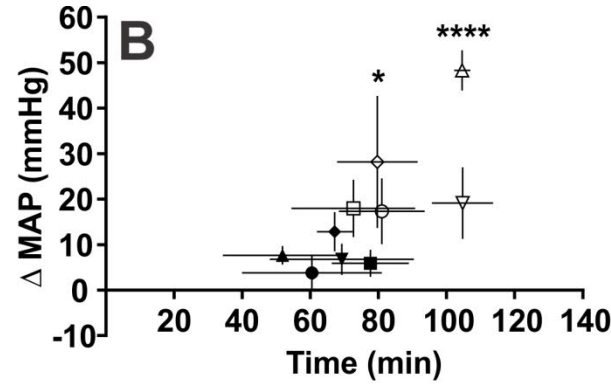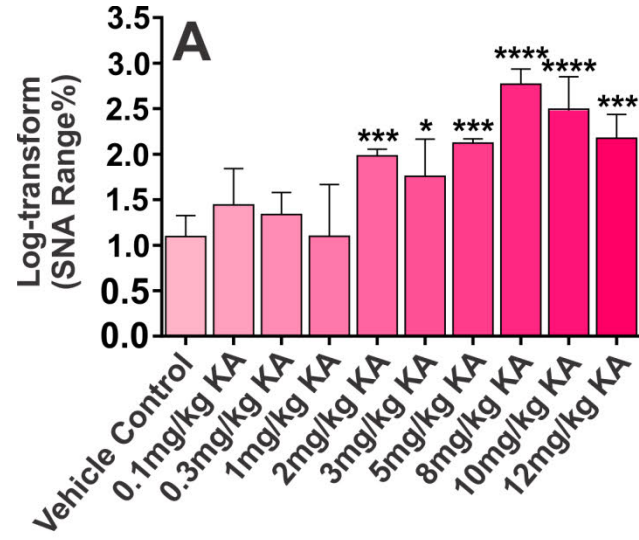
Figure 3. 3: *In vivo* effects of IT PACAP(6-38) and PACAP-38 in 2 mg/kg KA-induced seizure rats.

Change in SNA (% range) (A), maximum change in MAP (on y-axis) at respective time point after i.p. PBS or KA injection (on x-axis) (B), maximum change in HR (on y-axis) at respective time point after i.p. PBS or KA injection (on x-axis) (C), and log transform of percentage change in AUC of EEG activity at 60 and 120 min after i.p. PBS or KA injection (D) in different groups of rats after development of seizure. In all groups, $n = 5$. Statistical significance was determined using one-way ANOVA followed by t tests with a Holm-Šídák correction. Data are expressed as mean ± SEM. **** $p \leq 0.0001$; *** $p \leq 0.001$; ** $p \leq 0.01$; * $p \leq 0.05$ compared with vehicle control group; ## $p \leq 0.01$ and # $p \leq 0.05$ compared with KA control group.
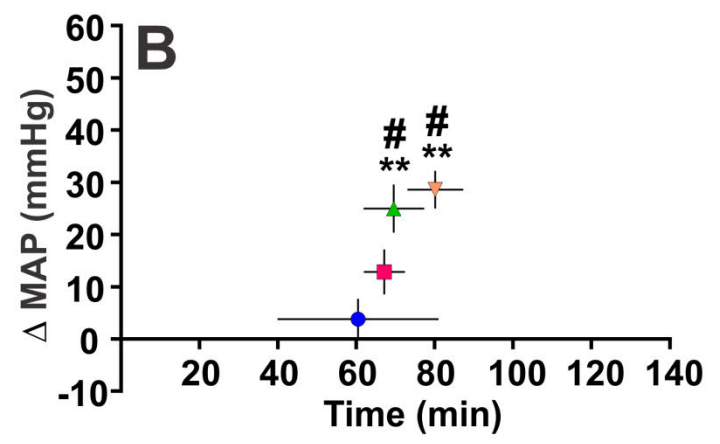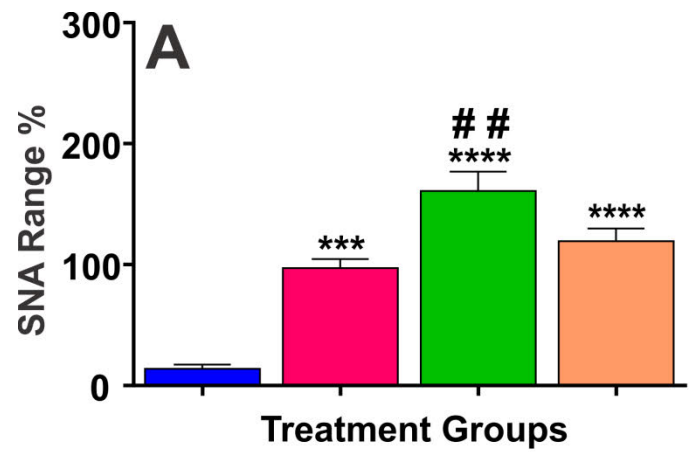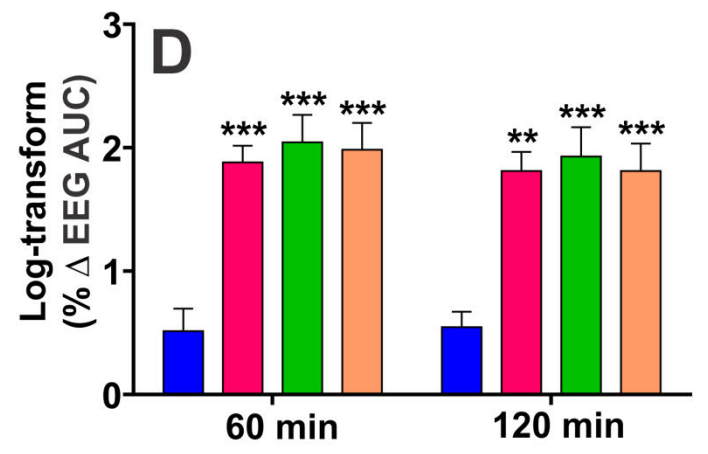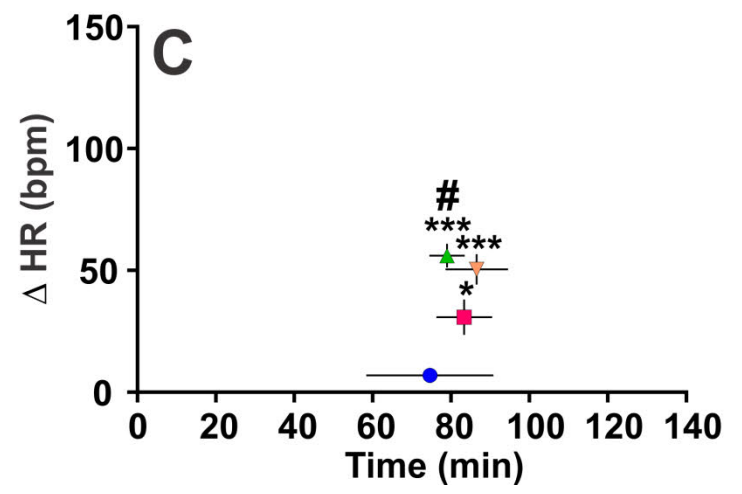
Figure 3. 4: *In vivo* effects of IT minocycline and doxycycline in 2 mg/kg KA-induced seizure rats and vehicle control rats.

Change in SNA (% range) (A), maximum change in MAP (on y-axis) at respective time point after i.p. PBS or KA injection (on x-axis) (B), maximum change in HR (on y-axis) at respective time point after i.p. PBS or KA injection (on x-axis) (C), and log transform of percentage change in AUC of EEG activity at 60 and 120 after i.p. PBS or KA injection (D) in different groups of rats after development of seizure. In all groups, $n = 5$. Statistical significance was determined using one-way ANOVA followed by t tests with a Holm-Šídák correction. Data are expressed as mean $\pm$ SEM. **** $p \leq$ 0.0001; *** $p \leq 0.001$; ** $p \leq 0.01$; * $p \leq 0.05$ compared with vehicle control group; ## $p \leq 0.01$ and # $p \leq 0.05$ compared with KA control group.
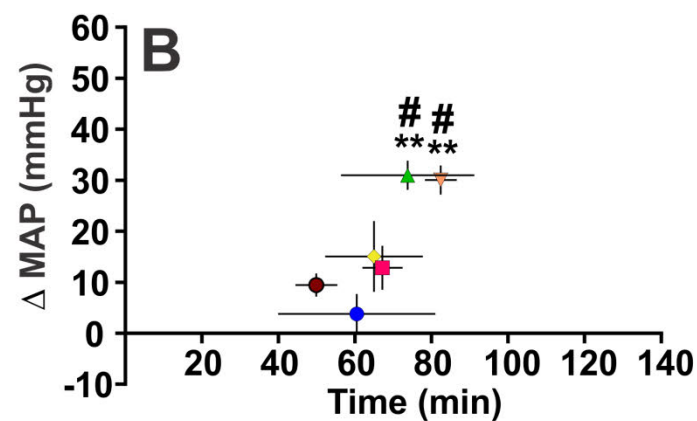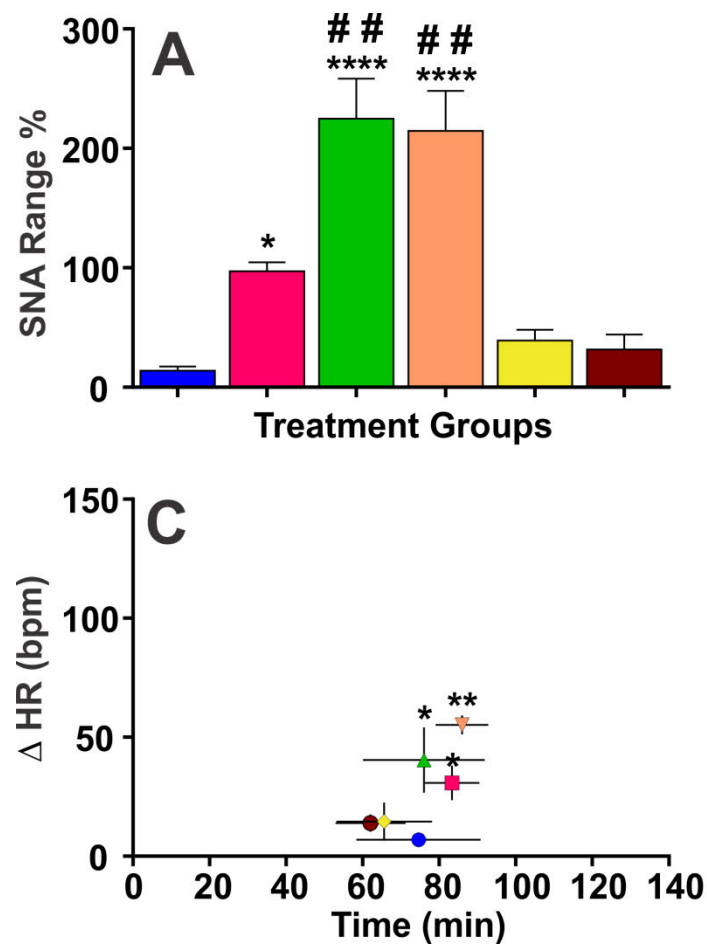
Figure 3. 5: Representative Poincare plots illustrate the increase in QT interval after KA-induced seizures in individual rats.

Black box symbols show pre-PBS or KA and red plus symbols show 120 min post-PBS or KA i.p. injection in the respective groups. A, Pre- (black) and 120 min post- (red) vehicle. B, Pre- (black) and 120 min post- (red) KA. C, Pre- (black) and 120 min post-KA with IT PACAP (6-38) (red). D, Pre- (black) and 120 min post-KA with IT PACAP-38 (red). E, Pre- (black) and 120 min post-KA with IT minocycline (red). F, Pre- (black) and 120 min post-KA with IT doxycycline (red). Scale bar in milliseconds. HR triggered ECG was drawn pre- and post-treatment and is shown in the right corner of each box (continuous black and dotted red lines represent pre-treatment and post-treatment ECG). ST segment elevation is shown with an arrow (C).
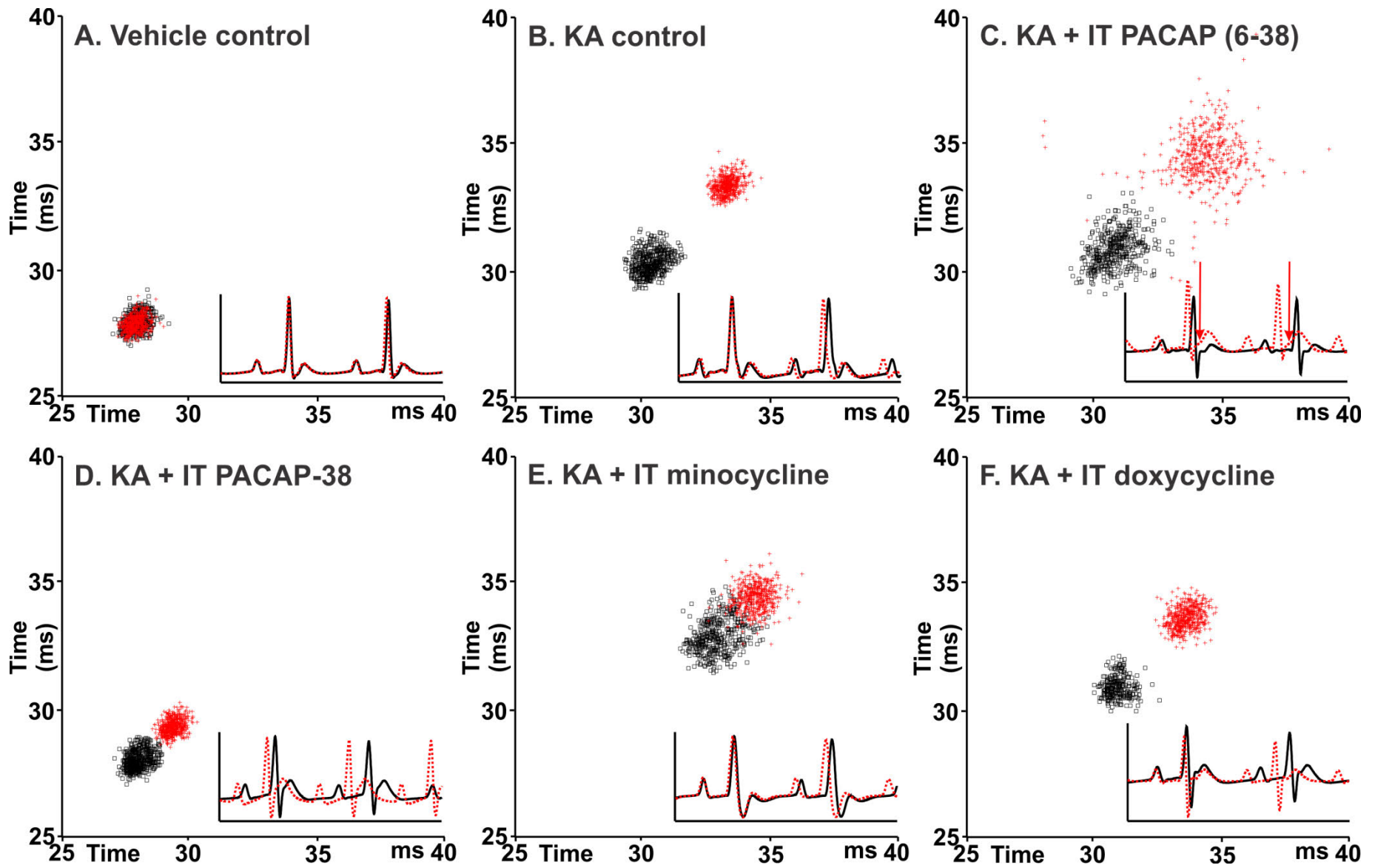
3.4.3. Microglial antagonism worsens the cardiovascular dysfunction in seizure

The effect of blocking microglial activation on seizure-induced cardiovascular responses was evaluated at the spinal cord level. IT injection of microglial antagonists minocycline and doxycycline in KA-induced seizure rats more than doubled the sympathoexcitatory and MAP responses, but did not affect HR. Microglial antagonists alone had no effect on measured cardiovascular parameters in vehicle-treated control rats (Figure 3. 4A-C). These results indicate that microglia have a neuroprotective or anti-inflammatory role during seizure. IT minocycline significantly increased sympathoexcitation in KA-induced seizure rats compared with the KA control group (SNA high: $314.1 \pm 33.4\%$; $p \le 0.01$, SNA range: $224.8 \pm 33.6\%$; $p \le 0.01$, Figure 3. 4A; and SNA slope: $0.04 \pm 0.006\%/s$; $p \le 0.05$). A similar response was observed with IT doxycycline which augmented the sympathoexcitation in KA-induced seizure rats compared with the KA control group (SNA high: $313.2 \pm 31.0\%$; $p \le 0.01$, SNA range: $214.5 \pm 33.6\%$; $p \le 0.01$, Figure 3. 4A; and SNA slope: $0.05 \pm 0.008\%/s$; $p \le 0.01$). MAP was also significantly increased in both minocycline- and doxycycline-treated rats after KA treatment compared with the KA control group (ΔMAP: 31.0 ± 2.9 mmHg; $p \le 0.05$ and 30.0 ± 2.9 mmHg; $p \le 0.05$, respectively; Figure 3. 4B). HR response were not different between the IT microglial antagonist treated seizure-induced group and the KA control group (Figure 3. 4C). IT minocycline and doxycycline treatment in the KA-induced seizure group had no effect on EEG activity compared with KA control (Figure 3. 4D).

3.4.4. Proarrhythmogenic changes in ECG after seizure

In vehicle-treated rats, the change in QTc interval (ΔQTc) duration between pre-treatment and 120 min after injection was 2.5 ± 1.0 ms (Figure 3. 6). The ΔQTc interval was significantly increased in seizure-induced rats compared with vehicle control (13.1 ± 1.5 ms; $p \le 0.001$; Figure 3. 6). Compared with the vehicle control group, the ΔQTc interval duration was significantly increased in the KA control, IT PACAP-38, PACAP(6-38), and doxycycline-treated groups, but not in the minocycline-treated group (Figure 3. 6). The QT interval was prolonged in KA control, PACAP(6-38), PACAP-38, and doxycycline-treated rats compared with vehicle treatment (Figure 3. 5). PACAP antagonist treatment not only prolongs the QT interval but also causes a clear ST-segment elevation (Figure 3. 5C, arrows), both of which are prominent proarrhythmogenic changes (HR triggered ECG was drawn pre-treatment and post-treatment and shown in the right side corner of each graph, Figure 3. 5). IT minocycline treatment in the KA-treated group showed significant differences in ΔQTc interval compared with the KA control group ($p \le 0.01$, Figure 3. 6).
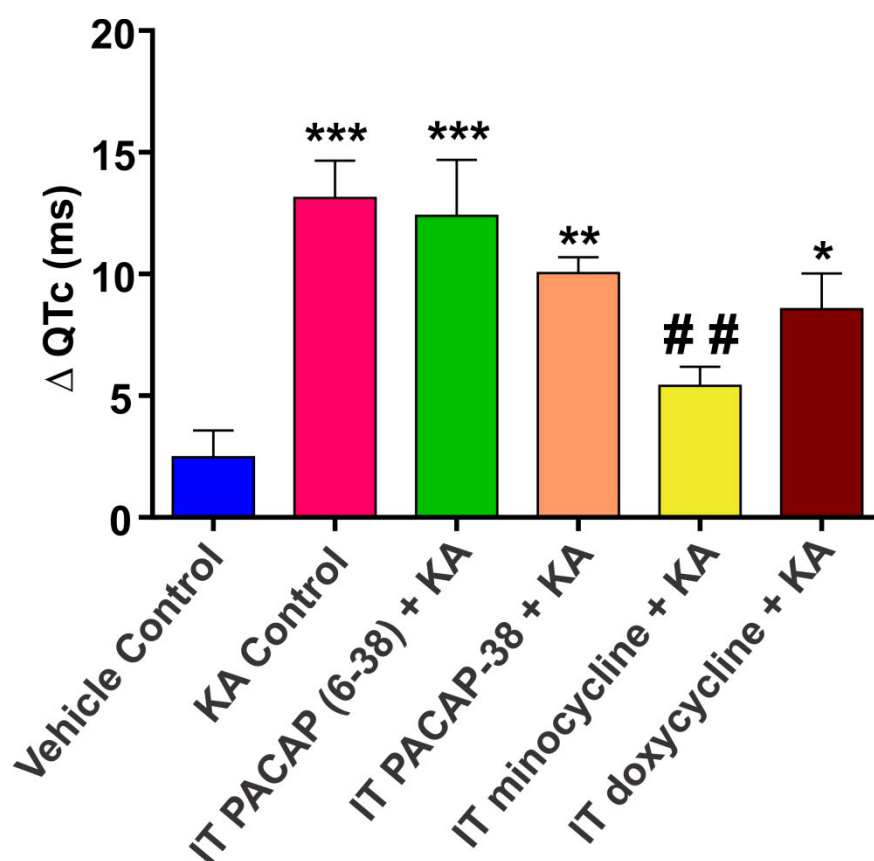
Figure 3. 6: Group data showing changes in QTc interval 120 min after i.p. injection of KA or PBS in the different groups of rats.

Statistical significance was determined using one-way ANOVA followed by t tests with a Holm-Šídák correction. Data are expressed as mean ± SEM. **** $p \leq 0.0001$; *** $p \leq 0.001$; ** $p \leq 0.01$; * $p \leq 0.05$ compared with vehicle control group; ## $p \leq 0.01$ compared with the KA control group.

3.5. <u>Discussion</u>

The main findings of the study are, first, that SNA begins to rise several minutes after the start of a seizure. Second, we find that induction of seizure activity in the hippocampal EEG that follows i.p. KA is associated with significant and dose-dependent increases in SNA, MAP, and HR and a prolongation of the QT interval. Third, in KA-induced seizure rats, IT administration of the PACAP antagonist, PACAP(6-38), exacerbates the cardiovascular responses, whereas IT administration of PACAP has no beneficial effect. Fourth, IT infusion of tetracycline-derived microglial antagonists exacerbate the cardiovascular responses after the induction of seizures. Overall, antagonism of PACAP or microglia tends to worsen the sympathoexcitatory effects of seizures.

Findings demonstrate that KA-induced seizure has a powerful effect on the cardiovascular system. It increases SNA, MAP, and HR; prolongs QTc; and, after PACAP antagonist, causes ST elevation. Together, these changes markedly increase the risk of arrhythmia. The present study revealed a neuroprotective role of endogenous PACAP that is antagonised by IT infusion of PACAP(6-38) in KA-induced seizure rats. Therefore, PACAP attenuates KA seizure-induced sympathoexcitation. The failure to see a beneficial effect of PACAP agonist infusion may be due to an inadequate dose being provided. Alternatively, local neurons secreting PACAP may cause a maximal effect on local PACAP receptors so that additional IT doses of PACAP provided exogenously have no effect. This creates the need for further study of the effect of PACAP during seizure on catecholaminergic and other bulbospinal sympathoexcitatory neurons in the rostral ventrolateral medulla (RVLM) (Schreihofer and Guyenet, 1997). It is possible that microinjection of low doses of exogenous PACAP in RVLM might provide an additional neuroprotective effect during seizure and inhibit the sympathoexcitation. Microglia are activated by increased phosphorylation of the MAPK pathway. PACAP act on microglia via membrane-associated PAC1 and VPAC1 (PACAP) receptors, causing the release of substances such as IL-10 or TGF-β, compounds that protect neurons from overexcitation (Figure 3. 7). The finding that an increase in sympathetic activity after PACAP antagonism with PACAP(6-38) or of microglial antagonism (doxycycline and minocycline) suggests that, in this model of epilepsy, there is strong activation of a neuroprotective PACAP and microglial pathway. The physiological effect of PACAP on microglia may act to dampen the sympathoexcitatory effects of seizure, an idea that is strengthened by the finding that tetracycline drugs had no effect in vehicle-treated animals.
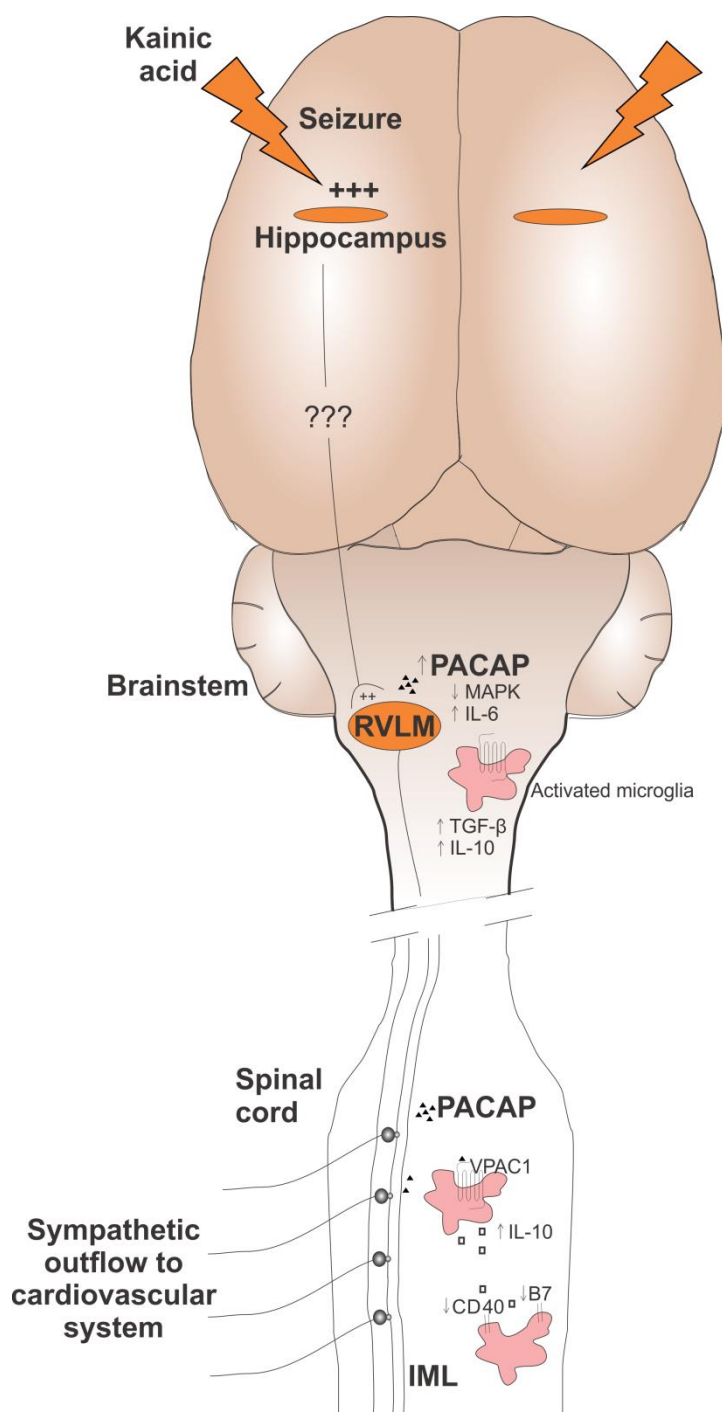
Figure 3. 7: A proposed mechanism by which PACAP and microglia may have protective effects on sympathetic neurons in the brainstem and spinal cord during seizure.

Seizure activates brainstem presympathetic neurons and changes cardiac and vascular reactivity. In seizure, microglia respond by changing from a quiescent surveillance state toward a more activated state. Activated microglia produce neurotrophic and anti-apoptotic molecules, including TGF-β and IL-10. These molecules have protective effects on sympathetic neurons. Seizure increases the expression of PACAP, which inhibits the activation of MAPK and stimulates the secretion of IL-6 into the CSF. PACAP then acts on microglial PAC1 and VPAC1 receptors to cause increased IL-10 protein expression, followed by downregulation of the expression of the pro-inflammatory receptors CD10 and B7.

To investigate the role of sympathoexcitation in acute seizure, we used a urethane-anesthetised, KA-induced model of seizure in rat. A single injection of KA in the range of 6-15 mg/kg, leads to a syndrome of recurrent status epilepticus (SE), with each seizure lasting 30 min or longer over a prolonged period in conscious rats (Lévesque and Avoli, 2013). At these doses, it is well known that seizure activity causes autonomic dysfunction with acute cardiovascular changes (Sakamoto et al., 2008; Hotta et al., 2009). Here, we aimed to determine the lowest dose of KA that elicited seizure and sympathoexcitation. It is possible that this sympathoexcitation might be responsible for the progressive deterioration of cardiovascular function in susceptible individuals and ultimately SUDEP. Several studies in human subjects during electroconvulsive therapy reported changes in ECG that are proarrhythmogenic or ischemic. Because patients having seizures during electroconvulsive therapy are under general anesthetic and neuromuscular blockade (Mokriski et al., 1992; Luckhaus et al., 2008), it is likely that any autonomic features would be blunted. Nevertheless, the finding that changes do occur suggests that seizures occurring during daily life would exhibit worse changes in ECG.

We aimed to elucidate PACAP-dependent differences in seizure-induced sympathoexcitation and a neuroprotective role of PACAP. PACAP exerts its autocrine neuroprotective (Shioda et al., 1998; Ringer et al., 2013) and paracrine anti-inflammatory (Shioda et al., 2006; Ringer et al., 2013) effects in two ways. PACAP not only inhibits the activation of members of the MAPK family such as c-Jun N-terminal kinase (JNK) (Shioda et al., 1998) but also stimulates the secretion of IL-6 in CSF (Gottschall et al., 1994; Shioda et al., 1998). This effect may be the mechanism of action of PACAP in attenuating seizure-induced sympathoexcitation (Figure 3. 7). An increased activity of MAPKs during seizures (Jeon et al., 2000; Ferrer et al., 2002) is associated with cell death in several experimental paradigms (Chan et al., 2003; Sakon et al., 2003). Although there are controversies about the pro-inflammatory and anti-inflammatory properties of IL-6, increased levels are reported to have neuroprotective effects on sympathetic neurons (März et al., 1998) and neuroprotective and anti-inflammatory effects in KA-induced seizure rats (Penkowa et al., 2001). Nomura et al. (2000) showed that PACAP gene expression increases in the PVN after KA-induced TLE in rats. Our findings suggest a mechanistic role for PACAP during epilepsy because blockade of PACAP activity during acute seizure has a detrimental effect on seizure-induced cardiovascular dysfunction. Microglia activated during seizure also express costimulatory molecules cluster of differentiation (CD)40 and B7 that may lead to further activation of microglia. PACAP, acting on microglial PAC1

and VPAC1 receptors (Delgado et al., 1999), increases IL-10 protein expression, causing a downregulation of CD40 and B7 messenger ribonucleic acid (mRNA) expression in activated microglia, thereby acting as a potent anti-inflammatory agent (Delgado et al., 1999; Kim et al., 2002). We propose that this effect of PACAP is a likely mechanism of action for the responses observed in this study (Figure 3. 7).

Microglia are the innate immune cells of the CNS and represent ~10% of the total brain cell population. Microglia can be either neuroprotective or neurodegenerative depending on circumstances (Mosser and Edwards, 2008; Loane and Byrnes, 2010; Benarroch, 2013; Biber et al., 2014). There is extensive microglial activation in animal models of seizure (Beach et al., 1995; Drage et al., 2002; Shapiro et al., 2008) and preconditioning of hippocampal microglia during the acute phase seizure results in a neuroprotective effect (Mirrione et al., 2010). Other studies report a neuroprotective role of microglia in different animal models of neurodegenerative diseases (Li et al., 2007; Lai and Todd, 2008; Mosser and Edwards, 2008; Neumann et al., 2008; Loane and Byrnes, 2010; Vinet et al., 2012; Benarroch, 2013; Biber et al., 2014), such as ischemic injury (Kitamura et al., 2004; Kitamura et al., 2005; Imai et al., 2007; Lalancette-Hébert et al., 2007) and chronic stress-induced depression (Kreisel et al., 2014). Until now, a role for microglia in seizure-induced cardiovascular responses was unclear. Our results demonstrate that inhibition of microglial activation and proliferation during KA-induced seizure worsens the sympathoexcitation. The microglial antagonists minocycline and doxycycline act by inhibiting the p38 MAPK pathway. Current findings suggest a neuroprotective potential of activated microglial cells on sympathetic preganglionic neurons. This neuroprotective effect of microglia may occur through an endogenous production of neurotrophic and anti-apoptotic molecules such as TGF-β and IL-10 (Benarroch, 2013) or by increased glutamate uptake (Persson and Rönnbäck, 2012). In this scenario, TGF-β and IL-10 mediated activation of microglia into regulatory or M2 type has potent anti-inflammatory and neuroprotective potential.

Resident microglia actively survey their environment and are referred to as surveilling microglia (Nimmerjahn et al., 2005). Activated microglia dynamically change into two different phenotypes, M1 or M2, that are generally considered to be inflammatory and protective respectively, and depending on the type of the stimulus and microenvironment, participate not only in mechanisms of injury, but also in neuroprotection, repair, and circuit refinement in the CNS (Mosser and Edwards, 2008). Our current findings suggest that acute seizure causes microglia to adopt the M2 phenotype and protect sympathetic neurons

from excitotoxicity. The neuroprotective effect on sympathetic neurons may be due to microglial production of IL-10. Inhibiting microglial activation with IT minocycline or doxycycline infusion in seizure-induced rats increased sympathoexcitation, leading to increased HR and BP. Recent phase 3 clinical trials of minocycline in amyotrophic lateral sclerosis patients showed that minocycline has a harmful effect on an amyotrophic lateral sclerosis functional rating scale and greater mortality during the 9-month treatment phase compared with placebo treatment (Gordon et al., 2007). These findings are consistent with our current findings, which suggest that microglial antagonists worsen the effect of cardiovascular dysfunction during seizure. Overall, we propose that microglial activation during acute seizure has a neuroprotective effect due to adoption of the M2 phenotype or "protective" state. Microglial inactivation during acute seizure produces more neuroexcitation and cardiovascular dysfunction.

In conclusion, low doses of KA, which are adequate to produce seizures, lead to slowly developing, but prolonged and significant increases in SNA, MAP, HR, and EEG activity and a prolongation of the QTc interval. This type of severe disruption in central autonomic function may ultimately lead to progressive deterioration of cardiovascular function and SUDEP.

The clinical implications of our findings are that PACAP may exert a protective role against known adverse cardiovascular effects of seizure because antagonism of the PACAP receptor exacerbated the seizure-induced cardiovascular effects. PACAP may exert neuroprotective effects by preventing the activation of MAPKs and increasing levels of IL-6 and by its action on microglia. Together, our findings suggest that targeting PACAP and microglial activation may provide new therapeutic avenues for the prevention of seizure-induced cardiovascular dysfunction and SUDEP.

3.6. <u>Supplementary results</u>

3.6.1. <u>Effects of KA-induced seizures on PNA and phrenic nerve frequency (PNF)</u>

The phrenic nerve frequency (PNF) did not change in KA-induced seizure group of rats, except 10 mg/kg, compared to vehicle control. 10 mg/kg KA-induced seizure rats showed significant increase in PNF compared to vehicle control at 60 min (ΔPNF: 31.6 ± 11.2; $p \leq 0.01$, Figure 3. 8A) and 120 min post-treatment (ΔPNF: 48.7 ± 19.8; $p \leq 0.01$, Figure 3. 8B). However, % change in PNA was not significant in any of the groups of rats treated with KA compared with vehicle-treated group, both at 60 (Figure 3. 8C) and 120 min (Figure 3. 8D) post-KA treatment.
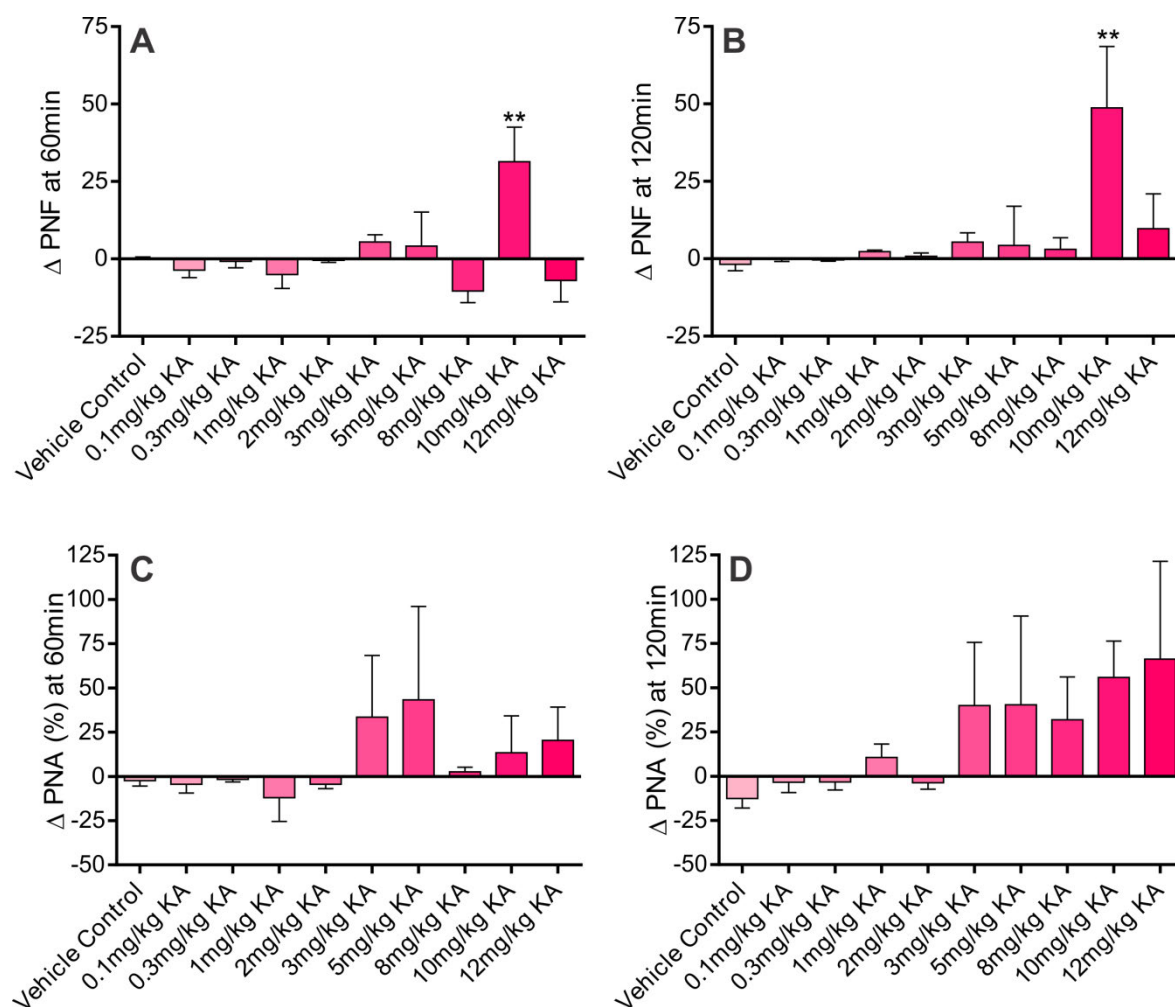
Figure 3. 8: *In vivo* effects of different doses of KA on PNF and PNA at 60 and 120 min post KA.

Change in PNF at 60 min (A), and at 120 min (B) and % change in PNA at 60 min (C), and at 120 min (D) post i.p. KA or PBS in different groups of rats. Statistical significance was determined using one-way ANOVA followed by t tests and Dunnett's correction to compare effects with the control value. Data are expressed as mean $\pm$ SEM. ** $p \leq 0.01$ compared with vehicle control group.

3.6.2. Confirmation of positions of recording EEG electrodes

A position of recording EEG electrodes was confirmed with cresyl violet staining (Figure 3. 9). A tip of electrodes was found into the area of the hippocampus.
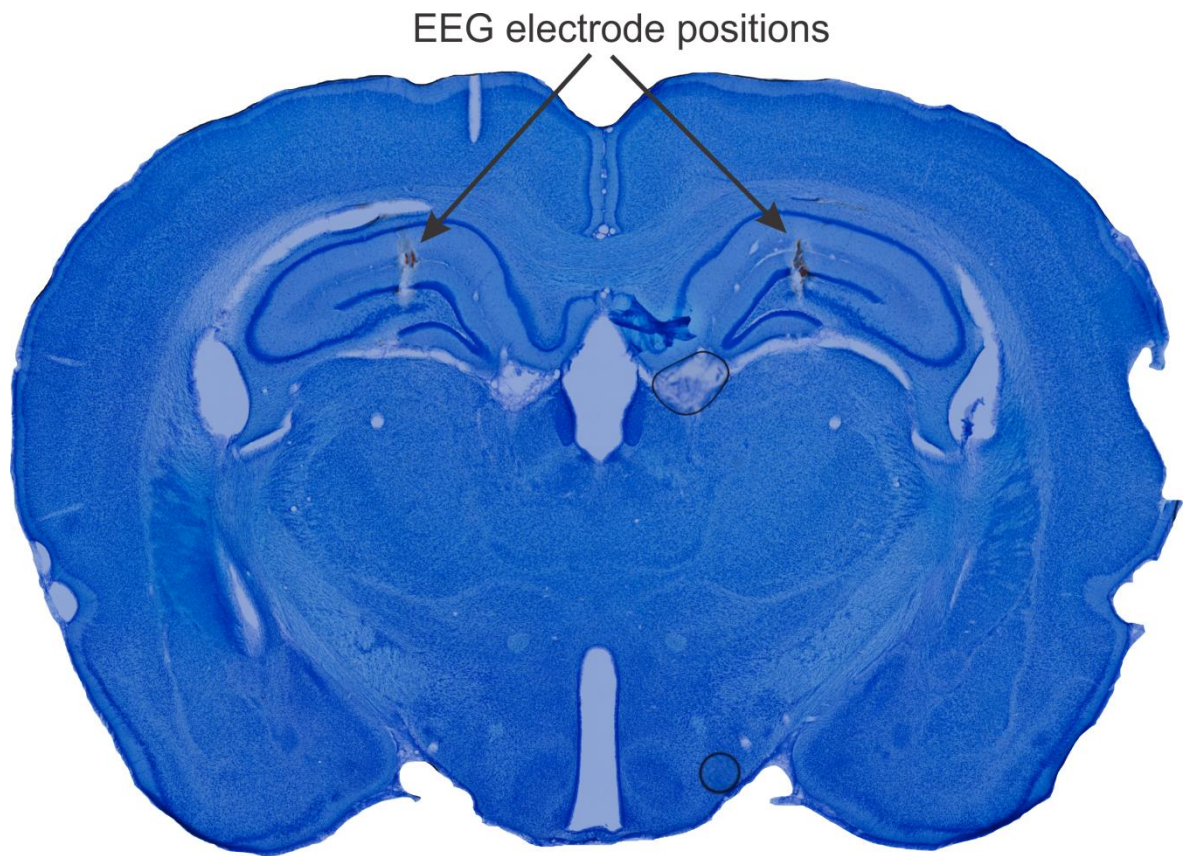
Figure 3. 9: Bilateral hippocampal EEG electrode positions.

Stereotaxic coordinates are 5.2 mm anterior to lambda, 3 mm lateral to midline and 2-3 mm below the skull surface.

Chapter 4
Activation of glutamatergic receptors in RVLM mediates sympathoexcitation during acute seizures that also causes proarrhythmogenic changes mediated by PACAP and microglia in rats

The work in this Chapter is published and fluorescence image is illustrated as a cover art for the "Journal of Neuroscience-An Official Journal of Society for Neuroscience" Issue: 13 January 2016: (36) 2.

Bhandare AM, Kapoor K, Pilowsky PM, Farnham MMJ (2016) Seizure-induced sympathoexcitation is caused by activation of glutamatergic receptors in RVLM that also causes proarrhythmogenic changes mediated by PACAP and microglia in rats. J Neurosci 36:506-517.

"The candidate designed experiments, performed all animal experiments, analysed data and interpreted results. Candidate was the major contributor to the manuscript writing, editing, figures drawing and revision. Paul Pilowsky and Melissa Farnham contributed to design of experiments, interpretation of results and editing, revision and final approval of manuscript. Komal Kapoor performed tissue extraction, immunohistochemistry experiments and analysis and processed cover art illustration image."

Table of Contents

4.1. <u>Abstract</u>

Cardiovascular autonomic dysfunction in seizure is a major cause of sudden unexpected death in epilepsy (SUDEP). The catecholaminergic neurons in the rostral ventrolateral medulla (RVLM) maintain sympathetic vasomotor tone and blood pressure (BP) through their direct excitatory projections to the intermediolateral cell column (IML). Glutamate, the principal excitatory neurotransmitter in the brain, is increased in seizures. Pituitary adenylate cyclase-activating polypeptide (PACAP) is an excitatory neuropeptide with neuroprotective properties whereas microglia are key players in inflammatory responses in the central nervous system (CNS). We investigated the roles of glutamate, PACAP and microglia on RVLM catecholaminergic neurons during the cardiovascular responses to 2 mg/kg kainic acid (KA)-induced seizures in urethane-anesthetised, male Sprague-Dawley (SD) rats. Microinjection of the glutamate antagonist, kynurenic acid (KYNA) (50 nl; 100 mM) into RVLM, blocked the seizure-induced $43.2 \pm 12.6\%$ sympathoexcitation ($p \leq 0.05$) and abolished the pressor responses, tachycardia, and QT interval prolongation. PACAP or microglial antagonists (50 nl), (PACAP(6-38) (15 picomoles); minocycline (10 mg/ml)), microinjected bilaterally into RVLM had no effect on seizure-induced sympathoexcitation, pressor responses or tachycardia, but abolished the prolongation of QT interval. The actions of PACAP or microglia on RVLM neurons do not cause sympathoexcitation, but they do elicit proarrhythmogenic changes. Microglia surrounding catecholaminergic neurons are in a surveillance state with no change in the number of M2 microglia (anti-inflammatory) in 2 and 10mg/kg KA-induced seizure rats. In conclusion, seizure-induced sympathoexcitation is caused by activation of glutamatergic receptors in RVLM that also cause proarrhythmogenic changes mediated by PACAP and microglia.

4.2. <u>Significance statement</u>

Sudden unexpected death in epilepsy (SUDEP) is a major cause of death in epilepsy. Generally, seizures are accompanied by changes in brain function leading to uncontrolled nerve activity causing high BP, rapid heart rate (HR), and abnormal heart rhythm. Nevertheless, the brain chemicals causing these cardiovascular changes are unknown. Chemicals, such as glutamate and PACAP, whose expression is increased after seizures, act on specific cardiovascular nuclei in the brain and influence the activity of the heart, and blood vessels. Microglia, which manage excitation in the brain, are commonly activated after seizure and produce pro-inflammatory and/or anti-inflammatory factors. Hence, we aimed to determine the effects of blocking glutamate, PACAP, and microglia in the RVLM and their contribution to cardiovascular autonomic dysfunction in seizure.

4.3. <u>Introduction</u>

Seizure-induced cardiovascular autonomic dysfunction is a common cause of SUDEP, which accounts for 5-17% deaths in people with epilepsy (Sakamoto et al., 2008; Surges et al., 2009; Bardai et al., 2012; Massey et al., 2014). The RVLM contains sympathetic premotor neurons (C1), which are a subset of catecholaminergic neurons that express all of the enzymes necessary for the synthesis of adrenaline (Schreihofer and Guyenet, 1997; Phillips et al., 2001). Sympathetic vasomotor tone and BP is regulated by C1 neurons, and another smaller population of neurons that is also located in the RVLM, through their direct projections to the IML (Ross et al., 1984b; Guyenet, 2006; Pilowsky et al., 2009). Seizure-induced increased activity of C1 catecholaminergic neurons (c-Fos) is well documented (Kanter, 1995; Silveira et al., 2000). Seizure causes an increase in sympathetic nerve activity (SNA) and has a significant effect on cardiac electrophysiology and HR (Nei et al., 2004; Metcalf et al., 2009b; Damasceno et al., 2013). There is no information about the neurotransmitters mediating activation of brainstem catecholaminergic neurons contributing to the autonomic manifestations that frequently accompany epileptic seizures.

As we have documented previously (Chapter 3), a low-dose KA-induced seizures in rat cause sympathoexcitation, increases in mean arterial pressure (MAP) and HR, and proarrhythmogenic changes, including prolongation of the QT interval (Bhandare et al., 2015). The evidence suggests that PACAP and microglia have a protective effect on sympathetic preganglionic neurons in the IML where they ameliorate the sympathoexcitatory effect of seizures. PACAP is well established to be neuroprotective (Shioda et al., 1998; Ohtaki et al., 2006), through its effect on microglia (Wada et al., 2013). Recently, we investigated the excitatory effect of PACAP in cardiovascular autonomic nuclei (Farnham et al., 2008; Farnham et al., 2012). KA-induced seizures dramatically increase PACAP expression in central autonomic nuclei (paraventricular nucleus (PVN)) (Nomura et al., 2000). Additionally, microglia can be pro-inflammatory or anti-inflammatory in some models of diseases, such as temporal lobe epilepsy (TLE) (Shapiro et al., 2008; Mirrione et al., 2010; Vinet et al., 2012). In seizure, there is extensive activation of microglia in patients and in animal models (Beach et al., 1995; Shapiro et al., 2008; Eyo et al., 2014). Moreover, there are reports suggesting that PACAP modulates the activated microglial state (Wada et al., 2013; Brifault et al., 2015). This important relationship between PACAP, microglia, and seizure-induced increase in its expression or activation in cardiovascular autonomic nuclei makes them a very promising target for the development of therapy for seizure-induced sympathoexcitation and cardiovascular

dysfunction. In addition, brain glutamate levels are increased in patients and animal models of TLE (Meldrum et al., 1999; Blümcke et al., 2000) and play a major pathogenic role for neuronal hyperexcitability. However, glutamatergic drive within RVLM neurons is not important for maintenance of basal tonic activity of catecholaminergic neurons or BP (Guyenet et al., 1987; Araujo et al., 1999; Sved et al., 2002). Collectively, the sympathoexcitation during seizure may be due to an increased glutamate turnover that could be reversed by glutamate antagonist microinjection into RVLM without affecting basal sympathetic output and BP.

Overall, the aims of this study were to identify the role of PACAP, microglia and glutamatergic receptors in the RVLM to regulate catecholaminergic neuronal hyperexcitability and other cardiovascular changes following low dose KA-induced seizures in rats. To achieve these aims we used a combination of electrophysiological and neuroanatomical approaches with KA-induced seizures in rats. Seizures were induced with 2 mg/kg intraperitoneal (i.p.) KA injection in urethane-anesthetised, vagotomised, paralysed and artificially ventilated rats and 50 nl of each PACAP antagonist, PACAP(6-38); microglial antagonist, minocycline; or glutamate antagonist, KYNA were microinjected into the RVLM of a different group of rats. The changes in microglial morphology and the expression of the anti-inflammatory M2 microglial phenotype in the vicinity of RVLM catecholaminergic neurons in response to 2 and 10 mg/kg KA-induced seizures in rats was analysed with immunohistochemistry.

4.4. **Materials and methods**

4.4.1. Animals

The animal usage and protocols were in accordance with the Australian code of practice for the care and use of animals for scientific purposes. The protocols were approved by the Animal Care and Ethics Committee of Macquarie University and the Sydney Local Health District (section 2.1.1; Appendix 3). All electrophysiology and histology experiments were conducted on adult male SD rats (250-350 g).

4.4.2. Surgical preparations

For electrophysiology experiments ($n = 31$) rats were anesthetised with 10% urethane (1.3-1.5 g/kg i.p.) (section 2.2.2.1) and for histology experiments ($n = 15$) with 3% sodium pentobarbital (50 mg/kg i.p.) (section 2.2.2.2) and the depth of anesthesia was monitored and maintained as specified in respective sections. Atropine sulfate (100 µg/kg) was administered with the first dose of anesthetics to prevent bronchial secretions. After the

completion of the general surgical procedures described below, rats were secured in a stereotaxic frame and body temperature was recorded and maintained between 36.5 and 37.5^{0}C throughout the experiment using a homeothermic blanket.

4.4.3. General surgical procedures and electroencephalogram (EEG) electrode placement

The right carotid artery and jugular vein were cannulated, as detailed in section 2.3.1, for the recording of BP, and for the administration of drugs and fluids, respectively, with a tracheostomy to enable mechanical ventilation (section 2.3.2). A three lead electrocardiogram (ECG) was recorded and HR was derived from it (section 2.3.4). Rats were vagotomised (section 2.3.5.1), artificially ventilated with oxygen-enriched room air and paralysed with pancuronium bromide (section 2.3.3). Arterial blood gases were analysed with an electrolyte and blood gas analyser and partial pressure of carbon dioxide (PaCO$_2$) was maintained at 40 ± 2 and pH between 7.35-7.45.

Two EEG electrodes were placed over the dorsal surface of the skull. A single electrode wire was inserted into each hole using stereotaxic manipulator (section 2.3.8). Signals were amplified, band-pass filtered from 1 Hz to 10 kHz, amplified 100X, and digitised at 20 kHz. Electrode positions were confirmed with cresyl violet staining (section 2.7.2).

4.4.4. Seizure induction

For electrophysiology experiments, seizures were induced by i.p. injection of 2 mg/kg KA in SD rats (section 2.2.6). In the histology study, two doses of KA (2 and 10 mg/kg; i.p.) were used to elicit mild and severe seizures in rats to analyse their effects on the morphology of microglia in the vicinity of catecholaminergic neurons in the RVLM (section 2.2.6). In the study, rats were paralysed and had no behavioural seizures. KA responses were recorded for 2 h post-KA injection, during which continuous monitoring of EEG was used to identify the development of seizures (section 2.2.6). To investigate the duration of seizure-induced cardiovascular responses, 2 mg/kg KA-induced seizures were recorded until cardiovascular parameters returned to baseline ($n = 4$) (section 2.5.8).

4.4.5. *In vivo* electrophysiology

4.4.5.1. Isolation and preparation of nerves

The left splanchnic sympathetic nerve and the left phrenic nerve were isolated, dissected and tied with 5/0 silk thread (sections 2.3.5.2 and 2.3.5.3). Nerve activity was recorded with bipolar stainless steel electrode and filtered with a 50/60-Hz line filter (section 2.3.6).

4.4.5.2. *RVLM site detection, confirmation, and microinjection*

The detailed procedure is explained in section 2.3.10. Briefly, the dorsal surface of the medulla oblongata was exposed by occipital craniotomy and the dura was removed. The bilateral RVLM stereotaxic coordinates were measured with respect to calamus scriptorius and confirmed if a 50 nl microinjection of 100 mM glutamate increased BP > 30 mmHg. After glutamate confirmation, stable baseline parameters were recorded at least for 30 min.

In vehicle and KA control groups of rats ($n = 5$), 50 nl of 10 mM phosphate-buffered saline (PBS) was microinjected bilaterally in the RVLM (section 2.3.10.2). PACAP(6-38) ($n = 6$), minocycline ($n = 5$) and KYNA ($n = 5$) (Miyawaki et al., 2002a) were bilaterally microinjected in the RVLM in a dose of 50 nl in a different group of rats. In all rats, microinjections were made 15 min before i.p. KA or PBS injection. Microinjections were not made in $n = 4$ rats that were used to investigate the duration of KA-induced cardiovascular effects. At the conclusion of the experiment, 50 nl of Chicago Sky Blue (2%) was microinjected at the site of the RVLM, and rats were either euthanised with 0.5 ml of 3 M potassium chloride (KCl; intravenous (i.v.)) (section 2.3.11), or deeply anesthetised and perfused with 400 ml of ice-cold 0.9% saline followed by 400 ml of 4% paraformaldehyde (PFA) solution (section 2.2.4). The brains were removed from the perfused rats and postfixed in the same fixative overnight. Cerebrum and brainstem were sectioned coronally (100 µm) and stained with cresyl violet for histological verification of the EEG electrode positions in hippocampus and microinjection site in the RVLM, respectively (section 2.7.2).

4.4.6. Histology

4.4.6.1. *Perfusions*

At the conclusion of the experiment, rats used for histology study (in all groups $n = 5$) were deeply anesthetised with an overdose of sodium pentobarbital and given 1 ml of heparin via the venous line. Rats were transcardially perfused with 400 ml of ice-cold 0.9% saline followed by 400 ml of 4% PFA solution as detailed in section 2.2.4. The brains were then removed and postfixed in the same fixative for 18-24 h.

4.4.6.2. *Sectioning and immunohistochemistry*

Immunohistochemical analysis was done in $n = 3$ out of 5 rats in each group and the methods are specified in detail in section 2.7.1 and 2.7.3. In brief, brainstems were sectioned coronally (40 µm thick) with a vibrating microtome and collected sequentially

into five different pots containing a cryoprotectant solution and stored at -20^0C until further processing. Free-floating sections were used for all histological procedures. Sections were rinsed, blocked and incubated in primary antibodies: mouse anti-tyrosine hydroxylase (TH) (1:500), rabbit anti-cluster of differentiation (CD)206 (1: 2,000) and goat anti-ionised calcium-binding adapter molecule-1(Iba1) (1: 1,000). After 48 h, sections were rinsed and TH, CD-206 and Iba1 immunoreactivity was subsequently revealed by overnight incubation with the following secondary antibodies at 1:500 dilutions: cyanine dye (Cy)5-conjugated donkey anti-mouse, Alexa Fluor 488-conjegated donkey anti-rabbit, and Cy3-conjugated donkey anti-goat (Table 2.4). Sections were rinsed, mounted sequentially on glass slides, and coverslipped with Vectashield.

4.4.7. Data acquisition and analysis

4.4.7.1. Electrophysiology data

Data were acquired using a CED 1401 ADC system and Spike2 acquisition and analysis software. The EEG activity raw data was DC removed. The power in the gamma frequency range was analysed, as mentioned in section 2.5.1. A power spectrum analysis was done from 5-min blocks taken 1 min before microinjection or i.p. injection and 60 and 120 min after i.p. injection. The percent change in power spectrum area was calculated for each rat at 60 and 120 min post i.p. injection compared to the pre-treatment area (taken as 100%) and grouped together. Phrenic nerve activity (PNA) was rectified and smoothed (τ 0.5 s) and the area under curve (AUC) was analysed from 1-min blocks taken 1 min before microinjection and 60 and 120 min after i.p. injection (section 2.5.2). SNA was rectified, and smoothed (τ 2 s), and normalised to zero by subtracting the residual activity 5-10 min after death. The integrated SNA trace was calibrated (baseline as 100%) and analysed for AUC between 60 to 120 min after i.p. KA or PBS injection as detailed in section 2.5.3. MAP and HR were analysed from 1-min blocks taken 1 min before microinjection or i.p. injection and 30, 60, 90 and 120 min after i.p. injection (only 120 min results are shown in graphs) (section 2.5.4). End-tidal CO_2 ($ETCO_2$), and core temperature were analysed from 1-min blocks taken 1 min before microinjection or i.p. injection and 30, 60, 90, and 120 min after i.p. injection of either KA or PBS (section 2.5.7). Arterial blood gas levels ($PaCO_2$, and pH) were measured 10 min before microinjection or i.p. injection and 120 min after KA or PBS injections in all animals. In the rats used to investigate the duration of KA-induced seizures, the duration of effect was analysed from the time of i.p. KA injection up to the point where SNA, MAP, and HR returned to baseline (section 2.5.8). Changes in EEG activity were analysed at the point where SNA returned to baseline and

compared to the pre-KA (control) and 60 min post-KA injection (seizure control) period. A log transformation was applied to EEG raw values since variances were not normally distributed, and/or heterogeneous. Statistical analysis was carried out in GraphPad Prism software. Statistical significance was determined using one-way analysis of variance (ANOVA) followed by t-tests with the Holm-Šídák correction. Multiple comparisons were done between groups. $p \leq 0.05$ was considered significant (section 2.6).

4.4.7.2. Histology imaging and analysis

All images were acquired using a Zeiss Axio Imager Z2. Images were captured at 20X and 40X magnifications (sections 2.8 and 2.9). A 0.16 mm^2 box was placed within the imaged RVLM and this area was used for analysis. The morphological analysis (branch length and number of endpoint processes) of Iba1-labelled microglia in the vicinity of TH-labelled RVLM neurons was carried out using ImageJ plugin software (section 2.9) and GraphPad Prism was used for chi-square test for goodness of fit (section 2.10). The proportions of CD206 labelled anti-inflammatory M2 microglia in the RVLM of 2 and 10 mg/kg KA-treated rats were compared with the vehicle-treated group. Statistical significance was determined using nonparametric Kruskal-Wallis test (Sokal and Rohlf, 2012).

4.4.8. Calculation of corrected QT (QTc) interval

QT, PR, and RR intervals were calculated from the ECG recordings. ECG raw data was processed (DC remove), wherever baseline fluctuations were prominent. QTc interval was calculated by dividing the QT interval in seconds by the square root of the RR interval in seconds (Bazett, 1920) (section 2.5.9). The QTc was obtained before and 120 min after vehicle or KA injection. The PR and QTc interval statistical analysis was carried out in GraphPad Prism software. Statistical significance was determined using one-way ANOVA between treatment groups followed by t-tests with the Holm-Šídák correction. Multiple comparisons were done between groups (section 2.6). $p \leq 0.05$ was considered significant.

4.5. Results

4.5.1. Sympathoexcitation, tachycardia, and pressor responses due to KA-induced seizures in rats

Intraperitoneal injection of 2 mg/kg KA induces seizures, and subsequently, increases HR, MAP, and SNA in KA control group of rats (Figure 4. 1A). Note that KA (2 mg/kg i.p.) leads to the development of hippocampal seizure activity within ~15-20 min. At this time, there are no changes in sympathetic activity (Figure 4. 2), BP or HR (Figure 4. 1A).

Figure 4. 1: Effect of bilateral RVLM microinjection of (A) PBS (50 nl) and (B) KYNA (50 nl; 100 mM) followed by 2 mg/kg i.p. KA in an anesthetised rat.

Showing the effect on: from the top, (i) HR (bpm), (ii) AP (mmHg), (iii) SNA (%), and (iv) EEG (μV). Arrow indicates time of RVLM microinjections and i.p. KA. Dotted arrows indicate the starting points for increase in EEG and/or SNA activity. Right side panels, Pre (a) and post (b) KA EEG represents the expanded waveform from respective period. Baseline (a), which is a pre-KA period with desynchronous waves, and (b) post-KA period with increased gamma range frequencies and followed by the data from the same EEG, drawn as a power spectrum (c, d, respectively) (during post-KA period gamma range frequencies, which is shown between two dotted lines) are increased. Increase in gamma range frequency (25-45 Hz) is characteristic property of KA-induced seizures (Olsson et al., 2006; Gurbanova et al., 2008).

A. RVLM PBS + 2 mg/kg KA IP

Right and left
RVLM 50 nl PBS
microinjection

2 mg/kg
IP KA

Start of
increase in
EEG activity

Start of
increase
in SNA

HR
bpm

570
500
420

AP
mmHG

180
150
100
50

ReSmSNA
%

200
150
100
50

EEG (uV)

1000
500
0
-500
-1000

30 min

a) Pre KA EEG
expanded on
right side

b) Post KA EEG
expanded on
right side

a) Pre KA EEG

500
0
-500
-1000

10 sec

b) Post KA EEG

500
0
-500
-1000

10 sec

c)

EEG (uV²)

250
200
150
100
50
0

0 10 20 30 40 50 60 70
Frequency (HZ)

d)

EEG (uV²)

250
200
150
100
50
0

0 10 20 30 40 50 60 70
Frequency (HZ)

B. RVLM KYNA + 2 mg/kg KA IP

Right and left
RVLM 50 nl KYNA
microinjection

2 mg/kg
IP KA

Start of
increase in
EEG activity

HR
bpm

570
500
420

AP
mmHG

180
150
100
50

ReSmSNA
%

200
150
100
50

EEG (uV)

500
250
0
-250
-500

30 min

a) Pre KA EEG
expanded on
right side

b) Post KA EEG
expanded on
right side

a) Pre KA EEG

500
0
-500

10 sec

b) Post KA EEG

500
0
-500

10 sec

c)

EEG (uV²)

6
5
4
3
2
1
0

0 10 20 30 40 50 60 70
Frequency (HZ)

d)

EEG (uV²)

6
5
4
3
2
1
0

0 10 20 30 40 50 60 70
Frequency (HZ)

Ten to fifteen minutes after the start of the hippocampal seizure activity, SNA, MAP and HR began to increase (Figure 4. 1A and Figure 4. 2). Autonomic changes are entirely downstream effects of hippocampal seizures as there was no seizure activity (increase in gamma frequency which is a typical sign of KA-induced seizures) in the sympathetic nerve recording until at least 70 min after KA injection whereas SNA started to increase 25-30 min after KA injection (Figure 4. 2). Taken together these findings indicate that central autonomic nuclei are not the source of KA-induced seizures. Between 60-120 min after KA injection, SNA AUC was increased by $43.2 \pm 12.6\%$ ($p = 0.04$) compared to the vehicle control group (Figure 4. 3A). In the KA-induced seizure group, MAP and HR were increased by 21 ± 4 mmHg ($p = 0.008$), and 32 ± 7 beats per minute (bpm) ($p = 0.0001$), respectively compared to the vehicle-treated group (Figure 4. 3B-C): the findings support the notion that seizure is the cause of the dramatic increase in SNA, tachycardia and pressor effects (Sakamoto et al., 2008; Bealer et al., 2010). Bilateral microinjection of PBS (50 nl) had a transient and non-significant effect on MAP, HR and SNA, that lasted for only a few minutes (Figure 4. 1A).

The induction of seizures was confirmed with hippocampal EEG recordings; the power spectra were obtained from the same expanded EEG waveforms as indicated (Figure 4. 1A). The spectral changes in EEG at 60 and 120 min after KA injection were obtained using Fourier analysis of 5 min EEG intervals and the AUC between gamma frequency range. The steep increase in gamma wave amplitude was observed at both 60 (Δ 1038 $\pm$ 402%, $p = 0.0001$) and 120 min (Δ 1329 $\pm$ 390%, $p = 0.0005$) after KA injection (Figure 4. 1A and Figure 4. 3D-E). This finding also shows that KA-induced seizures in rats continued for at least 120 min following KA injection which is consistent with results of the experiments performed to analyse the duration of seizure-induced cardiovascular effects.

Kainic acid (2 mg/kg)-induced seizures and its effects on SNA, MAP and HR lasted for approximately 3 h. After this time, SNA, MAP and HR returned to baseline values at 170, 196 and 160 min, respectively. At these time points EEG activity was significantly reduced compared to the seizure period (at 60 min post-KA) but did not return to baseline.

We did not observe any changes in PNA, expired CO_2 or body temperature in any of the groups (results not shown). Blood gas analysis confirmed that $PaCO_2$ and pH were within a normal physiological range ($PaCO_2$ was 40 ± 2 and pH between 7.35-7.45) throughout the experiment.
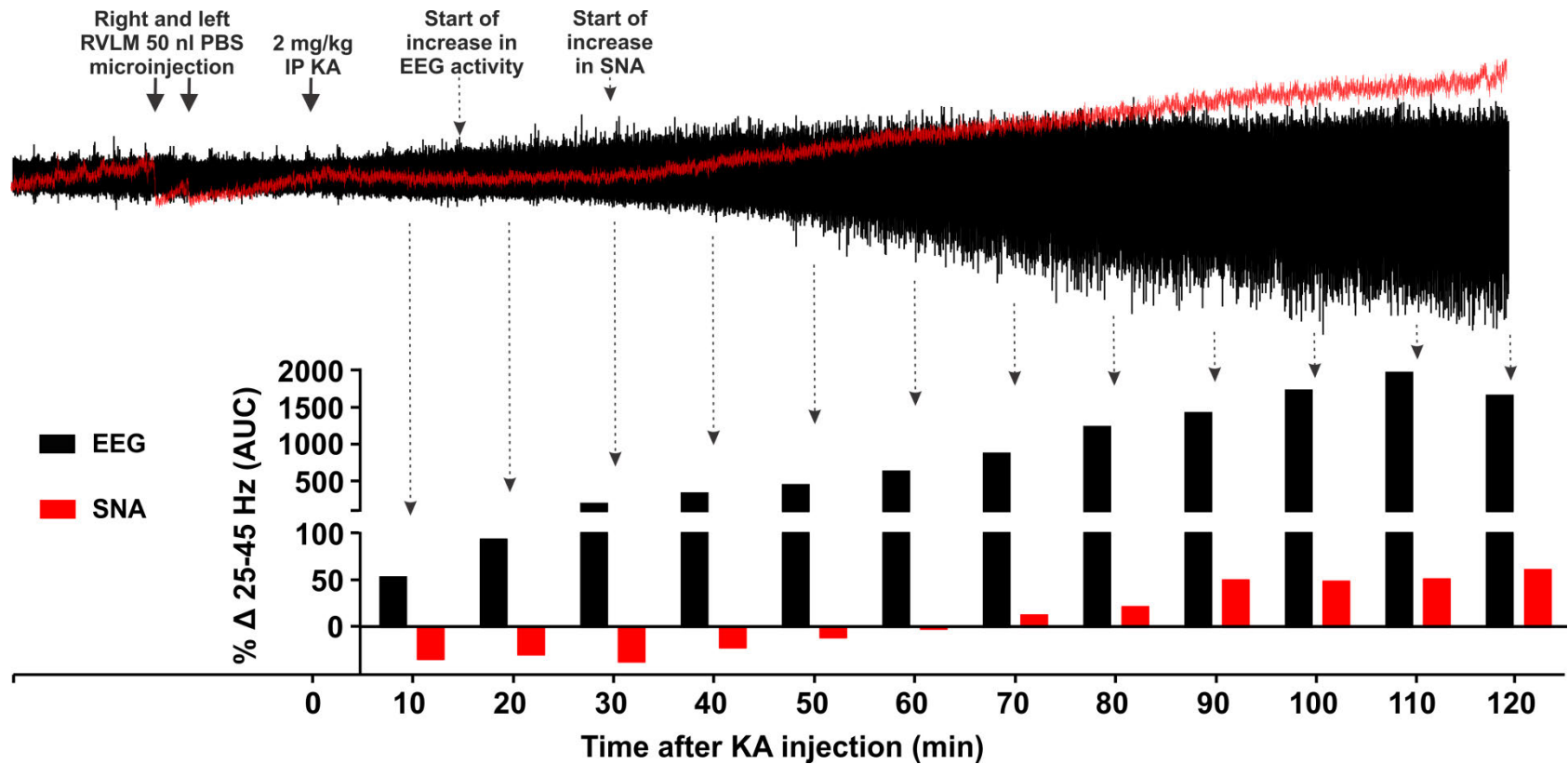
Figure 4. 2: Effects of KA treatment on induction of seizures in hippocampus and central autonomic nuclei.

Change in gamma range frequency (25-45 Hz) in hippocampal EEG and sympathetic nerve recordings every 10 min after 2 mg/kg KA injection. Arrow indicates time of RVLM microinjections and i.p. KA. Dotted arrows indicate the starting points for increase in EEG and/or SNA activity. Induction of seizure activity in SNA does not start at least until 70 min after KA injection, whereas hippocampal seizure activity starts ~15-20 min after KA injection followed by an increase in SNA at 25-30 min. Time-dependent increases in hippocampal seizure activity occur up to 110 min after KA injection followed by a fall.

4.5.2. <u>Sympathoexcitation, tachycardia, and pressor effects during seizure are caused by glutamatergic receptors in the RVLM and not by PACAP or microglial activation</u>

Our findings demonstrate that sympathoexcitation during seizure is caused by glutamatergic receptor activation in the RVLM, since bilateral microinjection of glutamate antagonist KYNA completely abolished the seizure-induced sympathoexcitation in rats (Figure 4. 1B and Figure 4. 3A). After microinjection of KYNA in five rats, KA-induced seizures were present (Figure 4. 1B and Figure 4. 3D-E), but pressor and HR responses were blocked ($p = 0.005$ and 0.001, respectively) compared to KA control group (Figure 4. 1B and Figure 4. 3B-C). The KA-induced seizures caused no change (Δ -1.0 ± 6.2%) in SNA after bilateral microinjection of KYNA and was significantly reduced compared to KA control group ($p = 0.04$) (Figure 4. 3A). In KYNA microinjected group of rats, MAP and HR were not significantly changed compared to vehicle-treated group (Δ -3 ± 5 mmHg and Δ -5 ± 7 bpm, respectively; Figure 4. 3B-C). The findings reveal that KA-induced sympathoexcitation, tachycardia, pressor responses along with changes in QT interval are downstream effects of seizure and do not have a direct effect on cardiomyocytes.

Bilateral microinjection of PACAP(6-38) into the RVLM of KA-induced seizure rats did not ameliorate the significant increase in SNA (Δ 53.7 ± 9.6%; $p = 0.007$) compared to the vehicle-treated group (Figure 4. 3A). The HR and MAP responses in PACAP(6-38) group were still significantly increased compared to the vehicle control group of rats (Figure 4. 3B-C). The lack of response to the PACAP antagonist (PACAP(6-38)), was replicated following bilateral RVLM microinjection of minocycline in seizure-induced rats. Following minocycline, there was significant increase in SNA (Δ 55.1 ± 13.8%; $p = 0.006$; Figure 4. 3A), as well as MAP and HR (Δ 16 ± 5 mmHg and Δ 14 ± 5 bpm; $p = 0.04$ and 0.02 respectively; Figure 4. 3B-C) compared to vehicle control group of rats.
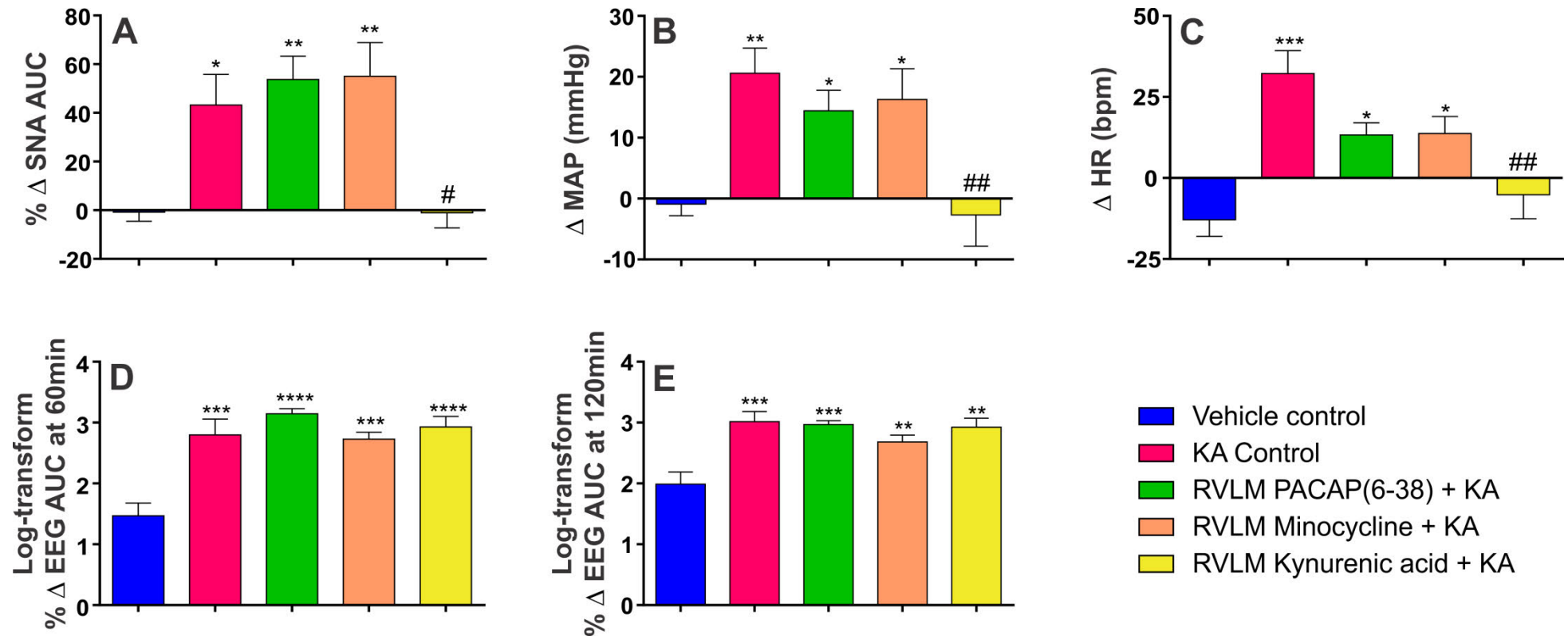
Figure 4. 3: *In vivo* **effects of RVLM microinjection of PBS, PACAP(6-38), minocycline, and KYNA in 2 mg/kg KA-induced seizure rats.**

Change in SNA (AUC) between 60-120 min post i.p. treatment (A), change in MAP 120 min post i.p. PBS or KA injection (B), change in HR at 120 min post i.p. PBS or KA injection (C) and log transform of % change in EEG activity (gamma frequency AUC), at 60 min (D) and 120 min (E) post i.p. PBS or KA injection in different groups of rats after development of seizure. Statistical significance was determined using one-way ANOVA followed by t-tests with a Holm-Šídák correction. Data expressed as mean ± SEM. ****$p \leq 0.0001$, ***$p \leq 0.001$, **$p \leq 0.01$ and *$p \leq 0.05$ compared with vehicle control group. #$p \leq 0.05$ compared with KA control group.

4.5.3. <u>After KA-induced seizures, microglia are in surveillance state in the vicinity of the RVLM neurons with no change in the proportion of M2 phenotype</u>

Immunohistochemical analysis was done in rats with vehicle treatment and 2 and 10 mg/kg i.p. KA ($n = 3$) to analyse the morphology of Iba1-labelled microglia and proportion of anti-inflammatory M2 phenotype in the vicinity of TH-labelled RVLM neurons. The effect of different doses of KA on MAP, HR and EEG are shown in Figure 4. 4 ($n = 5$). A 120 min after 2 and 10 mg/kg KA treatment, the MAP (Δ 18 ± 6 and Δ 29 ± 5; $p = 0.02$ and 0.001, respectively; Figure 4. 4A), HR (Δ 18 ± 18 and Δ 58 ± 19; $p = 0.05$, and 0.002, respectively; Figure 4. 4B), EEG activity at 60 min (Δ 1791 ± 622 and Δ 1651 ± 400; $p = 0.007$ and 0.007; respectively; Figure 4. 4C) and EEG activity at 120 min (Δ 4164 ± 2504 and Δ 1995 ± 563; $p = 0.04$ and 0.04; respectively; Figure 4. 4D) was significantly increased compared to vehicle-treated rats. The findings are consistent with *in vivo* electrophysiology data and results presented in Chapter 3.
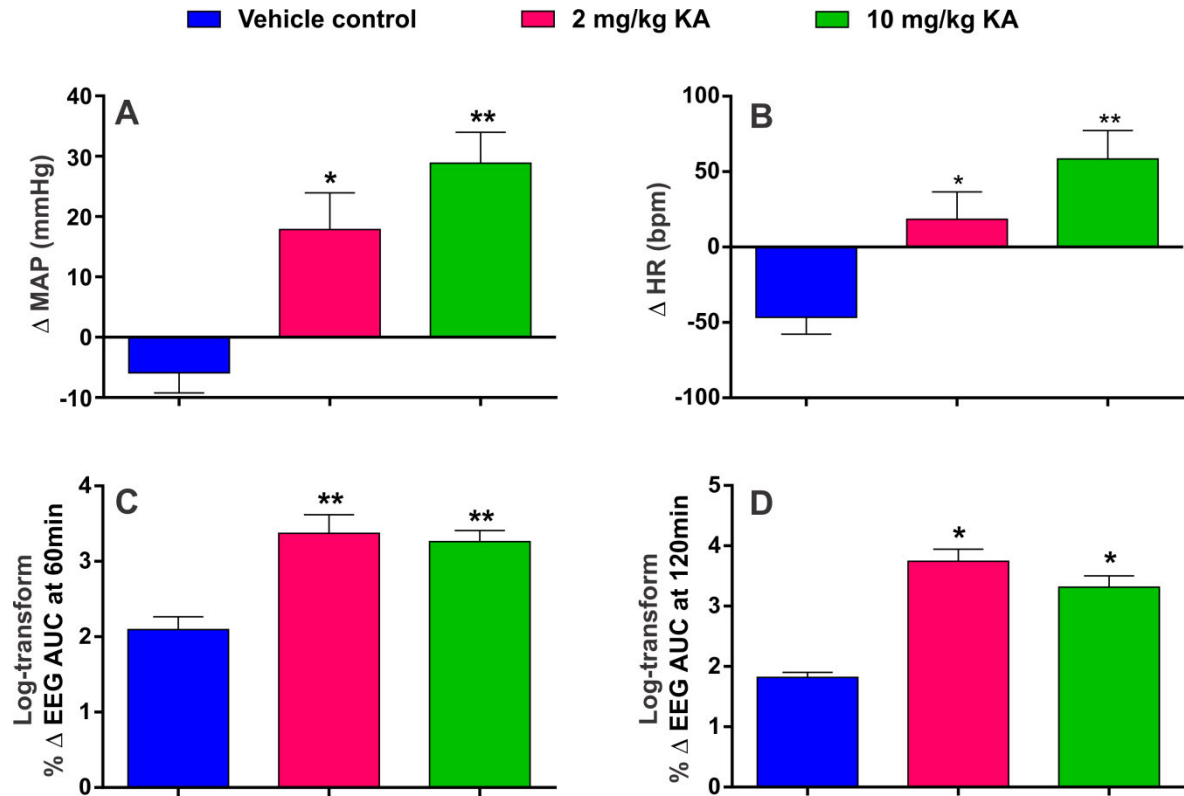
Figure 4. 4: *In vivo* **effects of PBS and KA-induced (2 and 10 mg/kg) seizures in rats studied for histology.**

Change in MAP (A) and HR (B), at 120 min post i.p. PBS or KA (2 and 10 mg/kg) injection and % change in EEG activity (gamma frequency AUC), at 60 (C) and 120 min (D) post i.p. PBS or KA (2 and 10 mg/kg) injection in different group of rats. In all groups $n = 5$. Statistical significance was determined using one-way ANOVA followed by t-tests with a Holm-Šídák correction. Data expressed as mean ± SEM. **$p \leq 0.01$ and *$p \leq 0.05$ compared with vehicle control group.

Immunohistochemical analysis revealed that TH-immunoreactive (ir) neurons were surrounded with typical resting microglial cells in all three groups (Figure 4. 5A-C). In all three groups, microglia appeared with a round cell body and processes that appeared normal with few ramifications (Figure 4. 5A-C). The total number of microglia in each group are shown in Figure 4. 5D. A branch length and a number of endpoint analysis was carried out to identify the activated microglia. There were no differences in the mean branch length, and a number of endpoint processes of Iba1 labelled microglia between the vehicle control and the seizure-induced rats (Figure 4. 5E-F). The proportion of anti-inflammatory M2 phenotype of microglia was $14.2 \pm 1.4\%$ in saline-treated rats which was similar in 2 and 10 mg/kg KA-treated rats ($10.1 \pm 2.5\%$ and $9.6 \pm 2.4\%$, respectively; Figure 4. 5G). The findings revealed that microglia are in a surveillance state with no differences in their morphology and proportion of M2 phenotype, at least in the RVLM, between the vehicle and seizure-induced groups. These results are consistent with our electrophysiology findings where microinjection of a microglial antagonist had no effect on the increase in SNA, MAP, and HR in KA-induced seizure rats.
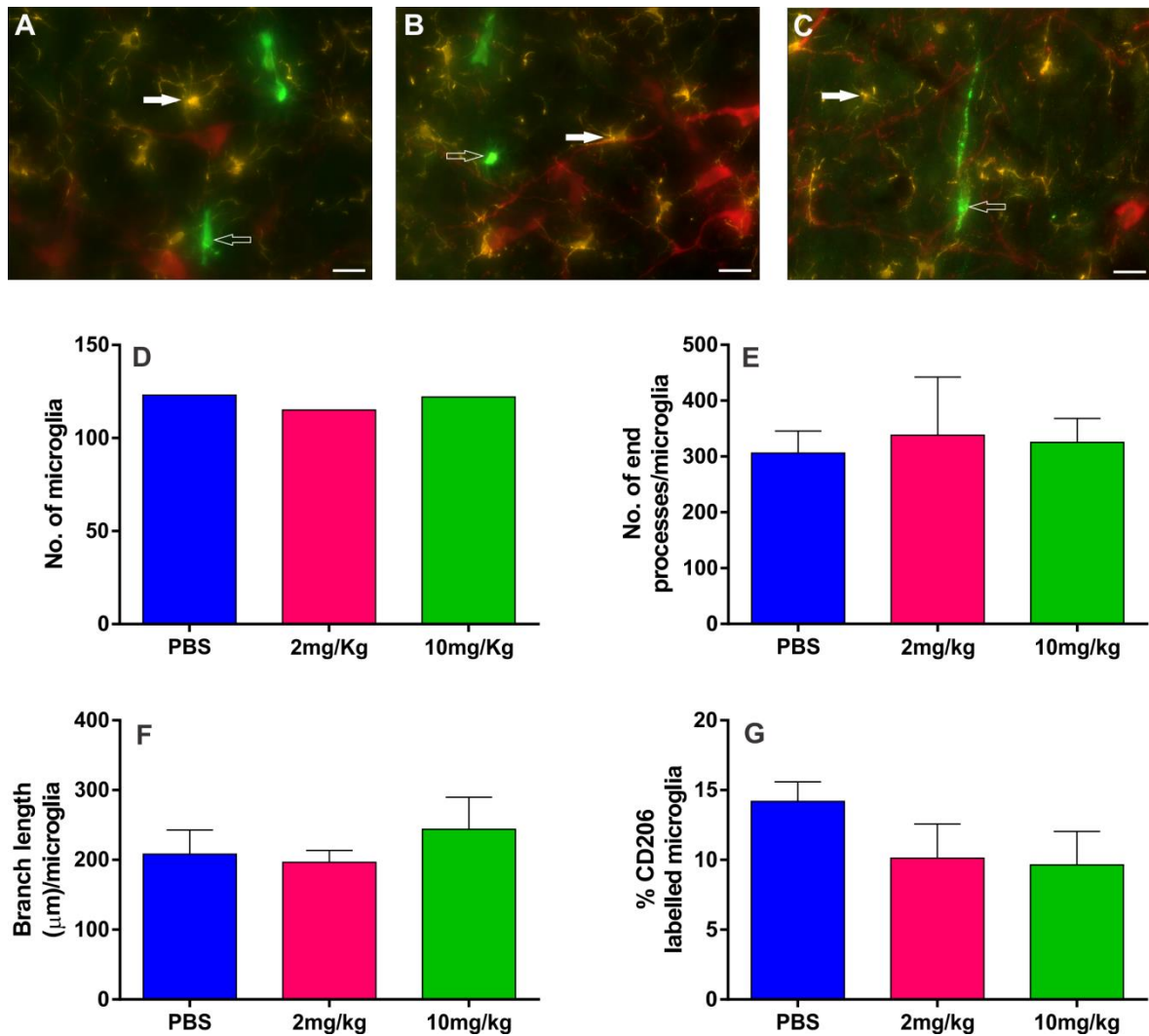
Figure 4. 5: Fluorescence images of RVLM and microglial analysis.

Fluorescence images of RVLM area containing TH[+]-ir (red), Iba1 labelled microglia (yellow) and CD206 labelled M2 microglial cells (green) and their morphological analysis in different treatment groups of rats. Scale bar = 20 µm. TH, Iba1 and CD206 immunoreactivity in RVLM in PBS (A), 2 mg/kg KA (B) and 10mg/kg KA (C) treated rats. In all of these three groups TH[+]-ir neurons (red) were surrounded with microglia with its round cell body and normal appearing processes with few ramifications (closed arrow) and no change in number of anti-inflammatory M2 microglia (open arrow). Quantitative analysis of number of microglial cells in mean square area (D), number of end processes/microglia (E), branch length (µm)/microglia of Iba1 labelled microglial cells (F) and percent of CD206 labelled M2 microglial cells (G) in the RVLM of vehicle treated and KA-induced seizure (2 and 10mg/kg i.p.) rats.

4.5.4. Proarrhythmogenic ECG changes during seizures are driven by activation of glutamatergic receptors, PACAP, and microglia

Two mg/kg KA-induced seizures caused prolongation of QT interval. The ΔQTc was significantly increased in KA control group (Δ 8.2 ± 2.5 ms; $p = 0.02$) compared with vehicle treatment group (Figure 4. 6A). These changes in QT interval are most clearly seen in Poincare plots before and after treatment; representative QT Poincare plots from each group are shown in (Figure 4. 7A). KA control group showed an almost complete dispersion of the QT interval along with arrhythmic behaviour in HR (multiple ellipses) (Figure 4. 7A-II). Despite this, there was no evidence of atrial fibrillation, although there was evidence of a dramatic decrease in PR interval after KA treatment (Figure 4. 6B and Figure 4. 7B-II). The prolongation of QT interval (ΔQTc) was completely blocked by administration of glutamate receptors antagonist KYNA in the RVLM ($p = 0.02$; Figure 4. 6A and Figure 4. 7A-V), nevertheless, the bilateral microinjection of KYNA has no effect on seizure-induced shortened PR interval (Figure 4. 6B and Figure 4. 7B-V). PACAP(6-38) and minocycline microinjections also significantly reduced ΔQTc interval compared to KA control group of rats (Δ 1.9 ± 1.5; $p = 0.03$ and Δ 1.5 ± 1.2; $p = 0.03$; Figure 4. 6A). In PACAP(6-38) and minocycline-treated groups, prolongation of QT interval and dysrhythmia is abolished. As shown in Figure 4. 7A, PACAP(6-38) and minocycline treatment in KA-induced seizure rats have an almost similar pattern of pre- and post-QT interval like vehicle-treated group (Figure 4. 7A-I, III, and IV). The seizure-induced prolongation of QT interval is very obvious in KA control, which was significantly blocked in PACAP(6-38) and minocycline microinjected rats. The PR interval was significantly reduced in the 2 mg/kg KA-induced seizure group compared to the vehicle control group of rats (Figure 4. 6B). This is clearly represented in Poincare plots (Figure 4. 7B). In contrast to the improvements seen in QT interval, RVLM microinjection of PACAP(6-38), minocycline or KYNA did not prevent changes in seizure-induced shortening of PR interval (Figure 4. 6B). However, PACAP(6-38) (Figure 4. 7B-III) and minocycline (Figure 4. 7B-IV) showed quantally dispersed PR intervals as evidenced by multiple ellipses, rather than complete RR dispersion, and an absence of P-waves, which is clearly not suggestive of atrial fibrillation.
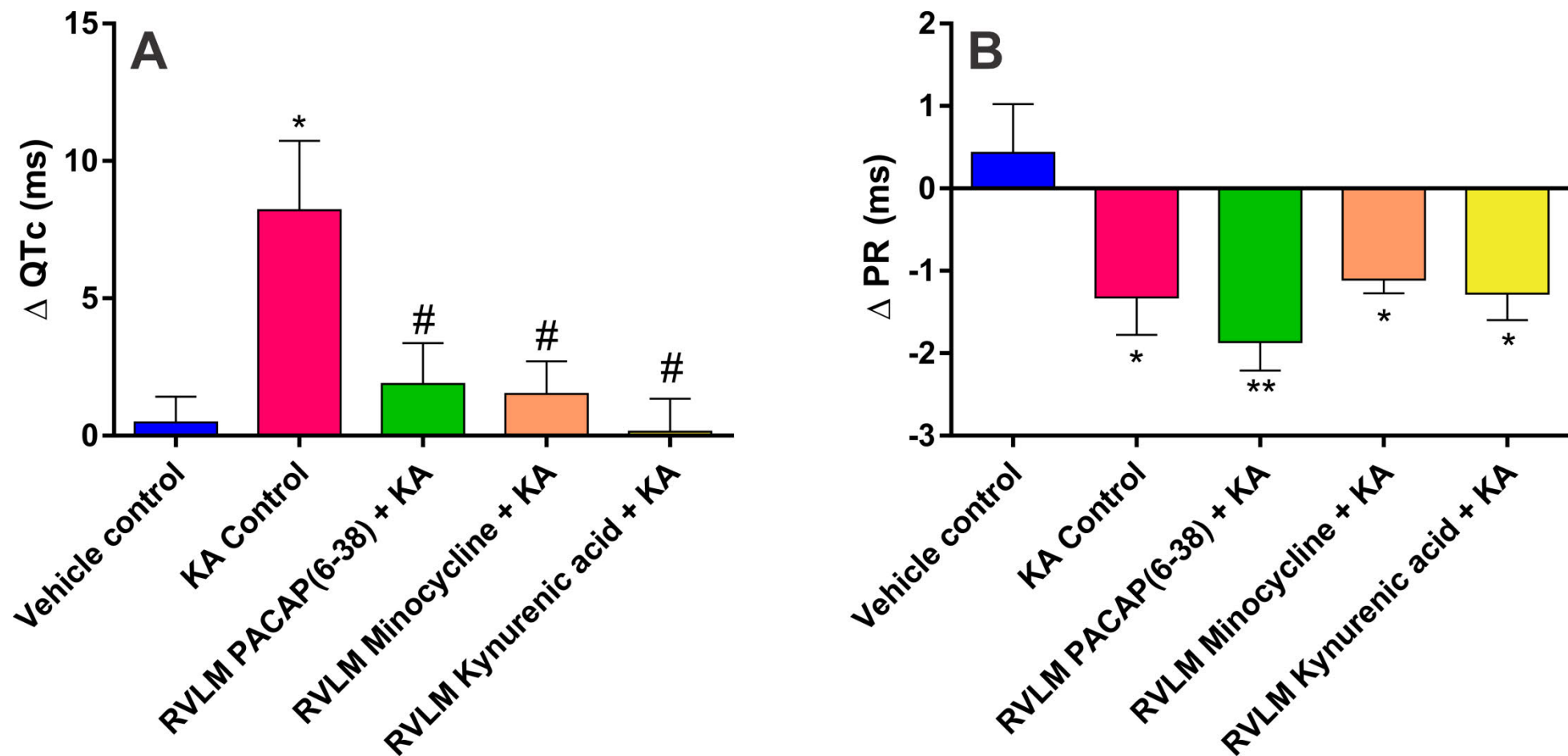
Figure 4. 6: Proarrhythmogenic effects of seizures.

Group data showing changes in QTc interval (A) and PR interval (B) 120 min after i.p. injection of PBS or KA in different groups of rats. Statistical significance was determined using one-way ANOVA followed by t-tests with a Holm-Šídák correction. Data expressed as mean ± SEM. $**p \leq 0.01$ and $*p \leq 0.05$ compared with vehicle control group and $\#p \leq 0.05$ compared with KA control group.

Figure 4. 7: Representative Poincare plots illustrate the changes in QT interval (A) and PR interval (B) following KA-induced seizures in rats.

A) Treatment with KA causes a dramatic dispersion in the QT interval (prolongation) and arrhythmic behaviour in the HR (multiple ellipses) (II). In rats treated with the PACAP antagonist (PACAP(6-38)) or with the microglial antagonist minocycline, prolongation of QT interval and the dysrhythmia is abolished (III-IV). Following treatment with KYNA, the HR and QT are restored to normal (V). HR triggered ECG was drawn pre and post treatment and shown in the right side corner of each box (Continuous black and dotted red lines represent pre and post treatment ECG). B) Induction of seizures with i.p. KA injection shortened the PR interval (II) compared to vehicle control. RVLM microinjection of PACAP (6-38) (III), minocycline (IV) or KYNA (V) did not show changes in seizure-induced short PR interval however PACAP (6-38) (III) and minocycline (IV) showed more dispersed PR interval with multiple ellipses. Scale bars are in milliseconds.
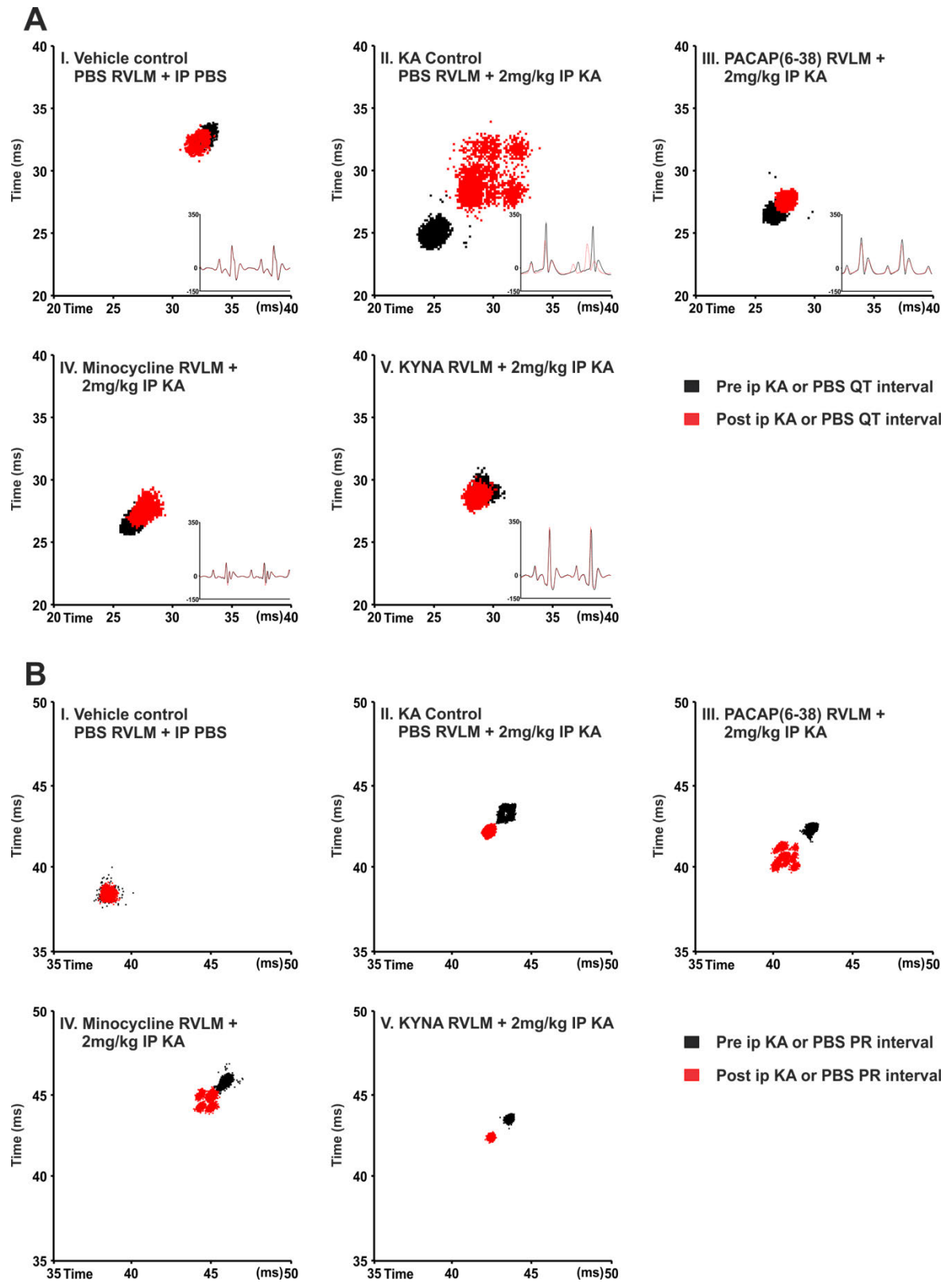
4.6. <u>Discussion</u>

This study provides the first direct evidence that the sympathoexcitation, tachycardia, pressor responses and proarrhythmogenic changes during seizures are driven by activation of glutamatergic receptors that leads to increased activity of the sympathetic premotor neurons in the RVLM. The sympathoexcitatory effect does not appear due to increases or decreases in PACAP secretion, or microglial activation. However, PACAP and microglial activity in the vicinity of RVLM neurons mediate the proarrhythmogenic changes during seizures. Central autonomic nuclei are not the source of KA-induced seizures (2 mg/kg). We confirm that the induction of seizures does not cause changes in the state of microglia within the RVLM and microglia remain in a surveillance state with no change in the number of M2 phenotypes; supporting our *in vivo* electrophysiology findings.

Our results strengthen the findings that seizures have devastating effects on the cardiovascular system (Sakamoto et al., 2008; Brotherstone et al., 2010; Bhandare et al., 2015), with immediate cardiovascular effects that last for approximately 3 h (Lothman et al., 1981). Importantly, these cardiovascular changes are downstream effects of seizure-induced autonomic overactivity and mediated by the action of the excitatory amino acid, glutamate, on sympathetic premotor neurons in the RVLM as the bilateral microinjection of the ionotropic glutamate receptors (iGluRs) antagonist KYNA completely abolished these changes. Glutamatergic synapses are important in the development of seizures, as seizure elevates the glutamate levels in the extracellular fluid of the rat hippocampus (Chapman, 1998; Ueda et al., 2001; Rainesalo et al., 2004; Kanamori and Ross, 2011). The RVLM contains sympathetic premotor neurons responsible for maintaining tonic excitation of sympathetic preganglionic neurons involved in cardiovascular regulation (Guyenet, 2006; Pilowsky et al., 2009). Increased activity of sympathetic premotor RVLM neurons has a significant effect on cardiac electrophysiology and is arrhythmogenic during seizures (Metcalf et al., 2009b; Damasceno et al., 2013). Microinjection of glutamate into the RVLM causes pressor responses and sympathoexcitation that is completely blocked with KYNA (Ito and Sved, 1997; Araujo et al., 1999; Dampney et al., 2003). KYNA microinjection into RVLM on its own does not affect basal BP and sympathetic activity (Guyenet et al., 1987; Kiely and Gordon, 1994; Araujo et al., 1999). Subsequently, Ito and Sved observed that if the caudal ventrolateral medulla (CVLM) (inhibitory drive to the RVLM) is inhibited first, subsequent blockade of glutamate receptor in the RVLM markedly reduces BP (Ito and Sved, 1997). In this paradigm, glutamatergic input to the RVLM directly excite presympathetic neurons and

indirectly inhibit gamma-aminobutyric acid (GABA)ergic inhibition of the RVLM, and the lack of change in arterial pressure (AP) with KYNA in the RVLM reflects the balance of these two actions. Miyawaki and colleagues also observed that after blockade of GABAergic input within the RVLM, injection of KYNA produced inhibition of splanchnic and lumbar SNA (Miyawaki et al., 2002a). Together these findings illustrate that there is a tonic glutamatergic input with the existence of additional sources of neurotransmitter drive to RVLM neurons. We hypothesised that the increased concentration of glutamate in the RVLM during seizure leads to sympathoexcitation, tachycardia and pressor responses. In turn, the responses can be antagonised by microinjection of KYNA into RVLM and indeed our findings support this hypothesis. The findings suggest that not only sympathoexcitation but also proarrhythmogenic changes during seizures are mediated through glutamatergic receptors activation in RVLM catecholaminergic neurons. RVLM microinjection of KYNA (as well as PACAP(6-38) and minocycline) were unable to block the reduction in PR interval. In this paradigm, it is possible that the KA-treatment had peripheral effects on dromotropy at the level of the AV node.

Generalised seizures in rats causes the expression of c-Fos, a protein marker of recently activated neurons (Minson et al., 1994), in brainstem catecholaminergic neurons in RVLM (Silveira et al., 2000). Earlier studies also suggest that C1 neurons are activated following seizure (Kanter, 1995); findings that were supported in previous, and current work (Bhandare et al., 2015), where KA-induced seizures in rats elicited sympathoexcitation, tachycardia and pressor responses. Together, the findings confirm that during seizure most of the excitatory effects of glutamate in RVLM are mediated by ionotropic receptors, since the broad-spectrum iGluRs (NMDA, AMPA, and kainate) antagonist (KYNA) completely abolished these effects.

PACAP is a 38 amino acid pleiotropic neuropeptide. The effects of PACAP are mediated via three different G-protein receptors (PAC1R, VPAC1R, and VPAC2R); all are positively coupled to adenylate cyclase. PACAP gene expression is increased in the PVN of the hypothalamus after KA-induced TLE in rats (Nomura et al., 2000). Whereas, PACAP is sympathoexcitatory (Lai et al., 1997; Farnham et al., 2008; Farnham et al., 2012; Gaede et al., 2012), anti-inflammatory and neuroprotective (Shioda et al., 1998) on sympathetic preganglionic neurons during seizure (Bhandare et al., 2015). Therefore, we aimed to determine whether or not PACAP also has a sympathoexcitatory or neuroprotective effect on RVLM sympathetic premotor neurons during seizures. The findings show that blockade of PACAP receptors (PAC1 and VPAC2), in the RVLM do

not affect seizure-induced sympathoexcitation, tachycardia, and hypertension, but do abolish prolongation of QT interval. This response to PACAP(6-38) suggests that the excitatory action of PACAP (Figure 4. 8) on RVLM sympathetic premotor neurons mediates proarrhythmogenic changes, but not seizure-induced sympathoexcitation. Possible explanations could be that PACAP expression in the RVLM at 2 h post 2 mg/kg KA injection may be insufficient to produce sympathoexcitation, but enough to induce proarrhythmogenic effects. This idea is supported by the findings that PACAP gene expression reaches a maximum at 12 h post 12 mg/kg KA-induced seizures in the PVN of the hypothalamus (Nomura et al., 2000).

Microglia are the principal resident immune cells of the CNS, contributing ~10% of the total brain cell population. Activated microglia respond to environmental perturbations by adopting either a "pro-inflammatory M1" or "anti-inflammatory M2" phenotype (Li et al., 2007; Lai and Todd, 2008; Pisanu et al., 2014). Seizure causes extensive microglial activation in patients (Beach et al., 1995), and in animal models (Drage et al., 2002). There is considerable controversy surrounding the pro-inflammatory (Shapiro et al., 2008) or anti-inflammatory (Mirrione et al., 2010; Eyo et al., 2014) role played by microglia during seizure. Our recent findings demonstrate that microglia are protective during seizure on sympathetic preganglionic neurons within spinal cord (Bhandare et al., 2015). The findings of the current study show that blockade of microglial activation with minocycline microinjection in RVLM abolishes the prolongation of QT interval caused by KA-induced seizures, but causes no change in sympathoexcitation, tachycardia or hypertension. Our immunohistochemical analysis revealed that there are no changes in microglial morphology or phenotype in the vicinity of RVLM neurons (branch length or number of endpoint processes) or proportion of the M2 phenotype following induction of seizures. The increased RVLM neuronal activity may have activated microglia (which might be insufficient to differentiate with immunohistochemistry) producing an excitatory effect and contributed to the seizure-induced prolongation of QT interval (Figure 4. 8).

A possible mechanism to explain the increased glutamate release from pre-synaptic cells during seizure, and sympathoexcitation, is proposed in Figure 4. 8. The oxidative stress and inflammation in RVLM during seizure (Tsai et al., 2012) could be mediated through increased glutamate levels or functional failure of glutamate transporters. Increased synthesis and release of PACAP during seizure acts via cyclic adenosine monophosphate (cAMP)-mediated protein kinase A (PKA) and/or protein kinase C (PKC) pathways that may have either excitatory effects through phosphorylation of TH at serine 40

(Bobrovskaya et al., 2007) or neuroprotective effects regulated through decreased caspase 3 (Dejda et al., 2011), increased glial-glutamate transporters and redirecting microglia towards anti-inflammatory M2 phenotype (Brifault et al., 2015). PACAP inhibits mitogen-activated protein kinase (MAPK) and increases interleukin (IL)-6 (Shioda et al., 1998) whereas its action on the PAC1 and VPAC1 receptors of activated microglia increase production of IL-10, transforming growth factor-β (TGF-β) and decrease tumor necrosis factor-α (TNF-α) (Wada et al., 2013). Whereas polarisation of activated microglia towards pro-inflammatory M1 phenotype increase IL-1β and TNF-α. Overall, depending on the type, severity and intensity of the stimulus, selective actions of PACAP and microglia regulate the physiological state of neurons. In the current study, both PACAP and microglia may regulate excitatory effects as their antagonism results in restoration of QT prolongation.

This is the first evidence to indicate that an increase in sympathetic nerve discharge and cardiovascular dysfunction in seizure is due to activation of glutamatergic receptors within the RVLM. Secondly, antagonism of PACAP and microglial activity in RVLM did not abolish the seizure-induced sympathoexcitation, hypertension, and tachycardia. Interestingly, minocycline, a drug that has central bioavailability following oral administration, and PACAP antagonist, restores the proarrhythmogenic effects of seizures to normal. This is the evidence for the physiological interaction between neurons and microglia. Thirdly, the finding that microglia are not activated, and there is no change in the proportion of M2 phenotype during seizures, is consistent with our physiological findings.

In summary, the implications of the current findings are that, in patients with seizure, targeting glutamatergic receptors in RVLM catecholaminergic neurons and tailoring activity of PACAP and microglia in the vicinity of sympathetic premotor neurons may have protective effects and lead to novel therapies for seizure-induced cardiovascular dysfunction and SUDEP.

Figure 4. 8: A proposed mechanism by which hippocampal seizures induce increased activity of sympathetic premotor neurons in the RVLM and role of glutamate, PACAP and microglia.

A) Seizure elevates synaptic glutamate release that can act on postsynaptic AMPA or NMDA receptors. Activation of AMPA or NMDA receptors leads to inhibition of cysteine uptake and influx of extracellular calcium which stimulates production of oxidants, NO and O^-. Under repetitive and extreme neuronal activation, neurotoxic effects are mediated through increased production of apoptotic factor like caspase-3. Glutamate transporters are expressed by astrocytes and play an important role in rapid clearance of the synaptically released glutamate, whose expression is down-regulated in seizure. Taken together, increased oxidative stress and cellular excitability causes increased activity of sympathetic premotor neurons. B) Increased PACAP expression can act via cAMP mediated PKA and/or PKC pathways and produce either excitatory effect through phosphorylation of TH at serine 40 or neuroprotective effect regulated through decreased caspase 3, increased glial-glutamate transporters and redirecting microglia towards anti-inflammatory M2 phenotype. In neurons, PACAP inhibits MAPK and increases IL-6 production. Microglia are activated by PACAP binding to PAC1 and VPAC1 receptors. Subsequently, microglia increase production and release of IL-10 and TGF-β and decrease production and release of TNF-α, as well as down-regulating CD40 and B7 surface protein expression, with a neuro-protective effect. Conversely, the pro-inflammatory phenotype of activated microglia can produce IL-1β and TNF-α that may increase the sensitivity of neurons to activation.

A) Excitatory effect of seizures on sympathetic neurons
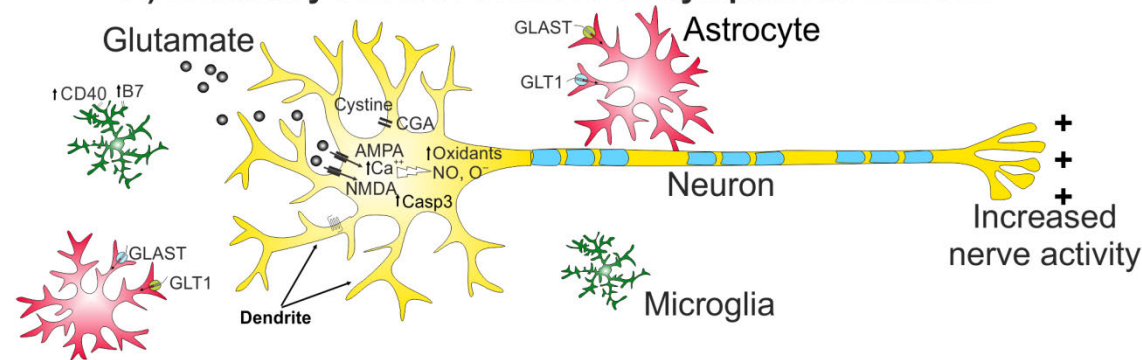
B) Possible effect of PACAP and microglia on sympathetic neurons during seizures
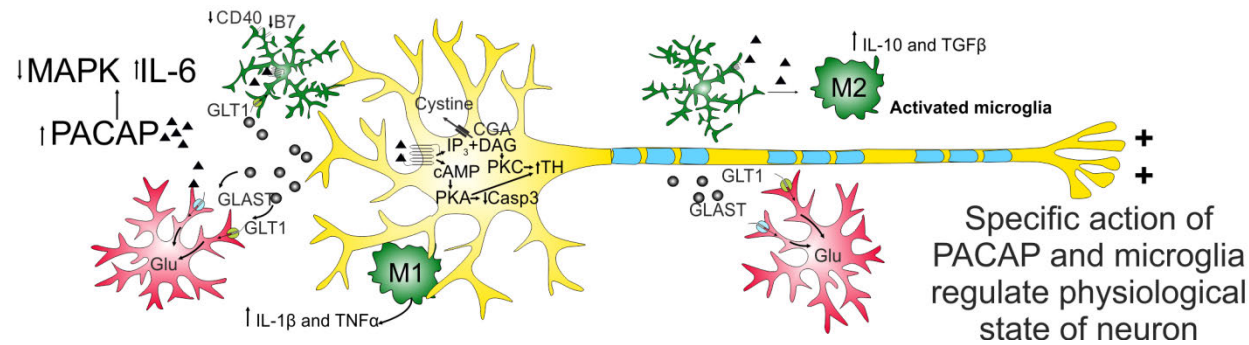
4.7. Supplementary results

4.7.1. Confirmation of site of RVLM microinjection

The RVLM microinjection site was confirmed with the cresyl violet staining (Figure 4. 9). The Chicago Sky Blue dye was evidenced in the RVLM nuclei as defined in section 2.8.
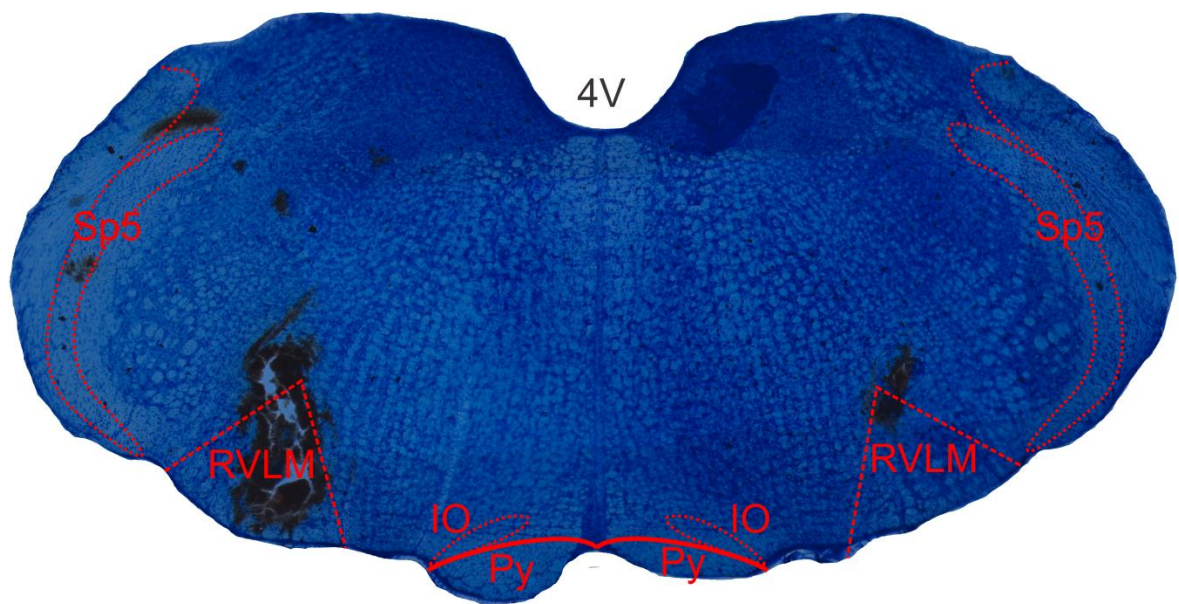
Figure 4. 9: Bilateral RVLM microinjection sites.

Chapter 5
Microglial activation in the spinal cord mediates sympathoexcitatory and proarrhythmogenic changes in rats with chronic temporal lobe epilepsy

The work in this Chapter is submitted in the "Journal of Neuroscience-An Official Journal of Society for Neuroscience" and is under review.

Bhandare AM, Kapoor K, Powell KL, Braine E, Casillas-Espinosa P, O'Brien TJ, Farnham MMJ, Pilowsky PM Microglial activation in the spinal cord mediates sympathoexcitatory and proarrhythmogenic changes in rats with chronic temporal lobe epilepsy. J Neurosci *Under review*.

"The candidate designed experiments, performed all physiology experiments, analysed data and interpreted results. Candidate was the major contributor to the manuscript writing, editing and figures drawing. Paul Pilowsky, Melissa Farnham, Terence O'Brien and Kim Powell contributed to design of experiments, interpretation of results and editing and final approval of manuscript. Emma Braine and Pablo Casillas-Espinosa performed induction of chronic seizure experiments and analysis of *in vivo* EEG-ECG data. Komal Kapoor performed immunohistochemistry experiments and analysed histology data."

Table of Contents

5.1. <u>Abstract</u>

The incidence of sudden unexpected death in epilepsy (SUDEP) is highest in people with chronic and drug resistant epilepsy. Chronic spontaneous recurrent seizures cause cardiorespiratory autonomic dysfunctions. Pituitary adenylate cyclase-activating polypeptide (PACAP) is neuroprotective, whereas microglia produce both pro-inflammatory and anti-inflammatory effects in the CNS. During acute seizures in rats, PACAP and microglia produce sympathoprotective effect at the intermediolateral cell column (IML), whereas their action on the presympathetic rostral ventrolateral medulla (RVLM) neurons mediates proarrhythmogenic changes. We evaluated the effect of PACAP and microglia at the IML on sympathetic nerve activity (SNA), cardiovascular reflex responses, and electrocardiographic changes in the post-status epilepticus (post-SE) model of acquired epilepsy, and control rats. Chronic spontaneous seizures in rats produced tachycardia with profound proarrhythmogenic effects (prolongation of QT interval). Antagonism of microglia, but not PACAP, significantly reduced the SNA and the corrected QT interval in post-SE rats. PACAP and microglia antagonists did not change baroreflex and peripheral or central chemoreflex responses with varied effect on somatosympathetic responses in post-SE and control rats. We did not notice changes in microglial morphology or changes in a number of M2 phenotype in epileptic nor control rats in the vicinity of RVLM neurons. Our findings establish that microglial activation, and not PACAP, at the IML accounts for higher SNA and proarrhythmogenic changes during chronic epilepsy in rats. This is the first experimental evidence to support a neurotoxic effect of microglia during chronic epilepsy, in contrast to their neuroprotective action during acute seizures.

5.2. <u>Significance statement</u>

Epilepsy-induced altered cardiovascular function, regulated by autonomic nervous system, is suggested as a major cause of death. However, we do not know the neurochemicals or brain cells responsible for these cardiovascular abnormalities. Our findings show that chronic spontaneous seizures in rats produce profound proarrhythmogenic effects. The proarrhythmogenic and sympathoexcitatory effects are mediated by the action of microglia (an immune cells of the CNS), but not PACAP, at the spinal cord in rats with chronic epilepsy. Conversely, neither PACAP nor microglia regulate the major cardiovascular reflex responses. Thus, modifying the activity of microglia at the spinal cord in individuals with chronic epilepsy might produce protective action on sympathetic neurons, and eventually cardioprotective effect.

5.3. <u>Introduction</u>

Epilepsy is a chronic brain disorder characterised by spontaneous recurrent seizures and carries a risk of sudden death that is 15-20 times higher than in normal population (Ficker et al., 1998; Nilsson et al., 1999; Eastaugh et al., 2015). Epilepsy affects about 50 million people worldwide (WHO, 2005); seizures can range from brief, barely noticeable loss of attention to major convulsions that affect the entire neuraxis. Epilepsy is associated with changes in autonomic functions, such as sympathovagal imbalance, sympathetic reflex dysfunction, tachycardia with concomitant arrhythmia or bradycardia with associated apnoea (Dütsch et al., 2006; Bateman et al., 2008; Ponnusamy et al., 2012; Massey et al., 2014; Powell et al., 2014c; Bhandare et al., 2015; Bhandare et al., 2016a). Seizure associated autonomic cardiorespiratory changes are well-documented and are thought to play an important role in a mechanism of SUDEP (Nei et al., 2004; Dlouhy et al., 2015). Interictal autonomic changes are also seen in patients with chronic epilepsy (Ansakorpi et al., 2000; Berilgen et al., 2004; Müngen et al., 2010; Lotufo et al., 2012). Nevertheless, the neuronal mechanisms causing autonomic cardiorespiratory dysfunction during chronic epilepsy are unknown.

Pituitary adenylate cyclase-activating polypeptide (PACAP), a 38 amino acid pleiotropic neuropeptide, produce neuroprotective effects (Shioda et al., 1998; Ohtaki et al., 2006; Bhandare et al., 2015) that are partly mediated through its action on microglia (Wada et al., 2013; Brifault et al., 2015). PACAP and microglia have a protective effect on sympathetic preganglionic neurons at the IML where they ameliorate the sympathoexcitatory effect of acute seizures (Bhandare et al., 2015). During acute seizures, PACAP and microglia act on presympathetic RVLM neurons in the brainstem to promote proarrhythmogenic changes, but not sympathoexcitation (Bhandare et al., 2016a). In many cardiovascular autonomic nuclei PACAP is pressor and sympathoexcitatory (Farnham et al., 2008; Farnham et al., 2011; Inglott et al., 2011; Inglott et al., 2012) and changes baroreflex response in trout (Lancien et al., 2011) but not in rats (Farnham et al., 2012). PACAP expression is increased in central autonomic nuclei (paraventricular nucleus) after kainic acid (KA)-induced seizures in rats (Nomura et al., 2000). Secondly, seizures produce microglial activation, and neuroinflammation in patients and animal models (Beach et al., 1995; Shapiro et al., 2008; Eyo et al., 2014), which persist for many years during chronic epilepsy (Beach et al., 1995; Papageorgiou et al., 2015). Microglia can be pro-inflammatory or anti-inflammatory in animal models of temporal lobe epilepsy (TLE) (Shapiro et al., 2008; Mirrione et al., 2010; Vinet et al., 2012; Devinsky et al., 2013).

Although the pro-inflammatory or anti-inflammatory state of activated microglia is a topic of debate, there is strong support for their dual role (Hanisch and Kettenmann, 2007). Short term microglial activation is considered beneficial (Mirrione et al., 2010; Vinet et al., 2012; Szalay et al., 2016), whereas chronic microglial activation is deleterious, and produces a damaging response to injury (Qin et al., 2007; Loane et al., 2014). During KA-induced acute seizures, spinal microglia have a protective effect on sympathetic preganglionic neurons (Bhandare et al., 2015), however, their role in chronic epilepsy is not known.

Thus, the aims of this study were to identify the role of PACAP and microglia in the spinal cord, during chronic epilepsy, in the regulation of central autonomic cardiovascular activity. To achieve these aims we used a model of acquired epilepsy in rats that manifest spontaneous seizures and many features of acquired epilepsy in humans- the KA-induced post-SE model (Morimoto et al., 2004; Powell et al., 2008a; Jupp et al., 2012). The effect of intrathecal (IT) infusion of the PACAP antagonist, PACAP(6-38), and the microglial antagonist, minocycline, on sympathetic activity, cardiovascular reflex responses, and the electrocardiogram (ECG) were analysed in chronically epileptic and control rats. Microglial morphology and their phenotype in the vicinity of RVLM neurons were analysed with immunohistochemistry in epileptic and control rats.

5.4. <u>Materials and methods</u>

5.4.1. <u>Animals</u>

The animal usage and protocols were in accordance with the Australian code of practice for the care and use of animals for scientific purposes. The protocols were approved by the Animal Care, and Ethics Committee of Macquarie University, The University of Melbourne, and the Sydney Local Health District (SLHD) (section 2.1.1; Appendix 3). The electroencephalogram (EEG)-ECG electrodes implant surgery was performed under isoflurane anesthesia on 17-19 weeks old adult control ($n = 9$), and post-SE ($n = 15$) male Wistar rats (section 2.3.7), whereas electrophysiology experiments were performed under urethane anesthesia.

5.4.2. <u>KA-induced post-SE rat model</u>

The post-SE model of acquired epilepsy was generated by intraperitoneal (i.p.) injection of the glutamate receptor agonist, KA, to induce a period of continuous seizure activity (status epilepticus (SE)) in non-epileptic rats as described previously (Hellier et al., 1998;

Powell et al., 2008b; Jupp et al., 2012; Powell et al., 2014c; Vivash et al., 2014) (section 2.2.5). Briefly, twelve week old Wistar rats were injected with repeated low doses of KA (5mg/kg, i.p., followed by 2.5 mg/kg, i.p., injections once per hour) until SE behaviour was observed. After four hours of SE, all rats were given diazepam injection (5mg/kg i.p.) to terminate the SE. Rats were then returned to their home cages in the animal house and maintained with normal animal house care and diet.

5.4.3. Implantation of EEG-ECG electrodes in post-SE and control rats

Seven weeks after KA-induced SE ($n = 15$) (or saline administered controls ($n = 9$)), two ECG electrodes and four EEG electrodes were implanted in each rat under isoflurane anesthesia (section 2.3.7). The electrodes were fixed to the skull using dental cement, and the animals observed until recovery.

5.4.4. *In vivo* EEG-ECG recordings

One week after recovery from the surgery, a continuous 24 h video-EEG-ECG recording was acquired for one week using Compumedics EEG acquisition software digitised at 2048 Hz as previously described (Powell et al., 2008b; Powell et al., 2014c). Each recording was reviewed for seizure activity, and the start and end of a seizure was manually marked on the EEG to allow quantification of the number of seizures and seizure duration as explained in section 2.2.7. Normally, all post-SE rats develop spontaneous seizures, and none were observed in control rats.

5.4.5. Non-invasive tail-cuff blood pressure (BP) recordings

A week after confirmation of spontaneous recurrent seizures in post-SE rats with video-EEG recordings and in age-matched controls, blood pressure (BP) was recorded with a non-invasive tail-cuff method (section 2.2.1). Rats were placed in an animal holder, pre-warmed at 32^0C, and acclimatised to the chamber. All animals were kept in the chamber for 10-15 min; a cuff was attached to their tail, and BP was recorded in triplicate and averaged. Heart rate (HR) and systolic, diastolic, and mean BP was derived from the BP waveform channel.

5.4.6. *In vivo* electrophysiology

5.4.6.1. *General surgical procedure*

Electrophysiology surgical procedures were carried out as described previously (Bhandare et al., 2015). Briefly, rats ($n = 24$) were anesthetised with 10% urethane (ethyl carbamate;

1.3-1.5 g/kg i.p.) (section 2.2.2.1). Atropine sulphate (100 µg/kg, i.p.) was administered with the first dose of anesthetic to prevent bronchial secretions.

The right carotid artery and jugular vein were cannulated for the recording of BP, and for the administration of drugs and fluids, respectively (section 2.3.1) with a tracheostomy to enable mechanical ventilation (section 2.3.2). A three lead ECG was recorded and HR was derived from it (section 2.3.4). EEG was recorded from the head mounted electrodes. Rats were vagotomised (section 2.3.5.1), artificially ventilated with oxygen-enriched room air, and paralysed with pancuronium bromide (section 2.3.3). Arterial blood gases were analysed with an electrolyte and blood gas analyser. Partial pressure of carbon dioxide ($PaCO_2$) was maintained at 40 ± 2, and pH between 7.35-7.45. After completion of the surgical procedures described above, rats were secured in a stereotaxic frame and body temperature was recorded, and maintained between 36.5 and 37.5^0C throughout the experiment using a rectal probe and a homeothermic blanket.

5.4.6.2. Intrathecal catheter placement

The atlanto-occipital junction was exposed, and a catheter with a dead space of ~6 µl was inserted into the IT space of all rats through a slit in the dura and advanced caudally to the level of T5/6 (section 2.3.9.1).

5.4.6.3. Intrathecal drug administration protocol

In all groups, IT infusions were made 10 min after baseline reflex responses recording and flushed in with 6µl of phosphate-buffered saline (PBS). Ten microliters of a control injection of 10 mM PBS, 1 mM PACAP(6-38) or 100µg/10µl minocycline was administered intrathecally in post-SE ($n = 5$) and control ($n = 3$) rats. All infusions were made over a 10 to 15 s period, as described previously (Bhandare et al., 2015) (sections 2.3.9.2 and 2.3.9.3).

5.4.6.4. Isolation and preparation of nerves

The left greater splanchnic sympathetic nerve at a site proximal to the coeliac ganglion and the left phrenic nerve were isolated, dissected, cut, and the distal end tied with 5/0 silk thread as detailed in section 2.3.5.2 and 2.3.5.3. Efferent nerve activity was recorded from the proximal end using bipolar stainless steel electrodes (section 2.3.6). Signals were amplified (sampling rate: 6 kHz, gain: 2,000, filtering: 30-3,000 Hz) and noise was removed with a 50/60-Hz line frequency filter. The sciatic nerve was isolated at the mid-thigh, tied with 5/0 silk thread, and cut distally (section 2.3.5.5). The left aortic

depressor nerve was isolated from the cervical vagus nerve at the level of the carotid bifurcation, tied with 5/0 silk thread and cut close to the chest (section 2.3.5.4).

5.4.6.5. Aortic depressor and sciatic nerve stimulation and chemoreflexes protocol

The effect of aortic depressor nerve and sciatic nerve stimulation on splanchnic SNA was assessed to estimate the baroreflex and somatosympathetic reflex function in post-SE and control rats as described in section 2.4.1. Stimuli were generated by isolated stimulators controlled by a Spike2 script. Stimulus threshold was determined by increasing or decreasing the stimulus voltage until no response was observed. During each experimental protocol, the aortic depressor nerve was stimulated at 4 times threshold, and the average SNA response was analysed before, and 60, 90 and 120 min after IT treatment (Figure 5. 1). The left sciatic nerve was stimulated to generate the somatosympathetic response. Stimulus threshold was determined as described above, and sciatic nerve was stimulated at 4 times threshold, and the average response of SNA was analysed before, and 60, 90 and 120 min after IT treatment (Figure 5. 1).

Peripheral chemoreceptors were stimulated by ventilating animals with 10% O_2 in N_2 for 45 s (section 2.4.2). Central chemoreceptors were stimulated by ventilating animals with 5% CO_2 / 95% O_2 for 3 min (section 2.4.2). Both the central and peripheral chemoreflex responses were generated prior to, and at 60 and 120 min after IT treatment (Figure 5. 1).

5.4.7. Collection of blood and plasma samples and catecholamine analysis

At the conclusion of the electrophysiology experiments, 3-4 ml of blood was withdrawn from the carotid artery and collected in heparinised tubes containing metabisulphite (section 2.2.3). Blood samples were immediately centrifuged at 4^0C for 10 min at 900g and plasma collected and stored at -20^0C until analysis. Plasma adrenaline and noradrenaline were extracted onto activated alumina, eluted, and analysed with reverse phase HPLC and electrochemical detection (section 2.2.3).

5.4.8. Histology

5.4.8.1. Perfusions

At the conclusion of the electrophysiology experiments, rats were injected with heparin (1 ml) via the venous line and then perfused transcardially with 400 ml of ice-cold 0.9% saline followed by 400 ml of 4% paraformaldehyde (PFA) solution (section 2.2.4). Brains were removed and post-fixed in the same fixative for 18-24 h.

5.4.8.2. Sectioning and immunohistochemistry

Immunohistochemical analysis was done in $n = 3$ rats from both post-SE and control groups treated with IT PBS (section 2.7.1 and 2.7.3). Brainstems were sectioned coronally (40 µm thick) with a vibrating microtome, and sections were collected sequentially into five different pots containing a cryoprotectant solution, and stored at -20^0C until further processing. Free-floating sections were used for all histological procedures. Sections were rinsed, blocked, and incubated in primary antibodies: mouse anti-tyrosine hydroxylase (TH) (1:100), rabbit anti-cluster of differentiation (CD)206 (1:2,000), and goat anti-ionised calcium-binding adapter molecule-1 (Iba1) (1:1,000) (Table 2.4). After 48 h, sections were rinsed and TH, CD206 and Iba1 immunoreactivity was subsequently revealed by overnight incubation with the following secondary antibodies at 1:500 dilutions: cyanine dye (Cy)5-conjugated donkey anti-mouse, Alexa Fluor 488-conjugated donkey anti-rabbit, and Cy3-conjugated donkey anti-goat (Table 2.4). Sections were rinsed, mounted sequentially on glass slides, and coverslipped with Vectashield.

5.4.9. Data acquisition and analysis

5.4.9.1. Electrophysiology data

Data were acquired using a CED 1401 ADC system, and Spike2 acquisition and analysis software. The EEG raw data were DC removed and the power in the gamma frequency range was analysed, as shown previously (Bhandare et al., 2016a), from 5 min blocks taken 1 min before IT treatment and 60 and 120 min post-treatment (section 2.5.1). The EEG data was also manually analysed in a blinded manner for detection of seizure activity as explained in section 2.2.7. Phrenic nerve activity (PNA) was rectified and smoothed (τ 0.5 s). PNA was analysed from 1-min blocks taken 1 min before, and 60 and 120 min after IT treatment (section 2.5.2). SNA was rectified and smoothed (τ 2 s), and normalised to zero by subtracting the residual activity 5-10 min after death. The integrated SNA trace was calibrated (baseline as 100% and death level as 0%) and analysed for AUC between 60 to 120 min after IT treatment (section 2.5.3). Mean arterial pressure (MAP) and HR were analysed from 1-min blocks taken 1 min before, and 30, 60, 90 and 120 min after IT infusion (only 120 min results are shown in graphs) (section 2.5.4). Baroreflex and somatosympathetic reflex responses were analysed before, and 60, 90 and 120 min after IT treatment (Figure 5. 1). The percent change in baroreflex response (AUC) was calculated considering pre-treatment response as 100% (section 2.5.5). The somatosympathetic reflex response was analysed with a sigmoid curve fit analysis (both fast conducting A-fibre and

slow conducting C-fibre response). The pre-treatment range is considered as 100% response, and percent change is calculated at 60, 90 and 120 min post-treatment.

Peripheral and central chemoreflex responses were analysed as percent change in the SNA AUC at 60 and 120 min post-treatment compared to the pre-treatment response (considered as 100%) (section 2.5.6).

End-tidal CO2 (ETCO$_2$), and core temperature were analysed from 1-min blocks taken 1 min before and 30, 60, 90, and 120 min after IT injection (section 2.5.7). Arterial blood gas levels (PaCO$_2$, and pH) were measured 10 min before the start of the protocol, and 120 min after IT treatment in all animals. Statistical analysis was carried out in GraphPad Prism software. Statistical significance was determined using one-way analysis of variance (ANOVA) followed by t-tests with the Holm-Šídák correction. Multiple comparisons were done between groups. $p \leq 0.05$ was considered significant (section 2.6).

5.4.9.2. Calculation of QTc interval

QTc was calculated as explained in section 2.5.9. QT, PR, and RR intervals were calculated from the ECG recordings. QTc interval was calculated by dividing the QT interval in seconds by the square root of the RR interval in seconds (Bazett, 1920). The QTc was obtained before, and 120 min after IT injection. The PR and QTc interval statistical analysis was carried out in GraphPad Prism software. Statistical significance was determined using one-way ANOVA between treatment groups followed by t-tests with the Holm-Šídák correction. Multiple comparisons were done between groups. $p \leq 0.05$ was considered significant.

5.4.9.3. Histology imaging and analysis

Histology images acquisition and analysis is performed as described previously (Bhandare et al., 2016a; Kapoor et al., 2016b; Kapoor et al., 2016c) (section 2.8 and 2.9). In brief, all images were acquired, at 20X and 40X magnifications, using a Zeiss Axio Imager Z2. A 0.16 mm^2 box was placed within the imaged RVLM, and this area was used for analysis. The branch length and a number of endpoint processes of Iba1-labelled microglia in the vicinity of TH-labelled RVLM neurons was analysed using ImageJ plugin software, and GraphPad Prism was used for chi-square test for goodness of fit. The proportions of CD206 labelled anti-inflammatory M2 microglia in the RVLM of post-SE rats were compared with control group. Statistical significance was determined using non-parametric Mann-Whitney test (Sokal and Rohlf, 2012).
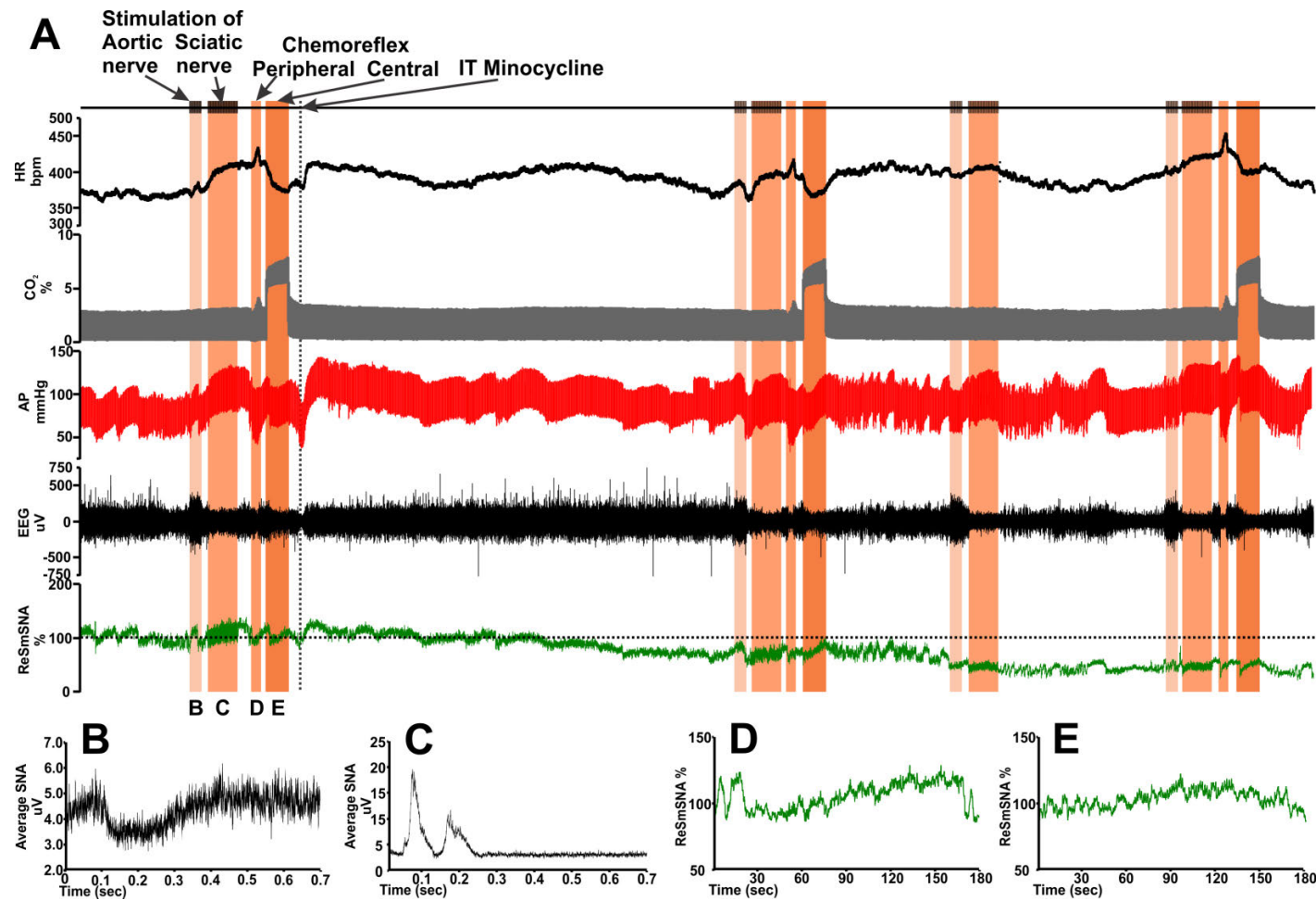
Figure 5. 1: *In vivo* **effects of IT minocycline treatment in post-SE rat on cardiovascular reflex responses.**

A typical response of stimulation of aortic depressor nerve (B), sciatic nerve (C), peripheral chemoreceptors (D) and central chemoreceptors (E) on the SNA and on HR, end-tidal CO_2, blood pressure, EEG and SNA activity (A). The protocol was repeated at 60, and/or 90 and 120 min after IT treatment.

5.5. <u>Results</u>

5.5.1. <u>Development of spontaneous recurrent seizures in post-SE rats</u>

A typical spontaneous seizure, with transition into ictal period, is shown in Figure 5. 2A and is characterised by high-amplitude and a new pattern of tracing. Video-EEG-ECG recordings confirmed that 9 weeks after induction of KA-induced SE, almost all rats developed spontaneous seizures with 0.44 ± 0.07 seizures per day (range 0-3) and with duration of 19.7 ± 3.3 sec per day. The seizure frequency and scores are highly variable across the post-SE rats as shown in (Figure 5. 2B-D). Whilst some of the post-SE animals may not have had seizures during recording period (a week), and is just could be due to the low frequency. None of the control rats (saline treatment) developed spontaneous seizures.

5.5.2. <u>Chronic seizure-induced tachycardia and proarrhythmogenic changes</u>

The *in vivo* EEG-ECG recordings in conscious chronic epileptic rats revealed that spontaneous seizure causes a dramatic tachycardia (~500 beats per minute (bpm) compared with ~300 bpm during pre-ictal period; Figure 5. 3A). The HR variability was increased from 91.8% to 98.2% in post-ictal period (Figure 5. 3F-I). HR was significantly unstable for more than one hour after the spontaneous seizure. Most significantly, the QTc interval was substantially prolonged during the ictal and post-ictal period. The pre-ictal QTc interval was 89.3 ms, which was massively prolonged by ~20% during the ictal period (110.3 ms) and persisted during the post-ictal period (94.9 ms, an hour after seizure). The uncorrected QT interval values during pre-ictal, ictal and post-ictal periods are 40.6, 41.2 and 41.9 ms, respectively (Figure 5. 3B-E). It suggests that despite the increased HR, which should decrease the QT interval in proportion, the QT interval was increased during the ictal and post-ictal period. Taken together, all these changes would contribute to the development of unstable, and possibly lethal arrhythmias.

5.5.3. <u>MAP, HR and plasma catecholamines in post-SE and control rats</u>

Non-invasive tail-cuff BP measurements confirmed non-significant differences in MAP and HR interictally between post-SE ($n = 15$), and control ($n = 9$) rats (Figure 5. 4A-B). The MAP and HR were 125.8 ± 4.5 mmHg and 310 ± 8 bpm in post-SE rats, respectively, compared to 129.3 ± 3.9 mmHg and 326 ± 10 bpm in controls, respectively (Figure 5. 4A-B). Plasma catecholamines were not significantly different between the groups. The plasma adrenaline was 1.6 ± 0.3 nmol/L and 1.9 ± 0.5 nmol/L in post-SE and control rats, respectively (Figure 5. 4C). Noradrenaline levels were also similar in both groups of rats; 3.4 ± 0.5 nmol/L in post-SE, and 3.9 ± 0.8 nmol/L in controls (Figure 5. 4D).
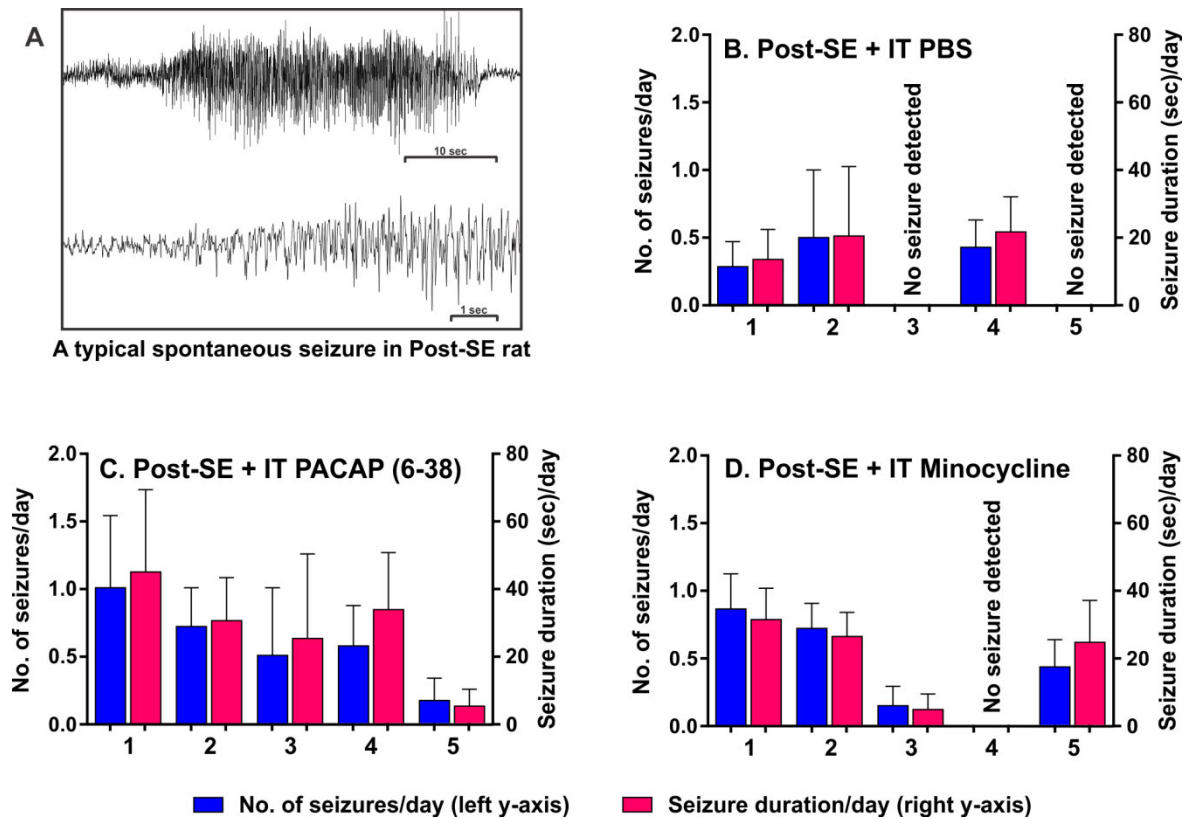
Figure 5. 2: Spontaneous seizure duration and frequency in post-SE chronic epileptic rats.

A typical spontaneous recurrent seizure (top-A) with a transition into ictal period (bottom-A) in epileptic rat. Seizure frequency and duration per day in IT PBS (B), PACAP(6-38) (C) and minocycline (D) treated post-SE rats. In each group $n = 5$. Data expressed as mean ± SEM.

5.5.4. Microglial activation, but not PACAP, mediates higher SNA and proarrhythmogenic changes in rats with spontaneous recurrent seizures

Our results showed that in chronically epileptic post-SE rats, the antagonism of microglial activation with minocycline at IT level significantly reduced SNA (Δ -25.0 $\pm$ 10.0%; $p \leq$ 0.05) compared to PBS-treated group (Δ 10.0 $\pm$ 7.7%) (Figure 5. 5AI). More interestingly, IT minocycline treatment in control rats (Δ -17.1 $\pm$ 18.5%) has a similar effect to PBS-treated control rats (Δ -17.8 $\pm$ 19.8%) (Figure 5. 5BI). IT PACAP(6-38) does not affect SNA activity in post-SE rats (Δ -15.3 $\pm$ 10.1%) compared with PBS treatment (Figure 5. 5AI). Similar results were obtained in control rats where changes in SNA were non-significant in IT PACAP(6-38) (Δ -18.5 $\pm$ 8.1%), and PBS treatments (Figure 5. 5BI). MAP and HR remained unchanged in both post-SE, and control rats treated with IT PBS, PACAP antagonist, and microglial antagonist (Figure 5. 5AII-III and Figure 5. 5BII-III). In post-SE rats, the HR changes were similar in PBS (Δ 0 $\pm$ 9 bpm), PACAP(6-38) (Δ -8 $\pm$ 5 bpm) and minocycline (Δ 1 $\pm$ 8 bpm) treated rats (Figure 5. 5AIII). There was a similar pattern in control rats (Figure 5. 5BIII) treated with PBS (Δ 3 $\pm$ 14 bpm), PACAP(6-38) (Δ 7 $\pm$ 10 bpm) and minocycline (Δ 1 $\pm$ 7 bpm). MAP was unaltered in post-SE (Figure 5. 5AII) and control rats (Figure 5. 5BII) treated with PBS (Δ 0.0 $\pm$ 2.0 mmHg and Δ 6.5 $\pm$ 4.3 mmHg, respectively), PACAP(6-38) (Δ 1.3 $\pm$ 6.7 mmHg and Δ 4.7 $\pm$ 1.4 mmHg, respectively), and minocycline (Δ -4.3 $\pm$ 4.2 mmHg and Δ 13.7 $\pm$ 8.4 mmHg, respectively).

The ECG findings in post-SE rats treated with IT minocycline showed a reduction in QTc interval duration (Figure 5. 6AI and Figure 5. 6CIII). In post-SE rats, the QTc interval was significantly reduced at 120 min after minocycline treatment compared to the pre-treatment period (Δ 3.0 $\pm$ 0.5 ms; $p \leq$ 0.05). The representative Poincare plot (Figure 5. 6CIII) clearly shows that IT minocycline treatment significantly reduced the QT interval. At 120 min post-treatment, the QTc interval in IT PBS and PACAP(6-38) treated groups did not change compared to the pre-treatment period (Δ 1.7 $\pm$ 1.1 ms and Δ 0.5 $\pm$ 1.3 ms, respectively; Figure 5. 6AI) (representative Poincare plot Figure 5. 6CI-II). In control rats, none of the treatments (IT PBS, PACAP(6-38) or minocycline) had a significant effect on QTc interval (Figure 5. 6BI). The IT PBS, PACAP(6-38) and minocycline do not alter the PR interval values in post-SE and control rats (Figure 5. 6AII and Figure 5. 6BII).

EEG activity, PNA, ETCO$_2$ or body temperature were not different in any of the groups (results not shown). None of the post-SE or control rats had spontaneous seizures under anaesthetised experimental conditions. Blood gas analysis confirmed that PaCO$_2$ and pH were within the normal physiological range (40 $\pm$ 2 and 7.35-7.45, respectively).
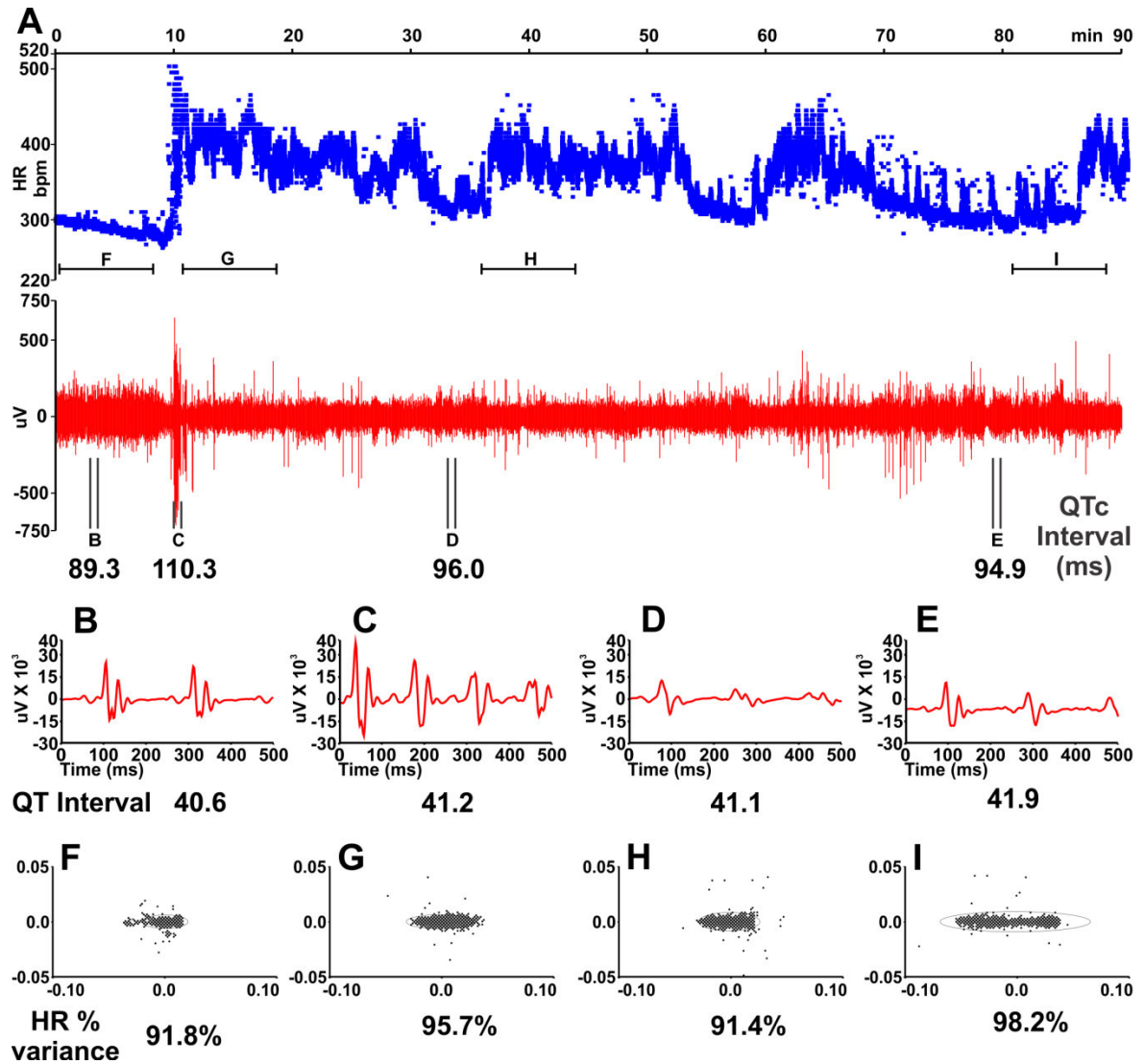
Figure 5. 3: The spontaneous seizure-induced tachycardia and prolongation of QT interval.

The effect of spontaneous seizure during *in vivo* EEG-ECG recordings in post-SE rats on HR (A), and QT interval during pre-ictal (B), ictal (C), and post-ictal (D-E) period in post-SE rats. The spontaneous seizure produced significant tachycardia along with increased variability in HR (F-I) during post-ictal period that was accompanied with prolongation of QT interval in ictal and post-ictal period.

5.5.5. <u>Neither microglia nor PACAP antagonists alter baroreflex, peripheral or central chemoreflex responses in epileptic post-SE or control rats, with varied effects on somatosympathetic responses</u>

A typical cardiovascular reflex response is shown in Figure 5. 1A. The protocol involved stimulation of aortic depressor nerve (baroreflex; Figure 5. 1B), stimulation of sciatic nerve (somatosympathetic; Figure 5. 1C), peripheral chemoreflex (Figure 5. 1D) and central chemoreflex responses (Figure 5. 1E), which were repeated at 60 and/or 90 and 120 min after IT treatment. Baroreflex responses were unaffected with the antagonism of PACAP or microglia in both post-SE, and control rats at 60 min, 90 min, and 120 min post-treatment (Figure 5. 7AI and Figure 5. 7BI).

The IT treatments in both post-SE and control rats produced varied effects on somtosympathetic reflex responses (Figure 5. 7AII-III and Figure 5. 7BII-III). Stimulation of sciatic nerve in post-SE rats treated with PBS showed significant decrease in fast (A-fibre; Figure 5. 7AII), and slow (C-fibre; Figure 5. 7AIII) conducting nerve fibre somatosympathetic responses over the time course (Δ -36.0 ± 8.3% and Δ -53.6 ± 14.3%, respectively at 120 min; $p \leq 0.05$). In post-SE rats, the A- and C-nerve fibre somatosympathetic responses were unaffected by IT PACAP(6-38) (Δ -29.8 ± 17.5% and Δ -40.8 ± 18.4%, respectively at 120 min) and minocycline (Δ -37.4 ± 16.3% and Δ -43.8 ± 21.9%, respectively at 120 min) treatment (Figure 5. 7AII-III). At 60, 90 and 120 min post-treatment, the fast conducting A-fibre somatosympathetic response was decreased in control rats treated with minocycline (Δ -61.0 ± 9.9%, at 120 min; $p \leq 0.001$; Figure 5. 7BII), whereas slow conducting C-fibre response was significantly reduced in rats treated with IT PBS (Δ -55.2 ± 9.6%, at 120 min; $p \leq 0.001$) and PACAP(6-38) (Δ -49.0 ± 3.1%, at 120 min; $p \leq 0.01$) (Figure 5. 7BIII).

The peripheral and central chemoreflex responses in post-SE, and control rats treated with IT PBS, PACAP(6-38), and minocycline were not altered at 60 or 120 min post treatment (Figure 5. 8). In post-SE rats, peripheral (Figure 5. 8AI) and central (Figure 5. 8AII) chemoreflex responses were unchanged in IT PBS (Δ 2.5 ± 10.0% and Δ 13.3 ± 3.7%, respectively), IT PACAP(6-38) (Δ 3.9 ± 3.7% and Δ -1.1 ± 3.1%, respectively), and IT minocycline (Δ 5.8 ± 2.9% and Δ 1.9 ± 3.3%, respectively) treated groups. Similar trend was noted in control rats where change in peripheral (Figure 5. 8BI) and central (Figure 5. 8BII) chemoreflex responses were Δ 3.7 ± 1.4% and Δ 3.2 ± 1.1% in IT PBS groups, respectively, Δ 5.7 ± 4.8% and Δ -10.8 ± 10.3% in IT PACAP(6-38) groups, respectively, and Δ 8.8 ± 10.0% and Δ 6.1 ± 1.8% in minocycline-treated groups, respectively.
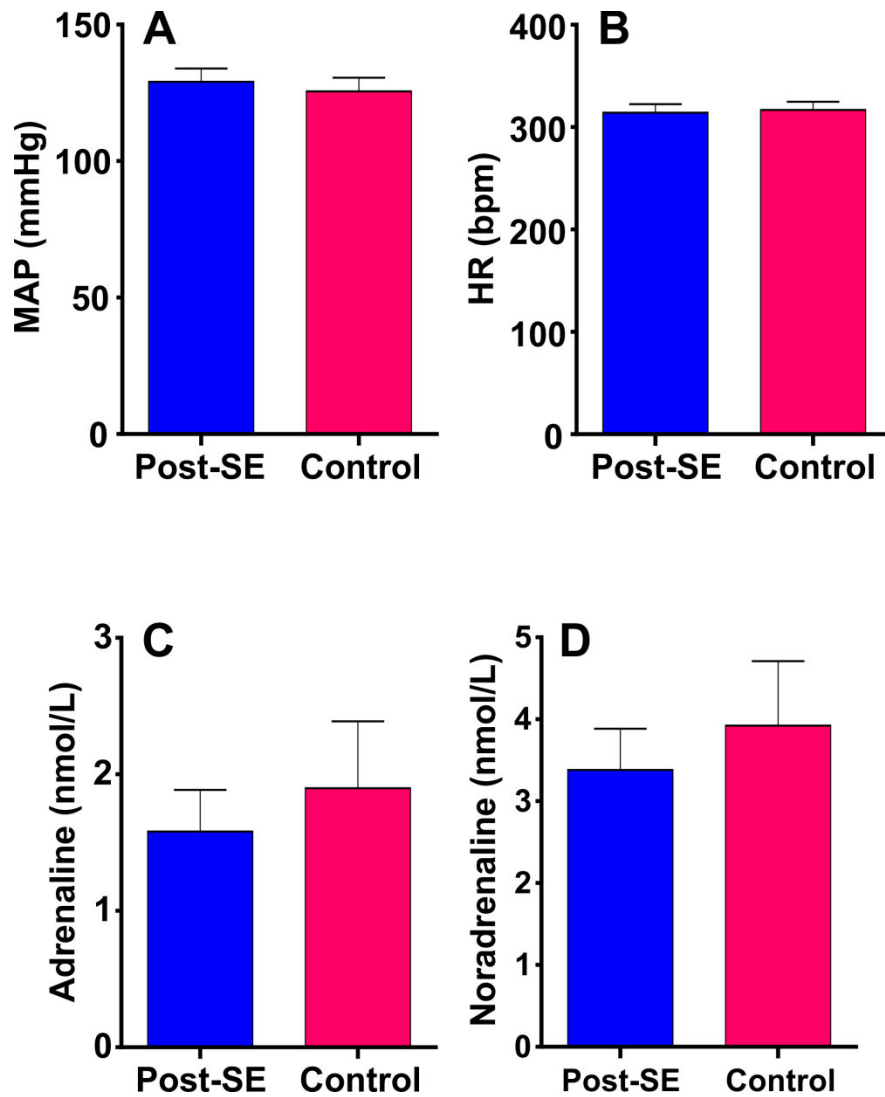
Figure 5. 4: The cardiovascular activity and catecholamine levels in post-SE chronic epileptic rats compared to control.

MAP (mmHg) (A) and HR (bpm) (B) in post-SE, and control rats recorded under conscious conditions. Plasma adrenaline (nmol/L) (C) and noradrenaline (nmol/L) (D) concentration in post-SE and control group of rats. Statistical significance was determined using unpaired t-test. Data expressed as mean ± SEM.

Figure 5. 5: *In vivo* **effects of IT PBS, PACAP(6-38) and minocycline treatment in post-SE and control rats.**

Change in SNA (AUC) between 60 and 120 min post treatment in post-SE (AI) and control (BI) rats. The changes in MAP (mmHg) at 120 min post IT treatment in post-SE (AII) and control (BII) rats, and HR (bpm) at 120 min after IT treatment in post-SE (AIII) and control (BIII) rats. Statistical significance was determined using one-way ANOVA followed by t-tests with a Holm-Šídák correction. Data expressed as mean ± SEM. *$p \leq 0.05$ compared with IT PBS treated post-SE group.
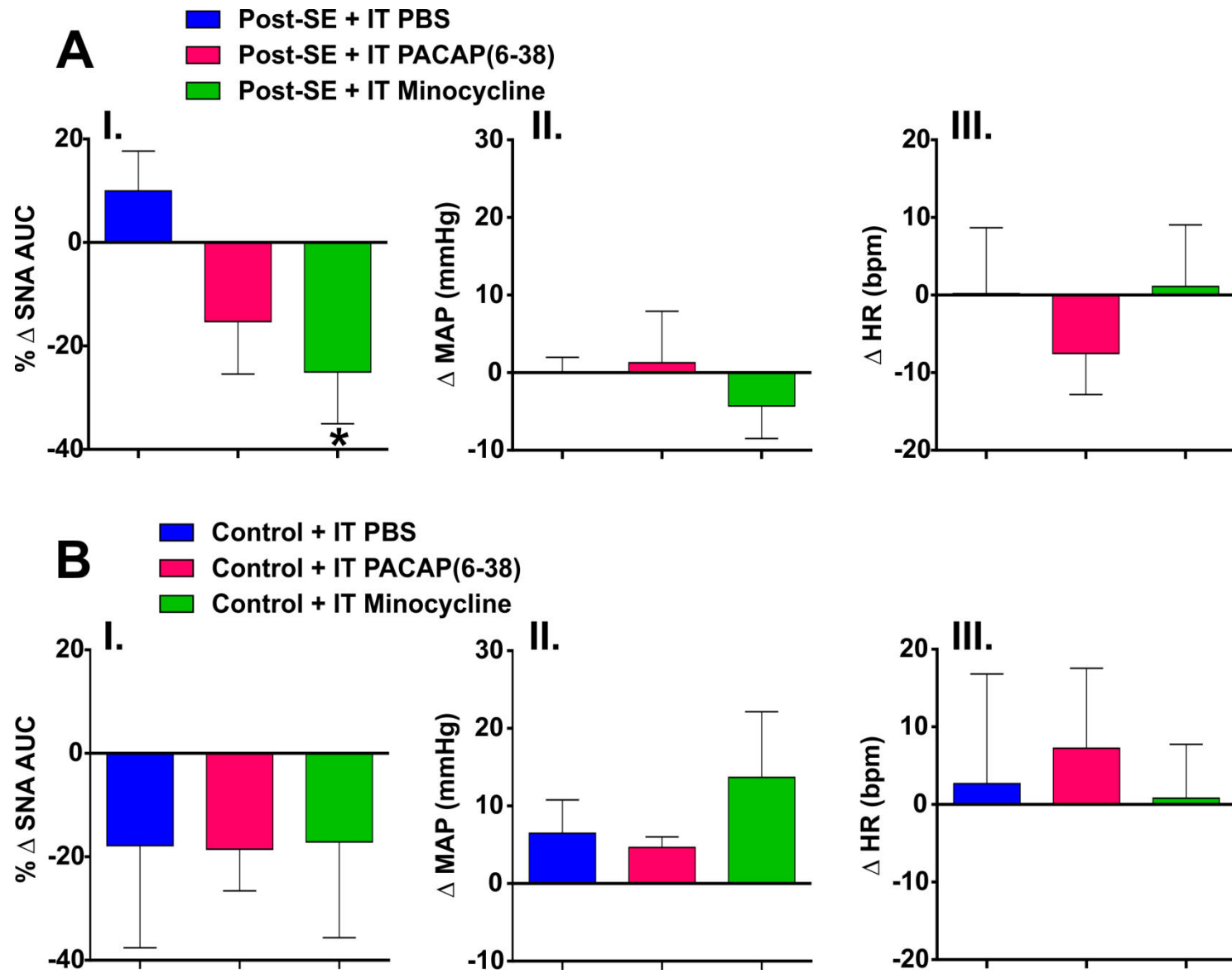
Figure 5. 6: *In vivo* **effects of IT PBS, PACAP(6-38) and minocycline treatment on ECG activity.**

Group data showing effect of IT PBS, PACAP(6-38) and minocycline treatment on: changes in corrected QT interval (Δ QTc) (ms) (AI) and PR interval (Δ PR) (ms) (AII) at 120 min post treatment compared to the pre-treatment period in post-SE rats; and changes in QTc interval (Δ QTc) (ms) (BI) and PR interval (Δ PR) (ms) (BII) at 120 min post treatment compared to the pre-treatment period in control rats. Representative Poincare plots illustrate changes in QT interval in post-SE rats from three different groups treated with IT PBS (CI), PACAP(6-38) (CII) and minocycline (CIII). IT PBS (CI) and PACAP(6-38) (CII) treatment in post-SE rats does not alter the QT interval, whereas antagonism of microglial activity significantly reduces the QT interval (CIII) in post-SE rats. Statistical significance was determined using one-way ANOVA followed by t-tests with a Holm-Šídák correction. Data expressed as mean ± SEM. *$p \leq 0.05$ compared with IT PBS treated post-SE group.

Figure 5. 7: *In vivo* effects of IT PBS, PACAP(6-38) and minocycline treatment on baroreflex and somatosympathetic reflex responses in post-SE and control rats.

The % change in baroreflex response at 60, 90 and 120 min post IT treatment compared to pre-treatment period in post-SE (AI) and control rats (BI). Effect of IT treatment on % change in fast conducting (A-fibre) somatosympathetic response at 60, 90 and 120 min post treatment compared to pre-treatment period in post-SE (AII) and control (BII) rats. The % change in slow conducting (C-fibre) somatosympathetic response at 60, 90 and 120 min post IT treatment compared to pre-treatment period in post-SE (AIII) and control (BIII) rats. Statistical significance was determined using one-way ANOVA followed by t-tests with a Holm-Šídák correction. Data expressed as mean ± SEM. *$p \leq 0.05$ compared with the pre-treatment time-point in post-SE group. ###$p \leq 0.001$, ##$p \leq 0.01$, #$p \leq 0.05$ compared with the pre-treatment time-point in control group.
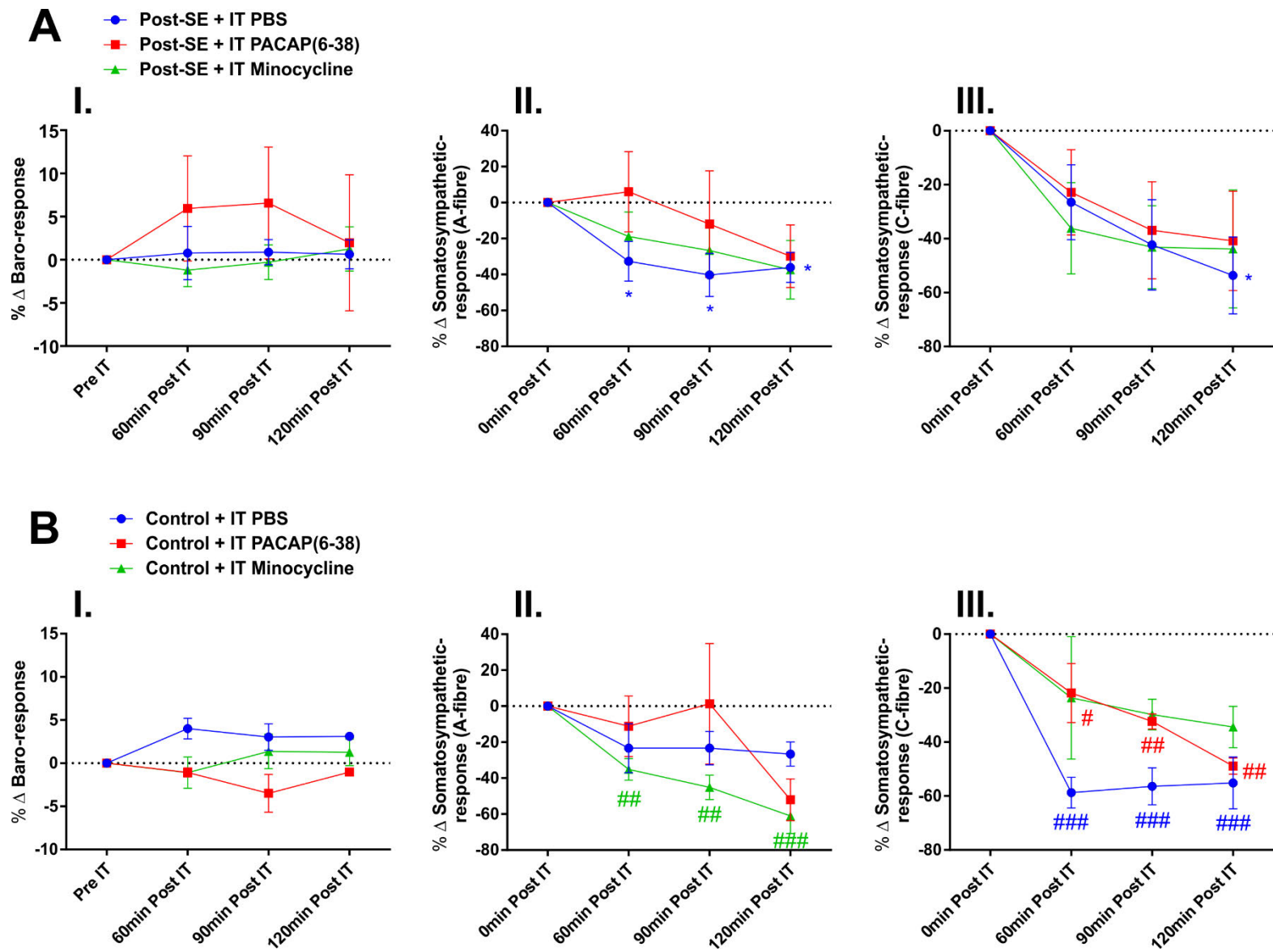
Figure 5. 8: *In vivo* effects of IT PBS, PACAP(6-38) and minocycline treatment on peripheral and central chemoreflex responses in post-SE and control rats.

The % change in peripheral (AI) and central (AII) chemoreflex response at 60 and 120 min post IT treatment compared to pre-treatment period in post-SE rats. The % change in peripheral (BI) and central (BI) chemoreflex response at 60 and 120 min post IT treatment compared to pre-treatment period in control rats. Statistical significance was determined using one-way ANOVA followed by t-tests with a Holm-Šídák correction. Data expressed as mean ± SEM.
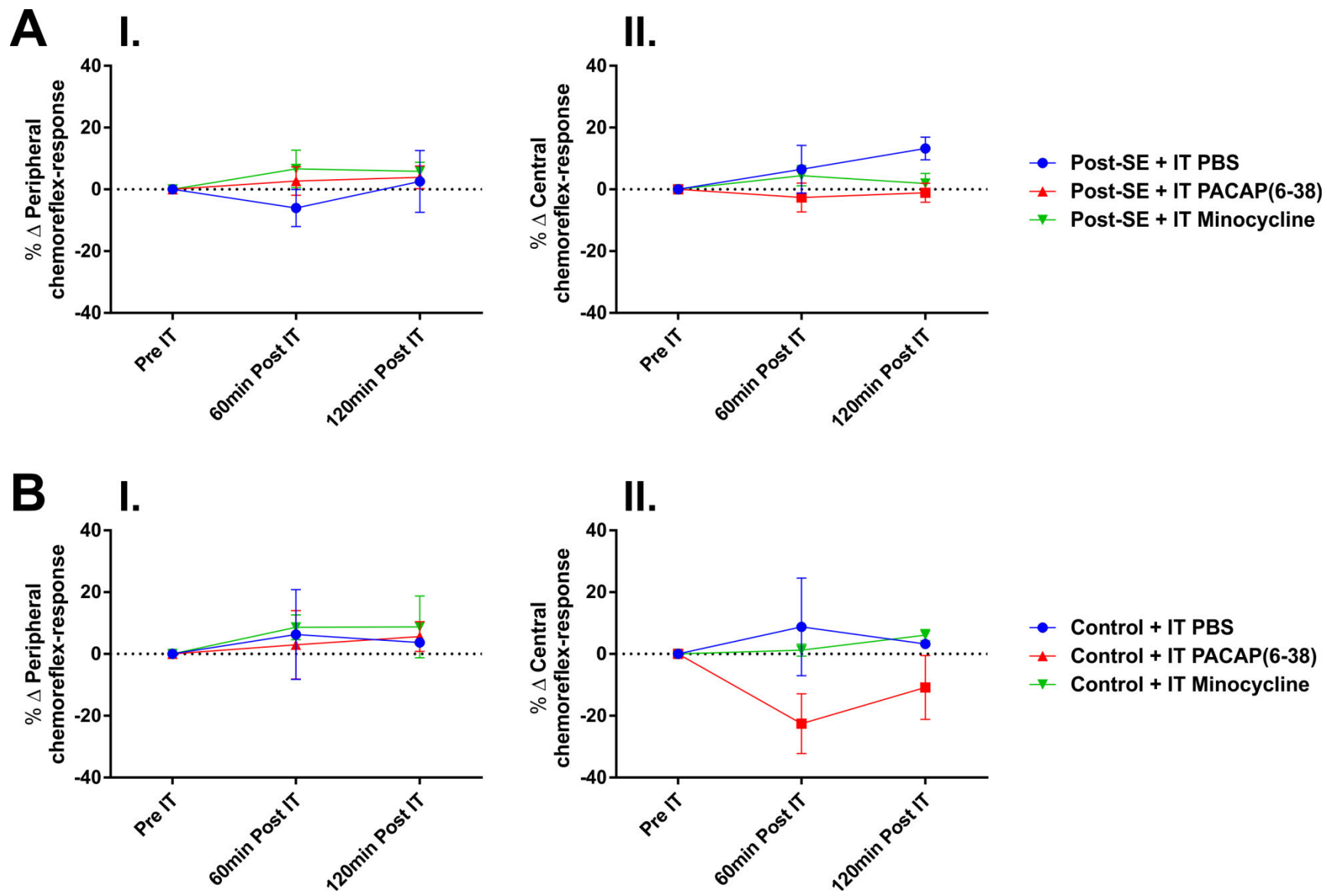
5.5.6. During spontaneous recurrent seizures, microglia are in surveillance state in the vicinity of the RVLM neurons

The morphological analysis of microglia was carried out in post-SE and control rats ($n = 3$) in the vicinity of the RVLM neurons. The brainstem sections, containing TH-immunoreactive (ir) RVLM neurons, were labelled with Iba1, which is a marker for all microglia and CD206-ir labelled anti-inflammatory M2 phenotype of microglia. Immunohistochemical analysis revealed that TH-ir neurons were surrounded with typical resting microglial cells in both groups (Figure 5. 9A-B). In both groups microglia appeared with a round cell body and processes that appeared normal with few ramifications (Figure 5. 9A-B). The total number of microglia in each group are shown in Figure 5. 9C. A branch length and a number of endpoint analysis, was carried out to identify the activated microglia. There were no significant differences in mean branch length and a number of endpoint processes of Iba1 labelled microglia between vehicle control and epileptic rats (Figure 5. 9D-E). The proportion of anti-inflammatory M2 phenotype of microglia was $12.2 \pm 4.0\%$ in post-SE rats, which was similar in controls ($8.9 \pm 2.1\%$; Figure 5. 9F). The findings revealed that microglia are in a surveillance state with no differences in their morphology and proportion of M2 phenotype, at least in the RVLM, between epileptic and control groups.
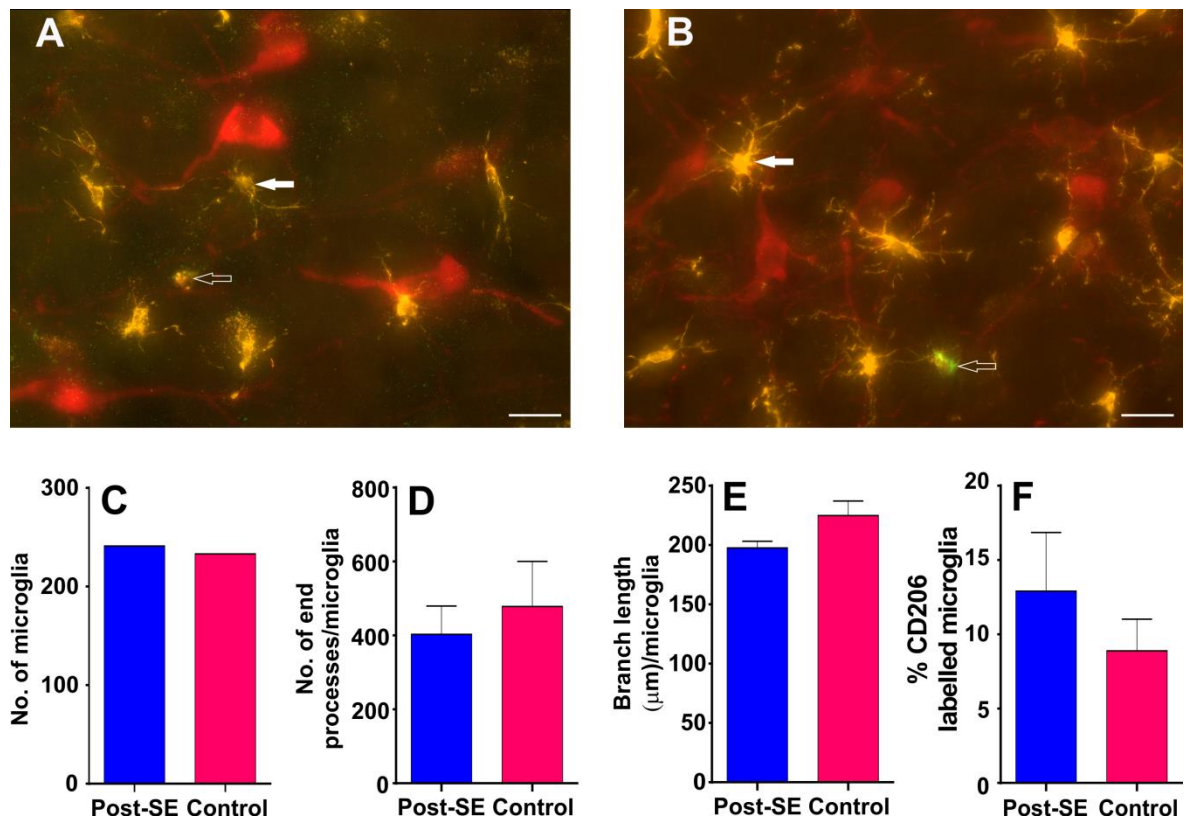
Figure 5. 9: Fluorescence images of the RVLM area containing TH+-ir (red), Iba-1 labelled microglia (yellow) and CD206-labelled M2 microglial cells (green) and their morphological analysis in post-SE and control rats.

Scale bar, 20 µm. TH, Iba1 and CD206 immunoreactivity in the RVLM of post-SE (A) and control (B) rats. In both groups TH+-ir neurons (red) were surrounded with microglia with its round cell body and normal appearing processes with few ramifications (closed arrow) and no change in number of anti-inflammatory M2 microglia (open arrow). Quantitative analysis of number of microglial cells in mean square area (C), number of end processes/microglia (D), branch length (µm)/microglia of Iba1 labelled microglial cells (E) and percent of CD206 labelled M2 microglial cells (F) in the RVLM of post-SE and control rats.

5.6. <u>Discussion</u>

The study provides direct evidence that microglia play a role in mediating increased SNA, and arrhythmogenic cardiac electrophysiological changes in chronic epileptic rats. First, spontaneous seizures cause severe tachycardia with prolongation of QT interval that persisted for more than one hour after the onset of a seizure. Secondly, antagonism of microglial activation, but not PACAP, in the spinal cord significantly reduces the SNA and seizure-induced prolongation of QTc interval in epileptic rats. Thirdly, neither spinal PACAP nor microglia regulate baroreflex or peripheral and central chemoreflex responses in epileptic and control rats, whereas PACAP or microglial antagonist decreases either A- or C-fibre somatosympathetic response in control rats and has no effect in post-SE rats. Fourthly, interictally epileptic rats, and controls, were normotensive with the plasma catecholamine levels in a normal range. Finally, our findings show that morphologically, microglia were in a surveillance stage in chronically epileptic rats with no difference in the number of an M2 phenotype compared with controls.

Microglia are the resident immune cells of the CNS, contributing ~10% of the total brain cell population. They respond to all types of pathological stimulus, including seizures, through activation, and adoption of either a "pro-inflammatory M1" or "anti-inflammatory M2" phenotype (Li et al., 2007; Lai and Todd, 2008; Loane and Byrnes, 2010; Kapoor et al., 2016a). Epileptic seizures cause extensive microglial activation in patients (Beach et al., 1995), and in animal models (Drage et al., 2002), but there is a considerable controversy surrounding the pro-inflammatory (Shapiro et al., 2008) or anti-inflammatory (Mirrione et al., 2010; Eyo et al., 2014) role of microglia during and following a seizure. Previous findings demonstrated that during acute seizures, microglia protect sympathetic preganglionic neurons from excitotoxicity (Bhandare et al., 2015). Our current findings show that the SNA and prolongation of QTc interval following spontaneous seizures were significantly reduced in epileptic rats, when the microglial activation was blocked at the IML. These novel findings strengthen the concept that during chronic pathological insult, such as spontaneous recurrent seizures, maladaptive responses of microglia may lead to a "deleterious" activation state (M1) that triggers the release of pro-inflammatory cytokines such as interleukin (IL)-1β and tumor necrosis factor-α (TNF-α) (Benson et al., 2015), in contrast to their beneficial activation during acute insult (Figure 5. 10). This concept has been proposed by others (Hanisch and Kettenmann, 2007; Gao et al., 2011), and is supported by previous studies (Bhandare et al., 2015), where during acute seizure, microglia can acquire a "beneficial" activation state (M2) to protect an overexcited

neurons, and restore the normal homeostatic condition to limit the further damage (Figure 5. 10).

Cardiovascular autonomic dysfunction with profound arrhythmogenic effects, including prolongation of QT interval, QT dispersion, "T"-wave inversion, and tachycardia or bradycardia, are major risks for SUDEP in humans and animals with spontaneous recurrent seizures (Opherk et al., 2002; Metcalf et al., 2009b; Brotherstone et al., 2010; Powell et al., 2014c; Eastaugh et al., 2015; Lamberts et al., 2015). Activated microglia are present in post-SE rats (Shapiro et al., 2008), and during chronic periods of epilepsy in humans (Beach et al., 1995) and animals (Shapiro et al., 2008). Our electrophysiology findings suggest that during chronic epilepsy ramified or activated microglia ("M1" phenotype) can produce pro-inflammatory cytokines, and contribute to a persistent neuroinflammation that lead to higher SNA and prolongation of QT interval (Figure 5. 10), which was seen even one hour after spontaneous seizure (Figure 5. 3). However, microglial morphological analysis revealed no change in their phenotype at least in the vicinity of the RVLM neurons. In this paradigm, as shown recently, physiological stimulus alert microglia (ramified) (Vinet et al., 2012), and change their spatial distribution and extent of end point processes contacting synapses without significant morphological changes (Kapoor et al., 2016c), which might be facilitating the pro-inflammatory effects during chronic epilepsy. Microglial activation into a deleterious phenotype in Parkinson's disease is responsible for chronic neuroinflammation, and progressive neurodegeneration of dopaminergic neurons (Gao et al., 2011). Thus, increased microglial activation or alertness during the post-seizure period in chronic epilepsy might mediate the expression and release of pro-inflammatory cytokines, and neuroinflammation in the IML. This might lead to severe cardiovascular autonomic dysfunction and a higher risk of malignant cardiac arrhythmias, and SUDEP, during chronic epilepsy (Figure 5. 10) (Kloster and Engelskjøn, 1999; Langan et al., 2000). Moreover, deleterious microglial response during chronic epilepsy might regulate the neurodegeneration, and neuronal loss in brainstem autonomic nuclei in SUDEP and TLE patients (Mueller et al., 2014). Collectively, chronic epilepsy-induced microglial activation contributes to sympathoexcitation and severe arrhythmogenic changes in rats.

Figure 5. 10: A proposed mechanism of action of microglia and PACAP on sympathetic neurons at the IML during acute and chronic seizures, and its possible outcomes.

Time scale on x-axis is variable from hours to days. Under normal conditions, highly motile surveilling microglia continuously survey their microenvironment through direct contact with neuronal synapses and exchange molecular signals. Microglia can immediately sense the disturbed functional and structural integrity of neurons during conditions, such as seizures. Upon detection of these trigger that are higher than the activation threshold, microglia respond through reorganisation of their processes and activity profile. During acute seizures, microglia might acquire "beneficial" activation state (M2) and produce neurotrophic factors, such as IL-10 and TGF-β, to protect the overexcited neurons, and limit further damage and restore normal homeostatic condition. Seizure also triggers synthesis and release of PACAP, which peaks at 12 h post seizure, and produce either neuroprotective or excitatory effects on sympathetic neurons at IML. However, chronic seizures may trigger more drastic changes in functional phenotype of microglia. During chronic seizures, maladaptive responses of microglia may lead to "deleterious" activation state (M1) that triggers release of inflammatory molecules such as IL-1β and TNF-α. This could be the mechanism for increased risk of SUDEP during chronic phase of epilepsy, and specifically during post-seizure period (as shown in orange) that is associated with central autonomic cardiovascular dysfunctions such as increased SNA and proarrhythmogenic changes.
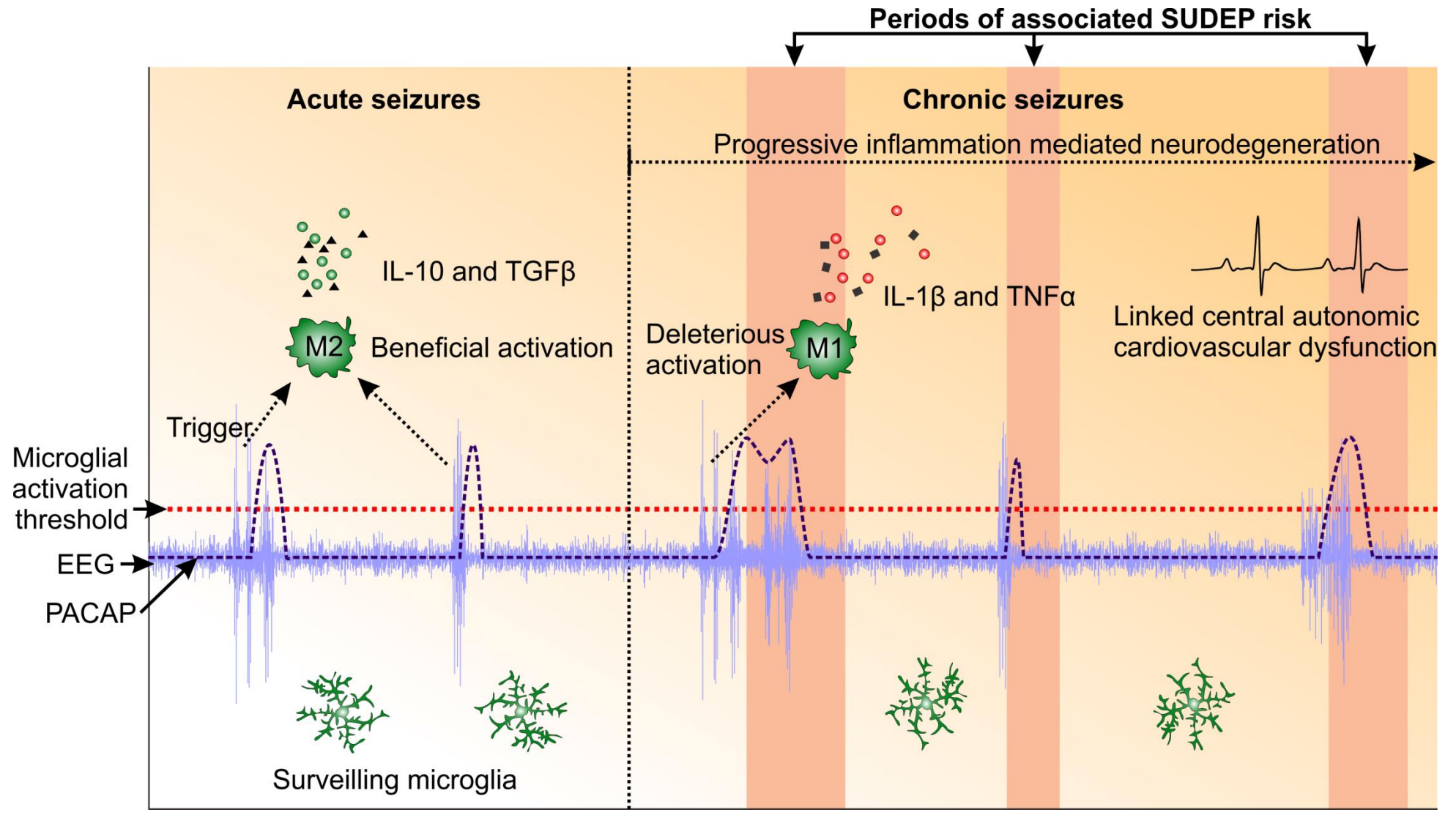
PACAP is a pleiotropic neuropeptide that achieves its effect through cyclic adenosine monophosphate (cAMP)-mediated mechanisms. PACAP produces neuroprotective effects (Shioda et al., 1998) as well as activates sympathetic efferent neurons (Farnham et al., 2008; Farnham et al., 2011; Inglott et al., 2011; Inglott et al., 2012). Antagonism of PACAP in the IML during acute seizures cause greater sympathoexcitation in rats (Bhandare et al., 2015), suggesting its neuroprotective effect during acute seizures. Microinjection of a PACAP receptor antagonist into the RVLM during acute seizures does not alter SNA but does ameliorate the seizure-induced arrhythmogenic effects (Bhandare et al., 2016a). Our results demonstrate that antagonism of PACAP at the IML during chronic epilepsy did not alter SNA or QTc interval, which suggests that PACAP is not modulating overall sympathetic output or arrhythmogenic effects in chronic epileptic rats. This might be due to low levels of PACAP in post-SE rats under our experimental conditions. PACAP gene expression increases after seizures, and reaches maximum at 12 h (Figure 5. 10) (Nomura et al., 2000). During electrophysiology experiments, we did not observe spontaneous seizures, which suggest that there might not be increased PACAP levels in post-SE rats during electrophysiology recordings. However, expression of PACAP can be upregulated after-seizures during the chronic epilepsy, which could produce either neuroprotective or excitatory effect on sympathetic preganglionic neurons as shown previously (Farnham et al., 2008; Farnham et al., 2011; Bhandare et al., 2015; Bhandare et al., 2016b; Bhandare et al., 2016a).

Cardiovascular reflexes (baroreflex, somatosympathetic-reflex and peripheral and central chemoreflex) are crucial for regulation of arterial BP, blood pH, and its chemical constituents (glucose, PaCO2 etc.) (section 1.2.5) (Pilowsky and Goodchild, 2002; Shahid et al., 2011). The baroreflex is the first line of defence during changes in BP and is impaired in epilepsy patients, and animal models (Sakamoto et al., 2005; Dütsch et al., 2006). Glutamate is a major excitatory neurotransmitter, and responsible for normal maintenance of reflex responses (Miyawaki et al., 1996a; Pilowsky and Goodchild, 2002; Pilowsky et al., 2009), which also plays an important role in the development of seizure (Casillas-Espinosa et al., 2012; Powell et al., 2014a; Bhandare et al., 2016b). Heart rate baroreflex sensitivity decreases with intracerebroventricular injection of PACAP in trout (Lancien et al., 2011), whereas in rats, PACAP agonist or antagonist microinjection into the RVLM produce no significant effect (Farnham et al., 2012). In spontaneously hypertensive rats, increased microglial activation, and pro-inflammatory cytokines in PVN causes autonomic (baroreflex) dysfunction (Masson et al., 2015). However, our findings

show that neither PACAP nor microglial antagonist affect the baroreflex, peripheral or central chemoreflex response in epileptic or control rats. In control rats, the microglial antagonist decreases the fast conducting, A-fibre, somatosympathetic response, whereas the PACAP antagonist decreases the slow conducting C-fibre somatosympathetic response; none of the antagonist treatments have effects in epileptic rats. The PACAP antagonist response is consistent with our other findings where PACAP(6-38) treatment did not alter the SNA and ECG findings in chronic epileptic or control rats.

Seizure activity is accompanied with increased sympathetic output, increased plasma noradrenaline levels, tachycardia and elevated BP (Read et al., 2015; Bhandare et al., 2016a). However, our non-invasive BP measurements and plasma catecholamine analysis did not reveal significant differences in MAP or plasma catecholamine levels interictally between epileptic and control rats. In epileptic rats, plasma catecholamine levels are reported to peak at 48 h post-seizure and then return to normal (Read et al., 2015). Differences in species, model, seizure type, seizure frequency, and duration might explain the non-significant differences in MAP and plasma catecholamines seen in epileptic and control rats.

Sudden cardiac death in chronic epilepsy (Kloster and Engelskjøn, 1999; Langan et al., 2000) as well as cardiorespiratory autonomic dysfunction (So et al., 2000; Opherk et al., 2002; Seyal et al., 2010) is almost always associated with seizures. Therefore, it is quite likely that activated microglia-mediated neuroinflammatory changes occurring after seizure are major contributors in central autonomic cardiorespiratory dysfunction, and potentially SUDEP (Figure 5. 10). Overall, the current findings suggest that spontaneous recurrent seizures in chronically epileptic rats produce tachycardia with long-term prolongation of QT interval. Microglial activation in the IML contributes to higher SNA and arrhythmogenic effects in chronic epileptic rats. These findings will help to understand the biphasic microglial response at different stages in epilepsy, and assist in tailoring treatment strategies for seizure-induced central autonomic cardiovascular dysfunction with potential implications to reduce the risk of SUDEP in patients with chronic epilepsy.

Chapter 6
General Discussion

Microglia, PACAP and glutamate modulate the seizure-induced central autonomic cardiovascular dysfunction

Epilepsy is a chronic paroxysmal neurological disorder characterized by seizures (WHO, 2005). Epilepsy is associated with spontaneous seizures, and changes in autonomic functions (Dütsch et al., 2006; Bateman et al., 2008; Metcalf et al., 2009a; Ponnusamy et al., 2012), which is established as a major cause of sudden unexpected death in epilepsy (SUDEP) (Figure 1. 1) (So et al., 2000; Nei et al., 2004; Bateman et al., 2010; Bermeo-Ovalle et al., 2015). The first evidence of SUDEP was published nearly 50 years ago (Hirsch and Martin, 1971), but the underlying mechanism still remains obscure.

The rostral ventrolateral medulla (RVLM) innervates pre-sympathetic neurons in the intermediolateral cell column (IML) of the spinal cord, which in turn control the sympathetic nerve activity (SNA) of post-ganglionic neurons and thus the cardiovascular system (Pilowsky and Goodchild, 2002; Guyenet, 2006).

Microglia are the principal resident immune cells of the central nervous system (CNS). They are the first defence mechanism that acts against every pathological or physiological disturbance in the brain (Hanisch and Kettenmann, 2007; Wake et al., 2009; Tremblay et al., 2010), such as a seizure (Beach et al., 1995; Shapiro et al., 2008; Luo and Chen, 2012; Eyo et al., 2014), to produce pro-inflammatory or anti-inflammatory effects (Figure 4. 8) (Pocock and Kettenmann, 2007; Kettenmann et al., 2011; Orihuela et al., 2016). Levels of the pituitary adenylate cyclase-activating polypeptide (PACAP) increase during and after seizures (Nomura et al., 2000), and it has neuroprotective as well as sympathoexcitatory properties (Lai et al., 1997; Shioda et al., 1998; Takei et al., 1998; Reglodi et al., 2000; Chen et al., 2006; Farnham et al., 2008; Baxter et al., 2011; Farnham et al., 2011; Inglott et al., 2011; Inglott et al., 2012). Glutamate, which is a principal cardiovascular autonomic neurotransmitter in the RVLM (Miyawaki et al., 1996a; Ito and Sved, 1997; Araujo et al., 1999; Sved et al., 2002; Horiuchi et al., 2004a), plays an important role in a development of seizure (Brines et al., 1997; Rainesalo et al., 2004; Kanamori and Ross, 2011).

The major aims of this thesis were to investigate the role of microglia, PACAP and glutamate in the RVLM and/or IML in the progression of seizure-induced autonomic cardiovascular dysfunction during acute and chronic epilepsy in rats.

The findings suggest that the kainic acid (KA)-induced acute seizures cause significant and dose-dependent increase in SNA, mean arterial pressure and heart rate and a prolongation of the QT interval in the ECG. Intrathecal (IT) infusion of PACAP antagonist (PACAP(6-

38)) or microglia antagonist (minocycline and doxycycline) worsened the cardiovascular responses of acute seizures, whereas IT PACAP agonist (PACAP-38) has no significant effect (Chapter 3). Acute seizure-induced cardiovascular responses, including prolongation of the QT interval, are driven by activation of glutamatergic receptors in the RVLM as these effects are abolished by microinjection of glutamate receptor antagonist (kynurenic acid). The activity of PACAP and microglia in the RVLM do not alter the SNA, but mediate prolongation of the QT interval. In the vicinity of the RVLM neurons, microglia remain in a surveillance state with no change in their number of anti-inflammatory M2 phenotype during acute seizures (Chapter 4). In rats with KA-induced chronic temporal lobe epilepsy, spontaneous seizures cause significant tachycardia with long-lasting prolongation of QT interval. The antagonism of microglial activation, but not PACAP, at the level of the IML significantly reduced SNA and proarrhythmogenic effects of chronic seizure activity. Neither PACAP nor microglia regulate baroreflex or peripheral and central chemoreflex responses during chronic epilepsy in rats. In chronic epileptic rats, microglia are in surveillance state and their number of anti-inflammatory M2 phenotype remain unchanged in the vicinity of the RVLM neurons (Chapter 5).

In summary, microglial activation and increased expression of PACAP during acute seizures is sympathoprotective and cardioprotective at the level of spinal cord. On the contrary, during chronic spontaneous seizures, maladaptive responses of microglia produce neurotoxic effects on spinal sympathetic neurons, and cause cardiovascular dysfunction. Thus, augmenting microglial activation and PACAP expression during acute epilepsy, whereas blocking their activation/expression during chronic epilepsy at the spinal cord might provide beneficial effects in people with epilepsy. Moreover, antagonism of glutamatergic receptors at the RVLM can produce protective effects on the presympathetic neurons during acute seizures, and offer a cardioprotection.

PACAP and microglia are protective at intrathecal (IT) level during acute seizures

Seizure causes increased expression of PACAP and microglial activation; however, their action as either neurotoxic or neuroprotective in brainstem and spinal cord cardiovascular nuclei remains unclear. Our findings support the idea that PACAP and its action on microglia at the level of the spinal cord elicit cardioprotective effects during seizures. Thus, therapeutic interventions targeting PACAP and microglia could be a promising strategy for prevention of cardiovascular dysfunction during acute seizures.

The findings during acute seizures, presented in Chapter 3, show that low dose kainic acid (KA) (2 mg/kg)-induced seizures produce strong activation of the SNS to cause pressor and tachycardia responses along with prolongation of QT interval in rats. Sympathetic nerve activity (SNA) begins to rise several minutes after the start of seizures in the hippocampus, confirming the observed autonomic changes are the consequence of seizure activity and not the peripheral or direct effect of KA. This study confirmed that the activated microglia and the increased expression of PACAP during acute seizures have a protective effect on sympathetic preganglionic neurons in the IML of the spinal cord. The seizure-induced sympathoexcitation was worsened in IT PACAP(6-38), minocycline and doxycycline treated group of rats. On the contrary, microglial activation at the spinal cord produces proarrhythmogenic effects that are blocked with minocycline treatment, but not with doxycycline. This could be due to the different pharmacokinetic properties of minocycline and doxycycline, where minocycline is three times more lipophilic than doxycycline (Barza et al., 1975). The opposite effects of microglial antagonism on QT interval compared to SNA might be attributed to their biphasic anti-inflammatory and pro-inflammatory responses (Beck et al., 2010). The early stimulus might polarise majority of microglia into beneficial M2 phenotype, blockade of which worsened the sympathoexcitation, and late stimulus might produce deleterious inflammatory M1 activation, antagonism of which might have reduced the prolongation of QT interval. However, this theory needs further investigation. IT PACAP antagonist treatment does not affect the seizure-induced prolongation of QT interval. The exogenous IT PACAP-38 treatment has no beneficial effects on seizure-induced cardiovascular autonomic disturbances. The failure to see a beneficial effect of exogenous PACAP may be due to an inadequate dose, or local neurons secreting PACAP may be causing a maximal effect so that additional doses of IT PACAP have no effect.

The increase in SNA following PACAP antagonism, or of microglial antagonism, suggests that in this model of acute epilepsy there is a strong activation of a neuroprotective PACAP and microglial pathway. PACAP inhibits the activation of members of mitogen-activated protein kinase (MAPK) family such as c-Jun N-terminal kinase (JNK) (Shioda et al., 1998) and stimulates the secretion of interleukin (IL)-6 in cerebrospinal fluid (CSF) (Gottschall et al., 1994; Shioda et al., 1998). This might be the mechanism of action of PACAP in attenuating seizure-induced sympathoexcitation (Figure 3. 7), as increased MAPK during seizure causes cell death (Jeon et al., 2000; Ferrer et al., 2002), whereas IL-6 has sympathoprotective properties (März et al., 1998; Penkowa et al., 2001). In addition,

PACAP acts on microglial PAC1 and VPAC1 receptors (Delgado et al., 1999) to increase IL-10 expression, causing a down-regulation of cluster of differentiation (CD)40 and B7 mRNA expression in activated microglia that most probably inhibits late phase (deleterious) activation of microglia, thereby acting as a potent anti-inflammatory agent (Figure 3. 7) (Delgado et al., 1999; Kim et al., 2002). On the other hand, the neuroprotective effect of activated microglia may occur through their polarisation towards a protective M2 phenotype and an endogenous production of neurotrophic and anti-apoptotic molecules, such as transforming growth factor-β (TGF-β) and IL-10 (Benarroch, 2013) or by increased glutamate uptake (Persson and Rönnbäck, 2012). The current findings suggest that during acute seizures, microglia and PACAP are neuroprotective, and defend spinal sympathetic preganglionic neurons from excitotoxicity.

During acute seizure, activation of iGluRs at presympathetic RVLM neurons mediates sympathoexcitation, which also causes proarrhythmogenic effects mediated by PACAP and microglia

The activity of the RVLM sympathetic premotor neurons (C1) is increased during seizures (Kanter, 1995; Silveira et al., 2000). However, there is no information about the neurotransmitters mediating activation of brainstem catecholaminergic neurons contributing to the autonomic manifestations that frequently accompany epileptic seizures. Findings suggest that an increase in sympathetic nerve discharge and cardiovascular dysfunction in seizure is due to activation of glutamatergic receptors within the RVLM, which also causes proarrhythmogenic effects mediated PACAP and microglia. In summary, inhibition of glutmategic receptor activation of the C1 sympathetic premotor neurons during acute seizure might produce a significant sympathoprotective and cardioprotective effects.

The study detailed in Chapter 4, investigated the effect of PACAP, microglia and glutamate during acute seizures on the RVLM presympathetic neurons, and clarified the significance of glutamatergic receptor activation in mediating cardiovascular autonomic dysfunction. The study has strengthened the finding that cardiovascular changes are downstream effects of seizure-induced autonomic overactivity and not the direct effect of KA or induction of seizure in autonomic nuclei. The sympathoexcitation, tachycardia, pressor responses and proarrhythmogenic changes during seizure are driven by the action of the excitatory amino acid, glutamate, on sympathetic premotor neurons in the RVLM, as the bilateral microinjection of the ionotropic glutamate receptors (iGluRs) antagonist, kynurenic acid (KYNA), completely abolished these changes. The sympathoexcitatory

effect does not appear to be due to increases or decreases in PACAP secretion or microglial activation in the vicinity of the RVLM neurons. However, PACAP and microglial activity in the vicinity of the RVLM neurons mediates the proarrhythmogenic changes during acute seizures. In addition, the induction of mild or severe seizures (2 and 10 mg/kg KA) does not cause changes in the state of microglia within the RVLM, and microglia remain in a surveillance state with no change in the number of M2 phenotypes that supports *in vivo* electrophysiology findings.

Glutamatergic synapses are important in the development of seizures (Ueda et al., 2001; Rainesalo et al., 2004; Kanamori and Ross, 2011). The sympathetic premotor neurons (C1- and non-C1) in the RVLM maintain tonic excitation of preganglionic neurons (Ito and Sved, 1997; Horiuchi et al., 2004a; Guyenet, 2006; Pilowsky et al., 2009; Turner et al., 2013). Microinjection of glutamate into the RVLM causes pressor responses and sympathoexcitation that are completely blocked with KYNA (Ito and Sved, 1997; Araujo et al., 1999; Dampney et al., 2003), suggesting the significance of glutamate in the regulation of the SNA. The activity of C1 neurons is increased following seizure (Kanter, 1995; Kanter et al., 1996), and is also supported by the findings presented in Chapter 3 and 4, where KA-induced seizures in rats elicited sympathoexcitation, tachycardia and pressor responses. These changes are driven by the excitatory action of glutamate in the RVLM and mediated by ionotropic receptors since the broad-spectrum iGluRs (NMDA, AMPA, and kainate) antagonist (KYNA) completely abolished these effects. In addition, the proarrhythmogenic changes are also abolished with KYNA treatment. On the other hand, the response to PACAP(6-38) microinjection suggests that the excitatory action of PACAP on the RVLM sympathetic premotor neurons mediates proarrhythmogenic changes, but not the seizure-induced sympathoexcitation. A possible explanation could be that the PACAP expression in the RVLM at 2 h post 2 mg/kg KA injection may be insufficient to produce sympathoexcitation, but enough to induce proarrhythmogenic effects. This idea is supported by the findings that PACAP gene expression reaches a maximum at 12 h post 12 mg/kg KA-induced seizures in the paraventricular nucleus (PVN) (Nomura et al., 2000). Finally, the blockade of microglial activation with minocycline microinjection in the RVLM abolishes the prolongation of QT interval caused by KA-induced seizures. This provides the evidence for the physiological interaction between neurons and microglia. However, minocycline microinjection into the RVLM causes no change in sympathoexcitation, tachycardia or pressor responses. The immunohistochemical analysis revealed that there are no changes in microglial morphology or phenotype in the vicinity of

RVLM neurons (branch length or number of endpoint processes) or proportion of the M2 phenotype following induction of seizures. The increased RVLM neuronal activity might have activated microglia (which might be insufficient to differentiate with immunohistochemistry) producing an excitatory effect and contributed to the seizure-induced prolongation of QT interval, but not the sympathoexcitation.

Taken together, glutamatergic receptor activation causes sympathoexcitation during acute seizure, which might be also facilitated by oxidative stress and inflammation in the RVLM (Tsai et al., 2012) or functional failure of glutamate transporters (Figure 4. 8) (Tanaka et al., 1997; Ueda et al., 2001). It is possible that increased synthesis and release of PACAP, depending on the seizures severity, might produce either excitatory effects through phosphorylation of tyrosine hydroxylase (TH) at serine 40 (Bobrovskaya et al., 2007) or neuroprotective effects regulated through decreased caspase 3 (Dejda et al., 2011), increased glial-glutamate transporters (Figiel and Engele, 2000) and redirecting microglia towards anti-inflammatory M2 phenotype (Figure 4. 8) (Brifault et al., 2015). PACAP and its action on microglia also increase production of IL-10, TGF-β and decrease tumor necrosis factor-α (TNF-α) (Wada et al., 2013). In summary, depending on the type, severity and intensity of the stimulus, selective action of PACAP and microglia can regulate the physiological state of neurons. Present findings suggest that during acute seizures both PACAP and microglia regulate excitatory effects at the RVLM as their antagonism results in restoration of QT prolongation.

During chronic epilepsy, deleterious microglial activation at IT level mediates sympathoexcitatory and proarrhythmogenic effects

Interictal autonomic changes are well documented in patients with chronic epilepsy (Ansakorpi et al., 2000; Berilgen et al., 2004; Müngen et al., 2010; Lotufo et al., 2012). Nevertheless, the neuronal mechanisms causing autonomic cardiorespiratory dysfunction during chronic epilepsy are unknown. The findings presented in Chapter 5 establish that the microglial activation, and not PACAP, at the IML accounts for higher SNA and proarrhythmogenic changes during chronic epilepsy in rats. This is the first experimental evidence to support a neurotoxic effect of microglia during chronic epilepsy, in contrast to their neuroprotective action during acute seizures. Thus, owing to biphasic microglial response during acute and chronic epilepsy, ablation of microglial activation during chronic epilepsy might provide cardiovascular protection.

In the two earlier chapters (Chapter 3 and 4), the role of microglia, PACAP, and glutamate is evaluated at the spinal cord and/or at the presympathetic RVLM neurons during acute seizure. In Chapter 5, the role of microglia and PACAP is evaluated at the spinal cord during chronic epilepsy, as the incidence of SUDEP is highest in people with chronic epilepsy (Walczak et al., 2001; Tomson et al., 2005). The *in vivo* electroencephalogram (EEG) and electrocardiogram (ECG) recordings in chronic epileptic rats showed that the spontaneous seizure causes severe tachycardia with prolongation of QT interval that was seen even an hour after an end of seizure. The electrophysiology findings provide the direct evidence for the role of microglia in mediating higher SNA and arrhythmogenic changes during chronic epilepsy in rats. The antagonism of microglial activation, but not PACAP, at the level of IML significantly reduced the SNA and prolongation of QT interval in chronic epileptic rats. These novel findings strengthen the concept that during a chronic pathological insult, such as recurring spontaneous seizures, maladaptive responses of microglia may lead to a "deleterious" activation state (M1) that triggers the release of pro-inflammatory cytokines such as IL-1β and TNF-α, in contrast to their beneficial activation during acute insult (Figure 5. 10). This concept has been proposed by others (Hanisch and Kettenmann, 2007; Gao et al., 2011), and supported by findings from Chapter 3, where during acute seizure, microglia can acquire a "beneficial" activation state (M2) and produce neurotrophic factors, such as IL-10 and TGF-β, to protect overexcited neurons, and restore the normal homeostatic condition to limit the further damage (Figure 5. 10).

Activated microglia have been evidenced during chronic epilepsy both in rats (Shapiro et al., 2008) and humans (Beach et al., 1995). Our findings suggest that during chronic epilepsy, microglia might acquire pro-inflammatory "M1" phenotype, and contribute to persistent neuroinflammation that may lead to higher SNA and prolongation of QT interval (Figure 5. 10). However, microglial morphological analysis revealed no change in their phenotype at least in the vicinity of the RVLM neurons. In this paradigm, as shown recently, physiological stimulus alert microglia (ramified) (Vinet et al., 2012), and change their spatial distribution and extent of end point processes contacting synapses without significant morphological changes (Kapoor et al., 2016c), which might be facilitating the pro-inflammatory effects during chronic epilepsy. It has been shown that microglial activation into deleterious phenotype in Parkinson's disease is responsible for chronic neuroinflammation, and progressive neurodegeneration of dopaminergic neurons (Gao et al., 2011). Thus, increased microglial activation during post-seizure period in chronic

epilepsy might be responsible for augmented pro-inflammatory cytokines, and neuroinflammation at the IML that might lead to severe cardiovascular autonomic dysfunction, and associated risk of SUDEP during post-seizure period (Figure 5. 10) (Kloster and Engelskjøn, 1999; Langan et al., 2000). In addition, activated microglia-induced neuroinflammation during chronic epilepsy might cause neurodegeneration, and neuronal loss in brainstem autonomic nuclei in SUDEP and temporal lobe epilepsy (TLE) patients (Mueller et al., 2014). Collectively, chronic epilepsy-induced microglial activation contributes to sympathoexcitation as well as severe arrhythmogenic changes in post-status epilepticus (post-SE) rats.

Technical limitations

The electrophysiology and histology studies were performed on rats under anesthesia. Anesthesia could influence the activity of the CNS as well as the seizure frequency and SNA. The most important point to be noted is that during electrophysiology experiments our rats were paralysed, and were having no tonic-clonic seizures. Tonic-clonic seizures are the major pathological feature found in the SUDEP cases, and therefore under non-paralytic conditions seizures might have a more devastating effect on the cardiovascular system (as seen during *in vivo* EEG-ECG recordings; Figure 5. 3) than we noticed in our electrophysiology studies. Anesthetics might have influenced the microglial response, as they respond to every change in homeostatic condition and are activated with both "ON" and "OFF" signalling (Bhandare et al., 2016b; Kapoor et al., 2016a). The microglial responses observed during acute seizure RVLM microinjection study might have been influenced by multiple factors such as, the microinjection of either vehicle, PACAP(6-38) or minocycline, and damage incurred by the micropipette during microinjection. Microglia are exquisitely alert for neuronal damage and might have responded differently to acute seizure due to the additional neuronal damage occurred during microinjection.

However, with our well-designed experimental conditions we tried to substantially limit or reduce these variables. We have included the control group of rats for each recorded parameters under similar conditions. This allowed us to evaluate the effects of seizures and eliminate the possible variables in our findings.

The rat model of KA-induced seizure to study the cardiorespiratory electrophysiology mechanisms under anesthesia does not represent the best model of SUDEP. However, our

findings provide the possible role of microglia, PACAP and glutamate in cardiovascular autonomic dysfunction during seizure, which is the major cause of SUDEP.

Concluding remarks

In summary, during acute seizure, microglial activation produces protective effect possibly mediated through the adoption of anti-inflammatory "M2" phenotype at the IML. The activity of microglia at the RVLM presympathetic neurons during acute seizures causes proarrhythmogenic changes but not sympathoexcitation. However, during chronic epilepsy, maladaptive responses of microglia lead to a "deleterious" activation state (M1) that might be causing further neuroinflammation and neurodegeneration. Although PACAP and its action on microglia during acute seizure at the IML produce cardioprotective effects, it has proarrhythmogenic and possibly an excitatory effect on presympathetic RVLM neurons. The expression of PACAP reaches maximum at 12 h post-seizure (Nomura et al., 2000), and might have a significant effect on the cardiovascular system 12 h post-seizure period in chronic epilepsy. However, our study revealed PACAP does not modulate the cardiovascular function in chronic epilepsy, which could attribute to their insufficient expression during the experimental period. Glutamatergic receptor activation at the RVLM neurons is devastating and primarily responsible for cardiovascular dysfunction during acute seizures.

Potential clinical applications

Potential clinical applications of these findings might include: 1) Augmenting microglial activation during acute epilepsy, whereas blocking their activation during chronic epilepsy at the spinal cord might provide beneficial effects in people with epilepsy. 2) During acute epilepsy antagonism of glutamatergic receptors at presympathetic RVLM neurons might provide a very potent cardioprotective effect by blocking sympathoexcitation and proarrhythmogenic changes. 3) PACAP agonist might provide protective effect at the spinal cord during acute seizure and not at the RVLM neurons as it might produce an excitatory effect on presympathetic neurons.

Future directions

The study has been able to investigate the microglial and neurochemical mechanisms of central autonomic cardiovascular dysfunction during acute and chronic epilepsy. This will help to understand the mechanism of SUDEP. However, there are still critical studies needed to be performed to understand the role of microglia, PACAP and glutamate in mediating protective and/or destructive responses during seizure. Future studies can

include and are not limited to: 1) The role of microglia, PACAP and glutamate at the RVLM presympathetic neurons during chronic seizure in the regulation of cardiovascular and autonomic activity. 2) Effect of PACAP treatment during acute and chronic seizures on the microglial polarisation towards different phenotype, and changes in expression of pro-inflammatory and anti-inflammatory cytokines, and its significance in the regulation of autonomic cardiovascular system. 3) More specific studies are required to eliminate any possible off target effects of pharmacological treatments and strengthen the current microglial findings, such as genetic model of CSF1R knockout mice, pharmaco-genetically inducible models using either CD11b-HSVTK or CD11b-DTR mice etc.

References

Abbott SBG, Pilowsky PM (2009) Galanin microinjection into rostral ventrolateral medulla of the rat is hypotensive and attenuates sympathetic chemoreflex. Am J Physiol-Reg I 296:1019-1026.

Agarwal SK, Gelsema AJ, Calaresu FR (1990) Inhibition of rostral VLM by barorecptor activation is relayed through caudal VLM. Am J Physiol-Reg I 258:1271-1278.

Ahmadi A, Sayyah M, Khoshkholgh-Sima B, Choopani S, Kazemi J, Sadegh M, Moradpour F, Nahrevanian H (2013) Intra-hippocampal injection of lipopolysaccharide inhibits kindled seizures and retards kindling rate in adult rats. Exp Brain Res 226:107-120.

Aiba I, Noebels JL (2015) Spreading depolarization in the brainstem mediates sudden cardiorespiratory arrest in mouse SUDEP models. Sci Transl Med 7:282ra246.

Ajmone-Cat MA, Nicolini A, Minghetti L (2003) Prolonged exposure of microglia to lipopolysaccharide modifies the intracellular signaling pathways and selectively promotes prostaglandin E2 synthesis. J Neurochem 87:1193-1203.

Ákos Szabó C, Knape KD, Michelle Leland M, Feldman J, McCoy KJM, Hubbard GB, Williams JT (2009) Mortality in captive baboons with seizures: A new model for SUDEP? Epilepsia 50:1995-1998.

Alexander GM, Godwin DW (2006a) Metabotropic glutamate receptors as a strategic target for the treatment of epilepsy. Epilepsy Res 71:1-22.

Alexander GM, Godwin DW (2006b) Unique presynaptic and postsynaptic roles of group II metabotropic glutamate receptors in the modulation of thalamic network activity. Neurosci 141:501-513.

Alexandre D, Anouar Y, Jegou S, Fournier A, Vaudry H (1999) A cloned frog vasoactive intestinal polypeptide/pituitary adenylate cyclase-activating polypeptide receptor exhibits pharmacological and tissue distribution characteristics of both VPAC1 and VPAC2 receptors in mammals. Endocrinology 140:1285-1293.

Allen AM (2002) Inhibition of the hypothalamic paraventricular nucleus in spontaneously hypertensive rats dramatically reduces sympathetic vasomotor tone. Hypertension 39:275-280.

Almado CEL, Leão RM, Machado BH (2014) Intrinsic properties of rostral ventrolateral medulla presympathetic and bulbospinal respiratory neurons of juvenile rats are not affected by chronic intermittent hypoxia. Exp Physiol 99:937-950.

Amiel J, Dubreuil V, Ramanantsoa N, Fortin G, Gallego J, Brunet JF, Goridis C (2009) PHOX2B in respiratory control: Lessons from congenital central hypoventilation syndrome and its mouse models. Respir Physiol Neurobiol 168:125-132.

Andresen MC, Doyle MW, Jin YH, Bailey TW (2001) Cellular mechanisms of baroreceptor integration at the nucleus tractus solitarius. Ann N Y Acad Sci 940:132-141.

Annegers JF, Hauser WA, Coan SP, Rocca WA (1998) A population-based study of seizures after traumatic brain injuries. N Engl J Med 338:20-24.

Ansakorpi H, Korpelainen JT, Suominen K, Tolonen U, Myllylä VV, Isojärvi JIT (2000) Interictal cardiovascular autonomic responses in patients with temporal lobe epilepsy. Epilepsia 41:42-47.

Anwyl R (1999) Metabotropic glutamate receptors: Electrophysiological properties and role in plasticity. Brain Res Rev 29:83-120.

Araujo GC, Lopes OU, Campos RR (1999) Importance of glycinergic and glutamatergic synapses within the rostral ventrolateral medulla for blood pressure regulation in conscious rats. Hypertension 34:752-755.

Arias RL, Tasse JRP, Bowlby MR (1999) Neuroprotective interaction effects of NMDA and AMPA receptor antagonists in an in vitro model of cerebral ischemia. Brain Res 816:299-308.

Armitage JA, Burke SL, Prior LJ, Barzel B, Eikelis N, Lim K, Head GA (2012) Rapid onset of renal sympathetic nerve activation in Rabbits fed a high-fat diet. Hypertension 60:163-171.

Artinian J, Peret A, Marti G, Epsztein J, Crépel V (2011) Synaptic kainate receptors in interplay with INaP shift the sparse firing of dentate granule cells to a sustained rhythmic mode in temporal lobe epilepsy. J Neurosci 31:10811-10818.

Auerbach DS, Jones J, Clawson BC, Offord J, Lenk GM, Ogiwara I, Yamakawa K, Meisler MH, Parent JM, Isom LL (2013) Altered cardiac electrophysiology and SUDEP in a model of Dravet syndrome. PLoS One 8:e77843.

Averill DB, Tsuchihashi T, Khosla MC, Ferrario CM (1994) Losartan, nonpeptide angiotensin II-type 1 (AT1) receptor antagonist, attenuates pressor and sympathoexcitatory responses evoked by angiotensin II and L-glutamate in rostral ventrolateral medulla. Brain Res 665:245-252.

Awasaki T, Ito K (2004) Engulfing action of glial cells is required for programmed axon pruning during Drosophila metamorphosis. Curr Biol 14:668-677.

Ayala GF, Matsumoto H, Gumnit RJ (1970) Excitability changes and inhibitory mechanisms in neocortical neurons during seizures. J Neurophysiol 33:73-85.

Ayoub AE, Salm AK (2003) Increased morphological diversity of microglia in the activated hypothalamic supraoptic nucleus. J Neurosci 23:7759-7766.

Bai L, Xu H, Collins JF, Ghishan FK (2001) Molecular and functional analysis of a novel neuronal vesicular glutamate transporter. J Biol Chem 276:36764-36769.

Bal-Price A, Brown GC (2001) Inflammatory neurodegeneration mediated by nitric oxide from activated glia-inhibiting neuronal respiration, causing glutamate release and excitotoxicity. J Neurosci 21:6480-6491.

Bardai A, Lamberts RJ, Blom MT, Spanjaart AM, Berdowski J, van der Staal SR, Brouwer HJ, Koster RW, Sander JW, Thijs RD, Tan HL (2012) Epilepsy is a risk factor for sudden cardiac arrest in the general population. PLoS One 7:e42749.

Barman SM, Gebber GL (1985) Axonal projection patterns of ventrolateral medullospinal sympathoexcitatory neurons. J Neurophysiol 53:1551-1566.

Barza M, Brown RB, Shanks C, Gamble C, Weinstein L (1975) Relation between lipophilicity and pharmacological behavior of minocycline, doxycycline, tetracycline, and oxytetracycline in dogs. Antimicrob Agents Chemother 8:713-720.

Bateman LM, Li CS, Seyal M (2008) Ictal hypoxemia in localization-related epilepsy: Analysis of incidence, severity and risk factors. Brain 131:3239-3245.

Bateman LM, Spitz M, Seyal M (2010) Ictal hypoventilation contributes to cardiac arrhythmia and SUDEP: Report on two deaths in video-EEG-monitored patients. Epilepsia 51:916-920.

Baxter PS, Martel MA, McMahon A, Kind PC, Hardingham GE (2011) Pituitary adenylate cyclase-activating peptide induces long-lasting neuroprotection through the induction of activity-dependent signaling via the cyclic AMP response element-binding protein-regulated transcription co-activator 1. J Neurochem 118:365-378.

Bazett HC (1920) An analysis of the time-relations of electrocardiograms. Heart 7:353-370.

Beach TG, Woodhurst WB, MacDonald DB, Jones MW (1995) Reactive microglia in hippocampal sclerosis associated with human temporal lobe epilepsy. Neurosci Lett 191:27-30.

Bealer SL, Little JG, Metcalf CS, Brewster AL, Anderson AE (2010) Autonomic and cellular mechanisms mediating detrimental cardiac effects of status epilepticus. Epilepsy Res 91:66-73.

Beaumont A, Whittle IR (2000) The pathogenesis of tumour associated epilepsy. Acta Neurochir 142:1-15.

Beck KD, Nguyen HX, Galvan MD, Salazar DL, Woodruff TM, Anderson AJ (2010) Quantitative analysis of cellular inflammation after traumatic spinal cord injury: evidence for a multiphasic inflammatory response in the acute to chronic environment. Brain 133:433-447.

Ben-Ari Y (1985) Limbic seizure and brain damage produced by kainic acid: Mechanisms and relevance to human temporal lobe epilepsy. Neurosci 14:375-403.

Ben-Ari Y, Cossart R (2000) Kainate, a double agent that generates seizures: Two decades of progress. Trends Neurosci 23:580-587.

Ben-Ari Y, Tremblay E, Riche D, Ghilini G, Naquet R (1981) Electrographic, clinical and pathological alterations following systemic administration of kainic acid, bicuculline or pentetrazole: Metabolic mapping using the deoxyglucose method with special reference to the pathology of epilepsy. Neurosci 6:1361-1391.

Benarroch EE (2013) Microglia: Multiple roles in surveillance, circuit shaping, and response to injury. Neurology 81:1079-1088.

Benson MJ, Manzanero S, Borges K (2015) Complex alterations in microglial M1/M2 markers during the development of epilepsy in two mouse models. Epilepsia 56:895-905.

Berg AT, Berkovic SF, Brodie MJ, Buchhalter J, Cross JH, Van Emde Boas W, Engel J, French J, Glauser TA, Mathern GW, Moshé SL, Nordli D, Plouin P, Scheffer IE (2010) Revised terminology and concepts for organization of seizures and epilepsies: Report of the ILAE Commission on Classification and Terminology, 2005-2009. Epilepsia 51:676-685.

Berilgen MS, Sari T, Bulut S, Mungen B (2004) Effects of epilepsy on autonomic nervous system and respiratory function tests. Epilepsy Behav 5:513-516.

Bermeo-Ovalle AC, Kennedy JD, Schuele SU (2015) Cardiac and autonomic mechanisms contributing to SUDEP. J Clin Neurophysiol 32:21-29.

Bhandare AM, Mohammed S, Pilowsky PM, Farnham MMJ (2015) Antagonism of PACAP or microglia function worsens the cardiovascular consequences of kainic-acid-induced seizures in rats. J Neurosci 35:2191-2199.

Bhandare AM, Kapoor K, Pilowsky PM, Farnham MMJ (2016a) Seizure-induced sympathoexcitation is caused by activation of glutamatergic receptors in RVLM that also causes proarrhythmogenic changes mediated by PACAP and microglia in rats. J Neurosci 36:506-517.

Bhandare AM, Kapoor K, Farnham MMJ, Pilowsky PM (2016b) Microglia PACAP and glutamate: Friends or foes in seizure-induced autonomic dysfunction and SUDEP? Respir Physiol Neurobiol 226:39-50.

Biber K, Owens T, Boddeke E (2014) What is microglia neurotoxicity (Not)? Glia 62:841-854.

Biber K, Laurie DJ, Berthele A, Sommer B, Tölle TR, Gebicke-Härter PJ, Van Calker D, Boddeke HWGM (1999) Expression and signaling of group I metabotropic glutamate receptors in astrocytes and microglia. J Neurochem 72:1671-1680.

Biet M, Morin N, Lessard-Beaudoin M, Graham RK, Duss S, Gagné J, Sanon NT, Carmant L, Dumaine R (2015) Prolongation of action potential duration and QT interval during epilepsy linked to increased contribution of neuronal sodium channels to cardiac late Na + current. Circ Arrhythm Electrophysiol 8:912-920.

Billman GE, Schwartz PJ, Stone HL (1982) Baroreceptor reflex control of heart rate: A predictor of sudden cardiac death. Circulation 66:874-880.

Blair ML, Mickelsen D (2006) Activation of lateral parabrachial nucleus neurons restores blood pressure and sympathetic vasomotor drive after hypotensive hemorrhage. Am J Physiol-Reg I 291:742-750.

Blümcke I, Becker AJ, Klein C, Scheiwe C, Lie AA, Beck H, Waha A, Friedl MG, Kuhn R, Emson P, Elger C, Wiestler OD (2000) Temporal lobe epilepsy associated up-regulation of metabotropic glutamate receptors: Correlated changes in mGluR1 mRNA and protein expression in experimental animals and human patients. J Neuropathol Exp Neurol 59:1-10.

Bobrovskaya L, Gelain DP, Gilligan C, Dickson PW, Dunkley PR (2007) PACAP stimulates the sustained phosphorylation of tyrosine hydroxylase at serine 40. Cell Signal 19:1141-1149.

Boillée S, Yamanaka K, Lobsiger CS, Copeland NG, Jenkins NA, Kassiotis G, Kollias G, Cleveland DW (2006) Onset and progression in inherited ALS determined by motor neurons and microglia. Science 312:1389-1392.

Borges K, Gearing M, McDermott DL, Smith AB, Almonte AG, Wainer BH, Dingledine R (2003) Neuronal and glial pathological changes during epileptogenesis in the mouse pilocarpine model. Exp Neurol 182:21-34.

Bouilleret V, Cardamone L, Liu C, Koe AS, Fang K, Williams JP, Myers DE, O'Brien TJ, Jones NC (2011) Confounding neurodegenerative effects of manganese for in vivo MR imaging in rat models of brain insults. J Magn Reson Imaging 34:774-784.

Boulter J, Hollmann M, O'Shea-Greenfield A, Hartley M, Deneris E, Maron C, Heinemann S (1990) Molecular cloning and functional expression of glutamate receptor subunit genes. Science 249:1033-1037.

Brifault C, Gras M, Liot D, May V, Vaudry D, Wurtz O (2015) Delayed pituitary adenylate cyclase-activating polypeptide delivery after brain stroke improves functional recovery by inducing M2 microglia/macrophage polarization. Stroke 46:520-528.

Brines ML, Sundaresan S, Spencer DD, de Lanerolle NC (1997) Quantitative autoradiographic analysis of ionotropic glutamate receptor subtypes in human temporal lobe epilepsy: Up-regulation in reorganized epileptogenic hippocampus. Eur J Neurosci 9:2035-2044.

Brotherstone R, Blackhall B, McLellan A (2010) Lengthening of corrected QT during epileptic seizures. Epilepsia 51:221-232.

Browne TR, Holmes GL (2008) Handbook of epilepsy, Fourth Edition. Philadelphia, PA: Lippincott Williams and Wilkins.

Burguillos MA, Deierborg T, Kavanagh E, Persson A, Hajji N, Garcia-Quintanilla A, Cano J, Brundin P, Englund E, Venero JL, Joseph B (2011) Caspase signalling controls microglia activation and neurotoxicity. Nature 472:319-324.

Burman KJ, Sartor DM, Verberne AJM, Llewellyn-Smith IJ (2004) Cocaine- and amphetamine-regulated transcript in catecholamine and noncatecholamine presympathetic vasomotor neurons of rat rostral ventrolateral medulla. J Comp Neurol 476:19-31.

Buscail L, Gourlet P, Cauvin A, De Neef P, Gossen D, Arimura A, Miyata A, Coy DH, Robberecht P, Christophe J (1990) Presence of highly selective receptors for PACAP (pituitary adenylate cyclase activating peptide) in membranes from the rat pancreatic acinar cell line AR 4-2J. FEBS Lett 262:77-81.

Byrum CE, Stornetta R, Guyenet PG (1984) Electrophysiological properties of spinally-projecting A5 noradrenergic neurons. Brain Res 303:15-29.

Callera JC, Sévoz C, Laguzzi R, Machado BH (1997) Microinjection of a serotonin3 receptor agonist into the NTS of unanesthetized rats inhibits the bradycardia evoked by activation of the baro- and chemoreflexes. J Autonom Nerv Syst 63:127-136.

Cano G, Sved AF, Rinaman L, Rabin BS, Card JP (2001) Characterization of the central nervous system innervation of the rat spleen using viral transneuronal tracing. J Comp Neurol 439:1-18.

Cano G, Passerin AM, Schiltz JC, Card JP, Morrison SF, Sved AF (2003) Anatomical substrates for the central control of sympathetic outflow to interscapular adipose tissue during cold exposure. J Comp Neurol 460:303-326.

Cao WH, Morrison SF (2003) Disinhibition of rostral raphe pallidus neurons increases cardiac sympathetic nerve activity and heart rate. Brain Res 980:1-10.

Card JP, Sved JC, Craig B, Raizada M, Vazquez J, Sveb AF (2006) Efferent projections of rat rostroventrolateral medulla C1 catecholamine neurons: Implications for the central control of cardiovascular regulation. J Comp Neurol 499:840-859.

Cardona AE, Pioro EP, Sasse ME, Kostenko V, Cardona SM, Dijkstra IM, Huang D, Kidd G, Dombrowski S, Dutta R, Lee JC, Cook DN, Jung S, Lira SA, Littman DR, Ransohoff RM (2006) Control of microglial neurotoxicity by the fractalkine receptor. Nat Neurosci 9:917-924.

Carta M, Fièvre S, Gorlewicz A, Mulle C (2014) Kainate receptors in the hippocampus. Eur J Neurosci 39:1835-1844.

Casillas-Espinosa PM, Powell KL, O'Brien TJ (2012) Regulators of synaptic transmission: roles in the pathogenesis and treatment of epilepsy. Epilepsia 53 Suppl 9:41-58.

Castle M, Comoli E, Loewy AD (2005) Autonomic brainstem nuclei are linked to the hippocampus. Neurosci 134:657-669.

Caulder EH, Riegle MA, Godwin DW (2014) Activation of Group 2 metabotropic glutamate receptors reduces behavioral and electrographic correlates of pilocarpine induced status epilepticus. Epilepsy Res 108:171-181.

Chalmers J, Pilowsky P (1991) Brainstem and bulbospinal neurotransmitter systems in the control of blood pressure. J Hypertens 9:675-694.

Chamberlin NL, Saper CB (1992) Topographic organization of cardiovascular responses to electrical and glutamate microstimulation of the parabrachial nucleus in the rat. J Comp Neurol 326:245-262.

Chan RKW, Sawchenko PE (1998) Organization and transmitter specificity of medullary neurons activated by sustained hypertension: Implications for understanding baroreceptor reflex circuitry. J Neurosci 18:371-387.

Chan UPF, Lee JFY, Wang SH, Leung KL, Chen GG (2003) Induction of colon cancer cell death by 7-hydroxystaurosporine (UCN-01) is associated with increased p38 MAPK and decreased Bcl-xL. Anticancer Drugs 14:761-766.

Chang JY, Korolev VV (1997) Cyclic AMP and sympathetic neuronal programmed cell death. Neurochem Int 31:161-167.

Chapman AG (1998) Glutamate receptors in epilepsy. Prog Brain Res 116:371-383.

Chen MJ, Yang MH, Han WJ, An SC, Liu YH, Liu ZQ, Ren W (2014) Individual aortic baroreceptors are sensitive to different ranges of blood pressures. Sci China Life Sci 57:502-509.

Chen QH, Toney GM (2010) In vivo discharge properties of hypothalamic paraventricular nucleus neurons with axonal projections to the rostral ventrolateral medulla. J Neurophysiol 103:4-15.

Chen S, Aston-Jones G (1995) Anatomical evidence for inputs to ventrolateral medullary catecholaminergic neurons from the midbrain periaqueductal gray of the rat. Neurosci Lett 195:140-144.

Chen Y, Samal B, Hamelink CR, Xiang CC, Chen Y, Chen M, Vaudry D, Brownstein MJ, Hallenbeck JM, Eiden LE (2006) Neuroprotection by endogenous and exogenous PACAP following stroke. Regul Peptides 137:4-19.

Chepurnova NE, Ponomarenko AA, Chepurnov SA (2002) Peptidergic mechanisms of hyperthermia-evoked convulsions in rats in early postnatal ontogenesis. Neurosci Behav Physiol 32:505-511.

Chiba T, Tanaka K, Tatsuoka H, Dun SL, Dun NJ (1996) The synaptic structure of PACAP immunoreactive axons in the intermediolateral nucleus of the rat. Neurosci Lett 214:65-68.

Chitravanshi VC, Sapru HN (1999) Phrenic nerve responses to chemical stimulation of the subregions of ventral medullary respiratory neuronal group in the rat. Brain Res 821:443-460.

Chrétien F, Le Pavec G, Vallat-Decouvelaere AV, Delisle MB, Uro-Coste E, Ironside JW, Gambetti P, Parchi P, Créminon C, Dormont D, Mikol J, Gray F, Gras G (2004) Expression of excitatory amino acid transporter-1 (EAAT-1) in brain macrophages and microglia of patients with prion diseases. J Neuropath Exp Neur 63:1058-1071.

Conn PJ, Pin JP (1997) Pharmacology and functions of metabotropic glutamate receptors. Annu Rev Pharmacol Toxicol 37:205-237.

Coulter DA, Eid T (2012) Astrocytic regulation of glutamate homeostasis in epilepsy. Glia 60:1215-1226.

Coyle JT, Puttfarcken P (1993) Oxidative stress, glutamate, and neurodegenerative disorders. Science 262:689-695.

Cravo SL, Morrison SF (1993) The caudal ventrolateral medulla is a source of tonic sympathoinhibition. Brain Res 621:133-136.

Cunningham C, Wilcockson DC, Campion S, Lunnon K, Perry VH (2005) Central and systemic endotoxin challenges exacerbate the local inflammatory response and increase neuronal death during chronic neurodegeneration. J Neurosci 25:9275-9284.

Cunningham Jr ET, Bohn MC, Sawchenko PE (1990) Organization of adrenergic inputs to the paraventricular and supraoptic nuclei of the hypothalamus in the rat. J Comp Neurol 292:651-667.

Damasceno DD, Savergnini SQ, Gomes ERM, Guatimosim S, Ferreira AJ, Doretto MC, Almeida AP (2013) Cardiac dysfunction in rats prone to audiogenic epileptic seizures. Seizure 22:259-266.

Dampney RAL, Horiuchi J, Tagawa T, Fontes MAP, Potts PD, Polson JW (2003) Medullary and supramedullary mechanisms regulating sympathetic vasomotor tone. Acta Physiol Scand 177:209-218.

Danbolt NC (2001) Glutamate uptake. Prog Neurobiol 65:1-105.

Darbin O, Casebeer DJ, Naritoku DK (2002) Cardiac dysrhythmia associated with the immediate postictal state after maximal electroshock in freely moving rat. Epilepsia 43:336-341.

Darstein M, Petralia RS, Swanson GT, Wenthold RJ, Heinemann SF (2003) Distribution of kainate receptor subunits at hippocampal mossy fiber synapses. J Neurosci 23:8013-8019.

Das M, Vihlen CS, Legradi G (2007) Hypothalamic and brainstem sources of pituitary adenylate cyclase-activating polypeptide nerve fibers innervating the hypothalamic paraventricular nucleus in the rat. J Comp Neurol 500:761-776.

Davalos D, Grutzendler J, Yang G, Kim JV, Zuo Y, Jung S, Littman DR, Dustin ML, Gan WB (2005) ATP mediates rapid microglial response to local brain injury in vivo. Nat Neurosci 8:752-758.

Day TA, Sibbald JR, Smith DW (1992) A1 neurons and excitatory amino acid receptors in rat caudal medulla mediate vagal excitation of supraoptic vasopressin cells. Brain Res 594:244-252.

De Sousa Buck H, Caous CA, Lindsey CJ (2001) Projections of the paratrigeminal nucleus to the ambiguus, rostroventrolateral and lateral reticular nuclei, and the solitary tract. Auton Neurosci-Basic 87:187-200.

Dean C (2004) Hemorrhagic sympathoinhibition mediated through the periaqueductal gray in the rat. Neurosci Lett 354:79-83.

Dejda A, Seaborn T, Bourgault S, Touzani O, Fournier A, Vaudry H, Vaudry D (2011) PACAP and a novel stable analog protect rat brain from ischemia: Insight into the mechanisms of action. Peptides 32:1207-1216.

Delgado M (2002a) Vasoactive intestinal peptide and pituitary adenylate cyclase-activating polypeptide inhibit CBP–NF-κB interaction in activated microglia. Biochem Bioph Res Co 297:1181-1185.

Delgado M (2002b) Vasoactive intestinal peptide and pituitary adenylate cyclase-activating polypeptide inhibit the MEKK1/MEK4/JNK signaling pathway in endotoxin-activated microglia. Biochem Bioph Res Co 293:771-776.

Delgado M, Munoz-Elias EJ, Gomariz RP, Ganea D (1999) Vasoactive intestinal peptide and pituitary adenylate cyclase-activating polypeptide enhance IL-10 production by murine macrophages: In vitro and in vivo studies. J Immunol 162:1707-1716.

Delogu AB, Spinelli A, Battaglia D, Dravet C, De Nisco A, Saracino A, Romagnoli C, Lanza GA, Crea F (2011) Electrical and autonomic cardiac function in patients with Dravet syndrome. Epilepsia 52:55-58.

Dembowsky K, Lackner K, Czachurski J, Seller H (1981) Tonic catecholaminergic inhibition of the spinal somato-sympathetic reflexes originating in the ventrolateral medulla oblongata. J Auton Nerv Syst 3:277-290.

Deshpande LS, Lou JK, Mian A, Blair RE, Sombati S, Attkisson E, DeLorenzo RJ (2008) Time course and mechanism of hippocampal neuronal death in an in vitro model of status epilepticus: Role of NMDA receptor activation and NMDA dependent calcium entry. Eur J Pharmacol 583:73-83.

Devinsky O, Perrine K, Theodore WH (1994) Interictal autonomic nervous system function in patients with epilepsy. Epilepsia 35:199-204.

Devinsky O, Vezzani A, Najjar S, De Lanerolle NC, Rogawski MA (2013) Glia and epilepsy: Excitability and inflammation. Trends Neurosci 36:174-184.

DiBona GF (1986) Neural mechanisms in body fluid homeostasis. Fed Proc 45:2871-2877.

Dickson L, Finlayson K (2009) VPAC and PAC receptors: From ligands to function. Pharmacol Ther 121:294-316.

DiMicco JA, Samuels BC, Zaretskaia MV, Zaretsky DV (2002) The dorsomedial hypothalamus and the response to stress: Part renaissance, part revolution. Pharmacol Biochem Behav 71:469-480.

Dlouhy BJ, Gehlbach BK, Kreple CJ, Kawasaki H, Oya H, Buzza C, Granner MA, Welsh MJ, Howard MA, Wemmie JA, Richerson GB (2015) Breathing inhibited when seizures spread to the amygdala and upon amygdala stimulation. J Neurosci 35:10281-10289.

Domann R, Westerhoff CHA, Witte OW (1994) Inhibitory mechanisms terminating paroxysmal depolarization shifts in hippocampal neurons of rats. Neurosci Lett 176:71-74.

Dong HW, Swanson LW (2006) Projections from bed nuclei of the stria terminalis, dorsomedial nucleus: Implications for cerebral hemisphere integration of neuroendocrine, autonomic, and drinking responses. J Comp Neurol 494:75-107.

Drage MG, Holmes GL, Seyfried TN (2002) Hippocampal neurons and glia in epileptic EL mice. J Neurocytol 31:681-692.

Dreifuss FE, Bancaud J, Henriksen O (1981) Proposal for revised clinical and electroencephalographic classification of epileptic seizures. Epilepsia 22:489-501.

Drexel M, Preidt AP, Sperk G (2012) Sequel of spontaneous seizures after kainic acid-induced status epilepticus and associated neuropathological changes in the subiculum and entorhinal cortex. Neuropharmacology 63:806-817.

Du D, Jiang M, Liu M, Wang J, Xia C, Guan R, Shen L, Ji Y, Zhu D (2015) Microglial P2X7 receptor in the hypothalamic paraventricular nuclei contributes to sympathoexcitatory responses in acute myocardial infarction rat. Neurosci Lett 587:22-28.

Dürr K, Norsted E, Gömüç B, Suarez E, Hannibal J, Meister B (2007) Presence of pituitary adenylate cyclase-activating polypeptide (PACAP) defines a subpopulation of hypothalamic POMC neurons. Brain Res 1186:203-211.

Dütsch M, Hilz MJ, Devinsky O (2006) Impaired baroreflex function in temporal lobe epilepsy. J Neurol 253:1300-1308.

Eastaugh AJ, Thompson T, Vohra JK, O'Brien TJ, Winship I (2015) Sudden unexpected death, epilepsy and familial cardiac pathology. J Clin Neurosci 22:1594-1600.

El Khoury J, Toft M, Hickman SE, Means TK, Terada K, Geula C, Luster AD (2007) Ccr2 deficiency impairs microglial accumulation and accelerates progression of Alzheimer-like disease. Nat Med 13:432-438.

Eleuteri S, Polazzi E, Contestabile A (2008) Neuroprotection of microglia conditioned media from apoptotic death induced by staurosporine and glutamate in cultures of rat cerebellar granule cells. Neurosci Lett 448:74-78.

Epsztein J, Represa A, Jorquera I, Ben-Ari Y, Crépel V (2005) Recurrent mossy fibers establish aberrant kainate receptor-operated synapses on granule cells from epileptic rats. J Neurosci 25:8229-8239.

Eyo UB, Peng J, Swiatkowski P, Mukherjee A, Bispo A, Wu LJ (2014) Neuronal hyperactivity recruits microglial processes via neuronal NMDA receptors and microglial P2Y12 receptors after status epilepticus. J Neurosci 34:10528-10540.

Faingold CL, Naritoku a DK, Copley CA, Randall ME, Riaz A, Anderson CAB, Arneric SP (1992) Glutamate in the inferior colliculus plays a critical role in audiogenic seizure initiation. Epilepsy Res 13:95-105.

Fan W, Schild JH, Andresen MC (1999) Graded and dynamic reflex summation of myelinated and unmyelinated rat aortic baroreceptors. Am J Physiol-Reg I 277:748-756.

Farkas E, Jansen ASP, Loewy AD (1998) Periaqueductal gray matter input to cardiac-related sympathetic premotor neurons. Brain Res 792:179-192.

Farnham MM, Lung MS, Tallapragada VJ, Pilowsky PM (2012) PACAP causes PAC1/VPAC2 receptor mediated hypertension and sympathoexcitation in normal and hypertensive rats. Am J Physiol-Heart C 303:910-917.

Farnham MMJ, Inglott MA, Pilowsky PM (2011) Intrathecal PACAP-38 causes increases in sympathetic nerve activity and heart rate but not blood pressure in the spontaneously hypertensive rat. Am J Physiol-Heart C 300:214-222.

Farnham MMJ, Li Q, Goodchild AK, Pilowsky PM (2008) PACAP is expressed in sympathoexcitatory bulbospinal C1 neurons of the brain stem and increases sympathetic nerve activity in vivo. Am J Physiol-Reg I 294:1304-1311.

Ferrer I, Carmona M, Puig B, Domínguez I, Viñals F (2002) Active, phosphorylation-dependent MAP kinases, MAPK/ERK, SAPK/JNK and p38, and specific transcription factor substrates are differentially expressed following systemic administration of kainic acid to the adult rat. Acta Neuropathol 103:391-407.

Ficker DM, So EL, Shen WK, Annegers JF, O'Brien PC, Cascino GD, Belau PO (1998) Population-based study of the incidence of sudden unexplained death in epilepsy. Neurology 51:1270-1274.

Figiel M, Engele J (2000) Pituitary adenylate cyclase-activating polypeptide (PACAP), a neuron- derived peptide regulating glial glutamate transport and metabolism. J Neurosci 20:3596-3605.

Filipovic R, Zecevic N (2008) Neuroprotective role of minocycline in co-cultures of human fetal neurons and microglia. Exp Neurol 211:41-51.

Finley JCW, Katz DM (1992) The central organization of carotid body afferent projections to the brainstem of the rat. Brain Res 572:108-116.

Florence G, Dahlem MA, Almeida ACG, Bassani JWM, Kurths J (2009) The role of extracellular potassium dynamics in the different stages of ictal bursting and spreading depression: A computational study. J Theor Biol 258:219-228.

Fulwiler CE, Saper CB (1984) Subnuclear organization of the efferent connections of the parabrachial nucleus in the rat. Brain Res Rev 7:229-259.

Gabbott PLA, Warner T, Busby SJ (2007) Catecholaminergic neurons in medullary nuclei are among the post-synaptic targets of descending projections from infralimbic area 25 of the rat medial prefrontal cortex. Neurosci 144:623-635.

Gabbott PLA, Warner TA, Jays PRL, Salway P, Busby SJ (2005) Prefrontal cortex in the rat: Projections to subcortical autonomic, motor, and limbic centers. J Comp Neurol 492:145-177.

Gaede AH, Inglott MA, Farnham MMJ, Pilowsky PM (2012) Catestatin has an unexpected effect on the intrathecal actions of PACAP dramatically reducing blood pressure. Am J Physiol-Reg I 303:719-726.

Gao HM, Zhou H, Zhang F, Wilson BC, Kam W, Hong JS (2011) HMGB1 acts on microglia Mac1 to mediate chronic neuroinflammation that drives progressive neurodegeneration. J Neurosci 31:1081-1092.

Ghauri M, Chapman AG, Meldrum BS (1996) Convulsant and anticonvulsant actions of agonists and antagonists of group III mGluRs. Neuroreport 7:1469-1474.

Gieroba ZJ, Shapoval LN, Blessing WW (1994) Inhibition of the A1 area prevents hemorrhage-induced secretion of vasopressin in rats. Brain Res 657:330-332.

Glasscock E, Yoo JW, Chen TT, Klassen TL, Noebels JL (2010) Kv1.1 potassium channel deficiency reveals brain-driven cardiac dysfunction as a candidate mechanism for sudden unexplained death in epilepsy. J Neurosci 30:5167-5175.

Goldman AM, Glasscock E, Yoo J, Chen TT, Klassen TL, Noebels JL (2009) Arrhythmia in heart and brain: KCNQ1 mutations link epilepsy and sudden unexplained death. Sci Transl Med 1:2ra6.

Gonzalez C, Almaraz L, Obeso A, Rigual R (1994) Carotid body chemoreceptors: From natural stimuli to sensory discharges. Physiol Rev 74:829-898.

Gordon PH, Moore DH, Miller RG, Florence JM, Verheijde JL, Doorish C, Hilton JF, Spitalny GM, MacArthur RB, Mitsumoto H, Neville HE, Boylan K, Mozaffar T, Belsh JM, Ravits J, Bedlack RS, Graves MC, McCluskey LF, Barohn RJ, Tandan R (2007) Efficacy of minocycline in patients with amyotrophic lateral sclerosis: a phase III randomised trial. Lancet Neurol 6:1045-1053.

Gottlieb M, Matute C (1997) Expression of ionotropic glutamate receptor subunits in glial cells of the hippocampal CA1 area following transient forebrain ischemia. J Cereb Blood Flow Metab 17:290-300.

Gottschall PE, Tatsuno I, Arimura A (1994) Regulation of interleukin-6 (IL-6) secretion in primary cultured rat astrocytes: Synergism of interleukin-1 (IL-1) and pituitary adenylate cyclase activating polypeptide (PACAP). Brain Res 637:197-203.

Guo GB, Thames MD, Abboud FM (1982) Differential baroreflex control of heart rate and vascular resistance in rabbits. Relative role of carotid, aortic, and cardiopulmonary baroreceptors. Circ Res 50:554-565.

Guo Z-L, Lai H-C, Longhurst JC (2002) Medullary pathways involved in cardiac sympathoexcitatory reflexes in the cat. Brain Res 925:55-66.

Guo Z-L, Tjen-A-Looi SC, Fu L-W, Longhurst JC (2009) Nitric oxide in rostral ventrolateral medulla regulates cardiac-sympathetic reflexes: role of synthase isoforms. Am J Physiol-Heart C 297:1478-1486.

Gurbanova AA, Aker RG, Sirvanci S, Demiralp T, Onat FY (2008) Intra-amygdaloid injection of kainic acid in rats with genetic absence epilepsy: The relationship of typical absence epilepsy and temporal lobe epilepsy. J Neurosci 28:7828-7836.

Guyenet PG (2006) The sympathetic control of blood pressure. Nat Rev Neurosci 7:335-346.

Guyenet PG (2014) Regulation of breathing and autonomic outflows by chemoreceptors. Compr Physiol 4:1511-1562.

Guyenet PG, Filtz TM, Donaldson SR (1987) Role of excitatory amino acids in rat vagal and sympathetic baroreflexes. Brain Res 407:272-284.

Guyenet PG, Haselton JR, Sun MK (1989) Sympathoexcitatory neurons of the rostroventrolateral medulla and the origin of the sympathetic vasomotor tone. Prog Brain Res 81:105-116.

Guyenet PG, Stornetta RL, Bochorishvili G, DePuy SD, Burke PGR, Abbott SBG (2013) C1 neurons: The body's EMTs. Am J Physiol-Reg I 305:187-204.

Guyenet PG, Stornetta RL, Schreihofer AM, Pelaez NM, Hayar A, Aicher S, Llewellyn-Smith IJ (2002) Opioid signalling in the rat rostral ventrolateral medulla. Clin Exp Pharmacol Physiol 29:238-242.

Hackett ML, Glozier NS, Martiniuk AL, Jan S, Anderson CS (2011) Sydney epilepsy incidence study to measure illness consequences: The SESIMIC observational epilepsy study protocol. BMC Neurol 11:1-11.

Hagino Y, Kariura Y, Manago Y, Amano T, Wang B, Sekiguchi M, Nishikawa K, Aoki S, Wada K, Noda M (2004) Heterogeneity and potentiation of AMPA type of glutamate receptors in rat cultured microglia. Glia 47:68-77.

Hanisch U-K, Kettenmann H (2007) Microglia: active sensor and versatile effector cells in the normal and pathologic brain. Nat Neurosci 10:1387-1394.

Hannibal J, Mikkelsen JD, Clausen H, Holst JJ, Wulff BS, Fahrenkrug J (1995) Gene expression of pituitary adenylate cyclase activating polypeptide (PACAP) in the rat hypothalamus. Regul Peptides 55:133-148.

Hara M, Sasa M, Kawabata A, Serikawa T, Yamada T, Yamada J, Takaori S (1993) Decreased dopamine and increased norepinephrine levels in the spontaneously epileptic rat, a double mutant rat. Epilepsia 34:433-440.

Hartley DM, Kurth MC, Bjerkness L, Weiss JH, Choi DW (1993) Glutamate receptor-induced 45Ca2+ accumulation in cortical cell culture correlates with subsequent neuronal degeneration. J Neurosci 13:1993-2000.

Hasegawa D, Matsuki N, Fujita M, Ono K, Orima H (2004) Kinetics of glutamate and γ-aminobutyric acid in cerebrospinal fluid in a canine model of complex partial status epilepticus induced by kainic acid. J Vet Med Sci 66:1555-1559.

Haxhiu MA, Jansen ASP, Cherniack NS, Loewy AD (1993) CNS innervation of airway-related parasympathetic preganglionic neurons: a transneuronal labeling study using pseudorabies virus. Brain Res 618:115-134.

He Y, Appel S, Le W (2001) Minocycline inhibits microglial activation and protects nigral cells after 6-hydroxydopamine injection into mouse striatum. Brain Res 909:187-193.

Heeringa J, Berkenbosch A, De Goede J, Olievier CN (1979) Relative contribution of central and peripheral chemoreceptors to the ventilatory response to CO2 during hyperoxia. Resp Physiol 37:365-379.

Hellier JL, Patrylo PR, Buckmaster PS, Dudek FE (1998) Recurrent spontaneous motor seizures after repeated low-dose systemic treatment with kainate: Assessment of a rat model of temporal lobe epilepsy. Epilepsy Res 31:73-84.

Hellwig S, Heinrich A, Biber K (2013) The brain's best friend: Microglial neurotoxicity revisited. Front Cell Neurosci 7:1-11.

Herbert H, Saper CB (1992) Organization of medullary adrenergic and noradrenergic projections to the periaqueductal gray matter in the rat. J Comp Neurol 315:34-52.

Herman ST (2002) Epilepsy after brain insult: Targeting epileptogenesis. Neurology 59:S21-S26.

Hermann DM, Luppi PH, Peyron C, Hinckel P, Jouvet M (1997) Afferent projections to the rat nuclei raphe magnus, raphe pallidus and reticularis gigantocellularis pars α demonstrated by iontophoretic application of choleratoxin (subunit b). J Chem Neuroanat 13:1-21.

Hermes SM, Mitchell JL, Aicher SA (2006) Most neurons in the nucleus tractus solitarii do not send collateral projections to multiple autonomic targets in the rat brain. Exp Neurol 198:539-551.

Hirooka Y, Potts PD, Dampney RAL (1997a) Role of angiotensin II receptor subtypes in mediating the sympathoexcitatory effects of exogenous and endogenous angiotensin peptides in the rostral ventrolateral medulla of the rabbit. Brain Res 772:107-114.

Hirooka Y, Polson JW, Potts PD, Dampney RAL (1997b) Hypoxia-induced fos expression in neurons projecting to the pressor region in the rostral ventrolateral medulla. Neurosci 80:1209-1224.

Hirsch CS, Martin DL (1971) Unexpected death in young epileptics. Neurology 21:682-690.

Ho YH, Lin YT, Wu CWJ, Chao YM, Chang AYW, Chan JYH (2015) Peripheral inflammation increases seizure susceptibility via the induction of neuroinflammation and oxidative stress in the hippocampus. J Biomed Sci 22.

Hodges MR, Wehner M, Aungst J, Smith JC, Richerson GB (2009) Transgenic mice lacking serotonin neurons have severe apnea and high mortality during development. J Neurosci 29:10341-10349.

Hodges MR, Tattersall GJ, Harris MB, McEvoy SD, Richerson DN, Deneris ES, Johnson RL, Chen ZF, Richerson GB (2008) Defects in breathing and thermoregulation in mice with near-complete absence of central serotonin neurons. J Neurosci 28:2495-2505.

Holighaus Y, Mustafa T, Eiden LE (2011) PAC1hop, null and hip receptors mediate differential signaling through cyclic AMP and calcium leading to splice variant-specific gene induction in neural cells. Peptides 32:1647-1655.

Holloway BB, Stornetta RL, Bochorishvili G, Erisir A, Viar KE, Guyenet PG (2013) Monosynaptic glutamatergic activation of locus coeruleus and other lower brainstem noradrenergic neurons by the C1 cells in mice. J Neurosci 33:18792-18805.

Holst AG, Winkel BG, Risgaard B, Nielsen JB, Rasmussen PV, Haunsø S, Sabers A, Uldall P, Tfelt-Hansen J (2013) Epilepsy and risk of death and sudden unexpected death in the young: A nationwide study. Epilepsia 54:1613-1620.

Horiuchi J, Killinger S, Dampney RAL (2004a) Contribution to sympathetic vasomotor tone of tonic glutamatergic inputs to neurons in the RVLM. Am J Physiol-Reg I 287:1335-1343.

Horiuchi J, McAllen RM, Allen AM, Killinger S, Fontes MAP, Dampney RAL (2004b) Descending vasomotor pathways from the dorsomedial hypothalamic nucleus: Role of medullary raphe and RVLM. Am J Physiol-Reg I 287:824-832.

Horton RW, Prestwich SA, Meldrum BS (1982) γ-Aminobutyric acid and benzodiazepine binding sites in audiogenic seizure-susceptible mice. J Neurochem 39:865-870.

Hotta H, Koizumi K, Stewart M (2009) Cardiac sympathetic nerve activity during kainic acid-induced limbic cortical seizures in rats. Epilepsia 50:923-927.

Hua XY, Svensson CI, Matsui T, Fitzsimmons B, Yaksh TL, Webb M (2005) Intrathecal minocycline attenuates peripheral inflammation-induced hyperalgesia by inhibiting p38 MAPK in spinal microglia. Eur J Neurosci 22:2431-2440.

Imai F, Suzuki H, Oda J, Ninomiya T, Ono K, Sano H, Sawada M (2007) Neuroprotective effect of exogenous microglia in global brain ischemia. J Cerebr Blood F Met 27:488-500.

Inglott MA, Farnham MMJ, Pilowsky PM (2011) Intrathecal PACAP-38 causes prolonged widespread sympathoexcitation via a spinally mediated mechanism and increases in basal metabolic rate in anesthetized rat. Am J Physiol-Heart C 300:2300-2307.

Inglott MA, Lerner EA, Pilowsky PM, Farnham MMJ (2012) Activation of PAC1 and VPAC receptor subtypes elicits differential physiological responses from sympathetic preganglionic neurons in the anaesthetized rat. Br J Pharmacol 167:1089-1098.

Ito S, Sved AF (1997) Tonic glutamate-mediated control of rostral ventrolateral medulla and sympathetic vasomotor tone. Am J Physiol-Reg I 273:487-494.

Ivy CM, Scott GR (2015) Control of breathing and the circulation in high-altitude mammals and birds. Comp Biochem Physiol A Mol Integr Physiol 186:66-74.

Jansen ASP, Wessendorf MW, Loewy AD (1995a) Transneuronal labeling of CNS neuropeptide and monoamine neurons after pseudorabies virus injections into the stellate ganglion. Brain Res 683:1-24.

Jansen ASP, Van Nguyen X, Karpitskiy V, Mettenleiter TC, Loewy AD (1995b) Central command neurons of the sympathetic nervous system: Basis of the fight-or-flight response. Science 270:644-646.

Jefferys JGR, Menendez de la Prida L, Wendling F, Bragin A, Avoli M, Timofeev I, Lopes da Silva FH (2012) Mechanisms of physiological and epileptic HFO generation. Prog Neurobiol 98:250-264.

Jeon SH, Kim YS, Bae CD, Park JB (2000) Activation of JNK and p38 in rat hippocampus after kainic acid induced seizure. Exp Mol Med 32:227-230.

Johnston SC, Horn JK, Valente J, Simon RP (1995) The role of hypoventilation in a sheep model of epileptic sudden death. Ann Neurol 37:531-537.

Johnston SC, Siedenberg R, Min JK, Jerome EH, Laxer KD (1997) Central apnea and acute cardiac ischemia in a sheep model of epileptic sudden death. Ann Neurol 42:588-594.

Jones JFX, Wang Y, Jordan D (1998) Activity of C fibre cardiac vagal efferents in anaesthetized cats and rats. J Physiol 507:869-880.

Joo KM, Chung YH, Kim MK, Nam RH, Lee BL, Lee KH, Cha CI (2004) Distribution of vasoactive intestinal peptide and pituitary adenylate cyclase-activating polypeptide receptors (VPAC1, VPAC2, and PAC1 receptor) in the rat brain. J Comp Neurol 476:388-413.

Jupp B, Williams J, Binns D, Hicks RJ, Cardamone L, Jones N, Rees S, O'Brien TJ (2012) Hypometabolism precedes limbic atrophy and spontaneous recurrent seizures in a rat model of TLE. Epilepsia 53:1233-1244.

Kåhlin J, Mkrtchian S, Ebberyd A, Hammarstedt-Nordenvall L, Nordlander B, Yoshitake T, Kehr J, Prabhakar N, Poellinger L, Fagerlund MJ, Eriksson LI (2014) The human carotid body releases acetylcholine, ATP and cytokines during hypoxia. Exp Physiol 99:1089-1098.

Kaila K, Lamsa K, Smirnov S, Taira T, Voipio J (1997) Long-lasting GABA-mediated depolarization evoked by high-frequency stimulation in pyramidal neurons of rat hippocampal slice is attributable to a network-driven, bicarbonate-dependent K+ transient. J Neurosci 17:7662-7672.

Kalume F, Westenbroek RE, Cheah CS, Yu FH, Oakley JC, Scheuer T, Catterall WA (2013) Sudden unexpected death in a mouse model of Dravet syndrome. J Clin Invest 123:1798-1808.

Kanamori K, Ross BD (2011) Chronic electrographic seizure reduces glutamine and elevates glutamate in the extracellular fluid of rat brain. Brain Res 1371:180-191.

Kangrga IM, Loewy AD (1995) Whole-cell recordings from visualized C1 adrenergic bulbospinal neurons: ionic mechanisms underlying vasomotor tone. Brain Res 670:215-232.

Kanter RK (1995) Seizure-induced c-fos expression in rat medulla oblongata is not dependent on associated elevation of blood pressure. Neurosci Lett 194:201-204.

Kanter RK, Strauss JA, Sauro MD (1996) Comparison of neurons in rat medulla oblongata with Fos immunoreactivity evoked by seizures, chemoreceptor, or baroreceptor stimulation. Neurosci 73:807-816.

Kapoor K, Bhandare AM, Farnham MMJ, Pilowsky PM (2016a) Alerted microglia and the sympathetic nervous system: A novel form of microglia in the development of hypertension. Respir Physiol Neurobiol 226:51-62.

Kapoor K, Bhandare AM, Mohammed S, Farnham MMJ, Pilowsky PM (2016b) Microglial number is related to the number of tyrosine hydroxylase neurons in SHR and normotensive rats. Auton Neurosci-Basic 198:10-18.

Kapoor K, Bhandare AM, Nedoboy PE, Mohammed S, Farnham MMJ, Pilowsky PM (2016c) Dynamic changes in the relationship of microglia to cardiovascular neurons in response to increases and decreases in blood pressure. Neurosci 329:12-29.

Kashihara K, McMullan S, Lonergan T, Goodchild AK, Pilowsky PM (2008) Neuropeptide Y in the rostral ventrolateral medulla blocks somatosympathetic reflexes in anesthetized rats. Auton Neurosci-Basic 142:64-70.

Kasting NW, Veale WL, Cooper KE, Lederis K (1981) Vasopressin may mediate febrile convulsions. Brain Res 213:327-333.

Kato K, Yokoyama T, Yamaguchi-Yamada M, Yamamoto Y (2013) Short-term hypoxia transiently increases dopamine β-hydroxylase immunoreactivity in glomus cells of the rat carotid body. J Histochem Cytochem 61:55-62.

Katz LC, Shatz CJ (1996) Synaptic activity and the construction of cortical circuits. Science 274:1133-1138.

Kennedy JD, Hardin KA, Parikh P, Li CS, Seyal M (2015) Pulmonary edema following generalized tonic clonic seizures is directly associated with seizure duration. Seizure 27:19-24.

Kettenmann H, Hanisch UK, Noda M, Verkhratsky A (2011) Physiology of microglia. Physiol Rev 91:461-553.

Kharatishvili I, Nissinen JP, McIntosh TK, Pitkänen A (2006) A model of posttraumatic epilepsy induced by lateral fluid-percussion brain injury in rats. Neurosci 140:685-697.

Kiely JM, Gordon FJ (1993) Non-NMDA receptors in the rostral ventrolateral medulla mediate somatosympathetic pressor responses. J Auton Nerv Syst 43:231-239.

Kiely JM, Gordon FJ (1994) Role of rostral ventrolateral medulla in centrally mediated pressor responses. Am J Physiol Heart Circ Physiol 267:1549-1556.

Kim W-K, Kan Y, Ganea D, Hart RP, Gozes I, Jonakait GM (2000) Vasoactive intestinal peptide and pituitary adenylyl cyclase-activating polypeptide inhibit tumor necrosis factor-α production in injured spinal cord and in activated microglia via a cAMP-dependent pathway. J Neurosci 20:3622-3630.

Kim WK, Ganea D, Jonakait GM (2002) Inhibition of microglial CD40 expression by pituitary adenylate cyclase-activating polypeptide is mediated by interleukin-10. J Neuroimmunol 126:16-24.

Kitamura Y, Takata K, Inden M, Tsuchiya D, Yanagisawa D, Nakata J, Taniguchi T (2004) Intracerebroventricular injection of microglia protects against focal brain ischemia. J Pharmacol Sci 94:203-206.

Kitamura Y, Yanagisawa D, Inden M, Takata K, Tsuchiya D, Kawasaki T, Taniguchi T, Shimohama S (2005) Recovery of focal brain ischemia-induced behavioral dysfunction by intracerebroventricular injection of microglia. J Pharmacol Sci 97:289-293.

Kloster R, Engelskjøn T (1999) Sudden unexpected death in epilepsy (SUDEP): A clinical perspective and a search for risk factors. J Neurol Neurosurg Psychiatry 67:439-444.

Koshiya N, Guyenet PG (1994) A5 noradrenergic neurons and the carotid sympathetic chemoreflex. Am J Physiol-Reg I 267:519-526.

Koshiya N, Guyenet PG (1996) NTS neurons with carotid chemoreceptor inputs arborize in the rostral ventrolateral medulla. Am J Physiol-Reg I 270:1273-1278.

Koshiya N, Huangfu D, Guyenet PG (1993) Ventrolateral medulla and sympathetic chemoreflex in the rat. Brain Res 609:174-184.

Kreisel T, Frank MG, Licht T, Reshef R, Ben-Menachem-Zidon O, Baratta MV, Maier SF, Yirmiya R (2014) Dynamic microglial alterations underlie stress-induced depressive-like behavior and suppressed neurogenesis. Mol Psychiatr 19:699-709.

Kung LH, Glasgow J, Ruszaj A, Gray T, Scrogin KE (2010) Serotonin neurons of the caudal raphe nuclei contribute to sympathetic recovery following hypotensive hemorrhage. Am J Physiol-Reg I 298:939-953.

Kuri BA, Chan SA, Smith CB (2009) PACAP regulates immediate catecholamine release from adrenal chromaffin cells in an activity-dependent manner through a protein kinase C-dependent pathway. J Neurochem 110:1214-1225.

Lai AY, Todd KG (2008) Differential regulation of trophic and proinflammatory microglial effectors is dependent on severity of neuronal injury. Glia 56:259-270.

Lai CC, Wu SY, Lin HH, Dun NJ (1997) Excitatory action of pituitary adenylate cyclase activating polypeptide on rat sympathetic preganglionic neurons in vivo and in vitro. Brain Res 748:189-194.

Lalancette-Hébert M, Gowing G, Simard A, Yuan CW, Kriz J (2007) Selective ablation of proliferating microglial cells exacerbates ischemic injury in the brain. J Neurosci 27:2596-2605.

Lamberts RJ, Blom MT, Novy J, Belluzzo M, Seldenrijk A, Penninx BW, Sander JW, Tan HL, Thijs RD (2015) Increased prevalence of ECG markers for sudden cardiac arrest in refractory epilepsy. J Neurol Neurosurg Psychiatry 86:309-313.

Lancien F, Mimassi N, Conlon JM, Mével JCL (2011) Central pituitary adenylate cyclase-activating polypeptide (PACAP) and vasoactive intestinal peptide (VIP) decrease the baroreflex sensitivity in trout. Gen Comp Endocrinol 171:245-251.

Langan Y, Nashef L, Sander JWAS (2000) Sudden unexpected death in epilepsy: A series of witnessed deaths. J Neurol Neurosurg Psychiatry 68:211-213.

Lawrence AJ, Jarrott B (1996) Neurochemical modulation of cardiovascular control in the nucleus tractus solitarius. Prog Neurobiol 48:21-53.

LeBlanc BW, Zerah ML, Kadasi LM, Chai N, Saab CY (2011) Minocycline injection in the ventral posterolateral thalamus reverses microglial reactivity and thermal hyperalgesia secondary to sciatic neuropathy. Neurosci Lett 498:138-142.

Légrádi G, Shioda S, Arimura A (1994) Pituitary adenylate cyclase-activating polypeptide-like immunoreactivity in autonomic regulatory areas of the rat medulla oblongata. Neurosci Lett 176:193-196.

Lehre KP, Danbolt NC (1998) The number of glutamate transport subtype molecules at glutamatergic synapses: Chemical and stereological quantification in young adult rat brain. J Neurosci 18:8751-8757.

Lévesque M, Avoli M (2013) The kainic acid model of temporal lobe epilepsy. Neurosci Biobehav R 37:2887 - 2899.

Lévesque M, Langlois JMP, Lema P, Courtemanche R, Bilodeau GA, Carmant L (2009) Synchronized gamma oscillations (30-50 Hz) in the amygdalo-hippocampal network in relation with seizure propagation and severity. Neurobiol Dis 35:209-218.

Levy LM, Warr O, Attwell D (1998) Stoichiometry of the glial glutamate transporter GLT-1 expressed inducibly in a Chinese hamster ovary cell line selected for low endogenous Na+-dependent glutamate uptake. J Neurosci 18:9620-9628.

Li JM, Zeng YJ, Peng F, Li L, Yang TH, Hong Z, Lei D, Chen Z, Zhou D (2010) Aberrant glutamate receptor 5 expression in temporal lobe epilepsy lesions. Brain Res 1311:166-174.

Li L, Lu J, Tay SSW, Moochhala SM, He BP (2007) The function of microglia, either neuroprotection or neurotoxicity, is determined by the equilibrium among factors released from activated microglia in vitro. Brain Res 1159:8-17.

Li YW, Gieroba ZJ, Blessing WW (1992a) Chemoreceptor and baroreceptor responses of A1 area neurons projecting to supraoptic nucleus. Am J Physiol-Reg I 263:310-317.

Li YW, Wesselingh SL, Blessing WW (1992b) Projections from rabbit caudal medulla to C1 and A5 sympathetic premotor neurons, demonstrated with phaseolus leucoagglutinin and herpes simplex virus. J Comp Neurol 317:379-395.

Li Z, Mi X, Xiong Y, Xu X, Wang X, Wang L (2015) Elevated expression of the delta-subunit of epithelial sodium channel in temporal lobe epilepsy patients and rat model. J Mol Neurosci 57:510-518.

Lipski J, Kanjhan R, Kruszewska B, Rong W (1996) Properties of presympathetic neurones in the rostral ventrolateral medulla in the rat: An intracellular study 'in vivo'. J Physiol 490:729-744.

Lipski J, Lin J, Teo MY, Van Wyk M (2002) The network vs. pacemaker theory of the activity of RVL presympathetic neurons-a comparison with another putative pacemaker system. Auton Neurosci-Basic 98:85-89.

Loane DJ, Byrnes KR (2010) Role of microglia in neurotrauma. Neurotherapeutics 7:366-377.

Loane DJ, Kumar A, Stoica BA, Cabatbat R, Faden AI (2014) Progressive neurodegeneration after experimental brain trauma: Association with chronic microglial activation. J Neuropathol Exp Neurol 73:14-29.

López-Redondo F, Nakajima K, Honda S, Kohsaka S (2000) Glutamate transporter GLT-1 is highly expressed in activated microglia following facial nerve axotomy. Mol Brain Res 76:429-435.

Lortet S, Samuel D, Had-Aissouni L, Masmejean F, Kerkerian-Le Goff L, Pisano P (1999) Effects of PKA and PKC modulators on high affinity glutamate uptake in primary neuronal cell cultures from rat cerebral cortex. Neuropharmacology 38:395-402.

Löscher W, Schwark WS (1987) Further evidence for abnormal GABAergic circuits in amygdala-kindled rats. Brain Res 420:385-390.

Lothman EW, Collins RC (1981) Kainic acid induced limbic seizures: metabolic, behavioral, electroencephalographic and neuropathological correlates. Brain Res 218:299-318.

Lothman EW, Collins RC, Ferrendelli JA (1981) Kainic acid-induced limbic seizures: Electrophysiologic studies. Neurology 31:806-812.

Lotufo PA, Valiengo L, Benseñor IM, Brunoni AR (2012) A systematic review and meta-analysis of heart rate variability in epilepsy and antiepileptic drugs. Epilepsia 53:272-282.

Luckhaus C, Hennersdorf M, Bell M, Agelink MW, Zielasek J, Cordes J (2008) Brugada syndrome as a potential cardiac risk factor during electroconvulsive therapy (ECT). World J Biol Psychia 9:150-153.

Ludwig A, Budde T, Stieber J, Moosmang S, Wahl C, Holthoff K, Langebartels A, Wotjak C, Munsch T, Zong X, Feil S, Feil R, Lancel M, Chien KR, Konnerth A, Pape HC, Biel M, Hofmann F (2003) Absence epilepsy and sinus dysrhythmia in mice lacking the pacemaker channel HCN2. EMBO J 22:216-224.

Luo XG, Chen SD (2012) The changing phenotype of microglia from homeostasis to disease. Transl Neurodegener 1:1-13.

Macdermott AB, Mayer ML, Westbrook GL, Smith SJ, Barker JL (1986) NMDA-receptor activation increases cytoplasmic calcium concentration in cultured spinal cord neurones. Nature 321:519-522.

Madden CJ, Sved AF (2003a) Cardiovascular regulation after destruction of the C1 cell group of the rostral ventrolateral medulla in rats. Am J Physiol Heart C 285:2734-2748.

Madden CJ, Sved AF (2003b) Rostral ventrolateral medulla C1 neurons and cardiovascular regulation. Cell Mol Neurobiol 23:739-749.

Maekawa F, Fujiwara K, Tsukahara S, Yada T (2006) Pituitary adenylate cyclase-activating polypeptide neurons of the ventromedial hypothalamus project to the midbrain central gray. Neuroreport 17:221-224.

Maggi CA, Meli A (1986) Suitability of urethane anesthesia for physiopharmacological investigations in various systems. Part 2: Cardiovascular system. Experientia 42:292-297.

Maiorov DN, Malpas SC, Head GA (2000) Influence of pontine A5 region on renal sympathetic nerve activity in conscious rabbits. Am J Physiol-Reg I 278:311-319.

Mandal M, Wei J, Zhong P, Cheng J, Duffney LJ, Liu W, Yuen EY, Twelvetrees AE, Li S, Li XJ, Kittler JT, Yan Z (2011) Impaired α-amino-3-hydroxy-5-methyl-4-isoxazolepropionic acid (AMPA) receptor trafficking and function by mutant Huntingtin. J Biol Chem 286:33719-33728.

Mandel DA, Schreihofer AM (2006) Central respiratory modulation of barosensitive neurones in rat caudal ventrolateral medulla. J Physiol 572:881-896.

Mandel DA, Schreihofer AM (2008) Glutamatergic inputs to the CVLM independent of the NTS promote tonic inhibition of sympathetic vasomotor tone in rats. Am J Physiol-Heart C 295:1772-1779.

März P, Cheng JG, Gadient RA, Patterson PH, Stoyan T, Otten U, Rose-John S (1998) Sympathetic neurons can produce and respond to interleukin 6. P Natl Acad Sci USA 95:3251-3256.

Massey CA, Sowers LP, Dlouhy BJ, Richerson GB (2014) Mechanisms of sudden unexpected death in epilepsy: The pathway to prevention. Nat Rev Neurol 10:271-282.

Massey CA, Iceman KE, Johansen SL, Wu Y, Harris MB, Richerson GB (2015) Isoflurane abolishes spontaneous firing of serotonin neurons and masks their pH/CO2 chemosensitivity. J Neurophysiol 113:2879-2888.

Masson GS, Nair AR, Soares PPS, Michelini LC, Francis J (2015) Aerobic training normalizes autonomic dysfunction, HMGB1 content, microglia activation and inflammation in hypothalamic paraventricular nucleus of SHR. Am J Physiol-Heart C 309:1115-1122.

Mayer ML, Miller RJ (1990) Excitatory amino acid receptors, second messengers and regulation of intracellular Ca2+ in mammalian neurons. Trends Pharmacol Sci 11:254-260.

McGrattan PA, Brown JH, Brown OM (1987) Parasympathetic effects on in vivo rat heart can be regulated through an α1-adrenergic receptor. Circ Res 60:465-471.

McKellar S, Loewy AD (1982) Efferent projections of the A1 catecholamine cell group in the rat: An autoradiographic study. Brain Res 241:11-29.

McMahon NC, Drinkhill MJ, Hainsworth R (1996) Reflex vascular responses from aortic arch, carotid sinus and coronary baroreceptors in the anaesthetized dog. Exp Physiol 81:397-408.

McMullan S, Pilowsky PM (2012) Sympathetic premotor neurones project to and are influenced by neurones in the contralateral rostral ventrolateral medulla of the rat in vivo. Brain Res 1439:34-43.

McMullan S, Pathmanandavel K, Pilowsky PM, Goodchild AK (2008) Somatic nerve stimulation evokes qualitatively different somatosympathetic responses in the cervical and splanchnic sympathetic nerves in the rat. Brain Res 1217:139-147.

McNamara JO (1994) Cellular and molecular basis of epilepsy. J Neurosci 14:3413-3425.

McNamara JO (1999) Emerging insights into the genesis of epilepsy. Nature 399:15-22.

Medvedev A, MacKenzie L, Hiscock JJ, Willoughby JO (2000) Kainic acid induces distinct types of epileptiform discharge with differential involvement of hippocampus and neocortex. Brain Res Bulletin 52:89-98.

Melander T, Hokfelt T, Rokaeus A (1986) Distribution of galaninlike immunoreactivity in the rat central nervous system. J Comp Neurol 248:475-517.

Meldrum BS (2000) Glutamate as a neurotransmitter in the brain: Review of physiology and pathology. J Nutr 130:1007S-1015S.

Meldrum BS, Akbar MT, Chapman AG (1999) Glutamate receptors and transporters in genetic and acquired models of epilepsy. Epilepsy Res 36:189-204.

Metcalf CS, Radwanski PB, Bealer SL (2009a) Status epilepticus produces chronic alterations in cardiac sympathovagal balance. Epilepsia 50:747-754.

Metcalf CS, Poelzing S, Little JG, Bealer SL (2009b) Status epilepticus induces cardiac myofilament damage and increased susceptibility to arrhythmias in rats. Am J Physiol-Heart C 297:2120-2127.

Michael Spyer K, Gourine AV (2009) Chemosensory pathways in the brainstem controlling cardiorespiratory activity. Philos Trans R Soc Lond B Biol Sci 364:2603-2610.

Michaels RL, Rothman SM (1990) Glutamate neurotoxicity in vitro: Antagonist pharmacology and intracellular calcium concentrations. J Neurosci 10:283-292.

Mikulecká A, Hliňák Z, Mareš P (1999) Behavioural effects of a subconvulsive dose of kainic acid in rats. Behav Brain Res 101:21-28.

Mills E, Minson J, Drolet G, Chalmers J (1990) Effect of intrathecal amino acid receptor antagonists on basal blood pressure and pressor responses to brainstem stimulation in normotensive and hypertensive rats. J Cardiovasc Pharmacol 15:877-883.

Minson J, Pilowsky P, Llewellyn-Smith I, Kaneko T, Kapoor V, Chalmers J (1991) Glutamate in spinally projecting neurons of the rostral ventral medulla. Brain Res 555:326-331.

Minson JB, Llewellyn-Smith IJ, Arnolda LF, Pilowsky PM, Oliver JR, Chalmers JP (1994) Disinhibition of the rostral ventral medulla increases blood pressure and Fos expression in bulbospinal neurons. Brain Res 646:44-52.

Mirrione MM, Konomos DK, Gravanis I, Dewey SL, Aguzzi A, Heppner FL, Tsirka SE (2010) Microglial ablation and lipopolysaccharide preconditioning affects pilocarpine-induced seizures in mice. Neurobiol Dis 39:85-97.

Miyata A, Arimura A, Dahl RR, Minamino N, Uehara A, Jiang L, Culler MD, Coy DH (1989) Isolation of a novel 38 residue-hypothalamic polypeptide which stimulates adenylate cyclase in pituitary cells. Biochem Biophys Res Commun 164:567-574.

Miyawaki T, Goodchild AK, Pilowsky PM (2001) Rostral ventral medulla 5-HT1A receptors selectively inhibit the somatosympathetic reflex. Am J Physiol-Reg I 280:1261-1268.

Miyawaki T, Goodchild AK, Pilowsky PM (2002a) Evidence for a tonic GABA-ergic inhibition of excitatory respiratory-related afferents to presympathetic neurons in the rostral ventrolateral medulla. Brain Res 924:56-62.

Miyawaki T, Goodchild AK, Pilowsky PM (2002b) Activation of mu-opioid receptors in rat ventrolateral medulla selectively blocks baroreceptor reflexes while activation of delta opioid receptors blocks somato-sympathetic reflexes. Neurosci 109:133-144.

Miyawaki T, Minson J, Arnolda L, Chalmers J, Llewellyn-Smith I, Pilowsky P (1996a) Role of excitatory amino acid receptors in cardiorespiratory coupling in ventrolateral medulla. Am J Physiol-Reg I 271:1221-1230.

Miyawaki T, Minson J, Arnolda L, Llewellyn-Smith I, Chalmers J, Pilowsky P (1996b) AMPA/kainate receptors mediate sympathetic chemoreceptor reflex in the rostral ventrolateral medulla. Brain Res 726:64-68.

Miyawaki T, Suzuki S, Minson J, Arnolda L, Chalmers J, Llewellyn-Smith I, Pilowsky P (1997) Role of AMPA/kainate receptors in transmission of the sympathetic baroreflex in rat CVLM. Am J Physiol- Reg I 272:800-812.

Mobley SC, Mandel DA, Schreihofer AM (2006) Systemic cholecystokinin differentially affects baro-activated GABAergic neurons in rat caudal ventrolateral medulla. J Neurophysiol 96:2760-2768.

Mokriski BK, Nagle SE, Papuchis GC, Cohen SM, Waxman GJ (1992) Electroconvulsive therapy-induced cardiac arrhythmias during anesthesia with methohexital, thiamylal, or thiopental sodium. J Clin Anesth 4:208-212.

Moraes DJA, Zoccal DB, Machado BH (2012) Sympathoexcitation during chemoreflex active expiration is mediated by L-glutamate in the RVLM/Bötzinger complex of rats. J Neurophysiol 108:610-623.

Moraes DJA, Bonagamba LGH, Costa KM, Costa-Silva JH, Zoccal DB, Machado BH (2014) Short-term sustained hypoxia induces changes in the coupling of sympathetic and respiratory activities in rats. J Physiol 592:2013-2033.

Moreira TS, Takakura AC, Colombari E, Guyenet PG (2006) Central chemoreceptors and sympathetic vasomotor outflow. J Physiol 577:369-386.

Moreira TS, Sato MA, Takakura ACT, Menani JV, Colombari E (2005) Role of pressor mechanisms from the NTS and CVLM in control of arterial pressure. Am J Physiol-Reg I 289:1416-1425.

Mori A, Hiramatsu M, Namba S, Nishimoto A, Ohmoto T, Mayanagi Y, Asakura T (1987) Decreased dopamine level in the epileptic focus. Res Commun Chem Pathol Pharmacol 56:157-164.

Morimoto K, Fahnestock M, Racine RJ (2004) Kindling and status epilepticus models of epilepsy: Rewiring the brain. Prog Neurobiol 73:1-60.

Morrison SF (2001) Differential control of sympathetic outflow. Am J Physiol-Reg I 281:683-698.

Morrison SF, Callaway J, Milner TA, Reis DJ (1991) Rostral ventrolateral medulla: a source of the glutamatergic innervation of the sympathetic intermediolateral nucleus. Brain Res 562:126-135.

Moseley BD, Wirrell EC, Nickels K, Johnson JN, Ackerman MJ, Britton J (2011) Electrocardiographic and oximetric changes during partial complex and generalized seizures. Epilepsy Res 95:237-245.

Mosser DM, Edwards JP (2008) Exploring the full spectrum of macrophage activation. Nat Rev Immunol 8:958-969.

Mueller SG, Bateman LM, Laxer KD (2014) Evidence for brainstem network disruption in temporal lobe epilepsy and sudden unexplained death in epilepsy. Neuroimage Clin 5:208-216.

Müngen B, Berilgen MS, Arikanoğlu A (2010) Autonomic nervous system functions in interictal and postictal periods of nonepileptic psychogenic seizures and its comparison with epileptic seizures. Seizure 19:269-273.

Mutolo D, Bongianni F, Nardone F, Pantaleo T (2005) Respiratory responses evoked by blockades of ionotropic glutamate receptors within the Bötzinger complex and the pre-Bötzinger complex of the rabbit. Eur J Neurosci 21:122-134.

Nadler JV (1981) Kainic acid as a tool for the study of temporal lobe epilepsy. Life Sci 29:2031-2042.

Nadler JV, Perry BW, Cotmon CW (1978) Intraventricular kainic acid preferentially destroys hippocampal pyramidal cells. Nature 271:676-677.

Naggar I, Lazar J, Kamran H, Orman R, Stewart M (2014) Relation of autonomic and cardiac abnormalities to ventricular fibrillation in a rat model of epilepsy. Epilepsy Res 108:44-56.

Nashef L (1997) Sudden unexpected death in epilepsy: Terminology and definitions. Epilepsia 38:S6-S8.

Nedoboy PE, Mohammed S, Kapoor K, Bhandare AM, Farnham MMJ, Pilowsky PM (2016) pSer40 tyrosine hydroxylase immunohistochemistry identifies the anatomical location of C1 neurons in rat RVLM that are activated by hypotension. Neurosci 317:162-172.

Nei M, Ho RT, Sperling MR (2000) EKG abnormalities during partial seizures in refractory epilepsy. Epilepsia 41:542-548.

Nei M, Ho RT, Abou-Khalil BW, Drislane FW, Liporace J, Romeo A, Sperling MR (2004) EEG and ECG in sudden unexplained death in epilepsy. Epilepsia 45:338-345.

Nellgard B, Wieloch T (1992) Postischemic blockade of AMPA but not NMDA receptors mitigates neuronal damage in the rat brain following transient severe cerebral ischemia. J Cereb Blood Flow Metab 12:2-11.

Neumann J, Sauerzweig S, Rönicke R, Gunzer F, Dinkel K, Ullrich O, Gunzer M, Reymann KG (2008) Microglia cells protect neurons by direct engulfment of invading neutrophil granulocytes: A new mechanism of CNS immune privilege. J Neurosci 28:5965-5975.

Nijs J, Daenen L, Cras P, Struyf F, Roussel N, Oostendorp RAB (2012) Nociception affects motor output: A review on sensory-motor interaction with focus on clinical implications. Clin J Pain 28:175-181.

Nilsson L, Farahmand BY, Persson PG, Thiblin I, Tomson T (1999) Risk factors for sudden unexpected death in epilepsy: a case-control study. Lancet 353:888-893.

Nimmerjahn A, Kirchhoff F, Helmchen F (2005) Resting microglial cells are highly dynamic surveillants of brain parenchyma in vivo. Science 308:1314-1318.

Niswender CM, Conn PJ (2010) Metabotropic glutamate receptors: Physiology, pharmacology, and disease. Annu Rev Pharmacol Toxicol 50:295-322.

Noda M, Nakanishi H, Nabekura J, Akaike N (2000) AMPA-kainate subtypes of glutamate receptor in rat cerebral microglia. J Neurosci 20:251-258.

Nomura M, Ueta Y, Hannibal J, Serino R, Yamamoto Y, Shibuya I, Matsumoto T, Yamashita H (2000) Induction of pituitary adenylate cyclase-activating polypeptide mRNA in the medial parvocellular part of the paraventricular nucleus of rats following kainic-acid-induced seizure. Neuroendocrinology 71:318-326.

Nunan R, Sivasathiaseelan H, Khan D, Zaben M, Gray W (2014) Microglial VPAC1R mediates a novel mechanism of neuroimmune-modulation of hippocampal precursor cells via IL-4 release. Glia 62:1313-1327.

Ohtaki H, Nakamachi T, Dohi K, Aizawa Y, Takaki A, Hodoyama K, Yofu S, Hashimoto H, Shintani N, Baba A, Kopf M, Iwakura Y, Matsuda K, Arimura A, Shioda S (2006) Pituitary adenylate cyclase-activating polypeptide (PACAP) decreases

ischemic neuronal cell death in association with IL-6. Proc Natl Acad Sci USA 103:7488-7493.

Olsson T, Broberg M, Pope KJ, Wallace A, Mackenzie L, Blomstrand F, Nilsson M, Willoughby JO (2006) Cell swelling, seizures and spreading depression: An impedance study. Neurosci 140:505-515.

Opherk C, Coromilas J, Hirsch LJ (2002) Heart rate and EKG changes in 102 seizures: Analysis of influencing factors. Epilepsy Res 52:117-127.

Orihuela R, McPherson CA, Harry GJ (2016) Microglial M1/M2 polarization and metabolic states. Br J Pharmacol 173:649-665.

Otis TS, Jahr CE (1998) Anion currents and predicted glutamate flux through a neuronal glutamate transporter. J Neurosci 18:7099-7110.

Pansani AP, Colugnati DB, Schoorlemmer GH, Sonoda EY, Cavalheiro EA, Arida RM, Scorza FA, Cravo SL (2011) Repeated amygdala-kindled seizures induce ictal rebound tachycardia in rats. Epilepsy Behav 22:442-449.

Paolicelli RC, Bolasco G, Pagani F, Maggi L, Scianni M, Panzanelli P, Giustetto M, Ferreira TA, Guiducci E, Dumas L, Ragozzino D, Gross CT (2011) Synaptic pruning by microglia is necessary for normal brain development. Science 333:1456-1458.

Papageorgiou IE, Fetani AF, Lewen A, Heinemann U, Kann O (2015) Widespread activation of microglial cells in the hippocampus of chronic epileptic rats correlates only partially with neurodegeneration. Brain Struct Func 220:2423-2439.

Pavlov I, Kaila K, Kullmann DM, Miles R (2013) Cortical inhibition, pH and cell excitability in epilepsy: What are optimal targets for antiepileptic interventions? J Physiol 591:765-774.

Paxinos G, Watson C (2007) The Rat Brain in stereotaxic coordinates, 6th Edition: Elsevier Inc.

Pellegrini-Giampietro DE, Gorter JA, Bennett MVL, Zukin RSU (1997) The GluR2 (GluR-B) hypothesis: Ca2+-permeable AMPA receptors in neurological disorders. Trends Neurosci 20:464-470.

Peltola J, Palmio J, Korhonen L, Suhonen J, Miettinen A, Hurme M, Lindholm D, Keränen T (2000) Interleukin-6 and interleukin-1 receptor antagonist in cerebrospinal fluid from patients with recent tonic-clonic seizures. Epilepsy Res 41:205-211.

Penkowa M, Molinero A, Carrasco J, Hidalgo J (2001) Interleukin-6 deficiency reduces the brain inflammatory response and increases oxidative stress and neurodegeneration after kainic acid-induced seizures. Neurosci 102:805-818.

Persson M, Rönnbäck L (2012) Microglial self-defence mediated through GLT-1 and glutathione. Amino Acids 42:207-219.

Persson M, Sandberg M, Hansson E, Rönnbäck L (2006) Microglial glutamate uptake is coupled to glutathione synthesis and glutamate release. Eur J Neurosci 24:1063-1070.

Persson M, Brantefjord M, Liljeqvist JÅ, Bergström T, Hansson E, Rönnbäck L (2007) Microglial GLT-1 is upregulated in response to herpes simplex virus infection to provide an antiviral defence via glutathione. Glia 55:1449-1458.

Petr GT, Sun Y, Frederick NM, Zhou Y, Dhamne SC, Hameed MQ, Miranda C, Bedoya EA, Fischer KD, Armsen W, Wang J, Danbolt NC, Rotenberg A, Aoki CJ, Rosenberg PA (2015) Conditional deletion of the glutamate transporter GLT-1 reveals that astrocytic GLT-1 protects against fatal epilepsy while neuronal GLT-1 contributes significantly to glutamate uptake into synaptosomes. J Neurosci 35:5187-5201.

Peyron C, Tighe DK, Van Den Pol AN, De Lecea L, Heller HC, Sutcliffe JG, Kilduff TS (1998) Neurons containing hypocretin (orexin) project to multiple neuronal systems. J Neurosci 18:9996-10015.

Phillips JK, Goodchild AK, Dubey R, Sesiashvili E, Takeda M, Chalmers J, Pilowsky PM, Lipski J (2001) Differential expression of catecholamine biosynthetic enzymes in the rat ventrolateral medulla. J Comp Neurol 432:20-34.

Piguet P, Schlichter R (1998) Lability of the pacemaker activity in the rat rostro-ventrolateral medulla: Effects of noradrenaline. Brain Res 796:1-12.

Pilowsky P, West M, Chalmers J (1985) Renal sympathetic nerve responses to stimulation, inhibition and destruction of the ventrolateral medulla in the rabbit. Neurosci Lett 60:51-55.

Pilowsky P, Sun QJ, Llewellyn-Smith I, Arnolda L, Chalmers J, Minson J (1997) Phosphate-activated glutaminase immunoreactivity in brainstem respiratory neurons. J Auton Nerv Syst 63:85-90.

Pilowsky PM, Goodchild AK (2002) Baroreceptor reflex pathways and neurotransmitters: 10 Years on. J Hypertens 20:1675-1688.

Pilowsky PM, Lung MSY, Spirovski D, McMullan S (2009) Differential regulation of the central neural cardiorespiratory system by metabotropic neurotransmitters. Philos T Roy Soc B 364:2537-2552.

Pisanu A, Lecca D, Mulas G, Wardas J, Simbula G, Spiga S, Carta AR (2014) Dynamic changes in pro-and anti-inflammatory cytokines in microglia after PPAR-γ agonist neuroprotective treatment in the MPTPp mouse model of progressive Parkinson's disease. Neurobiol Dis 71:280-291.

Pocock JM, Kettenmann H (2007) Neurotransmitter receptors on microglia. Trends Neurosci 30:527-535.

Ponnusamy A, Marques JLB, Reuber M (2012) Comparison of heart rate variability parameters during complex partial seizures and psychogenic nonepileptic seizures. Epilepsia 53:1314-1321.

Powell KL, Lukasiuk K, O'Brien TJ, Pitkänen A (2014a) Are alterations in transmitter receptor and ion channel expression responsible for epilepsies? Adv Exp Med Biol 813:211-229.

Powell KL, Ng C, O'Brien T, Xu SH, Williams DA, Foote S, Reid CA (2008a) Decreases in HCN mRNA expression in the hippocampus after kindling and status epilepticus in adult rats. Epilepsia 49:1686-1695.

Powell KL, Kyi M, Reid CA, Paradiso L, D'Abaco GM, Kaye AH, Foote SJ, O'Brien TJ (2008b) Genetic absence epilepsy rats from Strasbourg have increased corticothalamic expression of stargazin. Neurobiol Dis 31:261-265.

Powell KL, Tang H, Ng C, Guillemain I, Dieuset G, Dezsi G, Çarçak N, Onat F, Martin B, O'Brien TJ, Depaulis A, Jones NC (2014b) Seizure expression, behavior, and brain morphology differences in colonies of genetic absence epilepsy rats from Strasbourg. Epilepsia 55:1959-1968.

Powell KL, Jones NC, Kennard JT, Ng C, Urmaliya V, Lau S, Tran A, Zheng T, Ozturk E, Dezsi G, Megatia I, Delbridge LM, Pinault D, Reid CA, White PJ, O'Brien TJ (2014c) HCN channelopathy and cardiac electrophysiologic dysfunction in genetic and acquired rat epilepsy models. Epilepsia 55:609-620.

Przywara DA, Kulkarni JS, Wakade TD, Leontiev DV, Wakade AR (1998) Pituitary adenylyl cyclase-activating polypeptide and nerve growth factor use the proteasome to rescue nerve growth factor-deprived sympathetic neurons cultured from chick embryos. J Neurochem 71:1889-1897.

Pyner S, Coote JH (1999) Identification of an efferent projection from the paraventricular nucleus of the hypothalamus terminating close to spinally projecting rostral ventrolateral medullary neurons. Neurosci 88:949-957.

Pyner S, Coote JH (2000) Identification of branching paraventricular neurons of the hypothalamus that project to the rostroventrolateral medulla and spinal cord. Neurosci 100:549-556.

Qin L, Wu X, Block ML, Liu Y, Breese GR, Hong J-S, Knapp DJ, Crews FT (2007) Systemic LPS causes chronic neuroinflammation and progressive neurodegeneration. Glia 55:453-462.

Racine RJ (1972) Modification of seizure activity by electrical stimulation: II. Motor seizure. Electroencephalogr Clin Neurophysiol 32:281-294.

Rahman AA, Shahid IZ, Pilowsky PM (2011) Intrathecal neuromedin U induces biphasic effects on sympathetic vasomotor tone, increases respiratory drive and attenuates sympathetic reflexes in rat. Brit J Pharmacol 164:617-631.

Rainesalo S, Keränen T, Palmio J, Peltola J, Oja S, Saransaari P (2004) Plasma and cerebrospinal fluid amino acids in epileptic patients. Neurochem Res 29:319-324.

Read MI, McCann DM, Millen RN, Harrison JC, Kerr DS, Sammut IA (2015) Progressive development of cardiomyopathy following altered autonomic activity in status epilepticus. Am J Physiol-Heart C 309:1554-1564.

Reglodi D, Somogyvari-Vigh A, Vigh S, Kozicz T, Arimura A (2000) Delayed systemic administration of PACAP38 is neuroprotective in transient middle cerebral artery occlusion in the rat. Stroke 31:1411-1417.

Reis DJ, Granata AR, Perrone MH, Talman WT (1981) Evidence that glutamic acid is the neurotransmitter of baroreceptor afferents terminating in the nucleus tractus solitarius (NTS). J Auton Nerv Syst 3:321-334.

Rice AC, Delorenzo RJ (1998) NMDA receptor activation during status epilepticus is required for the development of epilepsy. Brain Res 782:240-247.

Ringer C, Büning L-S, Schäfer MKH, Eiden LE, Weihe E, Schütz B (2013) PACAP signaling exerts opposing effects on neuroprotection and neuroinflammation during disease progression in the SOD1(G93A) mouse model of amyotrophic lateral sclerosis. Neurobiol Dis 54:32-42.

Rosin DL, Chang DA, Guyenet PG (2006) Afferent and efferent connections of the rat retrotrapezoid nucleus. J Comp Neurol 499:64-89.

Ross C, Ruggiero D, Park D, Joh T, Sved A, Fernandez-Pardal J, Saavedra J, Reis D (1984a) Tonic vasomotor control by the rostral ventrolateral medulla: effect of electrical or chemical stimulation of the area containing C1 adrenaline neurons on arterial pressure, heart rate, and plasma catecholamines and vasopressin. J Neurosci 4:474-494.

Ross CA, Ruggiero DA, Joh TH, Park DH, Reis DJ (1984b) Rostral ventrolateral medulla: Selective projections to the thoracic autonomic cell column from the region containing C1 adrenaline neurons. J Comp Neurol 228:168-185.

Roy A, Derakhshan F, Wilson RJA (2013) Stress peptide PACAP engages multiple signaling pathways within the carotid body to initiate excitatory responses in respiratory and sympathetic chemosensory afferents. Am J Physiol-Reg I 304:1070-1084.

Ryvlin P et al. (2013) Incidence and mechanisms of cardiorespiratory arrests in epilepsy monitoring units (MORTEMUS): A retrospective study. The Lancet Neurology 12:966-977.

Sacaan AI, Schoepp DD (1992) Activation of hippocampal metabotropic excitatory amino acid receptors leads to seizures and neuronal damage. Neurosci Lett 139:77-82.

Sah P, Faber ESL, De Armentia ML, Power J (2003) The amygdaloid complex: Anatomy and physiology. Physiol Rev 83:803-834.

Sakamoto K, Koizumi K, Stewart M (2005) Kainic acid seizure-evoked parasympathetic and sympathetic nerve activity and altered baroreceptor reflex responses in urethane-anesthesized rats. Int Congr 1278:419-422.

Sakamoto K, Saito T, Orman R, Koizumi K, Lazar J, Salciccioli L, Stewart M (2008) Autonomic consequences of kainic acid-induced limbic cortical seizures in rats:

peripheral autonomic nerve activity, acute cardiovascular changes, and death. Epilepsia 49:982-996.

Sakima A, Yamazato M, Sesoko S, Muratani H, Fukiyama K (2000) Cardiovascular and sympathetic effects of L-glutamate and glycine injected into the rostral ventrolateral medulla of conscious rats. Hypertens Res 23:633-641.

Sakon S, Xue X, Takekawa M, Sasazuki T, Okazaki T, Kojima Y, Piao JH, Yagita H, Okumura K, Doi T, Nakano H (2003) NF-κB inhibits TNF-induced accumulation of ROS that mediate prolonged MAPK activation and necrotic cell death. EMBO J 22:3898-3909.

Sasaki M (2005) Role of Barrington's nucleus in micturition. J Comp Neurol 493:21-26.

Sato K, Morimoto K, Okamoto M, Nakamura Y, Otsuki S, Sato M (1990) An analysis of anticonvulsant actions of GABA agonists (progabide and baclofen) in the kindling model of epilepsy. Epilepsy Res 5:117-124.

Savic I, Svanborg E, Thorell JO (1996) Cortical benzodiazepine receptor changes are related to frequency of partial seizures: A positron emission tomography study. Epilepsia 37:236-244.

Schauwecker PE, Steward O (1997) Genetic determinants of susceptibility to excitotoxic cell death: Implications for gene targeting approaches. Proc Natl Acad Sci U S A 94:4103-4108.

Schreihofer AM, Guyenet PG (1997) Identification of C1 presympathetic neurons in rat rostral ventrolateral medulla by juxtacellular labeling in vivo. J Comp Neurol 387:524-536.

Schreihofer AM, Guyenet PG (2002) The baroreflex and beyond: Control of sympathetic vasomotor tone by gabaergic neurons in the ventrolateral medulla. Clin Exp Pharmacol Physiol 29:514-521.

Schreihofer AM, Guyenet PG (2003) Baro-activated neurons with pulse-modulated activity in the rat caudal ventrolateral medulla express GAD67 mRNA. J Neurophysiol 89:1265-1277.

Seaborn T, Masmoudi-Kouli O, Fournier A, Vaudry H, Vaudry D (2011) Protective effects of pituitary adenylate cyclase-activating polypeptide (PACAP) against apoptosis. Curr Pharm Design 17:204-214.

Seabrook TJ, Jiang L, Maier M, Lemere CA (2006) Minocycline affects microglia activation, Aβ deposition, and behavior in APP-tg mice. Glia 53:776-782.

Seagard JL, Gallenberg LA, Hopp FA, Dean C (1990) Acute resetting in two functionally different types of carotid baroreceptors. Circ Res 70:559-565.

Seidel JL, Faideau M, Aiba I, Pannasch U, Escartin C, Rouach N, Bonvento G, Shuttleworth CW (2015) Ciliary neurotrophic factor (CNTF) activation of astrocytes decreases spreading depolarization susceptibility and increases potassium clearance. Glia 63:91-103.

Seyal M, Bateman LM, Albertson TE, Lin TC, Li CS (2010) Respiratory changes with seizures in localization-related epilepsy: Analysis of periictal hypercapnia and airflow patterns. Epilepsia 51:1359-1364.

Seyedabadi M, Li Q, Padley JR, Pilowsky PM, Goodchild AK (2006) A novel pressor area at the medullo-cervical junction that is not dependent on the RVLM: Efferent pathways and chemical mediators. J Neurosci 26:5420-5427.

Shafton AD, Ryan A, Badoer E (1998) Neurons in the hypothalamic paraventricular nucleus send collaterals to the spinal cord and to the rostral ventrolateral medulla in the rat. Brain Res 801:239-243.

Shahid IZ, Rahman AA, Pilowsky PM (2011) Intrathecal orexin A increases sympathetic outflow and respiratory drive, enhances baroreflex sensitivity and blocks the somato-sympathetic reflex. Brit J Pharmacol 162:961-973.

Shapiro LA, Wang L, Ribak CE (2008) Rapid astrocyte and microglial activation following pilocarpine-induced seizures in rats. Epilepsia 49:33-41.

Sharma AK, Jordan WH, Reams RY, Greg Hall D, Snyder PW (2008) Temporal profile of clinical signs and histopathologic changes in an F-344 rat model of kainic acid-induced mesial temporal lobe epilepsy. Toxicol Pathol 36:932-943.

Sharma AK, Reams RY, Jordan WH, Miller MA, Thacker HL, Snyder PW (2007) Mesial temporal lobe epilepsy: pathogenesis, induced rodent models and lesions. Toxicol Pathol 35:984-999.

Sheardown MJ, Suzdak PD, Nordholm L (1993) AMPA, but not NMDA, receptor antagonism is neuroprotective in gerbil global ischaemia, even when delayed 24 h. Eur J Pharmacol 236:347-353.

Shi P, Diez-Freire C, Jun JY, Qi Y, Katovich MJ, Li Q, Sriramula S, Francis J, Sumners C, Raizada MK (2010) Brain microglial cytokines in neurogenic hypertension. Hypertension 56:297-303.

Shibasaki M, Umemoto Y, Kinoshita T, Ito T, Kouda K, Nakamura T, Crandall CG, Tajima F (2015) The role of cardiac sympathetic innervation and skin thermoreceptors on cardiac responses during heat stress. Am J Physiol-Heart C 308:1336-1342.

Shin JW, Geerling JC, Loewy AD (2008) Inputs to the ventrolateral bed nucleus of the stria terminalis. J Comp Neurol 511:628-657.

Shioda S, Ozawa H, Dohi K, Mizushima H, Matsumoto K, Nakajo S, Takaki A, Zhou CJ, Nakai Y, Arimura A (1998) PACAP protects hippocampal neurons against apoptosis: Involvement of JNK/SAPK signaling pathway. Ann NY Acad Sci 865:111-117.

Shioda S, Ohtaki H, Nakamachi T, Dohi K, Watanabe J, Nakajo S, Arata S, Kitamura S, Okuda H, Takenoya F, Kitamura Y (2006) Pleiotropic functions of PACAP in the CNS: Neuroprotection and neurodevelopment. Ann NY Acad Sci 1070:550-560.

Shoge K, Mishima HK, Saitoh T, Ishihara K, Tamura Y, Shiomi H, Sasa M (1999) Attenuation by PACAP of glutamate-induced neurotoxicity in cultured retinal neurons. Brain Res 839:66-73.

Silveira DC, Schachter SC, Schomer DL, Holmes GL (2000) Flurothyl-induced seizures in rats activate Fos in brainstem catecholaminergic neurons. Epilepsy Res 39:1-12.

Simmonds SS, Lay J, Stocker SD (2014) Dietary salt intake exaggerates sympathetic reflexes and increases blood pressure variability in normotensive rats. Hypertension 64:583-589.

Skoglösa Y, Takei N, Lindholm D (1999a) Distribution of pituitary adenylate cyclase activating polypeptide mRNA in the developing rat brain. Mol Brain Res 65:1-13.

Skoglösa Y, Lewén A, Takei N, Hillered L, Lindholm D (1999b) Regulation of pituitary adenylate cyclase activating polypeptide and its receptor type 1 after traumatic brain injury: Comparison with brain-derived neurotrophic factor and the induction of neuronal cell death. Neurosci 90:235-247.

Smolders I, Khan GM, Manil J, Ebinger G, Michotte Y (1997) NMDA receptor-mediated pilocarpine-induced seizures: Characterization in freely moving rats by microdialysis. Br J Pharmacol 121:1171-1179.

So EL, Sam MC, Lagerlund TL (2000) Postictal central apnea as a cause of SUDEP: Evidence from near-SUDEP incident. Epilepsia 41:1494-1497.

Sokal RR, Rohlf FJ (2012) Biometry, Fourth Edition. New York: W.H. Freeman and Company.

Spengler D, Waeber C, Pantaloni C, Holsboer F, Bockaert J, Seeburg PH, Journot L (1993) Differential signal transduction by five splice variants of the PACAP receptor. Nature 365:170-175.

Sperk G, Lassmann H, Baran H, Kish SJ, Seitelberger F, Hornykiewicz O (1983) Kainic acid induced seizures: Neurochemical and histopathological changes. Neurosci 10:1301-1315.

Stagg CJ, Lang B, Best JG, McKnight K, Cavey A, Johansen-Berg H, Vincent A, Palace J (2010) Autoantibodies to glutamic acid decarboxylase in patients with epilepsy are associated with low cortical GABA levels. Epilepsia 51:1898-1901.

Stornetta RL, Sevigny CP, Guyenet PG (2002a) Vesicular glutamate transporter DNPI/VGLUT2 mRNA is present in C1 and several other groups of brainstem catecholaminergic neurons. J Comp Neurol 444:191-206.

Stornetta RL, Sevigny CP, Schreihofer AM, Rosin DL, Guyenet PG (2002b) Vesicular glutamate transporter DNPI/VGLUT2 is expressed by both C1 adrenergic and nonaminergic presympathetic vasomotor neurons of the rat medulla. J Comp Neurol 444:207-220.

Strack AM, Sawyer WB, Platt KB, Loewy AD (1989a) CNS cell groups regulating the sympathetic outflow to adrenal gland as revealed by transneuronal cell body labelling with pseudorabies virus. Brain Res 491:274-296.

Strack AM, Sawyer WB, Hughes JH, Platt KB, Loewy AD (1989b) A general pattern of CNS innervation of the sympathetic outflow demonstrated by transneuronal pseudorabies viral infections. Brain Res 491:156-162.

Suk K, Park J-H, Lee W-H (2004) Neuropeptide PACAP inhibits hypoxic activation of brain microglia: a protective mechanism against microglial neurotoxicity in ischemia. Brain Res 1026:151-156.

Sun DA, Sombati S, DeLorenzo RJ (2001) Glutamate injury-induced epileptogenesis in hippocampal neurons: An in vitro model of stroke-induced "epilepsy". Stroke 32:2344-2350.

Sun MK (1995) Central neural organization and control of sympathetic nervous system in mammals. Prog Neurobiol 47:157-233.

Sun MK, Hackett JT, Guyenet PG (1988a) Sympathoexcitatory neurons of rostral ventrolateral medulla exhibit pacemaker properties in the presence of a glutamate-receptor antagonist. Brain Res 438:23-40.

Sun MK, Young BS, Hackett JT, Guyenet PG (1988b) Reticulospinal pacemaker neurons of the rat rostral ventrolateral medulla with putative sympathoexcitatory function: an intracellular study in vitro. Brain Res 442:229-239.

Sun W, Panneton WM (2005) Defining projections from the caudal pressor area of the caudal ventrolateral medulla. J Comp Neurol 482:273-293.

Sun X, Shi X, Lu L, Jiang Y, Liu B (2016) Stimulus-dependent neuronal cell responses in SH-SY5Y neuroblastoma cells. Mol Med Rep 13:2215-2220.

Sundler F, Ekblad E, Hannibal J, Moller K, Zhang YZ, Mulder H, Elsås T, Grunditz T, Danielsen N, Fahrenkrug J, Uddman R (1996) Pituitary adenylate cyclase-activating peptide in sensory and autonomic ganglia: Localization and regulation. Ann N Y Acad Sci 805:410-428.

Surges R, Thijs RD, Tan HL, Sander JW (2009) Sudden unexpected death in epilepsy: Risk factors and potential pathomechanisms. Nat Rev Neurol 5:492-504.

Sutter R, Kaplan PW, Rüegg S (2013) Outcome predictors for status epilepticus - What really counts. Nat Rev Neurol 9:525-534.

Suzuki H, Imai F, Kanno T, Sawada M (2001) Preservation of neurotrophin expression in microglia that migrate into the gerbil's brain across the blood-brain barrier. Neurosci Lett 312:95-98.

Suzuki T, Takayama K, Miura M (1997) Distribution and projection of the medullary cardiovascular control neurons containing glutamate, glutamic acid decarboxylase, tyrosine hydroxylase and phenylethanolamine N-methyltransferase in rats. Neurosci Res 27:9-19.

Sved AF (1989) PNMT-containing catecholaminergic neurons are not necessarily adrenergic. Brain Res 481:113-118.

Sved AF, Cano G, Patrick Card J (2001) Neuroanatomical specificity of the circuits controlling sympathetic outflow to different targets. Clin Exp Pharmacol Physiol 28:115-119.

Sved AF, Ito S, Yajima Y (2002) Role of excitatory amino acid inputs to the rostral ventrolateral medulla in cardiovascular regulation. Clin Exp Pharmacol Physiol 29:503-506.

Swanson LW, Sawchenko PE, Berod A, Hartman BK, Helle KB, Vanorden DE (1981) An immunohistochemical study of the organization of catecholaminergic cells and terminal fields in the paraventricular and supraoptic nuclei of the hypothalamus. J Comp Neurol 196:271-285.

Swanson RA, Liu J, Miller JW, Rothstein JD, Farrell K, Stein BA, Longuemare MC (1997) Neuronal regulation of glutamate transporter subtype expression in astrocytes. J Neurosci 17:932-940.

Szalay G, Martinecz B, Lenart N, Kornyei Z, Orsolits B, Judak L, Csaszar E, Fekete R, West BL, Katona G, Rozsa B, Denes A (2016) Microglia protect against brain injury and their selective elimination dysregulates neuronal network activity after stroke. Nat Commun 7:11499.

Szot P, Reigel CE, White SS, Veith RC (1996) Alterations in mRNA expression of systems that regulate neurotransmitter synaptic content in seizure-naive genetically epilepsy-prone rat (GEPR): Transporter proteins and rate-limiting synthesizing enzymes for norepinephrine, dopamine and serotonin. Mol Brain Res 43:233-245.

Takayama K, Suzuki T, Miura M (1994) The comparison of effects of various anesthetics on expression of Fos protein in the rat brain. Neurosci Lett 176:59-62.

Takei N, Skoglösa Y, Lindholm D (1998) Neurotrophic and neuroprotective effects of pituitary adenylate cyclase- activating polypeptide (PACAP) on mesencephalic dopaminergic neurons. J Neurosci Res 54:698-706.

Takeuchi H, Jin S, Suzuki H, Doi Y, Liang J, Kawanokuchi J, Mizuno T, Sawada M, Suzumura A (2008) Blockade of microglial glutamate release protects against ischemic brain injury. Exp Neurol 214:144-146.

Tanaka K, Watase K, Manabe T, Yamada K, Watanabe M, Takahashi K, Iwama H, Nishikawa T, Ichihara N, Kikuchi T, Okuyama S, Kawashima N, Hori S, Takimoto M, Wada K (1997) Epilepsy and exacerbation of brain injury in mice lacking the glutamate transporter GLT-1. Science 276:1699-1702.

Tang X, Neckel ND, Schramm LP (2004) Spinal interneurons infected by renal injection of pseudorabies virus in the rat. Brain Res 1004:1-7.

Taylor DL, Diemel LT, Pocock JM (2003) Activation of microglial group III metabotropic glutamate receptors protects neurons against microglial neurotoxicity. J Neurosci 23:2150-2160.

Taylor DL, Diemel LT, Cuzner ML, Pocock JM (2002) Activation of group II metabotropic glutamate receptors underlies microglial reactivity and neurotoxicity following stimulation with chromogranin A, a peptide up-regulated in Alzheimer's disease. J Neurochem 82:1179-1191.

Taylor DL, Jones F, Kubota ESFCS, Pocock JM (2005) Stimulation of microglial metabotropic glutamate receptor mGlu2 triggers tumor necrosis factor α-induced neurotoxicity in concert with microglial-derived Fas ligand. J Neurosci 25:2952-2964.

Ter Horst GJ, Hautvast RWM, De Jongste MJL, Korf J (1996) Neuroanatomy of cardiac activity-regulating circuitry: A transneuronal retrograde viral labelling study in the rat. Eur J Neurosci 8:2029-2041.

Tikka T, Fiebich BL, Goldsteins G, Keinänen R, Koistinaho J (2001) Minocycline, a tetracycline derivative, is neuroprotective against excitotoxicity by inhibiting activation and proliferation of microglia. J Neurosci 21:2580-2588.

Tizzano JP, Griffey KI, Schoepp DD (1995) Induction or protection of limbic seizures in mice by mGluR subtype selective agonists. Neuropharmacology 34:1063-1067.

Tolstykh GP, Cavazos JE (2013) Potential mechanisms of sudden unexpected death in epilepsy. Epilepsy Behav 26:410-414.

Tomson T, Walczak T, Sillanpaa M, Sander JWAS (2005) Sudden unexpected death in epilepsy: A review of incidence and risk factors. Epilepsia 46:54-61.

Tóth IE, Tóth DE, Boldogkoi Z, Hornyák Á, Palkovits M, Blessing WW (2006) Serotonin-synthesizing neurons in the rostral medullary raphé/parapyramidal region transneuronally labelled after injection of pseudorabies virus into the rat tail. Neurochem Res 31:277-286.

Traub RD, Whittington MA, Stanford IM, Jefferys JGR (1996) A mechanism for generation of long-range synchronous fast oscillations in the cortex. Nature 383:621-224.

Tremblay ME, Lowery RL, Majewska AK (2010) Microglial interactions with synapses are modulated by visual experience. PLoS Biol 8:e1000527.

Tsai C-Y, Chan JYH, Hsu K-s, Chang AYW, Chan SHH (2012) Brain-derived neurotrophic factor ameliorates brain stem cardiovascular dysregulation during experimental temporal lobe status epilepticus. PLoS One 7:e33527.

Tupal S, Faingold CL (2006) Evidence supporting a role of serotonin in modulation of sudden death induced by seizures in DBA/2 mice. Epilepsia 47:21-26.

Turner A, Kumar N, Farnham M, Lung M, Pilowsky P, McMullan S (2013) Rostroventrolateral medulla neurons with commissural projections provide input to sympathetic premotor neurons: Anatomical And Functional Evidence. Eur J Neurosci 38:2504-2515.

Ueda Y, Doi T, Tokumaru J, Yokoyama H, Nakajima A, Mitsuyama Y, Ohya-Nishiguchi H, Kamada H, James Willmore L (2001) Collapse of extracellular glutamate regulation during epileptogenesis: Down-regulation and functional failure of glutamate transporter function in rats with chronic seizures induced by kainic acid. J Neurochem 76:892-900.

Ueno M, Fujita Y, Tanaka T, Nakamura Y, Kikuta J, Ishii M, Yamashita T (2013) Layer v cortical neurons require microglial support for survival during postnatal development. Nat Neurosci 16:543-551.

Unnerstall JR, Wamsley JK (1983) Autoradiographic localization of high-affinity [3H]kainic acid binding sites in the rat forebrain. Eur J Pharmacol 86:361-371.

Van Landeghem FKH, Stover JF, Bechmann I, Brck W, Unterberg A, Bhrer C, Von Deimling A (2001) Early expression of glutamate transporter proteins in ramified microglia after controlled cortical impact injury in the rat. Glia 35:167-179.

Van Vliet EA, Araújo SDC, Redeker S, Van Schaik R, Aronica E, Gorter JA (2007) Blood-brain barrier leakage may lead to progression of temporal lobe epilepsy. Brain 130:521-534.

Vandenberghe W, Robberecht W, Brorson JR (2000) AMPA receptor calcium permeability, GluR2 expression, and selective motoneuron vulnerability. J Neurosci 20:123-132.

Vaudry D, Gonzalez BJ, Basille M, Anouar Y, Fournier A, Vaudry H (1998) Pituitary adenylate cyclase-activating polypeptide stimulates both c-fos gene expression and cell survival in rat cerebellar granule neurons through activation of the protein kinase A pathway. Neurosci 84:801-812.

Venit EL, Shepard BD, Seyfried TN (2004) Oxygenation prevents sudden death in seizure-prone mice. Epilepsia 45:993-996.

Vilhardt F (2005) Microglia: Phagocyte and glia cell. Int J Biochem Cell Biol 37:17-21.

Vincent P, Mulle C (2009) Kainate receptors in epilepsy and excitotoxicity. Neurosci 158:309-323.

Vinet J, van Weering HRJ, Heinrich A, Kälin RE, Wegner A, Brouwer N, Heppner FL, van Rooijen N, Boddeke HWGM, Biber K (2012) Neuroprotective function for ramified microglia in hippocampal excitotoxicity. J Neuroinflamm 9:27.

Vivash L, Gregoire MC, Bouilleret V, Berard A, Wimberley C, Binns D, Roselt P, Katsifis A, Myers DE, Hicks RJ, O'Brien TJ, Dedeurwaerdere S (2014) In vivo measurement of hippocampal GABAa/cBZR density with [18F]-flumazenil PET for the study of disease progression in an animal model of temporal lobe epilepsy. PLoS One 9:e86722.

Wada Y, Nakamachi T, Endo K, Seki T, Ohtaki H, Tsuchikawa D, Hori M, Tsuchida M, Yoshikawa A, Matkovits A, Kagami N, Imai N, Fujisaka S, Usui I, Tobe K, Koide R, Takahashi H, Shioda S (2013) PACAP attenuates NMDA-induced retinal damage in association with modulation of the microglia/macrophage status into an acquired deactivation subtype. J Mol Neurosci 51:493-502.

Wagster MV, Hedreen JC, Peyser CE, Folstein SE, Ross CA (1994) Selective loss of [3H]kainic acid and [3H]AMPA binding in layer VI of frontal cortex in huntington's disease. Exp Neurol 127:70-75.

Wake H, Moorhouse AJ, Jinno S, Kohsaka S, Nabekura J (2009) Resting microglia directly monitor the functional state of synapses in vivo and determine the fate of ischemic terminals. J Neurosci 29:3974-3980.

Walczak TS, Leppik IE, D'Amelio M, Rarick J, So E, Ahman P, Ruggles K, Cascino GD, Annegers JF, Hauser WA (2001) Incidence and risk factors in sudden unexpected death in epilepsy. Neurology 56:519-525.

Wang L, Meng X, Yuchi Z, Zhao Z, Xu D, Fedida D, Wang Z, Huang C (2015) De novo mutation in the SCN5A gene associated with brugada syndrome. Cell Physiol Biochem 36:2250-2262.

Wang Q, Yu S, Simonyi A, Sun GY, Sun AY (2005) Kainic acid-mediated excitotoxicity as a model for neurodegeneration. Mol Neurobiol 31:3-16.

Wannamaker BB (1985) Autonomic nervous system and epilepsy. Epilepsia 26:S31-S39.

Weinshenker D, Szot P (2002) The role of catecholamines in seizure susceptibility: new results using genetically engineered mice. Pharmacol Ther 94:213-233.

Wendling F, Hernandez A, Bellanger JJ, Chauvel P, Bartolomei F (2005) Interictal to ictal transition in human temporal lobe epilepsy: Insights from a computational model of intracerebral EEG. J Clin Neurophysiol 22:343-356.

Wenker IC, Kréneisz O, Nishiyama A, Mulkey DK (2010) Astrocytes in the retrotrapezoid nucleus sense H+ by inhibition of a Kir4.1-Kir5.1-like current and may contribute to chemoreception by a purinergic mechanism. J Neurophysiol 104:3042-3052.

Westerhaus MJ, Loewy AD (2001) Central representation of the sympathetic nervous system in the cerebral cortex. Brain Res 903:117-127.

White A, Williams PA, Hellier JL, Clark S, Dudek FE, Staley KJ (2010) EEG spike activity precedes epilepsy after kainate-induced status epilepticus. Epilepsia 51:371-383.

WHO (2005) Atlas: Epilepsy care in the world. In: (Department of Mental Health and Substance Abuse WHO, ed). Geneva.

Willette RN, Punnen-Grandy S, Krieger AJ, Sapru HN (1987) Differential regulation of regional vascular resistance by the rostral and caudal ventrolateral medulla in the rat. J Auton Nerv Syst 18:143-151.

Williams MR, De-Spenza T, Jr., Li M, Gulledge AT, Luikart BW (2015) Hyperactivity of newborn pten knock-out neurons results from increased excitatory synaptic drive. J Neurosci 35:943-959.

Wisden W, Seeburg PH (1993) A complex mosaic of high-affinity kainate receptors in rat brain. J Neurosci 13:3582-3598.

Wong M (2005) Advances in the pathophysiology of developmental epilepsies. Semin Pediatr Neurol 12:72-87.

Woulfe JM, Flumerfelt BA, Hrycyshyn AW (1990) Efferent connections of the A1 noradrenergic cell group: A DBH immunohistochemical and PHA-L anterograde tracing study. Exp Neurol 109:308-322.

Wyneken U, Smalla KH, Marengo JJ, Soto D, De la Cerda A, Tischmeyer W, Grimm R, Boeckers TM, Wolf G, Orrego F, Gundelfinger ED (2001) Kainate-induced seizures alter protein composition and N-methyl-D-aspartate receptor function of rat forebrain postsynaptic densities. Neurosci 102:65-74.

Yaari Y, Yue C, Su H (2007) Recruitment of apical dendritic T-type Ca2+ channels by backpropagating spikes underlies de novo intrinsic bursting in hippocampal epileptogenesis. J Physiol 580:435-450.

Yang Z, Coote JH (1999) The influence of the paraventricular nucleus on baroreceptor dependent caudal ventrolateral medullary neurones of the rat. Pflugers Arch 438:47-52.

Yokoyama T, Nakamuta N, Kusakabe T, Yamamoto Y (2015) Sympathetic regulation of vascular tone via noradrenaline and serotonin in the rat carotid body as revealed by intracellular calcium imaging. Brain Res 1596:126-135.

Yrjänheikki J, Keinänen R, Pellikka M, Hökfelt T, Koistinaho J (1998) Tetracyclines inhibit microglial activation and are neuroprotective in global brain ischemia. Proc Natl Acad Sci U S A 95:15769-15774.

Zahner MR, Schramm LP (2011) Spinal regions involved in baroreflex control of renal sympathetic nerve activity in the rat. Am J Physiol-Reg I 300:910-916.

Zanzinger J, Doutheil J, Czachurski J, Seller H (1994a) Excitatory somato-sympathetic reflexes are relayed in the caudal ventrolateral medulla in the cat. Neurosci Lett 179:71-74.

Zanzinger J, Czachurski J, Offner B, Seller H (1994b) Somato-sympathetic reflex transmission in the ventrolateral medulla oblongata: spatial organization and receptor types. Brain Res 656:353-358.

Zhang YZ, Hannibal J, Zhao Q, Moller K, Danielsen N, Fahrenkrug J, Sundler F (1996) Pituitary adenylate cyclase activating peptide expression in the rat dorsal root ganglia: Up-regulation after peripheral nerve injury. Neurosci 74:1099-1110.

Zhang ZH, Francis J, Weiss RM, Felder RB (2002) The renin-angiotensin-aldosterone system excites hypothalamic paraventricular nucleus neurons in heart failure. Am J Physiol-Heart C 283:423-433.

Zhao W, Chuang SC, Young SR, Bianchi R, Wong RK (2015) Extracellular glutamate exposure facilitates group I mGluR-mediated epileptogenesis in the hippocampus. J Neurosci 35:308-315.

Zhuo L, Zhang Y, Zielke HR, Levine B, Zhang X, Chang L, Fowler D, Li L (2012) Sudden unexpected death in epilepsy: Evaluation of forensic autopsy cases. Forensic Sci Int 223:171-175.

Appendix 1
Published manuscripts directly related to thesis that are produced during the course of candidature
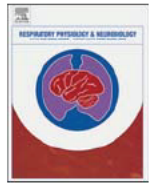
Contents lists available at ScienceDirect

Respiratory Physiology & Neurobiology

journal homepage: www.elsevier.com/locate/resphysiol

Microglia PACAP and glutamate: Friends or foes in seizure-induced autonomic dysfunction and SUDEP?

Amol M. Bhandare [a,b], Komal Kapoor [a,b], Melissa M.J. Farnham [b,c], Paul M. Pilowsky [b,c,*]

[a] Department of Biomedical Sciences, Faculty of Medicine and Health Sciences, Macquarie University, Sydney 2109 New South Wales, Australia
[b] The Heart Research Institute, 7 Eliza Street, Sydney 2042 New South Wales, Australia
[c] Department of Physiology, University of Sydney, Sydney 2006 New South Wales, Australia

ABSTRACT

Seizure-induced cardiorespiratory autonomic dysfunction is a major cause of sudden unexpected death in epilepsy (SUDEP), and the underlying mechanism is unclear. Seizures lead to increased synthesis, and release of glutamate, pituitary adenylate cyclase activating polypeptide (PACAP), and other neurotransmitters, and cause extensive activation of microglia at multiple regions in the brain including central autonomic cardiorespiratory brainstem nuclei. Glutamate contributes to neurodegeneration, and inflammation in epilepsy. PACAP has neuroprotective, and anti-inflammatory properties, whereas microglia are key players in inflammatory responses in CNS. Seizure-induced increase in PACAP is neuroprotective. PACAP produces neuroprotective effects acting on microglial PAC1 and VPAC1 receptors. Microglia also express glutamate transporters, and their expression can be increased by PACAP in response to harmful or stressful situations such as seizures. Here we discuss the mechanism of autonomic cardiorespiratory dysfunction in seizure, and the role of PACAP, glutamate and microglia in regulating cardiorespiratory brainstem neurons in their physiological state that could provide future therapeutic options for SUDEP.

© 2016 Elsevier B.V. All rights reserved.

1. Introduction

Epilepsy affects about 50 million people worldwide (WHO, 2005). Sudden unexpected death in epilepsy (SUDEP) is an important but poorly-appreciated disorder (Massey et al., 2014) that accounts for 5–17% of deaths in people with epilepsy, and 50% in refractory epilepsy (Ficker et al., 1998; Holst et al., 2013). The first evidence of SUDEP was published nearly 50 years ago (Hirsch and Martin, 1971), but the underlying mechanism remains obscure. The classical mechanism of SUDEP is extensively studied, and accounts for seizure-induced central autonomic and cardiorespiratory dysfunction (Figs. 1–2). Maximal electroshock applied by two ear electrodes, in freely moving rats, leads to seizure causing cardiac arrhythmia that is precisely correlated with the ictal period (Darbin et al., 2002). In human, seizure is commonly associated with profound apnoea and oxygen desaturation (Bateman et al., 2008; Dlouhy et al., 2015). Here we survey new data and propose a role for microglia (innate immune cells of the CNS), and the neurotransmitters, pituitary adenylate cyclase activating polypeptide

(PACAP), and glutamate in the context of seizure induced cardiorespiratory dysfunction (Fig. 3). These novel findings suggest probable mechanisms of cardiorespiratory dysfunction in seizure, and point to future therapeutic strategies that may help in the management, and prevention of SUDEP.

Cardiorespiratory disturbances such as arrhythmia and apnoea that occur during, and after seizures are the leading cause of SUDEP in both humans, and animals (Fig. 1) (Dlouhy et al., 2015; Johnston et al., 1997; Metcalf et al., 2009; Naggar et al., 2014). Cardiac sympathovagal imbalances with sympathetic dominance, baroreflex dysfunction, tachycardia or bradycardia with severe ictal ECG abnormalities are common in patients and animals (Bhandare et al., 2015; Nei et al., 2000; Opherk et al., 2002; Ponnusamy et al., 2012; Sakamoto et al., 2008). Seizure-related respiratory dysfunction, with associated hypoxaemia, is common, as seen in video-electroencephalogram (EEG) telemetry (Fig. 4), from patients in epilepsy monitoring units (Bateman et al., 2008; Dlouhy et al., 2015; Seyal et al., 2010).

Recent studies have uncovered a novel mechanism of seizure-induced cardiorespiratory dysfunction in animal models of seizure and epilepsy that involves three important mediators: microglia, which are immune cells in the CNS, PACAP, a pleiotropic neuropeptide, and glutamate, a major excitatory neurotransmitter in the brain (Fig. 3).

* Corresponding author at: The Heart Research Institute, 7 Eliza Street, Sydney 2042 New South Wales, Australia.
E-mail address: paul.pilowsky@hri.org.au (P.M. Pilowsky).
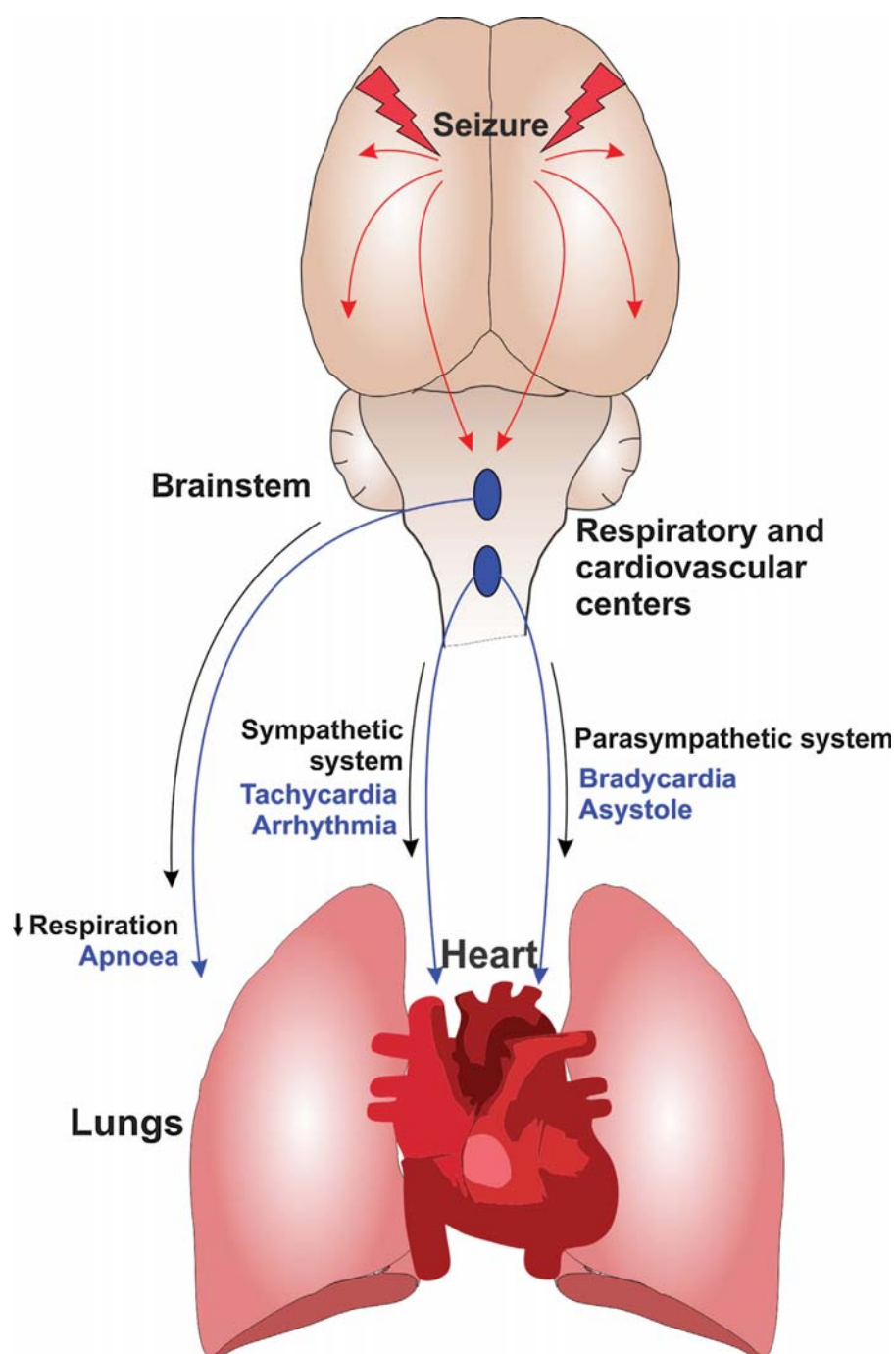
Fig. 1. A schematic diagram of mechanism of seizure-induced central autonomic cardiorespiratory dysfunction. Seizures propagate from higher brain region into the cardiorespiratory brainstem autonomic nuclei, and disturb the normal cardiorespiratory activity and reflexes. Seizure-induced excitation of sympathetic neurons leads to tachycardia and arrhythmia, whereas activation of parasympathetic system causes bradycardia and asystole. Moreover, spread of seizures could results in postictal coma, and loss of protective airway reflexes eventually causing decreased respiratory drive, apnoea and hypoventilation.

Microglia are ubiquitously distributed throughout the CNS, including in the vicinity of sympathetic premotor rostral ventro-lateral medullary (RVLM) neurons (Fig. 5) (Kapoor et al., 2016). Microglia can be either neuroprotective or neurodegenerative, depending on circumstances (Li et al., 2007; Vinet et al., 2012). Extensive microglial activation is evident in animal models of seizure (Beach et al., 1995; Drage et al., 2002; Shapiro et al., 2008).

During the acute phase of seizure, preconditioning of hippocampal microglia reduces the seizure score in mice (Mirrione et al., 2010). Moreover, antagonism of microglia activation, with intrathecal administration of minocycline, during acute phase seizures in rats produces more sympathoexcitation (Bhandare et al., 2015).

PACAP expression increases in the paraventricular nucleus (PVN) of the hypothalamus, after kainic acid-induced seizure in
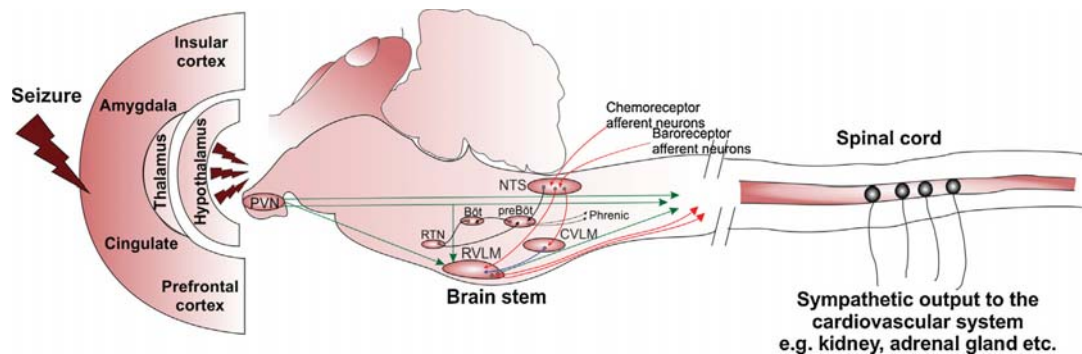
Fig. 2. The classical mechanism of seizure-induced central autonomic and cardiorespiratory dysfunction. Cardiorespiratory homeostasis is maintained by autonomic output, which is determined by balance of medullary reflexes, and influence of cerebral cortex. The sympathetic output to the heart is mediated by neurons from the RVLM through their direct projections to the IML cell column (red). The PVN affects sympathetic output through three different pathways; first, a direct descending projections to the IML, secondly, a projection to the vasomotor neurons of the RVLM, and thirdly, collateral projections to both IML and RVLM (green). Arterial baroreceptors are situated in the aortic arch and carotid sinus, and peripheral chemoreceptors are located in carotid and aortic bodies, providing afferent signals to NTS (red). The NTS integrates afferent information and relays it to activate (red) inhibitory neurons in the CVLM that in turn inhibit (blue) neurons in the RVLM. Astrocytes, and RTN neurons, act as central respiratory chemoreceptors that are exquisitely sensitive to changes in CO_2. Peripheral chemosensory afferent in NTS provide information to the pre-Bötzinger complex influencing the rate and shape of respiratory rhythm, which in turn regulates respiratory motoneurons including the phrenic, intercostal and hypoglossal neurons. Bulbar respiratory interneurons also modulate the activity of cardiovascular neurons. During seizures, electrical disturbances occur, and excitation propagates throughout the central autonomic network, disturbing the normal autonomic control of vital cardiorespiratory functions.

rats (Nomura et al., 2000). PACAP is sympathoexcitatory and pressor when injected into the subarachnoid space or into the RVLM (Farnham et al., 2012, 2011). During seizures, infusion of PACAP antagonist into the intrathecal space produces more sympathoexcitation (Bhandare et al., 2015), where PACAP may be reducing neurotoxicity, a possibility that requires further investigation. The multifaceted findings of PACAP make it a promising player in the central autonomic cardiorespiratory dysfunction in seizure.

Finally, glutamate, the principal excitatory neurotransmitter in brain, is increased in rat hippocampus following seizures (Kanamori and Ross, 2011), suggesting that glutamatergic synapses play an important role in the development of seizures (Ueda et al., 2001). Activation of glutamatergic receptors in RVLM mediate sympathoexcitation as well as proarrhythmogenic changes during seizure in rats (Bhandare et al., 2016), making them an attractive target for SUDEP therapy. Very recently, a role for microglia, PACAP, and glutamate, in seizure-induced cardiorespiratory responses is becoming a topic of considerable interest (Fig. 3).

2. Autonomic control of cardiorespiratory function

Normally, short-term cardiorespiratory homeostasis is tightly regulated by a balance between the sympathetic and parasympathetic activity (Young, 2010). The overall autonomic output to the cardiorespiratory system is determined by medullary reflexes, and the influence of the cerebral cortex (Fig. 2) (Guo et al., 2002; Westerhaus and Loewy, 2001). Findings in rats after pseudorabies virus injection in cardiac sympathetic target organs, such as adrenal gland and stellate ganglion, showed that higher brain centres exert a descending control on autonomic outflow to the heart (Fig. 2) (Westerhaus and Loewy, 2001). Stimulation of cardiac sympathetic afferents in cats, which evokes excitatory cardiovascular reflexes, confirmed that the neurons in the medulla, especially ventrolateral medulla, regulate the cardiovascular sympathetic reflexes (Guo et al., 2002). Medullary neurons regulate automatism of the sinus node, atrioventricular conduction, ventricular excitability and contractility. Sympathetic reflexes (baro, chemo and somatosympathetic) and blood pressure is regulated by C1, and non-C1, neurons in the RVLM, via direct projections to the IML cell column (intermediolateral cell column) (Madden and Sved, 2003; Nedoboy et al., 2016; Ross et al., 1984a,b). The PVN integrates the specific afferent inputs to generate a differential sympathetic out-

put. The PVN affects the sympathetic output (Allen, 2002) through three different pathways; projections to RVLM (Pyner and Coote, 1999), direct descending projections to IML, and collateral projections to both IML and RVLM (Fig. 2) (Pyner and Coote, 2000; Shafton et al., 1998). Arterial baroreceptors, situated in the aortic arch and carotid sinus, respond to changes in BP (Guo et al., 1982). Parasympathetic output to the heart is mediated by the vagus nerve, which originates from the dorsal motor nucleus, and more ventrally located nucleus ambiguus in the medulla (ter Horst et al., 1984). Respiratory centres in the brainstem provide an input to vagal efferents, which increases their activity decreasing heart rate, atrio-ventricular conduction, and ventricular excitability (Jones et al., 1998).

Brainstem neurons are also responsible for generating respiratory rhythm (Chitravanshi and Sapru, 1999; Mutolo et al., 2005). The findings in rabbits show that the respiratory rhythm is generated by glutamatergic interneurons, where the broad spectrum glutamate receptor antagonist, kynurenic acid, microinjection in pre-Bötzinger or Bötzinger complex induces a pattern of breathing characterised by low-amplitude, high-frequency irregular oscillations, superimposed on tonic phrenic nerve activity (Mutolo et al., 2005). The respiratory interneurons project to bulbar, phrenic, and other spinal motoneurons (Chitravanshi and Sapru, 1999). Peripheral chemoreceptors are located in the carotid and aortic bodies, and monitor blood chemicals (e.g. CO_2, O_2, H+, glucose) to maintain their homeostasis through initiation of respiratory, and cardiovascular reflexes (Heeringa et al., 1979; Moraes et al., 2014). Astrocytes, and neurons in the retrotrapezoid nucleus (RTN) act as central respiratory chemoreceptors (Wenker et al., 2010). Serotonin (5-hydroxytryptamine (5-HT)) (Massey et al., 2015) and many neuropeptides (Pilowsky et al., 2009; Rahman et al., 2011) can modify the excitability of central chemoreceptors. 5-HT neurons have projections to all parts of the CNS, and are important in arousal. The arousal response to hypercapnia is significantly diminished in genetically modified mice lacking 5-HT neurons (Hodges et al., 2008; Hodges et al., 2009).

The nucleus of the solitary tract (NTS) acts as a relay centre for both peripheral chemoreceptors, and baroreceptors (Callera et al., 1997). Suzuki and colleagues conducted experiments in rats, and showed that the glutamatergic NTS neurons excite both the RVLM and CVLM neurons, and the GABAergic (γ-aminobutyric acid) NTS and CVLM neurons inhibit the sympathetic activity of RVLM neu-
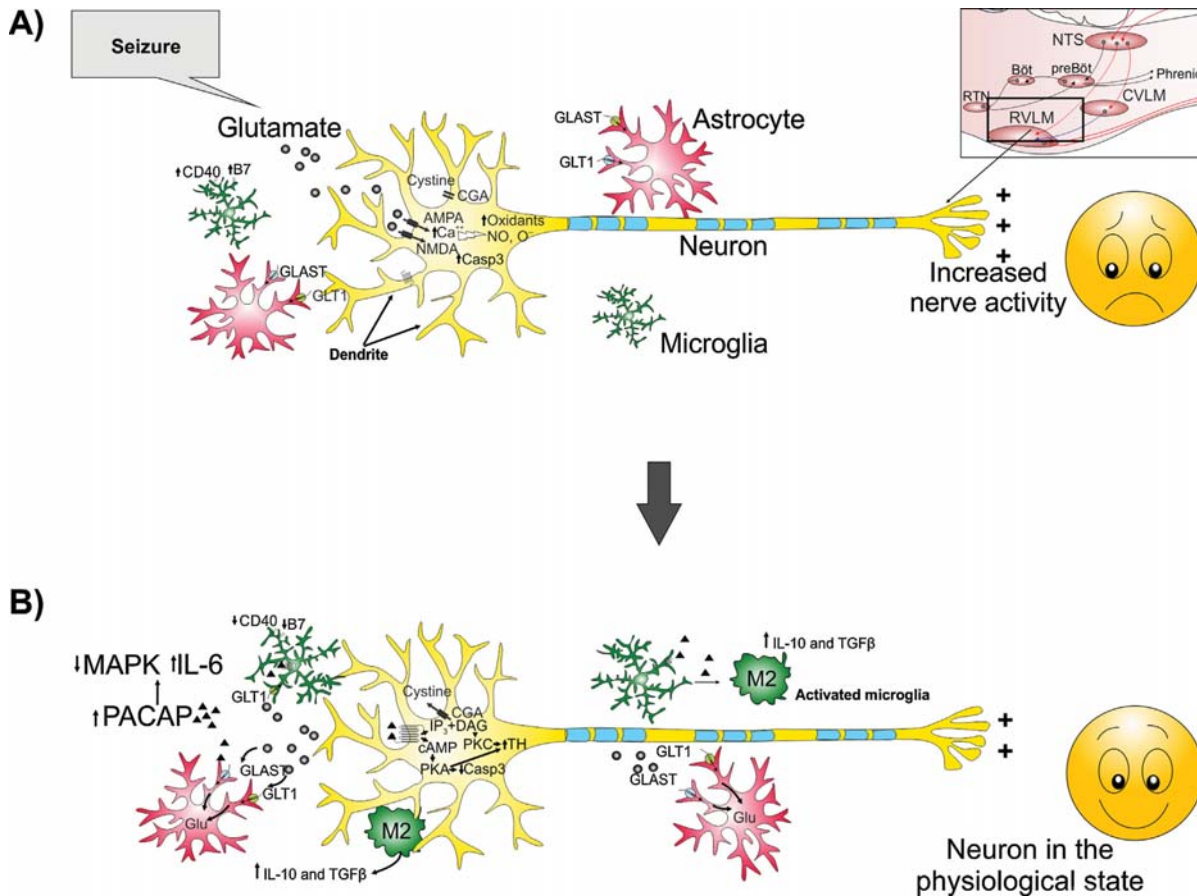
Fig. 3. A proposed model of the possible effect of PACAP, microglia, and glutamate on cardiorespiratory brainstem neurons during seizure. A) During seizures-induced intense neuronal hyperactivity, neurons release glutamate from presynaptic terminals that can act on postsynaptic AMPA or NMDA receptors. Activation of AMPA or NMDA receptors inhibits cysteine uptake, and influx of calcium stimulating production of oxidants, NO, and O^-. Under repetitive and extreme neuronal activation, neurotoxic effects are mediated through increased production of apoptotic factors such as caspase-3. Glutamate transporters expressed by astrocytes, play an important role in the rapid clearance of synaptically released glutamate. Expression of astrocytic glutamate transporters is downregulated in seizure. Altogether, increased oxidative stress, and cellular excitability, causes increased activity of cardiorespiratory neurons, and in extreme situations neuronal death. B) Increased PACAP expression during seizure may produce a neuroprotective effect on microglia in several ways. PACAP acts on neuronal PAC1 or VPAC2 receptors, to increase intracellular cAMP. PACAP can inhibit increases in caspase 3, via PKA and PKC pathways. Increased cAMP mimics the effect of glial glutamate transporter expression to further enhance glutamate clearance from the synaptic cleft. Microglia also express glutamate transporters in response to harmful or stressful situations such as seizures. PACAP can redirect the microglia towards the neuroprotective M2 phenotype. PACAP achieves its effects via actions on the MAP kinase family (and by inhibiting activation of JNK/SAPK, while it activate ERK), and increasing IL-6. Activation of PAC1 and VPAC1 receptors on activated microglia increases the production of IL-10, TGF-β, and decreases TNF-α as well as downregulating CD40, and B7 surface protein expression. Taken together, the action of PACAP and microglia may lead to protective effects on cardiorespiratory brainstem neuron to keep them in a physiological state.

rons (Suzuki et al., 1997). NTS plays a critical integrative role in regulation of cardiovascular, and respiratory system since it is the initial step in processing barosensory, and chemosensory information that culminates in homeostatic reflex responses (Callera et al., 1997). It is important to note that seizure upregulates the c-fos expression in brainstem cardiorespiratory nuclei including RVLM, and NTS (Sakamoto et al., 2008; Silveira et al., 2000). These findings confirm that seizure activates the neurons in the major cardiorespiratory nuclei in brainstem, and causes cardiorespiratory and autonomic dysfunction.

3. Cardiorespiratory dysfunction in seizure and SUDEP

There are many different types of epilepsy depending on signs, symptoms and origin of seizures (WHO, 2005). SUDEP is operationally defined as "sudden, unexpected, witnessed or unwitnessed, non-traumatic and non-drowning death in patients with epilepsy, with or without evidence of a seizure, and excluding documented status epilepticus, where post-mortem examination does not reveal a toxicological or anatomical cause of death" (Nashef, 1997). The mechanism of SUDEP is still unknown, and is the major hurdle in finding the best therapeutic solution for its prevention. Plausible mechanisms of SUDEP (Fig. 1) include ictal arrhythmias (Auerbach et al., 2013; Darbin et al., 2002), ictal and postictal central apnoea (Bateman et al., 2008; Seyal et al., 2010), acute neurogenic pulmonary edema (Kennedy et al., 2015), and autonomic dysfunction (Naggar et al., 2014) for each of which a case report has been documented and described further in detail. It therefore seems unlikely that SUDEP is a failure of a single system; rather it is more likely to be due to the collapse of multiple systems leading to fatal cardiac and respiratory dysfunction (Fig. 1).

Findings in SUDEP and temporal lobe epilepsy patients compared to controls shows that there is a significant volume loss in specific cardiorespiratory brainstem autonomic nuclei such as the periaqueductal gray, colliculi, raphe and reticular formation extending into the diencephalon particularly the medial posterior thalamus (Mueller et al., 2014). More importantly, in contrast to temporal lobe epilepsy patients, this volume loss was not only

more severe in SUDEP but also more widespread and extended into the dorsal section of the pons and even upper medulla. These findings specifically suggest that the neurodegeneration in central cardiorespiratory autonomic nuclei could be the mechanism for SUDEP (Mueller et al., 2014).

3.1. Cardiovascular dysfunction

3.1.1. Acute cardiac changes in epilepsy

Studies into the mechanisms of SUDEP, in human and animal, show that seizure causes major cardiovascular changes with significant sympathovagal imbalance, tachy- or brady- cardia, and abnormal changes in the electrocardiogram (ECG) (Fig. 1) (Bhandare et al., 2016, 2015; Naggar et al., 2014; Ponnusamy et al., 2012). Acute seizure causes a ∼100% increase in sympathetic activity, pressor effects, tachycardia, and prolongation of QT interval in rat (Bhandare et al., 2016, 2015; Naggar et al., 2014; Sakamoto et al., 2008). Increase in both sympathetic and parasympathetic activity, baro-reflex dysfunction, and hypoperfusion of brain and heart is evidenced as the major cause of death in seizure-induced rats (Sakamoto et al., 2008). Pilocarpine-induced status epilepticus causes severe shifts in sympathovagal balance towards a sympathetic predominance in rats (Metcalf et al., 2009). Kainic acid-induced chronic seizures in rats showed decreased vagal tone, increased QT dispersion, and eccentric cardiac hypertrophy without significant cardiac fibrosis (Naggar et al., 2014). Peri-ictal and ictal ECG changes are potential that can be used to detect seizure risk. In patients with refractory or well controlled temporal lobe epilepsy, heart rate variation during normal breathing, and tilting was lower, compared to control subjects (Ansakorpi et al., 2000). In temporal lobe epilepsy patients, heart rate variability changes (RR interval, low and high frequency domain analysed from ictal ECG recording) were significantly lower, and cardiosympathetic index was higher, compared to patients with psychogenic nonepileptic seizures (Ponnusamy et al., 2012). SUDEP is closely linked to ictal cardiovascular changes. ECG abnormalities, including ST segment elevation or depression, and T-wave inversion, occur in around 49% of patients during or after epileptic discharges, and are common in generalised seizure (Nei et al., 2000; Opherk et al., 2002). Tachycardia is present in 76–99% patients in epilepsy monitoring unit, suggestive of most probable clinical sign of convulsive and non-convulsive seizures (Moseley et al., 2011; Opherk et al., 2002). Activation of the central autonomic cardiovascular network, including the RVLM, causes cardiac changes observed in epilepsy (Silveira et al., 2000; Tsai et al., 2012). Overall, epileptic discharges are thought to propagate to the central autonomic nuclei in the brainstem, and disturb the normal autonomic control through sympathetic and parasympathetic pathways (Figs. 1–2). Our findings reveal that cardiovascular changes are always preceded by induction of seizures in rats (Bhandare et al., 2016, 2015). Temporal lobe epileptic discharges are also associated with ictal bradycardia, and asystole in 2–4% of seizure cases (Nei et al., 2000), and may occur due to the collapse of multiple systems.

3.1.2. Chronic cardiac changes in epilepsy

Neurocardiac channelopathies are the most significant chronic cardiovascular changes in patients with epilepsy. These changes lead to altered membrane excitability both in the brain and the heart (Ludwig et al., 2003), and pose an increased risk of autonomic dysfunction, and cardiac arrhythmia (Biet et al., 2015). Patch-clamp recordings reveal that, as in brain, epilepsy is associated with an increased expression of the neuronal isoform Nav1.1 in cardiomyocytes (Biet et al., 2015). In mice, the HCN channel plays a physiological role in regulating the resting membrane potential, required for regular cardiac and neuronal rhythmicity (Ludwig et al., 2003). In Genetic Absence Epilepsy Rats from Strasbourg (GAERS) and acquired temporal lobe epilepsy rats, the significant reduction in HCN2 mRNA and protein expression is the mechanism for abnormal cardiac electrophysiology (Powell et al., 2014).

Genetic mutations in the KCNQ1 gene cause familial long QT syndrome due to prolonged cardiac action potential (Goldman et al., 2009). Mutations in the KCNQ1 gene in forebrain neuronal networks, and in brainstem autonomic nuclei can produce seizures, and dysregulate the autonomic control of heart (Goldman et al., 2009).

Dravet syndrome is associated with a loss of function mutation in gene SCN1A encoding for voltage-gated sodium channel Nav1.5 that leads to ECG abnormalities. Increased excitability, prolongation of action potential duration, and triggered activity was recorded in isolated Dravet syndrome ventricular myocytes (Auerbach et al., 2013). Patients with Dravet syndrome have reduced heart rate variability (HRV) that shows imbalance in autonomic cardiac function (Delogu et al., 2011). The findings in SCN1A heterozygous knockout mice show that increase in parasympathetic activity following tonic-clonic seizures causes bradycardia and subsequently SUDEP (Kalume et al., 2013). SCN1A mutant mice have lower threshold for spreading depression that causes bradycardia, apnoea and SUDEP (Aiba and Noebels, 2015).

Loss of function mutations of the SCN5A gene causes Brugada syndrome, and is characterised with ECG abnormalities including ST segment elevation, syncope as well as seizures, and sleep abnormalities (Wang et al., 2015).

HRV is used as a functional tool to investigate the state of the autonomic nervous system. Reduced HRV is seen in epilepsy patients compared to their controls (Ponnusamy et al., 2012), and is associated with increased mortality in patients with heart failure. Abnormal blood pressure variability with higher vasomotor tone is observed in patients with chronic epilepsy (Devinsky et al., 1994).

3.2. Respiratory dysfunction

In epilepsy patients with severe respiratory dysfunction, as demonstrated using video-EEG telemetry, the ictal period is associated with a severe poikilocapnic hypoxia (Fig. 4) (Bateman et al., 2008; Seyal et al., 2010). Ictal and post- ictal ETCO$_2$ increased above 50 mmHg in 11 out of the 33 epilepsy patients with the post- ictal increase in respiratory rate, and amplitude (Seyal et al., 2010). In human, peri-ictal respiratory disturbances are likely to play a critical role in the pathophysiology of SUDEP (Dlouhy et al., 2015). Central apnoea is common in a sheep model of epileptic sudden death (Johnston et al., 1997). In audiogenic seizure-prone DBA/2 mice death due to respiratory arrest can be prevented by mechanical ventilation (Venit et al., 2004). Interestingly SUDEP in DBA/2 mice can also be prevented by treatment with a selective serotonin reuptake inhibitor (Tupal and Faingold, 2006). Serotonergic and/or glutamatergic neuronal abnormalities are associated with central respiratory dysfunction (Hodges et al., 2008, 2009). Impaired ventilatory responses to hypercapnia may lead to SUDEP by adversely affecting patients' ability to reposition their head when prone after convulsion.

Clinical evidence suggests that post-ictal pulmonary edema, which may be mediated by vasoconstriction induced by a massive seizure-related sympathetic outburst with increased pulmonary vascular resistance, could be associated with the pathophysiology of SUDEP (Kennedy et al., 2015). Forensic autopsies of 52 cases of SUDEP showed marked pulmonary congestion, and edema with an average combined lung weight of 1182 g, compared with the normal average combined lung weight of 840 g in men (Zhuo et al., 2012). In epileptic baboons that died suddenly without apparent cause, 96% had pulmonary congestion or edema, whereas only 12%
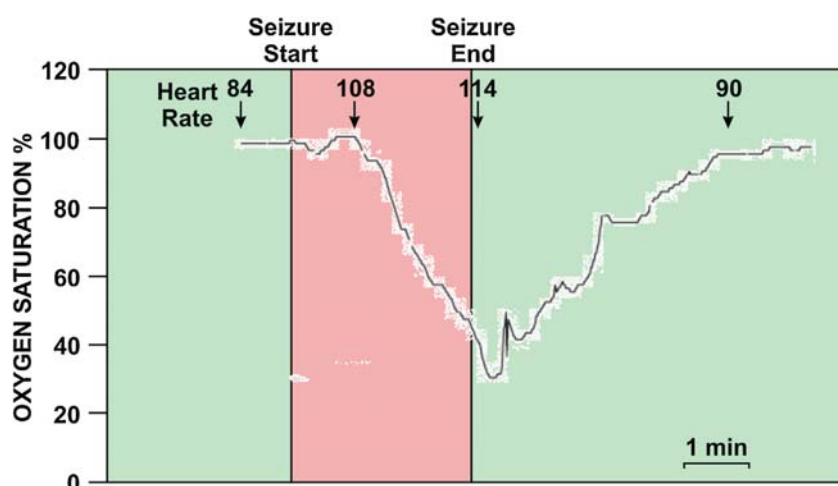
Fig. 4. Oxygen saturation falling below 40% in a 19 year old male patient with a complex partial seizure without generalisation. Seizure duration is shown in red with heart rate in the top panel. (With permission from Guarantors of Brain/Oxford University Press from- Bateman, L.M., Li, C.S., Seyal, M., 2008. Ictal hypoxemia in localization-related epilepsy: Analysis of incidence, severity and risk factors. Brain 131, 3239–3245).

of the control animals had pulmonary edema (Ákos Szabó et al., 2009).

4. Neurotransmitters in cardiorespiratory control

Glutamate, GABA and glycine are the three major ionotropic neurotransmitters within the central nervous system that are responsible for regulating cardiorespiratory activity and reflexes (Ross et al., 1984a; Suzuki et al., 1997). Antagonism of any of these three neurotransmitter systems causes major, or even complete, disruption of central cardiorespiratory control (Ross et al., 1984a). Microinjection of the broad spectrum ionotropic glutamate receptor antagonist, kynurenic acid, into either NTS or ventrolateral medulla reduces the vagal and sympathetic baroreflex (Guyenet et al., 1987). Selective inhibition of NMDA and AMPA/kainate receptors in the CVLM has a similar effect (Miyawaki et al., 1996a,b, 1997). On the other hand, other neurotransmitters and peptides, such as serotonin, catecholamines, PACAP, opioids, substance P, neuropeptide Y, somatostatin, galanin, orexin and angiotensin II also play significant roles in modulating cardiorespiratory function, and reflexes (Callera et al., 1997; Farnham et al., 2011; Kashihara et al., 2008; Miyawaki et al., 2002a; Pilowsky et al., 2009; Rahman et al., 2011; Shahid et al., 2011). Here we discuss the potential role of PACAP, and glutamate on brainstem cardiorespiratory neurons, in relation to seizure, and SUDEP.

4.1. Pituitary Adenylate Cyclase Activating Polypeptide (PACAP)

PACAP is a 38 amino acid pleiotropic neuropeptide that acts through three different G-protein coupled receptors (PAC1, VPAC1 and VPAC2) (Joo et al., 2004) to stimulate adenylate cyclase activity (Vaudry et al., 1998). It belongs to the glucagon-secretin-vasoactive intestinal polypeptide (VIP) super family of peptides. Since the discovery of PACAP, many studies have emphasised its neuroprotective, and anti-inflammatory role in *in vivo*, and in *in vitro*, models of neurodegenerative diseases (Bhandare et al., 2015; Brifault et al., 2015; Delgado et al., 1999; Shioda et al., 1998). PACAP is positively coupled to act on its membrane bound receptors and activate adenylyl cyclase and generate increased intracellular levels of cAMP. Subsequently, the increased level of cAMP leads to enhanced phosphorylation and changes intracellular proteins expressions such as the MAP kinase proteins (inhibit activation of Jun N-

terminal kinase (JNK)/stress activated protein kinase (SAPK), while it activate extracellular signal-regulated kinase (ERK)), and stimulates IL-6 secretion (Shioda et al., 1998; Shoge et al., 1999). PACAP administration after permanent cerebral ischemia by electrocauterization of middle cerebral artery improves function and recovery in mice by redirecting the microglial response toward a neuroprotective M2 phenotype (Brifault et al., 2015). In cardiovascular regulation, PACAP acts as an excitatory neurotransmitter at central autonomic nuclei in brainstem, and spinal cord (Farnham et al., 2012, 2011, 2008). PACAP is present in the brainstem, and spinal cord autonomic nuclei that are important in central cardiorespiratory regulation (Farnham et al., 2008). The PAC1 receptor is specific for PACAP with a 1000 times lower affinity for VIP, whereas VPAC1 and VPAC2 receptors have equal affinity for PACAP and VIP (Buscail et al., 1990; Miyata et al., 1989). PAC and VPAC receptors are present at specific locations throughout the CNS, on both neurons and microglia (Joo et al., 2004). PAC1 and VPAC1 (but not VPAC2) receptors are present on microglia (Delgado, 2002a,b; Kim et al., 2000; Nunan et al., 2014; Pocock and Kettenmann, 2007). PACAP immunoreactivity is found in regions of the brainstem and spinal cord, including the PVN (Hannibal et al., 1995). PACAP immunoreactive fibers innervate the PVN (Das et al., 2007), the RVLM (Farnham et al., 2008), the ventromedial hypothalamus (Maekawa et al., 2006), the arcuate nucleus (Dürr et al., 2007), and in the IML cell column (Chiba et al., 1996), which are major autonomic nuclei.

Kainic acid-induced seizure increases PACAP expression in PVN of the hypothalamus in rats (Nomura et al., 2000). Previously we found that low dose kainic acid-induced seizures in rats causes sympathoexcitation, increased mean arterial pressure and heart rate, and pro-arrhythmogenic changes including prolongation of the QT interval. The evidence suggests that PACAP has a protective effect on sympathetic preganglionic neurons in the IML cell column during seizures (Bhandare et al., 2015). In patients with epilepsy and SUDEP, PACAP might have "neuroprotective" or "excitatory" effect on sympathetic neurons, which depends on multiple factors, and leads to non-fatal or fatal seizure consequences. The outcome of seizure depends on the type and severity of seizure, the path of spread of seizure to autonomic nuclei, duration of seizure history, the presence of other cardiorespiratory complications etc. (Dlouhy et al., 2015; Hitiris et al., 2007). During seizures, the location of PACAP secretion and its concentration play an important role in modifying sympathetic activity and overall seizure outcome, e.g.

PACAP has different effects on sympathetic neurons at the RVLM and the IML cell column during seizures in rats (Bhandare et al., 2016, 2015).

There are a number of possibilities that could explain the way in which PACAP is exerting its effects, and contributing to either decrease or increase the seizure-induced sympathoexcitation. First, PACAP maintains the sympathetic neuronal firing threshold under control through inhibition of MAP kinase (Shioda et al., 1998), and synaptic glutamate levels (Figiel and Engele, 2000; Shoge et al., 1999) to keep them in healthy condition. Secondly, activation of PACAP on microglial PAC1, and VPAC1 receptors may polarise microglia toward an M2 (anti-inflammatory) phenotype, and increase the endogenous production of the anti-inflammatory cytokines, TGF-β, and IL-10 (Brifault et al., 2015; Suk et al., 2004). Thirdly, as reported earlier, PACAP may produce excitatory effect on the catecholaminergic neurons, and mediate sympathoexcitatory responses along with major effects on the ECG (Farnham et al., 2008; Lai et al., 1997). There is strong evidence that PACAP may play a neuroprotective role.

First, PACAP is anti-inflammatory, and protects neurons against various *in vitro* toxic insults (Delgado et al., 1999; Kim et al., 2000). Following ischemia, PACAP treatment inhibits the activation of JNK/SAPK, and increases secretion of IL-6, which further inhibits activation of JNK/SAPK (Shioda et al., 1998). The protective effect of PACAP is also seen in *in vivo* models of cerebral ischemia where its expression was increased after ischemic injury in rats and mice (Chen et al., 2006; Skoglösa et al., 1999a). PACAP is upregulated following sciatic nerve injury, suggesting a role for PACAP in post-injury recovery of nervous system (Zhang et al., 1996). PACAP also influences the development of the nervous system; specifically it has neurotrophic action on mesencephalic dopaminergic primary culture of neurons (Skoglösa et al., 1999b; Takei et al., 1998). The survival of the immature sympathetic neurons depends on NGF, and in its absence neurons undergo a decrease in intracellular cAMP levels, and programmed cell death (Chang and Korolev, 1997; Przywara et al., 1998). However, treatment with PACAP can increase the cAMP levels, and delay neuronal death caused by NGF deprivation. PACAP can rescue chick embryonic sympathetic neurons from apoptosis when the supply of NGF is compromised (Przywara et al., 1998). These findings indicate that under normal conditions, PACAP might not play a major role as a neurotropic molecule for sympathetic neuroblasts because NGF is sufficient, and is a dominant neurotropic factor. However, if neurons become vulnerable as a result of unavailable NGF, PACAP released from presynaptic sites could prevent neurons from apoptosis. Also the caspases 3, 6 and 7 cleave protein substrates within cell to trigger the final phase of apoptosis. PACAP inhibits the caspase 3 in NGF-deprived chicken sympathetic embryonic neuroblasts, which could be mediated through PKA and PKC, but not by ERK-type MAPK transduction pathways (Dejda et al., 2011; Vaudry et al., 1998).

PACAP has a protective effect against glutamate induced toxicity *in vitro* (Shoge et al., 1999). In cultured retinal neurons, a 10 min exposure to 1 mM glutamate followed by a further 24-h incubation significantly decreases cell viability. Application of PACAP simultaneously with glutamate attenuates the glutamate induced neurotoxicity, and prevents the decrease in viability, via cAMP/PKA/MAPK pathways (Shoge et al., 1999). Glutamate transporters play an important role in the rapid clearance of synaptically released excess glutamate. RT-PCR analysis of PACAP mRNA shows that PACAP is synthesised exclusively by neurons, and not by glia, and exposure of cortical astroglia to PACAP increases the maximal velocity of glutamate uptake by promoting the expression of GLT-1 and GLAST transporters (Figiel and Engele, 2000). PACAP also induces expression of glutamine synthetase, which metabolises glutamate into glu-

tamine. PACAP induced increased expression of glial glutamate transporter by astrocytes is likely mediated through activation of cAMP-dependant pathways (Figiel and Engele, 2000; Swanson et al., 1997). The results suggest that PACAP regulates glutamate transport, and metabolism that may contribute to its neuroprotective effect on cardiorespiratory neurons during seizure. Overall PACAP reduces the excessive firing of sympathetic neurons during seizures through the cAMP mediated mechanism, and needs further investigation, which inhibits JNK/SAPK, activates ERK, increases IL-6, inhibits caspase-3, and increases glutamate uptake via astrocytes (Fig. 3).

Secondly, PACAP can produce neuroprotective effects through its action on microglial PAC1 and VPAC1 receptors (Kim et al., 2000); causing release of substances such as IL-10, and TGF-β; compounds that protect neurons from overexcitation. PACAP suppresses NMDA-induced cell loss in the ganglion cell layer of the retina, and significantly elevates the mRNA levels of anti-inflammatory cytokines IL-10, and TGF-β by increasing the number of microglia and macrophages (Wada et al., 2013). PACAP inhibits activated microglia induced production of TNF-α by a cAMP dependent pathway in *in vivo*, and *in vitro* (Kim et al., 2000). The action of PACAP on microglial cell surface receptors increases IL-10 protein expression, causing downregulation of CD40, and B7 mRNA in activated microglia, thereby acting as a potent anti-inflammatory agent (Delgado et al., 1999; Kim et al., 2002). PACAP inhibits the activation of the MAPK family such as JNK (Delgado, 2002b; Shioda et al., 1998), and stimulates the secretion of IL-6 in CSF (Gottschall et al., 1994; Shioda et al., 1998). Under hypoxic condition, PACAP attenuates activation of inflammatory microglia, and protects co-cultured PC12 cells from microglial neurotoxicity via reduction of hypoxia induced activation of p38 MAPK (Suk et al., 2004). As explained later in detail, activated microglia can polarise into two different phenotypes depending on the type of stimulus, and participate in either neuroprotection or neurotoxicity. However, PACAP treatment can redirect the microglial response toward a neuroprotective M2 phenotype in the late phase of brain ischemia, suggesting that PACAP has a neuroprotective effect on activated microglia (Brifault et al., 2015). Altogether, the actions of PACAP may produce neuroprotective effect on cardiorespiratory neurons in the brainstem during neurotoxic insults such as epilepsy.

A third possibility that is also very promising occurs when increased PACAP expression during seizures may excite catecholaminergic neurons, and mediate sympathoexcitatory responses along with ECG abnormalities. PACAP infusion into the intrathecal space (Farnham et al., 2011; Lai et al., 1997), or microinjection into RVLM (Farnham et al., 2012) has long lasting sympathoexcitatory effects along with variable pressor responses in rats. Systemic administration of low doses of PACAP in rats decreases the threshold for the development of febrile convulsions. Conversely, administration of higher doses of PACAP increased the threshold (Chepurnova et al., 2002). The observed effect is most likely to be an indirect effect of PACAP-induced arginine vasopressin expression, where arginine vasopressin is known to mediate the hypothermia-induced seizures (Kasting et al., 1981). In these circumstances PACAP seems to mediate the induction of seizures, and acts as an excitatory neurotransmitter, which may cause further sympathoexcitatory effects.

4.2. Glutamate

Glutamate is the principal excitatory neurotransmitter of the CNS. Glutamate induced activation of the ionotropic NMDA and AMPA receptors leads to influx of Ca^{++} and Na^{+}. During prolonged excitation, glutamate causes neurotoxic insults through disruption of ionic homeostasis, and increases in oxidative stress (Fig. 3) (Hoyt et al., 1998). Glutamate transporters play an important role in
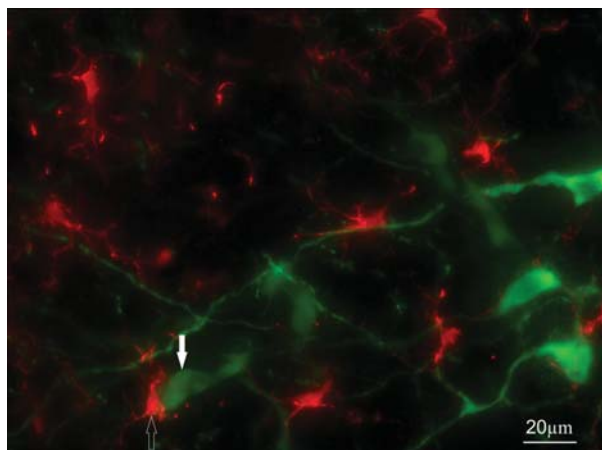
Fig. 5. Microglia (Iba1 immunoreactive; red) with a round cell body and normal processes with few ramifications are distributed in the vicinity of premotor tyrosine hydroxylase-immuno-reactive RVLM neurons (green). Sympathetic premotor RVLM neurons (green) are shown with a closed arrow and microglia (red) with open arrow.

rapid clearance of the synaptically released glutamate. High affinity sodium-dependant glutamate transporters include GLAST/EAAT1, GLT-1/EAAT2, EAAC1/EAAT3, EAAT4, and EAAT5. The GLAST1 and GLT-1 are expressed predominantly by glia (Swanson et al., 1997). Astrocytes are known to perform the majority of glutamate uptake in the brain, and unlike neurons, are capable of metabolising incorporated glutamate into glutamine by glutamine synthetase (Figiel et al., 2003).

Glutamate is the primary fast neurotransmitter of sympathetic premotor RVLM neurons, as all of these neurons express vesicular glutamate transporter 2 mRNA (Stornetta et al., 2002a,b), and phosphate activated glutaminase is present in both respiratory (Pilowsky et al., 1997) and cardiovascular neurons (Minson et al., 1991). Physiological findings confirmed that bulbospinal RVLM neurons use glutamate as their major neurotransmitter. Microinjection of L-glutamate into the RVLM produces pressor responses along with sympathoexcitation that are completely blocked by kynurenic acid (Araujo et al., 1999; Ito and Sved, 1997). Kynurenic acid microinjection into RVLM on its own has no effect on basal blood pressure, suggesting that glutamatergic synapses have little input to the RVLM in maintaining basal blood pressure, and sympathetic activity. On the other hand, the increase in blood pressure and sympathetic activity that follows blockade of inputs from CVLM to RVLM is dramatically attenuated by blocking glutamatergic excitation into the RVLM (Ito and Sved, 1997; Miyawaki et al., 2002b). Collectively, findings suggest that there is a glutamatergic input to the RVLM neurons and that this glutamatergic input is in balance with inhibitory pathways from CVLM.

Glutamatergic pathways are involved in acute and chronic neurodegenerative diseases including epilepsy, where it is more specific only in some types such as temporal lobe epilepsy (Mueller et al., 2014; Thom, 2004). Activation of both ionotropic and metabotropic glutamate receptors is pro-convulsant (Chapman, 1998). Seizure elevates glutamate levels in the extracellular fluid of the rat hippocampus (Kanamori and Ross, 2011), and produces down-regulation, and functional failure of glutamate transporters (Ueda et al., 2001). The RVLM contains sympathetic premotor neurons responsible for maintaining tonic excitation of sympathetic preganglionic neurons involved in cardiovascular regulation (Madden and Sved, 2003). The activity of pre-sympathetic RVLM neurons is directly correlated with sympathetic nerve activity, and stimulation of neuronal cell bodies in the RVLM with glutamate produces dose-dependent increases in arterial pres-

sure, that is sympathetically mediated (Madden and Sved, 2003). Seizure-induced sympathoexcitation is caused by activation of glutamatergic receptors in RVLM that also causes proarrhythmogenic changes in rats (Bhandare et al., 2016). Seizure-related increased glutamate expression causes autonomic cardiovascular changes, since the microinjection of kynurenic acid, completely abolished these effects.

It is most likely that increased glutamate levels during seizure induces excito-neurotoxicity of pre-synaptic RVLM neurons, and may contribute to neurodegeneration, and inflammation in epilepsy that might contribute to SUDEP (Mueller et al., 2014). Increased oxidative stress, and inflammation in RVLM during seizure (Tsai et al., 2012) could be mediated through increased glutamate levels or functional failure of glutamate transporters on astrocytes (Ueda et al., 2001). Extracellular glutamate activates either AMPA, NMDA or group I metabotropic receptors, resulting in oxidative stress and cellular excitability (Coyle and Puttfarcken, 1993), and causes sympathoexcitation. Group I metabotropic receptors (mGlu1 and mGlu5) are predominantly located post-synaptically, and activate phospholipase C, which catalyse the production of inositol trisphosphate, and thereby trigger the release of Ca^{2+} from intracellular stores. Mitochondrial activation is a plausible event in glutamate induced oxidative stress, and cellular excitability causing sympathoexcitation (Fig. 3) (Coyle and Puttfarcken, 1993).

5. Microglia and their effect on the physiological state of cardiorespiratory neurons during seizure

Microglia are the principal resident immune cells of the CNS, contributing ∼10% of total brain population (Benarroch, 2013; Helmut et al., 2011). Since the first morphological characterisation of microglia, enormous research is conducted, and still their precise role in the healthy and diseased CNS remains unclear. Initially, microglia were classified into two types, "resting" microglia, which are "inactive", and present in uninjured CNS; and "activated" microglia that are present in response to injury. However, recent work suggests that this classical active/inactive classification is misleading. Using *in vivo* two photon imaging of fluorescent-labelled neurons and microglia in mice, it is shown that resting microglia continuously survey their microenvironment for the homeostatic conditions by making brief, and direct contact with synapses. The frequency of microglial contact is directly proportional to neuronal activity, and also reflects the functional status of the synapses (Wake et al., 2009). On the other hand, resting microglia undergo drastic changes, and transform into an activated state. Activated microglia are ramified, with an amoeboid morphology, and acquire their phenotype depending on the type of stimulus; participating in either neuroprotection or neurotoxicity (Ayoub and Salm, 2003). Thus the important role of highly dynamic microglial cells is to maintain synaptic and neuronal homeostasis during both normal and diseased CNS conditions (Helmut et al., 2011; Wake et al., 2009).

Extensive microglial activation is well described in animal models of seizure (Drage et al., 2002; Shapiro et al., 2008), as well as in humans (Beach et al., 1995). Patients with intractable seizures display an 11-fold increase in microglial reactivity in the hippocampus suggesting that microglia change their state in response to altered neuronal activity (Beach et al., 1995). As explained earlier, brainstem and spinal cord autonomic nuclei are important in central cardiorespiratory regulation whose function is disturbed in seizure cases (Bhandare et al., 2015; Naggar et al., 2014; Sakamoto et al., 2008). Microglia are closely associated with sympathetic premotor RVLM neurons (Fig. 5) (Kapoor et al., 2016), and help to maintain a normal homeostatic state. During seizure, microglial responses are

not necessarily neurotoxic. Ablation of preconditioned hippocampal microglia in mice causes significant increases in acute seizure scores compared to non-ablated and preconditioned microglia in control mice, suggestive of a protective effect of microglia (Mirrione et al., 2010). Other studies reported a neuroprotective role of microglia in different animal models of neurodegenerative diseases. In TNF-α and IL-1β-deficient mice, sodium nitroprusside-induced acute neurotoxicity was increased, which supports a neuroprotective role for pro-inflammatory cytokines released by microglia (Turrin and Rivest, 2006). Marked increases in infarct size and neuronal apoptosis was evident when proliferation of resident microglia was selectively ablated in a mouse model of cerebral ischemia (Lalancette-Hébert et al., 2007). Similar findings were observed in *in vitro* studies, where ablation of ramified microglia severely enhanced NMDA induced neuronal cell death (Vinet et al., 2012). However, neurotoxic effects of microglia occur in cases of overshooting, and uncontrolled stimulation, and are widely attributed to release of cytokines such as caspases, TNF-α and IL-1β (Burguillos, 2011; Li et al., 2007). Activated microglia are major contributors to neuroinflammation, via secretion of pro-inflammatory cytokines, and chemokines, in addition to non-specific inflammatory mediators such as ROS, and NO. Fresh frozen tissue samples from autism patients showed marked activation of microglia with significant increase in proinflammatory cytokines profile in CSF (Vargas et al., 2005). However, there is little information available about the effect of seizure on microglial activation in brainstem, and spinal cord cardiorespiratory autonomic nuclei, and their possible neuroprotective or neurotoxic effect.

Recent findings provide increasing evidence for microglial communication with neurons (Wake et al., 2009). During early development, microglia clear apoptotic neurons, promote survival of cortical neurons, and prune synapses (Awasaki and Ito, 2004) whereas in the mature CNS they perform highly dynamic functions. Exquisitely motile process and stationary somata of microglial cells make contacts with neurons, and synapses to constantly survey the microenvironment (Fig. 5) (Wake et al., 2009). As explained earlier, glutamate plays a crucial role in development of seizure, and is a major neurotransmitter in cardiorespiratory reflexes. Increased glutamate levels in seizure activates neuronal NMDA receptors followed by calcium influx, and ATP release, which attracts microglial processes through activation of P2Y12 receptors (Eyo et al., 2014). Normally, astroglial glutamate transporters, GLT-1 and GLAST, perform the majority of glutamate uptake in the brain to mediate a high signal to noise ratio in synaptic signaling. However, in pathological conditions such as epilepsy, astroglial glutamate transporter proteins are downregulated, causing excitotoxicity (Ueda et al., 2001). It is possible that microglia may be neuroprotective during seizure by increasing glutamate transporter (GLT-1) expression, and reducing synaptic glutamate concentrations, as demonstrated during facial nerve axotomy (López-Redondo et al., 2000), infectious diseases (Persson et al., 2007), and neurodegenerative diseases (Chrétien et al., 2004). Collectively, the findings support the notion that during seizures, microglia may exert a neuroprotective effect on cardiorespiratory neurons in brainstem that is in part mediated by PACAP (Fig. 3).

6. Conclusion

In epilepsy, the increased expression of glutamate contributes to neurodegeneration, and inflammation. PACAP, and its action on microglia may mediate the neuroprotective effect on central cardiorespiratory neurons in the brainstem. PACAP is neuroprotective by causing production of anti-inflammatory factors such as TGF-β, and IL-6. Additionally, PACAP not only increases the expression of glutamate transporters on microglia, which accelerate glutamate

clearance from the synaptic cleft, but also polarise microglia toward an anti-inflammatory M2 phenotype. Hence, tailoring the effect of PACAP and microglia in the vicinity of cardiorespiratory brainstem neurons may be neuroprotective, and lead to possible novel therapeutic approaches for SUDEP.

References

Aiba, I., Noebels, J.L., 2015. Spreading depolarization in the brainstem mediates sudden cardiorespiratory arrest in mouse SUDEP models. Sci. Transl. Med. 7, 282ra46.

Ákos Szabó, C., Knape MichelleLeland, K.D.M., Feldman, J., McCoy, K.J.M., Hubbard, G.B., Williams, J.T., 2009. Mortality in captive baboons with seizures: a new model for SUDEP? Epilepsia 50, 1995–1998.

Allen, A.M., 2002. Inhibition of the hypothalamic paraventricular nucleus in spontaneously hypertensive rats dramatically reduces sympathetic vasomotor tone. Hypertension 39, 275–280.

Ansakorpi, H., Korpelainen, J.T., Suominen, K., Tolonen, U., Myllylä, V.V., Isojärvi, J.I.T., 2000. Interictal cardiovascular autonomic responses in patients with temporal lobe epilepsy. Epilepsia 41, 42–47.

Araujo, G.C., Lopes, O.U., Campos, R.R., 1999. Importance of glycinergic and glutamatergic synapses within the rostral ventrolateral medulla for blood pressure regulation in conscious rats. Hypertension 34, 752–755.

Auerbach, D.S., Jones, J., Clawson, B.C., Offord, J., Lenk, G.M., Ogiwara, I., Yamakawa, K., Meisler, M.H., Parent, J.M., Isom, L.L., 2013. Altered cardiac electrophysiology and SUDEP in a model of Dravet syndrome. PLoS One 8, e77843.

Awasaki, T., Ito, K., 2004. Engulfing action of glial cells is required for programmed axon pruning during Drosophila metamorphosis. Curr. Biol. 14, 668–677.

Ayoub, A.E., Salm, A.K., 2003. Increased morphological diversity of microglia in the activated hypothalamic supraoptic nucleus. J. Neurosci. 23, 7759–7766.

Bateman, L.M., Li, C.S., Seyal, M., 2008. Ictal hypoxemia in localization-related epilepsy: analysis of incidence, severity and risk factors. Brain 131, 3239–3245.

Beach, T.G., Woodhurst, W.B., MacDonald, D.B., Jones, M.W., 1995. Reactive microglia in hippocampal sclerosis associated with human temporal lobe epilepsy. Neurosci Lett. 191, 27–30.

Benarroch, E.E., 2013. Microglia: Multiple roles in surveillance, circuit shaping, and response to injury. Neurology 81, 1079–1088.

Bhandare, A.M., Kapoor, K., Pilowsky, P.M., Farnham, M.M.J., 2016. Seizure-Induced Sympathoexcitation Is Caused by Activation of Glutamatergic Receptors in RVLM That Also Causes Proarrhythmogenic Changes Mediated by PACAP and Microglia in Rats. J. Neurosci. 36, 506–517.

Bhandare, A.M., Mohammed, S., Pilowsky, P.M., Farnham, M.M.J., 2015. Antagonism of PACAP or microglia function worsens the cardiovascular consequences of kainic-acid-induced seizures in rats. J. Neurosci. 35, 2191–2199.

Biet, M., Morin, N., Lessard-Beaudoin, M., Graham, R.K., Duss, S., Gagné, J., Sanon, N.T., Carmant, L., Dumaine, R., 2015. Prolongation of action potential duration and QT interval during epilepsy linked to increased contribution of neuronal sodium channels to cardiac late Na + current. Circ-Arrhythmia Electrophysiol 8, 912–920.

Brifault, C., Gras, M., Liot, D., May, V., Vaudry, D., Wurtz, O., 2015. Delayed pituitary adenylate cyclase–activating polypeptide delivery after brain stroke improves functional recovery by inducing M2 microglia/macrophage polarization. Stroke 46, 520–528.

Burguillos, M.A.D.T.E.A.N.-Q.A.J.P.E.J.L.J.B., 2011. Caspase signalling controls microglia activation and neurotoxicity. Nature 472, 319–324.

Buscail, L., Gourlet, P., Cauvin, A., De Neef, P., Gossen, D., Arimura, A., Miyata, A., Coy, D.H., Robberecht, P., Christophe, J., 1990. Presence of highly selective receptors for PACAP (pituitary adenylate cyclase activating peptide) in membranes from the rat pancreatic acinar cell line AR 4-2J. FEBS Lett. 262, 77–81.

Callera, J.C., Sévoz, C., Laguzzi, R., Machado, B.H., 1997. Microinjection of a serotonin3 receptor agonist into the NTS of unanesthetized rats inhibits the bradycardia evoked by activation of the baro- and chemoreflexes. J. Autonom. Nerv. Syst. 63, 127–136.

Chang, J.Y., Korolev, V.V., 1997. Cyclic AMP and sympathetic neuronal programmed cell death. Neurochem. Int. 31, 161–167.

Chapman, A.G., 1998. Glutamate receptors in epilepsy. Prog. Brain Res. 116, 371–383.

Chen, Y., Samal, B., Hamelink, C.R., Xiang, C.C., Chen, Y., Chen, M., Vaudry, D., Brownstein, M.J., Hallenbeck, J.M., Eiden, L.E., 2006. Neuroprotection by endogenous and exogenous PACAP following stroke. Regul. Peptides 137, 4–19.

Chepurnova, N.E., Ponomarenko, A.A., Chepurnov, S.A., 2002. Peptidergic mechanisms of hyperthermia-evoked convulsions in rats in early postnatal ontogenesis. Neurosci. Behav. Physiol. 32, 505–511.

Chiba, T., Tanaka, K., Tatsuoka, H., Dun, S.L., Dun, N.J., 1996. The synaptic structure of PACAP immunoreactive axons in the intermediolateral nucleus of the rat. Neurosci. Lett. 214, 65–68.

Chitravanshi, V.C., Sapru, H.N., 1999. Phrenic nerve responses to chemical stimulation of the subregions of ventral medullary respiratory neuronal group in the rat. Brain Res. 821, 443–460.

Chrétien, F., Le Pavec, G., Vallat-Decouvelaere, A.V., Delisle, M.B., Uro-Coste, E., Ironside, J.W., Gambetti, P., Parchi, P., Créminon, C., Dormont, D., Mikol, J., Gray, F., Gras, G., 2004. Expression of excitatory amino acid transporter-1 (EAAT-1) in brain macrophages and microglia of patients with prion diseases. J. Neuropath. Exp. Neur. 63, 1058–1071.

Coyle, J.T., Puttfarcken, P., 1993. Oxidative stress, glutamate, and neurodegenerative disorders. Science 262, 689–695.

Darbin, O., Casebeer, D.J., Naritoku, D.K., 2002. Cardiac dysrhythmia associated with the immediate postictal state after maximal electroshock in freely moving rat. Epilepsia 43, 336–341.

Das, M., Vihlen, C.S., Legradi, G., 2007. Hypothalamic and brainstem sources of pituitary adenylate cyclase-activating polypeptide nerve fibers innervating the hypothalamic paraventricular nucleus in the rat. J. Comp. Neurol. 500, 761–776.

Dejda, A., Seaborn, T., Bourgault, S., Touzani, O., Fournier, A., Vaudry, H., Vaudry, D., 2011. PACAP and a novel stable analog protect rat brain from ischemia: Insight into the mechanisms of action. Peptides 32, 1207–1216.

Delgado, M., 2002a. Vasoactive intestinal peptide and pituitary adenylate cyclase-activating polypeptide inhibit CBP–NF-(B interaction in activated microglia. Biochem. Bioph. Res. Commun. 297, 1181–1185.

Delgado, M., 2002b. Vasoactive intestinal peptide and pituitary adenylate cyclase-activating polypeptide inhibit the MEKK1/MEK4/JNK signaling pathway in endotoxin-activated microglia. Biochem. Bioph. Res. Commun. 293, 771–776.

Delgado, M., Munoz-Elias, E.J., Gomariz, R.P., Ganea, D., 1999. Vasoactive intestinal peptide and pituitary adenylate cyclase-activating polypeptide enhance IL-10 production by murine macrophages: in vitro and in vivo studies. J. Immunol 162, 1707–1716.

Delogu, A.B., Spinelli, A., Battaglia, D., Dravet, C., De Nisco, A., Saracino, A., Romagnoli, C., Lanza, G.A., Crea, F., 2011. Electrical and autonomic cardiac function in patients with Dravet syndrome. Epilepsia 52, 55–58.

Devinsky, O., Perrine, K., Theodore, W.H., 1994. Interictal autonomic nervous system function in patients with epilepsy. Epilepsia 35, 199–204.

Dlouhy, B.J., Gehlbach, B.K., Kreple, C.J., Kawasaki, H., Oya, H., Buzza, C., Granner, M.A., Welsh, M.J., Howard, M.A., Wemmie, J.A., Richerson, G.B., 2015. Breathing inhibited when seizures spread to the amygdala and upon amygdala stimulation. J. Neurosci. 35, 10281–10289.

Drage, M.G., Holmes, G.L., Seyfried, T.N., 2002. Hippocampal neurons and glia in epileptic EL mice. J. Neurocytol. 31, 681–692.

Dürr, K., Norsted, E., Gömüç, B., Suarez, E., Hannibal, J., Meister, B., 2007. Presence of pituitary adenylate cyclase-activating polypeptide (PACAP) defines a subpopulation of hypothalamic POMC neurons. Brain Res. 1186, 203–211.

Eyo, U.B., Peng, J., Swiatkowski, P., Mukherjee, A., Bispo, A., Wu, L.J., 2014. Neuronal hyperactivity recruits microglial processes via neuronal NMDA receptors and microglial P2Y12 receptors after status epilepticus. J. Neurosci. 34, 10528–10540.

Farnham, M.M., Lung, M.S., Tallapragada, V.J., Pilowsky, P.M., 2012. PACAP causes PAC1/VPAC2 receptor mediated hypertension and sympathoexcitation in normal and hypertensive rats. Am. J. Physiol-Heart C 303, 910–917.

Farnham, M.M.J., Inglott, M.A., Pilowsky, P.M., 2011. Intrathecal PACAP-38 causes increases in sympathetic nerve activity and heart rate but not blood pressure in the spontaneously hypertensive rat. Am. J. Physiol-Heart C 300, 214–222.

Farnham, M.M.J., Li, Q., Goodchild, A.K., Pilowsky, P.M., 2008. PACAP is expressed in sympathoexcitatory bulbospinal C1 neurons of the brain stem and increases sympathetic nerve activity in vivo. Am. J. Physiol-Regul. I 294, 1304–1311.

Ficker, D.M., So, E.L., Shen, W.K., Annegers, J.F., O'Brien, P.C., Cascino, G.D., Belau, P.O., 1998. Population-based study of the incidence of sudden unexplained death in epilepsy. Neurology 51, 1270–1274.

Figiel, M., Engele, J., 2000. Pituitary adenylate cyclase-activating polypeptide (PACAP), a neuron- derived peptide regulating glial glutamate transport and metabolism. J. Neurosci. 20, 3596–3605.

Figiel, M., Maucher, T., Rozyczka, J., Bayatti, N., Engele, J., 2003. Regulation of glial glutamate transporter expression by growth factors. Exp. Neurol. 183, 124–135.

Goldman, A.M., Glasscock, E., Yoo, J., Chen, T.T., Klassen, T.L., Noebels, J.L., 2009. Arrhythmia in heart and brain: KCNQ1 mutations link epilepsy and sudden unexplained death. Sci. Transl. Med. 1, 2ra6.

Gottschall, P.E., Tatsuno, I., Arimura, A., 1994. Regulation of interleukin-6 (IL-6) secretion in primary cultured rat astrocytes: Synergism of interleukin-1 (IL-1) and pituitary adenylate cyclase activating polypeptide (PACAP). Brain Res. 637, 197–203.

Guo, G.B., Thames, M.D., Abboud, F.M., 1982. Differential baroreflex control of heart rate and vascular resistance in rabbits. Relative role of carotid aortic, and cardiopulmonary baroreceptors. Circ. Res. 50, 554–565.

Guo, Z.-L., Lai, H.-C., Longhurst, J.C., 2002. Medullary pathways involved in cardiac sympathoexcitatory reflexes in the cat. Brain Res. 925, 55–66.

Guyenet, P.G., Filtz, T.M., Donaldson, S.R., 1987. Role of excitatory amino acids in rat vagal and sympathetic baroreflexes. Brain Res. 407, 272–284.

Hannibal, J., Mikkelsen, J.D., Clausen, H., Holst, J.J., Wulff, B.S., Fahrenkrug, J., 1995. Gene expression of pituitary adenylate cyclase activating polypeptide (PACAP) in the rat hypothalamus. Regul. Peptides 55, 133–148.

Heeringa, J., Berkenbosch, A., De Goede, J., Olievier, C.N., 1979. Relative contribution of central and peripheral chemoreceptors to the ventilatory response to CO2 during hyperoxia. Resp. Physiol. 37, 365–379.

Helmut, K., Hanisch, U.K., Noda, M., Verkhratsky, A., 2011. Physiology of microglia. Physiol. Rev. 91, 461–553.

Hirsch, C.S., Martin, D.L., 1971. Unexpected death in young epileptics. Neurology 21, 682–690.

Hitiris, N., Suratman, S., Kelly, K., Stephen, L.J., Sills, G.J., Brodie, M.J., 2007. Sudden unexpected death in epilepsy: a search for risk factors. Epilepsy Behav. 10, 138–141.

Hodges, M.R., Tattersall, G.J., Harris, M.B., McEvoy, S.D., Richerson, D.N., Deneris, E.S., Johnson, R.L., Chen, Z.F., Richerson, G.B., 2008. Defects in breathing and thermoregulation in mice with near-complete absence of central serotonin neurons. J. Neurosci. 28, 2495–2505.

Hodges, M.R., Wehner, M., Aungst, J., Smith, J.C., Richerson, G.B., 2009. Transgenic mice lacking serotonin neurons have severe apnea and high mortality during development. J. Neurosci. 29, 10341–10349.

Holst, A.G., Winkel, B.G., Risgaard, B., Nielsen, J.B., Rasmussen, P.V., Haunsø, S., Sabers, A., Uldall, P., Tfelt-Hansen, J., 2013. Epilepsy and risk of death and sudden unexpected death in the young: a nationwide study. Epilepsia 54, 1613–1620.

Hoyt, K.R., Arden, S.R., Aizenman, E., Reynolds, I.J., 1998. Reverse Na+/Ca2+ exchange contributes to glutamate-induced intracellular Ca2+ concentration increases in cultured rat forebrain neurons. Mol. Pharmacol. 53, 742–749.

Ito, S., Sved, A.F., 1997. Tonic glutamate-mediated control of rostral ventrolateral medulla and sympathetic vasomotor tone. Am. J. Physiol-Regul. I 273, 487–494.

Johnston, S.C., Siedenberg, R., Min, J.K., Jerome, E.H., Laxer, K.D., 1997. Central apnea and acute cardiac ischemia in a sheep model of epileptic sudden death. Ann. Neurol. 42, 588–594.

Jones, J.F.X., Wang, Y., Jordan, D., 1998. Activity of C fibre cardiac vagal efferents in anaesthetized cats and rats. J. Physiol. 507, 869–880.

Joo, K.M., Chung, Y.H., Kim, M.K., Nam, R.H., Lee, B.L., Lee, K.H., Cha, C.I., 2004. Distribution of vasoactive intestinal peptide and pituitary adenylate cyclase-activating polypeptide receptors (VPAC1, VPAC2, and PAC1 receptor) in the rat brain. J. Comp. Neurol. 476, 388–413.

Kalume, F., Westenbroek, R.E., Cheah, C.S., Yu, F.H., Oakley, J.C., Scheuer, T., Catterall, W.A., 2013. Sudden unexpected death in a mouse model of Dravet syndrome. J. Clin. Invest. 123, 1798–1808.

Kanamori, K., Ross, B.D., 2011. Chronic electrographic seizure reduces glutamine and elevates glutamate in the extracellular fluid of rat brain. Brain Res. 1371, 180–191.

Kapoor, K., Bhandare, A.M., Farnham, M.M.J., Pilowsky, P.M., 2016. Alerted microglia and the sympathetic nervous system: A novel form of microglia in the development of hypertension. Respir. Physiol. Neurobiol. 226, 51–62.

Kashihara, K., McMullan, S., Lonergan, T., Goodchild, A.K., Pilowsky, P.M., 2008. Neuropeptide Y in the rostral ventrolateral medulla blocks somatosympathetic reflexes in anesthetized rats. Auton. Neurosci-Basic 142, 64–70.

Kasting, N.W., Veale, W.L., Cooper, K.E., Lederis, K., 1981. Vasopressin may mediate febrile convulsions. Brain Res. 213, 327–333.

Kennedy, J.D., Hardin, K.A., Parikh, P., Li, C.S., Seyal, M., 2015. Pulmonary edema following generalized tonic clonic seizures is directly associated with seizure duration. Seizure 27, 19–24.

Kim, W.-K., Kan, Y., Ganea, D., Hart, R.P., Gozes, I., Jonakait, G.M., 2000. Vasoactive intestinal peptide and pituitary adenylyl cyclase-activating polypeptide inhibit tumor necrosis factor-α production in injured spinal cord and in activated microglia via a cAMP-dependent pathway. J. Neurosci. 20, 3622–3630.

Kim, W.K., Ganea, D., Jonakait, G.M., 2002. Inhibition of microglial CD40 expression by pituitary adenylate cyclase-activating polypeptide is mediated by interleukin-10. J. Neuroimmunol. 126, 16–24.

Lai, C.C., Wu, S.Y., Lin, H.H., Dun, N.J., 1997. Excitatory action of pituitary adenylate cyclase activating polypeptide on rat sympathetic preganglionic neurons in vivo and in vitro. Brain Res. 748, 189–194.

Lalancette-Hébert, M., Gowing, G., Simard, A., Yuan, C.W., Kriz, J., 2007. Selective ablation of proliferating microglial cells exacerbates ischemic injury in the brain. J. Neurosci. 27, 2596–2605.

Li, L., Lu, J., Tay, S.S.W., Moochhala, S.M., He, B.P., 2007. The function of microglia, either neuroprotection or neurotoxicity, is determined by the equilibrium among factors released from activated microglia in vitro. Brain Res. 1159, 8–17.

López-Redondo, F., Nakajima, K., Honda, S., Kohsaka, S., 2000. Glutamate transporter GLT-1 is highly expressed in activated microglia following facial nerve axotomy. Mol. Brain Res. 76, 429–435.

Ludwig, A., Budde, T., Stieber, J., Moosmang, S., Wahl, C., Holthoff, K., Langebartels, A., Wotjak, C., Munsch, T., Zong, X., Feil, S., Feil, R., Lancel, M., Chien, K.R., Konnerth, A., Pape, H.C., Biel, M., Hofmann, F., 2003. Absence epilepsy and sinus dysrhythmia in mice lacking the pacemaker channel HCN2. EMBO J. 22, 216–224.

Madden, C.J., Sved, A.F., 2003. Cardiovascular regulation after destruction of the C1 cell group of the rostral ventrolateral medulla in rats. Am. J. Physiol. Heart C 285, 2734–2748.

Maekawa, F., Fujiwara, K., Tsukahara, S., Yada, T., 2006. Pituitary adenylate cyclase-activating polypeptide neurons of the ventromedial hypothalamus project to the midbrain central gray. Neuroreport 17, 221–224.

Massey, C.A., Iceman, K.E., Johansen, S.L., Wu, Y., Harris, M.B., Richerson, G.B., 2015. Isoflurane abolishes spontaneous firing of serotonin neurons and masks their pH/CO2 chemosensitivity. J. Neurophysiol. 113, 2879–2888.

Massey, C.A., Sowers, L.P., Dlouhy, B.J., Richerson, G.B., 2014. Mechanisms of sudden unexpected death in epilepsy: The pathway to prevention. Nat. Rev. Neurol. 10, 271–282.

Metcalf, C.S., Radwanski, P.B., Bealer, S.L., 2009. Status epilepticus produces chronic alterations in cardiac sympathovagal balance. Epilepsia 50, 747–754.

Minson, J., Pilowsky, P., Llewellyn-Smith, I., Kaneko, T., Kapoor, V., Chalmers, J., 1991. Glutamate in spinally projecting neurons of the rostral ventral medulla. Brain Res. 555, 326–331.

Mirrione, M.M., Konomos, D.K., Gravanis, I., Dewey, S.L., Aguzzi, A., Heppner, F.L., Tsirka, S.E., 2010. Microglial ablation and lipopolysaccharide preconditioning affects pilocarpine-induced seizures in mice. Neurobiol. Dis. 39, 85–97.

Miyata, A., Arimura, A., Dahl, R.R., Minamino, N., Uehara, A., Jiang, L., Culler, M.D., Coy, D.H., 1989. Isolation of a novel 38 residue-hypothalamic polypeptide which stimulates adenylate cyclase in pituitary cells. Biochem. Bioph. Res. Commun. 164, 567–574.

Miyawaki, T., Goodchild, A.K., Pilowsky, P.M., 2002a. Activation of mu-opioid receptors in rat ventrolateral medulla selectively blocks baroreceptor reflexes while activation of delta opioid receptors blocks somato-sympathetic reflexes. Neuroscience 109, 133–144.

Miyawaki, T., Goodchild, A.K., Pilowsky, P.M., 2002b. Evidence for a tonic GABA-ergic inhibition of excitatory respiratory-related afferents to presympathetic neurons in the rostral ventrolateral medulla. Brain Res. 924, 56–62.

Miyawaki, T., Minson, J., Arnolda, L., Chalmers, J., Llewellyn-Smith, I., Pilowsky, P., 1996a. Role of excitatory amino acid receptors in cardiorespiratory coupling in ventrolateral medulla. Am. J. Physiol-Regul. I 271, 1221–1230.

Miyawaki, T., Minson, J., Arnolda, L., Llewellyn-Smith, I., Chalmers, J., Pilowsky, P., 1996b. AMPA/kainate receptors mediate sympathetic chemoreceptor reflex in the rostral ventrolateral medulla. Brain Res. 726, 64–68.

Miyawaki, T., Suzuki, S., Minson, J., Arnolda, L., Chalmers, J., Llewellyn-Smith, I., Pilowsky, P., 1997. Role of AMPA/kainate receptors in transmission of the sympathetic baroreflex in rat CVLM. Am. J. Physiol-Regul. I 272, 800–812.

Moraes, D.J.A., Bonagamba, L.G.H., Costa, K.M., Costa-Silva, J.H., Zoccal, D.B., Machado, B.H., 2014. Short-term sustained hypoxia induces changes in the coupling of sympathetic and respiratory activities in rats. J. Physiol. 592, 2013–2033.

Moseley, B.D., Wirrell, E.C., Nickels, K., Johnson, J.N., Ackerman, M.J., Britton, J., 2011. Electrocardiographic and oximetric changes during partial complex and generalized seizures. Epilepsy Res. 95, 237–245.

Mueller, S.G., Bateman, L.M., Laxer, K.D., 2014. Evidence for brainstem network disruption in temporal lobe epilepsy and sudden unexplained death in epilepsy. Neuroimage Clin. 5, 208–216.

Mutolo, D., Bongianni, F., Nardone, F., Pantaleo, T., 2005. Respiratory responses evoked by blockades of ionotropic glutamate receptors within the Bötzinger complex and the pre-Bötzinger complex of the rabbit. Eur. J. Neurosci. 21, 122–134.

Naggar, I., Lazar, J., Kamran, H., Orman, R., Stewart, M., 2014. Relation of autonomic and cardiac abnormalities to ventricular fibrillation in a rat model of epilepsy. Epilepsy Res. 108, 44–56.

Nashef, L., 1997. Sudden unexpected death in epilepsy: terminology and definitions. Epilepsia 38, S6–S8.

Nedoboy, P.E., Mohammed, S., Kapoor, K., Bhandare, A.M., Farnham, M.M.J., Pilowsky, P.M., 2016. pSer40 tyrosine hydroxylase immunohistochemistry identifies the anatomical location of C1 neurons in rat RVLM that are activated by hypotension. Neuroscience 317, 162–172, http://dx.doi.org/10.1016/j.neuroscience.2016.01.012.

Nei, M., Ho, R.T., Sperling, M.R., 2000. EKG abnormalities during partial seizures in refractory epilepsy. Epilepsia 41, 542–548.

Nomura, M., Ueta, Y., Hannibal, J., Serino, R., Yamamoto, Y., Shibuya, I., Matsumoto, T., Yamashita, H., 2000. Induction of pituitary adenylate cyclase-activating polypeptide mRNA in the medial parvocellular part of the paraventricular nucleus of rats following kainic-acid-induced seizure. Neuroendocrinology 71, 318–326.

Nunan, R., Sivasathiaseelan, H., Khan, D., Zaben, M., Gray, W., 2014. Microglial VPAC1R mediates a novel mechanism of neuroimmune-modulation of hippocampal precursor cells via IL-4 release. Glia 62, 1313–1327.

Opherk, C., Coromilas, J., Hirsch, L.J., 2002. Heart rate and EKG changes in 102 seizures: Analysis of influencing factors. Epilepsy Res. 52, 117–127.

Persson, M., Brantefjord, M., Liljeqvist, J.Å., Bergström, T., Hansson, E., Rönnbäck, L., 2007. Microglial GLT-1 is upregulated in response to herpes simplex virus infection to provide an antiviral defence via glutathione. Glia 55, 1449–1458.

Pilowsky, P., Sun, Q.J., Llewellyn-Smith, I., Arnolda, L., Chalmers, J., Minson, J., 1997. Phosphate-activated glutaminase immunoreactivity in brainstem respiratory neurons. J. Auton. Nerv. Syst. 63, 85–90.

Pilowsky, P.M., Lung, M.S.Y., Spirovski, D., McMullan, S., 2009. Differential regulation of the central neural cardiorespiratory system by metabotropic neurotransmitters. Philos. T Roy Soc. B 364, 2537–2552.

Pocock, J.M., Kettenmann, H., 2007. Neurotransmitter receptors on microglia. Trends Neurosci. 30, 527–535.

Ponnusamy, A., Marques, J.L.B., Reuber, M., 2012. Comparison of heart rate variability parameters during complex partial seizures and psychogenic nonepileptic seizures. Epilepsia 53, 1314–1321.

Powell, K.L., Jones, N.C., Kennard, J.T., Ng, C., Urmaliya, V., Lau, S., Tran, A., Zheng, T., Ozturk, E., Dezsi, G., Megatia, I., Delbridge, L.M., Pinault, D., Reid, C.A., White, P.J., O'Brien, T.J., 2014. HCN channelopathy and cardiac electrophysiologic dysfunction in genetic and acquired rat epilepsy models. Epilepsia 55, 609–620.

Przywara, D.A., Kulkarni, J.S., Wakade, T.D., Leontiev, D.V., Wakade, A.R., 1998. Pituitary adenylyl cyclase-activating polypeptide and nerve growth factor use the proteasome to rescue nerve growth factor-deprived sympathetic neurons cultured from chick embryos. J. Neurochem. 71, 1889–1897.

Pyner, S., Coote, J.H., 1999. Identification of an efferent projection from the paraventricular nucleus of the hypothalamus terminating close to spinally projecting rostral ventrolateral medullary neurons. Neuroscience 88, 949–957.

Pyner, S., Coote, J.H., 2000. Identification of branching paraventricular neurons of the hypothalamus that project to the rostroventrolateral medulla and spinal cord. Neuroscience 100, 549–556.

Rahman, A.A., Shahid, I.Z., Pilowsky, P.M., 2011. Intrathecal neuromedin U induces biphasic effects on sympathetic vasomotor tone, increases respiratory drive and attenuates sympathetic reflexes in rat. Brit. J. Pharmacol. 164, 617–631.

Ross, C., Ruggiero, D., Park, D., Joh, T., Sved, A., Fernandez-Pardal, J., Saavedra, J., Reis, D., 1984a. Tonic vasomotor control by the rostral ventrolateral medulla: effect of electrical or chemical stimulation of the area containing C1 adrenaline neurons on arterial pressure, heart rate, and plasma catecholamines and vasopressin. J. Neurosci. 4, 474–494.

Ross, C.A., Ruggiero, D.A., Joh, T.H., Park, D.H., Reis, D.J., 1984b. Rostral ventrolateral medulla: Selective projections to the thoracic autonomic cell column from the region containing C1 adrenaline neurons. J. Comp. Neurol. 228, 168–185.

Sakamoto, K., Saito, T., Orman, R., Koizumi, K., Lazar, J., Salciccioli, L., Stewart, M., 2008. Autonomic consequences of kainic acid-induced limbic cortical seizures in rats: peripheral autonomic nerve activity, acute cardiovascular changes, and death. Epilepsia 49, 982–996.

Seyal, M., Bateman, L.M., Albertson, T.E., Lin, T.C., Li, C.S., 2010. Respiratory changes with seizures in localization-related epilepsy: analysis of periictal hypercapnia and airflow patterns. Epilepsia 51, 1359–1364.

Shafton, A.D., Ryan, A., Badoer, E., 1998. Neurons in the hypothalamic paraventricular nucleus send collaterals to the spinal cord and to the rostral ventrolateral medulla in the rat. Brain Res. 801, 239–243.

Shahid, I.Z., Rahman, A.A., Pilowsky, P.M., 2011. Intrathecal orexin A increases sympathetic outflow and respiratory drive, enhances baroreflex sensitivity and blocks the somato-sympathetic reflex. Brit. J. Pharmacol. 162, 961–973.

Shapiro, L.A., Wang, L., Ribak, C.E., 2008. Rapid astrocyte and microglial activation following pilocarpine-induced seizures in rats. Epilepsia 49, 33–41.

Shioda, S., Ozawa, H., Dohi, K., Mizushima, H., Matsumoto, K., Nakajo, S., Takaki, A., Zhou, C.J., Nakai, Y., Arimura, A., 1998. PACAP protects hippocampal neurons against apoptosis: Involvement of JNK/SAPK signaling pathway. Ann. NY Acad. Sci. 865, 111–117.

Shoge, K., Mishima, H.K., Saitoh, T., Ishihara, K., Tamura, Y., Shiomi, H., Sasa, M., 1999. Attenuation by PACAP of glutamate-induced neurotoxicity in cultured retinal neurons. Brain Res. 839, 66–73.

Silveira, D.C., Schachter, S.C., Schomer, D.L., Holmes, G.L., 2000. Flurothyl-induced seizures in rats activate Fos in brainstem catecholaminergic neurons. Epilepsy Res. 39, 1–12.

Skoglösa, Y., Lewén, A., Takei, N., Hillered, L., Lindholm, D., 1999a. Regulation of pituitary adenylate cyclase activating polypeptide and its receptor type 1 after traumatic brain injury: Comparison with brain-derived neurotrophic factor and the induction of neuronal cell death. Neuroscience 90, 235–247.

Skoglösa, Y., Takei, N., Lindholm, D., 1999b. Distribution of pituitary adenylate cyclase activating polypeptide mRNA in the developing rat brain. Mol. Brain Res. 65, 1–13.

Stornetta, R.L., Sevigny, C.P., Guyenet, P.G., 2002a. Vesicular glutamate transporter DNPI/VGLUT2 mRNA is present in C1 and several other groups of brainstem catecholaminergic neurons. J. Comp. Neurol. 444, 191–206.

Stornetta, R.L., Sevigny, C.P., Schreihofer, A.M., Rosin, D.L., Guyenet, P.G., 2002b. Vesicular glutamate transporter DNPI/VGLUT2 is expressed by both C1 adrenergic and nonaminergic presympathetic vasomotor neurons of the rat medulla. J. Comp. Neurol. 444, 207–220.

Suk, K., Park, J.-H., Lee, W.-H., 2004. Neuropeptide PACAP inhibits hypoxic activation of brain microglia: a protective mechanism against microglial neurotoxicity in ischemia. Brain Res. 1026, 151–156.

Suzuki, T., Takayama, K., Miura, M., 1997. Distribution and projection of the medullary cardiovascular control neurons containing glutamate, glutamic acid decarboxylase, tyrosine hydroxylase and phenylethanolamine N-methyltransferase in rats. Neurosci Res. 27, 9–19.

Swanson, R.A., Liu, J., Miller, J.W., Rothstein, J.D., Farrell, K., Stein, B.A., Longuemare, M.C., 1997. Neuronal regulation of glutamate transporter subtype expression in astrocytes. J. Neurosci. 17, 932–940.

Takei, N., Skoglösa, Y., Lindholm, D., 1998. Neurotrophic and neuroprotective effects of pituitary adenylate cyclase- activating polypeptide (PACAP) on mesencephalic dopaminergic neurons. J. Neurosci. Res. 54, 698–706.

ter Horst, G.J., Luiten, P.G.M., Kuipers, F., 1984. Descending pathways from hypothalamus to dorsal motor vagus and ambiguus nuclei in the rat. J. Autonom. Nerv. Syst. 11, 59–75.

Thom, M., 2004. Neuropathological findings in epilepsy. Curr. Diagn. Pathol. 10, 93–105.

Tsai, C.-Y., Chan, J.Y.H., Hsu K.-s. Chang, A.Y.W., Chan, S.H.H., 2012. Brain-derived neurotrophic factor ameliorates brain stem cardiovascular dysregulation during experimental temporal lobe status epilepticus. PLoS One 7, e33527.

Tupal, S., Faingold, C.L., 2006. Evidence supporting a role of serotonin in modulation of sudden death induced by seizures in DBA/2 mice. Epilepsia 47, 21–26.

Turrin, N.P., Rivest, S., 2006. Tumor necrosis factor α but not interleukin 1β mediates neuroprotection in response to acute nitric oxide excitotoxicity. J. Neurosci. 26, 143–151.

Ueda, Y., Doi, T., Tokumaru, J., Yokoyama, H., Nakajima, A., Mitsuyama, Y., Ohya-Nishiguchi, H., Kamada, H., James Willmore, L., 2001. Collapse of extracellular glutamate regulation during epileptogenesis: Down-regulation and functional failure of glutamate transporter function in rats with chronic seizures induced by kainic acid. J. Neurochem. 76, 892–900.

Vargas, D.L., Nascimbene, C., Krishnan, C., Zimmerman, A.W., Pardo, C.A., 2005. Neuroglial activation and neuroinflammation in the brain of patients with autism. Ann. Neurol. 57, 67–81.

Vaudry, D., Gonzalez, B.J., Basille, M., Anouar, Y., Fournier, A., Vaudry, H., 1998. Pituitary adenylate cyclase-activating polypeptide stimulates both c- fos gene expression and cell survival in rat cerebellar granule neurons through activation of the protein kinase A pathway. Neuroscience 84, 801–812.

Venit, E.L., Shepard, B.D., Seyfried, T.N., 2004. Oxygenation prevents sudden death in seizure-prone mice. Epilepsia 45, 993–996.

Vinet, J., van Weering, H.R.J., Heinrich, A., Kälin, R.E., Wegner, A., Brouwer, N., Heppner, F.L., van Rooijen, N., Boddeke, H.W.G.M., Biber, K., 2012. Neuroprotective function for ramified microglia in hippocampal excitotoxicity. J. Neuroinflamm. 9, 27.

Wada, Y., Nakamachi, T., Endo, K., Seki, T., Ohtaki, H., Tsuchikawa, D., Hori, M., Tsuchida, M., Yoshikawa, A., Matkovits, A., Kagami, N., Imai, N., Fujisaka, S.,

Usui, I., Tobe, K., Koide, R., Takahashi, H., Shioda, S., 2013. PACAP attenuates NMDA-induced retinal damage in association with modulation of the microglia/macrophage status into an acquired deactivation subtype. J. Mol. Neurosci. 51, 493–502.

Wake, H., Moorhouse, A.J., Jinno, S., Kohsaka, S., Nabekura, J., 2009. Resting microglia directly monitor the functional state of synapses in vivo and determine the fate of ischemic terminals. J. Neurosci. 29, 3974–3980.

Wang, L., Meng, X., Yuchi, Z., Zhao, Z., Xu, D., Fedida, D., Wang, Z., Huang, C., 2015. De novo mutation in the SCN5A gene associated with brugada syndrome. Cell Physiol. Biochem. 36, 2250–2262.

Wenker, I.C., Kréneisz, O., Nishiyama, A., Mulkey, D.K., 2010. Astrocytes in the retrotrapezoid nucleus sense H+ by inhibition of a Kir4.1-Kir5.1-like current and may contribute to chemoreception by a purinergic mechanism. J. Neurophysiol. 104, 3042–3052.

Westerhaus, M.J., Loewy, A.D., 2001. Central representation of the sympathetic nervous system in the cerebral cortex. Brain Res. 903, 117–127.

WHO, 2005 Atlas: Epilepsy Care in the World Department of Mental Health and Substance Abuse, W.H.O. (Ed.), Geneva.

Young, D., 2010. Control of Cardiac Output. San Rafael: Morgan & Claypool Life Sciences. San Rafael.

Zhang, Y.Z., Hannibal, J., Zhao, Q., Moller, K., Danielsen, N., Fahrenkrug, J., Sundler, F., 1996. Pituitary adenylate cyclase activating peptide expression in the rat dorsal root ganglia: Up-regulation after peripheral nerve injury. Neuroscience 74, 1099–1110.

Zhuo, L., Zhang, Y., Zielke, H.R., Levine, B., Zhang, X., Chang, L., Fowler, D., Li, L., 2012. Sudden unexpected death in epilepsy: Evaluation of forensic autopsy cases. Forensic Sci. Int. 223, 171–175.

Systems/Circuits

Antagonism of PACAP or Microglia Function Worsens the Cardiovascular Consequences of Kainic-Acid-Induced Seizures in Rats

Amol M. Bhandare,[1,2] Suja Mohammed,[2] Paul M. Pilowsky,[2,3] and Melissa M.J. Farnham[1,2]

[1]Australian School of Advanced Medicine, Macquarie University, Sydney, 2109 New South Wales, Australia, [2]The Heart Research Institute, 2042 New South Wales, Australia, and [3]Department of Physiology, University of Sydney, Sydney, 2006 New South Wales, Australia

Seizures are accompanied by cardiovascular changes that are a major cause of sudden unexpected death in epilepsy (SUDEP). Seizures activate inflammatory responses in the cardiovascular nuclei of the medulla oblongata and increase neuronal excitability. Pituitary adenylate cyclase-activating polypeptide (PACAP) is a neuropeptide with autocrine and paracrine neuroprotective properties. Microglia are key players in inflammatory responses in the CNS. We sought to determine whether PACAP and microglia mitigate the adverse effects of seizure on cardiovascular function in a rat model of temporal lobe epilepsy. Kainic acid (KA)-induced seizures increased splanchnic sympathetic nerve activity by 97%, accompanied by increase in heart rate (HR) but not blood pressure (BP). Intrathecal infusion of the PACAP antagonist PACAP(6–38) or the microglia antagonists minocycline and doxycycline augmented sympathetic responses to KA-induced seizures. PACAP(6–38) caused a 161% increase, whereas minocycline and doxycycline caused a 225% and 215% increase, respectively. In intrathecal PACAP-antagonist-treated rats, both BP and HR increased, whereas after treatment with microglial antagonists, only BP was significantly increased compared with control. Our findings support the idea that PACAP and its action on microglia at the level of the spinal cord elicit cardioprotective effects during seizure. However, intrathecal PACAP did not show additive effects, suggesting that the agonist effect was at maximum. The protective effect of microglia may occur by adoption of an M2 phenotype and expression of factors such as TGF-β and IL-10 that promote neuronal quiescence. In summary, therapeutic interventions targeting PACAP and microglia could be a promising strategy for preventing SUDEP.

Key words: kainic acid; microglia; PACAP; seizure; SUDEP; sympathetic nerve activity

Introduction

Epileptic seizures are commonly accompanied by autonomic changes that include disturbances in blood pressure (BP), heart rate (HR), and heart rhythm (Wannamaker, 1985; Darbin et al., 2002; Müngen et al., 2010; Pansani et al., 2011). These cardiovascular changes may be dramatic and lead to "sudden unexpected death in epilepsy" (SUDEP), a syndrome that accounts for 5–17% of deaths in people with epilepsy (Sakamoto et al., 2008; Brotherstone et al., 2010; Tolstykh and Cavazos, 2013).

Pituitary adenylate cyclase-activating polypeptide (PACAP) is a 38 aa peptide that activates three receptors: PAC1R, VPAC1R, and VPAC2R. The canonical pathway in each case is activation of

adenylate cyclase, leading to two main effects on neurons. First, it is able to act as an excitatory neurotransmitter (Lai et al., 1997; Farnham et al., 2008; Farnham et al., 2011; Farnham et al., 2012) and, second, as a neuroprotective and anti-inflammatory agent by inhibiting the activation of mitogen activated protein kinase (MAPK) family and by stimulating secretion of IL-6 (Shioda et al., 1998). During seizures, there is an upregulation of MAPK in hippocampus and, in patients who are recovering from tonic-clonic seizure, IL-6 is elevated in CSF (Peltola et al., 2000). Conversely, IL-6 knock-out mice are more susceptible to seizure-induced hippocampal damage (Penkowa et al., 2001), suggesting that IL-6 is neuroprotective. Nomura et al. (2000) showed that PACAP gene expression increases in the paraventricular nucleus of the hypothalamus after KA-induced temporal lobe epilepsy in rats. Based on these findings, we hypothesized that PACAP itself or its action on activated microglia has neuroprotective effects that inhibit seizure-induced neuronal excitation and protect against the adverse autonomic effects of seizure. Activated microglia are associated with neurodegeneration both in patients and animal models of temporal lobe epilepsy (Mirrione et al., 2010; Ahmadi et al., 2013); however, their action as either neurotoxic or neuroprotective in brainstem and spinal cord cardiovascular nuclei remains unclear. A number of recent studies suggest that microglia may acquire the neuroprotective

M2 phenotype, and increase endogenous production of TGF-β and IL-10 (Li et al., 2007; Mosser and Edwards, 2008; Neumann et al., 2008; Loane and Byrnes, 2010; Vinet et al., 2012). These findings led to our second hypothesis that microglia in cardiovascular nuclei may be neuroprotective and provide a defense mechanism by attenuating sympathoexcitatory cardiovascular responses during seizure.

This study therefore aimed to investigate the role of PACAP and microglia in seizure-induced cardiovascular responses. Specifically, the aims of this study were to determine the effect of intrathecal administration of PACAP and the PACAP antagonist PACAP(6–38) and the microglia antagonists minocycline and doxycycline on seizure-induced cardiovascular responses. We used *in vivo* physiological and pharmacological approaches in anesthetized rats using the KA-induced seizure model (Sakamoto et al., 2008).

Materials and Methods

Animals. All procedures and protocols were approved by the Animal Care and Ethics Committee of Macquarie University and the Sydney Local Health District. All experiments were conducted on adult male Sprague Dawley (SD) rats (250–350 g; Animal Resources Centre, Perth, Australia) in accordance with the Australian code of practice for the care and use of animals for scientific purposes.

Surgical preparation. Rats ($n = 64$) were anesthetized with 10% urethane (ethyl carbamate; 1.3–1.5 g/kg, i.p.; Sigma-Aldrich). The depth of anesthesia was monitored by observing reflex responses (withdrawal or pressor >10 mmHg) to nociceptive stimuli (periodic tail/paw pinches). Additional anesthetic was injected (30–40 mg, 10% urethane i.v.), if reflex responses were observed. Atropine sulfate (100 μg/kg, i.p.; Pfizer) was administered with the first dose of urethane to prevent bronchial secretions. After the completion of the general surgical procedures described below, rats were secured in a stereotaxic frame with their abdomen resting on a heating blanket (TC-1000; CWE). Core body temperature was monitored with a rectal thermometer and maintained between 36.5 and 37.5°C throughout the experiment.

General surgical procedures. The right carotid artery and jugular vein were cannulated with polyethylene tubing [internal diameter (I.D.) = 0.50 mm; outer diameter (O.D.) = 0.90 mm; Microtube Extrusions] for recording of blood pressure, and for administration of drugs and fluids, respectively. A tracheostomy enabled mechanical ventilation (rodent ventilator; UGO Basile Biological Research Apparatus) and recording of expired CO_2 (Capstar 100 CO_2 analyzer; CWE). Electrocardiogram (ECG) was recorded from leads connected to the forepaws of the rat and HR was derived from it. Rats were vagotomized, artificially ventilated with oxygen-enriched room air, and paralyzed with pancuronium bromide (0.4 mg given as a 0.2 ml bolus i.v. injection, followed by an infusion of 10% pancuronium in 0.9% saline at a rate of 2 ml/h; AstraZeneca). Arterial blood gases were analyzed with an electrolyte and blood gas analyzer (Vetstat; IDEXX). $PaCO_2$ was maintained at 40.0 $\pm$ 2 and pH between 7.35 and 7.45. The left greater splanchnic sympathetic nerve at a site proximal to the celiac ganglion and the left phrenic nerves were isolated, dissected, and tied with 5/0 silk thread. Nerve activity was recorded using bipolar stainless steel electrodes. Signals were amplified (BMA-931 Bioamplifiers; CWE; sampling rate: 6 kHz, gain: 2000, filtering: 30–3000 Hz) and filtered with a 50/60 Hz line frequency filter (Humbug; Quest Scientific).

Intrathecal catheter placement. The atlanto-occipital junction was exposed and a catheter (polyethylene tubing, O.D. = 0.50 mm; I.D. = 0.20 mm; Microtube Extrusions) with a dead space of ~6 μl was inserted into the intrathecal space of all rats through a slit in the dura and advanced caudally to the level of T5/6.

Electroencephalogram electrode placement. For the placement of electroencephalogram (EEG) electrodes, the scalp over the dorsal surface of the skull was incised, the skin retracted, and the periosteum scraped from the skull surface. Burr holes were drilled bilaterally for recording over the dorsal hippocampus (5.2 mm anterior to lambda, 3 mm lateral to mid-

line, and 2–3 mm below the skull surface) and electrode positions were confirmed with cresyl violet staining. A single electrode wire was inserted into each hole using stereotaxic manipulator. Electrodes were 75 μm Teflon-insulated stainless steel wires (A-M Systems). Signals were amplified (BMA-931 Bioamplifier; CWE), band-pass filtered from 1 Hz to 10 kHz, amplified 100×, and digitized at 6 kHz (see data acquisition below).

Seizure induction. Intraperitoneal injection of KA was used to generate a seizure/KA dose–response curve in SD rats (Figs. 1, 2). Responses were recorded for at least 2 h after KA injection, during which continuous monitoring of EEG was used to identify the development of seizures. To determine the presence or absence of seizure, the amplitude of the AUC of the EEG before and after KA administration was measured. A seizure was considered to have occurred if the AUC increased by at least 50%. In vehicle-treated rats, no change occurred. The log-transformed values of percent change in AUC at 60 and 120 min after injection relative to the AUC before injection in different groups are shown in the Results.

From the dose–response study, we found that 2 mg/kg KA was sufficient to induce seizure and a significant increase in splanchnic sympathetic nerve activity (Figs. 1, 2) and was used for the rest of the study. At the conclusion of the experiments, rats were either killed with 0.5 ml of 3 M potassium chloride (KCl, i.v.) or deeply anesthetized and perfused with 400 ml of ice-cold 0.9% saline followed by 400 ml of 4% paraformaldehyde solution. The brains were removed from the perfused rats and postfixed in the same fixative overnight. Brains were sectioned coronally (100 μm) and stained with cresyl violet for histological verification of the electrode positions.

Intrathecal drug administration protocol. In all dose–response studies, a control injection of 10 μl of 10 mmol/L PBS was washed in with 6 μl PBS 10 min before the intraperitoneal injection of KA. The same intrathecal PBS infusion protocol was followed for the vehicle control group of rats 10 min before intraperitoneal PBS injection.

The dose of PACAP-38 and the antagonist PACAP(6–38) (Auspep) for intrathecal infusion was selected from our previous study (Farnham et al., 2011). Ten microliters of 1 mmol/L PACAP(6–38) or 300 μmol/L PACAP was administered intrathecally and flushed in with 6 μl of PBS. Doses determined from a previous study (Hua et al., 2005) for minocycline (100 μg/10 μl) or doxycycline (100 μg/10 μl) were administered intrathecally and flushed in with 6 μl of PBS. In all groups of rats, intrathecal infusion was made 10 min before intraperitoneal KA or PBS injection. All infusions were made over a 10–15 s period, as described previously (Farnham et al., 2008). At the conclusion of experiments, the rats were killed as described above. Postmortem verification of the position of catheter tip was performed by exposing the spinal cord and checking its position with respect to the vertebra.

Data acquisition and analysis. Data were acquired using an ADC system (CED 1401; Cambridge Electronic Design) and Spike 2 acquisition and analysis software (version 8.01; Cambridge Electronic Design). The EEG activity raw data were DC removed. The amplitude of EEG activity (AUC) was analyzed in 5 min blocks taken 1 min before intrathecal infusion and 60 and 120 min after intraperitoneal injection of either KA or PBS. The percentage change in EEG AUC was calculated for each rat at 60 and 120 min after treatment compared with pretreatment area (taken as 100%) and grouped together. Phrenic nerve activity (PNA) was rectified and smoothed (τ 0.5 s). PNA was analyzed from 1 min blocks taken 1 min before intrathecal infusion and 60 and 120 min after intraperitoneal injection of either KA or PBS. The percent change in area under curve was analyzed at 60 and 120 min compared with pretreatment area (taken as 100%). SNA raw data were rectified and smoothed (τ 2 s) and normalized to zero by subtracting the residual activity 5–10 min after death. SNA was analyzed with a sigmoid curve-fit analysis method. A sigmoid curve was fitted to the processed SNA channel and the percentage low, percentage high, percentage range, and slope (%/s) were calculated (only percentage range is showed in graphs). Mean arterial pressure (MAP) and HR were analyzed from 1 min blocks taken 1 min before intrathecal infusion and the time at which it was peaked. End-tidal CO_2 and core temperature were analyzed from 1 min blocks taken 1 min before intrathecal infusion and intraperitoneal injection and 30, 60, 90, and 120 min after intraperitoneal injection of either KA or PBS. Arterial blood gas levels ($PaCO_2$ and pH) were measured 10 min before intrathe-
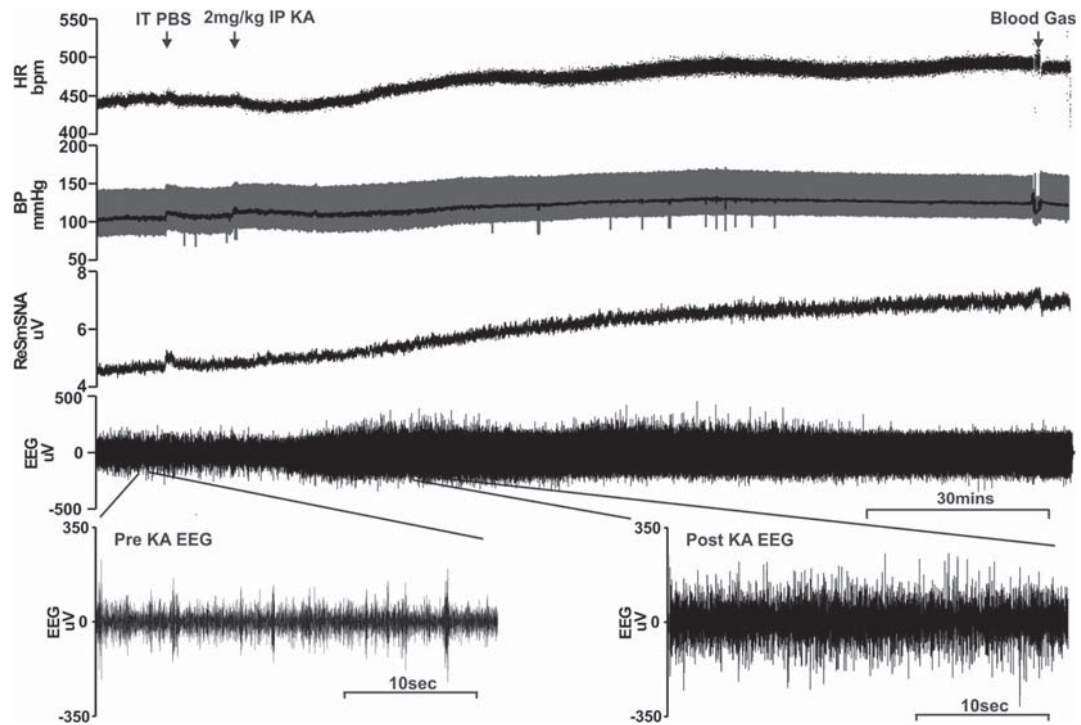
Figure 1. Effect of intrathecal (IT) PBS (10 μl) followed by 2 mg/kg intraperitoneal KA in an anesthetized rat (see Materials and Methods) on (from the top): HR (bpm), BP (mmHg), SNA (μV), and EEG (μV). Time of administration of IT PBS and intraperitoneal KA are marked with an arrow. Pre-KA EEG and post-KA EEG refer to the expanded periods as indicated.
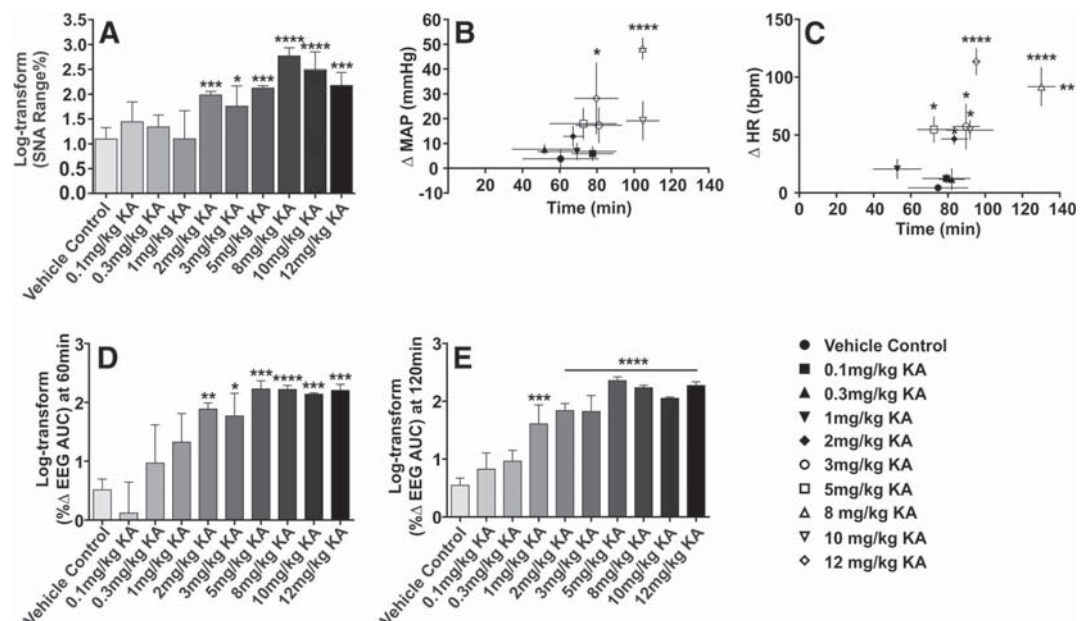
Figure 2. Dose–response curve for intraperitoneal KA. Change in SNA (log transform of percentage range) (**A**), maximum change in MAP (on y-axis) at respective time point after intraperitoneal PBS or KA injection (on x-axis) (**B**), maximum change in HR (on y-axis) at respective time point after intraperitoneal PBS or KA injection (on x-axis) (**C**) and log transform of percentage change in AUC of EEG activity at 60 min (**D**) and 120 min (**E**) after intraperitoneal PBS or KA injection, in PBS ($n = 5$) and 0.1 ($n = 3$), 0.3 ($n = 3$), 1 ($n = 3$), 2 ($n = 5$), 3 ($n = 3$), 5 ($n = 3$), 8 ($n = 3$), 10 ($n = 3$), and 12 ($n = 3$) mg/kg intraperitoneal KA-treated rats. Statistical significance was determined using one-way ANOVA followed by t tests and Dunnett's correction to compare effects with the control value. Data are expressed as mean $\pm$ SEM. ****$p \leq 0.0001$;***$p \leq 0.001$;**$p \leq 0.01$ and *$p \leq 0.05$ compared with vehicle control group.

cal infusion and 120 min after KA or PBS injections in all animals. Log transformation was applied to EEG and SNA raw values where necessary if variances were not normally distributed or heterogeneous. Statistical analysis was performed in GraphPad Prism software (version 6.04).

Statistical significance was determined using one-way ANOVA followed by t tests with Dunnett's correction for dose–response studies and with the Holm–Sidak correction for the rest of the study. Multiple comparisons were done between groups. $p \leq 0.05$ was considered significant.
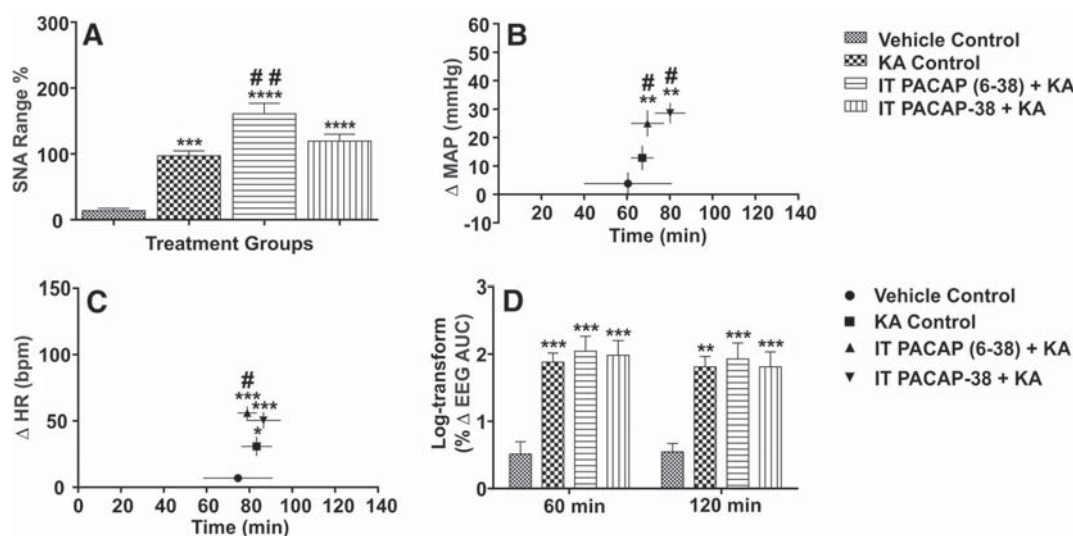
Figure 3. *In vivo* effects of intrathecal (IT) PACAP(6–38) and PACAP-38 in 2 mg/kg KA-induced seizure rats. Change in SNA (% range) (**A**), maximum change in MAP (on *y*-axis) at respective time point after intraperitoneal PBS or KA injection (on *x*-axis) (**B**), maximum change in HR (on *y*-axis) at respective time point after intraperitoneal PBS or KA injection (on *x*-axis) (**C**), and log transform of percentage change in AUC of EEG activity at 60 and 120 min after intraperitoneal PBS or KA injection (**D**) in different groups of rats after development of seizure. In all groups, $n = 5$. Statistical significance was determined using one-way ANOVA followed by *t* tests with a Holm–Sidak correction. Data are expressed as mean $\pm$ SEM. ****$p \leq 0.0001$; ***$p \leq 0.001$; **$p \leq 0.01$; *$p \leq 0.05$ compared with vehicle control group; ##$p \leq 0.01$ and #$p \leq 0.05$ compared with KA control group.

Calculation of corrected QT interval. Because the length of the QT interval can be affected by heart rate, corrected QT (QTc) interval was calculated by dividing the QT interval in seconds by the square root of the R-R interval in seconds (Bazett, 1920). The QTc was obtained in all rats before and after vehicle or KA injection.

Results

KA-induced seizures causes sympathoexcitation, tachycardia, and pressor responses

Intraperitoneal injection of KA in urethane anesthetized rats (Fig. 1) was used to determine the most effective dose for use in this study (Fig. 2). One-way ANOVA of peak EEG AUC responses revealed that the 2 mg/kg was the lowest dose of KA effective in significantly elevating EEG (120 min after KA: $64.0 \pm 17.7\%$; $p \leq 0.0001$; Fig. 2 *D*,*E*), SNA (% range: $97.2 \pm 7.4\%$; $p \leq 0.001$; Fig. 2*A*) and HR (ΔHR: 46.5 ± 4.8 bpm; $p \leq 0.05$; Fig. 2*C*). Therefore, a 2 mg/kg dose of KA was used in the rest of the study. SNA percentage low was same in all groups, whereas percentage high was significantly different in 2 mg/kg ($194.3 \pm 6.0\%$; $p \leq 0.05$) and in all higher doses of KA compared with vehicle-treated group. The change in MAP was significantly higher only in 8 (ΔMAP: 48.3 ± 4.5 mmHg; $p \leq 0.0001$) and 12 mg/kg (ΔMAP: 28.2 ± 14.6 mmHg; $p \leq 0.05$) doses of KA compared with vehicle control, whereas the change in HR was significantly different in 2 mg/kg and all higher doses of KA compared with vehicle control. There were no significant differences in PNA, expired CO_2, and rectal temperature in any of the groups studied (results not shown). Blood gas analysis revealed that blood $PaCO_2$ and pH were within normal physiological range in all animals ($PaCO_2$ was 40.0 ± 2 and pH between 7.35 and 7.45). There was no significant change in pretreatment and posttreatment blood $PaCO_2$ and pH levels (results not shown). A 2 mg/kg intraperitoneal injection of KA increased EEG amplitude beyond 50% of baseline and was classified as a seizure. The EEG seizure response was followed by an increase in SNA (Fig. 1). Importantly, SNA did not begin to increase before the first instance of seizure, eliminating the possibility of the increase in SNA being due to a peripheral effect of KA. The EEG activity started to increase at
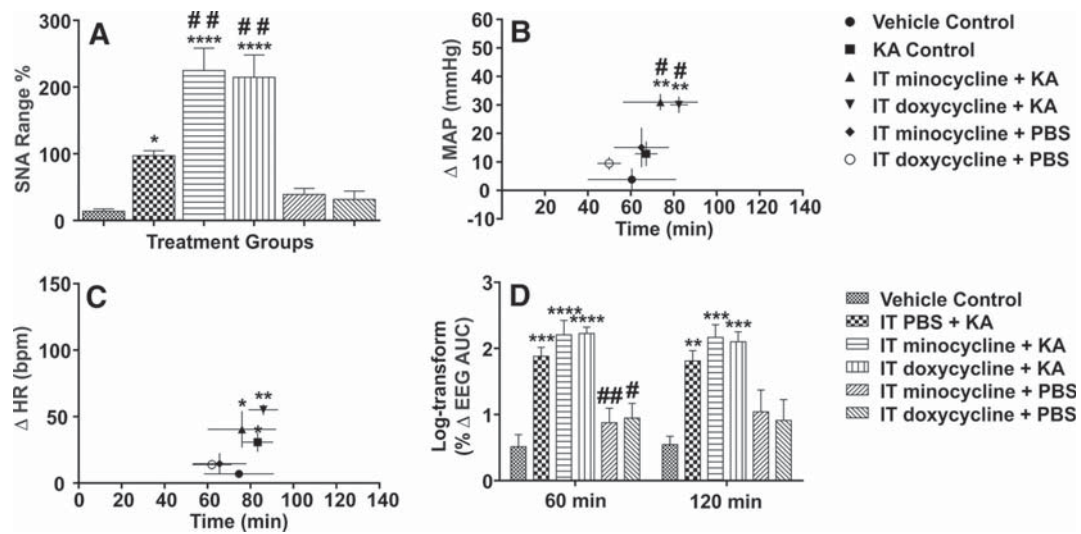
25.6 ± 3.6 min after KA injection, followed by SNA, MAP, and HR. SNA, EEG, and HR were significantly increased after KA injection compared with the vehicle-treated group.

Antagonism of PACAP exacerbates the cardiovascular effects of seizure

The PACAP antagonist PACAP(6–38) was administered intrathecally to test the hypothesis that PACAP has a neuroprotective and anti-inflammatory role in KA-induced seizure rats that might be responsible for attenuating the seizure-induced sympathoexcitation. The seizure-induced cardiovascular responses were significantly increased by infusing PACAP(6–38) 10 min before KA injection (Fig. 3*A*–*C*) compared with the KA control group (SNA high: $255.1 \pm 15.3\%$; $p \leq 0.01$, SNA range: $160.8 \pm 16.0\%$; $p \leq 0.01$, Fig. 3*A*; SNA slope: $0.043 \pm 0.0095\%/s$; $p \leq 0.01$, ΔMAP: 31.84 ± 3.5 mmHg; $p \leq 0.05$, Fig. 3*B*; and ΔHR: 56.1 ± 4.9 beats/min; $p \leq 0.05$, Fig. 3*C*). Intrathecal infusion of 300 μmol/L PACAP had no effect on the SNA increase in response to KA-induced seizure (Fig. 3*A*). Intrathecal PACAP agonist and antagonist treatment had no effect on EEG activity in seizure-induced rats compared with the KA control group (Fig. 3*D*).

Microglia antagonism worsens the cardiovascular dysfunction in seizure

The effect of blocking microglial activation on seizure-induced cardiovascular responses was evaluated at the spinal cord level. Intrathecal injection of the microglia antagonists minocycline and doxycycline in KA-induced seizure rats more than doubled the sympathoexcitatory and MAP responses, but did not affect HR. The microglia antagonists alone had no effect on measured cardiovascular parameters in vehicle-treated control rats (Fig. 4*A*–*C*). These results indicate that microglia have a neuroprotective or anti-inflammatory role during seizure. Intrathecal minocycline significantly increased sympathoexcitation in KA-induced seizure rats compared with the KA control group (SNA high: $314.1 \pm 33.4\%$; $p \leq 0.01$, SNA range: $224.8 \pm 33.6\%$;

Figure 4. *In vivo* effects of intrathecal (IT) minocycline and doxycycline in 2 mg/kg KA-induced seizure rats and vehicle control rats. Change in SNA (% range) (**A**), maximum change in MAP (on y-axis) at respective time point after intraperitoneal PBS or KA injection (on x-axis) (**B**), maximum change in HR (on y-axis) at respective time point after intraperitoneal PBS or KA injection (on x-axis) (**C**), and log transform of percentage change in AUC of EEG activity at 60 and 120 after intraperitoneal PBS or KA injection (**D**) in different groups of rats after development of seizure. In all groups, n = 5. Statistical significance was determined using one-way ANOVA followed by *t* tests with a Holm–Sidak correction. Data are expressed as mean ± SEM. ****$p \leq 0.0001$; ***$p \leq 0.001$; **$p \leq 0.01$; *$p \leq 0.05$ compared with vehicle control group; ##$p \leq 0.01$ and #$p \leq 0.05$ compared with KA control group.

$p \leq 0.01$, Fig. 4*A*; and SNA slope: 0.04 ± 0.006%/s; $p \leq 0.05$). A similar response was observed with intrathecal doxycycline, which augmented the sympathoexcitation in KA-induced seizure rats compared with the KA control group (SNA high: 313.2 ± 31.0%; $p \leq 0.01$, SNA range: 214.5 ± 33.6%; $p \leq 0.01$, Fig. 4*A*; and SNA slope: 0.05 ± 0.008%/s; $p \leq 0.01$). MAP was also significantly increased in both minocycline- and doxycycline-treated rats after KA treatment compared with the KA control group (ΔMAP: 31.0 ± 2.9 mmHg; $p \leq 0.05$ and 30.0 ± 2.9 mmHg; $p \leq 0.05$, respectively; Fig. 4*B*). There was no significant difference in the HR response between the intrathecal microglia antagonist treatment in the seizure-induced group and the KA control groups (Fig. 4*C*). Intrathecal minocycline and doxycycline treatment in the KA-induced seizure group had no effect on EEG activity compared with KA control (Fig. 4*D*).

Proarrhythmogenic changes in ECG after seizure
In vehicle-treated rats, changes in QTc interval (ΔQTc) duration between pretreatment intraperitoneal PBS injection and 120 min after injection was 2.5 ± 1.0 ms (Fig. 6). The ΔQTc interval was significantly increased in seizure-induced rats compared with vehicle control (13.1 ± 1.5 ms; $p \leq 0.001$; Fig. 6). Compared with the vehicle control group, the ΔQTc interval duration was significantly increased in the KA control, intrathecal PACAP-, PACAP (6–38)-, and doxycycline-treated groups, but not in the minocycline-treated group (also seen in Fig. 5). The QT interval was prolonged in KA control, PACAP (6–38)-, PACAP-, and doxycycline-treated rats compared with vehicle treatment (Fig. 5). PACAP antagonist treatment not only prolongs the QT interval, but also causes a clear ST segment elevation (Fig. 5*C*, arrows), both of which are prominent proarrhythmogenic changes (HR-triggered ECG was drawn pretreatment and posttreatment and shown in the right side corner of each graph; Fig. 5). Intrathecal minocycline treatment in the KA-treated group showed significant differences in ΔQTc interval compared with the KA control group ($p \leq 0.01$; Fig. 6).

Discussion
The main findings of the study are, first, that sympathetic nerve activity begins to rise several minutes after the start of a seizure. Second, we find that induction of seizure activity in the hippocampal EEG that follows intraperitoneal KA is associated with significant and dose-dependent increases in SNA, MAP, and HR and a prolongation of the QT interval. Third, in KA-induced seizure rats, intrathecal administration of the PACAP antagonist PACAP(6–38) exacerbates the cardiovascular responses, whereas intrathecal administration of PACAP has no beneficial effect. Fourth, intrathecal infusion of tetracycline-derived microglia antagonists exacerbates the cardiovascular responses after the induction of seizures. Overall, antagonism of PACAP or microglia tends to worsen the sympathoexcitatory effects of seizures.

Our work demonstrates that KA-induced seizure has a powerful effect on the cardiovascular system. It increases SNA, MAP, and HR; prolongs QTc; and, after PACAP antagonist, causes ST elevation. Together, these changes markedly increase the risk of arrhythmia. The present study revealed a neuroprotective role of endogenous PACAP that is antagonized by intrathecal infusion of PACAP(6–38) in KA-induced seizure rats. Therefore, PACAP attenuates KA seizure-induced sympathoexcitation. The failure to see a beneficial effect of PACAP agonist infusion may be due to an inadequate dose being provided. Alternatively, local neurons secreting PACAP may cause a maximal effect on local PACAP receptors so that additional intrathecal doses of PACAP provided exogenously have no effect. This creates the need for further study of the effect of PACAP during seizure on catecholaminergic and other bulbospinal sympathoexcitatory neurons in the rostral ventrolateral medulla (Schreihofer and Guyenet, 1997). It is possible that microinjection of low doses of exogenous PACAP in rostral ventrolateral medulla might provide an additional neuroprotective effect during seizure and inhibit the sympathoexcitation. Microglia are activated by increased phosphorylation of the MAPK pathway. PACAP act on microglia via membrane-
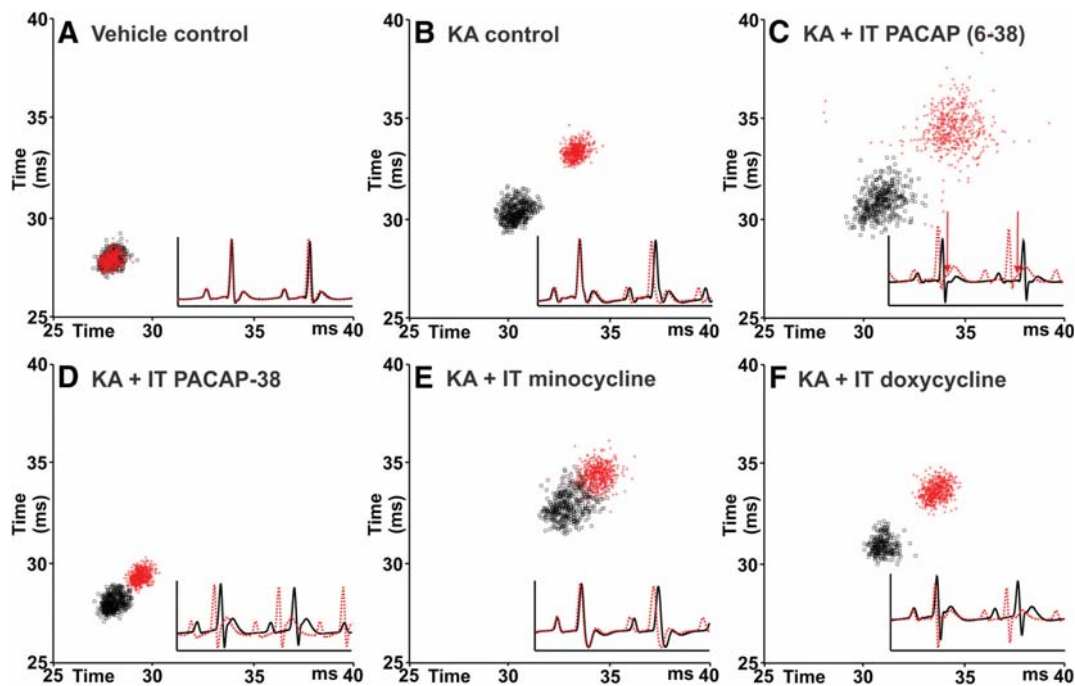
Figure 5. Representative Poincare plots illustrate the increase in QT interval after KA-induced seizures in individual rats (group data in Fig. 6). Black box symbols show pre-PBS and red plus symbols show 120 min post-PBS or KA intraperitoneal injection in the respective groups. *A*, Pre- (black) and 120 min post- (red) vehicle. *B*, Pre- (black) and 120 min post- (red) KA. *C*, Pre- (black) and 120 min post-KA with IT PACAP (6–38) (red). *D*, Pre- (black) and 120 min post-KA with IT PACAP-38 (red). *E*, Pre- (black) and 120 min post-KA with intrathecal (IT) minocycline (red). *F*, Pre- (black) and 120 min post-KA with IT doxycycline (red). Scale bar in milliseconds. HR-triggered ECG was drawn pre- and posttreatment and is shown in the right corner of each box (continuous black and dotted red lines represent pretreatment and posttreatment ECG). ST segment elevation is shown with an arrow (*C*).
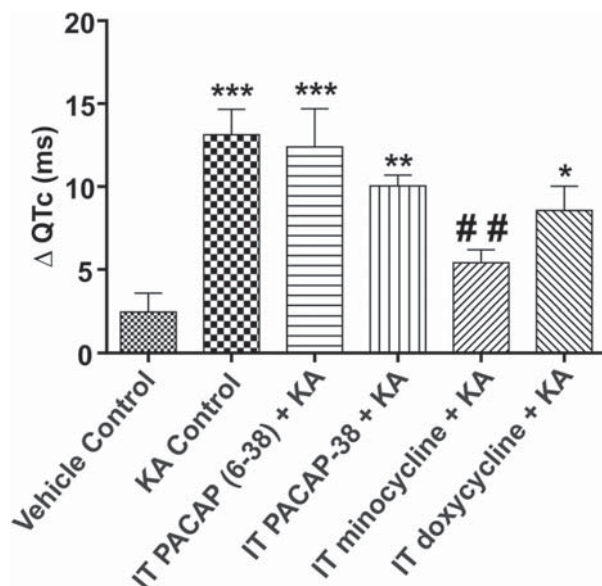
Figure 6. Group data showing increase in QTc interval 120 min after intraperitoneal injection of KA or PBS in the different groups of rats (see also Fig. 5). IT, Intrathecal. Statistical significance was determined using one-way ANOVA followed by *t* tests with a Holm–Sidak correction. Data are expressed as mean ± SEM. ****$p \leq 0.0001$; ***$p \leq 0.001$; **$p \leq 0.01$; *$p \leq 0.05$ compared with vehicle control group; ##$p \leq 0.01$ compared with the KA control group.

associated VPAC1 (PACAP) receptors, causing the release of substances such as IL-10 or TGF-β, compounds that protect neurons from overexcitation (Fig. 7). The finding that an increase in sympathetic activity after PACAP antagonism with PACAP(6–38) or

of microglial antagonism (doxycycline and minocycline) suggests that, in this model of epilepsy, there is strong activation of a neuroprotective PACAP and microglial pathway. The physiological effect of PACAP on microglia may act to dampen the sympathoexcitatory effects of seizure, an idea that is strengthened by the finding that tetracycline drugs had no effect in vehicle-treated animals.

To investigate the role of sympathoexcitation in acute seizure, we used a urethane-anesthetized, KA-induced model of seizure in rat. A single injection of KA in the range of 6–15 mg/kg, leads to a syndrome of recurrent status epilepticus, with each seizure lasting 30 min or longer over a prolonged period in conscious rats (Lévesque and Avoli, 2013). At these doses, it is well known that seizure activity causes autonomic dysfunction with acute cardiovascular changes (Sakamoto et al., 2008; Hotta et al., 2009). Here, we aimed to determine the lowest dose of KA that elicited seizure and sympathoexcitation. It is possible that this sympathoexcitation might be responsible for progressive deterioration of cardiovascular function in susceptible individuals and ultimately SUDEP. Several studies in human subjects during electroconvulsive therapy (ECT) reported changes in ECG that are proarrhythmogenic or ischemic. Because patients having seizures during ECT are under general anesthetic and neuromuscular blockade (Mokriski et al., 1992; Luckhaus et al., 2008), it is likely that any autonomic features would be blunted. Nevertheless, the finding that changes do occur suggests that seizures occurring during daily life would exhibit worse changes in ECG.

We aimed to elucidate PACAP-dependent differences in seizure-induced sympathoexcitation and a neuroprotective role of PACAP. PACAP exerts its autocrine neuroprotective (Shioda et al., 1998; Reglodi et al., 2000) and paracrine anti-inflammatory (Shioda et al., 2006; Ringer et al., 2013) effects in two ways.
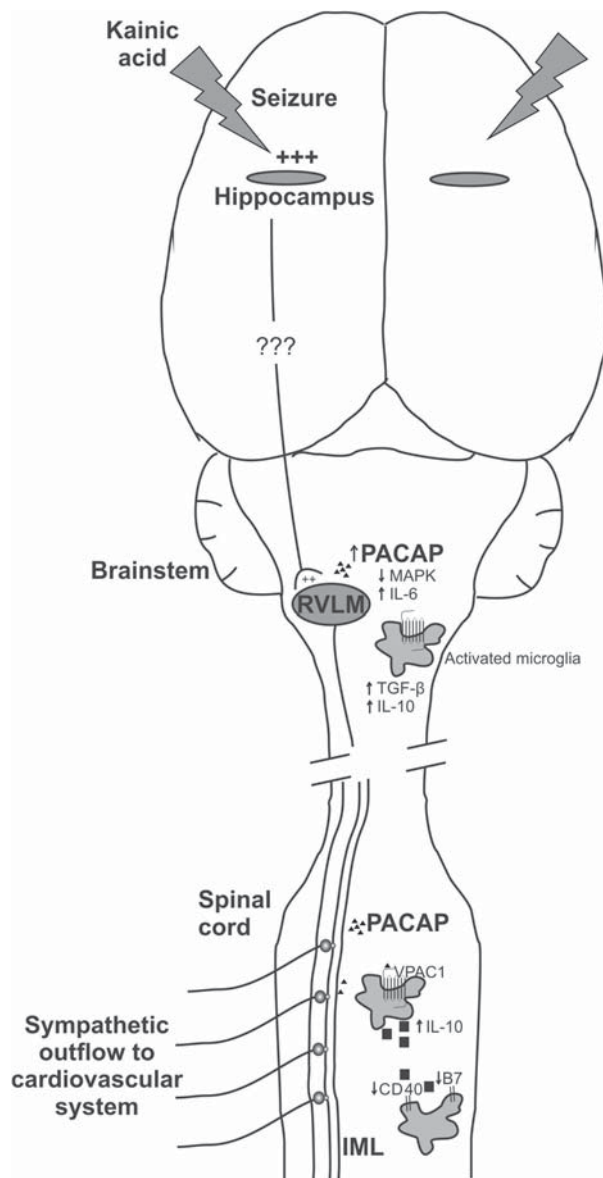
Figure 7. A proposed mechanism by which PACAP and microglia may have protective effects on sympathetic neurons in the brainstem and spinal cord during seizure. Seizure activates brainstem presympathetic neurons and changes cardiac and vascular reactivity. In seizure, microglia respond by changing from a quiescent surveillance state toward a more activated state. Activated microglia produce neurotropic and anti-apoptotic molecules, including TGF-β and IL-10. These molecules have protective effects on sympathetic neurons. Seizure increases the expression of PACAP, which inhibits the activation of MAPK and stimulates the secretion of IL-6 into the CSF. PACAP then acts on microglial VPAC1 receptors to cause increased IL-10 protein expression, followed by downregulation of the expression of the pro-inflammatory receptors CD10 and B7.

PACAP not only inhibits the activation of members of the MAPK family such as c-Jun N-terminal kinase (JNK) (Shioda et al., 1998), but also stimulates the secretion of IL-6 in CSF (Gottschall et al., 1994; Shioda et al., 1998). This effect may be the mechanism of action of PACAP in attenuating seizure-induced sympathoexcitation (Fig. 7). An increased activity of MAPKs in seizure (Jeon et al., 2000; Ferrer et al., 2002) is associated with cell death in several experimental paradigms (Chan et al., 2003; Sakon et al., 2003). Although there are controversies about the pro-

inflammatory and anti-inflammatory properties of IL-6, increased levels are reported to have neuroprotective effects on sympathetic neurons (März et al., 1998) and neuroprotective and anti-inflammatory effects in KA-induced seizure rats (Penkowa et al., 2001). Nomura et al. (2000) showed that PACAP gene expression increases in the paraventricular nucleus of the hypothalamus after KA-induced temporal lobe epilepsy in rats. Our findings suggest a mechanistic role for PACAP during epilepsy because blockade of PACAP activity during acute seizure has a detrimental effect on seizure-induced cardiovascular dysfunction. Microglia activated during seizure also express costimulatory molecules CD40 and B7 that may lead to further activation of microglia. PACAP, acting on microglial VPAC1 receptors (Delgado et al., 1999), increases IL-10 protein expression, causing a downregulation of CD40 and B7 mRNA expression in activated microglia, thereby acting as a potent anti-inflammatory agent (Delgado et al., 1999; Kim et al., 2002). We propose that this effect of PACAP is a likely mechanism of action for the responses observed in this study (Fig. 7).

Microglia are the innate immune cells of the CNS and represent ∼10% of the total brain cell population. Microglia can be either neuroprotective or neurodegenerative depending on circumstances (Mosser and Edwards, 2008; Loane and Byrnes, 2010; Benarroch, 2013; Biber et al., 2014). There is extensive microglial activation in animal models of seizure (Beach et al., 1995; Drage et al., 2002; Shapiro et al., 2008) and preconditioning of hippocampal microglia during the acute phase seizure results in a neuroprotective effect (Mirrione et al., 2010). Other studies report a neuroprotective role of microglia in different animal models of neurodegenerative diseases (Li et al., 2007; Lai and Todd, 2008; Mosser and Edwards, 2008; Neumann et al., 2008; Loane and Byrnes, 2010; Vinet et al., 2012; Benarroch, 2013; Biber et al., 2014) such as ischemic injury (Kitamura et al., 2004; Kitamura et al., 2005; Imai et al., 2007; Lalancette-Hébert et al., 2007) and chronic stress-induced depression (Kreisel et al., 2014). Until now, a role for microglia in seizure-induced cardiovascular responses was unclear. Our results demonstrate that inhibition of microglial activation and proliferation during KA-induced seizure worsens sympathoexcitation. The microglial antagonists minocycline and doxycycline act by inhibiting the p38 MAPK pathway. Current findings suggest a neuroprotective potential of activated microglial cells on sympathetic preganglionic neurons. This neuroprotective effect of microglia may occur through an endogenous production of neurotropic and anti-apoptotic molecules such as TGF-β and IL-10 (Benarroch, 2013) or by increased glutamate uptake (Persson and Rönnbäck, 2012). In this scenario, TGF-β- and IL-10-mediated activation of microglia into regulatory or M2 type has potent anti-inflammatory and neuroprotective potential.

Resident microglia actively survey their environment and are referred to as "surveilling microglia" (Nimmerjahn et al., 2005). Activated microglia dynamically change into two different phenotypes, M1 or M2, that are generally considered to be inflammatory and protective respectively depending on the type of stimulus and microenvironment, participating not only in mechanisms of injury, but also in neuroprotection, repair, and circuit refinement in the CNS (Mosser and Edwards, 2008). Our current findings suggest that acute seizure causes microglia to adopt the M2 phenotype and protect sympathetic neurons from excitotoxicity. The neuroprotective effect on sympathetic neurons may be due to microglial production of IL-10. Inhibiting microglial activation with intrathecal minocycline or doxycycline infusion in seizure-induced rats increased sympathoexcitation, leading to in-

creased HR and BP. Recent phase 3 clinical trials of minocycline in amyotrophic lateral sclerosis (ALS) patients showed that minocycline has a harmful effect on an ALS functional rating scale and greater mortality during the 9-month treatment phase compared with placebo treatment (Gordon et al., 2007). These findings are consistent with our current findings, which suggest that microglia antagonists worsen the effect of cardiovascular dysfunction during seizure. Overall, we propose that microglial activation during acute seizure has a neuroprotective effect due to adoption of the M2 phenotype or "protective" state. Microglial inactivation during acute seizure produces more neuroexcitation and cardiovascular dysfunction.

In conclusion, low doses of KA, which are adequate to produce seizures, lead to slowly developing, but prolonged and significant increases in SNA, MAP, HR, and EEG activity and a prolongation of the QTc interval. This type of severe disruption in central autonomic function may ultimately lead to progressive deterioration of cardiovascular function and SUDEP.

The clinical implications of our findings are that PACAP may exert a protective role against known adverse cardiovascular effects of seizure because antagonism of the PACAP receptor exacerbated the seizure-induced cardiovascular effects. PACAP may exert neuroprotective effects by preventing the activation of MAPKs and increasing levels of IL-6 and by its action on microglia. Together, our findings suggest that targeting PACAP and microglial activation may provide new therapeutic avenues in the prevention of seizure-induced cardiovascular dysfunction and SUDEP.

References

Ahmadi A, Sayyah M, Khoshkholgh-Sima B, Choopani S, Kazemi J, Sadegh M, Moradpour F, Nahrevanian H (2013) Intra-hippocampal injection of lipopolysaccharide inhibits kindled seizures and retards kindling rate in adult rats. Exp Brain Res 226:107–120. CrossRef Medline

Bazett HC (1920) An analysis of the time-relations of electrocardiograms. Heart 7:353–370.

Beach TG, Woodhurst WB, MacDonald DB, Jones MW (1995) Reactive microglia in hippocampal sclerosis associated with human temporal lobe epilepsy. Neurosci Lett 191:27–30. CrossRef Medline

Benarroch EE (2013) Microglia: multiple roles in surveillance, circuit shaping, and response to injury. Neurology 81:1079–1088. CrossRef Medline

Biber K, Owens T, Boddeke E (2014) What is microglia neurotoxicity (Not)? Glia 62:841–854. CrossRef Medline

Brotherstone R, Blackhall B, McLellan A (2010) Lengthening of corrected QT during epileptic seizures. Epilepsia 51:221–232. CrossRef Medline

Chan UPF, Lee JF, Wang SH, Leung KL, Chen GG (2003) Induction of colon cancer cell death by 7-hydroxystaurosporine (UCN-01) is associated with increased p38 MAPK and decreased Bcl-xL. Anticancer Drugs 14:761–766. Medline

Darbin O, Casebeer DJ, Naritoku DK (2002) Cardiac dysrhythmia associated with the immediate postictal state after maximal electroshock in freely moving rat. Epilepsia 43:336–341. CrossRef Medline

Delgado M, Munoz-Elias EJ, Gomariz RP, Ganea D (1999) Vasoactive intestinal peptide and pituitary adenylate cyclase-activating polypeptide enhance il-10 production by murine macrophages: in vitro and in vivo studies. J Immunol 162:1707–1716. Medline

Drage MG, Holmes GL, Seyfried TN (2002) Hippocampal neurons and glia in epileptic EL mice. J Neurocytol 31:681–692. CrossRef Medline

Farnham MMJ, Li Q, Goodchild AK, Pilowsky PM (2008) PACAP is expressed in sympathoexcitatory bulbospinal C1 neurons of the brain stem and increases sympathetic nerve activity in vivo. Am J Physiol 294:R1304–R1311. CrossRef Medline

Farnham MMJ, Inglott MA, Pilowsky PM (2011) Intrathecal PACAP-38 causes increases in sympathetic nerve activity and heart rate but not blood pressure in the spontaneously hypertensive rat. Am J Physiol 300:H214–H222. CrossRef Medline

Farnham MM, Lung MS, Tallapragada VJ, Pilowsky PM (2012) PACAP causes PAC1/VPAC2 receptor mediated hypertension and sympathoex-

citation in normal and hypertensive rats. Am J Physiol 303:H910–H917. CrossRef Medline

Ferrer I, Blanco R, Carmona M, Puig B, Domínguez I, Viñals F (2002) Active, phosphorylation-dependent MAP kinases, MAPK/ERK, SAPK/JNK and p38, and specific transcription factor substrates are differentially expressed following systemic administration of kainic acid to the adult rat. Acta Neuropathol 103:391–407. CrossRef Medline

Gordon PH, Moore DH, Miller RG, Florence JM, Verheijde JL, Doorish C, Hilton JF, Spitalny GM, MacArthur RB, Mitsumoto H, Neville HE, Boylan K, Mozaffar T, Belsh JM, Ravits J, Bedlack RS, Graves MC, McCluskey LF, Barohn RJ, Tandan R; Western ALS Study Group (2007) Efficacy of minocycline in patients with amyotrophic lateral sclerosis: a phase III randomised trial. Lancet Neurol 6:1045–1053. CrossRef Medline

Gottschall PE, Tatsuno I, Arimura A (1994) Regulation of interleukin-6 (IL-6) secretion in primary cultured rat astrocytes: Synergism of interleukin-1 (IL-1) and pituitary adenylate cyclase activating polypeptide (PACAP). Brain Res 637:197–203. CrossRef Medline

Hotta H, Koizumi K, Stewart M (2009) Cardiac sympathetic nerve activity during kainic acid-induced limbic cortical seizures in rats. Epilepsia 50:923–927. CrossRef Medline

Hua XY, Svensson CI, Matsui T, Fitzsimmons B, Yaksh TL, Webb M (2005) Intrathecal minocycline attenuates peripheral inflammation-induced hyperalgesia by inhibiting p38 MAPK in spinal microglia. Eur J Neurosci 22:2431–2440. CrossRef Medline

Imai F, Suzuki H, Oda J, Ninomiya T, Ono K, Sano H, Sawada M (2007) Neuroprotective effect of exogenous microglia in global brain ischemia. J Cereb Blood Flow Met 27:488–500. CrossRef Medline

Jeon SH, Kim YS, Bae CD, Park JB (2000) Activation of JNK and p38 in rat hippocampus after kainic acid induced seizure. Exp Mol Med 32:227–230. CrossRef Medline

Kim WK, Ganea D, Jonakait GM (2002) Inhibition of microglial CD40 expression by pituitary adenylate cyclase-activating polypeptide is mediated by interleukin-10. J Neuroimmunol 126:16–24. CrossRef Medline

Kitamura Y, Takata K, Inden M, Tsuchiya D, Yanagisawa D, Nakata J, Taniguchi T (2004) Intracerebroventricular injection of microglia protects against focal brain ischemia. J Pharmacol Sci 94:203–206. CrossRef Medline

Kitamura Y, Yanagisawa D, Inden M, Takata K, Tsuchiya D, Kawasaki T, Taniguchi T, Shimohama S (2005) Recovery of focal brain ischemia-induced behavioral dysfunction by intracerebroventricular injection of microglia. J Pharmacol Sci 97:289–293. CrossRef Medline

Kreisel T, Frank MG, Licht T, Reshef R, Ben-Menachem-Zidon O, Baratta MV, Maier SF, Yirmiya R (2014) Dynamic microglial alterations underlie stress-induced depressive-like behavior and suppressed neurogenesis. Mol Psychiatry 19:699–709. CrossRef Medline

Lai AY, Todd KG (2008) Differential regulation of trophic and proinflammatory microglial effectors is dependent on severity of neuronal injury. Glia 56:259–270. CrossRef Medline

Lai CC, Wu SY, Lin HH, Dun NJ (1997) Excitatory action of pituitary adenylate cyclase activating polypeptide on rat sympathetic preganglionic neurons in vivo and in vitro. Brain Res 748:189–194. CrossRef Medline

Lalancette-Hébert M, Gowing G, Simard A, Weng YC, Kriz J (2007) Selective ablation of proliferating microglial cells exacerbates ischemic injury in the brain. J Neurosci 27:2596–2605. CrossRef Medline

Lévesque M, Avoli M (2013) The kainic acid model of temporal lobe epilepsy. Neurosci Biobehav Rev 37:2887–2899. CrossRef Medline

Li L, Lu J, Tay SS, Moochhala SM, He BP (2007) The function of microglia, either neuroprotection or neurotoxicity, is determined by the equilibrium among factors released from activated microglia in vitro. Brain Res 1159:8–17. CrossRef Medline

Loane DJ, Byrnes KR (2010) Role of microglia in neurotrauma. Neurotherapeutics 7:366–377. CrossRef Medline

Luckhaus C, Hennersdorf M, Bell M, Agelink MW, Zielasek J, Cordes J (2008) Brugada syndrome as a potential cardiac risk factor during electroconvulsive therapy (ECT). World J Biol Psychiatry 9:150–153. CrossRef Medline

März P, Cheng JG, Gadient RA, Patterson PH, Stoyan T, Otten U, Rose-John S (1998) Sympathetic neurons can produce and respond to interleukin 6. Proc Natl Acad Sci U S A 95:3251–3256. CrossRef Medline

Mirrione MM, Konomos DK, Gravanis I, Dewey SL, Aguzzi A, Heppner FL, Tsirka SE (2010) Microglial ablation and lipopolysaccharide precondi-

tioning affects pilocarpine-induced seizures in mice. Neurobiol Dis 39: 85–97. CrossRef Medline

Mokriski BK, Nagle SE, Papuchis GC, Cohen SM, Waxman GJ (1992) Electroconvulsive therapy-induced cardiac arrhythmias during anesthesia with methohexital, thiamylal, or thiopental sodium. J Clin Anesth 4:208–212. CrossRef Medline

Mosser DM, Edwards JP (2008) Exploring the full spectrum of macrophage activation. Nat Rev Immunol 8:958–969. CrossRef Medline

Müngen B, Berilgen MS, Arikanoğlu A (2010) Autonomic nervous system functions in interictal and postictal periods of nonepileptic psychogenic seizures and its comparison with epileptic seizures. Seizure 19:269–273. CrossRef Medline

Neumann J, Sauerzweig S, Rönicke R, Gunzer F, Dinkel K, Ullrich O, Gunzer M, Reymann KG (2008) Microglia cells protect neurons by direct engulfment of invading neutrophil granulocytes: A new mechanism of CNS immune privilege. J Neurosci 28:5965–5975. CrossRef Medline

Nimmerjahn A, Kirchhoff F, Helmchen F (2005) Neuroscience: Resting microglial cells are highly dynamic surveillants of brain parenchyma in vivo. Science 308:1314–1318. CrossRef Medline

Nomura M, Ueta Y, Hannibal J, Serino R, Yamamoto Y, Shibuya I, Matsumoto T, Yamashita H (2000) Induction of pituitary adenylate cyclase-activating polypeptide mRNA in the medial parvocellular part of the paraventricular nucleus of rats following kainic-acid-induced seizure. Neuroendocrinology 71:318–326. CrossRef Medline

Pansani AP, Colugnati DB, Schoorlemmer GH, Sonoda EY, Cavalheiro EA, Arida RM, Scorza FA, Cravo SL (2011) Repeated amygdala-kindled seizures induce ictal rebound tachycardia in rats. Epilepsy Behav 22:442–449. CrossRef Medline

Peltola J, Palmio J, Korhonen L, Suhonen J, Miettinen A, Hurme M, Lindholm D, Keränen T (2000) Interleukin-6 and interleukin-1 receptor antagonist in cerebrospinal fluid from patients with recent tonic-clonic seizures. Epilepsy Res 41:205–211. CrossRef Medline

Penkowa M, Molinero A, Carrasco J, Hidalgo J (2001) Interleukin-6 deficiency reduces the brain inflammatory response and increases oxidative stress and neurodegeneration after kainic acid-induced seizures. Neuroscience 102:805–818. CrossRef Medline

Persson M, Rönnbäck L (2012) Microglial self-defence mediated through GLT-1 and glutathione. Amino Acids 42:207–219. CrossRef Medline

Reglodi D, Somogyvari-Vigh A, Vigh S, Kozicz T, Arimura A (2000) Delayed systemic administration of PACAP38 is neuroprotective in transient middle cerebral artery occlusion in the rat. Stroke 31:1411–1417. CrossRef Medline

Ringer C, Büning LS, Schäfer MK, Eiden LE, Weihe E, Schütz B (2013) PACAP signaling exerts opposing effects on neuroprotection and neuroinflammation during disease progression in the SOD1(G93A) mouse model of amyotrophic lateral sclerosis. Neurobiol Dis 54:32–42. CrossRef Medline

Sakamoto K, Saito T, Orman R, Koizumi K, Lazar J, Salciccioli L, Stewart M (2008) Autonomic consequences of kainic acid-induced limbic cortical seizures in rats: peripheral autonomic nerve activity, acute cardiovascular changes, and death. Epilepsia 49:982–996. CrossRef Medline

Sakon S, Xue X, Takekawa M, Sasazuki T, Okazaki T, Kojima Y, Piao JH, Yagita H, Okumura K, Doi T, Nakano H (2003) NF-κB inhibits TNF-induced accumulation of ROS that mediate prolonged MAPK activation and necrotic cell death. EMBO J 22:3898–3909. CrossRef Medline

Schreihofer AM, Guyenet PG (1997) Identification of C1 presympathetic neurons in rat rostral ventrolateral medulla by juxtacellular labeling in vivo. J Comp Neurol 387:524–536. CrossRef Medline

Shapiro LA, Wang L, Ribak CE (2008) Rapid astrocyte and microglial activation following pilocarpine-induced seizures in rats. Epilepsia 49:33–41. CrossRef Medline

Shioda S, Ozawa H, Dohi K, Mizushima H, Matsumoto K, Nakajo S, Takaki A, Zhou CJ, Nakai Y, Arimura A (1998) PACAP protects hippocampal neurons against apoptosis: Involvement of JNK/SAPK signaling pathway. Ann NY Acad Sci 865:111–117. CrossRef Medline

Shioda S, Ohtaki H, Nakamachi T, Dohi K, Watanabe J, Nakajo S, Arata S, Kitamura S, Okuda H, Takenoya F, Kitamura Y (2006) Pleiotropic functions of PACAP in the CNS: Neuroprotection and neurodevelopment. Ann NY Acad Sci 1070:550–560. CrossRef Medline

Tolstykh GP, Cavazos JE (2013) Potential mechanisms of sudden unexpected death in epilepsy. Epilepsy Behav 26:410–414. CrossRef Medline

Vinet J, Weering HR, Heinrich A, Kälin RE, Wegner A, Brouwer N, Heppner FL, Rooijen Nv, Boddeke HW, Biber K (2012) Neuroprotective function for ramified microglia in hippocampal excitotoxicity. J Neuroinflammation 9:27. CrossRef Medline

Wannamaker BB (1985) Autonomic nervous system and epilepsy. Epilepsia 26:S31–S39. CrossRef Medline

Systems/Circuits

Seizure-Induced Sympathoexcitation Is Caused by Activation of Glutamatergic Receptors in RVLM That Also Causes Proarrhythmogenic Changes Mediated by PACAP and Microglia in Rats

Amol M. Bhandare,[1,2] Komal Kapoor,[1,2] Paul M. Pilowsky,[1,3] and Melissa M.J. Farnham[1,3]

[1]The Heart Research Institute, Sydney 2042, New South Wales, Australia, [2]Faculty of Medicine and Health Sciences, Macquarie University, Sydney 2109, New South Wales, Australia, and [3]Department of Physiology, University of Sydney, Sydney 2006, New South Wales, Australia

Cardiovascular autonomic dysfunction in seizure is a major cause of sudden unexpected death in epilepsy. The catecholaminergic neurons in the rostral ventrolateral medulla (RVLM) maintain sympathetic vasomotor tone and blood pressure through their direct excitatory projections to the intermediolateral (IML) cell column. Glutamate, the principal excitatory neurotransmitter in brain, is increased in seizures. Pituitary adenylate cyclase activating polypeptide (PACAP) is an excitatory neuropeptide with neuroprotective properties, whereas microglia are key players in inflammatory responses in CNS. We investigated the roles of glutamate, PACAP, and microglia on RVLM catecholaminergic neurons during the cardiovascular responses to 2 mg/kg kainic acid (KA)-induced seizures in urethane anesthetized, male Sprague Dawley rats. Microinjection of the glutamate antagonist, kynurenic acid (50 nl; 100 mM) into RVLM, blocked the seizure-induced $43.2 \pm 12.6\%$ sympathoexcitation ($p \leq 0.05$), and abolished the pressor responses, tachycardia, and QT interval prolongation. PACAP or microglia antagonists (50 nl) (PACAP(6–38), 15 pmol; minocycline 10 mg/ml) microinjected bilaterally into RVLM had no effect on seizure-induced sympathoexcitation, pressor responses, or tachycardia but abolished the prolongation of QT interval. The actions of PACAP or microglia on RVLM neurons do not cause sympathoexcitation, but they do elicit proarrhythmogenic changes. An immunohistochemical analysis in 2 and 10 mg/kg KA-induced seizure rats revealed that microglia surrounding catecholaminergic neurons are in a "surveillance" state with no change in the number of M2 microglia (anti-inflammatory). In conclusion, seizure-induced sympathoexcitation is caused by activation of glutamatergic receptors in RVLM that also cause proarrhythmogenic changes mediated by PACAP and microglia.

Key words: glutamate; microglia; PACAP; rat; seizure; sympathetic

Significance Statement

Sudden unexpected death in epilepsy is a major cause of death in epilepsy. Generally, seizures are accompanied by changes in brain function leading to uncontrolled nerve activity causing high blood pressure, rapid heart rate, and abnormal heart rhythm. Nevertheless, the brain chemicals causing these cardiovascular changes are unknown. Chemicals, such as glutamate and pituitary adenylate cyclase activating polypeptide, whose expression is increased after seizures, act on specific cardiovascular nuclei in the brain and influence the activity of the heart, and blood vessels. Microglia, which manage excitation in the brain, are commonly activated after seizure and produce pro- and/or anti-inflammatory factors. Hence, we aimed to determine the effects of blocking glutamate, pituitary adenylate cyclase activating polypeptide, and microglia in the RVLM and their contribution to cardiovascular autonomic dysfunction in seizure.

Introduction

Seizure-induced cardiovascular autonomic dysfunction is a common cause of sudden unexpected death in epilepsy (SUDEP), which accounts for 5%–17% deaths in people with epilepsy (Sakamoto et al., 2008; Surges et al., 2009; Bardai et al., 2012; Massey et al., 2014). The rostral ventrolateral medulla (RVLM)

contains sympathetic premotor neurons (C1), which are a subset of catecholaminergic neurons that express all of the enzymes necessary for the synthesis of adrenaline (Schreihofer and Guyenet, 1997; Phillips et al., 2001). Sympathetic vasomotor tone and blood pressure are regulated by C1 neurons, and another smaller population of neurons that is also located in the RVLM, through their direct projections to the intermediolateral (IML) cell column (Ross et al., 1984; Guyenet, 2006; Pilowsky et al., 2009). Seizure-induced increased activity of C1 catecholaminergic neurons (c-fos) is well documented (Kanter et al., 1995; Silveira et al., 2000). Seizure causes an increase in sympathetic nerve activity (SNA) and has significant effect on cardiac electrophysiology and heart rate (HR) (Nei et al., 2004; Metcalf et al., 2009; Damasceno et al., 2013). There is no information about the neurotransmitters mediating activation of brainstem catecholaminergic neurons contributing to the autonomic manifestations that frequently accompany epileptic seizures.

As we have documented previously, low-dose kainic acid (KA)-induced seizures in rat cause sympathoexcitation, increases in mean arterial pressure (MAP) and HR, and proarrhythmogenic changes, including prolongation of the QT interval (Bhandare et al., 2015). The evidence suggests that pituitary adenylate cyclase activating polypeptide (PACAP) and microglia have a protective effect on sympathetic preganglionic neurons in the IML cell column where they ameliorate the sympathoexcitatory effect of seizures. PACAP is well established to be neuroprotective (Shioda et al., 1998; Ohtaki et al., 2006), through its effect on microglia (Wada et al., 2013). Recently, we investigated the excitatory effect of PACAP in cardiovascular autonomic nuclei (Farnham et al., 2008, 2012). KA-induced seizures dramatically increase PACAP expression in central autonomic nuclei (paraventricular nucleus) (Nomura et al., 2000). Additionally, microglia can be pro- or anti-inflammatory in some models of diseases, such as temporal lobe epilepsy (Shapiro et al., 2008; Mirrione et al., 2010; Vinet et al., 2012). In seizure, there is extensive activation of microglia in patients and in animal models (Beach et al., 1995; Shapiro et al., 2008; Eyo et al., 2014). Moreover, there are reports suggesting that PACAP modulates the activated microglial state (Wada et al., 2013; Brifault et al., 2015). This important relationship between PACAP, microglia, and seizure-induced increase in its expression or activation in cardiovascular autonomic nuclei makes them a very promising target in the development of therapy for seizure-induced sympathoexcitation and cardiovascular dysfunction. In addition, brain glutamate levels are increased in patients and animal models of temporal lobe epilepsy (Meldrum et al., 1999; Blümcke et al., 2000) and play a major pathogenic role for neuronal hyperexcitability. However, glutamatergic drive within RVLM neurons is not important for maintenance of basal tonic activity of catecholaminergic neurons or blood pressure (Guyenet et al., 1987; Araujo et al., 1999; Sved et al., 2002). Collectively, the sympathoexcitation during seizure may be due to an increased glutamate turnover that could be reversed by glutamate antagonist microinjection into RVLM without affecting basal sympathetic output and blood pressure.

Overall, the aims of this study were to identify the role of PACAP, microglia, and glutamatergic receptors in the RVLM to regulate catecholaminergic neuronal hyperexcitability and other

cardiovascular changes following low-dose KA-induced seizures in rats. To achieve these aims, we used a combination of electrophysiological and neuroanatomical approaches with KA-induced seizures in rats. Seizures were induced with 2 mg/kg intraperitoneal KA injection in urethane anesthetized, vagotomized, paralyzed, and artificially ventilated rats and 50 nl of each PACAP antagonist, PACAP(6–38); microglia antagonist, minocycline; or glutamate antagonist, kynurenic acid (KYNA) were microinjected into the RVLM of different group of rats. The changes in microglial morphology and the expression of the anti-inflammatory M2 microglial phenotype in the vicinity of RVLM catecholaminergic neurons in response to 2 and 10 mg/kg KA-induced seizures in rats were analyzed with immunohistochemistry.

Materials and Methods

Animals. The animal usage and protocols were in accordance with the Australian code of practice for the care and use of animals for scientific purposes. The protocols were approved by the Animal Care and Ethics Committee of Macquarie University and the Sydney Local Health District. All electrophysiology and histology experiments were conducted on adult male Sprague-Dawley rats (250–350 g; Animal Resources Centre).

Surgical preparations. For electrophysiology experiments ($n = 31$), rats were anesthetized with 10% urethane (ethyl carbamate; 1.3–1.5 g/kg i.p.; Sigma-Aldrich) and for histology experiments ($n = 15$) with 3% sodium pentobarbital (50 mg/kg i.p.; Virbac). The depth of anesthesia was monitored by observing reflex responses (withdrawal or pressor >10 mmHg) to nociceptive stimuli (periodic tail/paw pinches). Additional anesthetic was injected (30–40 mg, 10% urethane i.v. or 1.5–2.0 mg, sodium pentobarbital i.v.), if reflex responses were observed. Atropine sulfate (100 μg/kg, i.p.; Pfizer) was administered with the first dose of anesthetics to prevent bronchial secretions. After the completion of the general surgical procedures described below, rats were secured in a stereotaxic frame and body temperature was recorded and maintained between 36.5°C and 37.5°C throughout the experiment using a homeothermic blanket (TC-1000; CWE).

General surgical procedures and electroencephalogram (EEG) electrode placement. Procedures were performed as described previously (Bhandare et al., 2015). Briefly, the right carotid artery and jugular vein were cannulated for recording of blood pressure, and for administration of drugs and fluids, respectively, with a tracheostomy to enable mechanical ventilation. A three lead electrocardiogram (ECG; front paws, hindpaw) was recorded, and HR was derived from it. Rats were vagotomized, artificially ventilated with oxygen-enriched room air, and paralyzed with pancuronium bromide. Arterial blood gases were analyzed with an electrolyte and blood gas analyzer (IDEXX, Vetstat). PaCO$_2$ was maintained at 40 ± 2 and pH between 7.35 and 7.45.

For the placement of EEG electrodes, burr holes were drilled bilaterally for recording over the dorsal hippocampus (5.2 mm anterior to lambda, 3 mm lateral to midline, and 2–3 mm below the skull surface), and electrode positions were confirmed with cresyl violet staining. A single 75 μm Teflon-insulated stainless steel wire (A-M Systems) was inserted into each hole using stereotaxic manipulator. The signals were amplified (CWE, BMA-931 Bioamplifier), bandpass filtered from 1 Hz to 10 kHz, and digitized at 20 kHz with a 100× gain.

Seizure induction. For electrophysiology experiments, seizures were induced by intraperitoneal injection of 2 mg/kg KA in Sprague Dawley rats (Bhandare et al., 2015). In the histology study, two doses of KA (2 and 10 mg/kg; i.p.) were used to elicit mild and severe seizures in rats to analyze their effects on the morphology of microglia in the vicinity of catecholaminergic neurons in RVLM; 2 mg/kg is the lowest dose of KA required to induce seizure and sympathoexcitation (Bhandare et al., 2015), whereas 10 mg/kg KA induces status epilepticus with generalized tonic-clonic seizures in rats (Nadler, 1981; Sperk et al., 1983). However, in our study, rats were paralyzed and had no behavioral seizures. KA responses were recorded for 2 h after KA injection, during which continuous monitoring of EEG was used to identify the development of sei-

zures. To investigate the duration of seizure-induced cardiovascular responses, 2 mg/kg KA-induced seizures were recorded until cardiovascular parameters returned to baseline ($n = 4$).

In vivo *electrophysiology: isolation and preparation of nerves*. The left greater splanchnic sympathetic nerve at a site proximal to the celiac ganglion, and the left phrenic nerve were isolated, dissected, and tied with 5/0 silk thread. Nerve activity was recorded using bipolar stainless steel electrodes. Signals were amplified (CWE, BMA-931 Bioamplifiers) (sampling rate: 6 kHz, gain: 2000, filtering: 30 –3000 Hz) and filtered with a 50/60 Hz line frequency filter (Humbug; Quest Scientific).

RVLM site detection, confirmation and microinjection. The dorsal surface of the medulla oblongata was exposed by occipital craniotomy and the dura was removed. The bilateral RVLM stereotaxic coordinates were measured with respect to calamus scriptorius and confirmed if a 50 nl microinjection of 100 mmol/L glutamate increased blood pressure > 30 mmHg. After glutamate confirmation, stable baseline parameters were recorded for at least 30 min.

In vehicle and KA control groups of rats ($n = 5$), 50 nl of 10 mmol/L PBS was microinjected bilaterally in the RVLM; 50 nl of 15 pmol of PACAP(6–38) (150 μmol/L in 100 nl) (Auspep, Selleck) was microinjected bilaterally in the RVLM ($n = 6$) (Farnham et al., 2012). Minocycline (10 mg/ml) ($n = 6$) (LeBlanc et al., 2011) and KYNA (100 mM) ($n = 5$) (Miyawaki et al., 2002) were bilaterally microinjected in the RVLM in doses of 50 nl in different groups of rats. In all rats, microinjections were made 15 min before intraperitoneal KA or PBS injection. Microinjections were not made in $n = 4$ rats that were used to investigate the duration of KA-induced cardiovascular effects. At the conclusion of the experiment, 50 nl of Chicago Sky Blue (2%) was microinjected at the site of the RVLM, and rats were either killed with 0.5 ml of 3 M potassium chloride (KCl; i.v.) or deeply anesthetized and perfused with 400 ml of ice-cold 0.9% saline followed by 400 ml of 4% PFA solution. The brains were removed from the perfused rats and postfixed in the same fixative overnight. Cerebrum and brainstem were sectioned coronally (100 μm) and stained with cresyl violet for histological verification of the EEG electrode positions in hippocampus and microinjection site in RVLM, respectively.

Histology: perfusions. At the conclusion of the experiment, rats used for histology study (in all groups; $n = 5$) were deeply anesthetized with an overdose of sodium pentobarbital and given 1 ml of heparin via the venous line. Rats were transcardially perfused with 400 ml of ice-cold 0.9% saline followed by 400 ml of 4% PFA solution. The brains were then removed and postfixed in the same fixative for 18–24 h.

Sectioning and immunohistochemistry. Immunohistochemical analysis was done in $n = 3$ of 5 rats in each group. Brainstems were sectioned coronally (40 μm thick) with a vibrating microtome (Leica, VT1200S) and collected sequentially into five different pots containing a cryoprotectant solution and stored at −20°C until further processing. Free floating sections were used for all histological procedures. Sections were rinsed, blocked, and incubated in primary antibodies: mouse anti-tyrosine hydroxylase (TH) (1:500; Sigma-Aldrich), rabbit anti-CD206 (1:2000; Abcam), and goat anti-Iba1 (1:1000; Novus Biologicals). After 48 h, sections were rinsed and TH, CD-206, and Iba1 immunoreactivity was subsequently revealed by overnight incubation with the following secondary antibodies at 1:500 dilutions (Jackson ImmunoResearch Laboratories): Cy5-conjugated donkey anti-mouse, AlexaFluor-488-conjugated donkey anti-rabbit, and Cy3-conjugated donkey anti-goat. Sections were rinsed, mounted sequentially on glass slides, and coverslipped with Vectashield (Vector Laboratories).

Data acquisition and analysis: electrophysiology data. Data were acquired using a CED 1401 ADC system (Cambridge Electronic Design) and Spike 2 acquisition and analysis software (version 8.03; Cambridge Electronic Design). The EEG activity raw data were DC removed. The power in the "gamma" frequency range (25–45 Hz) was analyzed, as previously shown (Olsson et al., 2006; Gurbanova et al., 2008). A power spectrum analysis was done from 5 min blocks taken 1 min before microinjection or intraperitoneal injection and 60 and 120 min after intraperitoneal injection. The percentage change in power spectrum area was calculated for each rat at 60 and 120 min after intraperitoneal injection compared with pretreatment area (taken as 100%) and grouped together.

Phrenic nerve activity (PNA) was rectified and smoothed (τ 0.5 s). PNA was analyzed from 1 min blocks taken 1 min before microinjection and 60 and 120 min after intraperitoneal injection. The percentage change in PNA area under curve (AUC) was analyzed at 60 and 120 min and compared with the pretreatment area (taken as 100%). SNA was rectified, smoothed (τ 2 s), and normalized to zero by subtracting the residual activity 5–10 min after death. The integrated SNA trace was calibrated (baseline as 100%) and analyzed for AUC between 60 and 120 min after intraperitoneal KA or PBS injection. MAP and HR were analyzed from 1 min blocks taken 1 min before microinjection or intraperitoneal injection and 30, 60, 90, and 120 min after intraperitoneal injection (only 120 min results are shown in graphs). End-tidal CO_2 and core temperature were analyzed from 1 min blocks taken 1 min before microinjection or intraperitoneal injection and 30, 60, 90, and 120 min after intraperitoneal injection of either KA or PBS. Arterial blood gas levels ($PaCO_2$ and pH) were measured 10 min before microinjection or intraperitoneal injection and 120 min after intraperitoneal KA or PBS injections in all animals. In the rats used to investigate the duration of KA-induced seizures, the duration of effect was analyzed from the time of intraperitoneal KA injection up to the point where SNA, MAP, and HR returned to baseline. Changes in EEG activity were analyzed at the point where SNA returned to baseline and compared against the pre-KA (control) and 60 min post-KA injection (seizure control) period. A log transformation was applied to EEG raw values because variances were not normally distributed, and/or heterogeneous. Statistical analysis was performed in GraphPad Prism software (version 6.05). Statistical significance was determined using one-way ANOVA followed by t tests with the Holm-Šídák correction. Multiple comparisons were done between groups. $p \leq 0.05$ was considered significant.

Histology imaging and analysis. All images were acquired using a Zeiss Axio Imager Z2 (Zeiss). Images were captured at 20× and 40× magnifications. The RVLM is defined as a triangular area ventral to the nucleus ambiguus, medial to the spinal trigeminal tract, and lateral to the inferior olive or the pyramidal tracts. A 0.16 mm^2 box was then placed within the imaged RVLM, and this area was used for analysis. The morphological analysis (branch length and number of endpoint processes) of Iba1-labeled microglial cells in the vicinity of TH-labeled RVLM neurons was performed using ImageJ plugin software, and GraphPad Prism (version 6.05) was used for χ^2 test for goodness of fit. The proportions of CD206-labeled anti-inflammatory M2 microglia in the RVLM of 2 and 10 mg/kg KA treated rats were compared with the vehicle-treated group. The proportion of M2 microglia is equal to the number of M2 microglia divided by the total number of microglia multiplied by 100. Statistical significance was determined using nonparametric Kruskal–Wallis test (Sokal and Rohlf, 2012).

Calculation of corrected QT (QTc) interval. QT, PR, and RR intervals were calculated from the ECG recordings. ECG raw data were processed (DC remove), wherever baseline fluctuations were prominent. QTc interval was calculated by dividing the QT interval in seconds by the square root of the R-R interval in seconds (Bazett, 1920). The QTc was obtained before and 120 min after vehicle or KA injection. The PR and QTc interval statistical analysis was performed in GraphPad Prism software (version 6.05). Statistical significance was determined using one-way ANOVA between treatment groups followed by t tests with the Holm-Šídák correction. Multiple comparisons were done between groups. $p \leq$ 0.05 was considered significant.

Results

Sympathoexcitation, tachycardia, and pressor responses due to KA-induced seizures in rats

Intraperitoneal injection of 2 mg/kg KA induces seizures, and subsequently, increases HR, MAP, and SNA in KA control group of rats (Fig. 1A). KA (2 mg/kg i.p.) leads to development of hippocampal seizure activity within ~15–20 min. At this time, there are no changes in sympathetic activity (Fig. 2), blood pressure, or heart rate (Fig. 1A). Ten to 15 min after the start of the hippocampal seizure activity, SNA, MAP, and HR began to increase (Figs. 1A, 2). Autonomic changes are entirely downstream effects of hippocampal seizures as there was no seizure activity (increase in
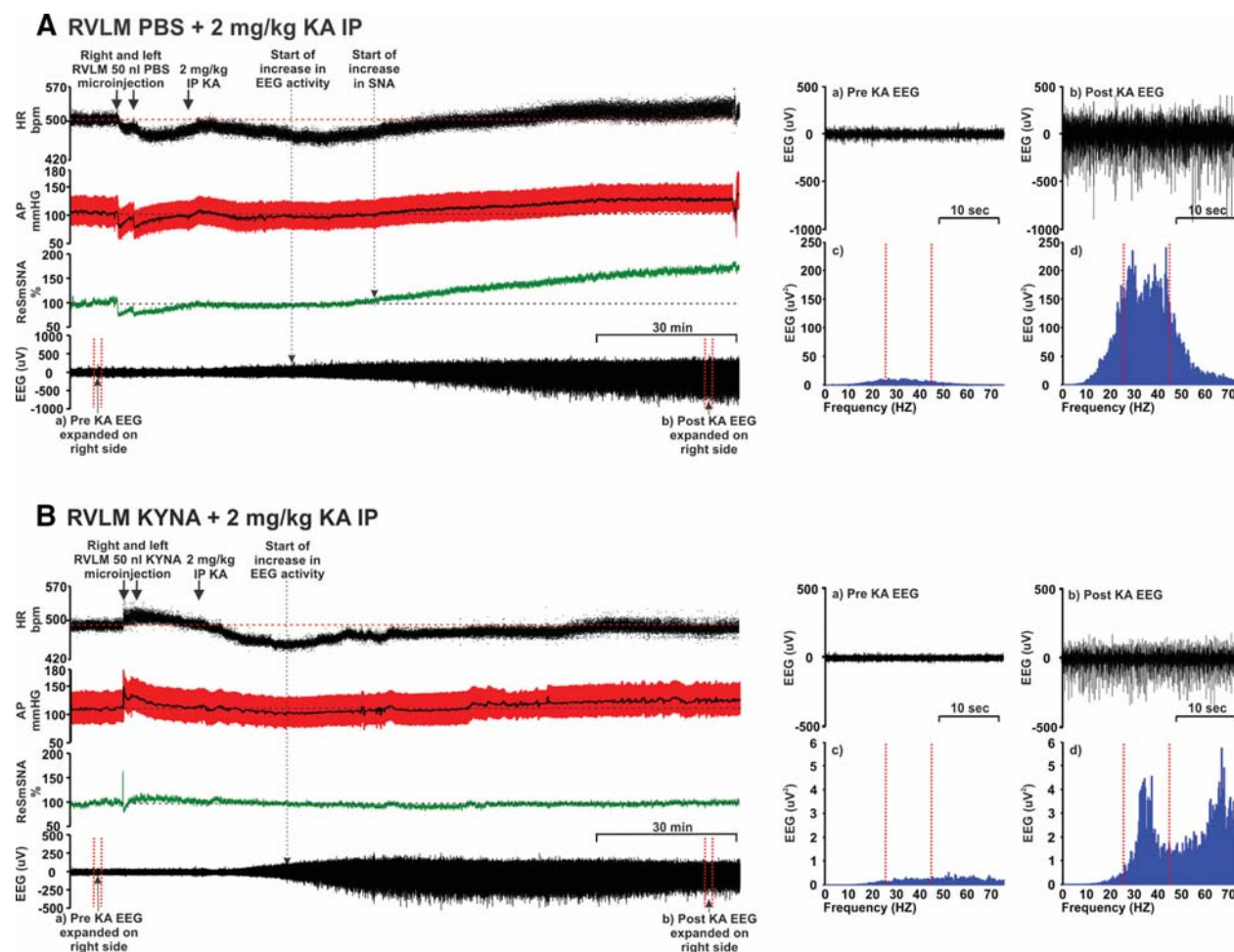
Figure 1. Effect of bilateral RVLM microinjection of (**A**) PBS (50 nl) and (**B**) KYNA (50 nl; 100 mM) followed by 2 mg/kg intraperitoneal KA in an anesthetized rat (see Materials and Methods) showing the effect on the following: from the top, (i) HR (bpm), (ii) AP (arterial pressure; mmHg), (iii) SNA (%), and (iv) EEG (μV). Arrow indicates time of RVLM microinjections and intraperitoneal KA. Dotted arrows indicate the starting points for increase in EEG and/or SNA activity. Right side panels, Pre (**a**) and post (**b**) KA EEG represents the expanded waveform from respective period. Baseline (**a**), which is a pre-KA period with desynchronous waves, and (**b**) post-KA period with increased γ range frequencies and followed by the data from the same EEG, drawn as a power spectrum (**c**, **d**, respectively) (during post-KA period γ range frequencies, which is shown between two dotted lines) are increased. Increase in gamma range frequency (25–45 Hz) is characteristic property of KA-induced seizures (Olsson et al., 2006; Gurbanova et al., 2008).

gamma frequency, which is typical sign of KA-induced seizures) in the sympathetic nerve recording until at least 70 min after KA injection, whereas SNA started to increase 25–30 min after KA injection (Fig. 2). Together, these findings indicate that central autonomic nuclei are not the source of KA-induced seizures. Between 60 and 120 min after KA injection, SNA AUC was increased by $43.2 \pm 12.6\%$ ($p = 0.04$) compared with the vehicle control group (Fig. 3A). In the KA-induced seizure group, MAP and HR were increased by 21 ± 4 mmHg ($p = 0.008$) and 32 ± 7 bpm ($p = 0.0001$), respectively, compared with the vehicle-treated group (Fig. 3B,C): the findings support the notion that seizure is the cause of the dramatic increase in sympathetic nerve activity, tachycardia, and pressor effects (Sakamoto et al., 2008; Bealer et al., 2010). Bilateral microinjection of PBS (50 nl) had a transient and nonsignificant effect on MAP, HR, and SNA, that lasted for only a few minutes (Fig. 1A).

The induction of seizures was confirmed with hippocampal EEG recordings; the power spectra were obtained from the same expanded EEG waveforms as indicated (Fig. 1A). The spectral

changes in EEG at 60 and 120 min after KA injection were obtained using Fourier analysis of 5 min EEG intervals and the AUC between gamma frequency range (25–45 Hz). The steep increase in γ wave amplitude was observed at both 60 (Δ $1038 \pm 402\%$, $p = 0.0001$) and 120 min (Δ $1329 \pm 390\%$, $p = 0.0005$) after KA injection (Figs. 1A, 3D,E). This finding also shows that KA-induced seizures in rats continued for at least 120 min following KA injection, which is consistent with results of the experiments performed to analyze the duration of seizure-induced cardiovascular effects.

KA (2 mg/kg)-induced seizures and its effects on SNA, MAP, and HR lasted for ~3 h. After this time, SNA, MAP, and HR returned to baseline values at 170, 196, and 160 min, respectively. At these time points, EEG activity was significantly reduced compared with the seizure period (at 60 min after KA) but did not return to baseline.

We did not observe any changes in PNA, expired CO_2, or body temperature in any of the groups (results not shown). Blood gas analysis confirmed that $PaCO_2$ and pH were within normal phys-
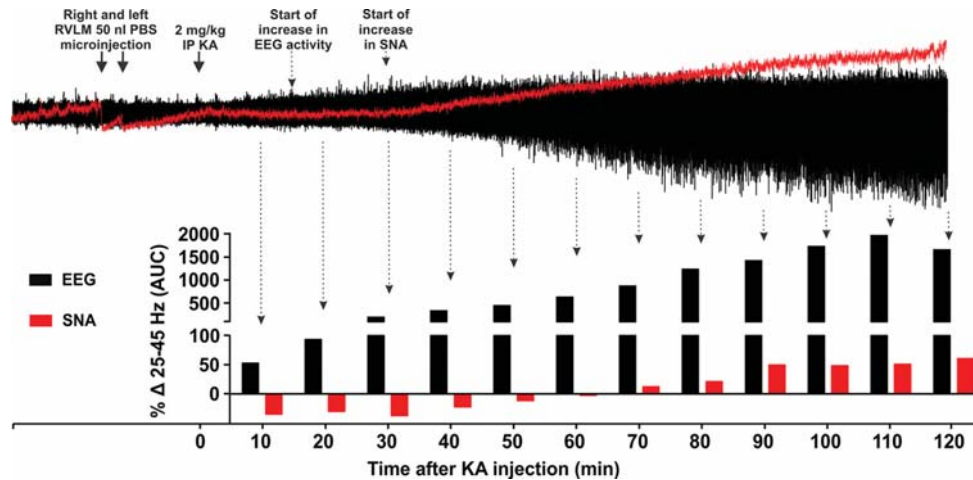
Figure 2. Effects of KA treatment on induction of seizures in hippocampus and central autonomic nuclei. Change in gamma range frequency (25–45 Hz) in hippocampal EEG and sympathetic nerve recordings every 10 min after 2 mg/kg KA injection. Arrow indicates time of RVLM microinjections and intraperitoneal KA. Dotted arrows indicate the starting points for increase in EEG and/or SNA activity. Induction of seizure activity in sympathetic nerve activity does not start at least until 70 min after KA injection, whereas hippocampal seizure activity starts ~15–20 min after KA injection followed by an increase in SNA at 25–30 min. Time-dependent increases in hippocampal seizure activity occur up to 110 min after KA injection followed by a fall.
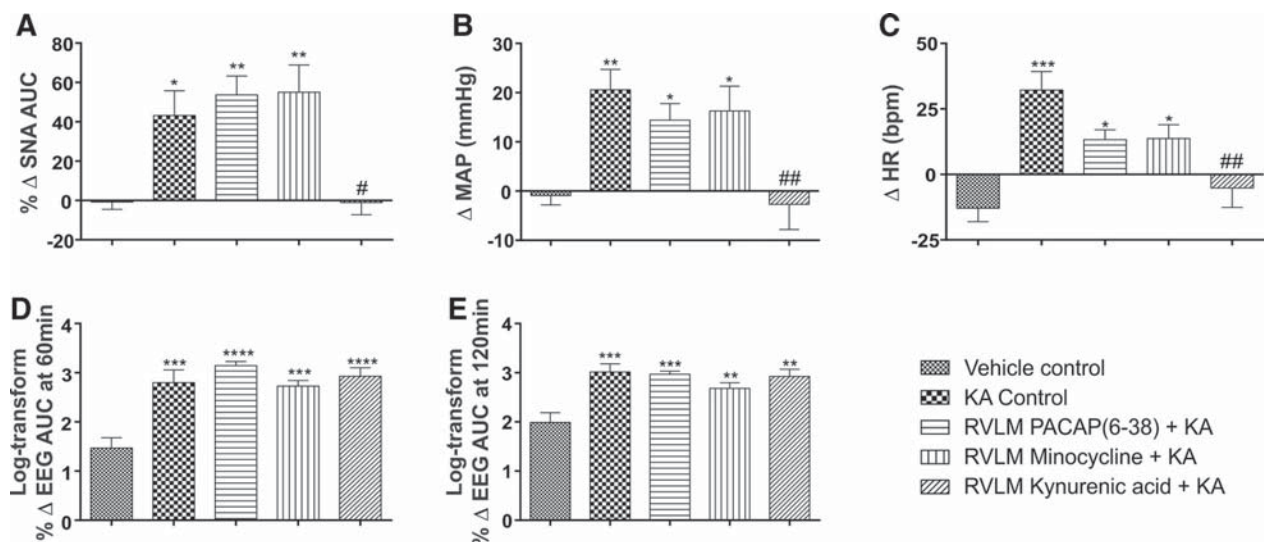
Figure 3. *In vivo* effects of RVLM microinjection of PBS, PACAP(6–38), minocycline, and KYNA in 2 mg/kg KA-induced seizure rats. Change in SNA (AUC) between 60 and 120 min after intraperitoneal treatment (*A*), change in MAP 120 min after intraperitoneal PBS or KA injection (*B*), change in HR at 120 min after intraperitoneal PBS or KA injection (*C*), and log transform of percentage change in EEG activity (gamma wave frequency AUC), at 60 min (*D*) and 120 min (*E*) after intraperitoneal PBS or KA injection in different groups of rats after development of seizure. Statistical significance was determined using one-way ANOVA followed by *t* tests with a Holm-Šídák correction. Data are mean ± SEM. ****$p \leq 0.0001$ compared with vehicle control group. ***$p \leq 0.001$ compared with vehicle control group. **$p \leq 0.01$ compared with vehicle control group. *$p \leq 0.05$ compared with vehicle control group. #$p \leq 0.05$ compared with KA control group. ##$p \leq 0.01$.

iological range ($PaCO_2$ was 40 ± 2 and pH between 7.35 and 7.45) throughout the experiment.

Sympathoexcitation, tachycardia, and pressor effects during seizure are caused by glutamatergic receptors in the RVLM and not by PACAP or microglial activation

Our findings demonstrate that sympathoexcitation during seizure is caused by glutamatergic receptor activation in the RVLM because bilateral microinjection of glutamate antagonist KYNA completely abolished the seizure-induced sympathoexcitation in rats (Figs. 1B, 3A). After microinjection of KYNA in five rats, KA-induced seizures were present (Figs. 1B, 3D,E), but pressor and heart rate responses were blocked (*p* = 0.005 and *p* = 0.001,

respectively) compared with KA control group (Figs. 1B, 3B,C). The KA-induced seizures caused no change (Δ −1.0 ± 6.2%) in SNA after bilateral microinjection of KYNA and was significantly reduced compared with KA control group (*p* = 0.04). In these groups of rats, MAP and HR were not significantly changed compared with the vehicle-treated group (Δ −3 ± 5 mmHg and Δ −5 ± 7 bpm, respectively; Fig. 3B,C). The findings reveal that KA-induced sympathoexcitation, tachycardia, pressor responses along with changes in QT interval are downstream effects of seizure and do not have a direct effect on cardiomyocytes.

Bilateral microinjection of PACAP(6–38) into the RVLM of KA-induced seizure rats did not ameliorate the significant in-
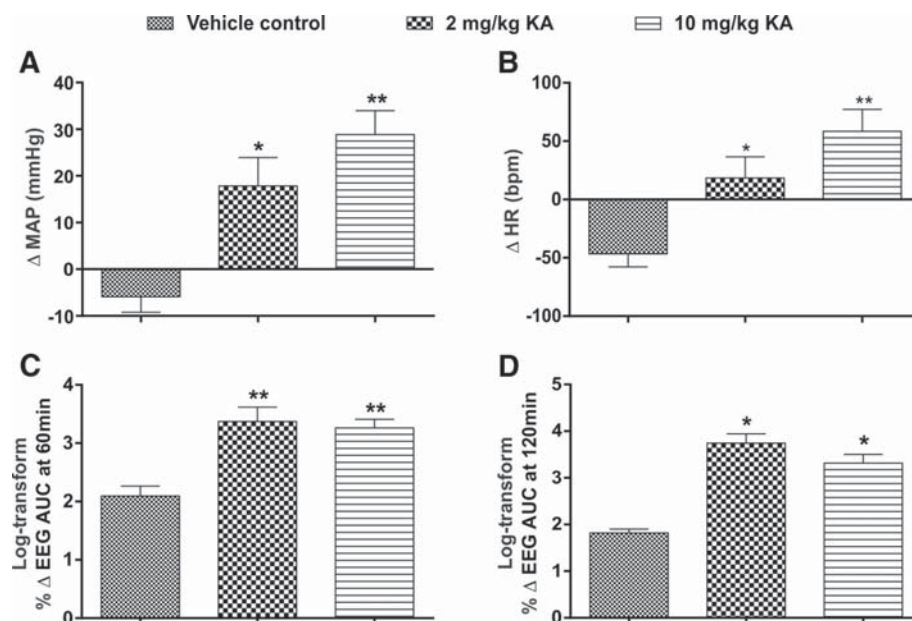
Figure 4. *In vivo* effects of PBS and KA-induced (2 and 10 mg/kg) seizures in rats studied for histology. Change in MAP (***A***) and HR (***B***), at 120 min after intraperitoneal PBS or KA (2 and 10 mg/kg) injection and percentage change in EEG activity (gamma wave frequency AUC), at 60 min (***C***) and 120 min (***D***) after intraperitoneal PBS or KA (2 and 10 mg/kg) injection in different groups of rats. In all groups, $n = 5$. Statistical significance was determined using one-way ANOVA followed by t tests with a Holm-Šídák correction. Data are mean $\pm$ SEM. **$p \leq 0.01$ compared with vehicle control group. *$p \leq 0.05$ compared with vehicle control group.

crease in SNA (Δ 53.7 $\pm$ 9.6%; $p = 0.007$) compared with the vehicle-treated group (Fig. 3A). The HR and MAP responses in PACAP(6–38) group were still significantly increased compared with the vehicle control group of rats (Fig. 3B,C). The lack of response to the PACAP antagonist (PACAP(6–38)) was replicated following bilateral RVLM microinjection of minocycline in seizure-induced rats. Following minocycline, there was a significant increase in SNA (Δ 55.1 $\pm$ 13.8%; $p = 0.006$; Fig. 3A), as well as MAP and HR (Δ 16 $\pm$ 5 mmHg and Δ 14 $\pm$ 5 bpm; $p = 0.04$ and $p = 0.02$, respectively; Fig. 3B,C) compared with vehicle control group of rats.

After KA induced seizures, microglia are in surveillance state in the vicinity of the RVLM neurons with no change in the proportion of M2 phenotype

Immunohistochemical analysis was done in rats with vehicle treatment and 2 and 10 mg/kg intraperitoneal KA ($n = 3$) to analyze the morphology of Iba1-labeled microglia and proportion of anti-inflammatory M2 phenotype in the vicinity of TH-labeled RVLM neurons. The effect of different doses of KA on MAP, HR, and EEG are shown in Figure 4 ($n = 5$). At 120 min after 2 and 10 mg/kg KA treatment, the MAP (Δ 18 $\pm$ 6 and Δ 29 $\pm$ 5; $p = 0.02$ and 0.001, respectively; Fig. 4A), HR (Δ 18 $\pm$ 18 and Δ 58 $\pm$ 19; $p = 0.05$, and 0.002, respectively; Fig. 4B), EEG activity at 60 min (Δ 1791 $\pm$ 622 and Δ 1651 $\pm$ 400; $p = 0.007$ and 0.007; respectively; Fig. 4C), and EEG activity at 120 min (Δ 4164 $\pm$ 2504 and Δ 1995 $\pm$ 563; $p = 0.04$ and 0.04; respectively; Fig. 4D) were significantly increased compared with vehicle-treated rats. The findings are consistent with *in vivo* electrophysiology data and our previous studies. Immunohistochemical analysis revealed that TH-immunoreactive (ir) neurons were surrounded with typical resting microglial cells in all three groups (Fig. 5A–C). In all three groups, microglia appeared with a round cell body and processes that appeared normal with few ramifications (Fig. 5A–C). The total number of microglia in each group

are shown in Figure 5D. A branch length, and number of endpoint analysis, was performed to identify the activated microglia. There were no differences in mean branch length, and number of endpoint processes of Iba1-labeled microglia between vehicle control and seizure-induced rats (Fig. 5E,F). The proportion of anti-inflammatory M2 phenotype of microglia was 14.2 $\pm$ 1.4% in saline-treated rats, which was similar in 2 and 10 mg/kg KA-treated rats (10.1 $\pm$ 2.5% and 9.6 $\pm$ 2.4%, respectively; Fig. 5G). The findings revealed that microglia are in a surveillance state with no differences in their morphology and proportion of M2 phenotype, at least in the RVLM, between vehicle and seizure-induced groups. These results are consistent with our electrophysiology findings where microinjection of a microglia antagonist had no effect on increase in SNA, MAP, and HR in KA-induced seizure rats.

Proarrhythmogenic ECG changes during seizures are driven by activation of glutamatergic receptors, PACAP, and microglia

The 2 mg/kg KA-induced seizures caused prolongation of QT interval. The ΔQTc was significantly increased in KA control group (Δ 8.2 $\pm$ 2.5 ms; $p = 0.02$) compared with vehicle treatment (Fig. 6A). These changes in QT interval are most clearly seen in Poincare plots before and after treatment; representative QT Poincare plots from each group are shown in Fig. 7A. KA control group showed almost complete dispersion of the QT interval along with arrhythmic behavior in heart rate (multiple ellipses) (Fig. 7AII). Despite this, there was no evidence of atrial fibrillation, although there was evidence of dramatic decrease in PR interval after KA treatment (Figs. 6B, 7BII). The prolongation of QT interval (ΔQTc) was completely blocked by administration of glutamate receptors antagonist KYNA in the RVLM ($p = 0.02$; Figs. 6A, 7AV); nevertheless, bilateral microinjection of KYNA has no effect on seizure-induced shortened PR interval (Figs. 6B, 7BV). PACAP(6–38) and minocycline microinjections also
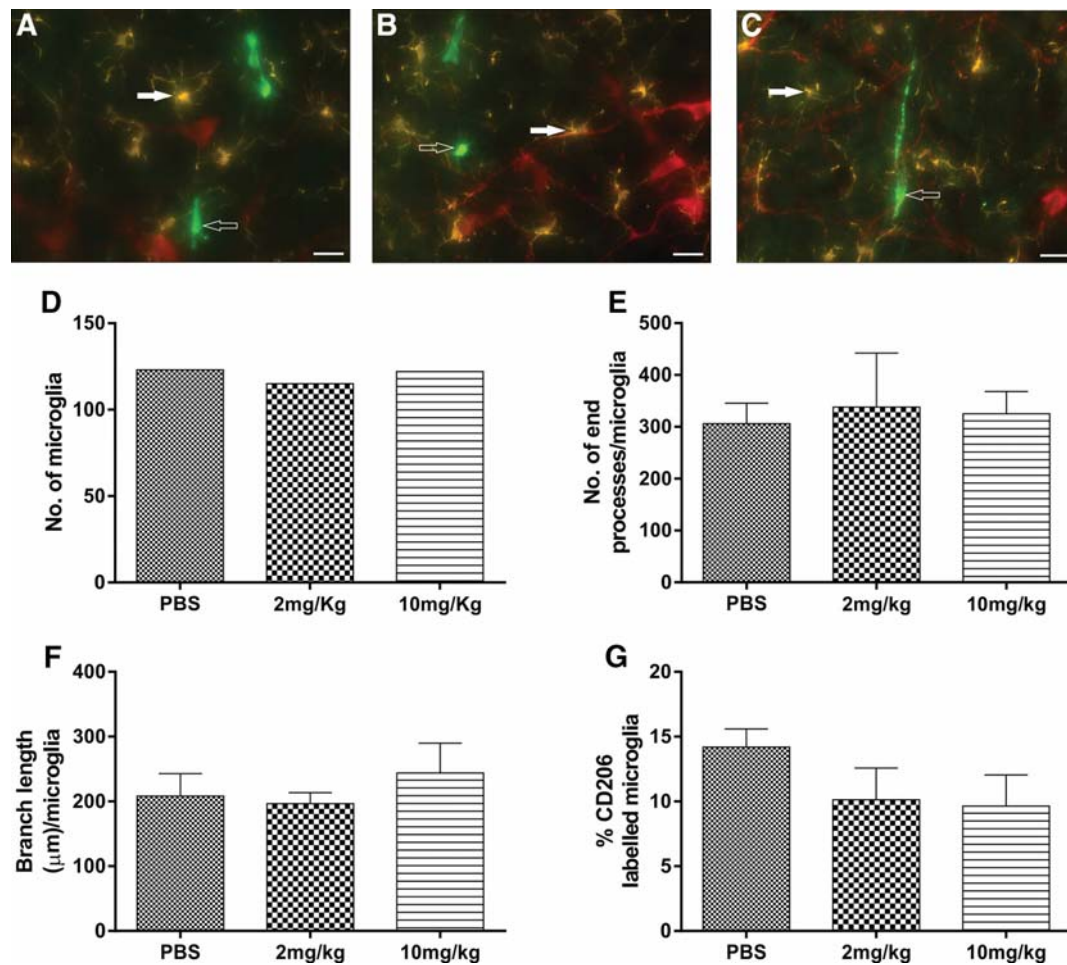
Figure 5. Fluorescence images of RVLM area containing TH $^+$-ir (red), Iba1-labeled microglia (yellow), and CD206-labeled M2 microglial cells (green) and their morphological analysis in different treatment groups of rats. Scale bar, 20 μm. TH, Iba1 and CD206 immunoreactivity in RVLM in PBS (**A**), 2 mg/kg KA (**B**), and 10 mg/kg KA (**C**) treated rats. In all of these three groups, TH $^+$-ir neurons (red) were surrounded with microglia with its round cell body and normal appearing processes with few ramifications (closed arrow) and no change in number of anti-inflammatory M2 microglia (open arrow). Quantitative analysis of number of microglial cells in mean square area (**D**), number of end processes/microglia (**E**), branch length (μm)/microglia of Iba1-labeled microglial cells (**F**), and percentage of CD206-labeled M2 microglial cells (**G**) in the RVLM of vehicle-treated and KA-induced seizure (2 and 10 mg/kg i.p.) rats.
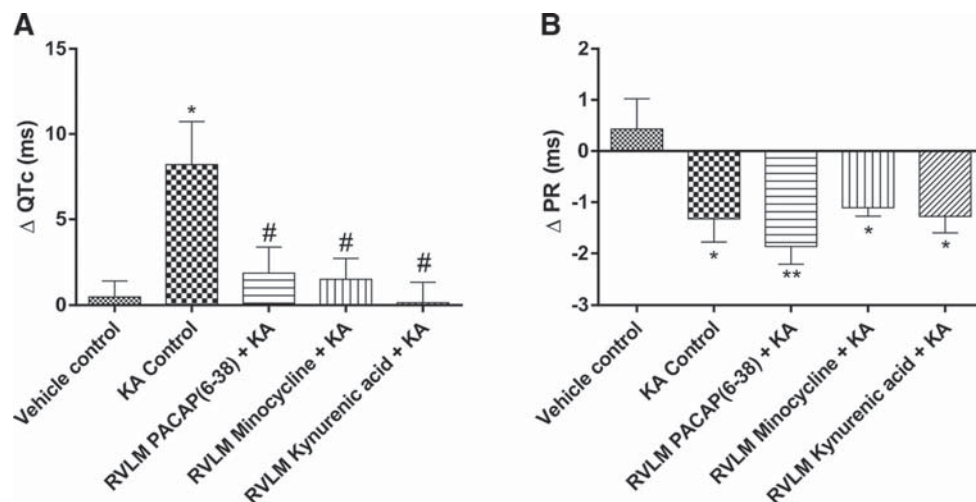
Figure 6. Proarrhythmogenic effects of seizures. Group data showing changes in QTc interval (**A**) and PR interval (**B**) 120 min after intraperitoneal injection of PBS or KA in different groups of rats. Statistical significance was determined using one-way ANOVA followed by t tests with a Holm-Šídák correction. Data are mean ± SEM. **$p \leq 0.01$ compared with vehicle control group. *$p \leq 0.05$ compared with vehicle control group. #$p \leq 0.05$ compared with KA control group.
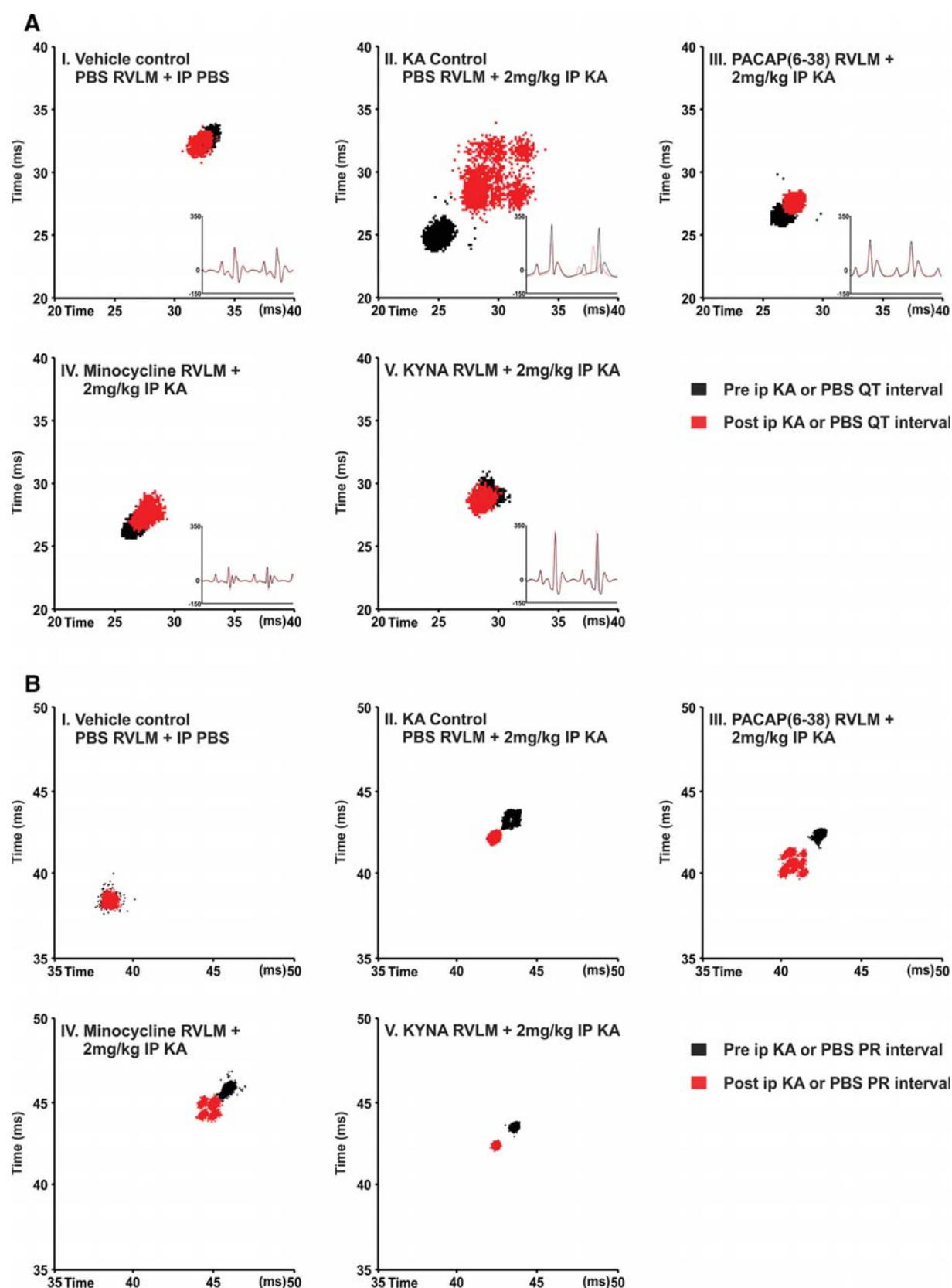
Figure 7. Representative Poincare plots illustrate the changes in QT interval (**A**) and PR interval (**B**) following KA-induced seizures in rats. **A**, Treatment with KA causes a dramatic dispersion in the QT interval (prolongation) and arrhythmic behavior in the heart rate (multiple ellipses) (**II**). In rats treated with the PACAP antagonist (PACAP(6 –38)) or (*Figure legend continues.*)

significantly reduced ΔQTc interval compared with KA control group of rats (Δ 1.9 ± 1.5; $p = 0.03$ and Δ 1.5 ± 1.2; $p = 0.03$; Fig. 6A). In PACAP(6–38) and minocycline-treated groups, prolongation of QT interval and dysrhythmia is abolished. As shown in Figure 7A, PACAP(6–38) and minocycline treatment in KA-induced seizure rats has almost similar patterns of pre- and post-QT interval as the vehicle-treated group (Fig. 7AI,III,IV). The seizure-induced prolongation of QT interval is very obvious in KA control, which was significantly blocked in PACAP(6–38) and minocycline-microinjected rats. The PR interval was significantly reduced in the 2 mg/kg KA-induced seizure group compared with the vehicle control group of rats (Fig. 6B). This is clearly represented in Poincare plots (Fig. 7B). In contrast to the improvements seen in the QT interval, RVLM microinjection of PACAP(6–38), minocycline, or KYNA did not prevent changes in seizure-induced shortening of PR interval (Fig. 6B). However, PACAP(6–38) (Fig. 7BIII) and minocycline (Fig. 7BIV) showed quantally dispersed PR intervals as evidenced by multiple ellipses, rather than complete R-R dispersion, and an absence of P-waves, which is clearly not suggestive of atrial fibrillation.

Discussion

This study provides the first direct evidence that the sympathoexcitation, tachycardia, pressor responses, and proarrhythmogenic changes during seizures are driven by activation of glutamatergic receptors, which leads to increased activity of the sympathetic premotor neurons in the RVLM. The sympathoexcitatory effect does not appear due to increases or decreases in PACAP secretion, or microglial activation. However, PACAP and microglial activity in the vicinity of RVLM neurons mediate the proarrhythmogenic changes during seizures. Central autonomic nuclei are not the source of KA-induced seizures (2 mg/kg). We confirm that the induction of seizures does not cause changes in the state of microglia within the RVLM, and microglia remain in a surveillance state with no change in the number of M2 phenotypes, supporting our *in vivo* electrophysiology findings.

Our results strengthen the findings that seizures have a devastating effects on the cardiovascular system (Sakamoto et al., 2008; Brotherstone et al., 2010; Bhandare et al., 2015), with immediate cardiovascular effects that last for ~3 h (Lothman et al., 1981). Importantly, these cardiovascular changes are downstream effects of seizure-induced autonomic overactivity and mediated by the action of the excitatory amino acid, L-glutamate, on sympathetic premotor neurons in the RVLM as the bilateral microinjection of ionotropic glutamate receptor antagonist KYNA completely abolished these changes. Glutamatergic synapses are important in the development of seizures, as seizure elevates the glutamate levels in the extracellular fluid of the rat hippocampus (Chapman, 1998; Faingold and Casebeer, 1999; Ueda et al., 2001; Kanamori and Ross, 2011). The RVLM contains sympathetic premotor neurons responsible for maintaining tonic excitation of sympathetic preganglionic neurons involved in cardiovascular

←

with the microglial antagonist minocycline, prolongation of QT interval and the dysrhythmia is abolished (*III*, *IV*). Following treatment with KYNA, the HR and QT are restored to normal (*V*). HR-triggered ECG was drawn before and after treatment and shown in the right side corner of each box. Continuous black and dotted red lines indicate pretreatment and post-treatment ECG, respectively. *B*, Induction of seizures with intraperitoneal KA injection shortened the PR interval (*II*) compared with vehicle control. RVLM microinjection of PACAP(6–38) (*III*), minocycline (*IV*), or KYNA (*V*) did not show changes in seizure-induced short PR interval; however, PACAP(6–38) (*III*) and minocycline (*IV*) showed more dispersed PR interval with multiple ellipses. Scale bars are in milliseconds.
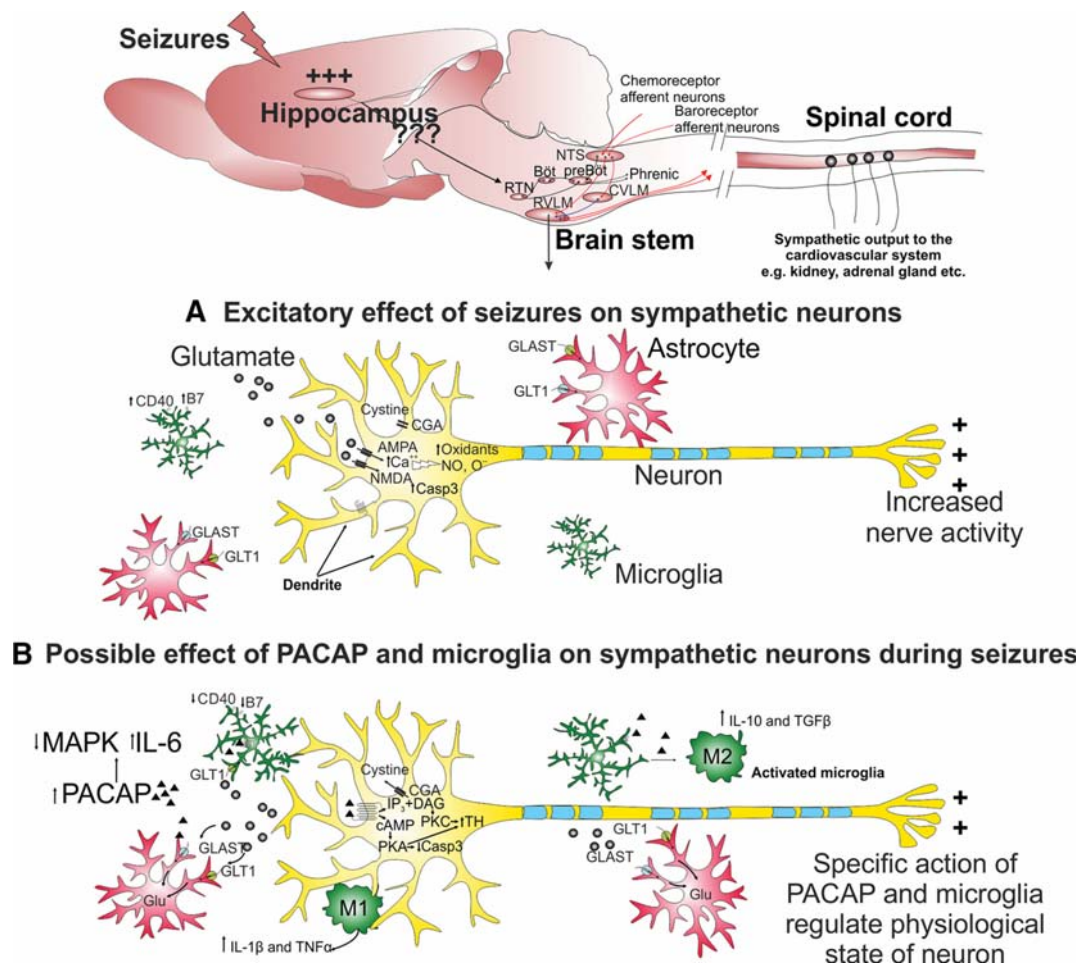
regulation (Guyenet, 2006; Pilowsky et al., 2009). Increased activity of sympathetic premotor RVLM neurons has significant effect on cardiac electrophysiology and is arrhythmogenic during seizures (Metcalf et al., 2009; Damasceno et al., 2013). Microinjection of L-glutamate into the RVLM causes pressor responses and sympathoexcitation that is completely blocked with KYNA (Ito and Sved, 1997; Araujo et al., 1999; Dampney et al., 2003). KYNA microinjection into RVLM on its own does not affect basal blood pressure and sympathetic activity (Guyenet et al., 1987; Kiely and Gordon, 1994; Araujo et al., 1999). Subsequently, Ito and Sved (1997) observed that, if the caudal ventrolateral medulla (inhibitory drive to the RVLM) is inhibited first, subsequent blockade of glutamate receptor in the RVLM markedly reduces blood pressure. In this paradigm, glutamatergic input to the RVLM directly excites presympathetic neurons and indirectly inhibit gamma-GABAergic inhibition of the RVLM, and the lack of change in arterial pressure with KYNA in the RVLM reflects the balance of these two actions. Miyawaki et al. (2002) also observed that, after blockade of GABAergic input within the RVLM, injection of KYNA produced inhibition of splanchnic and lumbar sympathetic nerve activity. Together, these findings illustrate that there is a tonic glutamatergic input with the existence of additional sources of neurotransmitter drive to RVLM neurons. We hypothesized that the increased concentration of glutamate in the RVLM during seizure leads to sympathoexcitation, tachycardia, and pressor responses. In turn, the responses can be antagonized by microinjection of KYNA into RVLM; indeed, our findings support this hypothesis. The findings suggest that not only sympathoexcitation but also proarrhythmogenic changes during seizures are mediated through glutamatergic receptor activation in RVLM catecholaminergic neurons. RVLM microinjection of KYNA (as well as PACAP(6–38) and minocycline) was unable to block the reduction in PR interval. In this paradigm, it is possible that the KA treatment had peripheral effects on dromotropy at the level of the AV node.

Generalized seizures in rats cause the expression of Fos, a protein marker of recently activated neurons (Minson et al., 1994), in brainstem catecholaminergic neurons in RVLM (Silveira et al., 2000). Earlier studies also suggests that C1 neurons are activated following seizure (Kanter et al., 1995), findings that were supported in our previous, and current work (Bhandare et al., 2015), where KA-induced seizures in rats elicited sympathoexcitation, tachycardia, and pressor responses. Together, the findings confirm that during seizure most of the excitatory effects of glutamate in RVLM are mediated by ionotropic receptors because the broad-spectrum ionotropic glutamate receptor (NMDA, AMPA, and kainate) antagonist (KYNA) completely abolished these effects.

PACAP is a 38 amino acid pleotropic neuropeptide. The effects of PACAP are mediated via three different G-protein receptors (PAC1R, VPAC1R, and VPAC2R); all are positively coupled to adenylate cyclase. PACAP gene expression is increased in the paraventricular nucleus of the hypothalamus after KA-induced temporal lobe epilepsy in rats (Nomura et al., 2000), whereas PACAP is sympathoexcitatory (Lai et al., 1997; Farnham et al., 2008, 2012; Gaede et al., 2012), anti-inflammatory, and neuroprotective (Shioda et al., 1998) on sympathetic preganglionic neurons during seizure (Bhandare et al., 2015). Therefore, we aimed to determine whether or not PACAP also has a sympathoexcitatory or neuroprotective effect on RVLM sympathetic premotor neurons during seizures. The findings show that blockade of PACAP receptors (PAC1 and VPAC2) in the RVLM does not affect seizure-induced sympathoexcitation, tachycardia, and hypertension but does abolish prolongation of the QT

Figure 8. A proposed mechanism by which hippocampal seizures induce increased activity of sympathetic premotor neurons in the RVLM and role of glutamate, PACAP, and microglia. ***A***, Seizure elevates synaptic glutamate release that can act on postsynaptic AMPA or NMDA receptors. Activation of AMPA or NMDA receptors leads to inhibition of cysteine uptake and influx of extracellular calcium, which stimulates production of oxidants, NO and O^-. Under repetitive and extreme neuronal activation, neurotoxic effects are mediated through increased production of apoptotic factor-like caspase-3. Glutamate transporters are expressed by astrocytes and play an important role in rapid clearance of the synaptically released glutamate, whose expression is downregulated in seizure. Together, increased oxidative stress and cellular excitability cause increased activity of sympathetic premotor neurons. ***B***, Increased PACAP expression can act via cAMP-mediated PKA and/or PKC pathways and produce either excitatory effect through phosphorylation of TH at serine 40 or neuroprotective effect regulated through decreased caspase 3, increased glial-glutamate transporters, and redirecting microglia toward anti-inflammatory M2 phenotype. In neurons, PACAP inhibits MAPK and increases IL-6 production. Microglia are activated by PACAP binding to PAC1 and VPAC1 receptors. Subsequently, microglia increase production and release of IL-10 and TGF-β and decrease production and release of TNF-α, as well as downregulating CD40 and B7 surface protein expression, with a neuroprotective effect. Conversely, the pro-inflammatory phenotype of activated microglia can produce IL-1β and TNF-α that may increase the sensitivity of neurons to activation.

interval. This response to PACAP(6–38) suggests that the excitatory action of PACAP (Fig. 8) on RVLM sympathetic premotor neurons mediates proarrhythmogenic changes, but not seizure-induced sympathoexcitation. Possible explanations could be that PACAP expression in the RVLM at 2 h after 2 mg/kg KA injection may be insufficient to produce sympathoexcitation, but enough to induce proarrhythmogenic effects. This idea is supported by the findings that PACAP gene expression reaches a maximum at 12 h after 12 mg/kg KA-induced seizures in the paraventricular nucleus of the hypothalamus (Nomura et al., 2000).

Microglia are the principal resident immune cells of the CNS, contributing ~10% of the total brain cell population. Activated microglia respond to environmental perturbations by adopting either a "pro-inflammatory M1" or "anti-inflammatory M2" phenotype (Li et al., 2007; Lai and Todd, 2008; Pisanu et al., 2014). Seizure causes extensive microglial activation in patients (Beach et al., 1995), and in animal models (Drage et al., 2002). There is considerable controversy surrounding the pro- (Shapiro

et al., 2008) or anti-inflammatory (Mirrione et al., 2010; Eyo et al., 2014) role played by microglia during seizure. Our recent findings demonstrate that microglia are protective during seizure on sympathetic preganglionic neurons within spinal cord (Bhandare et al., 2015). The findings of the current study show that blockade of microglial activation with minocycline microinjection in RVLM abolishes the prolongation of QT interval caused by KA-induced seizures but causes no change in sympathoexcitation, tachycardia, or hypertension. Our immunohistochemical analysis revealed that there are no changes in microglial morphology or phenotype in the vicinity of RVLM neurons (branch length or number of endpoint processes) or proportion of the M2 phenotype following induction of seizures. The increased RVLM neuronal activity may have activated microglia (which might be insufficient to differentiate with immunohistochemistry) producing an excitatory effect and contributed to the seizure-induced prolongation of QT interval (Fig. 8).

A possible mechanism to explain the increased glutamate release from presynaptic cells during seizure, and sympathoexcitation, is

proposed in Figure 8. The oxidative stress and inflammation in RVLM during seizure (Tsai et al., 2012) could be mediated through increased glutamate levels or functional failure of glutamate transporters. Increased synthesis and release of PACAP during seizure acts via cAMP-mediated PKA and/or PKC pathways that may have either excitatory effects through phosphorylation of TH at serine 40 (Bobrovskaya et al., 2007) or neuroprotective effects regulated through decreased caspase 3 (Dejda et al., 2011), increased glial-glutamate transporters, and redirecting microglia toward anti-inflammatory M2 phenotype (Brifault et al., 2015). PACAP inhibits MAPK and increases IL-6 (Shioda et al., 1998), whereas its action on the PAC1 and VPAC1 receptors of activated microglia increase production of IL-10, TGF-β and decrease TNF-α (Wada et al., 2013). Whereas polarization of activated microglia toward pro-inflammatory M1 phenotype increase IL-1β and TNF-α. Overall, depending on the type, severity, and intensity of stimulus, selective actions of PACAP and microglia regulate the physiological state of neurons. In the current study, both PACAP and microglia may regulate excitatory effects as their antagonism results in restoration of QT prolongation.

This is the first evidence to indicate that an increase in sympathetic nerve discharge and cardiovascular dysfunction in seizure is due to activation of glutamatergic receptors within the RVLM. Second, antagonism of PACAP and microglial activity in RVLM did not abolish the seizure-induced sympathoexcitation, hypertension, and tachycardia. Interestingly, minocycline, a drug that has central bioavailability following oral administration, and PACAP antagonist, restores the proarrhythmogenic effects of seizures to normal. This is the evidence for the physiological interaction between neurons and microglia. Third, the finding that microglia are not activated, and there is no change in the proportion of M2 phenotype during seizures, is consistent with our physiological findings.

In conclusion, the implications of the current findings are that, in patients with seizure, targeting glutamatergic receptors in RVLM catecholaminergic neurons and tailoring activity of PACAP and microglia in the vicinity of sympathetic premotor neurons may have protective effects and lead to novel therapies for seizure-induced cardiovascular dysfunction and SUDEP.

References

Araujo GC, Lopes OU, Campos RR (1999) Importance of glycinergic and glutamatergic synapses within the rostral ventrolateral medulla for blood pressure regulation in conscious rats. Hypertension 34:752–755. CrossRef Medline

Bardai A, Lamberts RJ, Blom MT, Spanjaart AM, Berdowski J, van der Staal SR, Brouwer HJ, Koster RW, Sander JW, Thijs RD, Tan HL (2012) Epilepsy is a risk factor for sudden cardiac arrest in the general population. PLoS One 7:e42749. CrossRef Medline

Bazett HC (1920) An analysis of the time-relations of electrocardiograms. Heart 7:353–370.

Beach TG, Woodhurst WB, MacDonald DB, Jones MW (1995) Reactive microglia in hippocampal sclerosis associated with human temporal lobe epilepsy. Neurosci Lett 191:27–30. CrossRef Medline

Bealer SL, Little JG, Metcalf CS, Brewster AL, Anderson AE (2010) Autonomic and cellular mechanisms mediating detrimental cardiac effects of status epilepticus. Epilepsy Res 91:66–73. CrossRef Medline

Bhandare AM, Mohammed S, Pilowsky PM, Farnham MM (2015) Antagonism of PACAP or microglia function worsens the cardiovascular consequences of kainic-acid-induced seizures in rats. J Neurosci 35:2191–2199. CrossRef Medline

Blümcke I, Becker AJ, Klein C, Scheiwe C, Lie AA, Beck H, Waha A, Friedl MG, Kuhn R, Emson P, Elger C, Wiestler OD (2000) Temporal lobe epilepsy associated upregulation of metabotropic glutamate receptors: correlated changes in mGluR1 mRNA and protein expression in experimental animals and human patients. J Neuropathol Exp Neurol 59:1–10. Medline

Bobrovskaya L, Gelain DP, Gilligan C, Dickson PW, Dunkley PR (2007) PACAP stimulates the sustained phosphorylation of tyrosine hydroxylase at serine 40. Cell Signal 19:1141–1149. CrossRef Medline

Brifault C, Gras M, Liot D, May V, Vaudry D, Wurtz O (2015) Delayed pituitary adenylate cyclase-activating polypeptide delivery after brain stroke improves functional recovery by inducing M2 microglia/macrophage polarization. Stroke 46:520–528. CrossRef Medline

Brotherstone R, Blackhall B, McLellan A (2010) Lengthening of corrected QT during epileptic seizures. Epilepsia 51:221–232. CrossRef Medline

Chapman AG (1998) Glutamate receptors in epilepsy. Prog Brain Res 116:371–383. CrossRef Medline

Damasceno DD, Savergnini SQ, Gomes ER, Guatimosim S, Ferreira AJ, Doretto MC, Almeida AP (2013) Cardiac dysfunction in rats prone to audiogenic epileptic seizures. Seizure 22:259–266. CrossRef Medline

Dampney RA, Horiuchi J, Tagawa T, Fontes MA, Potts PD, Polson JW (2003) Medullary and supramedullary mechanisms regulating sympathetic vasomotor tone. Acta Physiol Scand 177:209–218. CrossRef Medline

Dejda A, Seaborn T, Bourgault S, Touzani O, Fournier A, Vaudry H, Vaudry D (2011) PACAP and a novel stable analog protect rat brain from ischemia: insight into the mechanisms of action. Peptides 32:1207–1216. CrossRef Medline

Drage MG, Holmes GL, Seyfried TN (2002) Hippocampal neurons and glia in epileptic EL mice. J Neurocytol 31:681–692. CrossRef Medline

Eyo UB, Peng J, Swiatkowski P, Mukherjee A, Bispo A, Wu LJ (2014) Neuronal hyperactivity recruits microglial processes via neuronal NMDA receptors and microglial P2Y12 receptors after status epilepticus. J Neurosci 34:10528–10540. CrossRef Medline

Faingold C, Casebeer D (1999) Modulation of the audiogenic seizure network by noradrenergic and glutamatergic receptors of the deep layers of superior colliculus. Brain Res 821:392–399. CrossRef Medline

Farnham MMJ, Li Q, Goodchild AK, Pilowsky PM (2008) PACAP is expressed in sympathoexcitatory bulbospinal C1 neurons of the brain stem and increases sympathetic nerve activity in vivo. Am J Physiol Regul Integr Comp Physiol 294:1304–1311. CrossRef Medline

Farnham MM, Lung MS, Tallapragada VJ, Pilowsky PM (2012) PACAP causes PAC1/VPAC2 receptor mediated hypertension and sympathoexcitation in normal and hypertensive rats. Am J Physiol Heart Circ Physiol 303:910–917. CrossRef Medline

Gaede AH, Inglott MA, Farnham MM, Pilowsky PM (2012) Catestatin has an unexpected effect on the intrathecal actions of PACAP dramatically reducing blood pressure. Am J Physiol Regul Integr Comp Physiol 303:R719–R726. CrossRef Medline

Gurbanova AA, Aker RG, Sirvanci S, Demiralp T, Onat FY (2008) Intra-amygdaloid injection of kainic acid in rats with genetic absence epilepsy: the relationship of typical absence epilepsy and temporal lobe epilepsy. J Neurosci 28:7828–7836. CrossRef Medline

Guyenet PG (2006) The sympathetic control of blood pressure. Nat Rev Neurosci 7:335–346. CrossRef Medline

Guyenet PG, Filtz TM, Donaldson SR (1987) Role of excitatory amino acids in rat vagal and sympathetic baroreflexes. Brain Res 407:272–284. CrossRef Medline

Ito S, Sved AF (1997) Tonic glutamate-mediated control of rostral ventrolateral medulla and sympathetic vasomotor tone. Am J Physiol Regul Integr Comp Physiol 273:487–494. Medline

Kanamori K, Ross BD (2011) Chronic electrographic seizure reduces glutamine and elevates glutamate in the extracellular fluid of rat brain. Brain Res 1371:180–191. CrossRef Medline

Kanter RK, Strauss JA, Sauro MD (1995) Seizure-induced c-fos expression in rat medulla oblongata is not dependent on associated elevation of blood pressure. Neurosci Lett 194:201–204. CrossRef Medline

Kiely JM, Gordon FJ (1994) Role of rostral ventrolateral medulla in centrally mediated pressor responses. Am J Physiol Heart Circ Physiol 267:H1549–H1556. Medline

Lai AY, Todd KG (2008) Differential regulation of trophic and proinflammatory microglial effectors is dependent on severity of neuronal injury. Glia 56:259–270. CrossRef Medline

Lai CC, Wu SY, Lin HH, Dun NJ (1997) Excitatory action of pituitary adenylate cyclase activating polypeptide on rat sympathetic preganglionic neurons in vivo and in vitro. Brain Res 748:189–194. CrossRef Medline

LeBlanc BW, Zerah ML, Kadasi LM, Chai N, Saab CY (2011) Minocycline injection in the ventral posterolateral thalamus reverses microglial reac-

tivity and thermal hyperalgesia secondary to sciatic neuropathy. Neurosci Lett 498:138–142. CrossRef Medline

Li L, Lu J, Tay SS, Moochhala SM, He BP (2007) The function of microglia, either neuroprotection or neurotoxicity, is determined by the equilibrium among factors released from activated microglia in vitro. Brain Res 1159: 8–17. CrossRef Medline

Lothman EW, Collins RC, Ferrendelli JA (1981) Kainic acid-induced limbic seizures: electrophysiologic studies. Neurology 31:806–812. CrossRef Medline

Massey CA, Sowers LP, Dlouhy BJ, Richerson GB (2014) Mechanisms of sudden unexpected death in epilepsy: the pathway to prevention. Nat Rev Neurol 10:271–282. CrossRef Medline

Meldrum BS, Akbar MT, Chapman AG (1999) Glutamate receptors and transporters in genetic and acquired models of epilepsy. Epilepsy Res 36:189–204. CrossRef Medline

Metcalf CS, Poelzing S, Little JG, Bealer SL (2009) Status epilepticus induces cardiac myofilament damage and increased susceptibility to arrhythmias in rats. Am J Physiol Heart Circ Physiol 297:H2120–H2127. CrossRef Medline

Minson JB, Llewellyn-Smith IJ, Arnolda LF, Pilowsky PM, Oliver JR, Chalmers JP (1994) Disinhibition of the rostral ventral medulla increases blood pressure and Fos expression in bulbospinal neurons. Brain Res 646:44–52. CrossRef Medline

Mirrione MM, Konomos DK, Gravanis I, Dewey SL, Aguzzi A, Heppner FL, Tsirka SE (2010) Microglial ablation and lipopolysaccharide preconditioning affects pilocarpine-induced seizures in mice. Neurobiol Dis 39: 85–97. CrossRef Medline

Miyawaki T, Goodchild AK, Pilowsky PM (2002) Evidence for a tonic GABA-ergic inhibition of excitatory respiratory-related afferents to presympathetic neurons in the rostral ventrolateral medulla. Brain Res 924: 56–62. CrossRef Medline

Nadler JV (1981) Kainic acid as a tool for the study of temporal lobe epilepsy. Life Sci 29:2031–2042. CrossRef Medline

Nei M, Ho RT, Abou-Khalil BW, Drislane FW, Liporace J, Romeo A, Sperling MR (2004) EEG and ECG in sudden unexplained death in epilepsy. Epilepsia 45:338–345. CrossRef Medline

Nomura M, Ueta Y, Hannibal J, Serino R, Yamamoto Y, Shibuya I, Matsumoto T, Yamashita H (2000) Induction of pituitary adenylate cyclase-activating polypeptide mRNA in the medial parvocellular part of the paraventricular nucleus of rats following kainic-acid-induced seizure. Neuroendocrinology 71:318–326. CrossRef Medline

Ohtaki H, Nakamachi T, Dohi K, Aizawa Y, Takaki A, Hodoyama K, Yofu S, Hashimoto H, Shintani N, Baba A, Kopf M, Iwakura Y, Matsuda K, Arimura A, Shioda S (2006) Pituitary adenylate cyclase-activating polypeptide (PACAP) decreases ischemic neuronal cell death in association with IL-6. Proc Natl Acad Sci U S A 103:7488–7493. CrossRef Medline

Olsson T, Broberg M, Pope KJ, Wallace A, Mackenzie L, Blomstrand F, Nilsson M, Willoughby JO (2006) Cell swelling, seizures and spreading depression: an impedance study. Neuroscience 140:505–515. CrossRef Medline

Phillips JK, Goodchild AK, Dubey R, Sesiashvili E, Takeda M, Chalmers J, Pilowsky PM, Lipski J (2001) Differential expression of catecholamine biosynthetic enzymes in the rat ventrolateral medulla. J Comp Neurol 432:20–34. CrossRef Medline

Pilowsky PM, Lung MS, Spirovski D, McMullan S (2009) Differential regulation of the central neural cardiorespiratory system by metabotropic neurotransmitters. Philos Trans R Soc Lond B Biol Sci 364:2537–2552. CrossRef Medline

Pisanu A, Lecca D, Mulas G, Wardas J, Simbula G, Spiga S, Carta AR (2014) Dynamic changes in pro-and anti-inflammatory cytokines in microglia after PPAR-γ agonist neuroprotective treatment in the MPTPp mouse model of progressive Parkinson's disease. Neurobiol Dis 71:280–291. CrossRef Medline

Ross CA, Ruggiero DA, Joh TH, Park DH, Reis DJ (1984) Rostral ventrolateral medulla: selective projections to the thoracic autonomic cell column from the region containing C1 adrenaline neurons. J Comp Neurol 228: 168–185. CrossRef Medline

Sakamoto K, Saito T, Orman R, Koizumi K, Lazar J, Salciccioli L, Stewart M (2008) Autonomic consequences of kainic acid-induced limbic cortical seizures in rats: peripheral autonomic nerve activity, acute cardiovascular changes, and death. Epilepsia 49:982–996. CrossRef Medline

Schreihofer AM, Guyenet PG (1997) Identification of C1 presympathetic neurons in rat rostral ventrolateral medulla by juxtacellular labeling in vivo. J Comp Neurol 387:524–536. CrossRef Medline

Shapiro LA, Wang L, Ribak CE (2008) Rapid astrocyte and microglial activation following pilocarpine-induced seizures in rats. Epilepsia 49:33–41. CrossRef Medline

Shioda S, Ozawa H, Dohi K, Mizushima H, Matsumoto K, Nakajo S, Takaki A, Zhou CJ, Nakai Y, Arimura A (1998) PACAP protects hippocampal neurons against apoptosis: involvement of JNK/SAPK signaling pathway. Ann N Y Acad Sci 865:111–117. CrossRef Medline

Silveira DC, Schachter SC, Schomer DL, Holmes GL (2000) Flurothyl-induced seizures in rats activate Fos in brainstem catecholaminergic neurons. Epilepsy Res 39:1–12. CrossRef Medline

Sokal RR, Rohlf FJ (2012) Biometry, Ed 4. New York: Freeman.

Sperk G, Lassmann H, Baran H, Kish SJ, Seitelberger F, Hornykiewicz O (1983) Kainic acid induced seizures: neurochemical and histopathological changes. Neuroscience 10:1301–1315. CrossRef Medline

Surges R, Thijs RD, Tan HL, Sander JW (2009) Sudden unexpected death in epilepsy: risk factors and potential pathomechanisms. Nat Rev Neurol 5:492–504. CrossRef Medline

Sved AF, Ito S, Yajima Y (2002) Role of excitatory amino acid inputs to the rostral ventrolateral medulla in cardiovascular regulation. Clin Exp Pharmacol Physiol 29:503–506. CrossRef Medline

Tsai CY, Chan JY, Hsu KS, Chang AY, Chan SH (2012) Brain-derived neurotrophic factor ameliorates brain stem cardiovascular dysregulation during experimental temporal lobe status epilepticus. PLoS One 7:e33527. CrossRef Medline

Ueda Y, Doi T, Tokumaru J, Yokoyama H, Nakajima A, Mitsuyama Y, Ohya-Nishiguchi H, Kamada H, Willmore LJ (2001) Collapse of extracellular glutamate regulation during epileptogenesis: down-regulation and functional failure of glutamate transporter function in rats with chronic seizures induced by kainic acid. J Neurochem 76:892–900. CrossRef Medline

Vinet J, van Weering HRJ, Heinrich A, Kälin RE, Wegner A, Brouwer N, Heppner FL, van Rooijen N, Boddeke HWGM, Biber K (2012) Neuroprotective function for ramified microglia in hippocampal excitotoxicity. J Neuroinflamm 9:27. CrossRef Medline

Wada Y, Nakamachi T, Endo K, Seki T, Ohtaki H, Tsuchikawa D, Hori M, Tsuchida M, Yoshikawa A, Matkovits A, Kagami N, Imai N, Fujisaka S, Usui I, Tobe K, Koide R, Takahashi H, Shioda S (2013) PACAP attenuates NMDA-induced retinal damage in association with modulation of the microglia/macrophage status into an acquired deactivation subtype. J Mol Neurosci 51:493–502. CrossRef Medline

This Week in The Journal

- Olfactory Tubercle Neurons Signal Reward
- Amygdala Activation Alters Fear Conditioning

SOCIETY for NEUROSCIENCE

Appendix 2
Details of the chemicals, reagents, materials, equipment and software

CED Spike2	Cambridge Electronic Design
Compumedics EEG-ECG acqusition	Profusion EEG 4 v4.3, Australia
CorelDraw	CorelDRAW X7, Version 17.6.0.1021
IITC- Non-invasive tail cuff BP measurement	Life Sciences Inc., California, USA
Prism	Prism 6 for Windows, Version 6.05
Pulser script	Cambridge Electronic Design
Zeiss ZEN	ZEN 2012 (blue edition), Carl Zeiss Microscopy GmbH, 2011

Table 1: Details of the software used.

Axio Imager 2 (Z2)	Carl Zeiss Pty Ltd, NSW, Australia
Bioamplifier (BMA-931)	Cambridge Electronic Design, Cambridge, UK
Cautery	RB Medical Engineering, Herefordshire, England
CED 1401 ADC system	Cambridge Electronic Design, Cambridge, UK
Centrifuge machine (ALLEGRA X-15R)	Beckman Coulter, NSW, Australia
CO_2 analyser	Cambridge Electronic Design, Cambridge, UK
Electrolytes and blood gas analyser	IDEXX Vetstat, West Brook, USA
Hamiltor microsyringe	Grace Discovery Sciences, VIC, Australia
Heater with magnetic stirrer	John Morris Scientific, NSW, Australia
Heating pad	Cambridge Electronic Design, Cambridge, UK
Homeothermic blanket (TC-1000)	Cambridge Electronic Design
Humbugs	Quest Scientific
Isoflurane anasthesia machine	Blease Medical Equipment Ltd., Chiltern District, England
Nerve stimulator	A.M.P.I., Jerusalem, Israel
Peristaltic pump	John Morris Scientific, NSW, Australia
Pipette puller (P-2000)	SDR Scientific Pty Ltd, NSW, Australia
Pre-amplifier	Cambridge Electronic Design, Cambridge, UK
Shaker	John Morris Scientific, NSW, Australia
Stereotaxic manipulator	Narishige International Inc, NY, USA
Surgical drill	Ozito Rotary Tools, Australia
Surgical Microscope	Carl Zeiss Pty Ltd, NSW, Australia
Tail-cuff machine	ADInstruments Australia, NSW, Australia
Ventilator	Ugo Basile S.R.L., Monvalle, VA, Italy
Vertex mixer	Ratek Instruments Pty Ltd, VIC, Australia
Vibrotome (VT1200S)	Leica Microsystems Pty Ltd, NSW, Australia

Table 2: Details of the instruments used.

Isoflurane	Pharmachem, QLD, Australia
Lignocaine gel	Pfizer Australia Pty Limited, NSW, Australia
Lignocaine solution	Pfizer Australia Pty Limited, NSW, Australia
Sodium pentobarbital	Virbac (Australia) Pty Limited
Urethane (ethyl carbamate)	Sigma-Aldrich, NSW, Australia

Table 3: Details of the anesthetics used.

Atropine sulphate	Pfizer Australia Pty Limited, NSW, Australia
Diazepam	Mayne Pharma, Adelaide, SA
Doxycycline	LKT Laboratories, Inc, MN, USA
Heparin	Pfizer Australia Pty Limited, NSW, Australia
Minocycline	Sigma-Aldrich, NSW, Australia
Pancuronium	AstraZenca Pty Ltd, NSW, Australia

Table 4: Details of the drugs used.

| PACAP-38 | Auspep, VIC, Australia and Selleck Chemicals, TX, USA |
| PACAP(6-38) | Auspep, VIC, Australia and Selleck Chemicals, TX, USA |

Table 5: Details of the peptides used.

Compound sodium lactate solution	Baxter, NSW, Australia
Chicago Sky Blue	Sigma-Aldrich, NSW, Australia
Chloroform	Sigma-Aldrich, NSW, Australia
Cresyl violet	Sigma-Aldrich, NSW, Australia
Etahnol	Sigma-Aldrich, NSW, Australia
Ethylene glycol	Sigma-Aldrich, NSW, Australia
Glacial acetic acid	Sigma-Aldrich, NSW, Australia
Glutamate	Sigma-Aldrich, NSW, Australia
Xylene	ROWE Scientific Pty Ltd, NSW, Australia
HCl	Sigma-Aldrich, NSW, Australia
Kainic acid	Sapphire Bioscience, NSW, Australia and Enzo Life Sciences, Farmingdale, NY, U.S.A.
Kynurenic acid	Sigma-Aldrich, NSW, Australia
Merthiolate	Sigma-Aldrich, NSW, Australia
Paraformaldehyde	Sigma-Aldrich, NSW, Australia
PBS tablets	Amresco, OH, USA
Polyvinylpyrrolidone	Sigma-Aldrich, NSW, Australia
Potassium chloride (KCl)	Chem-Supply, SA, Australia
Sodilum chloride (NaCl)	Chem-Supply, SA, Australia
Sodium hydroxide solution (NaOH; 1N)	Sigma-Aldrich, NSW, Australia
Sodium phosphate dibasic (NaH_2PO_4)	Sigma-Aldrich, NSW, Australia
Sodium phosphate monobasic (Na_2HPO_4)	Sigma-Aldrich, NSW, Australia
Sucrose	Sigma-Aldrich, NSW, Australia
Tris-HCl	Sigma-Aldrich, NSW, Australia
Triton-X	Sigma-Aldrich, NSW, Australia

Table 6: Details of the chemicals used.

75-µm Teflon-insulated stainless steel EEG wires	A-M Systems Inc., WA, USA
Catalyst	IMCD Australia Limited, VIC, Australia
Cotton swabs	Mcfarlane Medical Equipment (Holdings) Pty Ltd, NSW, Australia
Cover slips	Thermo Fisher Scientific, VIC, Australia
Dental cement	Vertex-Dental, Soesterberg, The Netherlands
Donkey serum	Sigma-Aldrich, NSW, Australia
DPX (dibutylphthalate polystyrene xylene)	Sigma-Aldrich, NSW, Australia
ECG leads	Plastics One, VA, USA
Extradural electrodes	Plastics One, VA, USA
Gelatinised slides	Thermo Fisher Scientific, VIC, Australia
Glass slides	Thermo Fisher Scientific Australia Pty Ltd, VIC, Australia
Needles	Diagnostic and Medical Pty Ltd, NSW, Australia
Parafin oil	Biotech Pharmaceuticals Pty Ltd, VIC, Australia
pH strips	Sigma-Aldrich, NSW, Australia
Pipettes	SDR Scientific Pty Ltd, NSW, Australia
Polyethylene tubing (arterial)	Microtube Extrusions Pty Ltd, NSW, Australia
Polyethylene tubing (IT)	Microtube Extrusions Pty Ltd, NSW, Australia
Sharpoint polypropylene, 4-0	eSuture.com, IL, USA
Silastic tubing (arterial)	Microtube Extrusions Pty Ltd, NSW, Australia
Silastic tubing (IT)	Microtube Extrusions Pty Ltd, NSW, Australia
Silgel Part-A and -B	Barnes Products Pty Ltd, NSW, Australia
Silk threads (2/0)	Pearsalls Embroidery, Wales, UK
Silk threads (5/0)	Pearsalls Embroidery, Wales, UK
Surgical tools	Fiine Scientific Tools, CA, USA
Syringes	Diagnostic and Medical Pty Ltd, NSW, Australia
Vectashield (H-1000)	Vector Laboratories, Burlingame, California, USA

Table 7: Details of the miscellaneous items used.

Appendix 3
Ethics Approval

ANIMAL RESEARCH AUTHORITY (ARA)

AEC Reference No.: 2013/017　　　　　　　　　**Date of Expiry:** 19 May 2014

Full Approval Duration: 20 May 2013 to 19 May 2016 (36 Months)

This ARA remains in force until the Date of Expiry (unless suspended, cancelled or surrendered) **and will only be renewed upon receipt of a satisfactory Progress Report before expiry (see Approval email for submission details).**

Principal Investigator:　　　　　　　　　　　**Associate Investigators:**
Professor Paul Pilowsky　　　　　　　　　　　　Amol Bhandare　　　　0406 896 534
School of Advanced Medicine　　　　　　　　　　Melissa Farnham　　　0415 821 096
Macquarie University, NSW 2109
paul.pilowsky@mq.edu.au
0431 500 553

<div style="border:1px solid red">

In case of emergency, please contact:
the Principal Investigator / Associate Investigator named above
or Manager, CAF: 9850 7780 / 0428 861 163 and **Animal Welfare Officer**: 9850 7758 / 0439 497 383

</div>

The above named are authorised by MACQUARIE UNIVERSITY ANIMAL ETHICS COMMITTEE to conduct the following research:

Title of the project: **Brain mediated cardiorespiratory dysfunction during chemically induced seizures in rats**

Purpose: 4　Research: Human or Animal Biology

Aims: **To identify brain chemicals (neurotransmitters) in the nuclei of the brain responsible for seizure-induced cardiovascular effects**

Surgical Procedures category: 2　Animal Unconscious without Recovery

All procedures must be performed as per the AEC-approved protocol, unless stated otherwise by the AEC and/or AWO.

Maximum numbers approved (for the Full Approval Duration):

Species	Strain	Age/Sex/Weight	Total	Supplier/Source
02-Rat	Sprague-Dawley	6-8wk / Male / 200-350g	274	ARC Perth
		TOTAL	**274**	

Location of research:

Location	Full street address
Central Animal Facility	Building F9A, Research Park Drive, Macquarie University, NSW 2109
ASAM	Level 1, F10A, 2 Technology Place, Macquarie University, NSW 2109

Amendments approved by the AEC since initial approval: N/A

Conditions of Approval: N/A

Being animal research carried out in accordance with the Code of Practice for a recognised research purpose and in connection with animals (other than exempt animals) that have been obtained from the holder of an animal suppliers licence.

_____
Professor Mark Connor (Chair, Animal Ethics Committee)　　　　　　**Approval Date:** 17 May 2013

Adapted from Form C (issued under part IV of the Animal Research Act, 1985)

Health
Sydney
Local Health District

4 December 2013

Professor P Pilowsky
High Blood Pressure Group
Heart Research Institute

Dear Professor Pilowsky,

Re: Protocol No 2013/082 - "Brain mediated cardiorespiratory dysfunction during chemically induced seizures in rats"

Thank you for submitting the above research proposal, which was considered by the SLHD Animal Welfare Committee, at its meetings of 31 October 2013 and 22 November 2013. Approval is given for this study to be undertaken.

Approval Number:	2013/082A
Approval Period:	1 December 2013 to 30 November 2014
Description of research:	This study will investigate brain chemicals (neurotransmitters) that can affect heart function and which may have a role in sudden unexplained death in epilepsy. Rats will undergo a number of invasive procedures under anaesthesia in one of two separate experiments, at the end of which the animals will be euthanased for collection of the brain for laboratory analysis.
Location of research:	Heart Research Institute – Animal House
Animals Approved:	Year 1: 74 male rat (Sprague Dawley)

ADDRESS FOR ALL CORRESPONDENCE
RESEARCH DEVELOPMENT OFFICE
ROYAL PRINCE ALFRED HOSPITAL
CAMPERDOWN NSW 2050

TELEPHONE: (
FACSIMILE: (__, ____ . . . .
EMAIL: l(
REFERENCE: 2014/024
3.2/Aug14

Health
Sydney
Local Health District

NSW
GOVERNMENT

1 September 2014

Professor P M Pilowsky
C/- Dr M Farnham
Heart Research Institute
¯
i
l'

Dear Professor Pilowsky,

Re: Protocol No 2014/024 - "Brain mediated cardiorespiratory dysfunction in kainic acid induced chronic seizures rats"

Thank you for submitting the above research proposal, which was considered by the SLHD Animal Welfare Committee, at its meeting of 28 August 2014. Approval is given for this study to be undertaken.

Approval Number: 2014/024A

Approval Period: September 2014 to August 2017

This is subject to receipt of timely and satisfactory annual reports.

Description of research: In a series of invasive experiments, this study will investigate the complex relationship between brain function, nerve activity and changes in blood pressure and heart rate and rhythm that occur during and after epileptic seizures. A rat model of epilepsy will be used in which epileptic seizures are induced by the gradual administration of kainic acid solution and then stopped by the anti-epileptic drug, diazepam. This results in a period of wellness of 10-11 weeks after which the animals achieved through immunohistochemical study of the brain and spinal cord removed from deeply anaesthetised animals, and through *in vivo* physiological studies on deeply anaesthetised animals. The latter involve non-recovery, invasive procedures over a four hour period. At the conclusion of the studies blood and tissue collected for the animals will undergo laboratory analysis.